RICHARD WEIR and CARL NELSON

US Patent 7,033,406 25th April 2006 Inventors: Richard Weir and Carl Nelson

ELECTRICAL-ENERGY-STORAGE UNIT UTILISING CERAMIC AND INTEGRATED-CIRCUIT TECHNOLOGIES FOR REPLACEMENT OF ELECTROCHEMICAL BATTERIES

This patent shows an electrical storage method which is reputed to power an electric car for a 500 mile trip on a charge taking only five minutes to complete. This document is a very slightly re-worded copy of the original. It has been pointed out by Mike Furness that while a five minute recharge is feasible, it is not practical, calling for cables with a six-inch diameter. Also, the concept of recharging stations as suggested is also rather improbable as the electrical supply needed would rival that of a power station. However, if the charging time were extended to night time, then it would allow substantial driving range during the day time.

ABSTRACT

An Electrical-Energy-Storage Unit (EESU) has as a basis material a high-permittivity, composition-modified barium titanate ceramic powder. This powder is double coated with the first coating being aluminium oxide and the second coating calcium magnesium aluminosilicate glass. The components of the EESU are manufactured with the use of classical ceramic fabrication techniques which include screen printing alternating multi-layers of nickel electrodes and high-permittivity composition-modified barium titanate powder, sintering to a closed-pore porous body, followed by hot-isostatic pressing to a void-free body. The components are configured into a multi-layer array with the use of a solder-bump technique as the enabling technology so as to provide a parallel configuration of components that has the capability to store electrical energy in the range of 52 kWH. The total weight of an EESU with this range of electrical energy storage is about 336 pounds.

BACKGROUND OF THE INVENTION

1. Field of the Invention

This invention relates generally to energy-storage devices, and relates more particularly to high-permittivity ceramic components utilised in an array configuration for application in ultra high electrical-energy storage devices.

2. Description of the Relevant Art

The internal-combustion-engine (ICE) powered vehicles have as their electrical energy sources a generator and battery system. This electrical system powers the vehicle accessories, which include the radio, lights, heating, and air conditioning. The generator is driven by a belt and pulley system and some of its power is also used to recharge the battery when the ICE is in operation. The battery initially provides the required electrical power to operate an electrical motor that is used to turn the ICE during the starting operation and the ignition system.

The most common batteries in use today are:
Flooded lead-acid,
Sealed gel lead-acid,
Nickel-Cadmium (Ni-Cad),
Nickel Metal Hydride (NiMH), and
Nickel-Zinc (Ni-Z).

References on the subject of electrolchemical batteries include the following:

Guardian, Inc., "Product Specification": Feb. 2, 2001;
K. A. Nishimura, "NiCd Battery", Science Electronics FAQ V1.00: Nov. 20, 1996;
Ovonics, Inc., "Product Data Sheet": no date;
Evercel, Inc., "Battery Data Sheet—Model 100": no date;
S. R. Ovshinsky et al., "Ovonics NiMH Batteries: The Enabling Technology for Heavy-Duty Electrical and Hybrid Electric Vehicles", Ovonics publication 2000-01-3108: Nov. 5, 1999;
B. Dickinson et al., "Issues and Benefits with Fast Charging Industrial Batteries", AeroVeronment, Inc. article: no date.

Each specific type of battery has characteristics, which make it either more or less desirable to use in a specific application. Cost is always a major factor and the NiMH battery tops the list in price with the flooded lead-acid battery being the most inexpensive. Evercel manufactures the Ni-Z battery and by a patented process, with the

claim to have the highest power-per-pound ratio of any battery. See Table 1 below for comparisons among the various batteries. What is lost in the cost translation is the fact that NiMH batteries yield nearly twice the performance (energy density per weight of the battery) than do conventional lead-acid batteries. A major drawback to the NiMH battery is the very high self-discharge rate of approximately 5% to 10% per day. This would make the battery useless in a few weeks. The Ni-Cad battery and the lead-acid battery also have self-discharge but it is in the range of about 1% per day and both contain hazardous materials such as acid or highly toxic cadmium. The Ni-Z and the NiMH batteries contain potassium hydroxide and this electrolyte in moderate and high concentrations is very caustic and will cause severe burns to tissue and corrosion to many metals such as beryllium, magnesium, aluminium, zinc, and tin.

Another factor that must be considered when making a battery comparison is the recharge time. Lead-acid batteries require a very long recharge period, as long as 6 to 8 hours. Lead-acid batteries, because of their chemical makeup, cannot sustain high current or voltage continuously during charging. The lead plates within the battery heat rapidly and cool very slowly. Too much heat results in a condition known as "gassing" where hydrogen and oxygen gases are released from the battery's vent cap. Over time, gassing reduces the effectiveness of the battery and also increases the need for battery maintenance, i.e., requiring periodic de-ionised or distilled water addition. Batteries such as Ni-Cad and NiMH are not as susceptible to heat and can be recharged in less time, allowing for high current or voltage changes which can bring the battery from a 20% state of charge to an 80% state of charge in just 20 minutes. The time to fully recharge these batteries can be more than an hour. Common to all present day batteries is a finite life, and if they are fully discharged and recharged on a regular basis their life is reduced considerably.

SUMMARY OF THE INVENTION

In accordance with the illustrated preferred embodiment, the present invention provides a unique electrical-energy-storage unit that has the capability to store ultra high amounts of energy.

One aspect of the present invention is that the materials used to produce the energy-storage unit, EESU, are not explosive, corrosive, or hazardous. The basis material, a high-permittivity calcined composition-modified barium titanate powder is an inert powder and is described in the following references: S. A. Bruno, D. K. Swanson, and I. Burn, J. Am Ceram. Soc. 76, 1233 (1993); P. Hansen, U.S. Pat. No. 6,078,494, issued Jun. 20, 2000. The most cost-effective metal that can be used for the conduction paths is nickel. Nickel as a metal is not hazardous and only becomes a problem if it is in solution such as in deposition of electroless nickel. None of the EESU materials will explode when being recharged or impacted. Thus the EESU is a safe product when used in electric vehicles, buses, bicycles, tractors, or any device that is used for transportation or to perform work. It could also be used for storing electrical power generated from solar voltaic cells or other alternative sources for residential, commercial, or industrial applications. The EESU will also allow power averaging of power plants utilising SPVC or wind technology and will have the capability to provide this function by storing sufficient electrical energy so that when the sun is not shinning or the wind is not blowing they can meet the energy requirements of residential, commercial, and industrial sites.

Another aspect of the present invention is that the EESU initial specifications will not degrade due to being fully discharged or recharged. Deep cycling the EESU through the life of any commercial product that may use it will not cause the EESU specifications to be degraded. The EESU can also be rapidly charged without damaging the material or reducing its life. The cycle time to fully charge a 52 kWH EESU would be in the range of 4 to 6 minutes with sufficient cooling of the power cables and connections. This and the ability of a bank of EESUs to store sufficient energy to supply 400 electric vehicles or more with a single charge will allow electrical energy stations that have the same features as the present day gasoline stations for the ICE cars. The bank of EESUs will store the energy being delivered to it from the present day utility power grid during the night when demand is low and then deliver the energy when the demand hits a peak. The EESU energy bank will be charging during the peak times but at a rate that is sufficient to provide a full charge of the bank over a 24-hour period or less. This method of electrical power averaging would reduce the number of power generating stations required and the charging energy could also come from alternative sources. These electrical-energy-delivery stations will not have the hazards of the explosive gasoline.

Yet another aspect of the present invention is that the coating of aluminium oxide and calcium magnesium aluminosilicate glass on calcined composition-modified barium titanate powder provides many enhancement features and manufacturing capabilities to the basis material. These coating materials have exceptional high voltage breakdown and when coated on to the above material will increase the breakdown voltage of ceramics comprised of the coated particles from 3×10^6 V/cm of the uncoated basis material to around 5×10^6 V/cm or higher. The following reference indicates the dielectric breakdown strength in V/cm of such materials: J. Kuwata et al., "Electrical Properties of Perovskite-Type Oxide Thin-Films Prepared by RF Sputtering", Jpn. J. Appl. Phys., Part 1, 1985, 24(Suppl. 24-2, Proc. Int. Meet. Ferroelectr., 6th), 413-15. This very high voltage breakdown assists in allowing the ceramic EESU to store a large amount of energy due to the following: Stored energy $E = CV^2 / 2$,

Formula 1, as indicated in F. Sears et al., "Capacitance-Properties of Dielectrics", University Physics, Addison-Wesley Publishing Company, Inc.: Dec. 1957: pp 468-486, where C is the capacitance, V is the voltage across the EESU terminals, and E is the stored energy. This indicates that the energy of the EESU increases with the square of the voltage. **Fig.1** indicates that a double array of 2230 energy storage components 9 in a parallel configuration that contain the calcined composition-modified barium titanate powder. Fully densified ceramic components of this powder coated with 100 Angstrom units of aluminium oxide as the first coating 8 and a 100 Angstrom units of calcium magnesium aluminosilicate glass as the second coating 8 can be safely charged to 3500 V. The number of components used in the double array depends on the electrical energy storage requirements of the application. The components used in the array can vary from 2 to 10,000 or more. The total capacitance of this particular array 9 is 31 F which will allow 52,220 W·h of energy to be stored as derived by Formula 1.

These coatings also assist in significantly lowering the leakage and ageing of ceramic components comprised of the calcined composition-modified barium titanate powder to a point where they will not effect the performance of the EESU. In fact, the discharge rate of the ceramic EESU will be lower than 0.1% per 30 days which is approximately an order of magnitude lower than the best electrochemical battery.

A significant advantage of the present invention is that the calcium magnesium aluminosilicate glass coating assists in lowering the sintering and hot-isostatic-pressing temperatures to 800^{O}C. This lower temperature eliminates the need to use expensive platinum, palladium, or palladium-silver alloy as the terminal metal. In fact, this temperature is in a safe range that allows nickel to be used, providing a major cost saving in material expense and also power usage during the hot-isostatic-pressing process. Also, since the glass becomes easily deformable and flowable at these temperatures it will assist in removing the voids from the EESU material during the hot-isostatic-pressing process. The manufacturer of such systems is Flow Autoclave Systems, Inc. For this product to be successful it is mandatory that all voids be removed to assist in ensuring that the high voltage breakdown can be obtained. Also, the method described in this patent of coating the calcium magnesium aluminosilicate glass ensures that the hot-isostatic-pressed double-coated composition-modified barium titanate high-relative-permittivity layer is uniform and homogeneous.

Yet another aspect of the present invention is that each component of the EESU is produced by screen-printing multiple layers of nickel electrodes with screening ink from nickel powder. Interleaved between nickel electrodes are dielectric layers with screening ink from calcined double-coated high-permittivity calcined composition-modified barium titanate powder. A unique independent dual screen-printing and layer-drying system is used for this procedure. Each screening ink contains appropriate plastic resins, surfactants, lubricants, and solvents, resulting in a proper rheology (the study of the deformation and flow of matter) for screen printing. The number of these layers can vary depending on the electrical energy storage requirements. Each layer is dried before the next layer is screen printed. Each nickel electrode layer **12** is alternately preferentially aligned to each of two opposite sides of the component automatically during this process as indicated in **Fig.2**. These layers are screen printed on top of one another in a continuous manner. When the specified number of layers is achieved, the component layers are then baked to obtain by further drying sufficient handling strength of the green plastic body. Then the array is cut into individual components to the specified sizes.

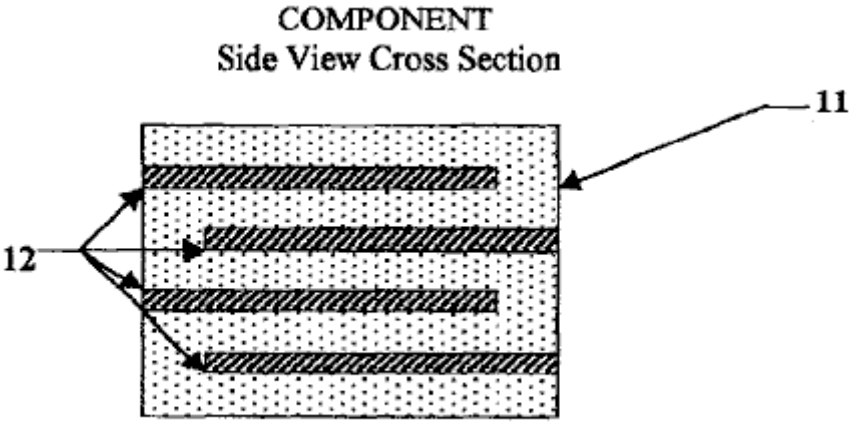

Figure 2

Alternatively, the dielectric powder is prepared by blending with plastic binders, surfactants, lubricants, and solvents to obtain a slurry with the proper rheology for tape casting. In tape casting, the powder-binder mixture is extruded by pressure through a narrow slit of appropriate aperture height for the thickness desired of the green plastic ceramic layer on to a moving plastic-tape carrier, known as a doctor-blade web coater. After drying, to develop sufficient handling strength of the green plastic ceramic layer, this layer is peeled away from the plastic-tape carrier. The green plastic ceramic layer is cut into sheets to fit the screen-printing frame in which the

electrode pattern is applied with nickel ink. After drying of the electrode pattern, the sheets are stacked and then pressed together to assure a well-bonded lamination. The laminate is then cut into components of the desired shape and size.

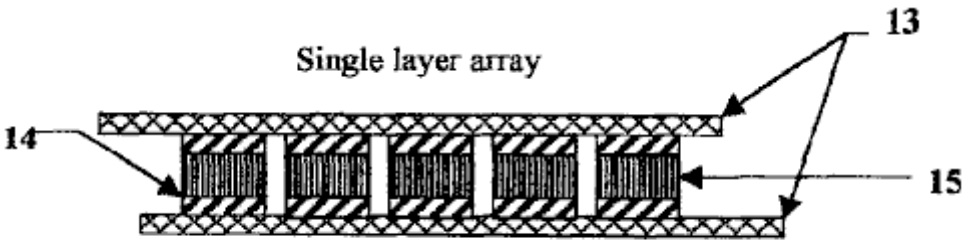

Figure 3

The components are treated for the binder-burnout and sintering steps. The furnace temperature is slowly ramped up to 350^{O}C and held for a specified length of time. This heating is accomplished over a period of several hours so as to avoid any cracking and delamination of the body. Then the temperature is ramped up to 850^{O}C and held for a specified length of time. After this process is completed the components are then properly prepared for the hot isostatic pressing at 700^{O}C and the specified pressure. This process will eliminate voids. After this process, the components are then side-lapped on the connection side to expose the preferentially aligned nickel electrodes **12**. Then these sides are dipped into ink from nickel powder that has been prepared to have the desired rheology. Then side conductors of nickel **14** are dipped into the same ink and then are clamped on to each side of the components **15** that have been dipped into the nickel powder ink. The components are then fired at 800^{O}C for 20 minutes to bond the nickel bars to the components as indicated in **Fig.3**. The components are then assembled into a first-level array, **Fig.3**, with the use of the proper tooling and solder-bump technology. Then the first-level arrays are assembled to form a second-level array, **Fig.4**, by stacking the first array layers on top of one another in a preferential mode. Then nickel bars **18** are attached on each side of the second array as indicated in **Fig.4**. Then the EESU is packaged to form its final assembly configuration.

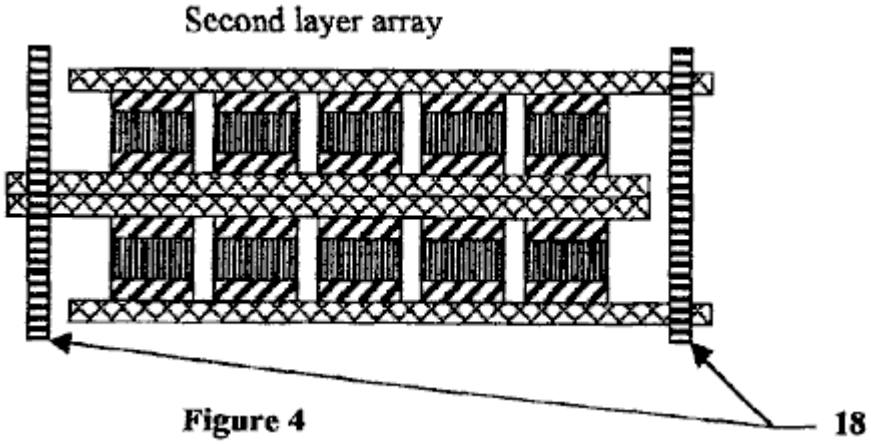

Figure 4

The features of this patent indicate that the ceramic EESU, as indicated in Table 1, outperforms the electrochemical battery in every parameter. This technology will provide mission-critical capability to many sections of the energy-storage industry.

TABLE 1
The parameters of each technology to store 52.2 kW · h of electrical energy
are indicated-(data as of February 2001 from manufacturer's specification sheets).

	NiMH	LA(Gel)	Ceramic EESU	Ni—Z
Weight (pounds)	1,716	3,646	336	1,920
Volume (cu. inch)	17,881	43,045	2,005	34,780
Discharge rate	5% in 30 days	1% in 30 days	0.1% in 30 days	1% in 30 days
Charging time (full)	1.5 hours	8.0 hours	3 to 6 minutes	1.5 hours
Life reduced with deep cycle use	moderate	high	none	moderate
Hazardous materials	Yes	Yes	None	Yes

This EESU will have the potential to revolutionise the electric vehicle (EV) industry, the storage and use of electrical energy generated from alternative sources with the present utility grid system as a backup source for residential, commercial, and industrial sites, and the electric energy point of sales to EVs. The EESU will replace the electrochemical battery in any of the applications that are associated with the above business areas or in any business area where its features are required.

The features and advantages described in the specifications are not all inclusive, and particularly, many additional features and advantages will be apparent to one of ordinary skill in the art in view of the description, specification and claims made here. Moreover, it should be noted that the language used in the specification has been principally selected for readability and instructional purposes, and may not have been selected to delineate or circumscribe the inventive subject matter, resort to the claims being necessary to determine such inventive subject matter.

BRIEF DESCRIPTION OF THE DRAWINGS

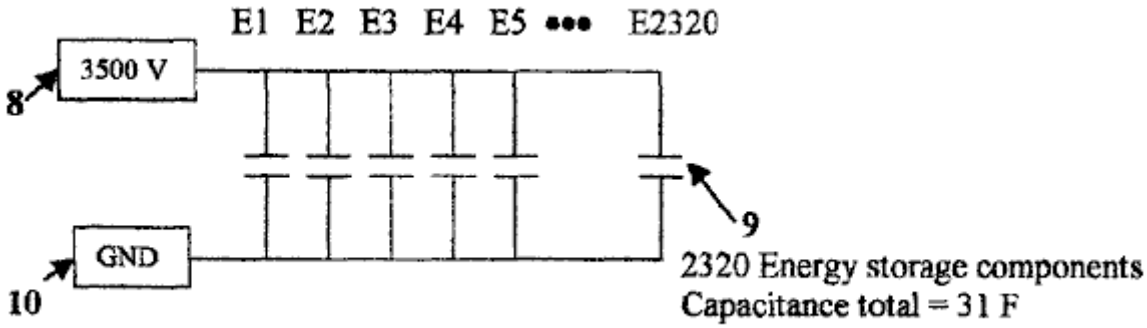

Figure 1

Fig.1 indicates a schematic of 2320 energy storage components **9** hooked up in parallel with a total capacitance of 31 Farads. The maximum charge voltage **8** of 3500 V is indicated with the cathode end of the energy storage components **9** hooked to system ground **10**.

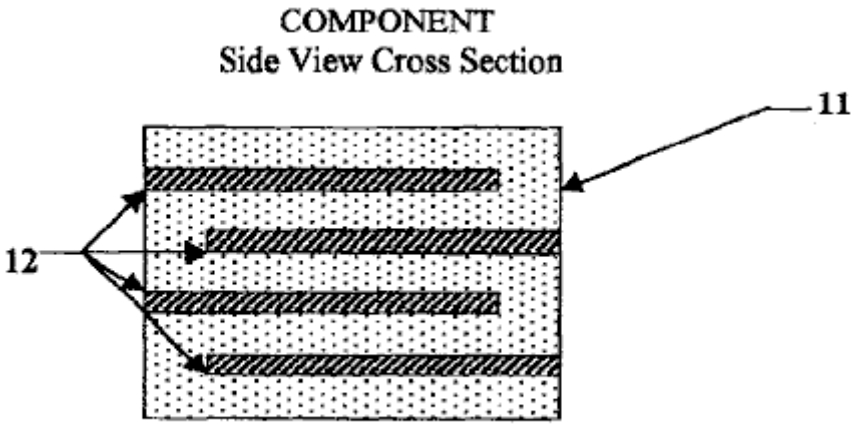

Figure 2

Fig.2 is a cross-section side view of the electrical-energy-storage unit component. This figure indicates the alternating layers of nickel electrode layers **12** and high-permittivity composition-modified barium titanate dielectric layers **11**. This figure also indicate the preferentially aligning concept of the nickel electrode layers **12** so that each storage layer can be hooked up in parallel.

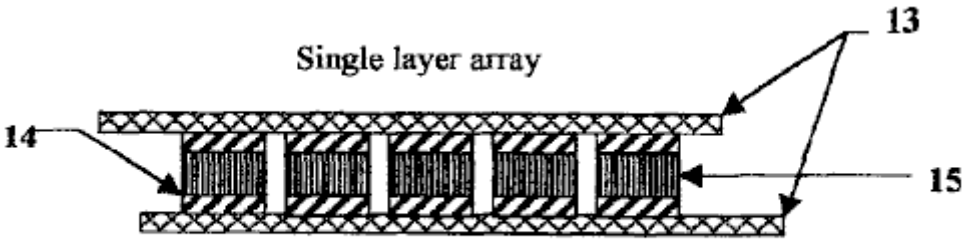

Figure 3

Fig.3 is side view of a single-layer array indicating the attachment of individual components **15** with the nickel side bars **14** attached to two preferentially aligned copper conducting sheets **13**.

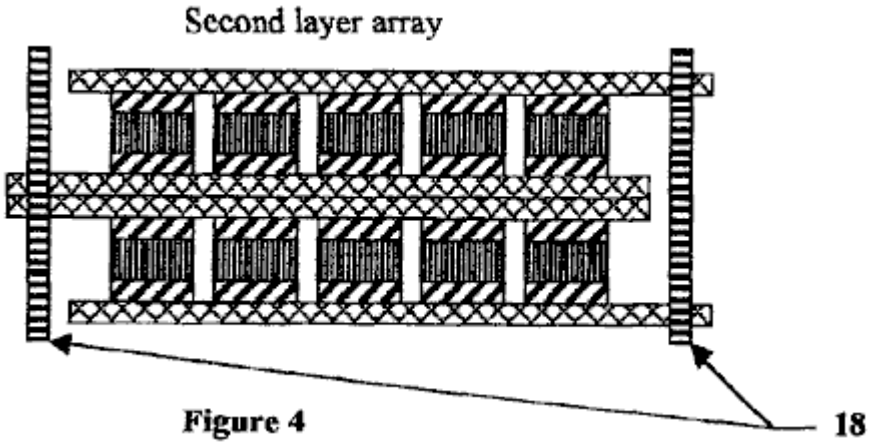

Figure 4

Fig.4 is a side view of a double-layer array with copper array connecting nickel bars **16** attaching the two arrays via the edges of the preferentially aligned copper conductor sheets **13**. This figure indicates the method of attaching the components in a multi-layer array to provide the required energy storage.

Reference No.	Refers to this in the drawings
8	System maximum voltage of 3500 V
9	2320 energy-storage components hooked up in parallel with a total capacitance of 31 Farad
10	System ground
11	High-permittivity calcined composition-modified barium titanate dielectric layers
12	Preferentially aligned nickel electrode layers
13	Copper conductor sheets
14	Nickel sidebars
15	Components
16	Copper array connecting nickel bars

DETAILED DESCRIPTION OF THE PREFERRED EMBODIMENTS

Fig.1, **Fig.2**, **Fig.3**, and **Fig.4** of the drawings and the following description depict various preferred embodiments of the present invention for purposes of illustration only. One skilled in the art will readily recognise from the following discussion those alternative embodiments of the structures and methods illustrated herein may be employed without departing from the principles of the invention described here. While the invention will be described in conjunction with the preferred embodiments, it will be understood that they are not intended to limit the invention to those embodiments. On the contrary, the invention is intended to cover alternatives, modifications, and equivalents, which may be included within the spirit and scope of the invention as defined by the claims.

Preparation of the high-permittivity calcined composition-modified barium titanate powder that is used to fabricate the EESU is explained as follows. Wet-chemical-prepared powders of high-purity as well as composition-modified barium titanate with narrow particle-size distribution have been produced with clear advantages over those prepared by solid-state reaction of mechanically mixed, ball-milled, and calcined powdered ingredients. The

compositional and particle-size uniformity attained with a coprecipitated-prepared powder is vastly superior to that with a conventional-prepared powder. The microstructures of ceramics formed from these calcined wet-chemical-prepared powders are uniform in grain size and can also result in smaller grain size. Electrical properties are improved so that higher relative permittivities and increased dielectric breakdown strengths can be obtained. Further improvement can be obtained by the elimination of voids within the sintered ceramic body with subsequent hot isostatic pressing.

High-relative-permittivity dielectrics have inherent problems, namely ageing, fatigue, degradation, and decay of the electrical properties, which limit their application. The use of surface-coated powders in which the surface region is comprised of one or two materials different in composition from that of the powder overcomes these problems provided that the compositions are appropriately chosen.

Among ceramics, alumina [aluminium oxide (Al_2O_3)], and among glasses, calcium magnesium aluminosilicate ($CaO.MgO.Al_2O_3.SiO_2$) glasses are the best dielectrics in terms of having the highest dielectric breakdown strengths and to seal the high-relative-permittivity dielectric powder particles so as to eliminate or significantly reduce their inherent problems.

A glass with a given composition at temperatures below its glass transition temperature range, which is in the neighbourhood of its strain-point temperature, is in a fully rigid condition, but at temperatures above this range is in a viscous-flow condition, its viscosity decreasing with increasing temperature. The application of hot isostatic pressing to a sintered closed-pore porous ceramic body comprised of sufficient-thickness glass-coated powder will lead to void elimination provided the glass is in the viscous-flow condition where it is easily deformable and flowable.

The wet-chemical-prepared and calcined composition-modified barium titanate powder is accordingly coated with these layers of, first, alumina, and second, a calcium magnesium aluminosilicate glass. After the first layer has been applied by wet-chemical means, the powder is calcined at $1050^{O}C$ to convert the precursor, aluminium nitrate nonahydrate [$Al(NO_3)_3.9H_2O$] to aluminium oxide (corundum) [α-Al_2O_3]. Then the second layer is applied by wet-chemical means with the use of the precursors in the appropriate amounts of each, and in absolute ethanol (CH_3CH_2OH) as the solvent, shown in the accompanying table. After drying, the powder is calcined at $500^{O}C$ to convert the precursor mixture to a calcium magnesium aluminosilicate glass. It is important that the calcining temperature is not higher than the strain point of the selected glass composition to prevent sticking together of the powder. The glass coating has the further advantage of acting as a sintering aid and allowing a substantially lower firing temperature for densification of the ceramic body particularly during the hot-isostatic-pressing step.

Another significant advantage of the calcium magnesium aluminosilicate glass coating is that sintering and densification temperatures are sufficiently lowered to allow the use of nickel conductor electrodes in place of the conventional expensive platinum, palladium, or palladium-silver alloy ones.

Preparation of the Calcined Composition-Modified Barium Titanate Powder is Indicated by the Following Process Steps.

A solution of the precursors: $Ba(NO_3)_2$, $Ca(NO_3)_2.4H_2O$, $Nd(NO_3)_3.6H_2O$, $Y(NO_3)_3.4H_2O$, $Mn(CH_3COO)_2.4H_2O$, $ZrO(NO_3)_2$, and $[CH_3CH(O—)COONH_4]2Ti(OH)_2$, as selected from the reference; Sigma-Aldrich, Corp., "Handbook of Fine Chemicals and Laboratory Equipment", 2000-2001, in de-ionised water heated to $80^{O}C$ is made in the proportionate amount in weight percent for each of the seven precursors as shown in the most right-hand column of Table 3. A separate solution of $(CH_3)4NOH$ somewhat in excess amount than required, as shown in Table 4, is made in de-ionised water, free of dissolved carbon dioxide (CO_2) and heated to 80^{O}-$85^{O}C$. The two solutions are mixed by pumping the heated ingredient streams simultaneously through a coaxial fluid jet mixer. A slurry of the co-precipitated powder is produced and collected in a drown-out vessel. The co-precipitated powder is refluxed in the drown-out vessel at 90°-95° C. for 12 hr and then filtered, de-ionised-water washed, and dried. Alternatively, the powder may be collected by centrifugal sedimentation. An advantage of $(CH_3)4NOH$ as the strong base reactant is that there are no metal element ion residuals to wash away anyway. Any residual $(CH_3)4NOH$, like any residual anions from the precursors, is harmless, because removal by volatilisation and decomposition occurs during the calcining step. The powder contained in a silica glass tray or tube is calcined at $1050^{O}C$ in air. Alternatively, an alumina ceramic tray can be used as the container for the powder during calcining.

TABLE 2

Composition-modified barium titanate with metal element atom fractions given for an optimum result, as demonstrated in the reference: P. Hansen, U.S. Pat. No. 6,078,494, issued Jan. 20, 2000.

Composition-modified barium titanate with
metal element atom fractions as follows:

Metal Element	Atom Fraction	Atomic Weight	Product	Weight %
Ba	0.9575	137.327	131.49060	98.52855
Ca	0.0400	40.078	1.60312	1.20125
Nd	0.0025	144.240	0.36060	0.27020
Total:	**1.0000**			**100.00000**
Ti	0.8150	47.867	39.01161	69.92390
Zr	0.1800	91.224	16.42032	29.43157
Mn	0.0025	54.93085	0.13733	0.24614
Y	0.0025	88.90585	0.22226	0.39839
Total:	**1.0000**			**100.00000**

TABLE 3
Water-soluble precursors and reactant strong base for wet-chemical-prepared powder of a composition-modified barium titanate by a coprecipitation procedure

Precursor	Formula	FW	Mol fraction	Product	Weight %	Multiplier factor	Product	Weight %
Barium nitrate	$Ba(NO_3)_2$	261.34	0.9575	250.233050	95.95748	1.0	95.95748	48.09898
Calcium nitrate tetrahydrate	$Ca(NO_3)_2.4H_2O$	236.15	0.0400	9.446000	3.62228	1.0	3.62228	1.81568
Neodymium nitrate hexahydrate	$Nd(NO_3)_3.6H_2O$	438.35	0.0025	1.095875	0.42024	1.0	0.42024	0.21065
Yttrium nitrate tetrahydrate	$Y(NO_3)_3.4H_2O$	346.98	0.0025	0.86745	0.30676	0.995	0.30523	0.15300
Manganese(II) acetate tetrahydrate	$Mn(CH_3COO)_2.4H_2O$	245.08	0.0025	0.61270	0.21667	0.995	0.21559	0.10806
Oxozirconium(IV) nitrate	$ZrO(NO_3)_2$	231.23	0.1800	41.62140	14.71882	0.995	14.64523	7.34097
Bis(ammonium lactato) dihydroxotitanium(IV)	$[CH_3CH(O—)COONH_4]2Ti(OH)_2$	294.08	0.8150	239.67520	84.75775	0.995	84.33396	42.27266
							Total:	100.0000
Reactant strong base Tetramethylammonium hydroxide	$(CH_3)_4NOH$	91.15						

TABLE 4

Calculation of minimum amount of $(CH_3)_4NOH$
required for 100 g of the precursor mixture

Precursor	FW	Wt %	Wt %/FW	Reactant base multiplier	Mol of base required
$Ba(NO_3)_2$	261.34	48.09898	0.184048	2	0.368095
$Ca(NO_3)_2.4H_2O$	236.15	1.81568	0.007689	2	0.015377
$Nd(NO_3)_3.6H_2O$	438.35	0.21065	0.000481	3	0.001442
$Y(NO_3)_3.4H_2O$	346.98	0.15300	0.000441	3	0.001323
$Mn(CH_3COO)_2.4H_2O$	245.08	0.10806	0.000441	2	0.000882
$ZrO(NO_3)_2$	231.23	7.34097	0.031747	2	0.063495
$[CH_3CH(O—)COONH_4]_2Ti(OH)_2$	294.08	42.27266	0.143745	2	0.287491
	Total:	100.00000			0.738105
Reactant strong base					
$(CH_3)_4NOH$	91.15				

Note: The weight of (CH3)4NOH required is accordingly a minimum of
(0.738105 mol) (91.15 g/mol) = 67.278 g for 100 g of the precursor mixture.
Tetramethylammonium hydroxide (CH3)4NOH is a strong base.

Coating of Aluminium Oxide on Calcined Modified Barium Titanate Powder

Barium titanate $BaTiO_3$	FW 233.19	d 6.080 g/cm3
Aluminium oxide Al_2O_3	FW 101.96	d 3.980 g/cm3

Precursor, aluminium nitrate nonahydrate, as selected from the reference: Sigma-Aldrich Corp., "Handbook of Fine Chemicals and Laboratory Equipment", 2000-2001. $Al(NO_3)_3.9H_2O$ FW 3.75.13

For Calcined Aluminium Oxide (Al_2O_3) Coating of 100 Angstrom units Thickness on Calcined Modified Barium Titanate Powder 100 Angstrom units = 10-6 cm 1.0 m^2 = 104 cm^2

area thickness of Al_2O_3 coating volume $(10^4\ cm^2/g)(10^{-6}\ cm) = 10^{-2}\ cm^3/g$ - - - of calcined powder

$$\frac{(10^{-2}\ \text{cm}^3\ \text{volume}\ Al_2O_3\ \text{coating}) \times (3.98\ \text{g/cm}^3\ \text{density of}\ Al_2O_3)}{\text{g of calcined powder}} = \frac{39.8 \times 10^{-3}\ \text{g of}\ Al_2O_3\ \text{coating}}{\text{g of calcined powder}}\ \text{or}$$

$$= \frac{39.8\ \text{mg of}\ Al_2O_3\ \text{coating}}{\text{g of calcined powder}}$$

$Al(NO_3)_3.9H_2O$ (FW 375.13)(2)=750.26

Al_2O_3 FW 101.96=101.96

750.26/101.96=7.358

$$\frac{(7.358)(39.8\ \text{mg of}\ Al_2O_3\ \text{coating})}{\text{g of calcined powder}} = \frac{292.848\ \text{mg of}\ Al(NO_3)_3 \cdot 9H_2O}{\text{g of calcined powder}}$$

For an aluminium oxide (Al_2O_3) coating of 100 Angstrom units thickness on calcined modified barium titanate powder with particle volume of 1.0 μm^3, 39.8 mg of Al_2O_3 are required per g of this powder, corresponding to 292.848 mg of the aluminium nitrate nonahydrate [$Al(NO_3)_3.9H_2O$] precursor required per g of this powder.

Coating of Calcium Magnesium Aluminosilicate Glass on Aluminium Oxide Coated
Calcined Modified Barium Titanate Powder

	FW g/mol	d g/cm^3
Barium titanate $BaTiO_3$	233.19	6.080

Calcium magnesium aluminosilicate (CaO.MgO.Al2O3.SiO2) glass precursors, as selected from the reference: Sigma-Aldrich, Corp., "Handbook of Fine Chemicals and Laboratory Equipment", 2000-2001.

Calcium methoxide	$(CH_3O)2Ca$	101.15
Calcium isopropoxide	$[(CH_3)_2CHO]_2Ca$	158.25
Magnesium methoxide	$(CH_3O)_2Mg$	86.37
Magnesium ethoxide	$(CH_3CH_2O)_2Mg$	114.43
Aluminium ethoxide	$(CH_3CH_2O)_3Al$	162.16
Aluminium isopropoxide	$[(CH_3)_2CHO]_3Al$	204.25
Aluminium butoxide	$[CH_3(CH_2)_3O]_3Al$	246.33
Tetraethyl orthosilicate	$Si(OCH_2CH_3)_4$	208.33

Select glass composition, e.g.,

$CaO.MgO.2Al_2O_3.8SiO_2$ and accordingly the precursors:

1 mol	(158.25 g) calcium isopropoxide
1 mol	(114.43 g) magnesium ethoxide
4 mol	(817.00 g) aluminum isopropoxide
8 mol	(1666.64 g) tetraethyl orthosilicate

2756.32 g for 1.0 mol glass

Prepare Mixture of these Precursors in Absolute Ethanol (to Avoid Hydrolysis) and in Dry-Air Environment (Dry Box) (also to Avoid Hydrolysis).

Glass Composition: $CaO.MgO.2Al_2O_3.8SiO_2$ or $CaMgAl_4Si_8O_{24}$

1 mol (56.08 g)	CaO
1 mol (40.30 g)	MgO
2 mol (101.96 g × 2 = 203.92 g)	Al_2O_3
8 mol (60.08 g × 8 = 480.64 g)	SiO_2

glass FW total 780.98 g/mol
Density of glass: about 2.50 g/cm^3

Calcined modified barium titanate powder
Particle volume: 1.0 μm^3 or $1.0(10^{-4}\ cm)^3 = 10^{-12}\ cm^3$;
so there are 10^{12} particles/cm^3 (assumption of no voids)
Particle area: 6 μm^2 or $(6)(10^{-4}\ cm)^2 = 6\times10^{-8}\ cm^3$;
Particle area/cm3 (no voids):
$(6\times10^{-8}\ cm^2/particle)(10^{12}\ particles/cm^3) = 6\times10^4\ cm^2/cm^3$ or 6 m^2/cm^3.

Then for density of 6 g/cm^3, the result is:

$$\frac{6\ m^2/cm^3}{6\ g/cm^3} = 1.0\ m^2/g$$

For Calcined Glass Coating of 100 Angstrom units Thickness on Calcined Powder:

100 Angstrom units = 10^{-6} cm 1.0 m^2 = 10^4 cm^2

(10^4 cm^2/g)(10^{-6} cm) = 10^{-2} cm^3/g of calcined powder of glass coating and then

$$\frac{(10^{-2}\ \text{cm}^3\ \text{of glass coating})}{\text{g of calcined powder}} \times (2.50\ \text{g/cm}^3\ \text{density of glass}) =$$

$$\frac{25.0\times10^{-3}\ \text{g of glass coating}}{\text{g of calcined powder}} \quad \text{or} \quad \frac{25.0\ \text{mg of glass coating}}{\text{g of calcined powder}}$$

Precursor mixture FW 2756.32 = 3.529
Glass FW 780.98

$$\frac{(3.529)(25.0\ \text{mg of glass coating})}{(\text{g of calcined powder})} = 88.228\ \text{mg of precursor mixture}$$

For a $CaMgAl_4Si_8O_{24}$ glass coating of 100 Angstrom units thickness on calcined modified barium titanate powder with particle volume of 1.0 μm3, 25.0 mg of this glass are required per g of this powder, corresponding to 88.228 mg of the precursor mixture required per g of this powder.

Particle Volume and Area

V particle = a^3 for cube
If a = 1.0 μm, V = 1.0 μm^3
A particle = $6a^2$ for cube
If a = 1.0 μm, A = 6 μm^2

Particle coating volume

($6\ a^2$)(t), if t = 100 Angstrom units = 10×10^3 μm, and 6 a^2=6.0 μm^2,
then (6.082 m^2)(10×10^{-3} μm) = 60×10^{-3} μm^3 = V coating

Ratio of particle coating volume to particle volume 60×10^{-3} μm^3/1.0 μm^3 = 60×10^{-3} = 0.06 or 6%

With the assumption of no voids and absolutely smooth surface, for an ideal cubic particle with volume of 1.0 μm3 and for a particle coating of 100 Angstrom units thickness, the coating volume is 60×10^{-3} μm3 or 6.0% that of the particle volume.

Calculations of the Electrical-Energy-Storage Unit's Weight, Stored Energy, Volume, and Configuration.

Assumptions:

The relative permittivity of the high-permittivity powder is nominally 33,500, as given in the reference: P. Hansen, U.S. Pat. No. 6,078,494, issued Jan. 20, 2000.

- The 100 ? coating of Al2O3 and 100 ? of calcium magnesium aluminosilicate glass will reduce the relative permittivity by 12%.
- K = 29,480

  Energy stored by a capacitor: E = CV^2/(2×3600 s/h) = W·h
- C = capacitance in farads
- V = voltage across the terminals of the capacitor

  It is estimated that is takes 14 hp, 746 watts per hp, to power an electric vehicle running at 60 mph with the lights, radio, and air conditioning on. The energy-storage unit must supply 52,220 W·h or 10,444 W for 5 hours to sustain this speed and energy usage and during this period the EV will have travelled 300 miles. Each energy-storage component has 1000 layers.

  $C = \varepsilon_o KA/t$

* ε_o = permittivity of free space
* K = relative permittivity of the material
* A = area of the energy-storage component layers
* t = thickness of the energy-storage component layers

Voltage breakdown of the energy-storage components material after coating with Al_2O_3 and calcium magnesium aluminosilicate glass will be in the range of 1.0×10^6 V/cm to 5×10^6 V/cm or higher. Using the proper voltage breakdown selected from this range could allow the voltage of the energy-storage unit to be 3500 V or higher.
One hp = 746 W

EXAMPLE

Capacitance of one layer = 8.854×10^{-12} F / m × 2.948×10^4 × 6.45×10^{-4} m^2 / 12.7×10^{-6} m

C = 0.000013235 F

With 1000 layers:

C = 0.013235 F

The required energy storage is

E_t = 14 hp × 746 W /hp × 5 h = 52,220 W·h

The total required capacitance of the energy-storage unit:

CT = E_t × 2 × 3600 s/h / V^2 = 52,220 W·h × 2 × 3600 s/h/(3500 V)^2 C_T = 31 F

Number of capacitance components required:

N_c = 31 F / 0.013235 F = 2320

Volume and weight of energy-storage unit:

Volume of the dielectric material:

Volume = area x thickness x number of layers
= 6.45 cm^2 x 12.72 x 10^{-4} cm x 1000
= 8.2 cm^3

Total volume = 8.2 cm^3 × number of components (2320) = 19,024 cm^3
Density of the dielectric material = 6.5 g/cm^3
Weight of each component = density × volume = 53.3 g
Total weight of the dielectric material = 53.3 g × 2320 / 454 g per pound = 272 pounds

Volume of the nickel conductor layers:
Thickness of the nickel layer is 1×10-6 m
Volume of each layer = 6.45 cm2×1.0×10-4 cm × 1000 = 0.645 cm3
Density of nickel = 8.902 g/cm3
Weight of nickel layers for each component = 5.742 g
Total weight of nickel = 34 pounds

Total number of capacitance layers and volume of the EESU:
Area required for each component to solder bump = 1.1 $inch^2$
A 12 × 12 array will allow 144 components for each layer of the first array
19 layers of the second array will provide 2736 components which are more than enough to meet the required 2320 components. The distance between the components will be adjusted so that 2320 components will be in each EESU. The second array area will remain the same.

The total weight of the EESU (est.) = 336 pounds
The total volume of the EESU (est.) = 13.5 inches × 13.5 inches × 11 inches = 2005 $inches^3$ which includes the weight of the container and connecting material.
The total stored energy of the EESU = 52,220 W·h

From the above description, it will be apparent that the invention disclosed herein provides a novel and advantageous electrical-energy-storage unit composed of unique materials and processes. The foregoing discussion discloses and describes merely exemplary methods and embodiments of the present invention. As will be understood by those familiar with the art, the invention may be embodied in other specific forms and utilise other materials without departing from the spirit or essential characteristics thereof. Accordingly, the disclosure of the present invention is intended to be illustrative, but not limiting, of the scope of the invention, which is set forth in the following claims.

CLAIMS

1. A method for making an electrical-energy-storage unit comprising components fabricated by the method steps as follow;

a) preparing a wet-chemical-prepared calcined composition-modified barium titanate powder derived from a solution of precursors: $Ba(NO_3)_2$, $Ca(NO_3)_2.4H_2O$, $Nd(NO_3)_3.6H_2O$, $Y(NO_3)_3.4H_2O$, $Mn(CH_3COO)_2.4H_2O$, $ZrO(N_3O)_2$, and $[CH_3CH(O—)COONH_4]_2Ti(OH)_2$ in de-ionised water heated to 80^OC, and a separate solution of $(CH_3)_4NOH$ made in de-ionised water and heated to 80^O-85^OC, then mixing the solutions by pumping the heated ingredient streams simultaneously through a coaxial fluid mixer producing co-precipitated powder, then collecting the co-precipitated powder in a drown-out vessel and refluxing at a temperature of 90^O-95^OC for 12 hours, then filtering, washing with de-ionised water, drying, and then calcining 1050^OC in air;

b) fabricating an aluminium oxide (Al_2O_3) coating of 100 Angstrom units thickness on to the wet-chemical-prepared calcined composition-modified barium titanate powder, with the use of aluminium nitrate nonahydrate precursor applied by wet chemical means, then calcining at 1050^OC, resulting in a single-coated calcined composition-modified barium titanate powder;

c) fabricating on to the alumina-coated composition-modified barium titanate powder, a second uniform coating of 100 Angstrom units of calcium magnesium aluminosilicate glass derived from alcohol-soluble precursors: calcium methoxide or calcium isopropoxide, magnesium methoxide or magnesium ethoxide, aluminium ethoxide or aluminium isopropoxide or aluminium isopropoxide, and tetraethyl orthosilicate are applied by wet chemical means which upon calcining at 500^OC results in a double-coated composition-modified barium titanate powder;

d) blending, this double-coated composition-modified barium titanate powder with a screen-printing ink containing appropriate plastic resins surfactants, lubricants, and solvents to provide a suitable rheology for screen printing;

e) screen-printing into interleaved multi-layers of alternating offset nickel electrode layers **12** and double-coated calcined composition-modified barium titanate high-relative-permittivity layers **11** with the use of screening inks having the proper rheology for each of the layers;

f) drying and cutting the screen-punted multi-layer components **15** into a specified rectangular area;

g) sintering the screen-printed multi-layer components **15**, first at a temperature of 350^OC for a specified length of time, then at 850^OC for a specified length of time, to form closed-pore porous ceramic bodies; and

h) hot isostatically pressing the closed-pore porous ceramic bodies, at a temperature of 700^OC with a specified pressure, into a void-free condition;

i) grinding and each side of the component to expose the alternating offset interleaved nickel electrodes **12**;

j) connecting nickel side bars **14** to each side of the components **15**, that have the interleaved and alternating offset nickel electrodes **12** exposed, by applying nickel ink with the proper rheology to each side and clamping the combinations together;

k) heating the components and side nickel bar combination **14-15** 800^OC, and time duration of 20 minutes to bond them together;

l) wave soldering each side of the conducting bars;

m) assembling the components **15** with the connected nickel side bars **14** into the first array, utilising unique tooling and solder-bump technology;

n) assembling the first arrays into the second array;

o) assembling the second arrays into the EESU final assembly.

2. The method of claim 1 wherein a second coating of glass is provided on to the double-coated composition-modified barium titanate powder being in contact with the nickel electrodes and having an applied working voltage of 3500 V across the parallel electrodes.

3. The method of claim 1 wherein a dielectric voltage breakdown strength of 5.0×10^6 V/cm was achieved across the electrodes of the components.

4. The method of claim 1 wherein the method provides an ease of manufacturing due to the softening temperature of the calcium magnesium aluminosilicate glass allowing the relatively low hot-isostatic-pressing temperatures of 700^{O}C which in turn provides a void-free ceramic body.

5. The method of claim 1 wherein the method provides an ease of fabrication due to the softening temperature of the calcium magnesium aluminosilicate glass allowing the relatively low hot-isostatic-pressing temperatures of 700^{O}C which in turn allows the use of nickel for the conduction-path electrodes rather than expensive platinum, palladium, or palladium-silver alloy.

6. The method of claim 1 wherein the method provides an ease of fabrication due to the softening temperature of the calcium magnesium aluminosilicate lass allowing the relatively low hot-isostatic-pressing temperatures of 700^{O}C, which feature along with the coating method provided a uniform-thickness shell of the calcium magnesium aluminosilicate glass and in turn provides hot-isostatic-pressed double-coated composition-modified barium titanate high-relative-permittivity layers that are uniform and homogeneous in microstructure.

7. The method of claim 1 wherein the method provides the double coating of the basis particles of the composition-modified barium titanate powder thereby reducing the leakage and ageing of this material by an order of magnitude of the specification of this basis material, thus reducing the discharge rate to 0.1% per 30 days.

8. The method of claim 1 wherein the method provides a double coating of the composition-modified barium titanate powder, the hot-isostatic-pressing process, the high-density solder-bump packaging, and along with the double-layered array configuration stored 52,220 W·h of electrical energy in a 2005 $inches^3$ container.

9. The method of claim 1 wherein the method provides materials used: water-soluble precursors of barium (Ba), calcium (Ca), titanium (Ti), zirconium (Zr), manganese (Mn), yttrium (Y), neodymium (Nd), forming the composition-modified barium titanate powder, and the metals: nickel (Ni), and copper (Cu), which are not explosive, corrosive, or hazardous.

10. The method of claim 1 wherein the method provides an EESU that is not explosive, corrosive, or hazardous and therefore is a safe product when used in electrical vehicles, which include bicycles, tractors, buses, cars, or any device used for transportation or to perform work.

11. The method of claim 1 wherein the method provides an EESU which can store electrical energy generated from solar voltaic cells or other alternative sources for residential, commercial, or industrial applications.

12. The method of claim 1 wherein the method provides an EESU which can store electrical energy from the present utility grid during the night when the demand for electrical power is low and then deliver the electrical energy during the peak power demand times and thus provide an effective power averaging function.

13. The method of claim 1 wherein the method provides a double coating of the composition-modified barium titanate powder and a hot-isostatic-pressing process which together assists in allowing an applied voltage of 3500 V to a dielectric thickness of 12.76×10-6 m to be achieved.

14. The method of claim 1 wherein the method provides a EESU which when fully discharged and recharged, the EESU's initial specifications are not degraded.

15. The method of claim 1 wherein the method provides a EESU which can be safely charged to 3500 V and store at least 52.22 kW·h of electrical energy.

16. The method of claim 1 wherein the method provides a EESU at has a total capacitance of at least 31 F.

17. The method of claim 1 wherein the method provides a EESU that can be rapidly charged without damaging the material or reducing its life.

HERMANN PLAUSTON

US Patent 1,540,998 9th June 1925 Inventor: Hermann Plauson

CONVERSION OF ATMOSPHERIC ELECTRIC ENERGY

Please note that this is a re-worded excerpt from this patent. It describes in considerable detail, different methods for abstracting useable electrical power from passive aerial systems. He describes a system with 100 kilowatt output as a “small” system.

Be it known that I, Hermann Plauson, Estonian subject, residing in Hamburg, Germany, have invented certain new and useful improvements in the Conversion of atmospheric Electric Energy, of which the following is a specification.

According to this invention, charges of atmospheric electricity are not directly converted into mechanical energy, and this forms the main difference from previous inventions, but the static electricity which runs to earth through aerial conductors in the form of direct current of very high voltage and low current strength is converted into electro-dynamic energy in the form of high frequency vibrations. Many advantages are thereby obtained and all disadvantages avoided.

The very high voltage of static electricity of a low current strength can be converted by this invention to voltages more suitable for technical purposes and of greater current strength. By the use of closed oscillatory circuits it is possible to obtain electromagnetic waves of various amplitudes and thereby to increase the degree of resonance of such current. Such resonance allows various values of inductance to be chosen which, by tuning the resonance between a motor and the transformer circuit, allows the control of machines driven by this system. Further, such currents have the property of being directly available for various uses, other than driving motors, including lighting, heating and use in electro-chemistry.

Further, with such currents, a series of apparatus may be fed without a direct current supply through conductors and the electro-magnetic high frequency currents may be converted by means of special motors, adapted for electro-magnetic oscillations, into alternating current of low frequency or even into high voltage direct current.

DESCRIPTION OF THE DRAWINGS

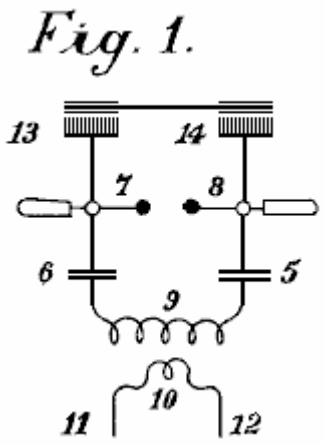

Fig.1 is an explanatory figure

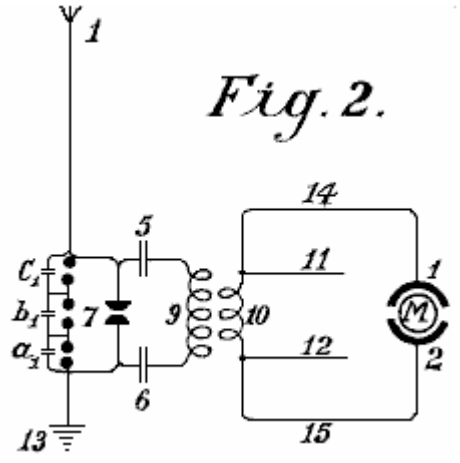

Fig.2 is a diagrammatic view of the most simple form.

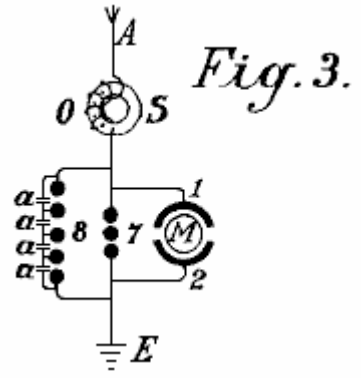

Fig.3 shows a method of converting atmospheric electrical energy into a form suitable for use with motors.

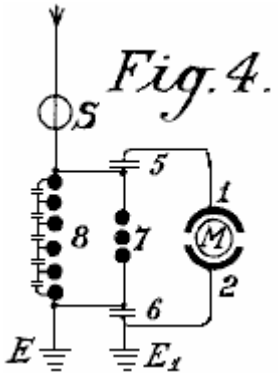

Fig.4 is a diagram showing the protective circuitry.

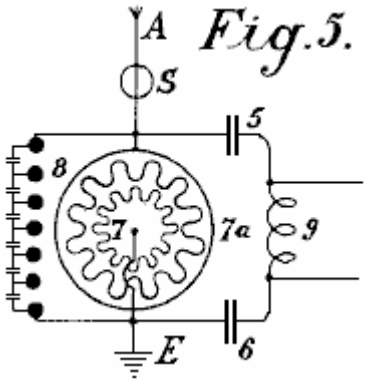

Fig.5.

Fig.5 is a diagram of an arrangement for providing control

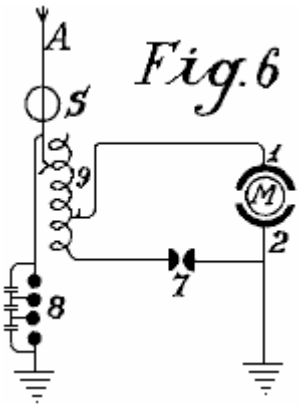

Fig.6

Fig.6 is an arrangement including a method of control

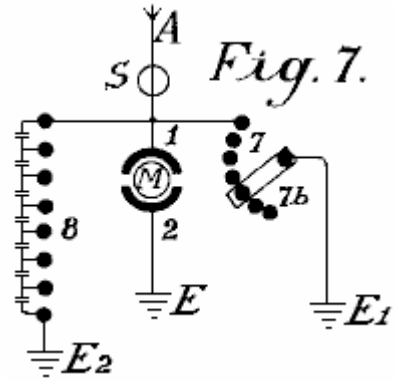

Fig. 7.

Fig.7 shows how the spark gap can be adjusted

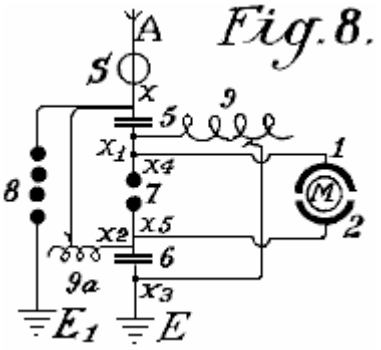

Fig.8 shows a unipolar connection for the motor

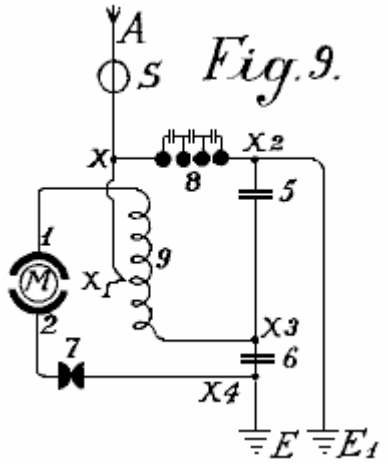

Fig.9 shows a weak coupled system suitable for use with small power motors

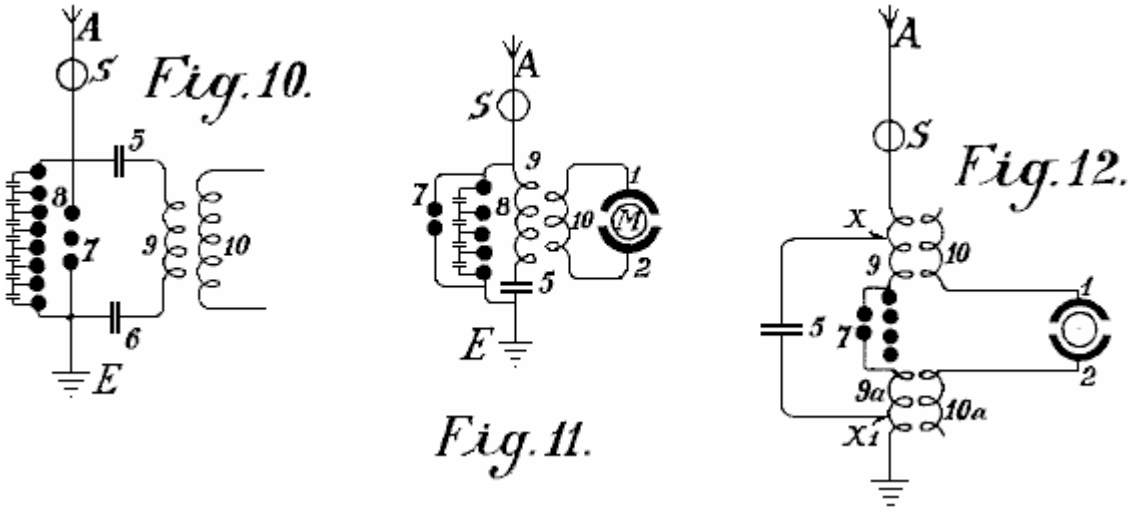

Fig.10, Fig.11 and Fig.12 show modified arrangements

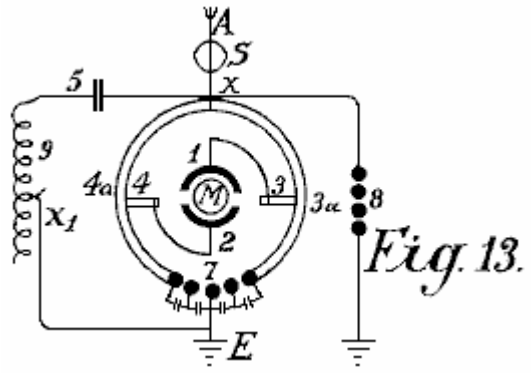

Fig.13 shows a form of inductive coupling for the motor circuit

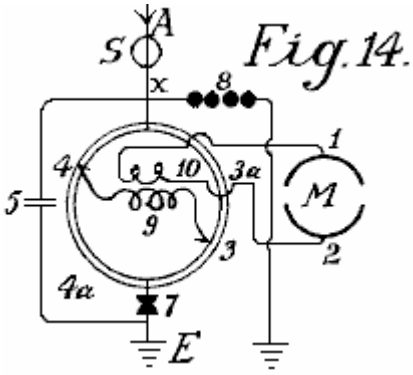

Fig.14 is a modified form of Fig.13 with inductive coupling.

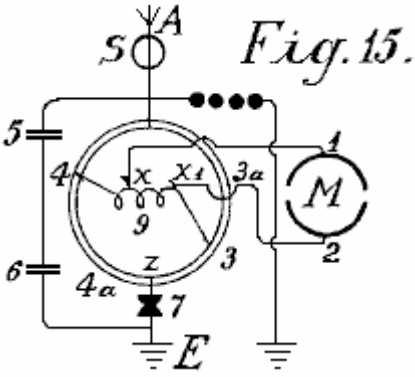

Fig.15 is an arrangement with non-inductive motor

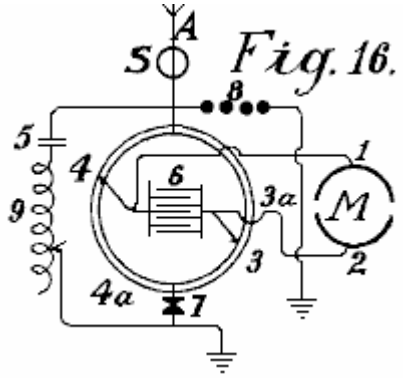

Fig.16 is an arrangement with coupling by capacitor.

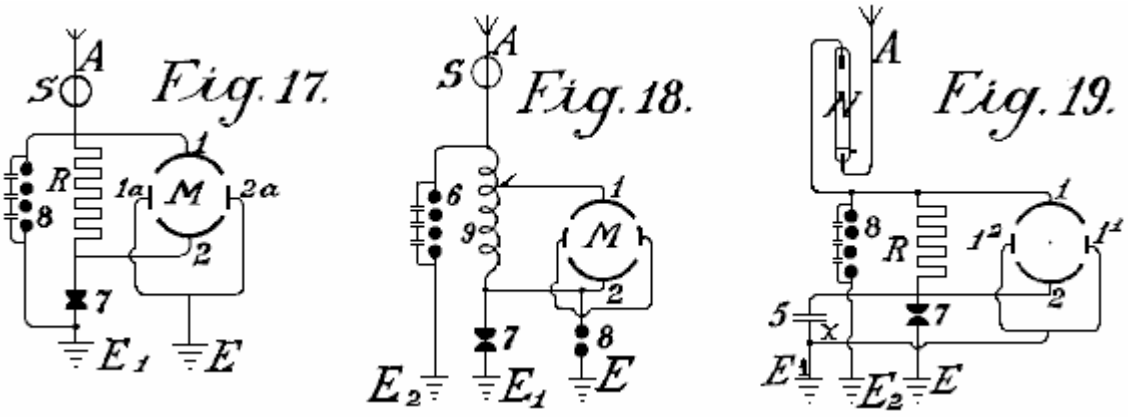

Fig.17, **Fig.18** and **Fig.19** are diagrams showing further modifications

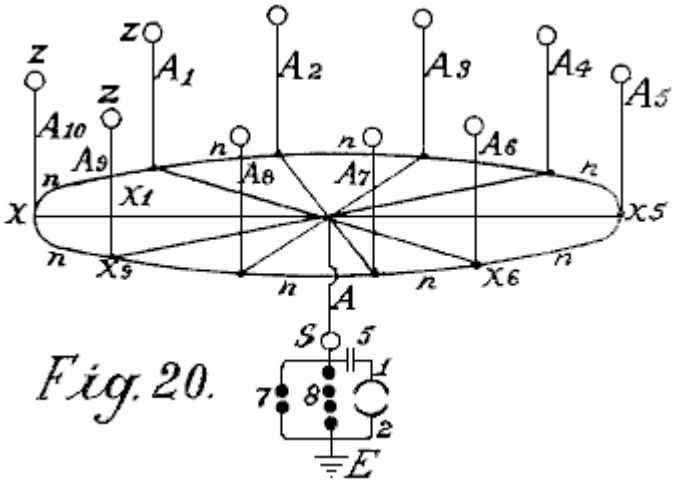

Fig.20 shows a simple form in which the aerial network is combined with special collectors

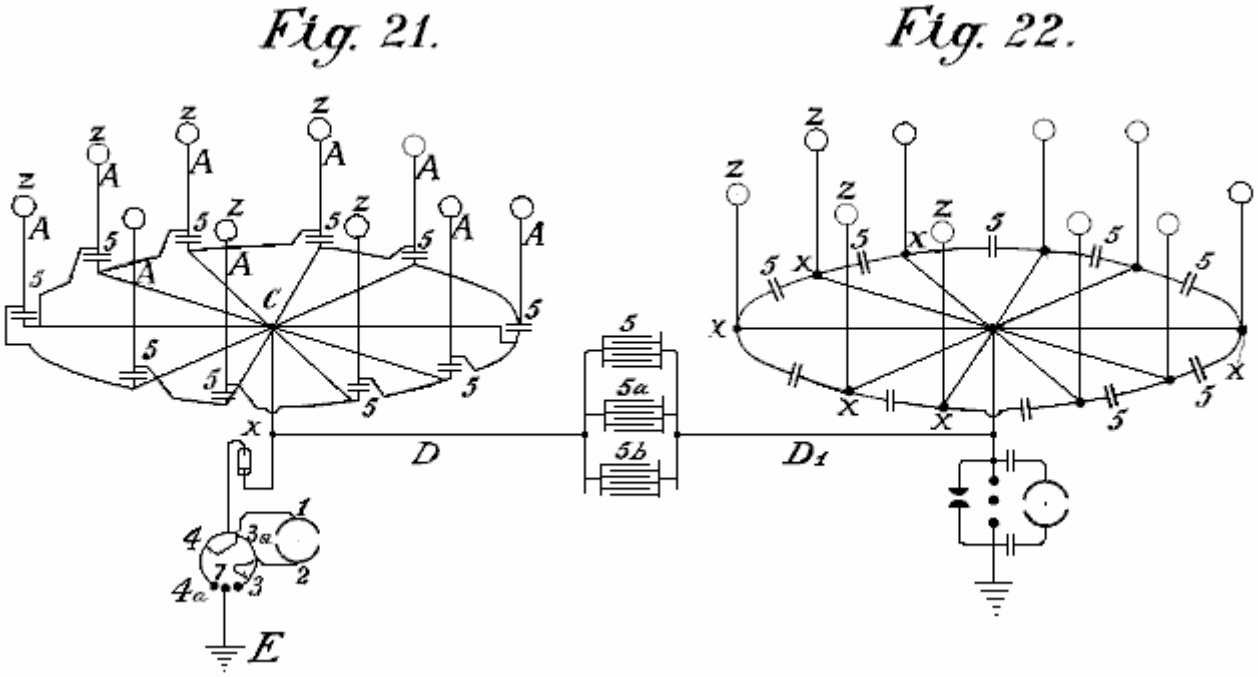

Fig.21 shows diagramatically, an arrangement suitable for collecting large quantities of energy.
Fig.22 is a modified arrangement having two rings of collectors

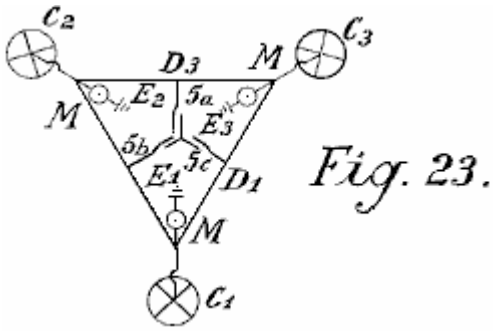

Fig. 23.

Fig.23 shows the connections for three rings of collectors

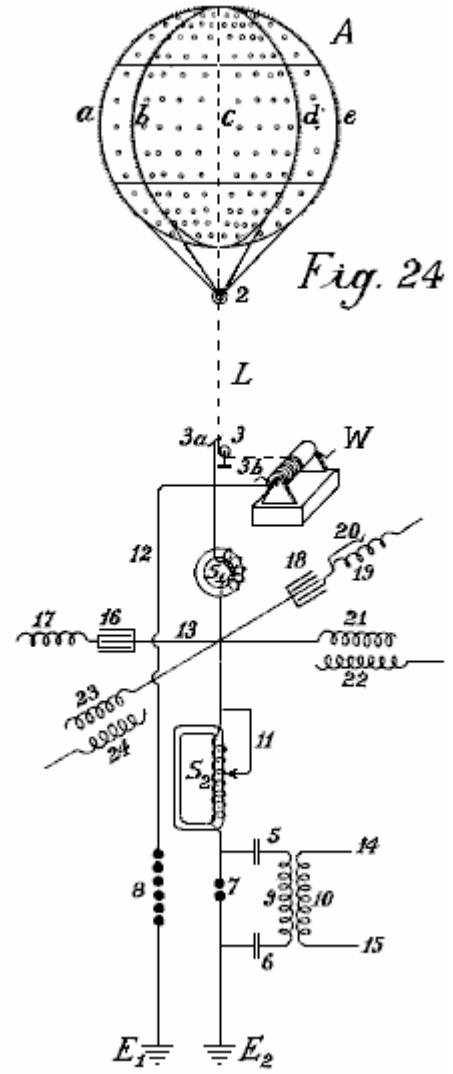

Fig. 24

Fig.24 shows a collecting balloon and diagram of its battery of capacitors

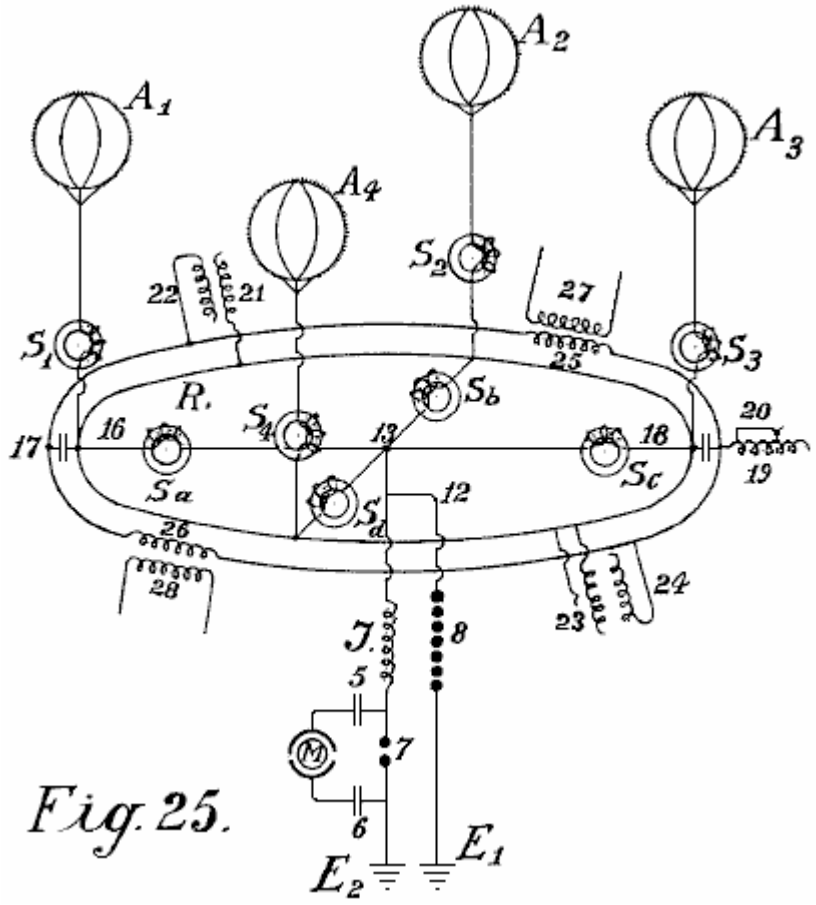

Fig. 25.

Fig.25 and Fig.26 show modified collector balloon arrangements.

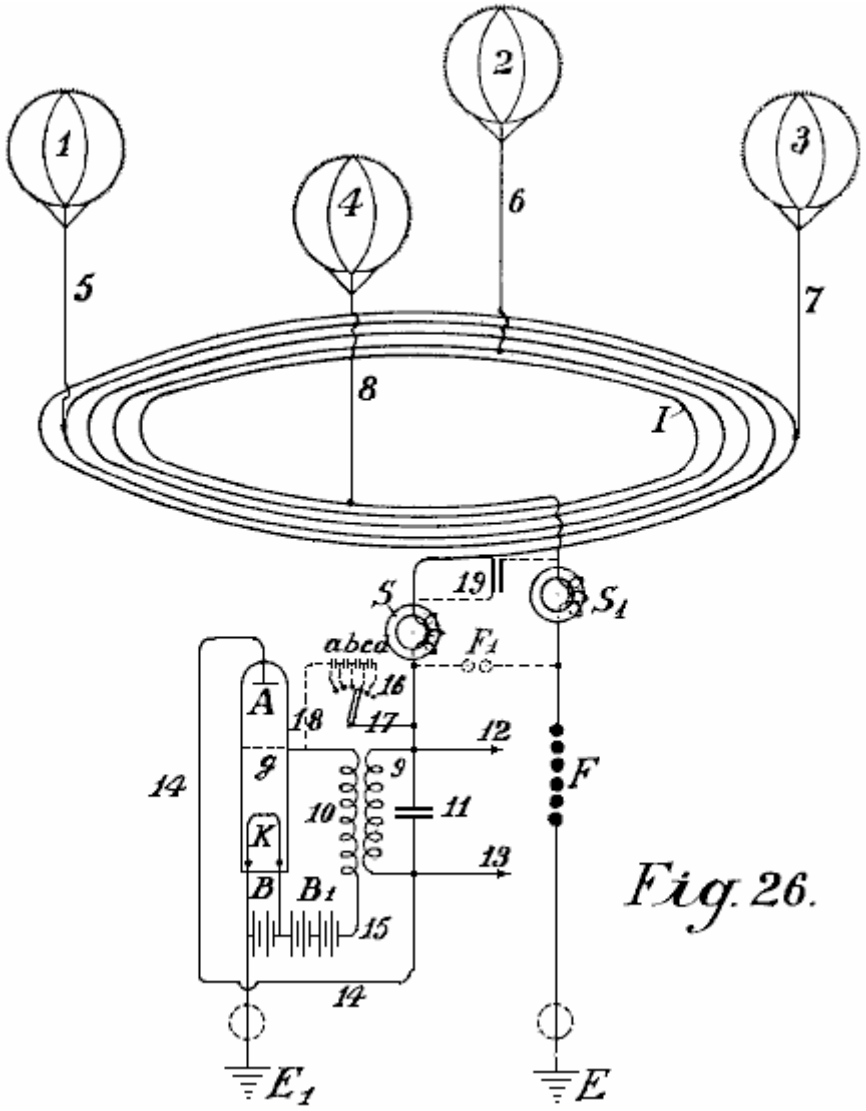
1
2
3
4
5
6
7
8
I
S
19
S1
abcd
F1
16
A
18
17
12
9
9
F
14
10
11
K
13
B
B1
15
14
E1
E

Fig. 26.

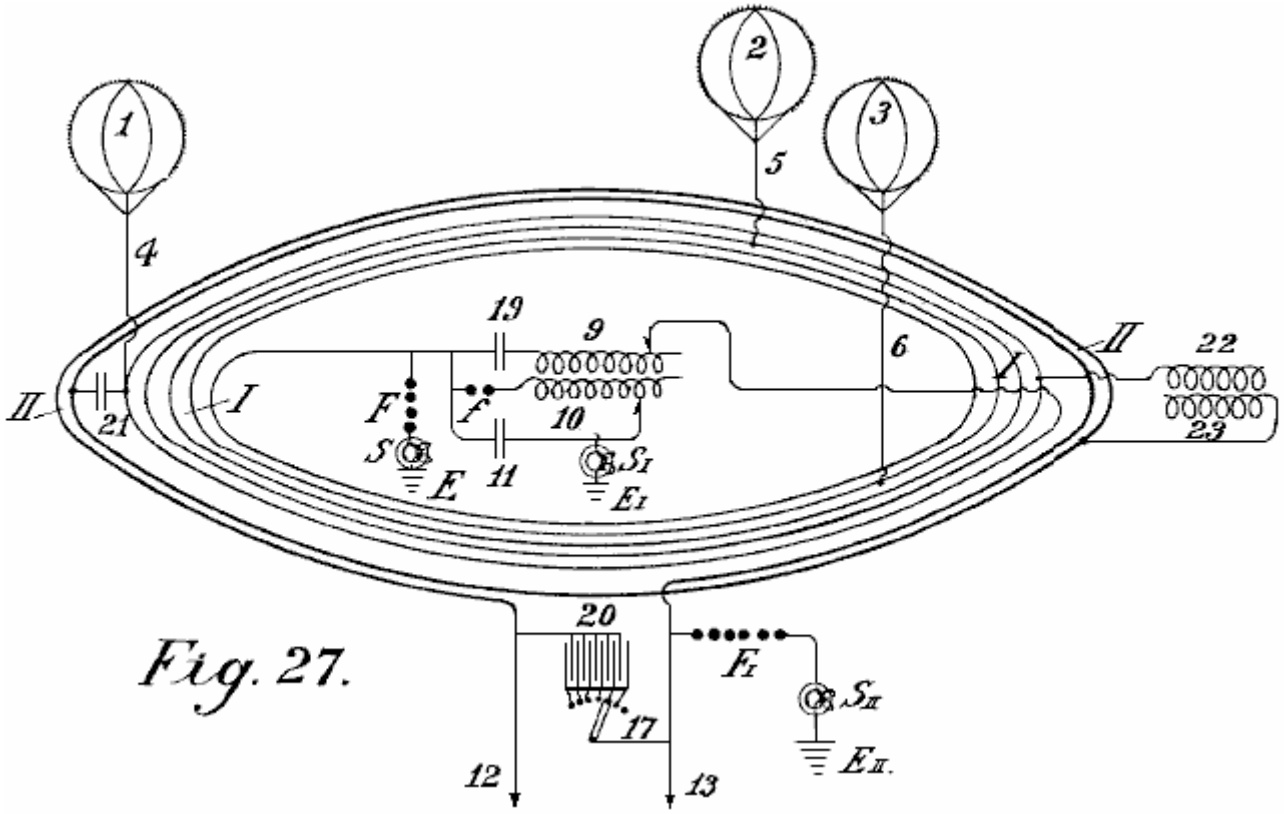

Fig. 27.

Fig.27 shows a second method of connecting conductors for the balloon aerials.

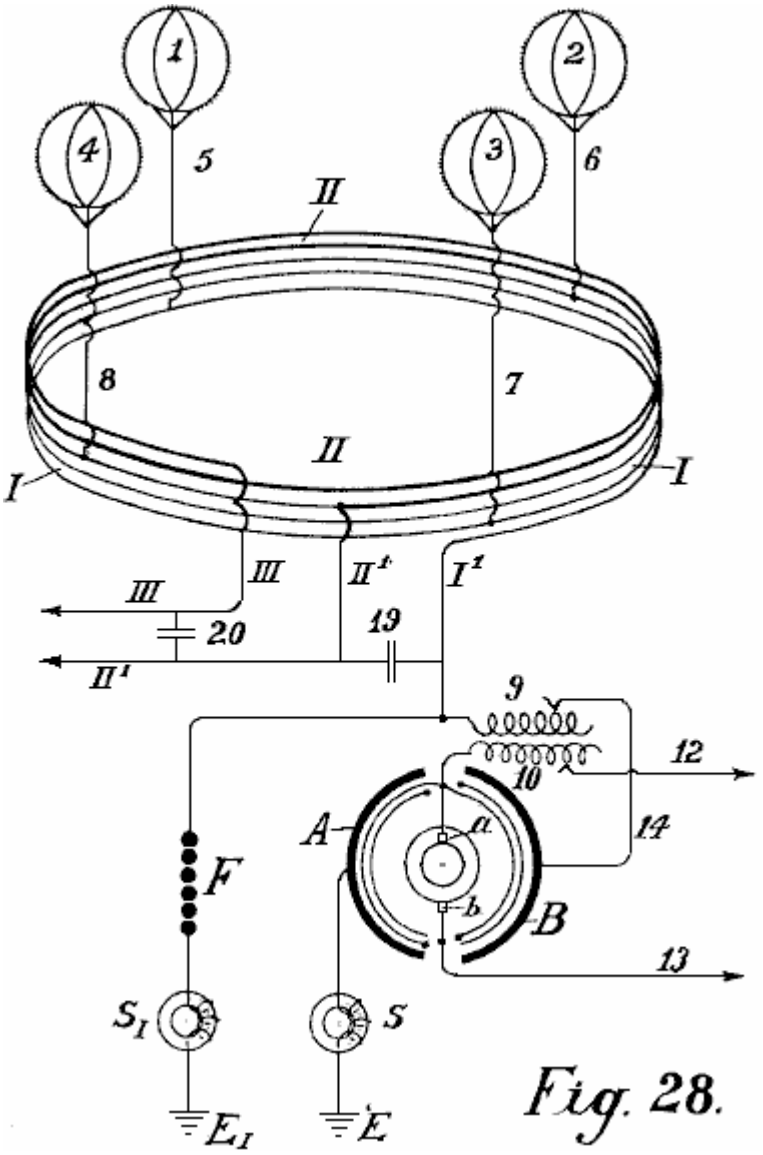

Fig. 28.

Fig.28 shows an auto-transformer method of connection.

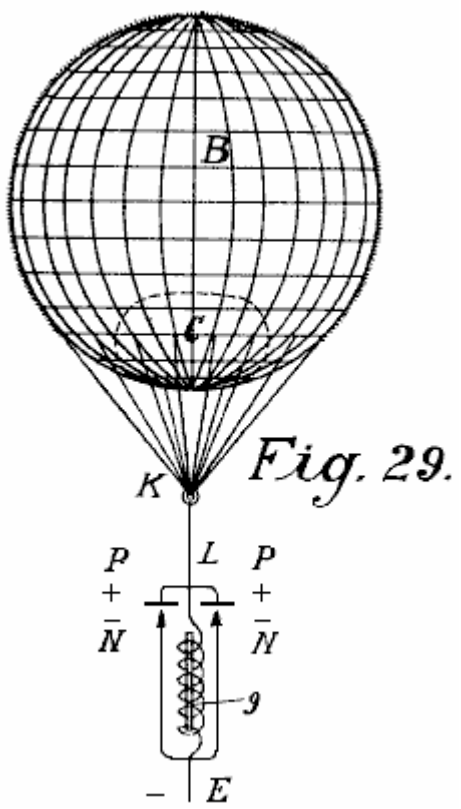

Fig. 29.

Fig.29 shows the simplest form of construction with incandescent cathode.

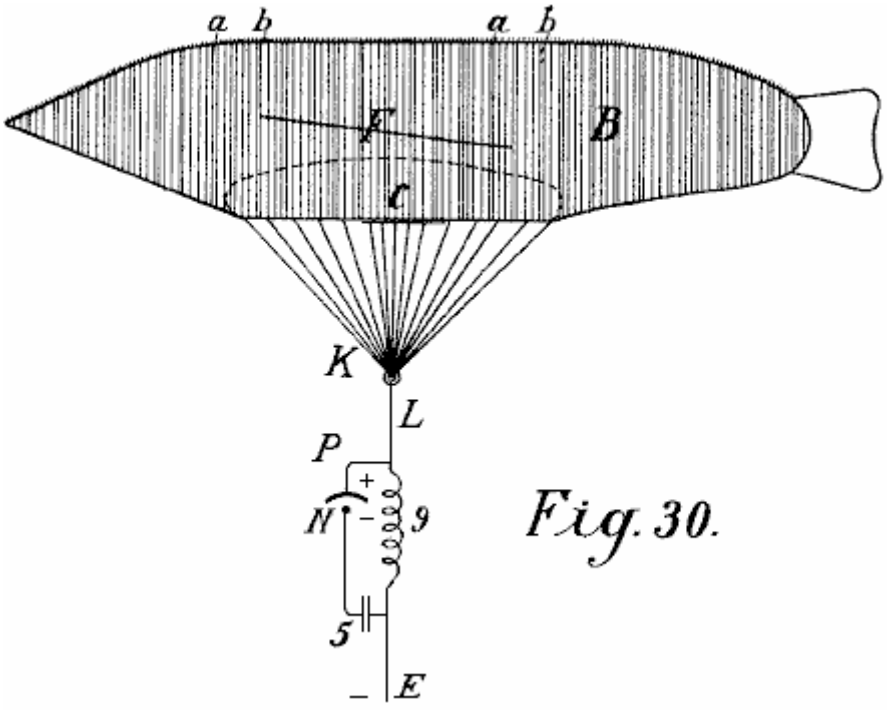

Fig. 30.

Fig.30 shows a form with a cigar-shaped balloon.

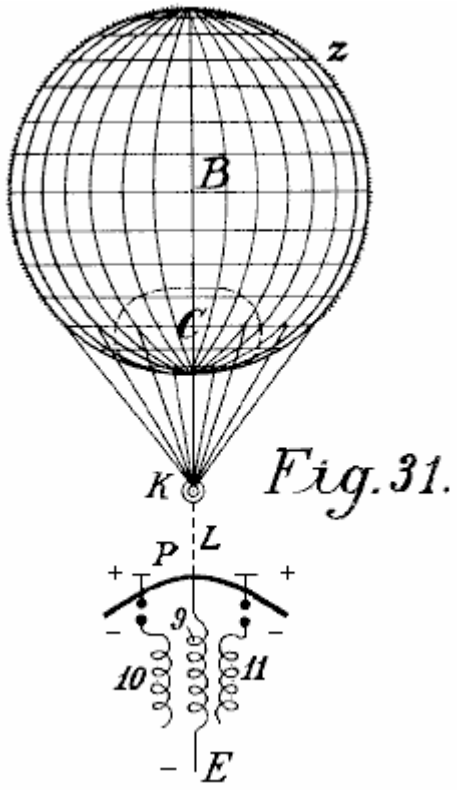

Fig. 31.

Fig.31 is a modified arrangement.

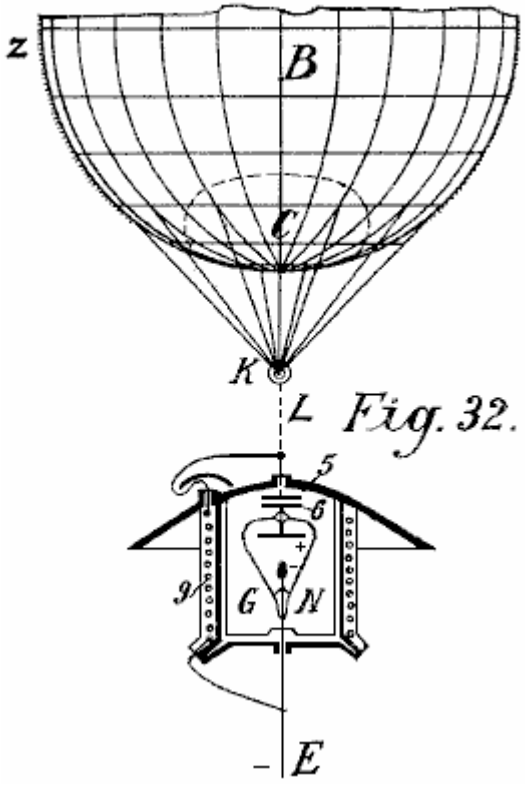

Fig. 32.

Fig.32 shows a form with cathode and electrode enclosed in a vacuum chamber.

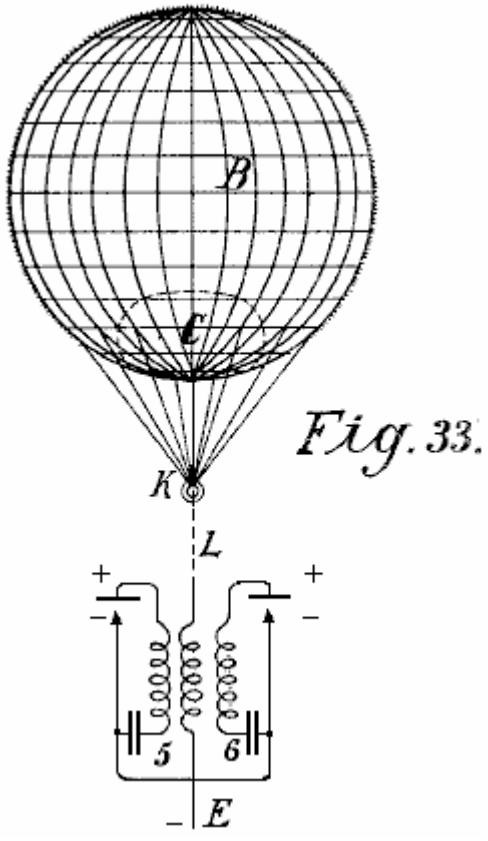

Fig. 33.

Fig.33 is a modified form of Fig.32

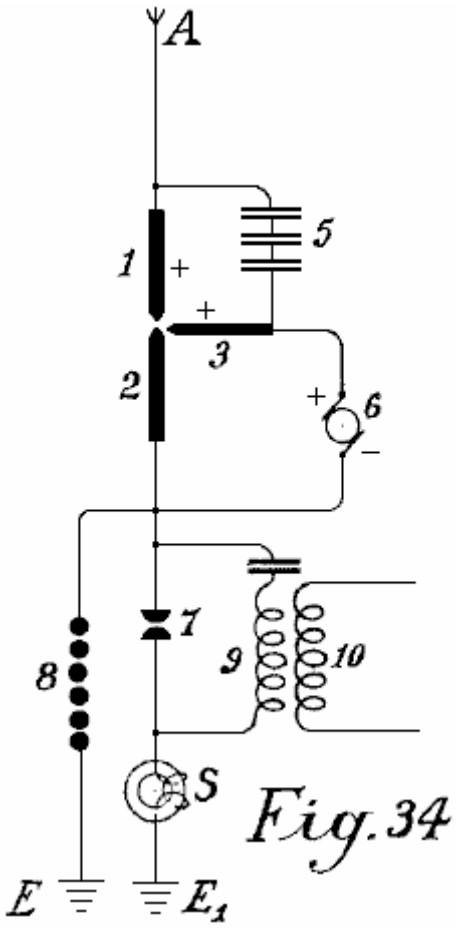

Fig. 34

Fig.34 shows an arc light collector.

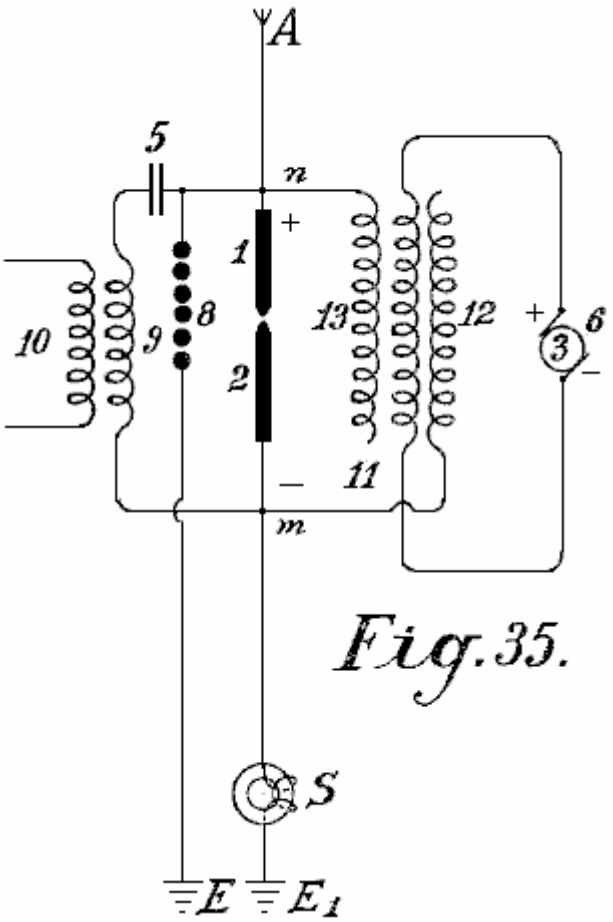

Fig. 35.

Fig.35 shows such an arrangement for alternating current

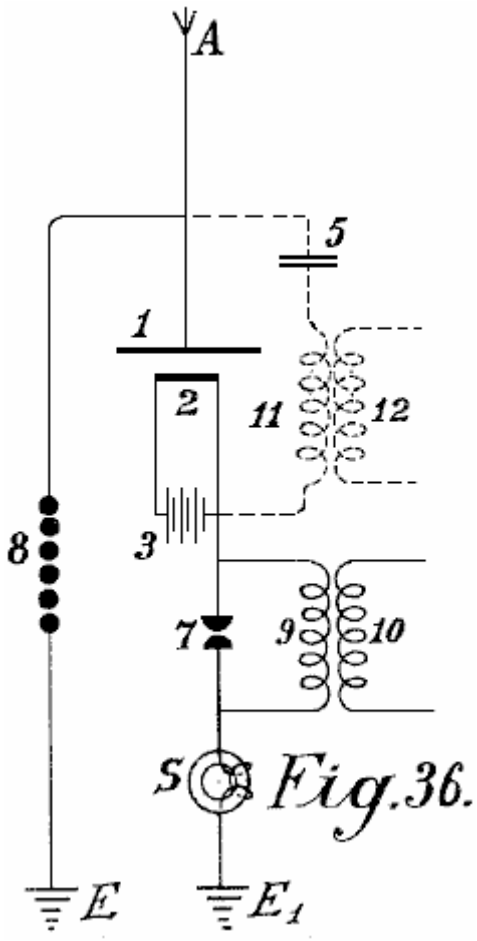

Fig.36.

Fig.36 shows an incandescent collector with Nernst lamp

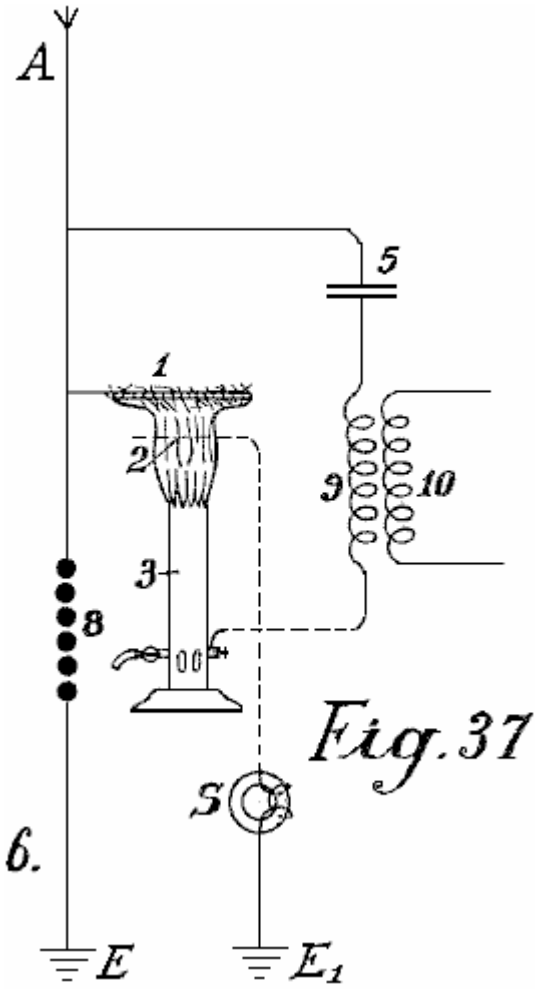

Fig.37 shows a form with a gas flame.

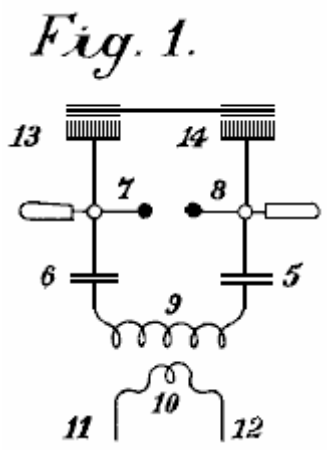

Fig.1 illustrates a simple diagram for converting static electricity into dynamic energy of a high number of oscillations. For the sake of clarity, a Wimshurst machine is assumed to be employed and not an aerial antenna. Items **13** and **14** are combs for collecting the static electricity of the influence machine. Items **7** and **8** are spark-discharging electrodes. Items **5** and **6** are capacitors, **9** is the primary winding of an inductive coil, **10** is the secondary winding whose ends are **11** and **12**. When the disc of the static influence machine is rotated by mechanical means, the combs collect the electric charges, one being positive and one negative and these charge the capacitors **5** and **6** until such a high voltage is developed across the spark gap **7-- 8** that the spark gap is jumped. As the spark gap forms a closed circuit with capacitors **5** and **6**, and inductive resistance **9**, as is well known, waves of high frequency electromagnetic oscillations will pass in this circuit.

The high frequency of the oscillations produced in the primary circuit induces waves of the same frequency in the secondary circuit. Thus, in the primary circuit, electromagnetic oscillations are formed by the spark and these oscillations are maintained by fresh charges of static electricity.

By suitably selecting the ratio between the number of turns in the primary and secondary windings, with regard to a correct application of the coefficients of resonance (capacitance, inductance and resistance) the high voltage of the primary circuit may be suitably converted into a low voltage high current output.

When the oscillatory discharges in the primary circuit become weaker or cease entirely, the capacitors are charged again by the static electricity until the accumulated charge again breaks down across the spark gap. All this is repeated as long as electricity is produced by the static machine through the application of mechanical energy to it.

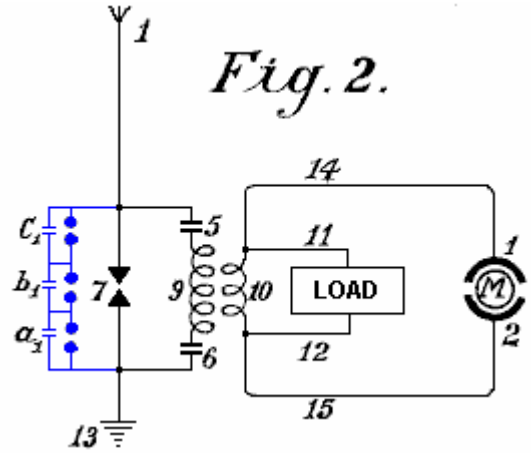

An elementary form of the invention is shown in **Fig.2** in which two spark gaps in parallel are used, one of which may be termed the working gap **7** while the second serves as a safety device for excess voltage and consists of a larger number of spark gaps than the working section, the gaps being arranged in series and which are bridged by very small capacitors a_1, b_1, c_1, which allow uniform sparking in the safety section.

1 is the aerial antenna for collecting charges of atmospheric electricity, **13** is the earth connection of the second part of the spark gap, **5** and **6** are capacitors and **9** is the primary coil winding. When the positive atmospheric electricity seeks to combine with the negative earth charge via aerial **1**, this is prevented by the air gap between the spark gaps. The resistance of spark gap **7** is lower than that of the safety spark gap set of three spark gaps connected in series a which consequently has three times greater air resistance.

Therefore, so long as the resistance of spark gap **7** is not overloaded, discharges take place only through it. However, if the voltage is increased by any influence to such a level that it might be dangerous for charging the capacitors **5** and **6**, or for the coil insulation of windings 9 and 10, the safety spark gap set will, if correctly set, discharge the voltage directly to earth without endangering the machine. Without this second spark gap arrangement, it is impossible to collect and render available large quantities of electrical energy.

The action of this closed oscillation circuit consisting of spark gap **7**, two capacitors **5** and **6**, primary coil **9** and secondary coil **10**, is exactly the same as that of **Fig.1** which uses a Wimshurst machine, the only difference being the provision of the safety spark gap. The high frequency electromagnetic alternating current can be tapped off through the conductors **11** and **12** for lighting and heating purposes. Special motors adapted for working with static electricity or high frequency oscillations may be connected at **14** and **15**.

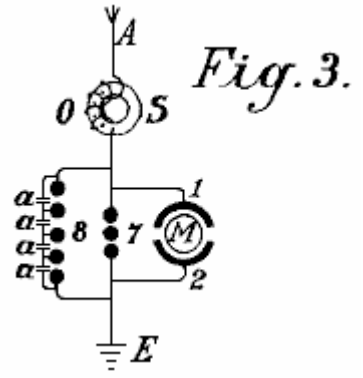

Fig. 3.

In addition to the use of spark gaps in parallel, a second measure of security is also necessary for taking the current from this circuit. This is the introduction of protective electromagnets or choking coils in the aerial circuit as shown by **S** in **Fig.3**. A single electromagnet having a core of the thinnest possible separate laminations is connected with the aerial. In the case of high voltages in the aerial network or at places where there are frequent thunderstorms, several such magnets may be connected in series.

In the case of large units, several such magnets can be employed in parallel or in series parallel. The windings of these electromagnets may be simply connected in series with the aerials. In this case, the winding preferably consists of several thin parallel wires, which together, make up the necessary cross-sectional area of wire. The winding may be made of primary and secondary windings in the form of a transformer. The primary winding will then be connected in series with the aerial network, and the secondary winding more or less short-circuited through a regulating resistor or an induction coil. In the latter case it is possible to regulate, to a certain extent, the effect of the choking coils. In the following circuit and constructional diagrams , the aerial electromagnet choke coil is indicated by a simple ring **S**.

Fig.3 shows the most simple way of converting atmospheric electricity into electromagnetic wave energy by the use of special motors adapted for high oscillatory currents or static charges of electrical energy. Recent improvements in motors for working with static energy and motors working by resonance, that is to say, having groups of tuned electromagnetic co-operating circuits render this possible but such do not form part of the present invention.

A motor adapted to operate with static charges, will for the sake of simplicity, be shown in the diagrams as two semi-circles **1** and **2** and the rotor of the motor by a ring **M** (**Fig.3**). **A** is a vertical aerial or aerial network. **S** is the safety choke or electromagnet with coil **O** as may be seen is connected with the aerial **A**. Adjacent to the electromagnet **S**, the aerial conductor is divided into three circuits, circuit **8** containing the safety spark gap, circuit **7** containing the working spark gap, and then a circuit containing the stator terminal **1**, the rotor and stator terminal **2** at which a connection is made to the earth wire. The two spark gaps are also connected metallically with the earth wire. The method of working in these diagrams is as follows:

The positive atmospheric electric charge collected tends to combine with the negative electricity (or earth electricity) connected via the earth wire. It travels along the aerial **A** through the electromagnet **S** without being checked as it flows in the same direction as the direct current. Further, its progress is arrested by two spark gaps placed in the way and the stator capacitors. These capacitors charge until their voltage exceeds that needed to jump the spark gap **7** when a spark occurs and an oscillatory charge is obtained via the closed oscillation circuit containing motor **M**. The motor here forms the capacity and the necessary inductance and resistance, which as is well known, are necessary for converting static electricity into electromagnetic wave energy.

The discharges are converted into mechanical energy in special motors and cannot reach the aerial network because of the electromagnet or choke. If, however, when a spark occurs at spark gap **7**, a greater quantity of atmospheric electricity tends to flow to earth, then a counter voltage is induced in the electromagnet, which is greater the more rapidly and strongly the flow of current direct to earth is. This opposing voltage causes the circuit to exhibit a sufficiently high resistance to prevent a short circuit between the atmospheric electricity and the earth.

The circuit containing spark gap **8**, having a different wave length which is not in resonance with the natural frequency of the motor, does not endanger the motor and serves as security against excess voltage, which, as practical experiments have shown, may still arise in certain cases.

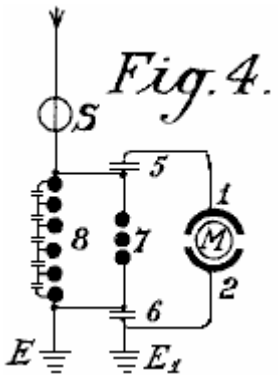

In **Fig.4**, spark gap **7** is shunted across capacitors **5** and **6** from the motor **M**. This arrangement provides improved over-voltage protection for the motor and it gives a uniform excitation through the spark gap **7**.

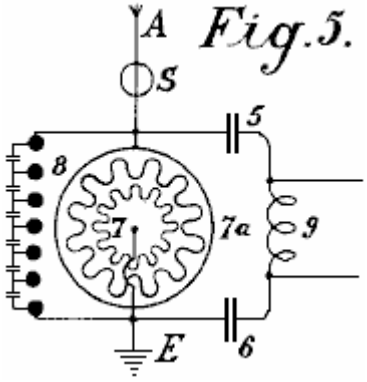

Fig.5 shows an arrangement for producing large currents which can be used direct without motors, to provide heating and lighting. The main difference here is that the spark gap consists of a star-shaped disc **7** which can rotate on its own axis and is rotated by a motor opposite similarly fitted electrodes **7a**. When separate points of starts face one another, discharges take place, thus forming an oscillation circuit with capacitors **5** and **6** and inductor **9**. It is evident that a motor may also be connected directly to the ends of inductor **9**.

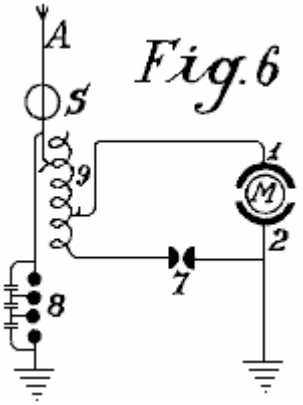

Fig.6 shows how the oscillation circuit may have a motor connected via a variable inductor which opposes any excess voltages which might be applied to the motor. By cutting the separate coils **9** (coupled inductively to the aerial) in or out, the inductive action on the motor may be more or less increased, or variable aerial action may be exerted on the oscillation circuit.

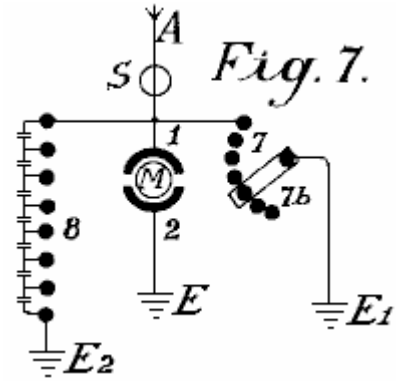

In **Fig.7** the oscillation circuit is closed through the earth (**E** and $\mathbf{E_1}$). The spark gap **7** may be increased or reduced by means of a contact arm **7b**.

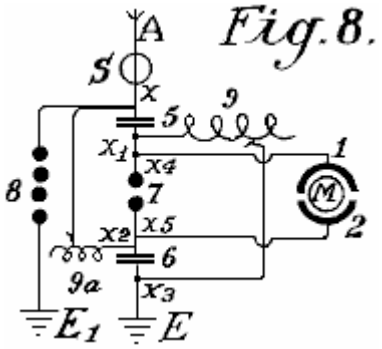

Fig.8 shows a unipolar connection of the motor with the aerial network. Here, two oscillation circuits are closed through the same motor. The first oscillation circuit passes from aerial **A** through electromagnet **S**, point **x**, inductance **9a** to the earth capacitor **6**, across spark gap **7** to the aerial capacitor **5** and back to point **x**. The second oscillation circuit starts from the aerial **5** at the point **x1** through inductor **9** to the earth capacitor **6** at the point **x3**, through capacitor **6**, across spark gap **7** back to point **x1**. The motor itself, is inserted between the two points of spark gap **7**. This arrangement produces slightly dampened oscillation wave currents.

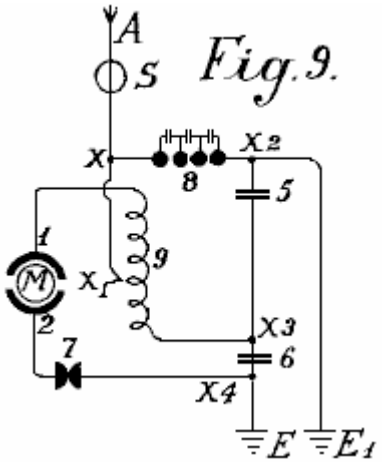

Fig.9 shows a loosely coupled system intended for small motors for measuring purposes. **A** is the serial, **S** is the electromagnet or aerial inductor, **9** the inductor, **7** the spark gap, **5** and **6** capacitors, **E** the earth, **M** the motor, and **1** and **2** the stator connections of the motor which is directly connected to the oscillator circuit.

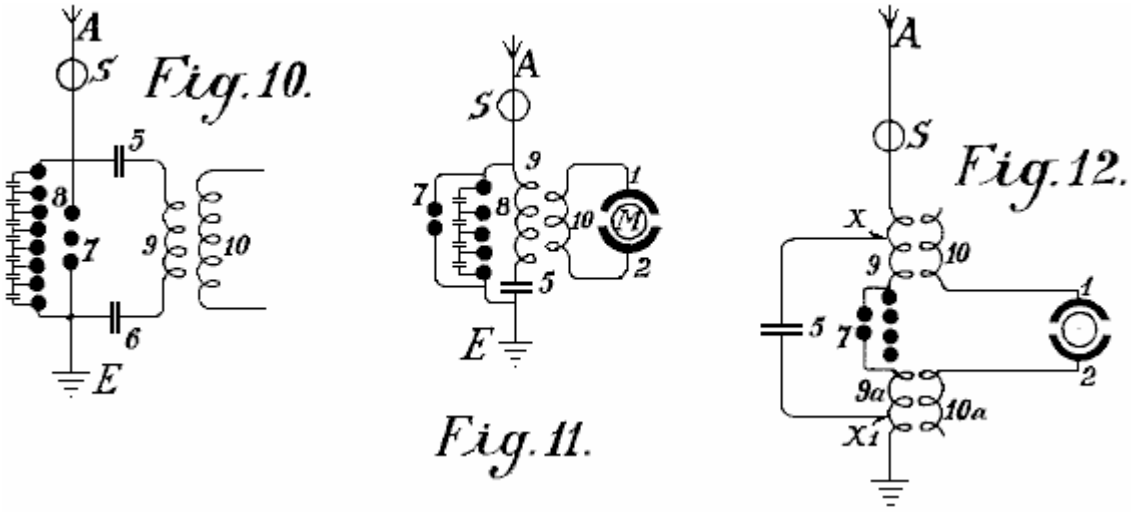

Fig.10 shows a motor circuit with purely inductive coupling. The motor is connected with the secondary wire **10** as may be seen in **Fig.11** in a somewhat modified circuit. The same applies to the circuit of **Fig.12**.

The circuit diagrams shown so far, allow motors of small to medium strength to be operated. For large aggregates, however, they are too inconvenient as the construction of two or more oscillation circuits for large amounts of energy is difficult; the governing is still more difficult and the danger in switching on or off is greater.

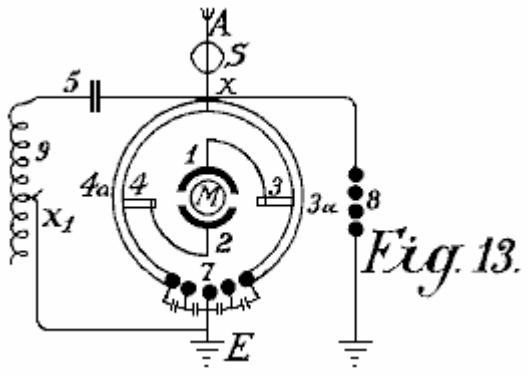

A means for overcoming such difficulties is shown in **Fig.13**. The oscillation circuit shown here, runs from point **x** over capacitor **5**, variable inductor **9**, spark gap **7** and the two segments **3a** and **3b** forming arms of a Wheatstone bridge, back to **x**. If the motor is connected by brushes **3** and **4** transversely to the two arms of the bridge as shown in the drawing, electromagnetic oscillations of equal sign are induced in the stator surfaces **1** and **2** and the motor does not revolve. If however, the brushes **3** and **4** are moved in common with the conducting wires **1** and **2** which connect the brushes with the stator poles, a certain alteration or displacement of the polarity is obtained and the motor commences to revolve.

The maximum action will result if one brush **3** comes on the central sparking contact **7** and the other brush **4** on the part **x**. In practice however, they are usually brought on to the central contact **7** but only held in the path of the bridge segments **4a** and **3a** in order to avoid connecting the spark gaps with the motor oscillation circuit.

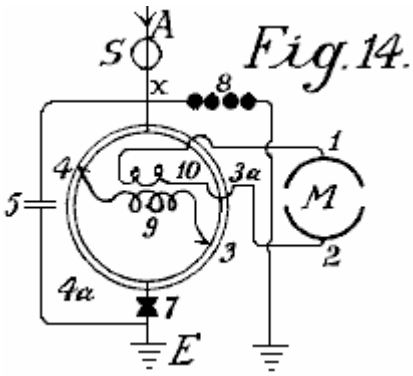

As this prevents the whole of the oscillation energy acting on the motor, it is better to adopt the modification shown in **Fig.14**. The only difference here is that the motor is not wired directly to the segments of the commutator, but instead it is wired to secondary coil **10** which receives induced current from primary coil **9**. This arrangement provides a good transforming action, a loose coupling and an oscillation circuit without a spark gap.

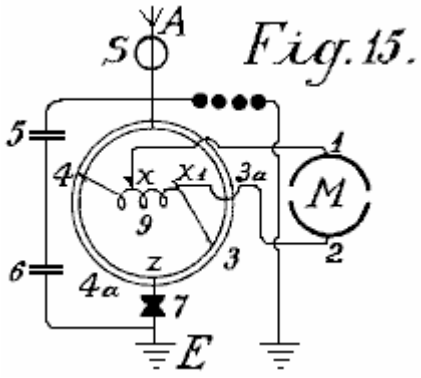

In **Fig.15**, the motor is wired directly to the primary coil at **x** and **x1** after the principle of the auto-transformer. In **Fig.16**, instead of an inductor, capacitor **6** replaces the inductance and is inserted between the segments **3a** and **4a**. This has the advantage that the segments **3a** and **4a** need not be made of solid metal, but may consist of spiral coils which allow a more exact regulation, and high inductance motors may be used.

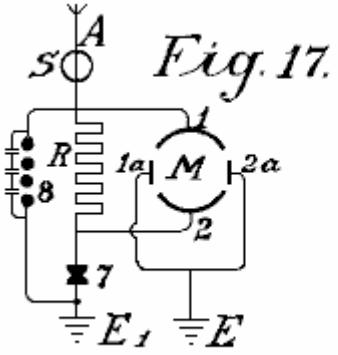

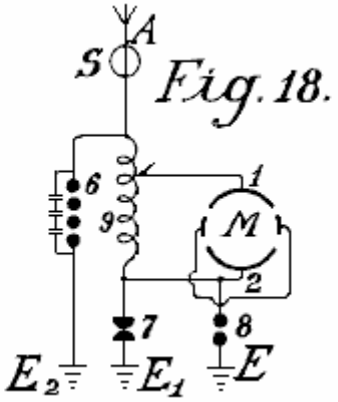

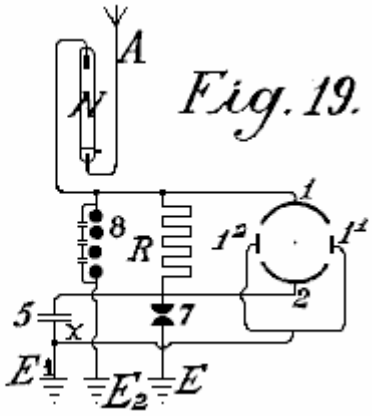

The circuits shown in **Fig.17**, **Fig.18** and **Fig.19** may be used with resonance and particularly with induction capacitor motors; between the large stator induction capacitor surfaces, small reversing pole capacitors are connected which are lead together to earth. Such reversing poles have the advantage that, with large quantities of electrical energy, the spark formation between the separate oscillation circuits ceases.

Fig.19 shows another method which prevents high frequency electromagnetic oscillations formed in the oscillation circuit, feeding back to the aerial. It is based on the well known principle that a mercury lamp, one electrode of which is formed of mercury, the other of solid metal such as steel, allows an electric charge to pass in only one direction: from the mercury to the steel and not vice versa. The mercury electrode of the vacuum tube **N** is therefore connected with the aerial conductor and the steel electrode with the oscillation circuit. Charges can then only pass from the aerial through the vacuum tube to the oscillation circuit and no flow occurs in the opposite direction. In practice, these vacuum tubes must be connected behind an electromagnet as the latter alone provides no protection against the danger of lightning.

As regards the use of spark gaps, all arrangements as used for wireless telegraphy may be used. Of course, the spark gaps in large machines must have a sufficiently large surface. In very large stations they are cooled in liquid carbonic acid or better still, in liquid nitrogen or hydrogen; in most cases the cooling may also take place by means of liquefied low homologues of the metal series or by means of hydrocarbons, the freezing point of which lies between -90^{o}C and -40^{0}C. The spark gap casing must also be insulated and be of sufficient strength to be able to resist any pressure which may arise. Any undesirable excess super-pressure which may be formed must

be let off automatically. I have employed with very good results, mercury electrodes which were frozen in liquid carbonic acid, the cooling being maintained during the operation from the outside, through the walls.

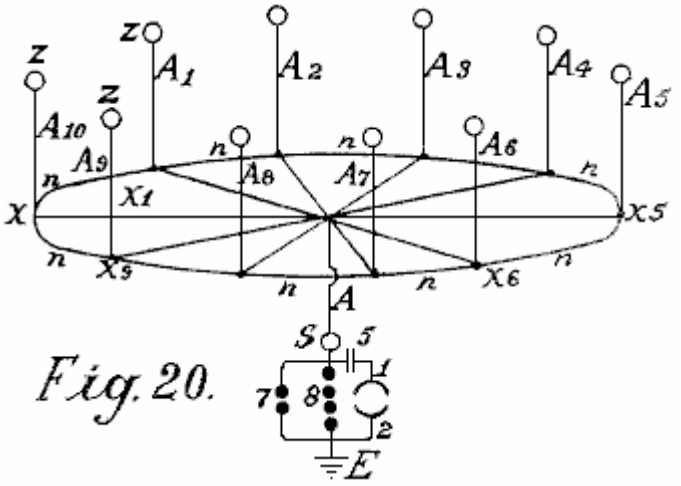

Fig. 20.

Fig.20 shows one of the most simple forms of construction of an aerial network in combination with collectors, transformers and the like. **E** is the earth wire, **8** the safety spark gap, **7** the working spark gap, **1** and **2** the stator surfaces of the motor, **5** a capacitor battery, **S** the protective magnet which is connected with the coil in the aerial conductor, $\mathbf{A^1}$ to $\mathbf{A^{10}}$ aerial antennae with collecting balloons, **N** horizontal collecting or connecting wires, from which, a number of connections run to the centre.

The actual collectors consist of metal sheaths, preferably made of an aluminium magnesium alloy, and are filled with hydrogen or helium, and are attached to copper-plated steel wires. The size of the balloon is selected so that the actual weight of the balloon and its conducting wire is supported by it. Aluminium spikes, made and gilded as described below, are arranged on top of the balloons in order to produce a conductor action. Small quantities of radium preparations, more particularly, polonium-ionium or mesothorium preparations, considerably increase the ionisation, and the performance of these collectors.

In addition to metal balloons, fabric balloons which are sprayed with a metallic coating according to Schoop's metal-spraying process may also be used. A metallic surface may also be produced by lacquering with metallic bronzes, preferably according to Schoop's spraying process, or lacquering with metallic bronze powders in two electrical series of widely different metals, because this produces a considerably increased collecting effect.

Instead of the ordinary round balloons, elongated cigar-shaped ones may be employed. In order also to utilise the frictional energy of the wind, patches or strips of non-conducting substances which produce electricity by friction, may be attached to the metallised balloon surfaces. The wind will impart a portion of its energy in the form of frictional electricity, to the balloon casing, thus substantially increasing the collection effect.

In practice however, very high towers of up to 300 metres may be employed as antennae. In these towers, copper tubes rise freely further above the top of the tower. A gas lamp secured against the wind is then lit at the point of the copper tube and a netting is secured to the copper tube over the flame of this lamp to form a collector. The gas is conveyed through the interior of the tube, up to the summit. The copper tube must be absolutely protected from moisture at the place where it enters the tower, and rain must be prevented from running down the walls of the tower, which might lead to a bad catastrophe. This is done by bell-shaped enlargements which expand downwards, being arranged in the tower in the form of high voltage insulators of Siamese pagodas.

Special attention must be devoted to the foundations of such towers. They must be well insulated from the ground, which may be achieved by first embedding a layer of concrete in a box form to a sufficient depth in the ground, and inserting in this, an asphalt lining and then glass bricks cast about 1 or 2 metres in thickness. Over this in turn, there is a ferro-concrete layer in which alone the metal foot of the tube is secured. This concrete block must be at least 2 metres from the ground and at the sides, be fully protected from moisture by a wooden covering. In the lower part of the tower, a wood or glass housing should be constructed to protect the capacitors and/or motors. In order to ensure that the ground lead connects to the water-table, a well insulated pit lined with vitreous bricks must be provided. Several such towers are erected at equal distances apart and connected with a horizontal conductor. The horizontal connecting wires may either run directly from tower to tower or be carried on bell-shaped insulators similar to those in use for high voltage electricity transmission lines. The width of the aerial tower network may be of any suitable size and the connection of the motors can take place at any convenient location.

Fig. 21.

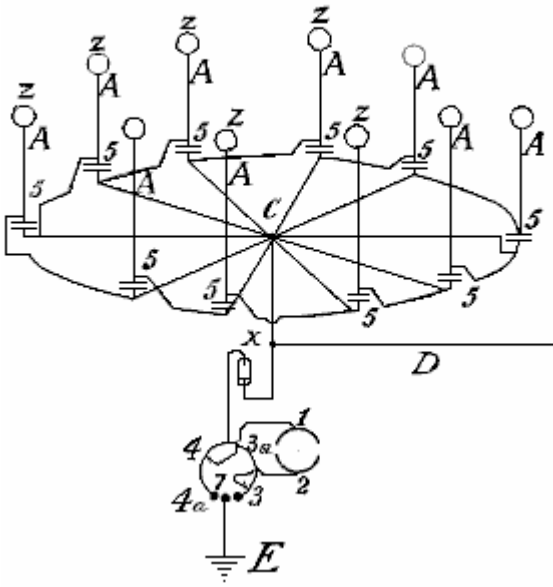

Fig. 22.

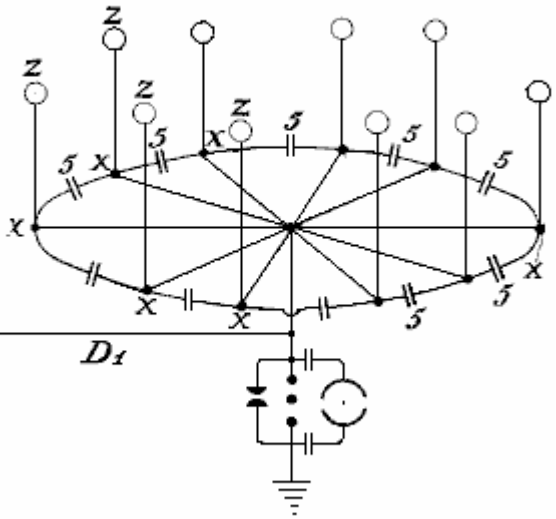

In order to collect large quantities of electricity with few aerials, it is as well to provide the aerial conductor with sets of capacitors as shown in the two methods of construction illustrated in **Fig.21** and **Fig.22**. In **Fig.21** the set of capacitors **5** is connected between the aerials **Z** via lead **A** and an annular conductor from which horizontal run to the connecting points **C** to which the earth wire is connected. **Fig.22** shows a similar arrangement.

Should two such series of antenna rings be shown by a voltmeter to have a large voltage difference (for example, one in the mountains and one on the plain) or even of a different polarity, these differences may be compensated for by connecting sufficiently large capacitor sets (**5, 5a, 5b**) by means of Maji star conductors **D** and **D[1]**. **Fig.23**, shows a connection of three such rings of collectors are positioned in a triangle with a central set of capacitors.

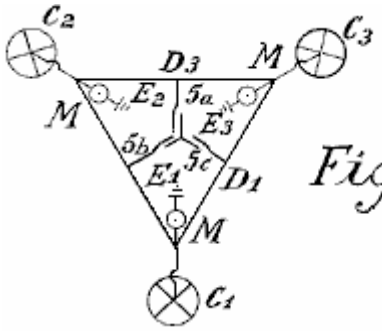

Fig. 23.

The capacitor sets of such large installations must be embedded in liquefied gasses or in liquids freezing at very low temperatures. In such cases, a portion of the atmospheric energy must be employed for liquefying these gasses. It is also preferable to employ pressure. By this means, the capacitor surfaces may be reduced in area and still allow the storage of large quantities of energy to be stored, secure against breakdown. For the smaller installations, the immersing of the capacitors in well insulated oil or the like, is sufficient. Solid substances, on the other hand, cannot be employed as insulators.

The arrangement in the diagrams shown earlier has always shown both poles of the capacitors connected to the aerial conductors. An improved method of connection has been found to be very advantageous. In this method, only one pole of each capacitor is connected to the collecting network. Such a method of connection is very important, as by means of it, a constant current and an increase in the normal working voltage is obtained. If, for example, a collecting balloon aerial which is allowed to rise to a height of 300 metres, shows 40,000 volts above earth voltage, in practice it has been found that the working voltage (with a withdrawal of the power as described earlier by means of oscillating spark gaps and the like) is only about 400 volts. If however, the capacity of the capacitor surfaces be increased, which capacity in the above mentioned case was equal to that of the collecting surface of the balloon aerials, to double the amount, by connecting the capacitors with only one pole, the voltage rises under an equal withdrawal of current up to and beyond 500 volts. This can only be ascribed to the favourable action of the connecting method.

In addition to this substantial improvement it has also been found preferable to insert double inductances with electromagnets and to place the capacitors preferably between two such electromagnets. It has also been found that the useful action of such capacitors can be further increased if an induction coil is connected as an inductive resistance to the unconnected pole of the capacitor, or still better if the capacitor itself be made as an induction capacitor. Such a capacitor may be compared to a spring, which when compressed, carries in itself accumulated force, which it gives off again when released. In charging, a charge with reversed sign is formed at the other free capacitor pole, and if a short circuit occurs through the spark gap, the accumulated energy is again given back since now new quantities of energy are induced at the capacitor pole connected to the conductor network, which in fact, charges with opposite sign to that at the free capacitor pole. The new induced charges have of course, the same sign as the collector network. The whole voltage energy in the aerial is thereby increased. In the same time interval, larger quantities of energy are accumulated than is the case without such capacitor sets being inserted.

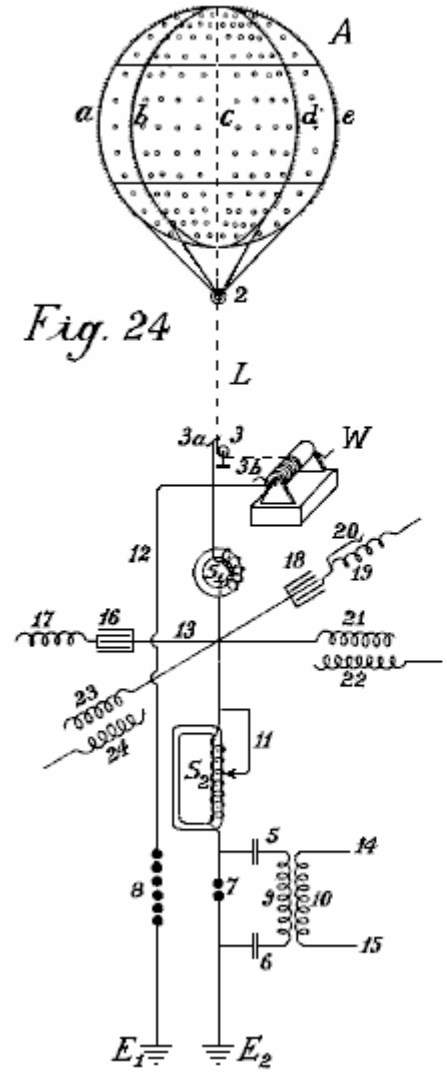

Fig. 24

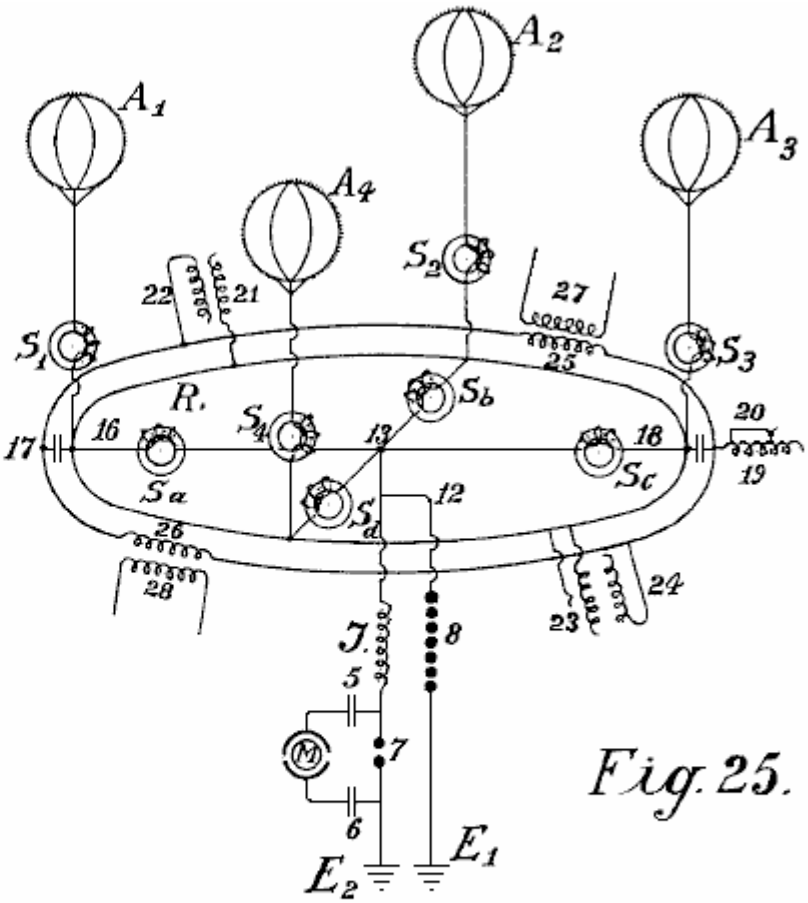

Fig. 25.

In **Fig.24** and **Fig.25**, two different connection diagrams are illustrated in more detail. **Fig.24** shows a collecting balloon along with its earth connections. **Fig.25** shows four collecting balloons and the parallel connection of their capacitor sets.

A is the collecting balloon made of an aluminium magnesium alloy (electron metal magnalium) of a specific gravity of 1.8 and a plate thickness of 0.1 mm to 0.2 mm. Inside, there are eight strong vertical ribs of T-shaped section of about 10 mm to 20 mm in height and about 3 mm in thickness, with the projecting part directed inwards (indicated by **a, b, c, d** and so forth). They are riveted together to form a firm skeleton and are stiffened in a horizontal direction by two cross ribs. The ribs are further connected to one another internally and transversely by means of thin steel wires, whereby the balloon obtains great strength and elasticity. Rolled plates of 0.1 mm to 0.2 mm in thickness made of magnalium alloy are then either soldered or riveted on to this skeleton so that a fully metallic casing with a smooth external surface is created. Well silvered or coppered aluminium plated steel wires run from each rib to the fastening ring **2**. Further, the coppered steel hawser **L**, preferably twisted out of separate thin wires (shown as dotted lines in **Fig.24**) and which must be long enough to allow the balloon to rise to the

desired height, leads to a metal roller or pulley **3** and on to a winch **W**, which must be well insulated from the earth. By means of this winch, the balloon which is filled with hydrogen or helium, can be allowed to rise to a suitable height of 300 to 5,000 metres, and brought to the ground for recharging or repairs.

The actual current is taken directly through a friction contact from the metal roller **3** or from the wire or even from the winch, or simultaneously from all three by means of brushes (**3**, **3a** and **3b**). Beyond the brushes, the conductor is divided, the paths being:- firstly, over **12** to the safety spark gap **8**, on to the earth conductor $\mathbf{E^1}$, and secondly over electromagnet $\mathbf{S^1}$, point **13**, to a second loose electromagnet having an adjustable coil $\mathbf{S^2}$, then to the spark gap **7** and to the second earth conductor $\mathbf{E^2}$. The actual working circuit is formed through the spark gap **7**, capacitors **5** and **6**, and through the primary coil **9**; here the static electricity formed by oscillatory discharges is accumulated and converted into high frequency electromagnetic oscillations. Between the electromagnets $\mathbf{S^1}$ and $\mathbf{S^2}$ at the crossing point **13**, four capacitor sets are introduced which are only indicated diagramatically in the drawings by a single capacitor. Two of these sets of capacitors (**16** and **18**) are made as plate capacitors and prolonged by regulating induction coils or spirals **17** and **19** while the two others (**21** and **23**) are induction capacitors. As may be seen from the drawings, each of the four capacitor sets, **16**, **18**, **21** and **23** is connected by only one pole to either the aerial or to the collector conductor. The second poles **17**, **19**, **22** and **24** are open. In the case of plate capacitors having no inductive resistance, an induction coil is inserted. The object of such a spiral or coil is the displacement of phase of the induction current by $^1/_4$ periods, whilst the charging current of the capacitor poles which lie free in the air, works back to the collector aerial. The consequence of this is that in discharges in the collector aerial, the back-inductive action of the free poles allows a higher voltage to be maintained in the aerial collecting conductor than would otherwise be the case. It has also been found that such a back action has an extremely favourable effect on the wear of the contacts. Of course, the inductive effect may be regulated at will within the limits of the size of the induction coil, the length of the coil in action being adjustable by means of wire connection without induction (see **Fig.24** No. **20**).

$\mathbf{S^1}$ and $\mathbf{S^2}$ may also be provided with such regulating devices, in the case of $\mathbf{S^2}$ illustrated by **11**. If excess voltage be formed, it is conducted to earth through wire **12** and spark gap **8**, or through any other suitable apparatus, since this voltage would be dangerous for the other components. The action of these capacitor sets has already been described.

The small circles on the collector balloon indicate places where small patches of extremely thin layers (0.01 to 0.05 mm thick) of zinc amalgam, gold amalgam or other photoelectric acting metals, are applied to the balloon casing of light metal. Such metallic patches may also be applied to the entire balloon as well as in greater thickness to the conducting network. The capacity of the collector is thereby considerably strengthened at the surface. The greatest possible effect in collecting may be obtained by polonium amalgams and the like. On the surface of the collector balloon, metal points or spikes are also fixed along the ribs. These spikes enhance the charge collection operation. Since it is well known that the sharper the spikes, the less the resistance of the spikes, it is therefore extremely important to use spikes which are as sharp as possible. Experiments have shown that the formation of the body of the spike or point also play a large part, for example, spikes made of bars or rollers with smooth surfaces, have point resistance many times greater than those with rough surfaces. Various kinds of spike bodies have been experimented with for the collector balloons and the best results were given with spikes which were made in the following way: Fine points made of steel, copper, nickel or copper and nickel alloys, were fastened together in bundles and then placed as anode with the points placed in a suitable electrolyte (preferably in hydrochloric acid or muriate of iron solutions) and so treated with weak current driven by 2 to 3 volts. After 2 to 3 hours, according to the thickness of the spikes, the points become extremely sharp and the bodies of the spikes have a rough surface. The bundle can then be removed and the acid washed off with water. The spikes are then placed as cathode in a bath containing a solution of gold, platinum, iridium, palladium or wolfram salts or their compounds, and coated at the cathode galvanically with a thin layer of precious metal, which mush however be sufficiently firm to protect them from atmospheric oxidation.

Such spikes act at a 20 fold lower voltage almost as well as the best and finest points made by mechanical means. Still better results are obtained if polonium or radium salts are added to the galvanic bath when forming the protective layer or coating. Such pins have low resistance at their points and have excellent collector action even at one volt or lower.

In **Fig.24**, the three unconnected poles are not connected with one another in parallel. That is quite possible in practice without altering the principle of the free pole. It is also preferable to interconnect a series of collecting aerials in parallel to a common collector network. **Fig.25** shows such an arrangement. $\mathbf{A^1, A^2, A^3, A^4}$ are four metal collector balloons with gold or platinum coated spikes which are electrolytically mad in the presence of polonium emanations or radium salts, the spikes being connected over four electromagnets $\mathbf{S^1, S^2, S^3, S^4}$, through an annular conductor **R**. From this annular conductor, four wires run over four further electromagnets $\mathbf{S^a, S^b, S^c, S^d}$, to the connecting point **13**. There, the conductor is divided, one branch passing over **12** and the safety spark gap **7** to the earth at $\mathbf{E^1}$, the other over inductive resistance **J** and working spark gap **7** to the earth at

E^2. The working circuit, consisting of the capacitors **5** and **6** and a resonance motor or a capacitor motor **M**, such as already described, is connected in proximity around the sparking gap section **7**. Of course, instead of connecting the capacitor motor directly, the primary circuit for high frequency oscillatory current may also be inserted.

The capacitor sets are connected by one pole to the annular conductor **R** and can be either inductionless (**16** and **18**) or made as induction capacitors as shown by **21** and **23**. The free poles of the inductionless capacitors are indicated by **17** and **19**, and those of the induction capacitors by **22** and **24**. As may be seen from the drawings, all of these poles **17, 22, 19** and **24** may be interconnected in parallel through a second annular conductor without any fear that thereby the principle of the free pole connection will be lost. In addition to the advantages already mentioned, the parallel connection also allows an equalisation of the working voltage in the entire collector network. Suitably calculated and constructed induction coils **25** and **26** may also be inserted in the annular conductor of the free poles, by means of which, a circuit may be formed in the secondary coils **27** and **28** which allows current produced in this annular conductor by fluctuations of the charges, to be measured or otherwise utilised.

According to what has already been stated, separate collector balloons may be connected at equidistant stations distributed over the whole country, either connected directly with one another metallically or by means of intermediate suitably connected capacitor sets through high voltage conductors insulated from earth. The static electricity is converted through a spark gap, into high frequency dynamic electricity which may be utilised as a source of energy by means of a suitable connection method, various precautions being observed, and with special regulations. The wires leading from the collector balloons, have up to now been connected through an annular conductor without this endless connection, which can be regarded as an endless induction coil, being able to exert any action on the whole conductor system.

It has now been found that if the network conductor connecting the aerial collector balloons with one another, is not made as a simple annular conductor, but preferably short-circuited in the form of coils over a capacitor set or spark gap or through thermionic valves, then the total collecting network exhibits quite new properties. The collection of atmospheric electricity is thereby not only increased but an alternating field may easily be produced in the collector network. Further, the atmospheric electrical forces showing themselves in the higher regions, may also be obtained directly by induction. In **Fig.26** and **Fig.28**, a form of construction is shown, on the basis of which, the further foundations of the method will be explained in more detail.

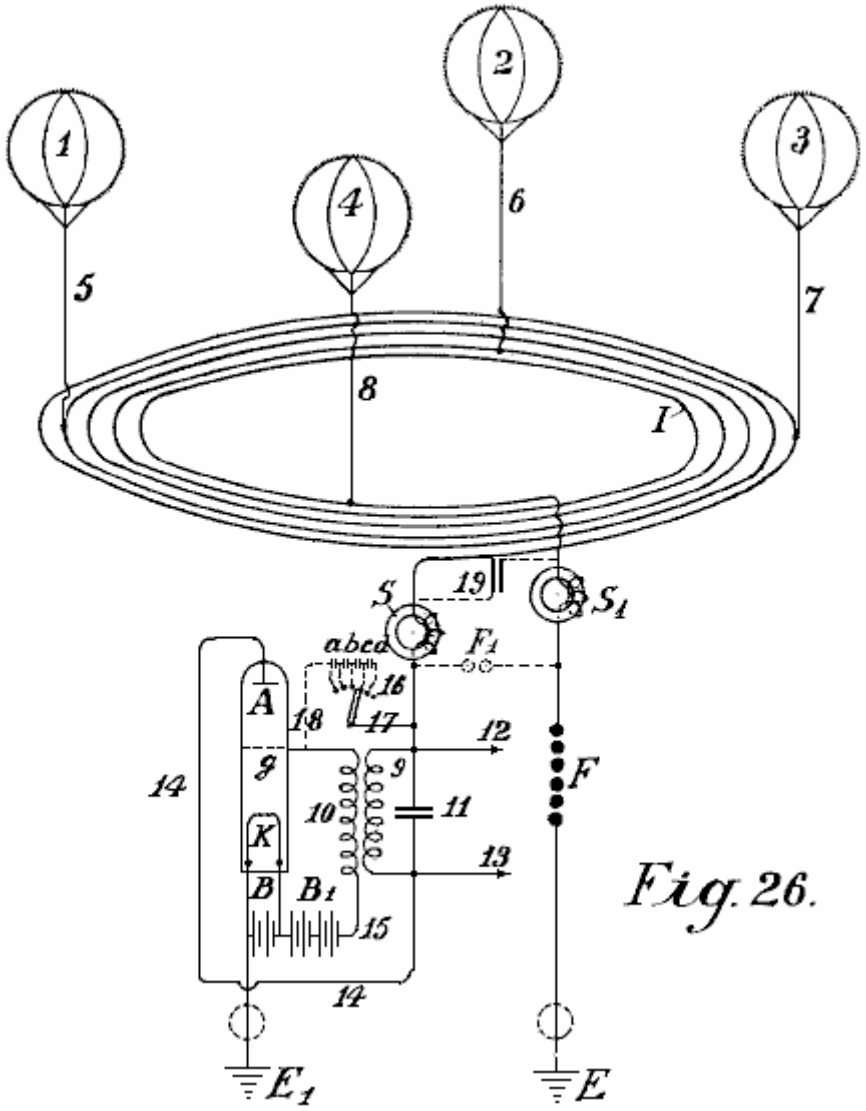

Fig. 26.

In **Fig.26, 1,2,3** and **4** are metallic collector balloons, with **5, 6, 7** and **8** their metallic aerial conductors and **I** the actual collector network. This consists of five coils and is mounted on high voltage insulators in the air, on high voltage masts (or with a suitable construction of cable, embedded in the earth). One coil has a diameter of 1 to 100 km. or more. **S** and **S^1** are two protective electromagnets, **F** is the second safety section against excess voltage, **E** its earth conductor and **E^1** the earth conductor of the working section. When an absorption of static atmospheric electricity is effected through the four balloon collectors, in order to reach the earth connection **E^1**, the current must flow spirally through the collector network, over the electromagnet **S**, primary induction coil **9**, conductor **14**, anode **A** of the audion tube, incandescent cathode **K**, as the way over the electromagnet and safety spark gap **F** offers considerably greater resistance. Owing to the fact that the accumulated current flows in one direction, an electromagnetic alternating field is produced in the interior of the collector network coil, whereby all of the free electrons are directed more or less into the interior of the coil. An increased ionisation of the atmosphere is therefore produced. Consequently, the points mounted on the collector balloon, show a considerably reduced resistance and therefore increased static charges are produced between the points on the balloon and the surrounding atmosphere. This results in a considerably increased collector effect.

A second effect, which could not be achieved in any other way, is obtained by the alternating electromagnetic field running parallel to the earth's surface, which acts more or less with a diminishing or increasing effect on the earth's magnetic field, whereby in the case of fluctuations in the current, a return induction current of reversed sign is always produced in the collector coil by earth magnetism. Now if a constantly pulsating, continuous alternating field is produced as stated in the collector network **I**, an alternating current of the same frequency is also produced in the collecting network coil. As the same alternating field is further transmitted to the aerial balloon, the resistance of its points is thereby considerably reduced, while the collector action is considerably increased. A further advantage is that positive charges which collect on the metal surfaces during the conversion into dynamic current, produce a so-called voltage drop in the collector area. As an alternating field is present, when discharge of the collector surfaces takes place, the negative ions surrounding the collector surfaces produce, by the law of induction, an induction of reversed sign on the collector surface - that is, a positive charge. In addition to the advantages already stated, the construction of connecting conductors in coil form, when of

sufficiently large diameter, allows a utilisation of energy arising in higher regions, also in the most simple way. As is well known, electric discharges frequently take place at very great elevations which may be observed, such as 'St. Elmo's fires' or 'northern lights'. These energy quantities have not been able to have been utilised before now. By this invention, all of these kinds of energy, as they are of electromagnetic nature and since the axis of the collector coils is at right angles to the earth's surface, can be absorbed in the same way as a radio absorbs distant radio signals. With a large diameter of the spiral, it is possible to connect large surfaces and thereby take up large quantities of energy.

It is well known that in the summer months and in the tropics, large radio stations are very frequently unable to receive signals due to interruptions caused by atmospheric electricity, and this takes place with vertical coils of only 40 to 100 metres in diameter. If, on the contrary, horizontal coils of 1 to 100 kilometres in diameter are used, very strong currents may be obtained through discharges which are constantly taking place in the atmosphere. Particularly in the tropics, or still better in the polar regions where the northern lights are constantly present, large quantities of energy may probably be obtained in this way. A coil with several windings should perform the best. In a similar manner, any alteration of the earth's magnetic field should act inductively on such a coil.

It is not at all unlikely that earthquakes and sunspots will also produce an induction in collector coils of that size. In similar manner, this collector conductor will react to earth currents more particularly when they are near the surface of the earth or even embedded in the earth. By combining the previous kind of current collectors, so far as they are adapted for the improved system with the improved possibilities of obtaining current, the quantities of free natural energy which are to be obtained in the form of electricity are considerably increased.

In order to produce uniform undamped current oscillations in the improved collector coil, so-called audion high vacuum or thermionic valves are used instead of the previous described spark gaps (**Fig.26, 9-18**). The main aerial current flows through electromagnet **S** (which in the case of a high number of alternations is not connected here but in the earth conductor $\mathbf{E^1}$) and may be conveyed over the primary coils in the induction winding through wire **14** to the anode **A** of the high vacuum grid valve. Parallel with the induction resistance **9**, a regulating capacity of suitable size, such as capacitor **11**, is inserted. In the lower part of the vacuum grid valve is the incandescent filament cathode **K** which is fed through a battery **B**. From the battery, two branches run, one to the earth conductor $\mathbf{E^1}$ and the other through battery $\mathbf{B^1}$ and secondary coil **10** to the grid anode **g** of the vacuum tube. By the method of connections shown in dotted lines, a desired voltage may also be produced at the grid electrode **g** through wire **17** which is branched off from the main current conductor through switches **16** and some small capacitors (**a, b, c, d**) connected in series, and conductor **18**, without the battery $\mathbf{B^1}$ being required. The action of the whole system is somewhat as follows:-

On the connecting conductor of the aerial collector network being short-circuited to earth, the capacitor pole **11** is charged, and slightly dampened oscillations are formed in the short-circuited oscillation circuit formed by capacitor **11** and self inductance **9**. Because of the coupling through coil **10**, voltage fluctuations of the same frequency take place in the grid circuit **15** and in turn, these fluctuations influence the strength of the electrode current passing through the high vacuum amplifying valve and thus produce current fluctuations of the same frequency in the anode circuit. A permanent supply of energy. Consequently, a permanent supply of energy is supplied to the oscillation circuits **9** and **10** takes place, until a balance is achieved where the oscillation energy consumed exactly matches the energy absorbed. This produces constant undamped oscillations in the oscillation circuits **9 - 11**.

For regular working of such oscillation producers, high vacuum strengthening tubes are necessary and it is also necessary that the grid and anode voltages shall have a phase difference of 180^0 so that if the grid is negatively charged, then the anode is positively charged and vice versa. This necessary difference of phase may be obtained by most varied connections, for example, by placing the oscillating circuit in the grid circuit or by separating the oscillation circuit and inductive coupling from the anodes and the grid circuit, and so forth.

A second important factor is that care must be taken that the grid and anode voltages have a certain relation to one another; the latter may be obtained by altering the coupling and a suitable selection of the self induction in the grid circuit, or as shown by the dotted lines **18, 17, 16** by means of a larger or smaller number of capacitors of suitable size connected in series; in this case, the battery $\mathbf{B^1}$ may be omitted. With a suitable selection of the grid potential, a glow discharge takes place between the grid **g** and the anode **A**, and accordingly at the grid there is a cathode drop and a dark space is formed. The size of this cathode drop is influenced by the ions which are emitted in the lower space in consequence of shock ionisation of the incandescent cathodes **K** and pass through the grid in the upper space. On the other hand, the number of the ions passing through the grid is dependent on the voltage between the grid and the cathode. Thus, if the grid voltage undergoes periodic fluctuations (as in the present case), the amount of the cathode drop at the grid fluctuates, and consequently, the internal resistance of the valve fluctuates correspondingly, so that when a back-coupling of the feed circuit with the grid circuit takes

place, the necessary means are in place for producing undamped oscillations and of taking current as required, from the collecting conductor.

With a suitably loose coupling, the frequency of the undamped oscillations produced is equal to the self-frequency of the oscillation circuits **9** and **10**. By selecting a suitable self-induction for coil **9** and capacitor **11**, it is possible to extend operation from frequencies which produce electromagnetic oscillations with a wavelength of only a few metres, down to the lowest practical alternating current frequency. For large installations, a suitable number of frequency producing tubes in the form of the well known high vacuum transmission tubes of 0.5 kW to 2 kW in size may be connected in parallel so that in this respect, no difficulty exists.

The use of such tubes for producing undamped oscillations, and the construction and method of inserting such transmission tubes in an accumulator or dynamo circuit is known, also, such oscillation producing tubes only work well at voltages of 1,000 volts up to 4,000 volts, so that on the contrary, their use at lower voltages is considerably more difficult. By the use of high voltage static electricity, this method of producing undamped oscillations as compared with that through spark gaps, must be regarded as an ideal solution, particularly for small installations with outputs from 1 kW to 100 kW.

By the application of safety spark gaps, with interpolation of electromagnets, not only is short-circuiting avoided but also the taking up of current is regulated. Oscillation producers inserted in the above way, form a constantly acting alternating electromagnetic field in the collector coil, whereby, as already stated, a considerable accumulating effect takes place. The withdrawal or 'working' wire is connected at **12** and **13**, but current may be taken by means of a secondary coil which is firmly or moveably mounted in any suitable way inside the large collector coil, i.e. in its alternating electromagnetic field, so long as the direction of its axis is parallel to that of the main current collecting coil.

In producing undamped oscillations of a high frequency (50 KHz and more) in the oscillation circuits **9** and **11**, electromagnets **S** and **S[1]** must be inserted if the high frequency oscillations are not to penetrate the collector coil, between the oscillation producers and the collector coil. In all other cases they are connected shortly before the earthing (as in **Fig.27** and **Fig.28**).

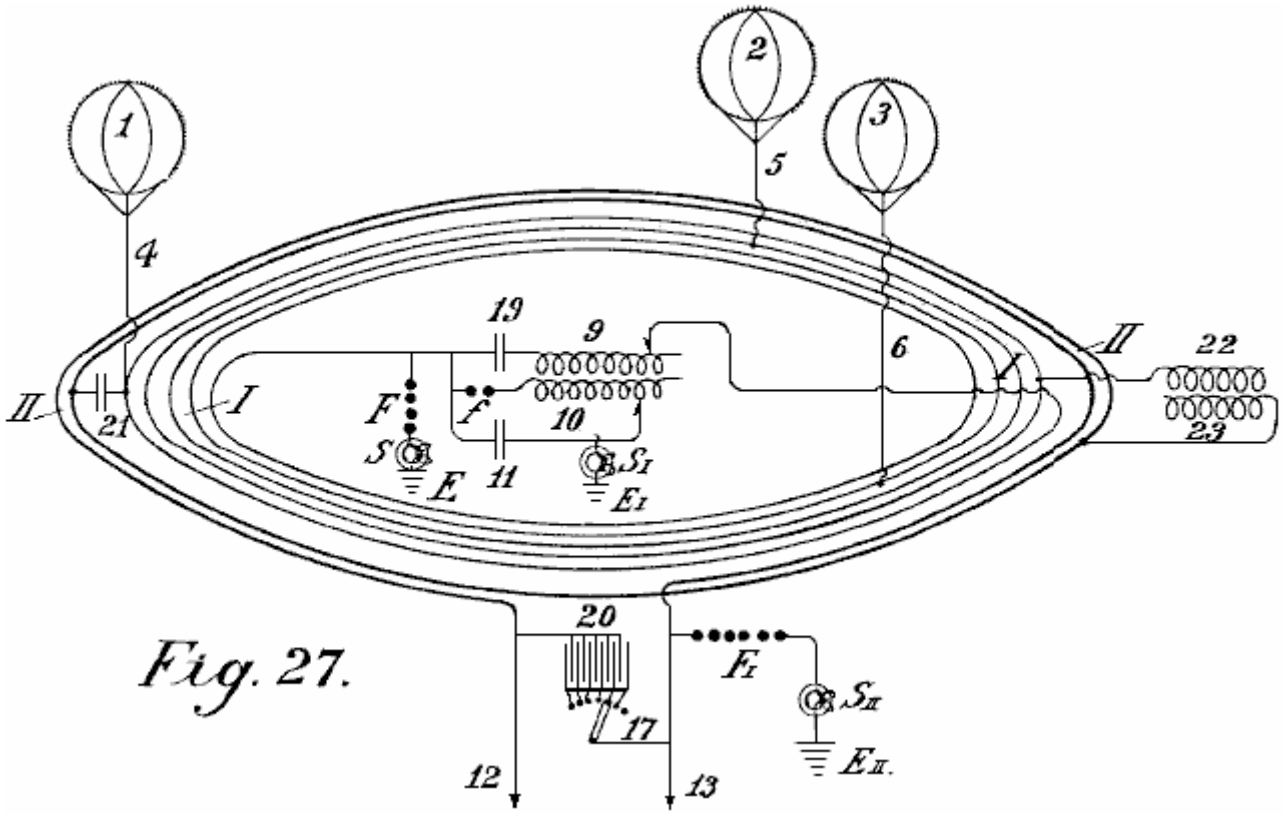

Fig. 27.

In **Fig.27** a second method of construction of the connecting conductor of the balloon aerials is illustrated in the form of a coil. The main difference is that in addition to the connecting conductor **I** another annular conductor **II** is inserted parallel to the former on the high voltage masts in the air (or embedded as a cable in the earth) but both in the form of a coil. The connecting wire of the balloon aerials is both a primary conductor and a current producing network while the coil is the consumption network and is not in unipolar connection with the current producing network.

In **Fig.27** the current producing network **I** is shown with three balloon collectors **1, 2, 3** and aerial conductors **4, 5, 6**; it is short-circuited through capacitor **19** and inductor **9**. The oscillation forming circuit consists of spark gap **f**, inductor **10** and capacitor **11**. The earth wire **E** is connected to earth through electromagnet S^1. F_I is the safety spark gap which is also connected to earth through a second electromagnet S_{II} at E_{II}. On connecting up the capacitor circuit **11** it is charged over the spark gap **f** and an oscillatory discharge is formed. This discharging current acts through inductor **10** on the inductively coupled secondary **9**, which causes a change in the producing network, by modifying the voltage on capacitor **19**. This causes oscillations in the coil-shaped producer network. These oscillations induce a current in the secondary circuit **II**, which has a smaller number of windings and lower resistance, consequently, this produces a lower voltage and higher current in it.

In order to convert the current thus obtained, into current of an undamped character, and to tune its wavelengths, a sufficiently large regulatable capacitor **20** is inserted between the ends **12** and **13** of the secondary conductor **II**. Here also, current may be taken without an earth conductor, but it is advisable to insert a safety spark gap E^1 and to connect this with the earth via electromagnet S^2. The producer network may be connected with the working network **II** over an inductionless capacitor **21** or over an induction capacitor **22, 23**. In this case, the secondary conductor is unipolarly connected with the energy conductor.

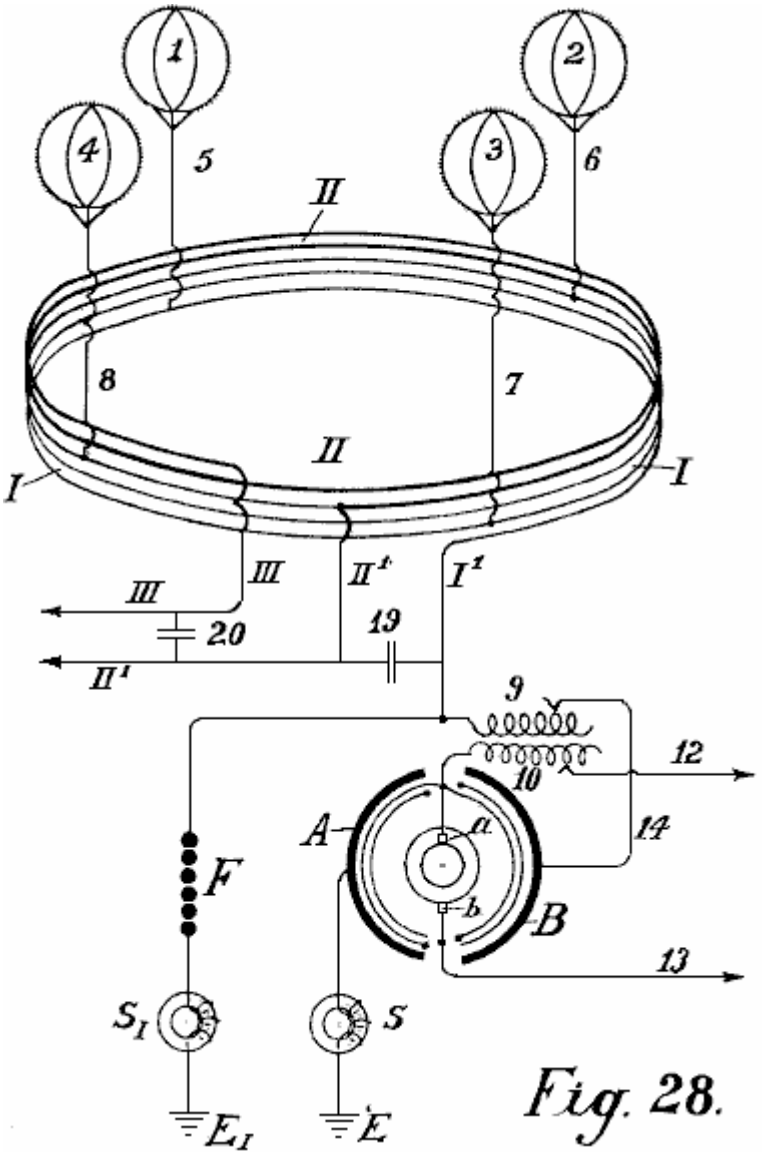

Fig. 28.

In **Fig.28**, the connecting conductor between the separate collecting balloons is carried out according to the autotransformer principle. The collecting coil connects four aerial balloons **1, 2, 3, 4**, the windings of which are not made side-by-side but one above the other. In **Fig.28**, the collector coil **I** is shown with a thin line and the metallically connected prolongation coils **II** with a thick line. Between the ends I^1 and II^1 of the energy network **I**, a regulating capacitor **19** is inserted. The wire I^1 is connected with the output wire and with the spark gap **F**.

As transformer of the atmospheric electricity, an arrangement is employed which consists of using rotary pairs of capacitors in which the stator surface **B** is connected with the main current, while the other **A** is connected to the earth pole. These pairs of short-circuited capacitors are caused to rotate and the converted current can be taken from them via two collector rings and brushes. This current is alternating current with a frequency dependent on the number of balloons and the rate of revolutions of the rotor. As the alternating current formed in the rotor can act through coils **10** on the inductor **9**, an increase or decrease of the feed current in **I** can be obtained according to the direction of the current by back-induction. Current oscillations of uniform rhythm are produced in the coil-shaped windings of the producer network.

As the ends of this conductor are short-circuited through the regulatable capacitor **19**, these rhythms produce short-circuited undamped oscillations in the energy conductor. The frequency of these oscillations can be altered at will by adjusting the capacitance of capacitor **19**. These currents may also be used as working current via the conductors **II**[1] and **III**. By inserting capacitor **20**, a connection between these conductors may also be made, whereby harmonic oscillations of desired wavelength are formed. By this means, quite new effects as regards current distribution are obtained. The withdrawal of current can even take place without direct wire connection if, at a suitable point in the interior of the producing network (quite immaterially whether this has a diameter of 1 or 100 km) a coil tuned to these wavelength and of the desired capacity, is firmly or moveably mounted in the aerial conductor in such a way that its axis is parallel with the axis of the collector coil. In this case, a current is induced in the producing network, the size of which is dependent on the total capacity and resistance and on the frequency selected. A future possibility is taking energy from the producer network by radio signals as in addition to atmospheric electricity, magnetic earth currents and energy from the upper atmosphere may be tapped.

Of course, vacuum tubes may be used to produce undamped oscillations anywhere spark gaps are shown in the circuits. The separate large-diameter coils of the producer network may be connected to one another through separate conductors all in parallel or all in series or in groups in series. By regulating the number of oscillations and the magnitude of the voltage, more or fewer large collector coils of this kind may be used. The coils may also be divided spirally over the entire section. The coils may be carried out in annular form or in triangular, quadrangular, hexagonal or octagonal form.

Of course, wires which form guides for the current waves, may be carried from a suitable place to the centre or also laterally. This is necessary when the currents have to be conducted over mountains and valleys and so forth. In all these cases, the current must be converted into a current of suitable frequency.

As already mentioned, separate collecting balloons may be directly metallically interconnected a equidistant stations distributed over the entire country, or may be connected by interpolation of suitable capacitor sets by means of high voltage conductors. The static electricity is converted through a spark gap into dynamic energy of high frequency and could then in that form be used as an energy source after special regulation.

According to this invention, in order to increase the collecting effect of the balloon in the aerial collector conductor or in the earth wire, radiating collectors are used. These consist of either incandescent metal or oxide electrodes in the form of vacuum grid valves, or electric arcs (mercury or similar electrodes), Nernst lamps, or flames of various kinds maybe simply connected with the respective conductor.

It is well known that energy can be drawn off from a cathode consisting of an incandescent body opposite an anode charged with positive electricity (vacuum grid tube). Hitherto however, a cathode was always first directly placed opposite an anode, and secondly, the system always consisted of a closed circuit.

Now if we dispense with the ordinary ideas in forming light or flame arcs in which a cathode must always stand directly opposite an anode charged to a high voltage or another body freely floating in the air, or consider the incandescent cathode to be only a source of unipolar discharge, (which represents group and point discharges in electro-static machines similar to unipolar discharges), it may be ascertained that incandescent cathodes and less perfectly, all incandescent radiators, flames and the like, have relatively large current densities and allow large quantities of electric energy to radiate into open space in the form of electron streams as transmitters.

The object of this invention is as described below, if such incandescent oxide electrodes or other incandescent radiators or flames are not freely suspended in space but instead are connected metallically with the earth so that they can be charged with negative terrestrial electricity, these radiators possess the property of absorbing the free positive electrical charges contained in the air space surrounding them (that is to say, of collecting them and conducting them to earth). They can therefore serve as collectors and have in comparison to the action of the spikes, a very large radius of action R; the effective capacity of these collectors is much greater than the geometrical capacity (R_0) calculated in an electro-static sense.

As is well known, our earth is surrounded with an electro-static field and the difference of potential dV/dh of the earth field according to the latest investigations, is in summer about 60 to 100 volts, and in winter, 300 to 500 volts

per metre difference in height, a simple calculation gives the result that when such a radiation collector or flame collector is arranged, for example, on the ground, and a second one is mounted vertically over it at a distance of 2,000 metres and both are connected by a conducting cable, there is a voltage difference in summer of about 2,000,000 volts and in winter 6,000,000 volts or more.

According to Stefan Boltzmann's law of radiation, the quantity of energy which an incandescent surface (temperature T) of 1 sq. cm. radiates in a unit of time into the open air (temperature T_0) is expressed by the following formula:

$$S = R (T^4 - T_0^4) \text{ watts per square centimetre}$$

and the universal radiation constant R, according to the latest researches of Ferry, is equal to 6.30×10^{-12} watts per square centimetre.

Now, if an incandescent surface of 1 sq. cm., as compared to the surrounding space, shows a periodic fall of potential dV, it radiates (independent of the direction of the current) in accordance with the above formula, for example at a temperature of 3715^0 C. an energy of 1.6 kW per square centimetre. As for the radiation, the same value can be calculated for the collection of energy, but reversed. Now, as carbon electrodes at the temperature of the electric arc, support a current density up to 60 to 65 amps per sq. cm., no difficulties will result in this direction in employing radiating collectors as accumulators.

If the earth be regarded as a cosmically insulated capacitor in the sense of geometrical electro-statics *x*, according to Chwolson, there results from the geometric capacity of the earth:

For negative charging 1.3×10^6 Coulomb For negative potential $V = 10 \times 10^8$ volts.

It follows from this that EJT is approximately equal to 24.7×10^{24} watts/sec. Now if it is desired to make a theoretical short circuit through an earthed flame collector, this would represent an electrical total work of about $79{,}500 \times 10^{10}$ kilowatt years. As the earth must be regarded as a rotating mechanism which is thermo-dynamically, electromagnetically and kinematically coupled with the sun and star system by cosmic radiation and gravitation, a reduction in the electric energy of the earth field is not to be feared. The energies which the incandescent collectors could withdraw from the earth field can only cause a lowering of the earth temperature. This is however, not the case as the earth does not represent a cosmically entirely insulated system. On the contrary, there is conveyed from the sun to the earth an energy of $18{,}500 \times 10^{10}$ kilowatts. Accordingly, any lowering of the earth temperature without a simultaneous lowering of the sun's temperature would contradict Stefan Boltzmann's law of radiation.

From this it must be concluded that if the earth temperature sinks, the total radiation absorbed by the earth increases, and further, the rate of cooling of the earth is directly dependent on that of the sun and the other radiators cosmically coupled with the sun.

The incandescent radiation collectors may, according to this invention, be used for collecting atmospheric electricity if they (1) are charged with the negative earth electricity (that is to say, when they are directly connected to the earth by means of a metallic conductor) and (2) if large capacities (metal surfaces) charged with electricity are mounted opposite them as positive poles in the air. This is regarded as the main feature of the present invention as without these inventive ideas it would not be possible to collect with an incandescent collector, sufficiently large quantities of the electrical charges contained in the atmosphere as technology requires; the radius of action of the flame collectors would also be too small, especially if it be considered that the very small surface density does not allow of large quantities of charge being absorbed from the atmosphere.

It has already been proposed to employ flame collectors for collecting atmospheric electricity and it is known that their collecting effect is substantially greater opposite the points. It is however, not known that the quantities of current which hitherto be obtained are too small for technical purposes. According to my experiments, the reason for this is to be found in the inadequate capacities of the collector conductor poles. If such flame or radiating collectors have no or only small positive surfaces, their radius of action for large technical purposes is too small. If the incandescent collectors be constantly kept in movement in the air, they may collect more according to the speed of the movement, but this is again not capable of being carried out in practice.

By this invention, the collector effect is considerably increased by a body charged with a positive potential and of the best possible capacity, being also held floating (without direct earth connection) opposite such an incandescent collector which is held floating in the air at a desired height. If, for example, a collecting balloon of sheet metal or metallised fabric, be caused to mount to 300 to 3,000 metres in the air, and as a positive pole it is brought opposite such a radiating collector connected by a conductor to earth, quite different results are obtained.

The metallic balloon shell which has a large surface area is charged to a high potential by atmospheric electricity. This potential is greater the higher the collecting balloon is above the incandescent collector. The positive electricity acts concentratedly on the anode floating in the air as it is attracted through the radiation shock ionisation, proceeding from the incandescent cathode. The consequence of this is that the radius of action of the incandescent cathode collector is considerably increased and so is the collecting effect of the balloon surface. Further, the large capacity of the anode floating in the air, plays therefore an important part because it allows the collection of large charges resulting in a more uniform current even when there is substantial current withdrawal - this cannot be the case with small surfaces.

In the present case, the metallic collecting balloon is a positive anode floating in the air and the end of the earth conductor of this balloon serves as positive pole surface opposite the surface of the radiating incandescent cathode, which in turn is charged with negative earth electricity as it is connected to the earth by a conductor. The process may be carried out by two such contacts (negative incandescent cathode and anode end of a capacity floating in the air) a capacitor and an inductive resistance being switched on in parallel, whereby simultaneously undamped oscillations may be formed.

In very large installations it is advisable to connect two such radiating collectors in series. Thus an arc light incandescent cathode may be placed below on the open ground and an incandescent cathode which is heated by special electro-magnetic currents, be located high in the air. Of course for this, the special vacuum Liebig tubes with or without grids may also be used. An ordinary arc lamp with oxide electrodes may be introduced on the ground and the positive pole is not directly connected with the collecting balloon, but through the upper incandescent cathode or over a capacitor. The method of connecting the incandescent cathode floating in the air may be seen in **Figs.29-33**.

B is the air balloon, **K** a Cardan ring (connection with the hawser) **C** the balloon, **L** a good conducting cable, **P** a positive pole, **N** negative incandescent cathode and **E** the earth conductor.

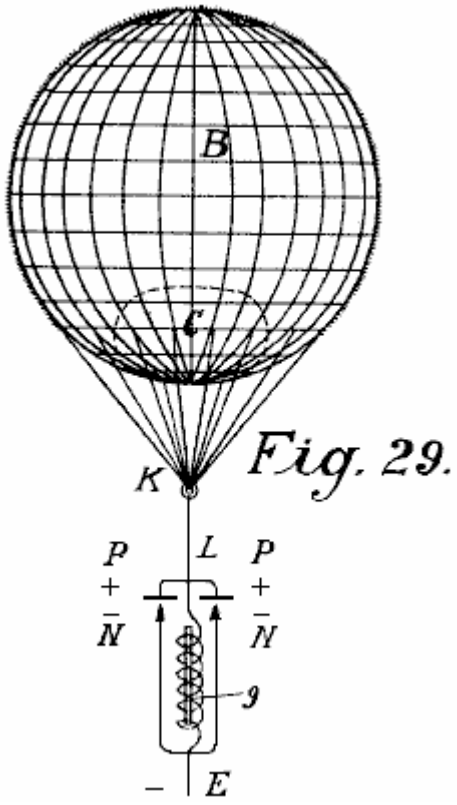

Fig. 29.

Fig.29 represents the simplest form of construction. If electric oscillations are produced below on the ground by means of a carbon arc lamp or in any other suitable way, a considerably greater electric resistance is opposed to that in the direct way by inserting an electrical inductive resistance **9**. Consequently, between **P** and **N**, a voltage is formed, and as, over **N** and **P** only an inductionless ohmic resistance is present, a spark will spring over so long as the separate induction coefficients and the like are correctly calculated. The consequence of this is that the oxide electrode (carbon or the like) is rendered incandescent and then shows as incandescent cathode, an increased collecting effect. The positive poles must be substantially larger than the negative in order that they may not also become incandescent. As they are further connected with the large balloon area which has a large capacity and is charged at high voltage, an incandescent body which is held floating in the air and a positive pole which can collect large capacities is thereby obtained in the simplest way. The incandescent cathode is first

caused to become incandescent by means of separate energy produced on the earth, and then maintained by the energy collected from the atmosphere.

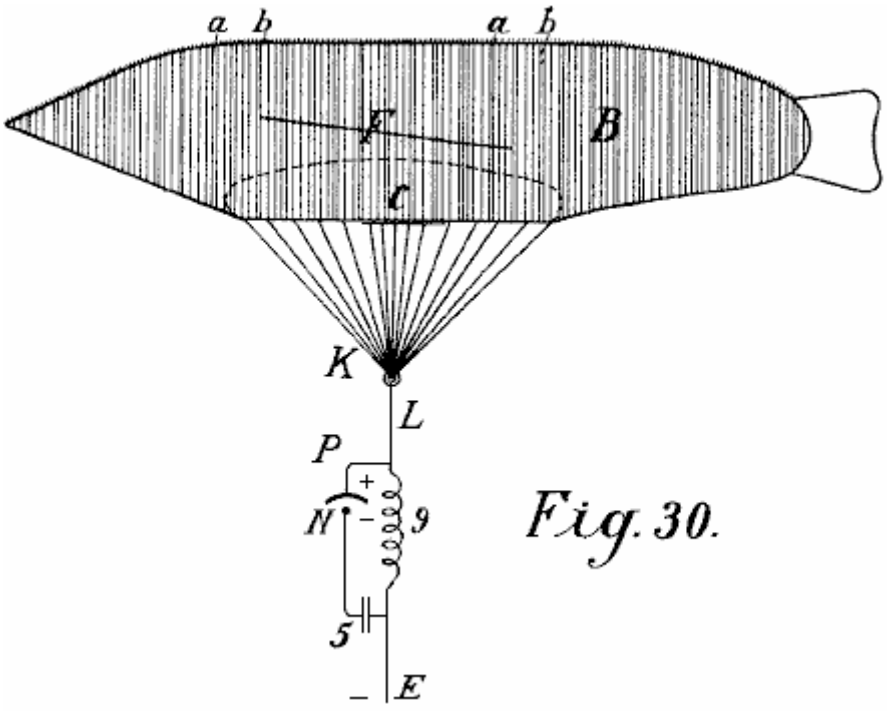

Fig. 30.

Fig.30 only shows the difference that instead of a round balloon, a cigar-shaped one may be used, also, a capacitor **5** is inserted between the incandescent cathode and the earth conductor so that a short-circuited oscillation circuit over **P N 5** and **9** is obtained. This has the advantage that quite small quantities of electricity cause the cathode to become incandescent and much larger cathode bodies may be made incandescent.

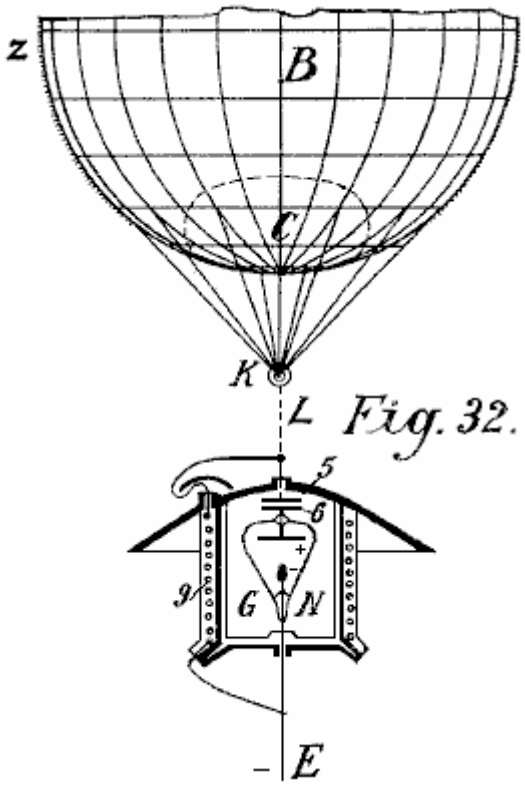

Fig. 32.

In this form of construction, both the incandescent cathode and the positive electrode may be enclosed in a vacuum chamber as shown in **Fig.32**. A cable **L** is carried well insulated through the cover of a vessel and ends in a capacitor disc **5**. The cover is arched in order to keep the rain off. The vessel is entirely or partially made of magnetic metal and well insulated inside and outside. Opposite disc **5** another disc **6** and on this again a metallic positive pole of the vacuum tube **g** with the incandescent cathode (oxide electrode) **N** is arranged. The negative electrode is on the one hand connected to the earth conductor **E**, and on the other hand with the inductive resistance **9** which is also connected with the cable **L** with the positive pole and wound around the vessel in coils.

The action is exactly the same as that in **Fig.29** only instead of an open incandescent cathode, one enclosed in vacuo is used. As in such collectors, only small bodies be brought to incandescence, in large installations a plurality of such vacuum tubes must be inserted in proximity to one another. According to the previous constructions **Fig.31** and **Fig.33** are quite self evident without further explanations.

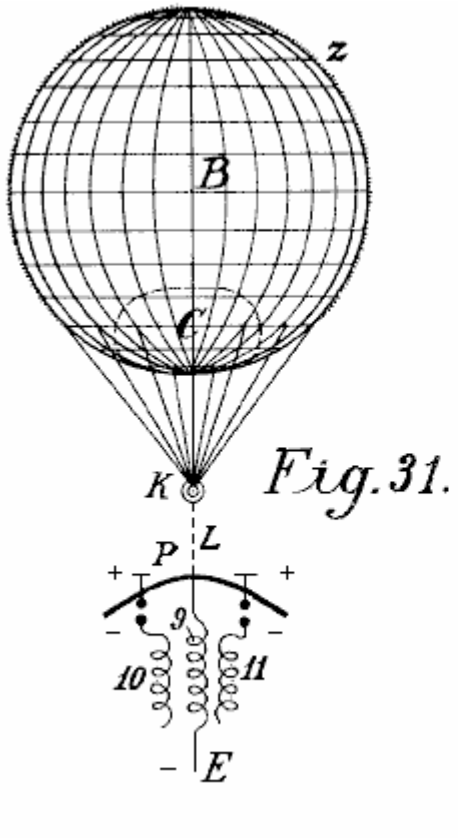

Fig. 31.

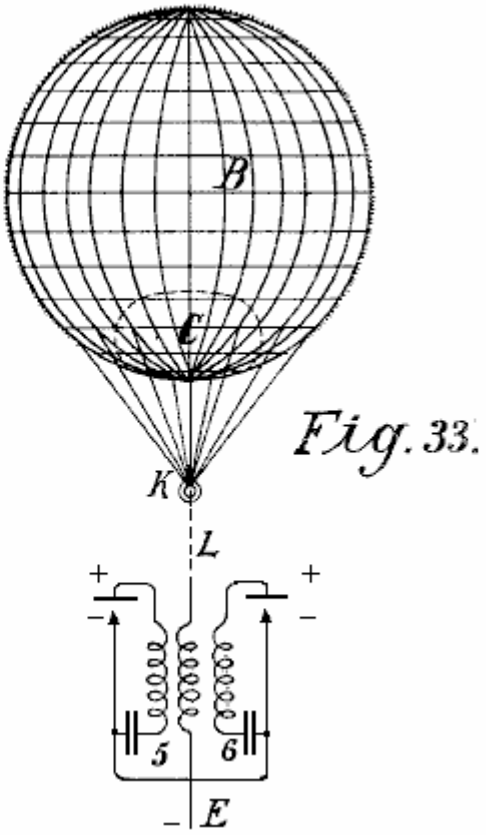

Fig. 33.

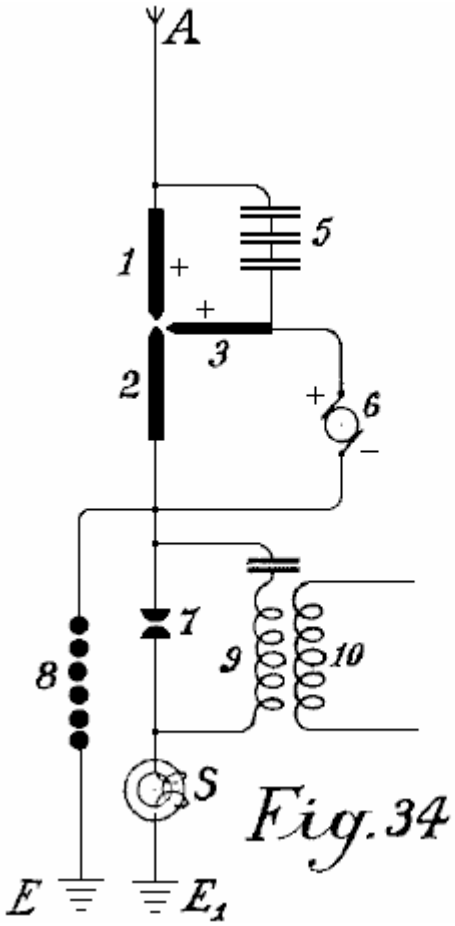

Fig. 34

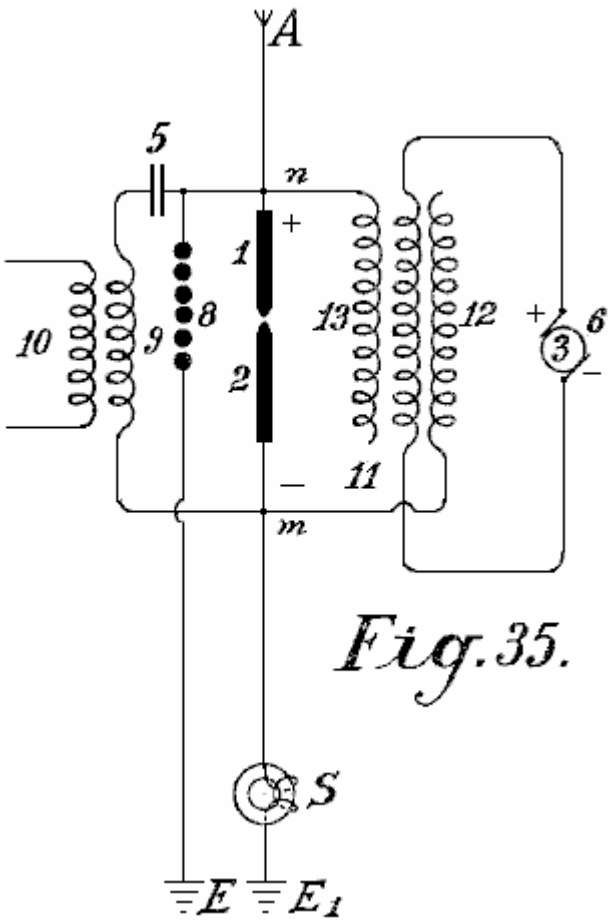

Fig. 35.

Figs.34-37 represent further diagrams of connections over radiating and flame collectors, and in fact, how they are to be arranged on the ground. **Fig.34** shows an arc light collector with oxide electrodes for direct current and its connection. **Fig.35** shows a similar one for alternating current. **Fig.36** an incandescent collector with a Nernst lamp and **Fig.37** a similar one with a gas flame.

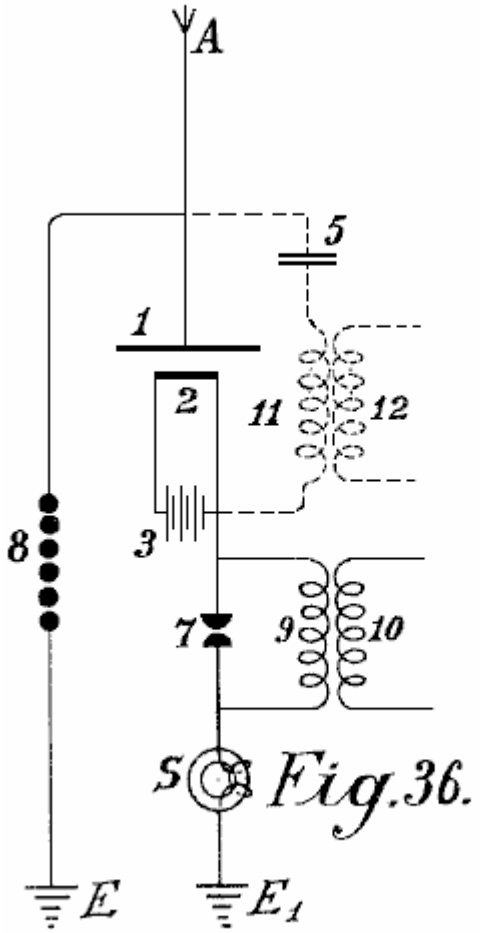

Fig.36.

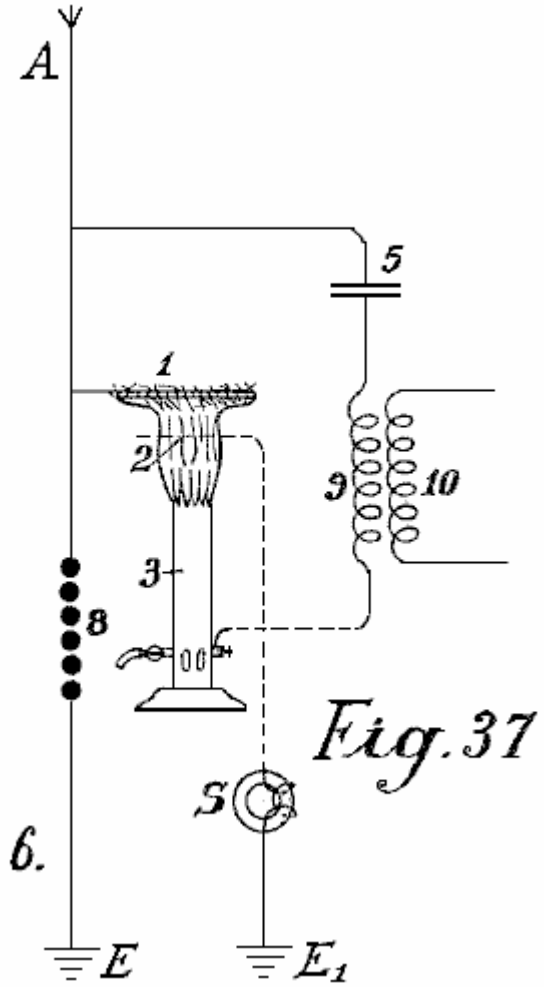

Fig.37

The positive pole **1** of the radiating collectors is always directly connected to the aerial collecting conductor **A**. In **Fig.34**, this is further connected over the capacitor set **5** with a second positive electrode **3**. The direct current dynamo **b** produces current which flows over between the electrodes **3** and **2** as an arc light. On the formation of an arc, the negative incandescent electrode **2** absorbs electricity from the positive poles standing opposite it and highly charged with atmospheric electricity which it conveys to the working circuit. The spark gap 7, inductive resistance **9** and induction coil **10** are like the ones previously described. The protective electromagnet **S** protects the installation from earth circuiting and the safety spark gap **8** from excess voltage or overcharging.

In **Fig.35**, the connection is so far altered that the alternating current dynamo feeds the excitation coil **11** of the induction capacitor. **12** is its negative and **13** its positive pole. If the coil **3** on the magnet core of the dynamo is correctly calculated and the frequency of the alternating current sufficiently high, then an arc light can be formed between poles **1** and **2**. As the cathode **2** is connected to the negatively charged earth, and therefore always acts as a negative pole, a form of rectification of the alternating current produced by the dynamo **3** is obtained, since the second half of the period is always suppressed. The working circuit may be carried out in the same way as in **Fig.34**; the working spark gap **7** may however be dispensed with, and instead of it, between the points **n** and **m**, a capacitor **5** and an induction resistance **9** may be inserted, from which, a current is taken inductively.

Fig.36 represents a form of construction similar to that shown in **Fig.34** except that here instead of an arc lamp, a Nernst incandescent body is used. The Nernst lamp is fed through the battery **3**. The working section is connected with the negative pole, the safety spark gap with the positive poles. The working spark gap **7** may also be dispensed with and the current for it taken at **12** over the oscillation circuit **5, 11** (shown in dotted lines).

Flame collectors (**Fig.37**) may also be employed according to this invention. The wire network **1** is connected with the aerial collector conductor **A** and the burner with the earth. At the upper end of the burner, long points are provided which project into the flame. The positive electrode is connected with the negative over a capacitor **5** and the induction coil **9** with the earth.

The novelty in this invention is:

(1) The use of incandescent cathodes opposite positive poles which are connected to large metallic capacities as automatic collecting surfaces.
(2) The connection of the incandescent cathodes to the earth whereby, in addition to the electricity conveyed to them from the battery of machine which causes the incandescing, also the negative charge of the earth potential is conveyed, and
(3) The connection of the positive and negative poles of the radiating collectors over a capacitor circuit alone or with the introduction of a suitable inductive resistance, whereby simultaneously an oscillatory oscillation circuit may be obtained. The collecting effect is by these methods quite considerably increased.

ROY MEYERS

Patent GB1913,01098 14th January 1914 Inventor: Roy J. Meyers

APPARATUS FOR PRODUCING ELECTRICITY

ABSTRACT

A rectifier for use with apparatus for producing electricity from the earth consists of mercury- vapour lamps constructed and arranged as shown in **Fig.4**. Each lamp comprises two wires **6<1>, 7<1>** wound around a steel tube **15** surrounding a mercury tube **11** preferably of copper. The coil **6<1>** is connected between the electrode **14** and the terminal **18**, and the coil **7<1>** between the terminals **19, 5**. The coils **6<1>, 7<1>** are preferably composed of soft iron.

DESCRIPTION

This invention relates to improvements in apparatus for the production of electrical currents, and the primary object in view is the production of a commercially serviceable electrical current without the employment of mechanical or chemical action. To this end the invention comprises means for producing what I believe to be dynamic electricity from the earth and its ambient elements.

I am, of course aware that it has been proposed to obtain static charges from upper strata of the atmosphere, but such charges are recognised as of widely variant potential and have thus far proved of no practical commercial value, and the present invention is distinguished from all such apparatus as has heretofore been employed for attracting static charges by the fact that this improved apparatus is not designed or employed to produce or generate irregular, fluctuating or other electrical charges which lack constancy, but on the other hand I have by actual test been able to produce from a very small apparatus at comparatively low elevation, say about 50 or 60 feet above the earth's surface, a substantially constant current at a commercially usable voltage and amperage.

This current I ascertained by repeated tests is capable of being readily increased by additions of the unit elements in the apparatus described below, and I am convinced from the constancy of the current obtained and its comparatively low potential that the current is dynamic and not static, although, of course, it is not impossible that certain static discharges occur and, in fact, I have found occasion to provide against the damage which might result from such discharge by the provision of lightning arresters and cut-out apparatus which assist in rendering the obtained current stable by eliminating sudden fluctuations which sometimes occur during conditions of high humidity from what I consider static discharges.

The nature of my invention is obviously such that I have been unable to establish authoritatively all of the principles involved, and some of the theories herein expressed may possibly prove erroneous, but I do know and am able to demonstrate that the apparatus which I have discovered does produce, generate, or otherwise acquire a difference of potential representing a current amperage as stated above.

The invention comprises the means for producing electrical currents of serviceable potential substantially without the employment of mechanical or chemical action, and in this connection I have been able to observe no chemical action whatever on the parts utilised although deterioration may possibly occur in some of the parts, but so far as I am able to determine such deterioration does not add to the current supply but is merely incidental to the effect of climatic action.

The invention more specifically comprises the employment of a magnet or magnets and a co-operating element, such as zinc positioned adjacent to the magnet or magnets and connected in such manner and arranged relative to the earth so as to produce current, my observation being that current is produced only when such magnets have their poles facing substantially to the north and south and the zincs are disposed substantially along the magnets.

The invention also comprehends other details of construction, combinations and arrangements of parts as will be fully set forth.

DESCRIPTION OF THE DRAWINGS

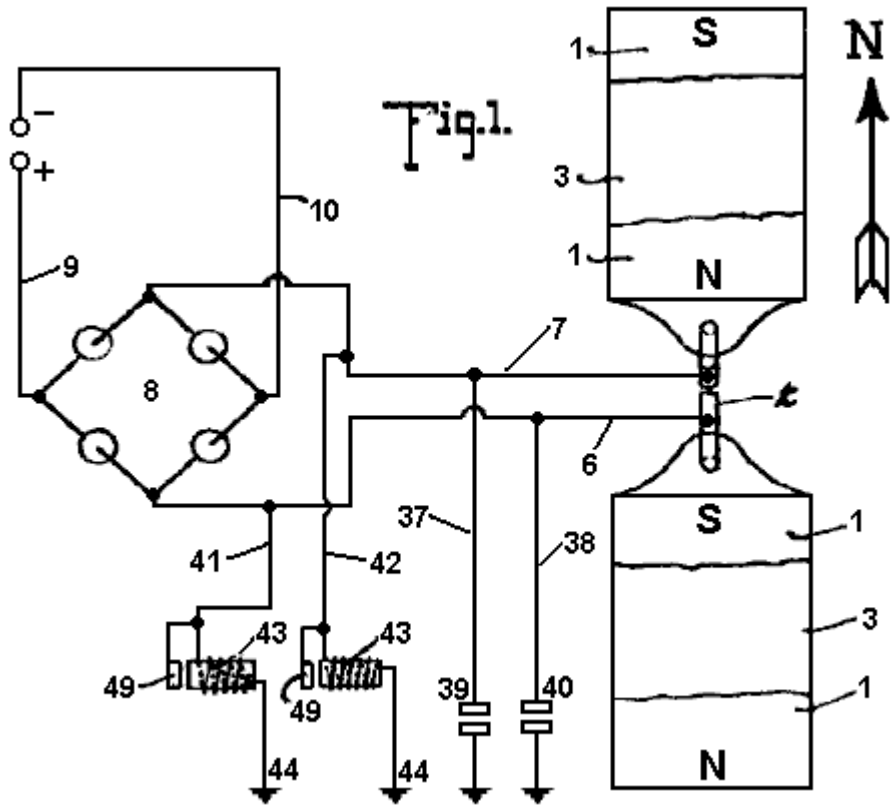

Fig.1 is a plan view of an apparatus embodying the features of the present invention, the arrow accompanying the figure indicating substantially the geographical north, parts of this figure are diagrammatic.

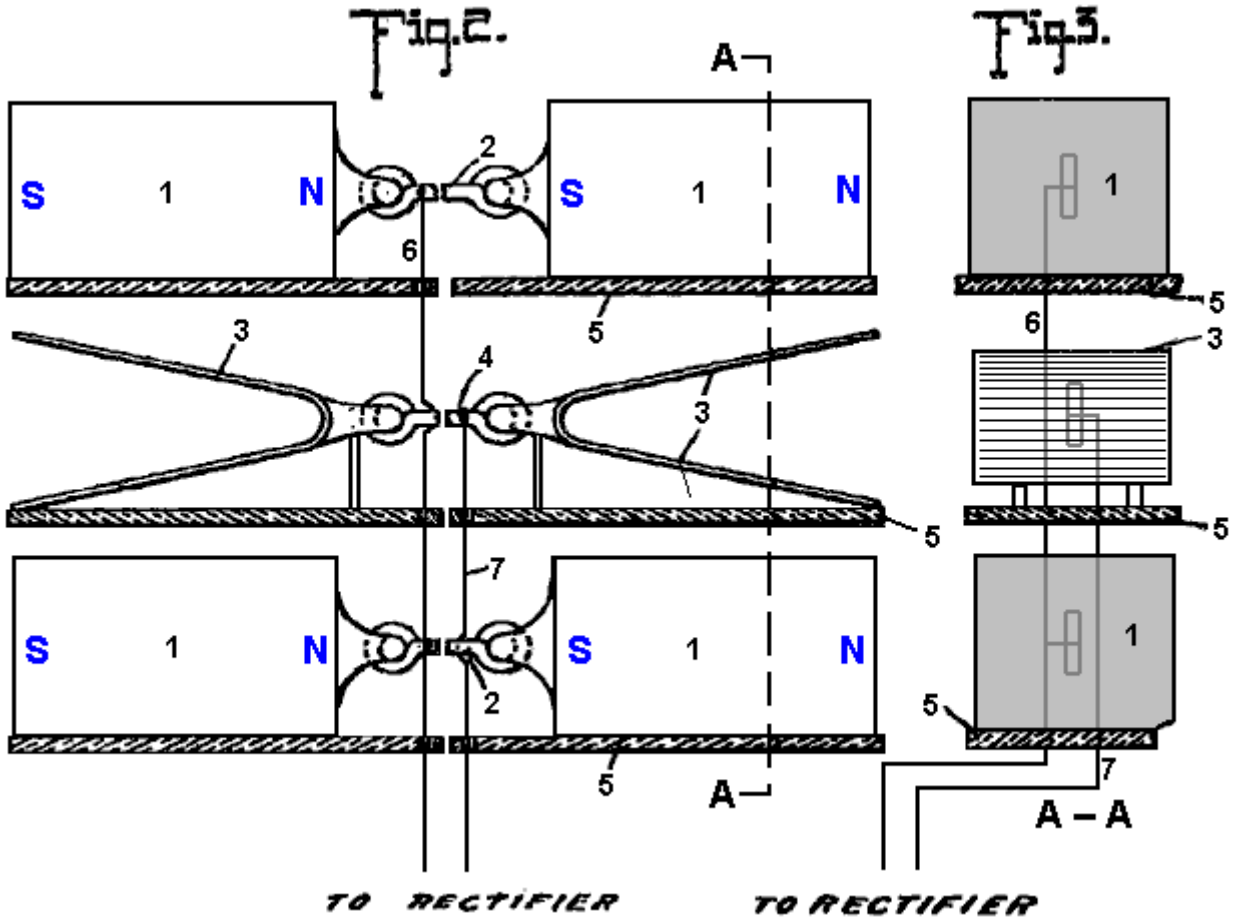

Fig.2 is a view is side elevation of the parts seen in plan in **Fig.1**
Fig.3 is a vertical section taken on the plane indicated by the line **A--A** of **Fig.2**.

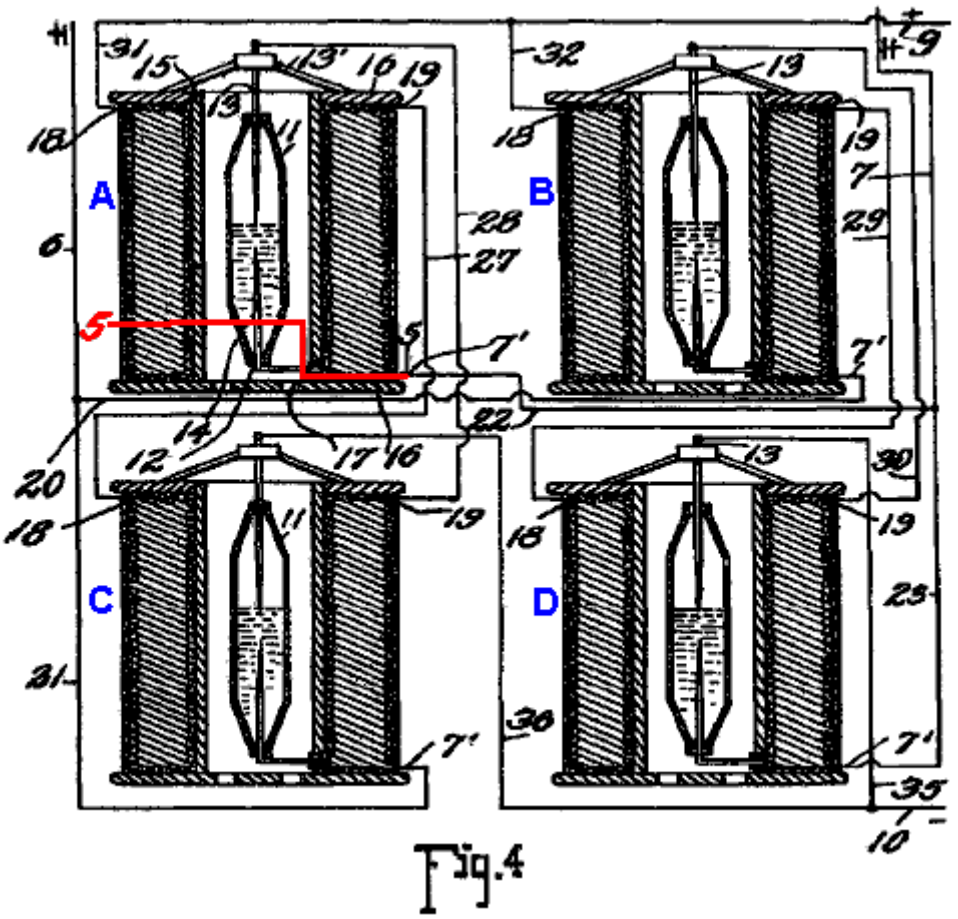

Fig.4

Fig.4 is a detail view, partly in elevation and partly in section, showing the connections of the converter and intensifier.

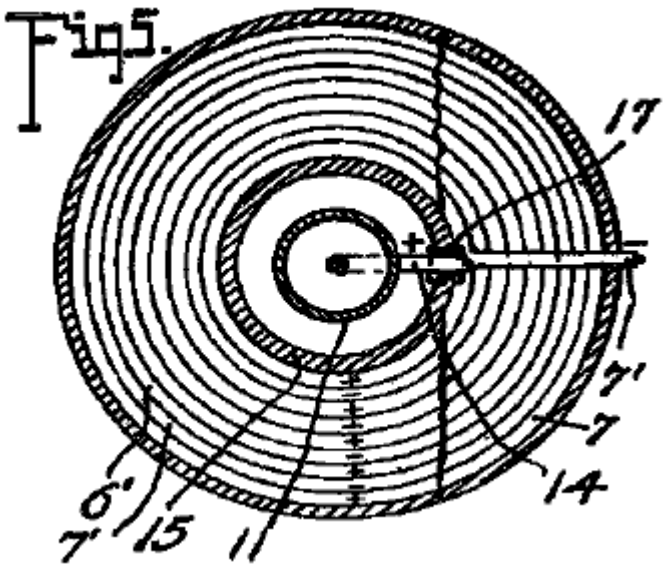

Fig.5.

Fig.5 is a transverse section taken on the planes indicated by line **5-5** of **Fig.4**, looking downwards.

Fig.6

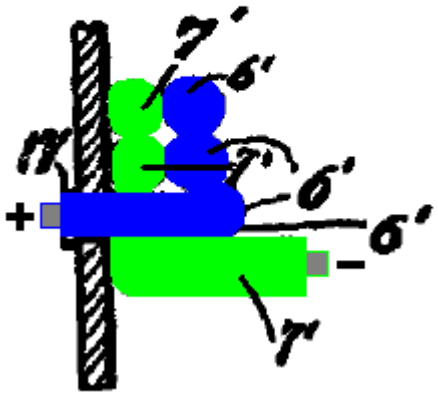

Fig.6 is an enlarged detail fragmentary section illustrating the parts at the junction of the conductors and one of the intensifiers.

Fig.7.

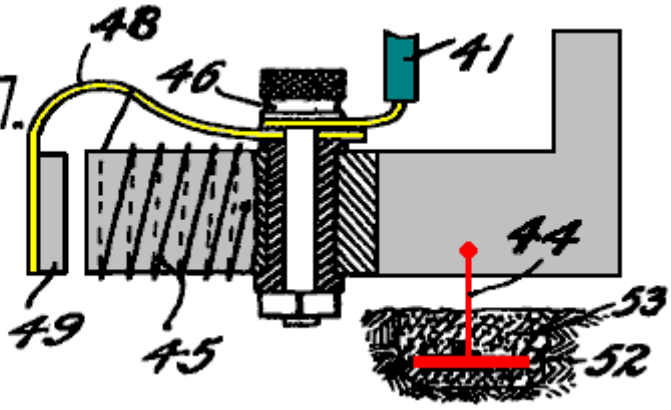

Fig.7 is an enlarged detail view partly in elevation and partly in section of one of the automatic cut-outs

Fig.8

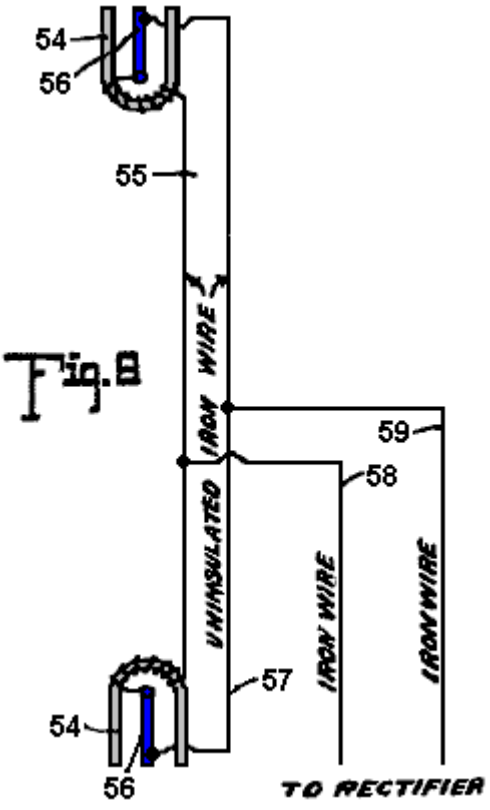

Fig.8 is a diagrammatic view of one of the simplest forms of embodiment of the invention.

Referring to the drawing by numerals, **1,1** indicates magnets connected by a magnetic substance **2**, preferably an iron wire. The magnets **1** are arranged in pairs, one pair being spaced beneath the other, and interposed between the magnets are zinc plates **3,3** connected by an iron wire conductor **4**. Suitable insulating supports **5** are arranged for sustaining the respective magnets **1** and plates **3,3**. Each plate **3** is preferably bent substantially into V form, as clearly seen in **Fig.1**, and the V of one of the plates opens or faces toward the North and the V of the other plate to the South. I have determined by experimentation that it is essential that the plates **3** be disposed substantially North and South with their flat faces approximately parallel to the adjacent faces of the co-operating magnets, although by experience I have not discovered any material difference in the current obtained when the plates are disposed slightly to one side of North and South, as for instance when the plates are disposed slightly to one side of North and South, as for instance when disposed in the line of the magnetic polarity of the earth. The same is true with respect to the magnets **1**, the said magnets being disposed substantially North and South for operative purposes, although I find that it is immaterial whether the North pole of one of the magnets is disposed to the North and the South pole to the South, or vice versa, and it is my conviction from experience that it is essential to have the magnets of each pair connected by magnetic material so that the magnets substantially become one with a pole exposed to the North and a pole exposed to the South.

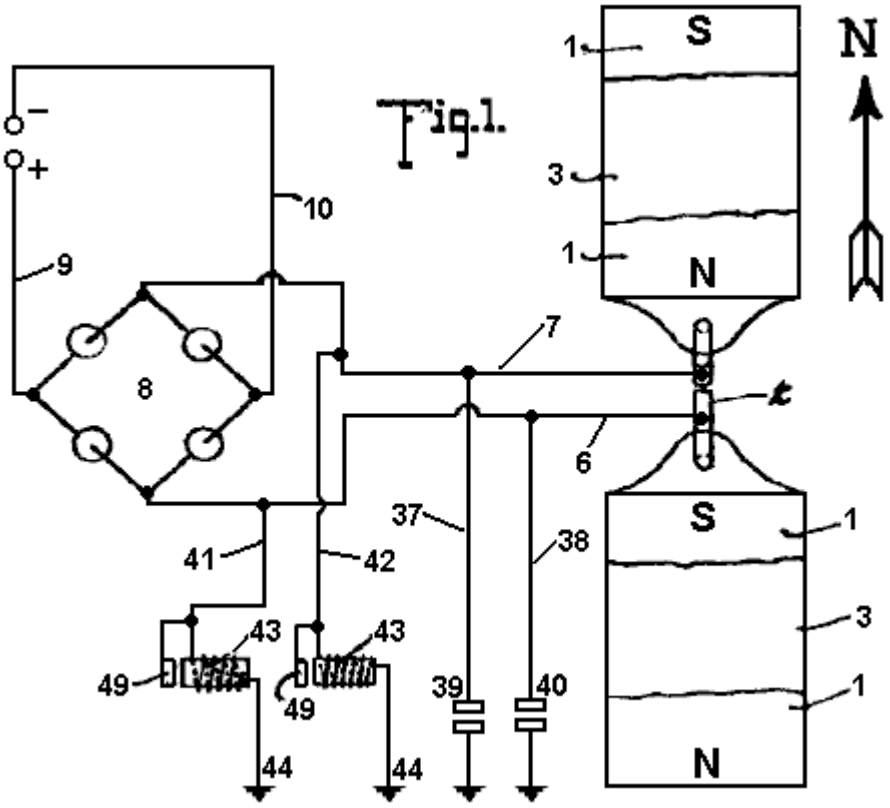

In **Fig.1**, I have indicated in full lines by the letters **8** and **N** the respective polarities of the magnets **1**, and have indicated in dotted lines the other pole of those magnets when the connection **2** is severed. I have found that the magnets and zinc plates operate to produce, (whether by collection or generation I am not certain), electrical currents when disposed substantially North and South, but when disposed substantially East and West, no such currents are produced. I also find that the question of elevation is by no means vital, but it is true that more efficient results are obtained by placing the zincs and magnets on elevated supports. I furthermore find from tests, that it is possible to obtain currents from the apparatus with the zincs and magnets disposed in a building or otherwise enclosed, although more efficient results are obtained by having them located in the open.

While in **Figures 1, 2,** and **3**, I have shown the magnets and the zinc plates as superimposed, it will be apparent, as described in detail below, that these elements may be repositioned in horizontal planes, and substantially the same results will be secured. Furthermore, the magnets **1** with the interposed zincs **3**, as shown in **Figures 1, 2** and **3** merely represent a unit which may be repeated either horizontally or vertically for increasing the current supply, and when the unit is repeated the zinc plates are arranged alternating with the magnets throughout the entire series as indicated below.

A conductor **6** is connected in multiple with the conductors **2** and a conductor **7** is connected with conductor **4**, the conductor **6** extending to one terminal of a rectifier which I have indicated by the general reference character **8**, and the conductor **7** extending to the other terminal of the rectifier. The rectifier as seen in the diagram **Fig.1** may

assume any of several well known embodiments of the electrical valve type and may consist of four asymmetric cells or Cooper-Hewitt mercury vapour lamps connected as indicated in **Fig.1** for permitting communication of the positive impulses from the conductor **6** only to the line conductor **9** and the negative impulses from conductor **6** on only to the line conductor **10**. The current from this rectifier may be delivered through the conductors **9** and **10** to any suitable source for consumption.

While the said rectifier **8** may consist of any of the known types, as above outlined, it preferably consists of a specially constructed rectifier which also has the capacity of intensifying the current and comprises specifically the elements shown in detail in **Figures 4, 5,** and **6** wherein I have disclosed the detail wiring of the rectifier when composed of four of the rectifying and intensify in elements instead of asymmetric cells or simple mercury vapour valves. As each of these structures is an exact embodiment of all the others, one only will be described, and the description will apply to all. The rectifying element of each construction consists of a mercury tube **11** which is preferably formed of glass or other suitable material, and comprises a cylinder having its end portions tapered and each terminating in an insulating plug or stopper **12**. Through the upper stopper **12** is extended the electrode **13** which extends well into the tube and preferably about one-half its length, to a point adjacent the inner end of an opposing electrode **14** which latter electrode extends from there down through the insulation **12** at the lower end of the tube. The tube **11** is supplied with mercury and is adapted to operate on the principle of the mercury vapour lamp, serving to rectify current by checking back impulses of one sign and permitting passage of impulses of the other.

To avoid the necessity for utilising a starter, as is common with the lamp type of electrical valve, the supply of mercury within the tube may be sufficient to contact with the lower end of the electrode **13** when current is not being supplied, so that as soon as current is passed from one electrode to the other sufficiently for volatilising that portion of the mercury immediately adjacent the lower end of electrode **13**, the structure begins its operation as a rectifier. The tube **11** is surrounded by a tube **15** which is preferably spaced from tube **11** sufficiently for allowing atmospheric or other cooling circulation to pass the tube **11**. In some instances, it may be desirable to cool the tube **11** by a surrounding body of liquid, as mentioned below. The tube **15** may be of insulating material but I find efficient results attained by the employment of a steel tube, and fixed to the ends of the of the tube are insulating disks **16**, **16** forming a spool on which are wound twin wires **6'** and **7'**, the wire **6'** being connected at the inner helix of the coil with the outer end of the electrode **14**, the lower portion of said electrode being extended to one side of the tube **11** and passed through an insulating sleeve **17** extending through the tube **15**, and at its outer end merging into the adjacent end of the wire **6'**. The wire **7'** extends directly from the outer portion of the spool through the several helices to a point adjacent to the junction of the electrode **14** with wire **6'** and thence continues parallel to the wire throughout the coil, the wire **6'** ending in a terminal **18** and the wire **7'** ending in a terminal **19**.

For the sake of convenience of description and of tracing the circuits, each of the apparatus just above described and herein known as an intensifier and rectifier will be mentioned as **A**, **B**, **C** and **D**, respectively. Conductor **6** is formed with branches **20** and **21** and conductor **7** is formed with similar branches **22** and **23**. Branch **20** from conductor **6** connects with conductor **7'** of intensifier **B** and branch **21** of conductor **6** connects with the conductor **7'** of intensifier **C**, while branch **22** of conductor **7** of intensifier **C**, while branch **22** of conductor **7** connects with conductor **7'** of intensifier **D**. A conductor **27** is connected to terminal **19** of intensifier **A** and extends to and is connected with the terminal **18** of intensifier **C**, and a conductor **7** connects with conductor **7'** of intensifier **D**. A conductor **27** is connected to terminal **19** of intensifier **A**, and extends to and is connected to terminal **18** of intensifier **C**, and a conductor **28** is connected to the terminal **19** of intensifier **C** and extends from the terminal **19** of intensifier **B** to the terminal **18** of intensifier **D** to electrode **13** of intensifier **B**. Each electrode **13** is supported on a spider **13'** resting on the upper disk **16** of the respective intensifier. Conductors **31** and **32** are connected to the terminals **18** of intensifiers **A** and **B** and are united to form the positive line wire **9** which co-operates with the negative line wire **10** and extends to any suitable point of consumption. The line wire **10** is provided with branches **35** and **36** extending to the electrodes **13** of intensifiers **C** and **D** to complete the negative side of the circuit.

Thus it will be seen that alternating currents produced in the wires **6** and **7** will be rectified and delivered in the form of a direct current through the line wires **9** and **10**, and I find by experiment that the wires **6** and **7** should be of iron, preferably soft, and may of course be insulated, the other wiring not specified as iron being of copper or other suitable material.

In carrying out the operation as stated, the circuits may be traced as follows: A positive impulse starting at the zincs **3** is directed along conductor **7** to branch **23** to conductor **7'** and the winding of the rectifier of intensifier **B** through the rectifier to the conductor **6'**, through its winding to the contact **18**, conductor **32** and to the line wire **9**. The next, or negative, impulse directed along conductor **7** cannot find its way along branch **23** and the circuit just above traced because it cannot pass across the rectifier of intensifier **B** but instead the negative impulse passes along conductor **22** to conductor **7** of intensifier **A** and its winding to the contact **19** and to conductor **27** to contact **18** of intensifier **C**, to the winding of the wire **6'** thereof to the electrode **14** through the rectifier to the of the

electrode **13** and conductor of intensifier **A**, electrode **14** thereof and conductor **6'** to contact **18** and wire **31** to line wire **9**.

Obviously the positive impulse cannot pass along the wire **20** because of its inverse approach to the rectifier of intensifier **B**. The next impulse or negative impulse delivered to conductor **6** cannot pass along conductor **21** because of its connection with electrode **13** of the rectifier of intensifier **A**, but instead passes along conductor **20** to the wire **7'** and its winding forming part of intensifier **B** to the contact **19** and conductor **29** to contact **18** and the winding of wire **6'** of intensifier **D** to the electrode **14** and through the rectifier to the electrode **13** and conductor **35** to line wire **10**. Thus the current is rectified and all positive impulses directed along one line and all negative impulses along the other lie s that the potential difference between the two lines will be maximum for the given current of the alternating circuit. It is, of course, apparent that a less number of intensifiers with their accompanying rectifier elements may be employed with a sacrifice of the impulses which are checked back from a lack of ability to pass the respective rectifier elements, and in fact I have secured efficient results by the use of a single intensifier with its rectifier elements, as shown below.

Grounding conductors **37** and **38** are connected respectively with the conductors **6** and **7** and are provided with the ordinary lightning arresters **39** and **40** respectively for protecting the circuit against high tension static charges.

Conductors **41** and **42** are connected respectively with the conductors **6** and **7** and each connects with an automatic cut-out **43** which is grounded as at **4**. Each of the automatic cut-outs is exactly like the other and one of the these is shown in detail in **Fig.7** and comprises the inductive resistance **45** provided with an insulated binding post **46** with which the respective conductor **6** or **7** is connected, the post also supporting a spring **48** which sustains an armature **49** adjacent to the core of the resistance **45**. The helix of resistance **45** is connected preferably through the spring to the binding post at one end and at the other end is grounded on the core of the resistance, the core being grounded by ground conductor **44** which extends to the metallic plate **52** embedded in moist carbon or other inductive material buried in the earth. Each of the conductors **41**, **42** and **44** is of iron, and in this connection I wish it understood that where I state the specific substance I am able to verify the accuracy of the statement by the results of tests which I have made, but of course I wish to include along with such substances all equivalents, as for instance, where iron is mentioned its by-products, such as steel, and its equivalents such as nickel and other magnetic substances are intended to be understood.

The cut-out apparatus seen in detail in **Fig.7** is employed particularly for insuring against high voltage currents, it being obvious from the structure shown that when potential rises beyond the limit established by the tension of the spring sustaining the armature **40**, the armature will be moved to a position contacting with the core of the cut-out device and thereby directly close the ground connection for line wire **41** with conductor **44**, eliminating the resistance of winding **45** and allowing the high voltage current to be discharged to the ground. Immediately upon such discharge the winding **45** losing its current will allow the core to become demagnetised and release the armature **49** whereby the ground connection is substantially broken leaving only the connection through the winding **45** the resistance of which is sufficient for insuring against loss of low voltage current.

In **Fig.8** I have illustrated an apparatus which though apparently primitive in construction and arrangement shows the first successful embodiment which I produced in the course of discovery of the present invention, and it will be observed that the essential features of the invention are shown there. The structure shown in the figure consists of horseshoe magnets **54**, **55**, one facing North and the other South, that is, each opening in the respective directions indicated and the two being connected by an iron wire **55** which is uninsulated and wrapped about the respective magnets each end portion of the wire **55** being extended from the respective magnets to and connected with, as by being soldered to, a zinc plate **56**, there being a plate **56** for each magnet and each plate being arranged longitudinally substantially parallel with the legs of the magnet and with the faces of the plate exposed toward the respective legs of the magnet, the plate being thus arranged endwise toward the North and South. An iron wire **57** connects the plates **56**, the ends of the wire being preferably connected adjacent the outer ends of the plates but from experiment I find that the wire may be connected at practically any point to the plate. Wires **58** and **59** are connected respectively with the wires **55** and **57** and supply an alternating current at a comparatively low voltage, and to control such current the wires **58** and **59** may be extended to a rectifier or combined rectifier and intensifier, as discussed above.

The tests which I have found successful with the apparatus seen in **Fig.8** were carried out by the employment first of horseshoe magnets approximately 4 inches in length, the bar comprising the horseshoe being about one inch square, the zincs being dimensioned proportionately and from this apparatus with the employment of a single intensifier and rectifier, as above stated, I was able to obtain a constant output of 8 volts.

It should be obvious that the magnets forming one of the electrodes of this apparatus may be permanent or may be electromagnets, or a combination of the two.

While the magnets mentioned throughout the above may be formed of any magnetic substance, I find the best results obtained by the employment of the nickel chrome steel.

While the successful operation of the various devices which I have constructed embodying the present invention have not enabled me to arrive definitely and positively at fixed conclusion relative to the principles and theories of operation and the source from which current is supplied, I wish it to be understood that I consider myself as the first inventor of the general type described above, capable of producing commercially serviceable electricity, for which reason my claims hereinafter appended contemplate that I may utilise a wide range of equivalents so far as concerns details of construction suggested as preferably employed.

The current which I am able to obtain is dynamic in the sense that it is not static and its production is accomplished without chemical or mechanical action either incident to the actual chemical or mechanical motion or incident to changing caloric conditions so that the elimination of necessity for the use of chemical or mechanical action is to be considered as including the elimination of the necessity for the use of heat or varying degrees thereof.

PAULO and ALEXANDRA CORREA

Pat. Application US 2006/0082,334 20th April 2006 Inventors: Paulo & Alexandra Correa

ENERGY CONVERSION SYSTEMS

This patent application shows the details of devices which can produce ordinary electricity from Tesla longitudinal waves. If these claims are correct (and there does not appear to be the slightest reason for believing that they are not), then implementations of this patent application are capable of producing free electrical power and the importance of this information is enormous.

ABSTRACT

This invention relates to apparatus for the conversion of mass-free energy into electrical or kinetic energy, which uses in its preferred form a transmitter and a receiver both incorporating Tesla coils, the distal ends of whose secondary windings are co-resonant and connected to plates of a chamber, preferably evacuated or filled with water, such that energy radiated by the transmitter may be picked up by the receiver, the receiver preferably further including a pulsed plasma reactor driven by the receiver coil and a split phase motor driven by the reactor. Preferably the reactor operates in pulsed abnormal gas discharge mode, and the motor is an inertially dampened drag motor. The invention also extends to apparatus in which an otherwise driven plasma reactor operating in pulsed abnormal gas discharge mode in turn used to drive an inertially dampened drag motor.

DESCRIPTION

This is a continuation of application Ser. No. 09/907,823, filed Jul. 19, 2001.

FIELD OF THE INVENTION

This invention relates to systems for the conversion of energy, inter alia in the form of what we will refer to for convenience as Tesla waves (see below), to conventional electrical energy.

BACKGROUND OF THE INVENTION

Energy converters that are fed by local or environmental energy are usually explained by taking recourse to the notion that they convert zero point electromagnetic radiation (ZPE) to electric energy. The ZPE theories have gained a life of their own, as T. Kuhn has pointed out (in his "Black Body Theory and the Quantum"), after emerging from Planck's second theory, specifically from the term ½ hυ in the new formula for oscillator energy. In 1913, Einstein and Stern suggested that motional frequencies contributing to specific heat fell into two categories--those that were independent of temperature and those that were not (e.g. rotational energy), leading them to conclude that zero-point energy on the order of ½ hυ was most likely. In the second part of their paper, however, they provided a derivation of Planck's Law without taking recourse to discontinuity, by assuming that the value of the ZPE was simply ha. It is worth noting that Einstein had already in 1905 ("Erzeugung und Verwandlung des Lichtes betreffenden heuristichen Gesichtspunkt",Ann. d. Phys, 17, 132) framed the problem of discontinuity, even if only heuristically, as one of placing limits upon the infinite energy of the vacuum state raised by the Rayleigh-Jeans dispersion law. According to Einstein, the Rayleigh-Jeans law would result in an impossibility, the existence of infinite energy in the radiation field, and this was precisely incompatible with Planck's discovery - which suggested instead, that at high frequencies the entropy of waves was replaced by the entropy of particles. Einstein, therefore, could only hope for a stochastic validation of Maxwell's equations at high frequencies "by supposing that electromagnetic theory yields correct time-average values of field quantities", and went on to assert that the vibration-energy of high frequency resonators is exclusively discontinuous (integral multiples of hυ).

Since then, ZPE theories have gone on a course independent from Planck's second theory. The more recent root of modern ZPE theories stems from the work of H. Casimir who, in 1948, apparently showed the existence of a force acting between two uncharged parallel plates. Fundamentally the Casimir effect is predicated upon the existence of a background field of energy permeating even the “vacuum”, which exerts a radiation pressure, homogeneously and from all directions in space, on every body bathed in it. Given two bodies or particles in proximity, they shield one another from this background radiation spectrum along the axis (i.e. the shortest distance) of their coupling, such that the radiation pressure on the facing surfaces of the two objects would be less than the radiation pressure experienced by all other surfaces and coming from all other directions in space. Under these conditions, the two objects are effectively pushed towards one another as if by an attractive force. As the distance separating the two objects diminishes, the force pushing them together increases until they collapse one on to the other. In this sense, the Casimir effect would be the macroscopic analogy of the microscopic van der Waals forces of attraction responsible for such dipole-dipole interactions as hydrogen bonding. However, it is worth noting that the van der Waals force is said to tend to establish its normal radius, or

the optimal distance between dipoles, as the distance where the greatest attractive force is exerted, beyond which the van der Waals forces of nuclear and electronic repulsion overtake the attraction force.

Subsequently, another Dutch physicist, M. Sparnaay, demonstrated that the Casimir force did not arise from thermal radiation and, in 1958, went on to attribute this force to the differential of radiation pressure between the ZPE radiation from the vacuum state surrounding the plates and the ZPE radiation present in the space between them. Sparnaay's proposal is that a classical, non-quantal, isotropic and ubiquitous electromagnetic zero-point energy exists in the vacuum, and even at a temperature of absolute zero. It is further assumed that since the ZPE radiation is invariant with respect to the Lorentz transformations, it obeys the rule that the intensity of its radiation is proportional to the cube of the frequency, resulting in an infinite energy density for its radiation spectrum.

What appeared to be the virtue of this reformulated theory was the notion that the vacuum no longer figured as pure space empty of energy, but rather as a space exposed to constantly fluctuating “fields of electromagnetic energy”.

Puthoff has utilised the isomorphism between van der Waals and Casimir forces to put forth the zero-point (ZP) energy theory of gravity, based on the interpretation that the virtual electromagnetic ZP field spectrum predicted by quantum electrodynamics (QED) is functionally equivalent to an actual vacuum state defined as a background of classical or Maxwellian electromagnetic radiation of random phases, and thus can be treated by stochastic electrodynamics (SED). Whereas in QED, the quanta are taken as virtual entities and the infinite energy of the vacuum has no physical reality, for SED, the ZPE spectrum results from the distortion of a real physical field and does not require particle creation. Gravity then, could be seen as only the macroscopic manifestation of the Casimir force.

We do not dispute the fact that even in space-absent matter, there is radiant energy present which is not of a thermal nature. But we claim that this energy is not electromagnetic, nor is its energy spectrum-infinite. That this is so, stems not just from our opinion that it is high time that Einstein's heuristic hypothesis should be taken as literally factual - in the dual sense that all electromagnetic energy is photon energy and all photons are local productions, but above all from the fact that it is apparent, from the experiments of Wang and his colleagues (Wang, Li, Kuzmich, A & Dogariu, A. "Gain-assisted superluminal light propagation", Nature 406; #6793; 277), that the photon stimulus can propagate at supraluminal speeds and lies therefore well outside of any scope of electromagnetic theory, be this Maxwell's classical approach taken up by ZPE theories, or Einstein's special relativistic phenomenology of Maxwell's theory. The fact is, that if the light stimulus can propagate at speeds greater than those of light, then what propagates is not light at all, and thus not energy configured electromagnetically. Light is solely a local production of photons in response to the propagation of a stimulus that itself is not electromagnetic.

It is critical to understand that the implication from this, that - aside from local electromagnetic radiation and from thermal radiation associated with the motions of molecules (thermo-mechanical energy), there is at least one other form of energy radiation which is everywhere present, even in space-absent matter. Undoubtedly, it is that energy which prevents any attainment of absolute zero, for any possible local outpumping of heat is matched by an immediate local conversion of some of this energy into a minimum thermal radiation required by the manifolds of Space and Time. Undoubtedly also, this radiation is ubiquitous and not subject to relativistic transformations (i.e. it is Lorentz invariant). What it is not, is electromagnetic radiation consisting of randomistic phases of transverse waves.

To understand this properly, one must summarise the differences from existing ZPE theories - and all these differences come down to the fact that this energy, which is neither electromagnetic nor thermal per se, (and is certainly not merely thermo-mechanical), has nevertheless identifiable characteristics both distributed across sub-types or variants and also common to all of them.

Essentially, the first sub-type or variant consists of longitudinal mass-free waves which deploy electric energy. They could well be called Tesla waves, since Tesla-type transformers can indeed be shown experimentally to radiate mass-free electric energy, in the form of longitudinal magnetic and electric waves having properties not reducible to photon energy nor to “electromagnetic waves”, and having speeds of displacement which can be much greater than the limit c for all strictly electromagnetic interactions.

One may well denote the second sub-type by the designation of mass-free thermal radiation, since it contributes to temperature changes - and, as obviously indicated by the impossibility of reaching an absolute zero of temperature, this contribution occurs independently of the presence of matter, or mass-energy, in Space. In other words, not all thermal radiation can be reduced to vibration, rotation and translation (drift motion) of molecules, i.e. to thermomechanical energy, because the properties of pressure and volume which determine temperature and affect matter, appear indeed to a great extent to be independent from matter, a fact which itself is responsible for the observed catastrophic and unexpected phase changes of matter and has required to this day the insufficient explanation offered semi-empirically by the Van der Waals Force Law.

Finally, the third sub-type may be designated latent mass-free energy radiation - since it deploys neither charge, nor thermal or baroscopic effects, and yet it is responsible for "true latent heat" or for the "intrinsic potential energy" of a molecule. It is also responsible for the kineto-regenerative phenomenon whereby an electroscope performs a variable charge-mediated work against the local gravitational field.

The common characteristic of all three sub-types of mass-free energy radiation is that they share the same non-classical fine structure, written as follows for any energy unit, where **c** is any speed of light wave function, and the wavelength λ and wave function W are interconnected as a function of the physical quality of the energy field under consideration: $E=\lambda cW$

In the instance of longitudinal electric radiation, this takes on the directly quantifiable form:

$$E=(\lambda_q c)W_v=p_e W_v=(h/\lambda_x)W_v=\int=qV$$

where:

W_V is the voltage-equivalent wave function corresponding to V,

P_e constitutes the linear momentum corresponding to the conventional q or e,

h is the Planck constant,

λ_x is the Duane-Hunt constant expressed as a wavelength,

λ_q is a wavelength constant; and the sign

$=\int=$ signifies exact equality between an expression in the conventional dimensions of length, mass and time, and an expression in length and time dimensions alone.

In the instance of mass-free thermal radiation (contributing to temperature changes), the transformation obeys Boltzmann's rule (**k** is now Boltzmann's constant and T is Kelvin-scale temperature):

$$E=\lambda_{n1}cW_{n1}=\lambda_{n1}(\pi_V\zeta_p)(\lambda_{n1})\sim=kT$$

and in the third instance - of latent mass-free radiation, the transformation obeys the rule:

$$E=\lambda_{n1}cW_{n1} = \lambda_{n1}(\lambda_{n1}\zeta_{n1})(\lambda_{n1}f_{n1}) = \lambda_{n1}{}^3\zeta_{n1}f_{n1}$$

where ζ and f are frequency functions, f being a specific gravitational frequency term, and f_{n1} being defined as equal to $(\lambda_{n1})^{-0.5}\text{meter}^{0.5}\text{sec}^{-1}$ and ζ_{n1} has the value of c/λ_{n1}

If the electric variant of mass-free radiation has a direct quantum equivalence, via the Duane-Hunt Law, none of the three primary aether energy variants possess either the classic form of electromagnetic energy which requires square superimposition of speed of light wave functions **c**, as $\mathbf{c^2}$, or the quantum form of energy, requiring $E = hu$. The critical first step in the right direction may well be attributed to Dr. W. Reich, as it regards the fact that mass-free energy couples two unequal wave functions, only one of which is electromagnetic and abides by the limit **c**. We then unravelled the threefold structure described above, and further showed that, in the case of longitudinal electric waves, the postulated equivalence $(q=\lambda_q c)$ is merely phenomenological, as these waves are not restricted by the function **c** in their conveying of electric charge across space. It can further be demonstrated that all black-body photons are bound by an upper frequency limit (64×10^{14} Hz), above which only ionising photons are produced, and that all black-body photons arise precisely from the interaction of mass-free electric radiation with molecules of matter (including light leptons), whereby the energy of that radiation is locally converted into photon or electromagnetic radiation. In other words, all non-ionising electromagnetic energy appears to be secondary energy which results locally from the interaction of matter with mass-free electric energy. It cannot therefore consist of the primary energy that is present in the vacuum, an energy that is neither virtual nor electromagnetic, but actual and concrete in its electric, thermal and antigravitic manifestations. Lastly, gravitational energy, being either the potential or the kinetic energy responsible for the force of attraction between units of matter, is a manifestation that also requires, much as electromagnetic radiation does, coupling of mass-free energy to matter or to mass-energy.

The Tesla coil is a generator of a mass-free electric energy flux which it transmits both by conduction through the atmosphere and by conduction through the ground. Tesla thought it did just that, but it has been since regarded instead (because of Maxwell, Hertz and Marconi) as a transmitter of electromagnetic energy. The transmitter operates by a consumption of mass-bound electric power in the primary, and by induction it generates in the

coupled secondary two electric fluxes, one mass-bound in the coil conductor, and the other mass-free in the body of the solenoid. Tesla also proposed and demonstrated a receiver for the mass-free energy flux in the form of a second Tesla coil resonant with the first. The receiver coil must be identical and tuned to the transmitter coil; the capacitance of the antenna plate must match that of the transmitter plate; both transmitter and receiver coils must be grounded; and the receiver coil input and output must be unipolar, as if the coil were wired in series.

The generators of mass-free energy with which we are concerned, provide current pulses associated with a dampened wave (DW) oscillation of much higher frequency than the pulse repetition frequency. A particular problem in recovering the mass-free energy content of such pulses is provided by the dampened wave oscillations. Although in our U.S. Pat. No. 5,416,391 we describe arrangements incorporating split phase motors to recover such energy, their efficiency is a great deal less than what should theoretically be attainable. Other workers such as Tesla and Reich, have encountered the same problem to an even greater degree.

In nineteenth century motor engineering terminology, dynamos capable of producing direct current by continuous homopolar induction were known as “unipolar” generators. The term “unipolar induction” appears to have originated with W. Weber, to designate homopolar machines where the conductor moves continuously to cut the magnetic lines of one kind of magnetic pole only, and thus require sliding contacts to collect the generated current. Faraday's rotating copper disc apparatus was, in this sense, a homopolar generator when the disc was driven manually, or a homopolar motor when the current was provided to it. Where the rotating conductor continuously cuts the magnetic field of alternatingly opposite magnetic poles, the operation of a machine, whether a generator or a motor, is said to be “heteropolar”. Unipolar machines went on to have a life of their own in the form of low voltage and high current DC generators - from Faraday, through Plucker, Varley, Siemens, Ferraris, Hummel, to Lord Kelvin, Pancinoti, Tesla and others - almost exclusively in the form of disc dynamos, but some having wound rotors.

In Mordey's alternator, and in so-called “inductor alternators”, however, homopolar generators were employed to obtain alternating currents, with the use of rotors wound back and forth across the field. Use of smooth, unwound rotors in AC induction motors (as opposed to AC synchronous motors, such as hysteresis motors) was a later development than homopolar dynamos. By 1888, Tesla and Ferraris amongst still others, had independently produced rotating magnetic fields in a motor, by employing two separate alternate currents with the same frequency but different phase. Single phase alternate current motors were developed later, and split-phase motors were developed last. Ferraris (Ferraris, G (1888) "Rotazioni elettrodynamiche", Turin Acad, March issue.) proposed the elementary theory of the 2-phase motor, where the current induced in the rotor is proportional to the slip (the difference between-the angular velocity of the magnetic field and that of the rotating cylinder), and the power of the motor is proportional to both the slip and the velocity of the rotor.

If an iron rotor is placed within the rotating magnetic field of a 2-phase stator, it will be set in rotation, but not synchronously, given that it is always attracted to the moving magnetic poles with a lag. But if an aluminium or copper rotor is used instead, it gets “dragged” around by the rotating stator field because of the eddy currents induced in it. If the aluminium or copper rotor were to rotate synchronously with the stator magnetic field, there would be no induced eddy currents and thus no motor action would result. The motor action depends, in this instance, upon the presence of asynchronous slip, since the function of the latter is to sustain the induction of those currents in the rotor that are responsible for the motor action of the dragged rotor. This then is the origin of the term “AC drag motors”. Once the drag rotor evolved from a cylinder to a hollow cup, they earned the epithet of “drag-cup motors”. Later, already in the 20th century, the cups were fitted over a central stator member, and the sleeve rotor 2-phase servo motor was born.

Tesla knew that impulse currents as well as CW (constant wave) sinusoidal currents could be used to drive AC motors. Regarding his invention of a hysteresis motor (which he called a “magnetic lag motor”), he stated: " . . . pulsatory as well as an alternating current might be used to drive these motors . . . " (Martin, T C (1894) "The inventions, researches and writings of Nikola Tesla", Chapter XII, p. 68). In his search for efficient utilisation of the high frequency DW (dampened wave) impulse currents of his induction coils, Tesla began by employing an AC disc induction motor as shown in Fig.17 of his famous 1892 address (Tesla, N (1892) "Experiments with alternate currents of high potential and high frequency", in "Nikola Tesla Lectures", 1956, Beograd, pp. L-70-71). This consisted of a copper or aluminium disc mounted vertically along the longitudinal axis of an iron core on which was wound a single motor coil which was series wired to the distal terminal of an induction coil at one end, and to a large suspended and insulated metal plate at the other. What was new about this was the implementation of an AC disc induction motor drive, where the exciting current travelled directly through the winding with just a unipolar connection to the coil secondary (under certain conditions, even the series connection to the plate could be removed, or replaced with a direct connection to the experimenter's body): "What I wish to show you is that this motor rotates with one single connection between it and the generator" (Tesla, N. (1892), op. cit., L-70, Tesla's emphasis). Indeed, he had just made a critical discovery that, unlike in the case of mass-bound charge where current flow requires depolarisation of a bipolar tension, mass-free charge engages current flow unipolarly as a mere matter of proper phase synchronisation:

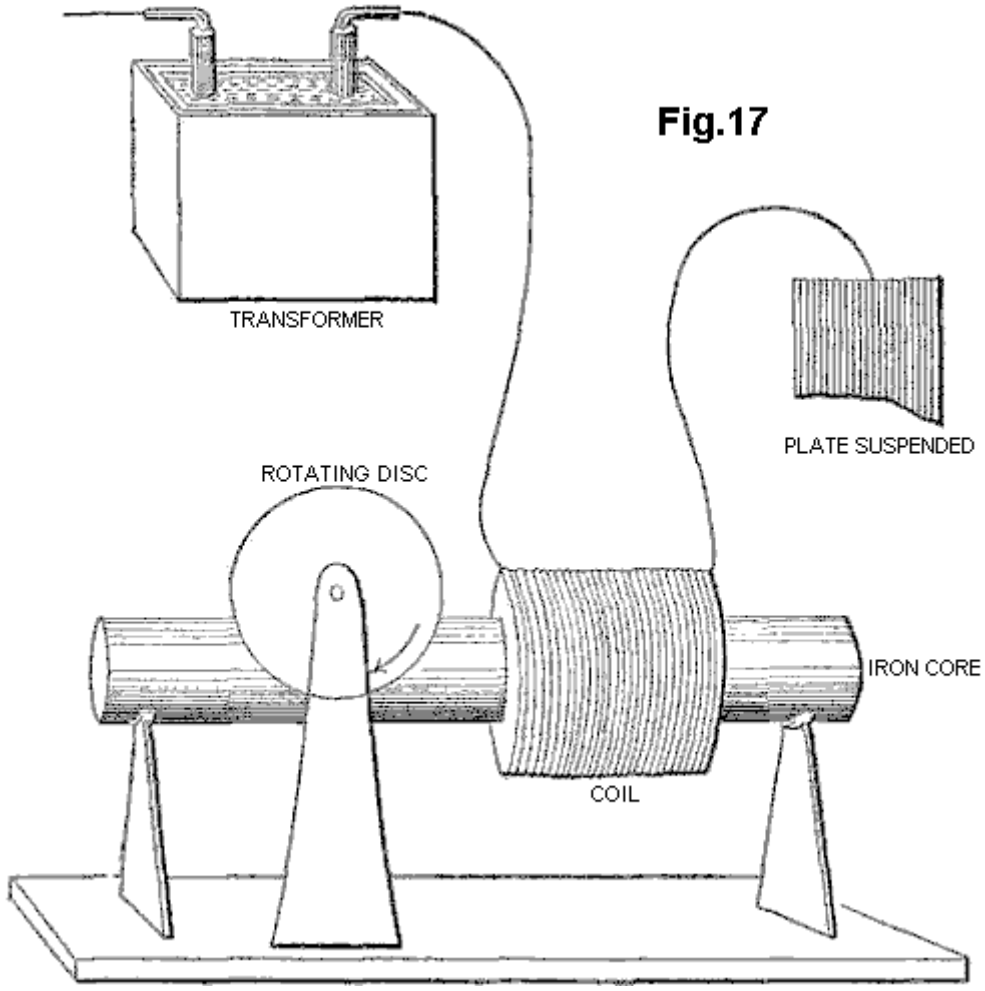

Fig.17

Tesla thought that his motor was particularly adequate to respond to windings which had “high-self-induction”, such as a single coil wound on an iron core. The basis of this self-induction is the magnetic reaction of a circuit, or an element of a circuit - an inductor - whereby it chokes, dims or dampens the amplitude of electric waves and retards their phase.

For the motor to respond to still higher frequencies, one needed to wind over the primary motor winding, a partial overlap secondary, closed through a capacitor, since "it is not at all easy to obtain rotation with excessive frequencies, as the secondary cuts off almost completely the lines of the primary" (Idem, L-71.).

Tesla stated that "an additional feature of interest about this motor" was that one could run it with a single connection to the earth ground, although in fact one end of the motor primary coil had to remain connected to the large, suspended metal plate, placed so as to receive or be bathed by "an alternating electrostatic field", while the other end was taken to ground. Thus Tesla had an ordinary induction coil that transmitted this "alternating electrostatic field", an untuned Tesla antenna receiving this "field", and a receiver circuit comprising his iron-core wound motor primary, a closely coupled, capacitatively closed secondary, and the coupled non-ferromagnetic disc rotor. Eventually, in his power transmission system, he would replace this transmitter with a Tesla coil, and place an identical receiving coil at the receiving end, to tune both systems and bring them into resonance. But his motor remained undeveloped, and so did the entire receiver system.

Tesla returned to this subject a year later, saying "on a former occasion I have described a simple form of motor comprising a single exciting coil, an iron core and disc" (Tesla, N (1893) "On light and other high frequency phenomena", in "Nikola Tesla Lectures", 1956, Beograd, pp. L-130, and L-131 with respect to Fig.16-II). He describes how he developed a variety of ways to operate such AC motors unipolarly from an induction transformer, and as well other arrangements for "operating a certain class of alternating motors founded on the action of currents of differing phase". Here, the connection to the induction transformer is altered so that the motor primary is driven from the coarse secondary of a transformer, whose finer primary is coupled, at one end, directly and with a single wire to the Tesla secondary, and at the other left unconnected. On this occasion, Tesla mentions that such a motor has been called a “magnetic lag motor”, but that this expression (which, incidentally, he had himself applied to his own invention of magnetic hysteresis motors) is objected to by "those who attribute the rotation of the disc to eddy currents when the core is finally subdivided" (Tesla, N (1893), op. cit., p. L-130).

In none of the other motor solutions, 2-phase or split-phase, that he suggests as unipolar couplings to the secondary of an induction coil, does the non-ferromagnetic disc rotor motor again figure. But he returns to it a page later, and indirectly so, by first addressing the disadvantages of ferromagnetic rotors: "Very high frequencies are of course not practicable with motors on account of the necessity of employing iron cores. But one may use sudden discharges of low frequency and thus obtain certain advantages of high-frequency currents-without rendering the iron core entirely incapable of following the changes and without entailing a very great expenditure of energy in the core. I have found it quite practicable to operate, with such low frequency disruptive discharges of condensers, alternating-current motors."

In other words--whereas his experiments with constant wave (CW) alternating currents, and as well with high-voltage dampened wave (DW) impulses from induction coils, indicated the existence of an upper frequency limit to iron core motor performance, one might employ instead high-current, DW impulses - of high DW frequencies but low impulse rates - to move these motors quite efficiently. Then he adds "A certain class of [AC] motors which I advanced a few years ago, that contain closed secondary circuits, will rotate quite vigorously when the discharges are directed through the exciting coils. One reason that such a motor operates so well with these discharges is that the difference of phase between the primary and secondary currents is 90 degrees, which is generally not the case with harmonically rising and falling currents of low frequency. It might not be without interest to show an experiment with a simple motor of this kind, inasmuch as it is commonly thought that disruptive discharges are unsuitable for such purposes."

What he proposes next, forms the basis of modern residential and industrial AC electric power meters, the AC copper disc motor whose rotor turns on the window of these meters, propelled forward by the supply frequency. But instead of employing any such Constant Wave input, Tesla uses the disruptive discharges of capacitors, incipiently operating as current rectifiers. With the proper conditions, e.g. correct voltage from the generator, adequate current from the capacitor, optimum capacitance for the firing rate, and tuned spark-gap, to mention a few, Tesla found that the non-ferromagnetic disc rotor turned but with considerable effort. But this hardly compared to the results obtained with a high-frequency CW alternator, which could drive the disc "with a much smaller effort". In summary then, Tesla went as far as being the first to devise a motor driven by Tesla waves, that employed a non-ferromagnetic rotor, and whose arrangement encompassed both transmitter and receiver circuits. For this purpose, he employed a single-phase method in which the signal is fed unipolarly to the winding, placed in series with a plate capacitance.

Tesla also later proposed driving a similar single-phase non-ferromagnetic disc motor from bipolar capacitative discharges through an atmospheric spark-gap now placed in parallel with the main motor winding, and again simulating a split-phase by a closely-wound secondary which was closed by a capacitance.

As Tesla admits, the results of all his AC eddy current motor solutions were meagre and limited by current and frequency problems. Likewise, the two-phase arrangements proposed by Reich for his OR motor, involving a superimposition of the Dampened Waves of a first phase on a fixed Continuous Wave second phase, require an external power source and a pulse amplifier circuit, and failed to meet Reich's own requirements.

We have previously proposed the use of squirrel cage motors with capacitative splitting of phase to convert the Dampened Wave output of plasma pulsers, but once a Squirrel Cage is introduced, the dampening effect which the non-ferromagnetic copper cage exerts in being dragged by the revolving stator field, is counteracted by the ferromagnetic cylinder of laminated iron, in which the copper cage is embedded, working to diminish the slip and bring the rotor to near synchronism. This is, in all likelihood, what limits Squirrel Cage motors responding to the DC component of the Dampened Wave impulse, and thus be limited to respond to fluxes of mass-bound charges. Historically, as we shall see, the obvious advantage of the Squirrel Cage servo motors lay in the fact that, in particular for 2-phase applications, they were far more efficient at performing work without evolution of heat. Indeed, if the eddy currents in the non-ferromagnetic rotor are permitted to circulate in non-ordered form, the rotor material and stator will heat up rapidly and consume much power in that heating. This is in fact considered to be a weakness of AC non-ferromagnetic-rotor induction motors.

SUMMARY OF THE INVENTION

The present invention is concerned with conversion to conventional electrical energy of the variants of mass-free energy radiation considered above, referred to for convenience as Tesla waves, mass-free thermal radiation and latent mass-free radiation. The first variant of such radiation was recognised, generated and at least partially disclosed by Tesla about a hundred years ago, although his work has been widely misinterpreted and also confused with his work on the transmission of radio or electromagnetic waves. The Tesla coil is a convenient generator of such radiation, and is used as such in many of the embodiments of our invention described below, but it should be clearly understood that our invention in its broadest sense is not restricted to the use of such a coil as a source of mass-free radiation and any natural or artificial source may be utilised. For example, the sun is

a natural source of such radiation, although interaction with the atmosphere means that it is largely unavailable at the earth's surface, limiting applications to locations outside of the earth's atmosphere.

According to the invention, a device for the conversion of mass-free radiation into electrical or mechanical energy comprises a transmitter of mass-free electrical radiation having a dampened wave component, a receiver of such radiation tuned to resonance with the dampened wave frequency of the transmitter, a co-resonant output circuit coupled into and extracting electrical or kinetic energy from the receiver, and at least one structure defining a transmission cavity between the transmitter and the receiver, a full-wave rectifier in the co-resonant output circuit, and an oscillatory pulsed plasma discharge device incorporated in the co-resonant output circuit. The output circuit preferably comprises a full-wave rectifier presenting a capacitance to the receiver, or an electric motor, preferably a split-phase motor, presenting inductance to the receiver. The transmitter and receiver each preferably comprise a Tesla coil and/or an autogenous pulsed abnormal glow discharge device. The transmission cavity is preferably at least partially evacuated, and comprises spaced plates connected respectively to the farthest out poles of the secondaries of Tesla coils incorporated in the transmitter and receiver respectively, the plates being parallel or concentric. The structure defining the cavity may be immersed in ion-containing water. The split-phase motor is preferably an inertially-dampened AC drag motor.

The invention, and experiments demonstrating its basis, are described further below with reference to the accompanying drawings.

SHORT DESCRIPTION OF THE DRAWINGS

Fig.1 is a schematic view of a Tesla coil connected to a full-wave rectifier to form an energy conversion device:

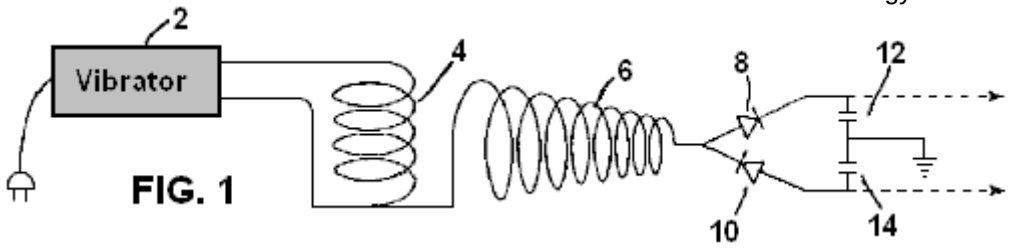

FIG. 1

Fig.2 is a schematic view of a Tesla coil connected to a gold leaf electrometer:

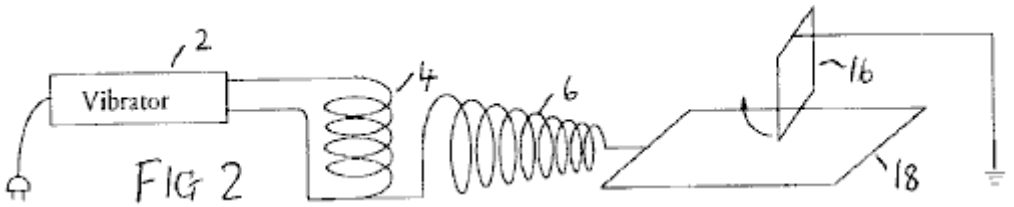

FIG 2

Fig.3 to Fig.6 show alternative electrometer configurations:

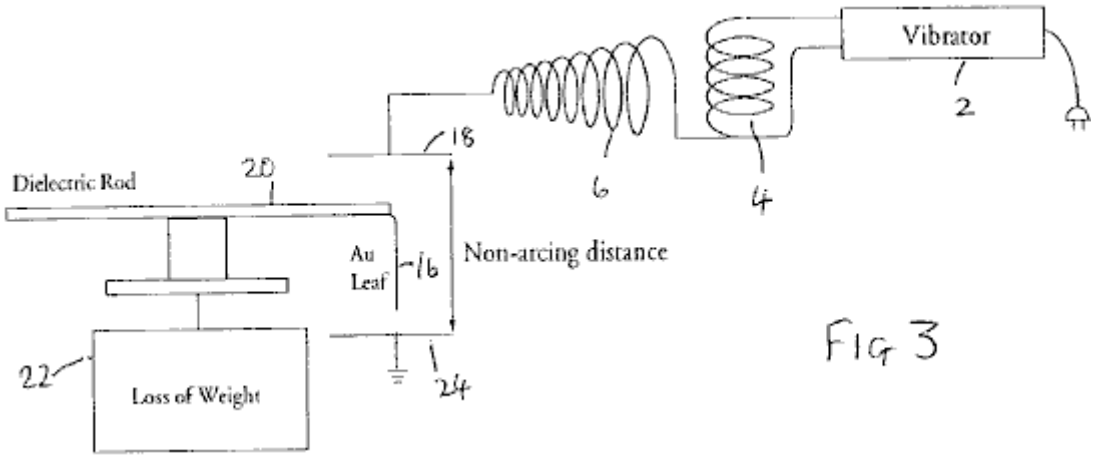

FIG 3

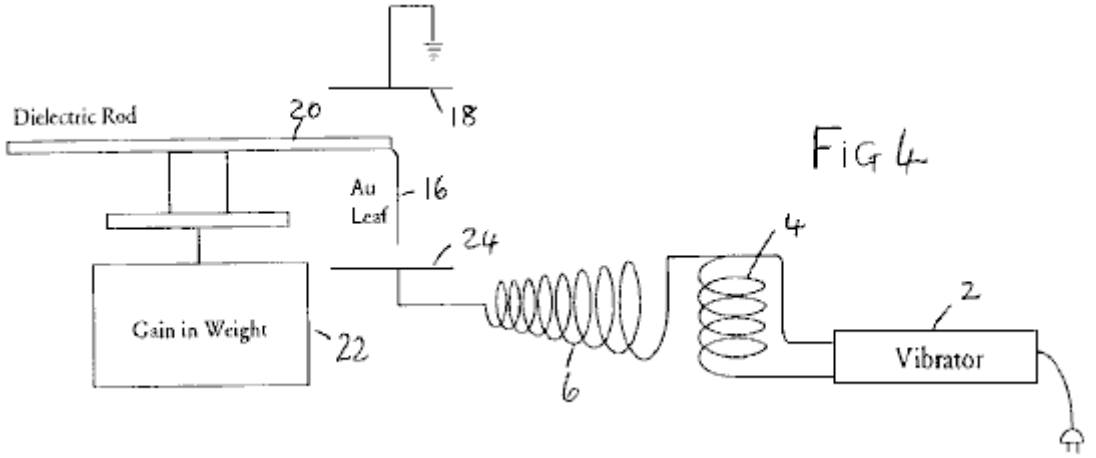

FIG 4

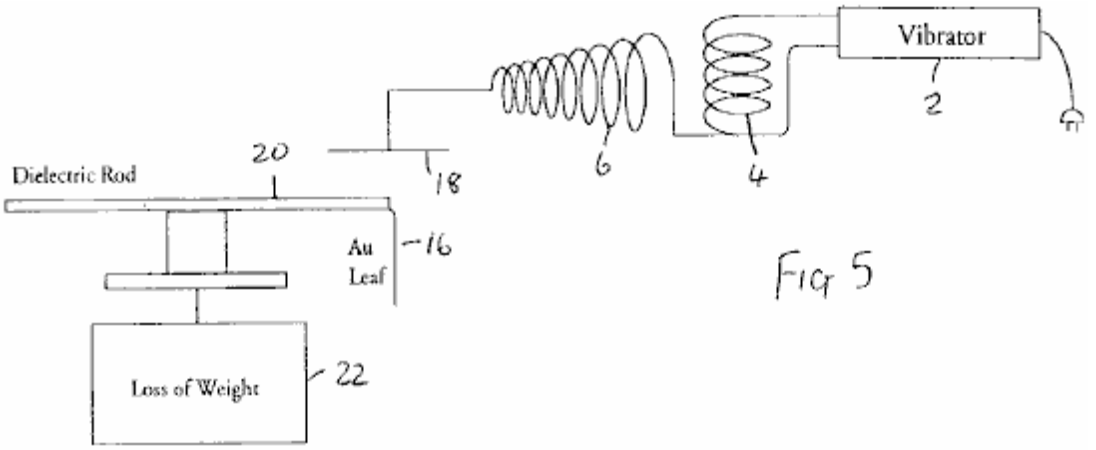

FIG 5

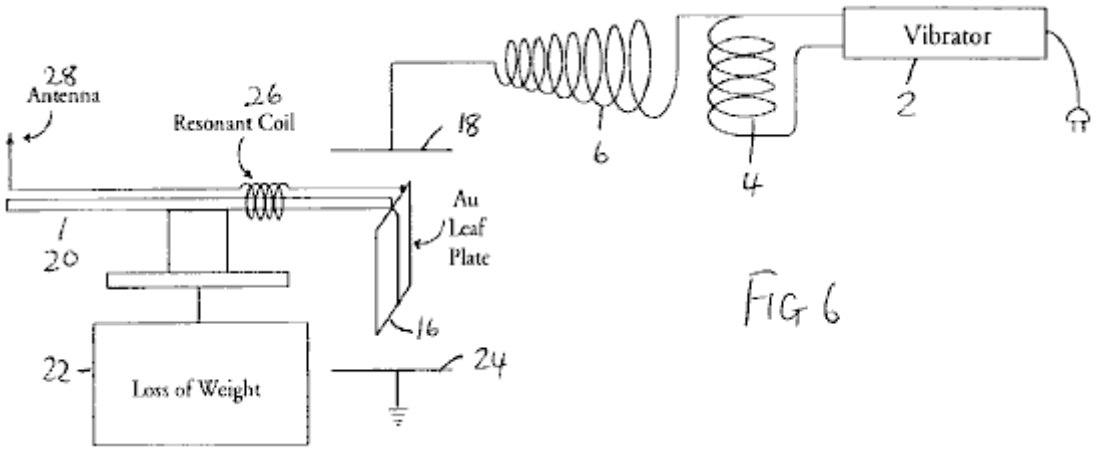

FIG 6

Fig.7 to Fig.11 show modifications of the circuit of **Fig.1**:

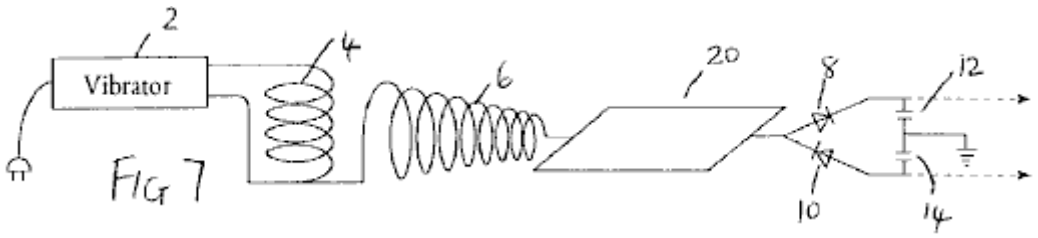

FIG 7

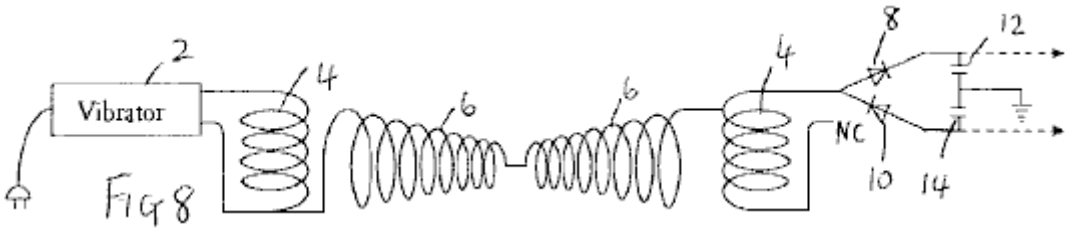

FIG 8

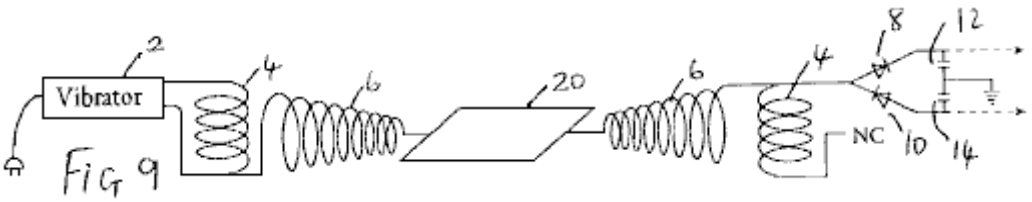

FIG 9

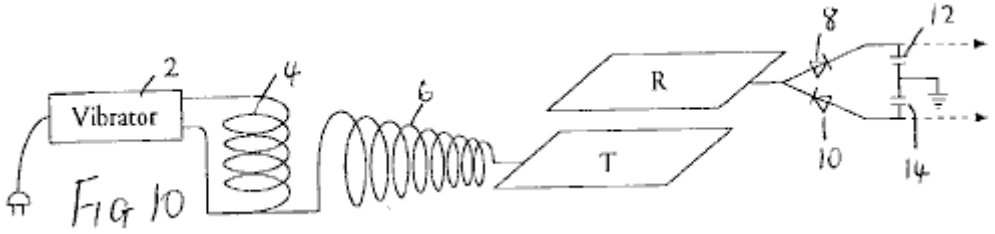

FIG 10

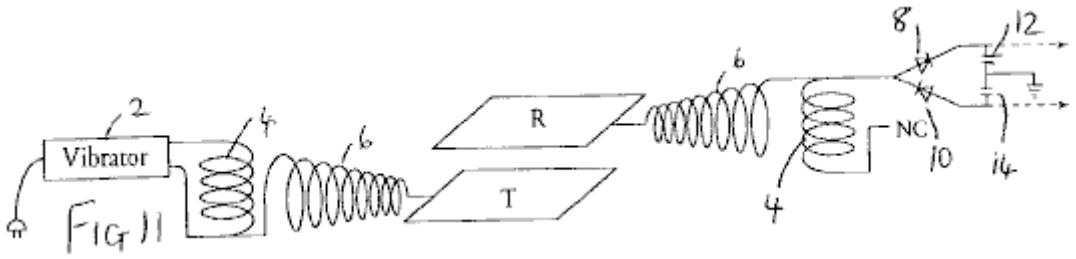

FIG 11

Fig.12 shows apparatus for investigating aspects of the experimental results obtained with the foregoing devices;

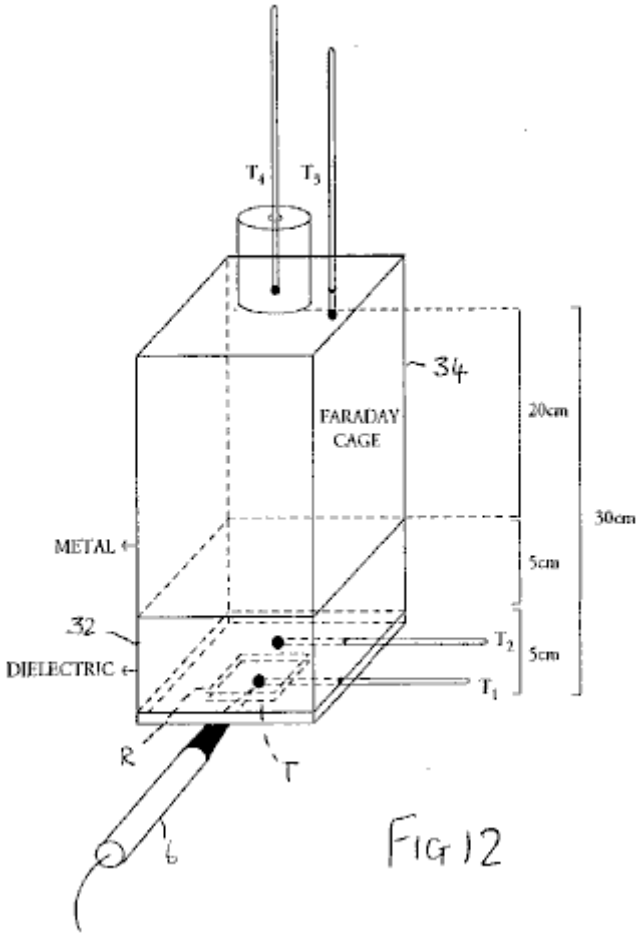

FIG 12

Fig.13 is a graph illustrating results obtained from the apparatus of **Fig.12**:

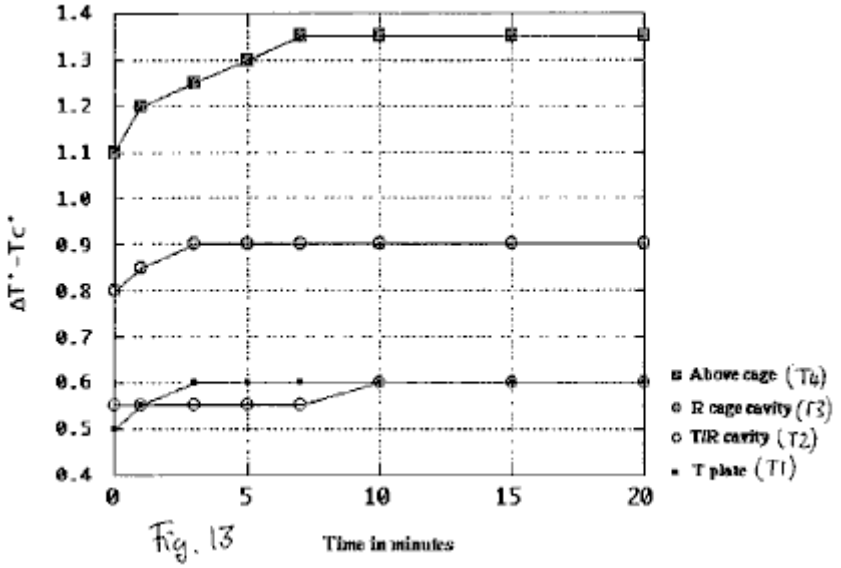

Fig. 13

Fig.14 to Fig.17 show schematic diagrams of embodiments of energy conversion devices:

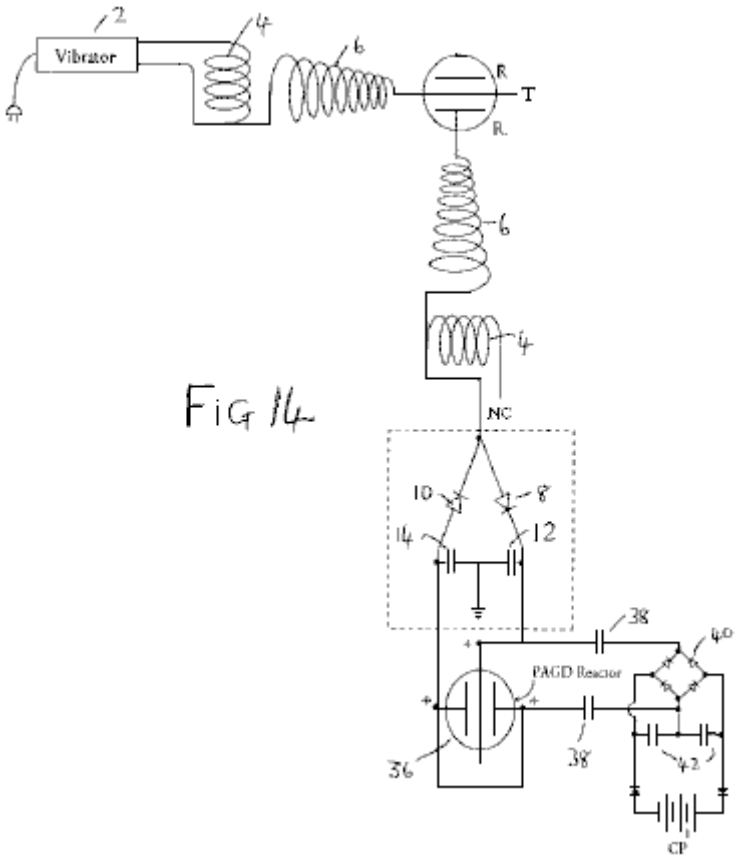

Fig 14

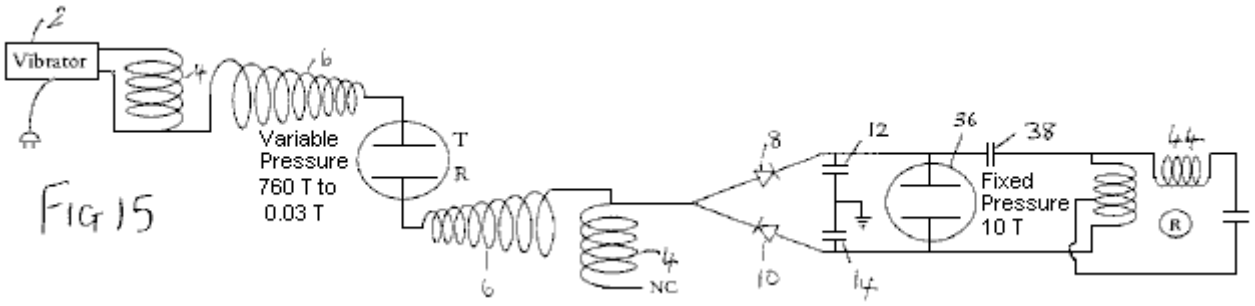

FIG 15

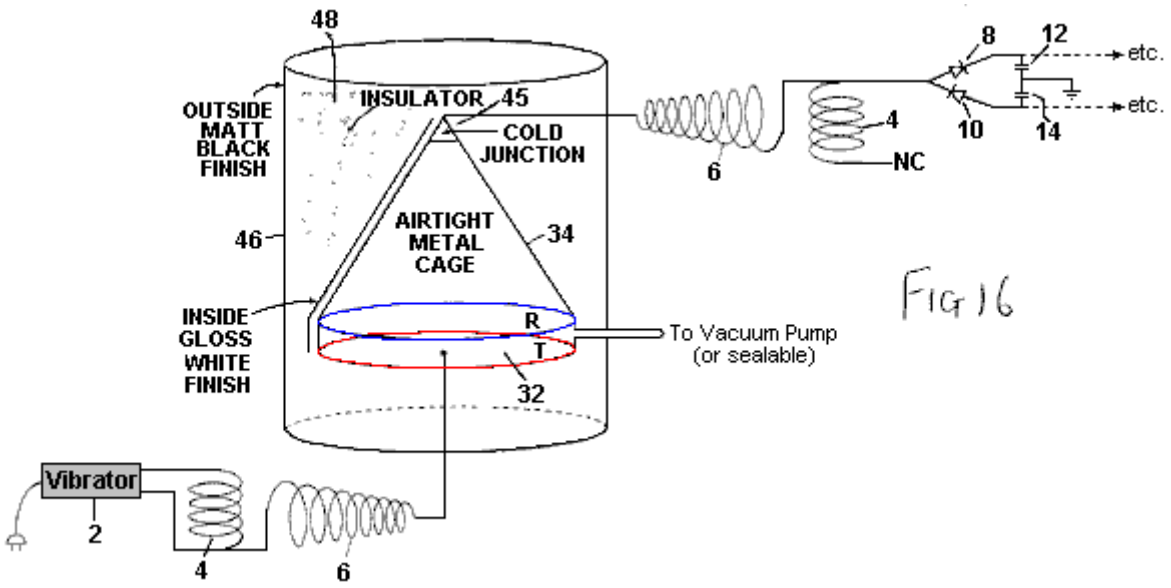

FIG 16

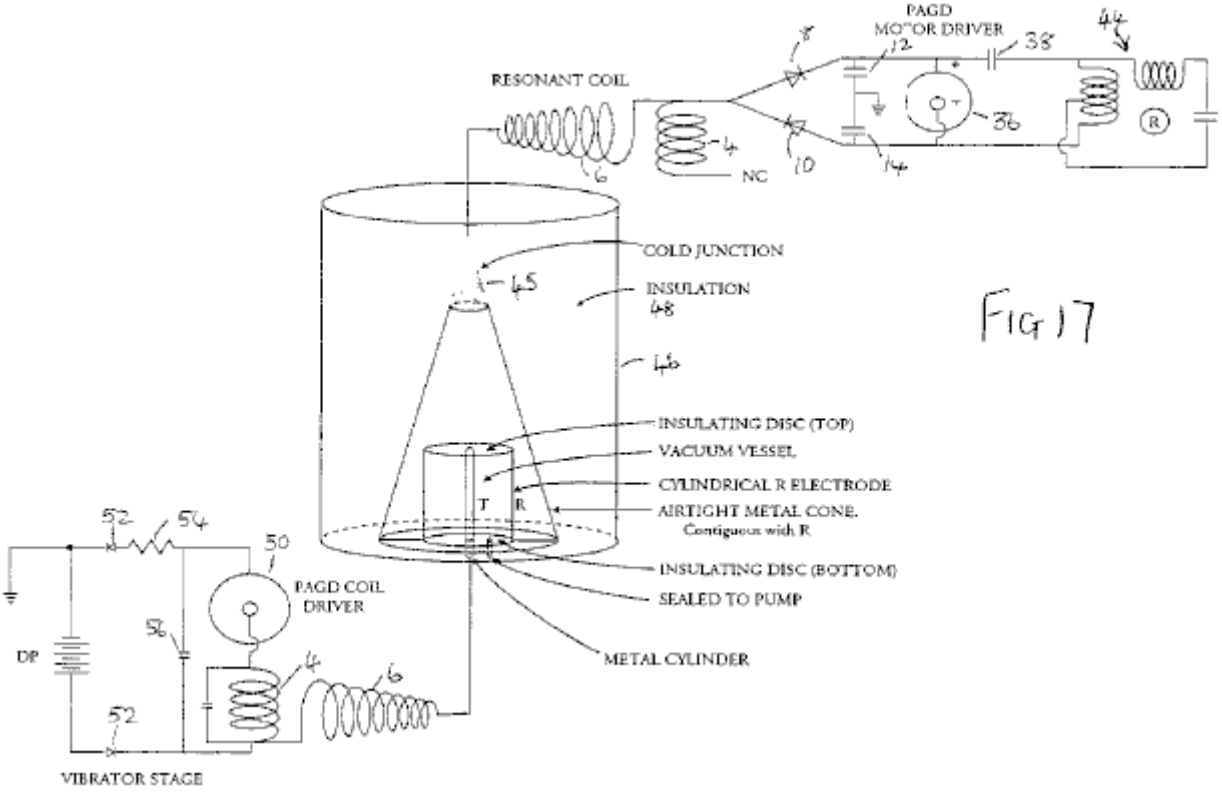

FIG 17

Fig.18 is a diagrammatic cross-section of an inertially dampened drag cup motor:

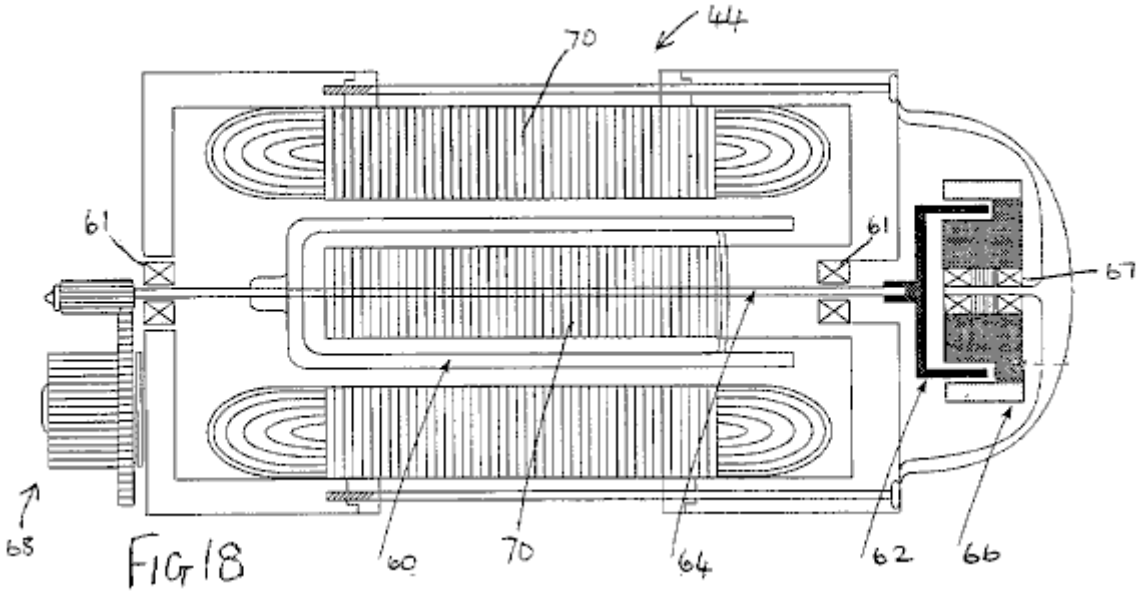

FIG 18

Fig.19 is a schematic diagram of a further embodiment of an energy conversion device incorporating such a motor:

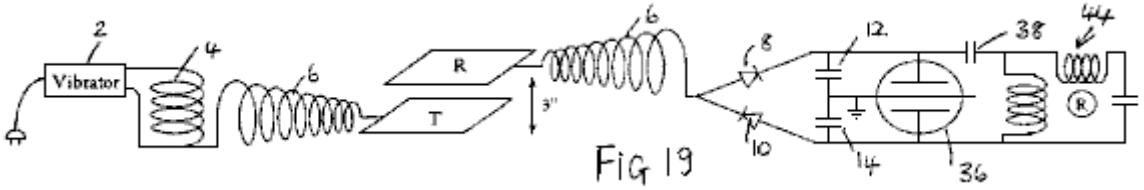

FIG 19

DESCRIPTION OF THE PREFERRED EMBODIMENTS

Based upon observations of weight loss in metallic matter as induced by exposure to high frequency alternating electric fields, we developed an experimental method to optimise this-weight loss, and from this a device that treats the forces causing weight loss as manifestations of intrinsic potential energy ΔU (or true "latent heat") of the molecules of matter, and converts both "true latent heat" energy present in the neighbourhood of a receiver, and "sensible" heat induced within that receiver, into electric energy which can be used to drive a motor, flywheel or charge batteries.

It is commonly believed that the output of the Tesla coil is ionising electromagnetic radiation. We have demonstrated that it is not, i.e. that it is neither electromagnetic radiation, nor ionising electromagnetic radiation. The output of an air-cored, sequentially-wound secondary, consists exclusively of electric energy: upon contact with the coil, a mass-bound AC current can be extracted at the resonant frequency, whilst across a non-sparking gap, mass-free AC-like electric wave radiation having the characteristics of longitudinal waves, can be intercepted anywhere in adjacent space. Accordingly, the radiation output from such coils is different to electromagnetic radiation.

The basic demonstration that the output of a Tesla coil does not consist of ionising radiation, is that it does not accelerate the spontaneous discharge rate of electroscopes, whether positively or negatively charged. In fact, in its immediate periphery, the coil only accelerates the spontaneous discharge rate of the negatively charged electroscope (i.e. the charge leakage rate), whereas it arrests the discharge of the positively charged electroscope (i.e. the charge seepage rate falls to zero). But this dual effect is not due to any emission of positive ions from the secondary, even if it can positively charge a discharged electroscope brought to its proximity. This charging effect is in fact an artifact, in that metals but not dielectrics are ready to lose their conduction and outer valence band electrons when exposed to the mass-free electric radiation of the coil.

This is simply demonstrated by the apparatus of **Fig.1**, in which the outer terminal of the secondary winding **6** of a Tesla coil having a primary winding **4** driven by a vibrator **2** is connected to the input of a full-wave voltage wave divider formed by diodes **8** and **10** and reservoir capacitors **12** and **14** (the same reference numerals are used for similar parts in subsequent diagrams). If the rectifiers employed are non-doped, then the coil appears to only charge the divider at the positive capacitance **10**, but if doped rectifiers are employed, the coil will be observed to charge both capacitances equally. Whereas positive ionises can charge either doped or un-doped dividers

positively, no positive ionise can charge a doped divider negatively, clearly demonstrating that the Tesla coil does not emit positive ions.

The basic demonstration that the output of a Tesla coil is not non-ionising electromagnetic radiation of high frequency, such as optical radiation, or of lower frequency, such as thermal photons, is also a simple one. Placement of a sensitive wide spectrum photoelectric cell (capable of detecting radiation to the limits of vacuum UV), wired in the traditional closed circuit manner from a battery supply, at any distance short of sparking from the outer terminal of the coil will show in the dark that the light output from the coil is negligible. This rules out optical radiation at high frequency. The demonstration that the sensible heat output from the Tesla coil is also negligible will be addressed below.

Our theory proposed the existence of physical processes whereby mass-free electric radiation can be converted into electromagnetic radiation. Such a process is at work whenever mass-free electric wave radiation interacts with electrons, such as those that remain in the valence bands of atoms. This mass-free electric energy interacts with charge carriers, such as electrons, to confer on them an electrokinetic energy which they shed in the form of light whenever that electrokinetic energy is dissociated from those carriers (e.g. by deceleration, collision or friction processes). Such a process is at work to a negligible extent in the coil itself and its usual terminal capacitance, hence the faint glow that can be seen to issue from it, but it can also be greatly amplified in the form of a corona discharge by connecting a large area plate to the output of the secondary, as Tesla himself did in his own experiments, and thus by increasing the capacitance of the coil system.

Now, what is interesting in this process is that, in the absence of virtually any I^2R losses at the plate, and if the plate thus introduced is bent at the edges so that it has no pointed edges, or if it is in the form of a bowl, or in any other manner that precludes sparking at edges and specially corners, and thus enhances the corona discharge, any electroscope, whether negatively or positively charged, now brought close to the plate will show a tendency to arrest its spontaneous discharge rate. One might say that this is simply the result obtained in a Faraday cage which disperses charge on its outside and electrically insulates its interior, and indeed if an electroscope is placed inside a Faraday cage no amount of Tesla radiation on the outside of that cage, save direct sparking, adversely affects the leakage or seepage rate of the electroscope. In fact, since the effect of such a cage can be shown to be that of, by itself, inducing arrest of either spontaneous electroscopic discharge, this effect simply remains or is magnified when the cage is bathed by Tesla radiation. However, a cage constitutes an electrically isolated environment, whereas a plate with or without curved or bent edges does not. Furthermore, the change observed in the properties of the output radiation from a Tesla coil when certain metal plates or surfaces are directly connected to the outer terminal of the secondary, takes place whilst the capacitance of the coil is increased by the connected plate, and thus the plate is an electrically active element of the circuit - and hence the opposite of an electrically isolated element.

For a long time, we believed that the anomalous cathode reaction forces observed in autoelectronic discharges (atmospheric sparks, autogenous PAGD (pulsed abnormal glow discharge) and vacuum arc discharges) were exclusive to an autoelectronic emission mechanism prompted by a direct potential between discharging electrodes. Sparking driven by AC potentials could sustain the same forces, but their mutual cancellation over time would not deploy a net force. In this sense, when a large gold leaf connected directly to the ground (via a water pipe or any other suitable connection) or to another large area plate suspended at some height above the ground, is vertically placed at a sparking distance above the surface of another plate connected to the secondary of a Tesla coil, one would not expect the AC spark to sustain any net force across the gap between the gold leaf and the plate. In terms of cathode reaction forces, one would expect their cancellation to be simply brought about by the high frequency of the current alternation in the coil, as both leaf and plate would alternate between being the emitting cathode or the receiving anode. However, this is not what is observed - instead, the gold leaf **16** lifts away from the plate **18** (**Fig.2**). If instead, the suspended gold leaf is connected to the coil terminal, and the bottom plate is connected to the ground in the same manner as described above, this also yields the same result.

Even more curious is the finding that this anomalous reaction force deployed by an alternate current of mass-bound charges in the arc, remains present when the sparking is prevented and instead the corona effect is enhanced (by employing a large plate connected to the outer pole of the secondary, and by employing a distance at which sparking ceases), as if the lift itself were the property of the corona underlying the spark channels and not the property per se of the autoelectronic emission mechanism.

By mounting the suspended leaf **16** (41 mg of hammered 99.9996% pure gold) directly at the end of a long dielectric rod **20** balanced at the centre and placed on a light stand over an electronic balance **22**, we sought to determine the observed lift of the leaf as weight lost. Surprisingly, and despite the most apparent lifting motion of the leaf, the balance registered a substantial weight gain, indicating the addition of 1 to 5 mg weight (with the same 14W input to the vibrator stage), independently of whether the leaf was connected to the terminal of the coil or instead to the earth ground via a water pipe. This suggested to us that, whether formed as a DC or AC spark channel, or whether in the form of a corona discharge, the electric gap develops an expansion force (exactly

opposite to a Casimir force) on both electrodes, independently of their polarity, which force is responsible for the observed repulsion. Yet, this expansion goes hand in hand with an increase in their weight such that some other process is at work in that electric gap.

To examine this problem further, we assembled a different experiment where the gold leaf **16** was suspended between two large metal plates **18** and **24** placed 20 cm apart, and the leaf was not electrically connected to them or to any other circuit, while attached to the dielectric rod employed to suspend it over the electronic balance. Given that the leaf is suitably and equally spaced from both plates, there is no arcing between it and either plate. The obvious expectation is that, since the electric field bathing the leaf alternates at high frequency (measured in hundreds of kilohertz), and the corona from both electrodes should equalise and balance any electric wind, no lift should be observed. In fact, no lift is apparent, but a most curious observation is made: depending upon which orientation is employed for the plates, the gold leaf either gains or loses 4-6% of its weight. This gain or loss is registered for as long as the coil is on. If the top plate is grounded and the bottom one connected to the different terminal of the secondary, a gain in weight is observed (**Fig.3**). If the connections are reversed, an equal weight loss is registered (**Fig.4**).

Furthermore, in this last instance, if the grounded plate **24** is entirely removed (**Fig.5**), and only the top plate remains connected to the outer terminal of the secondary, the observed loss of weight continues to occur such that in effect, this reaction can be obtained with unipolar electric fields of high frequency, and it provides a unidirectional force which, once exerted upon metallic objects bathed by its field, can be made to oppose or augment gravity.

Now, these effects can be greatly magnified, in the order of 10-fold, if the same gold leaf is made part of a simple series floating electric circuit where the leaf functions as a large area plate, and is wired in series with a coil **26** which, for best results, should be wound so as to be of a length resonant with the secondary of the Tesla-type coil employed; and this coil is connected in turn to a point antenna **28** upwardly oriented (**Fig.6**). The entire floating circuit is mounted on the rod **20** and this in turn, is mounted over the sensitive balance. If both plates are kept as in **Fig.3** and **Fig.4**, the observed weight loss and weight gain both vary between 30% and 95% of the total weight of the leaf. Again, the gain or loss of weight is registered for as long as the coil is on.

These anomalous findings suggested that, whatever is the nature of the energy responsible for the force observed in that high frequency alternating current gap, any metallic object placed in that gap will experience a force repelling it from the electric ground. This force will be maximised if the gap frequency is tuned to the elementary or molecular structure of the metallic object. If the electric ground is placed opposite the actual plane of the earth ground, that force will act in the direction of gravity. If, instead, the electric ground and the earth ground are made to coincide on the same plane, that force will act opposite the direction of gravity, i.e. will repel the metallic object from the ground.

No such weight alteration was observed with solid dielectrics, for instance with polyethylene and other thermoplastic sheets.

These facts rule out the possibility of a hidden electrostatic attraction force, acting between the plate connected to the different terminal of the secondary and the gold leaf. Firstly, such an attraction would be able to lift the gold leaf entirely, as is easily observed with the unipole of any electrostatic generator operating with a few milliwatts output with either negative or positive polarity; secondly, the same attraction, if it existed and were the product of an electric force, would surely be manifested independently from whether the experimental leaf was metallic or a dielectric (as again is observed with electrostatic generators).

The results suggest therefore, that whenever a large plate is connected to a Tesla-type coil, it induces in surrounding matter that is not part of its own circuit, a directional thrust which is oriented in a direction which is opposite to the electric ground and, if the electrical ground is on the same side as the surface of the Earth, then a thrust is produced which opposes gravity.

When this thrust is made to oppose gravity, we believe that its effect upon the gold leaf can be compared to the lifting power imparted to the water molecule when it transits from the liquid to the vapour state and which is associated with the increase in internal (or intrinsic) potential “thermal” energy ΔU (See Halliday D & ResnickR (1978) "Physics", Vol. 1, section 22-8, p. 489). The "specific latent heat" of water (m*L) contains indeed both an expression for the sensible radiant thermal work involving volume and pressure relations:
$W = P(V_V-V_L)$ where P = a pressure of 1 atmosphere, and V_V and V_L are the molar volumes in the vapour and liquid phases respectively, and an expression for a quantity of "latent" energy (ΔU) which is associated with the molecule in the more rarefied state. Hence, the relation for the latter with respect to water vapour is: $\Delta U = mL - P(V_V-V_L)$

We propose that likewise, if a very small portion of the energy of the mass-free electric waves is indirectly transformed by mass-bound charge carriers on that plate into blackbody photons (once those charge carriers shed their electrokinetic energy), the greater portion of those waves are directly transformed in the space adjacent to that plate into the latent energy equivalent to ΔU for the atoms of the surrounding air, and so on, until this process itself is also occurring for the atoms of that gold leaf, thus inducing their non-electrical weight loss and suggesting the existence of a non-thermal "antigravitokinetic" energy term previously unknown to mankind other than as "latent heat" or "internal potential energy".

From this viewpoint, the energy released by any Tesla-type coil to its surroundings, would be tantamount to a radiative injection of "internal potential energy" which would confer on local gas molecules a weight cancellation (a cancellation of gravitational mass occurring in the absence of any cancellation of inertial mass - a process which the inventors theorise is explained by the neutralisation of elementary gravitons), and the same process would be equally at work for metallic solids but not dielectric solids.

Gold vapour also deploys a substantial intrinsic potential energy. With an enthalpy of vaporisation on the order of H_V = 324 kJ mol^{-1}, the molar volumetric work performed by gold vapour at atmospheric pressure at the temperature of vaporisation T_V (2,856^{0}C., i.e. 3,129 degrees Kelvin) is:

$W = P\Delta V_{V\text{-}L}$ = 23.58 kJ $mol.^{-1}$ where $\Delta V_{V\text{-}L} = 0.2327 m^3$. The intrinsic potential energy of gold vapour is then given by:

$\Delta U = H_V - W$ = 300.4 kJ $mol.^{-1}$ i.e. 12.74 times greater than the volumetric work performed during the phase transition.

It is our contention that this intrinsic potential energy, associated with molecules as their "latent heat", has fine structure that in turn is altered if this energy is released from these molecules and fails to gain a "sensible" thermal form. What is suggested is that the fine structure of "latent heat" is not electromagnetic and obeys instead the molecular function:

$\Delta U / N_A = \lambda_{n2}^2 c f_{n2}$ where N_A is Avogadro's number, the wavelength denoted as λ_{n2} is the wavelength-equivalent of the mass of the molecule to which the "latent heat" is associated, obtained by a conversion method proposed in these inventors' theory, and the frequency term f is a non-electromagnetic frequency term, specifically in this case a gravitational frequency function.

Employing the conversion of Joules into m^3 sec^{-2} proposed by these inventors as being exactly:

$1J = 10\ N_A\ m^3\ sec^{-2}$, and putting the wavelength λ_{n2} down as the wavelength-equivalent of the mass of the gold atom, λ_{Au}, at 1.9698 m, that frequency term f_{n2} can be obtained as being equal to 2.6×10^{-3} sec^{-1}.

According to the present inventors' theory, the wave function c constitutive of the fine structure of "latent heat" associated with molecules of matter, carries the same wavelength λ_{Au} and its frequency is given in the usual manner by c/λ_{Au} = 1.52 x 103 sec^{-1}. The resultant frequency for the non-Planckian unit quantum of "latent energy" associated with each gold atom at the vaporisation temperature is then obtained by the geometric mean of the two synchronous frequency terms: $[(c/\lambda_{Au})\ f_{n2}]^{0.5}$ = 624 Hz. However, this is the signature of that intrinsic potential energy when associated with that gold atom at its vaporisation temperature. It is not the signature of the energy quantum itself if it is released from that molecule, nor prior to being absorbed (i.e. in transit), at that same temperature.

The fine structure of the same non-Planckian "latent" energy quantum varies to encompass different determinations of the constituent wavelength and frequency functions. The basic relation for the determination of the wavelength of a "latent thermal" energy quantum not associated with matter, but corresponding to one that is, is:

$\lambda_{n1} = [(\Delta U / N_A) / c]^{0.666}$ $meters^{-0.333}$ $seconds^{0.666}$

which gives 0.046478 m for the unbound equivalent of the "latent heat" unit quantum of vaporisation associated with the gold atom at a pressure of one atmosphere. The fine structure of the free quantum is still parallel, as given by:

$\Delta U / N_A = \lambda_{n1}^2 c f_{n1}$

but now notice how the frequency terms have changed value, with the f_{n1} function having the value 4.65 sec^{-1} and c / λ_{n1} yielding 6.48 x 10^9 sec^{-1}. The geometric mean of the superimposition of the two frequencies is then:

$[(c / \lambda_{n1}^2) f_{n1}]^{0.5}$ = 173.7 KHz

We contend that it is at this frequency that the atoms of gold vapour absorb "latent heat".

However, this is just the overall scenario of what happens at the temperature of vaporisation of gold. But at room temperature (e.g. 293 degrees Kelvin), and with respect to processes where there is no sublimation of the atoms of that gold leaf under way (and indeed, once the coil is turned off, the leaf returns to its normal weight), one must infer to a different phase of matter what portion of "latent heat" energy, if any, do the atoms of gold hold in the solid phase lattice. Assuming the same proportionality between the "sensible" and "latent" thermal energy terms for atoms of gold at room temperature, where the unit thermal energy is $N_A kT$ = 2.436 kJ mol^{-1}, we speculate that the gold atom could absorb up to 12.74 times the value of this "sensible" thermal energy, and thus hold $N_A kT$ = 31.053 kJ more energy in its own micro-atmosphere.

If this speculation is correct, and employing the above novel methodology, then the mean geometric frequency of the maximal "latent heat" energy quantum of a gold atom at room temperature would be 538 KHz (versus 174 KHz at the vaporisation temperature), and once absorbed its mean frequency mode would reduce to 201.5 Hz (versus 630 Hz once the atom has vaporised).

To test this hypothesis, we employed two different Tesla-type coils having output frequencies of 200 KHz and 394 KHz. The circuit tested was that shown in **Fig.6**, and both coils were operated at 50 KV outputs. Whereas the former coil, closer to the 174 KHz marker, could only systematically produce 10mg to 11 mg of weight cancellation in the gold leaf of the floating circuit, the second coil, closer to the speculated 538 KHz marker, could produce 15mg to 35 mg of weight cancellation in the same gold leaf. The empirical results appear therefore to suggest that our speculation may well be a valid one.

The above-mentioned full wave divider (see **Fig.1**) can be easily coupled to our autogenous Pulsed Abnormal Glow Discharge technology as described in our U.S. Pat. No. 5,416,391 to form an alternative source of direct current, ultimately powered by Tesla waves, and such a drive can equally be applied to any other vacuum device that can sustain endogenous oscillatory discharges, whether in the PAGD regime or any other pulsatory regime. For the purposes of experimental and visual determination of power outputs from the divider in question, we have utilised either 2 Torr vacuum tubes operating in the high-current PAGD regime, or 20-100 Torr spark tubes requiring high voltages (2 to 10 KV) for their spark breakdown. As taught in the above US Patent, the output from the full wave voltage divider can be assessed by the energy spent in driving the tube and the motor, whose rotary speed is proportional, within the limits chosen, to the power input.

Two separate sets of experiments presented in Table 1 below, showed that direct connection of the wave divider to the outer terminal of the coil (set constantly at 6 clicks on the vibrator stage in **Fig.1**) or to the same terminal but across a large (2 or 3 square feet) plate **30** that increased the capacitance of the secondary (**Fig.7**), presented the same power output in either case (the effect of the plate is to lower the voltage of the output proportional to the increase in current). A substantial increase in power output through the divider is observed only when an identically wound Tesla coil is connected in reverse (**Fig.8**) with the non-common end of its winding **4** not connected, in order to obtain a condition of resonance, and this observed increase is further augmented by now interposing either of the metal plates **18**, **24** between the two chirally connected and identical coils (**Fig.9**). The increase in plate area appears to have the effect of increasing the output for as long as the plate is isolated between the two chiral image coils. Throughout these experiments, the input power to the vibrator was fixed at 14W (60 Hz AC). [Note: 'Chirality', or 'handedness', is a property of objects which are not symmetrical. Chiral objects have a unique three-dimensional shape and as a result a chiral object and its mirror image are not completely identical - PJK].

TABLE 1

Status	Pulse rate (PPS)	Motor rotation (RPM), M ± SEM
Expt A		
Tesla coil (TC) to divider	2.6	582.5 ± 3.9 (n = 4)
TC to inverted TC, to divider	4.4	621 7.6 (n = 4)
TC to 2 ft^2 plate, to inverted TC, to divider	5	775.25 ± 23.6 (n = 4)
Expt B		
Tesla coil (TC) to divider	2.2	613 ± 5.6 (n = 12)
TC to 3 ft^2 plate, to divider	2.3	605 ± 2.6 (n = 12)
TC to inverted TC, to divider	2.3	722 ± 5.7 (n = 12)
TC to 3 ft^2 plate, to inverted TC, to divider	4.2	877.6 ± 6.5 (n = 12)

In our loss of weight experiments described above, we noted that the phenomenon of weight loss by a metallic body placed in proximity of the coil output continued to be observed when only the plate connected to the distal pole of the secondary was retained. The leaf, although not part of the circuit of the secondary, could however be seen as part of a circuit for the capture of ambient radiant energy, specifically that generated by the coil and, as well, that also possibly picked up, in the process, from other ambient sources. To determine whether the last consideration is a possibility at all, or whether the energy picked up by an analogue of our metallic body or gold leaf in the experiments described above, is entirely a by-product of the energy transmitted by the plate connected to the outer pole of the secondary, we next determined what would happen if the pick-up for the full-wave divider were placed, not at the output from the secondary coil, but from an, in all respects identical, plate (the Receiver plate **R**, as opposed to the Transmitter plate **T**) placed a distance away from, and above, the first one. In other words, the gold leaf is replaced by a receiver plate, and this carries an attached test circuit identical to the test circuit employed to directly assess the coil output.

TABLE 2

Status	T R distance	Pulse rate (PPS)	Motor rotation (RPM), M ± SEM
2 ft^2 plates			
R plate to inverted TC, to divider	3"	6.7	882 ± 17.5 (n = 4)
	4"	8	906 ± 12.1 (n = 4)
	6"	10	936 ± 46.1 (n = 9)
3 ft^2 plates			
TC to T plate, to divider	0	2.3	605 ± 2.6 (n = 12)
R plate to divider	6"	3.3	890.1 ± 3.8 (n = 12)
R plate to inverted TC, to divider	6"	5.1	1009.2 ± 4 (n = 12)
R plate to divider	8"	4.0	783.1 ± 11.3 (n = 12)
R plate to inverted TC, to divider	8"	5.1	1005.7 ± 6 (n = 12)

As shown in Table 2 above, the results of the experiment show that there is no loss of energy picked up at the **R** plate (**Fig.10**) when compared to the most favourable situation involving the plate **30** (**Fig.9**) interposed between the chirally connected coils. This observation is however not always the case. For best results one should employ iron, gold or silver plates placed parallel to the horizon, with the **T** plate underneath the **R** plate. In fact, if one employs instead aluminium plates and suspends these vertically, one can consistently register a loss of output at the divider when changing the divider input from the **T** to the **R** plates.

If however the plate **R** is connected in turn to a second identical coil, also wired in reverse, and this second coil in turn serves as input to the full-wave divider (**Fig.11**), then a most curious occurrence takes place - the power output increases considerably (see Table 2), as if the divider circuit had undergone an energy injection not present at the source. Note that the circuits are in fact resonant, but the energy injection contributing nearly 60-66% (for both plate areas in the previous experiment) of the input that we refer to, is not caused by inductive resonance, since the effect of resonance can be ascribed to the set-up described in **Fig.9**. The distance between the plates, as well as their orientation with respect to the local horizon system of the observer also appear to matter, best results being achieved at optimal distances (e.g. for 2 square feet plates the best gap, at 43% RH and room temperature, was at least 6 inches).

We tested the possibility that environmental heat produced by operation of the coil might be the source of the injected energy, the plate of the second system acting possibly as collector for the heat present in the gap. As it turned out, experiments showed repeatedly that in the gap between the **T** and **R** plates there was no significant thermal radiation propagating between one and the other. The more illustrative experiments are those in which we identified where the sensible thermal energy appears, and which involved coupling two cavities: the Transmitter-Receiver gap between plates **T** and **R**, and a Faraday cage enclosure **34** (see **Fig.12**). The first cavity appears to be much like that of a capacitor: the two identical parallel plates are surrounded by a thick dielectric insulator **32**, and a thermometer **T2** is inserted half-way through it. A thermometer **T1** is also fixed to the **T** plate, to measure it's temperature. The second cavity is a simple insulated metal cage with a thermometer **T3** inserted 2 cm into its top. Some 2-4 cm above the top of the cage there is placed a fourth thermometer **T4**, inside an insulated cylinder.

If the Tesla Coil is a source of thermal energy (e.g. IR radiation, microwaves, etc.) we would expect the **T** plate to be the hottest element from which, by radiation, thermal energy would reach the middle of the first cavity making the next thermometer **T2** second hottest, and that the third thermometer **T3** inside the second cavity, even if it might initially be slightly warmer than the other two, would, over time, become comparatively cooler than either one of the other two thermometers, despite the fact that the rising heat would still be seen to warm it up over time. One would expect a similar outcome for the fourth thermometer **T4**, above the cage. As shown by **Fig.13**, where only the temperature differences (ΔT^0 - $T_C{}^0$) between the experimental thermometers and the control thermometer reading the air temperature $T_C{}^0$ of the laboratory are shown, the surface of the **T** plate warms up by 0.1^0C. at 3 minutes after initiation of the run (closed squares), whereas in the space of the T/R gap a diminutive warming, by 0.05^0C., is registered after 10 minutes (open circles). Conversely, the temperature inside the cage, at the top (shaded circles) rises by 0.1^0C. also by the third minute, and the temperature above the cage itself (shaded squares) rises by a much greater difference of 0.35^0C., which remains stable after the eighth minute.

These results show that it is not sensible heat that radiates from the **T** plate. Instead, some other form of radiation traverses these cavities to generate sensible heat at their metallic boundaries, such that more heat is generated above the **R** plate (inside the cage) and again above the third plate, i.e. above the top of the cage, than is generated in the T/R gap, i.e. near the **T** plate. This clearly shows that the Tesla coil is not a significant source of thermal radiation, and that sensible heat can be detected inside and on top of the Faraday cage only as a further transformation of the radiant energy transmitted across the T/R cavity.

The same experiment also illustrates that, whatever is the nature of the additional environmental energy being injected at the surface of **R** plate (as shown by Table 2 results above), it is most likely not thermal radiation, at least not energy in the form of sensible heat. And whatever is the nature of this ambient radiant energy being mobilised by the electric radiant energy transmitted from the **T** plate, it can produce significant heat inside an enclosure adjacent to plate **R**.

Since we also know experimentally, that this observation of an ambient energy injection at the **R** plate or **R** cage depends upon relative humidity, being most easily observable when the latter is low (<50% Relative Humidity), and being virtually impossible to observe when air is saturated with water vapour, we can infer that water vapour is a good absorber of the electric mass-free radiant energy emitted from the **T** plate. This strongly suggests that this absorption process is tantamount to increasing the potential intrinsic energy ΔU of the water vapour molecules adjacent to the **T** plate. In the absence of significant quantities of water vapour, when the atmosphere is dry, one may speculate that this absorption process is replaced by what one presumes is a parallel process involving the various gaseous molecules of air. However, either because the air molecules involve molecular species that readily give off this potential energy, as one might speculate is the case with molecular oxygen, hydrogen and nitrogen, or because the air molecules absorb far less "latent" energy (as appears to be the case with inert gases), and therefore there is more of it in the molecularly unbound state (as we explicitly propose as a possibility) and thus available for absorption by the appropriately tuned receiver, the increased ΔU of air molecules conferred by the absorption of the mass-free electric radiation in the T/R gap is transferred to the **R** conductor together with the latent energy which those molecules already possessed before entering that gap. Hence the

energy injection and its dependency upon the partial pressure of water vapour, which absconds instead with this "latent" energy and succeeds in withholding it from transmission to the **R** plate.

If the T/R gap can mobilise ambient energy which is neither electromagnetic nor thermal in nature, but which "latent" energy becomes injected into the divider circuit in electric form, the heat (i.e. sensible thermal energy) produced inside and on top of the cage, can also be mobilised electrically as input into the divider circuit. The obvious place to look for the positioning of the cool junction which could convert sensible heat into electrokinetic energy of mass-bound charges is at the top of the cage, where it is warmest (See top curve of **Fig.13** in shaded squares). This is clearly observed from the results shown in Table 3 below, where the initial temperature difference between the top of the box and the **T** plate surface was 0.5^0C., and the top of the box temperature rose by 0.2^0C. after 2.5 minutes when the divider was connected at the junction, versus 0.35^0C. when it was not (and the transmitter coil was on).

TABLE 3

Status	TR distance inches	Pulse rate PPS	Motor rotation RPM, M ± SEM (n = 12)
3 ft^2 plates			
TC to T plate, to divider	NA	4.2	877.6 ± 6.5
R plate to inverted TC, to divider	6"	5.1	1009.2 ± 4
Top of naked R plate/ cage to divider	6"	5.4	1047.1 ± 5.7
Top of insulated R plate/cage exposed to sun, to divider	6"	6.1	1072.4 ± 8.7

For the run performed with the naked **R** cage, the temperature directly above the top of the cage was 24.3^0C., at the outset, versus the control room temperature of 23.9^0C. For the run performed with the insulated **R** cage exposed directly to the sun at midday, on a cool and clear August day, the temperature directly above the top of the cage was 33^0C., versus the control air temperature of 18.4^0C. The temperature of the cool junction at the top of the cage was 31.9^0C. while the run was performed.

It is apparent from the data of Table 3, how a second injection of energy has occurred in the apparatus. If, within the T/R gap, the energy injected appears to be on the order of absorption of "latent heat", at the top of the cage cavity, at the cool junction, the injection is one of radiant "sensible" heat. Moreover, this secondary energy addition could be further enhanced by placing strong insulation around the whole apparatus or the cage itself, and further so, by exposing the whole apparatus to solar radiation.

We next turned our attention to the T/R gap cavity with the intention of determining whether atmospheric conditions or vacua yield the same or different results. We could not, of course, test the same large area plates as have been employed for the studies undertaken at atmospheric pressures. For the present purpose we employed instead large area electrodes (ca 0.2 ft^2) made of high grade stainless steel or even aluminium. Preliminary results showed that these T/R gap tubes, when coupled to the divider circuit, yielded faster pulse rates in the secondary circuit when evacuated than at atmospheric pressure. The strength of the corona discharge also intensified, as it eventually became replaced by a normal glow discharge. For purposes of improved spatial capture of (1) the electric mass-free energy radiated from the **T** electrode and (2) the non-radiant latent thermal energy mobilised by it to be collected electrically at the **R** plate, an axial cylindrical T electrode was inserted inside a larger concentric cylinder or between two common plates of large surface area (e.g. >100 cm^2) functioning as the **R** electrode(s), in a dielectric container suitable for evacuation (glass, polycarbonate), at a typical distance of at least 3 cm between electrodes, and the entire device was tested at different pressures.

The secondary circuit connected downstream from the full-wave divider was as shown in **Fig.14** (employing an autogenous pulsed abnormal glow discharge, or PAGD, converter circuit), with the PAGD reactor **36** set at 10 Torr (in light of the high-voltage input, which varied between 1,500V and 3,200V) and gave the results presented in Table 4 below. We should remark also that these pulses charged the charge pack **CP** through the coupling

capacitors **38**, bridge rectifier **40** and reservoir capacitors **42**, and blocking diodes **44**, as expected from the prior art represented by our patents related to PAGD devices.

TABLE 4

T/R tube Pressure (Torr)	Pulse rate (PPS)
760	0.376
0.025	0.513

The effect of the vacuum in the T/R gap tube seems to be dual. By transforming the corona discharge into a normal glow discharge, it increases the local production of photons (probably associated to the formation and discharge of metastable states in the plasma), and at the same time, increases the pulse rate in the output circuit and thus, in all probability, the energy injected in the T/R gap cavity. But this did not yet permit us to confirm whether or not it is "latent heat" energy of the plasma molecules which is being tapped at the receiver plate, even if it be plausible in principle that plasmas may effect more efficient transfer of "latent heat" to tuned receivers than atmospheric gases.

The vacuum dependency of the pulse rate of the PAGD reactor employed as example in the secondary circuit downstream from the divider is also rather well marked, with the fastest pulse rates being registered at 1 Torr for the sample run shown in Table 5 below.

TABLE 5

T/R tube Pressure (Torr)	Pulse rate (PPS)	PAGD Reactor Pressure (Torr)	Voltage (across divider)
0.025	0.115	90	4.5 kV
0.025	0.1553	75	3.5 kV
0.025	0.183	60	3.3 kV
0.025	0.291	30	
0.025	0.513	15	1.6 kV
0.025	0.602	10	1.4 kV
0.025	2.9	2	0.53 kV
0.025	4.1	1	0.45 kV

It is worth noting here that the illustrated polarity of the wiring of the PAGD reactor tube, as shown in **Fig.14**, is best for purposes of sustaining regular auto-electronic emission at high voltage. The reverse configuration, with the centre electrode negative and the plates positive favours instead heating of the cathode and a lapse into a normal glow discharge.

We tested a similar arrangement to that shown in **Fig.14** above, but with a PAGD motor circuit (see our U.S. Pat. No. 5,416,391). A split-phase motor **44** replaces the rectifier and charge pack, and the PAGD reactor is operated at the same pressure of 15 Torr, as shown in **Fig.15**. The T/R gap tube tested had a longer plate distance (2''), with one plate now functioning as Transmitter and the other as Receiver. Note also the different wiring of the PAGD reactor. The results, as shown below in Table 6, present pulse per second (PPS) and motor revolutions per minute (RPM) curve trends that appear to be analogous and parallel to the well known Paschen curves for breakdown voltage in vacuum - such that the T/R gap performs better either in the atmospheric corona discharge mode, or in the high vacuum normal glow discharge (NGD) mode, than in the low breakdown voltage range of the curve where the discharge forms a narrow channel and takes on the appearance of an "aurora" transitional region discharge (TRD).

TABLE 6

T/R tube Pressure (Torr)	Pulse rate (PPS)	Motor rotation (RPM), M ± SEM (n = 17)	Discharge Type
760	2.8	751.2 ± 7.1	Corona
100	2.1	611.5 ± 5.1	TRD
20	2.4	701.9 ± 4.6	TRD
0.006	2.8	748.4 ± 9.3	NGD
0.003	3.0	819.4 ± 6.3	NGD

These results suggest that plasmas with high lateral dispersion, i.e. formed over large electrode areas (e.g. corona and NGD plasmas) and thus devoid of pinch, are more likely to mobilise electrically, the intrinsic potential energy of the molecular charges than pinch plasmas appear to be able to do (e.g. TRD plasmas). Apparently also, the greater the vacuum drawn from the T/R gap cavity, the more efficient does the transfer of this intrinsic potential energy become, i.e. the mass-bound latent heat, to the electrokinetic energy of the charges circulating in the receiver circuit. At about 0.06 Torr, this transfer in vacuo is comparable to that observed under atmospheric conditions and thus for a much greater density of molecules.

We investigated whether it Is possible to tap the latent heat energy of water molecules. It is possible that in the vapour phase they can effectively hold on to their latent energy - but could they give off some of it once closely packed in liquid phase? To test this hypothesis we immersed the T/R gap in a glass water tank. The motor employed for these tests was a high-speed 2-phase drag-cup motor (see **Fig.18** and associated description), wired in split-phase with two identical phase windings capacitatively balanced, and the galvanised iron plates each had an area of one square foot. The results are shown in Table 7 below, and clearly indicate that it is possible to tap - within the T/R cavity - the `latent heat` of water in the liquid phase. As observed, immersion of the T/R cavity in water increased the motor output speed 22% (12,117 / 9,888) x 100). This corresponds to a 50% increase in power output, from 18W at 9,888 rpm to 27W at 12,117 rpm:

TABLE 7

	Pulse rate PPS	Motor rotation RPM M ± SEM	T/R distance cm
Direct from TC	0.3	8076 ± 89.3	NA
TC to T plate	0.5	9888 ± 78.7	NA
R plate	2.75	12117 ± 29.8	30
R plate	2.9	12203 ± 55.9	60

Thus the use of ion-containing water or other ion-containing aqueous liquid in the cavity promotes long distance propagation and a greater injection of latent and thermal energies in the receiver circuit. Such a result is not achieved if the cavity is filled with deionised water.

The preceding results lead therefore to the design of a presently preferred apparatus, based on these findings, for the conversion of mass-free electric energy, "latent heat" energy and "sensible" heat energy into conventional electric energy, as shown in **Fig.16**, which integrates all of the separate findings and improvements. The winding **6** of the Tesla coil at the bottom is driven in the usual manner employing a vibrator stage **2** to pulse the primary coil **4**. The outer pole of the secondary **6** is then connected to a circular metal plate **T** which is one end of an evacuated cylindrical cavity, connected to a vacuum pump or sealed at a desired pressure, or which forms a still containing water or other aqueous solution or liquid. This cavity constitutes the transmitter/receiver gap, and is therefore bounded by a dielectric envelope and wall structure **32**, with the circular receiver plate **R** as its top surface. In turn this plate **R** serves as the base of a conical Faraday cage **34**, preferably air-tight and at atmospheric pressure, but which could also be subject to evacuation, which conical structure carries at its apex provisions for a cold junction **45** and any possible enhancement of the same junction by surface application of different metallic conductors that may optimise the Peltier-Seebeck effect. The output from the cold junction where sensible thermal energy is added to the electrokinetic energy of charge carriers, is also the input to the distal end of the winding **6** of the chiral coil arrangement that sustains resonant capture of all three energy flows ((1) mass-free electric waves of a longitudinal nature, (2) true "latent heat" or the intrinsic (thermal) potential energy, and (3) the thermokinetic energy of molecules, (i.e. "sensible" heat) and, placed in series with the input of

the full wave divider **8**, **10**, feeds the circuit output from the series capacitors **12**, **14** grounded at their common tap. In the T/R gap, the transmitted electric longitudinal wave energy is captured along with any intrinsic potential energy shed by molecules caught in the field. Within the **R** element, expanded into an enclosure that guides "sensible" radiant heat, the latter is generated and then recaptured at the cold junction.

The apparatus consisting of the cylindrical T/R gap cavity and the contiguous conical cage is then preferably finished in gloss white and cylindrically enveloped within a matt black container **46** by effective thermal insulation **48**, the latter terminating at the height of the bottom disc **T**. Apparatus (not shown) may be provided to move the plate **T** vertically to adjust the T/R gap.

Another alternative embodiment of the apparatus is shown in **Fig.17**. Here the circuit driving the apparatus is as we have set forth in our prior patents, which employs an autogenous pulsed abnormal glow discharge tube **50** in the configuration shown, supplied by a battery pack **DP** through blocking diodes **52** and an RC circuit formed by resistor **54** and capacitor **56** to drive the primary **2** of a first Tesla coil to obtain at the distal pole of the secondary **6** the energy to be injected to plate **T** in the form of a central electrode of a coaxial vacuum chamber (sealed or not), of which the cylindrical metallic envelope forms the receiver plate **R**, the latter being placed centrally inside the conical cage **34** and contiguous with its walls and base. The top and bottom of the coaxial chamber carries suitable insulating discs, preferably with O-ring type fittings. Again, the apparatus is enclosed in insulation within a cylindrical container **46**, and the input into the capture circuit driven from the full wave divider is taken from the cold junction **45** at the apex of the air-tight cage. The output circuit is similar to that of **Fig.15**.

We have found however that even when the component values in the motor driver and motor circuits are carefully selected so that these circuits are co-resonant with the dampened wave (DW) component of the motor driver pulses, the motor power output falls well short of that which should theoretically be attainable. In an endeavour to meet this problem, we replaced the squirrel-cage type induction motor **44** by a drag cup motor of type KS 8624 from Western Electric in the expectation that the low-inertia non-magnetic rotor would allow better response to the Dampened Wave component. This motor is similar to one of the types used by Reich in his experiments. Although results were much improved they still fell short of expectations. Replacement of this motor by an inertially dampened motor of type KS 9303, also from Western Electric, provided much better results as discussed below.

Fundamentally, the difficulties we encountered stemmed from the inability of motor couplings to respond efficiently and smoothly, and at the same time, to the pulse and wave components of Dampened Wave impulses: that is, simultaneously to the high-intensity peak current pulses (the front end event), the DC-like component, and to the dampened wave trains these cause, i.e. the pulse tails (or back end event)-or AC-like component. This difficulty is present even when we just seek to run induction motors from the DW impulses of a Tesla coil, the very difficulty that led Tesla to abandon his project of driving a non-ferromagnetic disc rotor mounted on an iron core bar stator with dampened waves.

We believe that the key to the capture of the mass-free energy flux output in electric form by Tesla transmitters, including any injected latent or thermal energy that have undergone conversion into electrical energy is to employ the tuned, unipolar, Y-fed, PAGD-plasma pulser driven split-phase motor drive we have invented (U.S. Pat. No. 5,416,391) in conjunction with an inertially dampened AC servomotor-generator (see **Fig.18**): this has a motor shaft **64** which couples a drag-cup motor rotor **60**, preferably of aluminium, silver, gold or molybdenum, directly to a drag-cup generator rotor **62** that drives a permanent magnet (PM) flywheel **66**, freely rotatable in bearings **67**, that provides inertial damping. The shaft **64**, journalled by bearings **61** in the casing of the motor **44**, provides a power output through optional gearing **68**. The phase windings of the motor **44** are wound on a stator core **70** having concentric elements between which the rotor or cup **60** rotates. This structure makes it ideal for the capture of the DW impulses, whether sourced in the transmitter, amplified in the T/R cavity or sourced in the plasma pulser, all in synchrony. Effectively the motor couples the damping action of the drag-cup sleeve motor rotor, which action, as we have already found for the KS-8624 motors, is quite effective at absorbing the front-end DC-like event, with the inertial damping of the PM flywheel upon the drag-cup sleeve generator rotor, that in turn is quite efficient at absorbing the back-end AC-like wavetrain event.

The KS-9154 motor used by Reich was not an inertial dampened AC drag-cup servomotor-generator. Had Reich succeeded in overcoming the limitations of his 2-phase OR Motor solution, as we have now shown it is possible to do (by applying the Function Y circuit to the PAGD split-phase motor drive which we invented), his motor would have suffered the same limitations which we encountered with the KS 8624 motor.

Any motor, by itself, has an internal or inherent damping whereby the acceleration only vanishes when the rotor is running at constant speed. For motors which operate on the basis of the drag principle, where the asynchronous slip is actually constitutive of the motor action, by inducing eddy currents in the rotor, the inherent damping is always more pronounced than for other induction motors. The damping or braking torque is produced when a

constant current flows through a rotating drag disc or cup.

Aside from this inherent braking, dampers can also be applied to servo motors to further stabilise their rotation. They absorb energy, and the power output and torque of the motor is thereby reduced. Optimal operation of servo motors requires both rapid response on the part of the rotor to changes in the variable or control phase, and a stable response that is free from oscillation, cogging and overshooting. The rapid response is assured by employing low inertia rotors, such as drag-cups or cast alloy squirrel-cages, and the overshooting and oscillation are reduced to a minimum by damping or a retarding torque that increases with increasing motor speed. Typically, in a viscous-dampened servomotor, the damper is a drag-cup generator mounted rigidly on the shaft of the motor rotor, and the generator drag-cup rotates against the stator field of a static permanent magnet field. The generator develops a retarding torque directly proportional to speed, and the energy absorbed by the damper is proportional to speed squared. The damping can be adjusted and, as it increases, the same amount of input power yields lower torque and motor speeds. Inertial-dampened servo motors differ from viscous dampened motors in that the permanent magnet stator of the drag-cup generator is now mounted in its own bearings, either in the motor shaft or on a separate aligned shaft, forming a high-inertia flywheel.

This means that, whereas the motor rotor always experiences a viscous damping in viscous-dampened servo motors, in inertial-dampened servo motors the drag cup motor rotor only experiences a viscous damping while accelerating the flywheel, with the damping torque always opposing any change in rotor speed. Once the flywheel rotates synchronously with the rotor, all damping ceases. Note that this viscous damping is carried out via the coupling of the drag-cup generator rotor, rigidly affixed to the motor rotor, to the PM flywheel, so that their relative motion generates the viscous torque proportional to the relative velocity. Use of drag-cup sleeve rotors in inertially dampened servo motors was largely supplanted by squirrel-cage rotors once the latter became produced as cast alloy rotors. Since inertially dampened motors can be used in open and closed-loop servo applications, and present better stability - even in the presence of non-linearities - and higher velocity characteristics than other induction motors do (Diamond, A (1965) "Inertially dampened servo motors, performance analysis", Electro-Technology, 7:28-32.), they have been employed in antenna tracking systems, stable inertial-guidance platforms, analogue to digital converters, tachometers and torque tables.

The typical operation of an inertially dampened servomotor is as follows: with the reference phase fully excited, the motor rotor -fixedly linked to the generator rotor, as well as the flywheel - remain immobile; once power is applied to the control phase, the motor rotor immediately responds but the flywheel remains at rest. However, as the drag-cup generator **62** is forced to move through the permanent magnetic field of the flywheel, it creates a drag torque that slows down the attached motor rotor proportionally to the acceleration that it imparts to the flywheel that it now sets into motion, thus creating the viscous damper. As the flywheel accelerates, the relative speed of the motor with respect to the flywheel, as well as the damping torque, decrease until both motor and flywheel rotate synchronously and no damping torque is exercised - at which point the drag on the motor cup exerted by the generator cup is negligible.

The KS-9303 motor is an inertial dampened servomotor but is differentiated with respect to other inertially dampened motors, in that (1) it employs a drag-cup sleeve motor rotor made of aluminium, very much like that of the KS-8624, but with slightly altered dimensions and with a shaft extension for the drag-cup copper generator rotor, and (2) the moving flywheel structure was journalled on a separate, fixed shaft, as already described with reference to **Fig.18**. Now, in principle, even application of minimal damping decreases motor efficiency, resulting in diminished torque and speed. Whether the inertial-dampened motor has a drag-cup rotor, a sleeve rotor or a squirrel-cage rotor, the damping increases the rotor slip. Laithwaite considers drag-cup motors as being "dynamically inferior to their cage counterparts" (Laithwaite, E R (1957) "Induction machines for special purposes", London, England, p. 323). If we now add a viscous damping and retarding torque, we should not be able to get much more than a 55% efficiency in the best of conditions. On the other hand, the inertial damping arrangement described will only abstract or supply energy when the motor rotor is accelerating or decelerating relative to the flywheel.

These drag-cup motors, whether inertially dampened or not, develop a constant torque at constant rpm for a given supply frequency and a suitable phase shift capacitance. For each frequency the motors respond to, there is an optimum resonant split-phase capacitance, but other values nearby are still suited for operation, and for each value of capacitance, there is an optimum frequency to which the motors respond. For example the KS-8624 motor responds best at 450 Hz when a 1 microfarad capacitance is employed, responds best at 250 Hz when a capacitance of 10 microfarads is employed, and responds best at 60 Hz, when a capacitance of 100 microfarads is employed. As the capacitance increases, the resonant CW frequency of the motor is displaced to lower values. If we fix the capacitance at a value (e.g. 10 microfarads) suitable for testing the frequency response at a fixed voltage of 12 VAC, the observed result for both the KS-8624 and KS-9303 motors show a response distribution of the motor rotary velocity that has an identical peak at 250 Hz for both motors, with the response decreasing to zero smoothly on both sides of the peak.

These results indicate that, when wired as a split-phase motor, the motor rotary velocity varies not as a function of voltage or current, but as a function of frequency when the phase-splitting capacitance is fixed within a suitable range, there being an optimum frequency mode for each value of suitable capacitance, with lower values of capacitance favouring higher frequency modes. For a given frequency and capacitance, the motor rotary velocity remains essentially constant and independent from voltage and current input, and thus at a plateau. Torque, in the same circuit arrangement, follows exactly the same pattern as rotary velocity, as a function of input frequency at a fixed potential. Torque is linearly proportional to rpm in these motors when they are split-phase wired, and rpm linearly proportional to CW frequency, which makes them ideal for experimentation and determination of power output computations. Moreover, since these are drag machines, the slip itself determines the rotor currents and these are susceptible to tuning such that their retardation and relative position in the field can find resonant modes for varying CW frequency and capacitance.

In the circuit of **Fig.17** when using the KS 9303 motor, the inertial damping of the flywheel coupling retards the motor rotor currents sufficiently to allow them to build up torque, with the entire motor assembly serving as the preferred sink for all of the energy, mass-free and mass-bound, captured by the receiving coil circuit with a drawing action established by the motor on the circuit, and providing satisfactory absorption by an inertial damper of the combined, synchronised, dampened wave impulses, those occurring at a low frequency as a result of the firing of the PAGD reactor, and those occurring at a higher superimposed frequency -sourced in the transmitter circuit and picked-up by the receiver plate and coil. The action of each DW impulse train itself generates two different events: the DC-like auto-electronic-like discontinuity which sets the motor in motion and initiates the rotor currents, and the AC-like dampened wavetrain which supports the consistency of those rotors. The concentration of current required to kick-start the motor is provided by the DW impulses of the PAGD reactor, whereas, once the motor is in motion, and particularly, once it is stabilised by the flywheel, the cumulative action of the higher frequency DW impulses makes itself felt by accelerating the rotor to an optimum rotary velocity.

For the next series of tests we employed the basic circuit diagram of the improved motor shown in **Fig.19**. The transmission station is the typical Tesla transmitter with a line-fed, 60 Hz vibrator stage. At the line input to the first stage, we place a calibrated AC wattmeter (Weston Model 432), and a Beckman 330B rms ammeter in series with the hot lead, we set the vibrator stage for 41 clicks, consuming between 28.5W and 35W, depending upon circumstances yet to be described. This consumption was confirmed by driving the coil from an inverter powered by a 12 volt battery. The inverter consumes 2.16 watts, and is 90% efficient. The total consumption from the battery was 42 watts (12V at 3.5A); once the 2.16 watts is deducted and the efficiency taken into account, we obtain the same 36W (vibrator stage at max., i.e. 47 clicks, in this experiment). The T/R gap is adjusted to 3", and 2 square foot plates are used. Transmitter and receiver coils are tuned, and so are the plate capacitances, to 250 kHz, also the capacitances of the Function Y circuit connected at the output of the receiving coil.

The rectified voltage and current generated by the transmitter secondary and by the transmitter plate was ascertained with a coil-tuned wave-divider (Function Y) circuit by loading it with different resistive values. The results constitute a measure of the mass-bound electrical power output directly from the transmitter apparatus. The same method was employed to ascertain the voltage, current and power of the mass-bound charges circulating in the receiving plate and coil circuit. The results are shown in Table 8 below:

TABLE 8

Massbound currents rectified by Function Y at the output of the Tesla transmitter, transmitter plate and receiver plate, as a function of the bleeding resistance employed in each of the function Y arms

	VDC (kilovolts)	ADC (amp)	WDC (watts)	R/arm (Mohm)
Direct from 2°	42–50	$3 * 10^{-5}$	1.26–1.5	500
From 2° (T) plate	26	$2 * 10^{-5}$	0.52	500
From 2° (R) plate	15.1	$1.25 * 10^{-5}$	0.189	500
Direct from 2°	20.4	$3.4 * 10^{-4}$	6.936	50
From 2° (T) plate	15.2	$2.4 * 10^{-4}$	3.648	50
From 2° (R) plate	9	$1.2 * 10^{-4}$	1.08	50
Direct from 2°	3.3	$1.75 * 10^{-3}$	5.775	1
From 2° (T) plate	3.5	$2 * 10^{-3}$	7.0	1
From 2° (R) plate	2.95	$1.6 * 10^{-3}$	4.72	1

The results indicate that the highest mass-bound power assembled by the secondary transmitter circuit does not exceed 7 watts - and this is directly output from the secondary **26** when the load is 50 Megohm, or from the transmitter plate when the load is 1 Megohm. The mass-bound electric power emulated by the receiving circuit (plate, coil and Function Y without the plasma pulser circuitry) never exceeds the mass-bound electric power outputted directly by the transmitter, and peaks when the resistive load value (1 Megohm) approaches the pre-breakdown resistance range of the vacuum tube, at 4.72W. These findings then indicate that when the transmitter circuit is consuming a maximum of 35W, a typical output from the secondary of the transmitter is 7W, and at 3" of distance within the proximal field of the latter, the pick-up by a tuned receiver will be of the order of 5W of mass-bound current duplicated within the receiving coil. The loss in the first stage is therefore on the order of sevenfold.

Continuing with the description of the circuit of **Fig.19**, a 128 cm^2 plate area, 6 cm gap PAGD reactor is used, connected as described in our prior art to a high-vacuum rotary pump (Correa, P & Correa, A (1995) "Energy conversion system", U.S. Pat. No. 5,449,989). Pressure readings were obtained with a thermocouple gauge during the operational runs. The KS-9303 motors to be tested are then connected to the PAGD reactor in the usual capacitatively-coupled, inverter fashion described in our prior art (Correa, P & Correa, A (1995) "Electromechanical transduction of plasma pulses", U.S. Pat. No 5,416.391). Their rpm is detected by a stroboscopic tachometer and fed to a Mac Performa 6400 running a motor algorithm program calculating the power output. Motor measurements were made at five minutes into each run for the unloaded motors, and at ten minutes for the inertially dampened motors.

All experiments were carried out in the same work session. The experimental determination of the continuous rotary power output as a function of the reactor pulse rate confirmed that the improved circuit develops maximum rotary capture of the mass-free energy in the receiver circuit at the lowest rates of pulsation, just as we have previously found for the conversion system of U.S. Pat. No. 5,449,989. Furthermore, the data showed that even motors of type KS-8624 are able to output power mechanically in excess of the mass-bound power output by the transmitter (7W) or captured by the receiver (5 to a max. of 7W), once the PAGD rate decreases to 1.5 PPS. Such an anomaly can only be explained by the system having become able to begin capturing the mass-free energy flux in the receiver circuit that we know already is output by the transmitter circuit. But this excess mechanical power is still less than the power input into the transmitter, and clearly so. It represents a power gain with respect to the secondary, but a loss with respect to the primary. The full breadth of the capture of the mass-free electric energy flux circulating in the receiver circuit is not seen until the motors are resonantly loaded because they are inertially dampened.

The KS-9303 motors, once inertially dampened, and thus loaded, are able to recover enough power from the mass-free energy field to develop a mechanical power, not just greatly in excess of the mass-bound power of the secondary, but also greatly in excess of the mass-bound power input to the vibrator stage and the primary, at 28 to 35W. Once the pulse rate approaches the same 1.5 PPS marker, mechanical power in excess of the mass-bound electric power input to the primary becomes evident, peaking at nearly three times that input. In fact, the highest output recorded was also obtained with the lowest input to the transmitter circuit, the highest exact coefficient observed in this experiment being 100.8W / 28W = 3.6. Furthermore, with respect to the secondary mass-bound output, the same mechanical rotary output represents a much greater overunity coefficient of performance, on the order of 14.4 times greater. This is at least partly the result of the receiver and motor capture of the mass-free electric energy output by the transmitter, and may be partly the result of mass-free energy engrafted by the PAGD regime in the PAGD reactor.

Reviewing the mechanical power output results as a function of increasing vacuum in the PAGD reactor and at different output power levels, any motor performance below the 5-7W limit of the traditional mass-bound output power of the secondary represents an output mechanical power loss with respect to both the mass-bound secondary output and the mass-bound primary input. All the results for pressures down to 0.03 Torr fall into this category, and thus represent a very inefficient coupling to the PAGD regime. Any motor performance between 7W and 28-35W represent a loss with respect to the electrical power input to the transmitter system, but a net gain of power with respect to the mass-bound secondary power output. None of the non-inertially dampened motors tested were able to perform outside of this area, under the test conditions. With more efficient primary to secondary couplings in the transmitter station, however, one could advantageously employ these motors alone to extract some of the mass-free power of the secondary or to operate them in enclosed vessels without conventional external electrical connections.

To reach satisfactory levels of recovery of mass-free energy, one must dampen the superimposed DW impulses. Hence, all results showing outputs in excess of 35W were obtained using the inertially dampened KS-9303 motors, and represent a net overunity power gain over both the power input to the primary and the mass-bound power output by the secondary, or the mass-bound power emulated by the receiver circuitry. This happens when the PAGD pulse rate falls to 2 PPS, with the rotary power output steeply increasing as the rate falls to 1 PPS.

One of the interesting features of the motor circuitry we have proposed is that it can operate with pulsed plasmas in both the TRD and the AGD regions, the least efficient response occurring in the NGD region near the Paschen minimum. One might think that the voltage depression would allow increased current intensity supplied to the motors, but in fact that is not observed, with the flashing of the NGD yielding erratic oscillations and low values of current. In keeping with the notion that the TRD plasma is mainly composed of lagging positive ions, whereas the PAGD plasma is mostly an electron plasma, the observed direction of rotation of the motors is opposite in the TRD region to that of the AGD region. The NGD region therefore marks the depression where the velocity vectors change direction. In the second or PAGD region, motor operation is very quiet, unlike what is observed in the TRD region.

Part and parcel of the tuning of the circuit components is the selection of the optimum capacitances employed to couple the PAGD reactor to the motor circuit and split the phase to feed the auxiliary winding of the motor. We have experimented with capacitances ranging from 0.5 to 100 microfarads, and found that best results (for the specific circuit in question - including the characteristics of the transmission), were such that the optimum value of the PAGD coupling capacitance lay near 4 microfarads, and the phase splitting capacitance, near 1 to 4 microfarads, depending upon weather conditions. In good weather days lower capacitance values can be used, while in bad weather days higher capacitances are needed. For ease of comparison in demonstrating the need to tune the circuit by employing optimum capacitances in those two couplings (reactor to motor, and motor phase coupling), we employed the same capacitances in both circuit locations.

A comparison of tests using 1 and 4 microfarad values shows the difference caused by changing those capacitances from their optimum value: across all discharge regions of the pressure range that was examined, the four motors tested, operated with greater motor speeds when the capacitances are set to 4 microfarads rather than to 1 microfarad. The less efficient performance obtained with 1 microfarad capacitance fits the inverse correlation of pulse power with increasing pulse frequency, such as we have found for the PAGD regime. This is made evident by a comparison of rpm versus pulse rate for the two capacitance values being considered. They demonstrate the higher pulse rates observed with the lower capacitance, that correlate with the lower motor speeds, and result in lower efficiency of the motor response. The results equally indicate that low capacitance values increase the pulse rate, but if this increase is out of tune with the rest of the circuit values, it results in power waste because it imposes a rate that is not optimum.

We have also determined experimentally that the efficiency of the system is affected by external weather conditions, higher efficiencies being noted on a fine bright day than under poor weather conditions even though the apparatus is not exposed to such conditions. This may reflect a diminution under poor weather conditions of latent mass-free energy that can be taken up by the system.

The observed high efficiency of circuits including inertially dampened motors indicates that the phenomenon does not reduce to a mere optimum capture of, DC-like pulses produced by the reactor in what is essentially an AC motor circuit. Effectively, the pulsed plasma discharge deploys a front-end, DC-like pulse, or discontinuity, but this is followed by an AC-like dampened wave of a characteristic frequency (having a half-cycle periodicity identical to that of the front-end pulse) to which the motor circuit also responds. Moreover, the mass-free electric radiation from the transmitter circuit itself induces, in the receiver antenna, coil and circuit, and in the reactor discharge itself, the train of finer dampened wave impulses responsible, after conversion through the wave-divider, for the mass-bound rectified current which is employed to charge the plasma reactor to begin with. Serving as trigger of the plasma discharges in the reactor are the DW impulses circulating in the receiver circuit, such that the two different lines of DW impulses, in the receiver circuit (for example 120 PPS for the pulses and 154 kHz for the waves) and from the reactor, are synchronised by interpolated coincidences, since their pulse and wave frequencies are different. Ideally, these two superimposed DW frequencies are harmonics or made identical. The receiver stage involves capture of the mass-free electric energy received from the transmitter, duplication of the mass-bound current in the receiver coil, and injection of latent and sensible thermal energy in the T/R gap cavity which augments the emulated mass-bound current.

The mass-bound current is employed to charge the wave-divider capacitance bridge and therefore the reactor. In turn, the plasma pulses from the reactor are superimposed with the DW impulses from the receiving coil, and together they are coupled to the split-phase motor drive. Hence the first receiver stage employs the totality of the energy captured in the T/R gap cavity - mass-free electric energy transmitted by the **T** plate, latent and sensible thermal energy injected at the surface of the **R** plate - and produces in the receiving coil a mass-bound current comparable to that assembled in the transmitter coil by the action of the primary. The mass-bound current is stored in the wave-divider bridge and used to drive the plasma reactor in the PAGD region. Subsequently, the autogenous disruptive discharge that employs a substantial electron plasma generates both a concentrated, intense flux of mass-bound charges in the output circuit, and a mass-free oscillation of its own. The dampened motor is therefore fed directly with (1) the intense mass-bound current output from the reactor; (2) the pulse and wave components of the mass-free electric energy captured by the receiver plate and coil (and matched by conduction through the earth), and which are gated through the wave-divider and the reactor for the duration of the PAGD channel; and (3) any mass-free latent energy taken up from the vacuum by the PAGD event. Once the

motor is set into motion, and is resonantly loaded with an inertial damper, we believe that it will also respond to the much weaker DW impulses captured by the receiver, since these impulses encompass both a DC-like front end - further enhanced by analytic separation through the wave-divider - and a dampened wave at 154 kHz.

Essentially, the DW impulses that are ultimately sourced in the transmitter - and received unipolarly through the T/R gap - have sufficient DC-like potential (plus all the other requisite physical characteristics, such as frequency) to contribute directly to the motor response, once the motor has gained substantial speed (for they lack the current to set it into motion, one of the contributions from the plasma pulser). This is the case, provided that the motor itself is suited for absorption of both DC-like pulses and AC-like dampened waves, which is precisely the case with motors of the type shown in **Fig.18** since the inertia of the flywheel is overcome through homopolar absorption of the dampened oscillations simultaneously in the motor drag-cup rotor and in the generator drag-cup rotor.

We also tested these inertially dampened motors in the traditional DC power supply-driven PAGD circuit we have taught in our previous patents, that is, circuits with an overt HV DC power source, and thus in the absence of any Function Y circuit or transmitter circuit. Here then, only the DW impulses generated by the PAGD reactor can account for the motor response. The tube employed (A31) had an area of 256 cm^2, and a gap distance of 4 cm. Coupling capacitances employed were 4 microfarads for the inverter coupling, and 1 microfarad for the split phase motor coupling. The DC power supply delivered up to 1 ampere of current between 150 and 1,000 VDC, and the ballast resistor was adjusted to 215 ohms. Having determined the basic physical characteristics of the reactor's behaviour in the circuit under consideration, we conducted our experiment in the PAGD region. We chose a pressure of 0.6 Torr, just off from the Paschen minimum, as we intended to benefit from the lower sustaining voltage which it affords.

The experiment basically consisted of increasing the sustaining voltage at this fixed pressure in the PAGD regime, and measuring the diverse physical parameters of the circuit and motor response in order to ultimately ascertain the difference between the input electric DC power and the output mechanical rotary power. We first looked at how the motor rpm response varied as a function of the sustaining voltage (V_S): the results illustrate the importance of starting close to the Paschen minimum in the pressure scale, since the KS-9303 motors reach plateau response (at 17,000 rpm) when the reactor output voltage nears 450V. Any further increase in potential is simply wasted. Likewise, the same happened when we measured motor speed as a function of increasing peak DC current, plateau response being reached at 0.1 ADC. Again, any further increase in current is wasted. Essentially then, the optimal power input to the reactor when the output of the latter is coupled to the motor, lies around 45 watts. This is a typical expenditure in driving a PAGD reactor. As for pulse rate we once again find a motor response that is frequency proportional in the low frequency range, between 10 and 40 PPS (all pulse rates now refer solely to PAGDs per sec), but once rates of >40 PPS are reached, the response of the motor also reaches a plateau.

The observed increment in speed from 40 to 60 PPS translates only into an increase of 1,000 RPM, from 16,000 to 17,000 RPM. So, we can place the optimal PAGD rate at ca 40 PPS. The DC electric power input to drive the PAGD reactor was next compared to the rotary mechanical power output by the inertially loaded motor, driven in turn by the reactor. This comparison was first carried out with respect to the PAGD rates. The motor response far exceeds the conventional input power, indicating that the whole system can be tuned to resonance such that optimal power capture inside the reactor takes place, the critical limit rate lying at around 60 PPS, when the motor response is firmly within the pulse response plateau. At this juncture, the break-even efficiency for the measured rates of energy flux over time reach 700% (overunity coefficient of 7), in keeping with the observations and the values we have made in the PAGD conversion system. In the proportional part of the curve, before the plateau is reached, even greater rates of break-even efficiency - up to >1,000% were registered.

These results constitute the first time we have been able to confirm the presence of output energy in excess of break-even over conventional mass-bound energy input in the PAGD inverter system, and the results are comparable to what we have observed and previously reported for the PAGD converter system. At pulse rates greater than 60 PPS a greater input power results in decreased efficiency, also translated into a noticeable heating of the reactor and motor. And this is all the more remarkable as experiments we have conducted with inductive tuning of PAGD reactors, or employing PAGD reactors as replacements for the primaries of Tesla coil assemblies, and still, more recently, with the PAGD inverter circuit driving motors, have all shown that it is possible to operate these reactors with minimal mirroring and heating, preserving essentially the cold-cathode conditions and yet focusing the plasma column so that deposition on the insulator is negligible. It appears that above a certain threshold of optimal efficiency, surplus input energy is just dissipated thermally by both the reactor and the motors.

It should be understood that the above described embodiments are merely exemplary of our invention, and are, with the exception of the embodiments of **Figs. 16 to 19** designed primarily to verify aspects of the basis of the invention. It should also be understood that in each of these embodiments, the transmitter portion may be omitted

if an external or natural source of Tesla waves is available, provided that the receiver is tuned to the mass-free radiation mode of the source. For example if solar radiation is available in which the mass-free component has not interacted with the earth's atmosphere (as in space applications), the receiver is tuned to the voltage wave of the mass-free radiation sourced in the sun, e.g. by using a Tesla coil in the receiver constructed to have an appropriate voltage wave close to the 51.1 kV characteristic of such radiation.

CLAIMS

1. A device for the conversion of mass-free radiation into electrical or electrokinetic energy comprising a transmitter of mass-free electrical radiation having a dampened wave component, a receiver of such radiation tuned to resonance with the dampened wave frequency of the transmitter, a co-resonant output circuit coupled into and extracting electrical or electrokinetic energy from the receiver, and at least one of a transmission cavity between the transmitter and the receiver, a full-wave rectifier in the co-resonant output circuit, and an oscillatory pulsed glow discharge device incorporated in the co-resonant output circuit.

2. A device according to claim 1, wherein the output circuit comprises a full wave rectifier presenting a capacitance to the receiver.

3. A device according to claim 2, wherein the output circuit comprises an electric motor presenting inductance to the receiver.

4. A device according to claim 3, wherein the motor is a split phase motor.

5. A device according to claim 4, wherein the motor is a drag motor having a non-magnetic conductive rotor.

6. A device according to claim 5, wherein the motor has inertial damping.

7. A device according to claim 6, wherein the motor has a shaft, a drag cup rotor on the shaft, and inertial damping is provided by a further drag cup on the shaft.

8. A device according to claim 6, wherein the transmitter and receiver each comprise at least one of a Tesla coil and an autogenous pulsed abnormal glow discharge device.

9. A device according to claim 8, wherein the transmitter and receiver both comprise Tesla coils, and further including a transmission cavity which comprises spaced plates connected respectively to the distal poles of the secondaries of Tesla coils incorporated in the transmitter and receiver respectively.

10. A device according to claim 9, wherein the plates are parallel.

11. A device according to claim 9, wherein the plates are concentric.

12. A device according to claim 9, wherein at least the receiver comprises a Tesla coil driving a plasma reactor operating In PAGD (pulsed abnormal glow discharge) mode.

13. A device according to claim 1, wherein the transmitter and receiver each comprise at least one of a Tesla coil and an autogenous pulsed abnormal glow discharge device.

14. A device according to claim 12, wherein the transmitter and receiver both comprise Tesla coils, and further Including a transmission cavity which comprises spaced plates connected respectively to the distal poles of the secondaries of Tesla coils incorporated in the transmitter and receiver respectively.

15-17. (cancelled)

18. A device according to claim 1 wherein a transmitter/receiver cavity is present and filled with an aqueous liquid.

19. A device for the conversion of mass-free radiation into electrical or electrokinetic energy comprising a receiver of such radiation from a source of mass-free electrical radiation having a dampened wave component, the receiver being tuned to resonance with the dampened wave frequency of the source, a co-resonant output circuit coupled into and extracting electrical or electrokinetic energy from the receiver, and at least one of a transmission cavity between the source and the receiver, a full-wave rectifier in the co-resonant output circuit, and an oscillatory pulsed glow discharge device incorporated in the co-resonant output circuit.

PAULO and ALEXANDRA CORREA

US Patent 5,449,989 **12th September 1995** **Inventors: Correa, Paulo and Alexandra**

ENERGY CONVERSION SYSTEM

This patent shows a method of extracting environmental energy for practical use. In the extensive test runs, an input of 58 watts produced an output of 400 watts (COP = 6.9). This document is a very slightly re-worded copy of the original.

ABSTRACT

An energy conversion device includes a discharge tube which is operated in a pulsed abnormal glow discharge regime in a double ported circuit. A direct current source connected to an input port provides electrical energy to initiate emission pulses, and a current sink in the form of an electrical energy storage or utilisation device connected to the output port captures at least a substantial proportion of energy released by collapse of the emission pulses.

US Patent References:

3205162	Sep, 1965	MacLean.
3471316	Oct, 1969	Manuel.
3705329	Dec, 1972	Vogeli.
3801202	Apr, 1974	Breaux.
3864640	Feb, 1975	Bennett.
3878429	Apr, 1975	Iwata.
4009416	Feb, 1977	Lowther.
4128788	Dec, 1978	Lowther.
4194239	Mar, 1980	Jayaram et al.
4443739	Apr, 1984	Woldring.
4489269	Dec, 1984	Edling et al.
4527044	Jul, 1985	Bruel et al.
4772816	Sep, 1988	Spence.
4896076	Jan, 1990	Hunter et al.
5126638	Jun, 1992	Dethlefsen.

Other References:

Tanberg, R. "On the Cathode of an Arc Drawn in Vacuum", (1930), Phys. Rev., 35:1080.

Kobel, E. "Pressure & High Vapour Jets at the Cathodes of a Mercury Vacuum Arc", (1930), Phys. Rev., 36:1636.

Aspden, H. (1969) "The Law of Electrodynamics", J. Franklin Inst., 287:179.

Aspden, H. (1983) "Planar Boundaries of the Space-Time Lattice" Lettere Al Nuovo Cimento, vol. 38, No. 7, pp. 243-246.

Aspden, H. (1980) "Physics Unified", Sabberton Publications, pp. 14-17, 42-45, 88-89, 190-193.

Pappas, P. T. (1983) "The Original Ampere Force and Bio-Savart & Lorentz Forces", Il Nuovo Cimento, 76B:189.

Graham, G. M. & Lahoz, D. G. (1980) "Observation of Static Electromagnetic Angular Momentum in Vacuo", Nature, vol. 285, pp. 154 & 155.

Sethlan, J. D. et al., "Anomalous Electron-Ion Energy Transfer in a Relativistic-Electron-Beam-Plasma" Phys. Rev. Letters, vol. 40, No. 7, pp. 451-454 (1978).

REFERENCE TO RELATED APPLICATIONS

This application is a continuation-in-part of U.S. application Ser. No. 07/922,863, filed Jul. 31, 1992 (abandoned), and is also a continuation-in-part of U.S. patent application Ser. No. 07/961,531, filed Oct. 15, 1992, now U.S. Pat. No. 5,416,391.

BACKGROUND OF THE INVENTION

1. Field of the Invention:

This invention relates to energy conversion circuits utilising discharge tubes operating in the pulsed abnormal glow discharge (PAGD) regime.

2. Review of the Art:

Such discharge tubes and circuits incorporating them are described in our co-pending U.S. patent application Ser. Nos. 07/922,863 and 07/961,531. The first of these applications discloses discharge tube constructions particularly suited for PAGD operation, and the second discloses certain practical applications of such tubes, particularly in electric motor control circuits. The review of the art contained in those applications is incorporated here by reference, as is their disclosure and drawings.

It is known that there are anomalous cathode reaction forces associated with the cathodic emissions responsible for vacuum arc discharges, the origin and explanation of which have been the subject of extensive discussion in scientific literature, being related as it is to on-going discussion of the relative merits of the laws of electrodynamics as variedly formulated by Ampere, Biot-Savart and Lorentz. Examples of literature on the subject are referenced later in this application.

SUMMARY OF THE INVENTION

The particular conditions which prevail in a discharge tube operated in the PAGD regime, in which a plasma eruption from the cathode is self-limiting and collapses before completion of a plasma channel to the anode gives rise to transient conditions which favour the exploitation of anomalous cathode reaction forces.

We have found that apparatus utilising discharge tubes operated in a self-sustaining pulsed abnormal glow discharge regime, in a double ported circuit designed so that energy input to the tube utilised to initiate a glow discharge pulse is handled by an input circuit substantially separate from an output circuit receiving energy from the tube during collapse of a pulse, provides valuable energy conversion capabilities.

The invention extends to a method of energy conversion, comprising initiating plasma eruptions from the cathode of a discharge tube operating in a pulsed abnormal glow discharge regime utilising electrical energy from a source in a first circuit connected to said discharge tube, and capturing electrical energy generated by the collapse of such eruptions in a second circuit connected to the discharge tube.

BRIEF DESCRIPTION OF THE DRAWINGS

The invention is described further with reference to the accompanying drawings, in which:

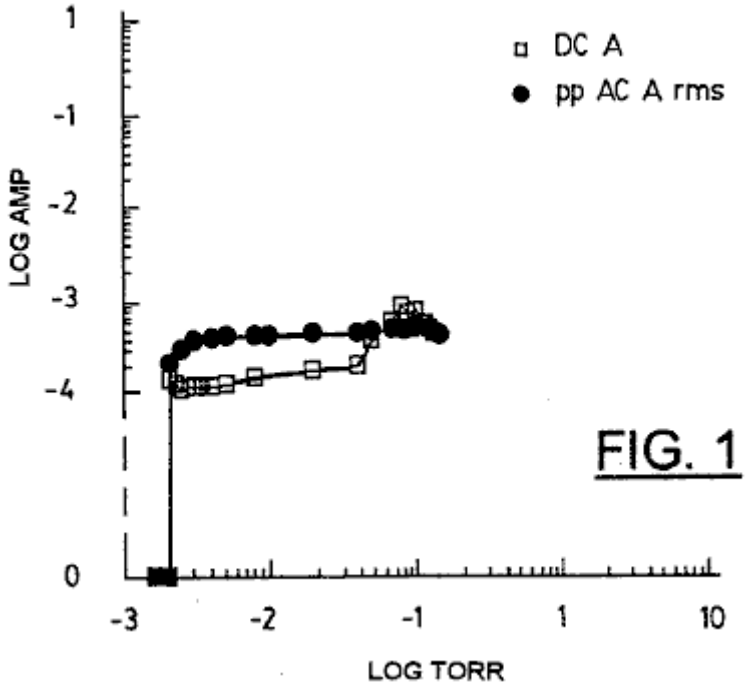

FIG. 1

Fig.1 shows variation of applied DC current and pulse AC rms currents characteristic of a low current PAGD regime, as a function of decreasing pressure, for a 128 cm^2 H34 aluminium plate pulse generator having a 5.5 cm gap length and being operated in the single or plate diode configuration of FIG. 11A, at about 600 V DC.

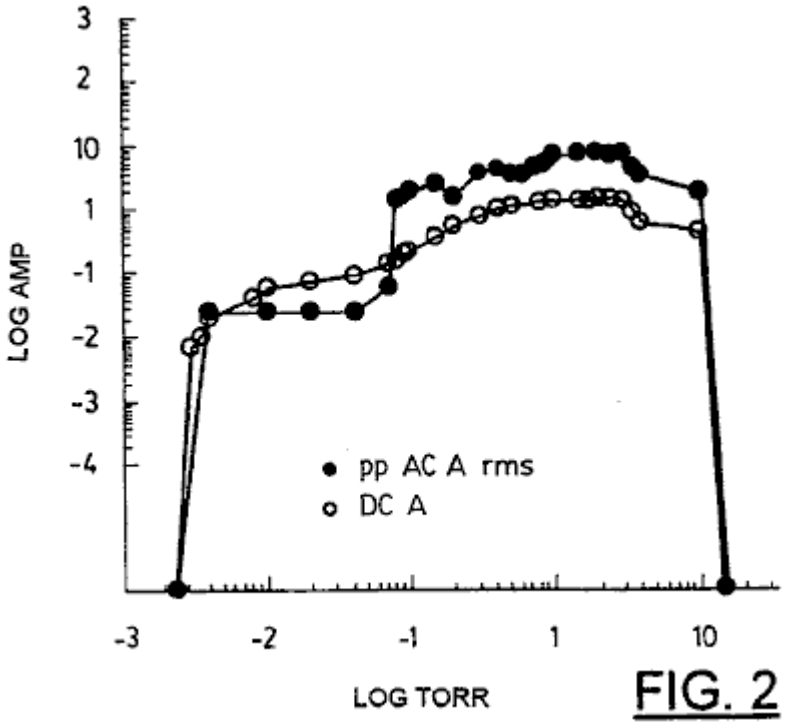

FIG. 2

Fig.2 shows variation of applied DC current and AC rms currents of a high current PAGD regime, as a function of the decreasing pressure, for a device identical to that of Fig.1, and operated at the same potential.

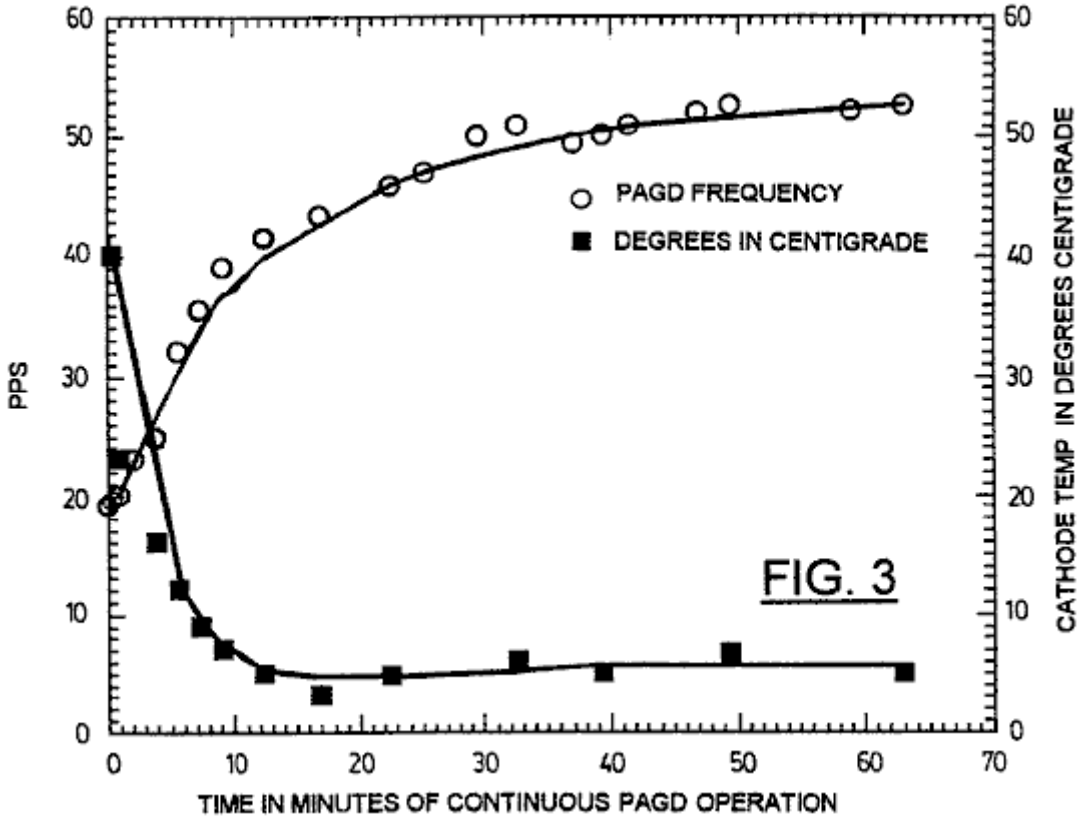

FIG. 3

Fig.3 shows PAGD rate vs pulse generator cathode temperature as a function of the time of continuous PAGD operation, for a pulse generator with 64 cm^2 plates having a 4 cm gap distance, operated at a DC voltage of 555 (av) and R1 = 600 ohms (see Fig.9).

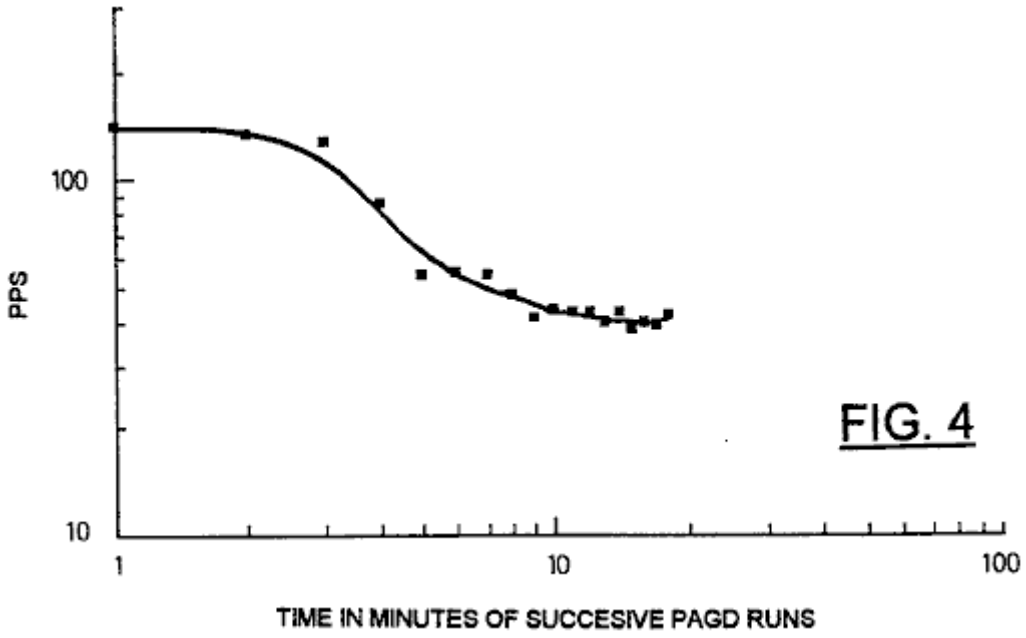

FIG. 4

Fig.4 shows PAGD frequency variation with time, for 18 successive spaced one-minute PAGD runs for a pulse generator with 128 cm^2 plates, and a 5.5 cm gap distance, operated at V DC = 560 (av) and R1 = 300 ohms.

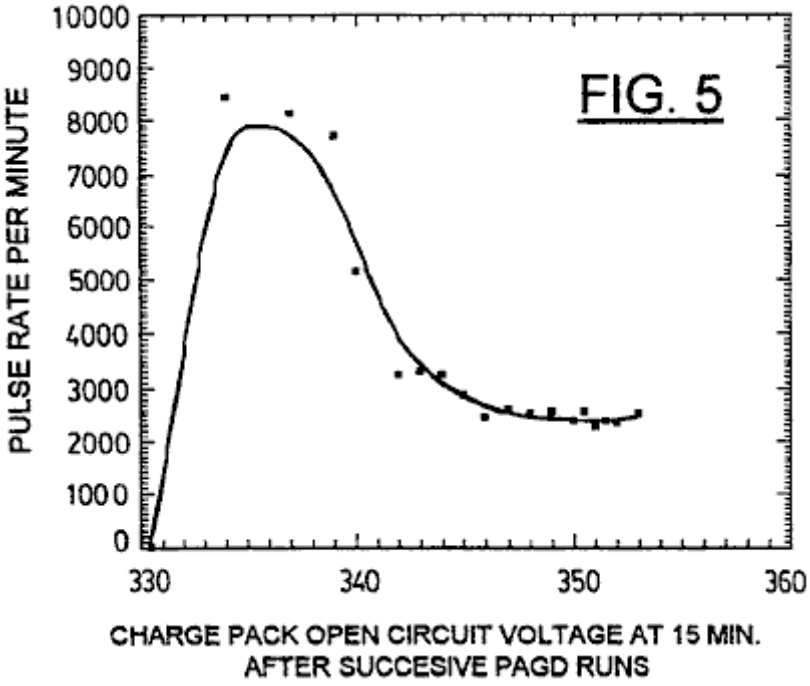

FIG. 5

Fig.5 shows variation of the PAGD frequency in pulses per minute (PPM) with increasing charge of a PAGD recovery charge pack (see Fig.9), as measured in terms of the open circuit voltage following 15 minutes of relaxation after each one minute long PAGD run, repeated 18 times in tandem, under similar conditions to Fig.4.

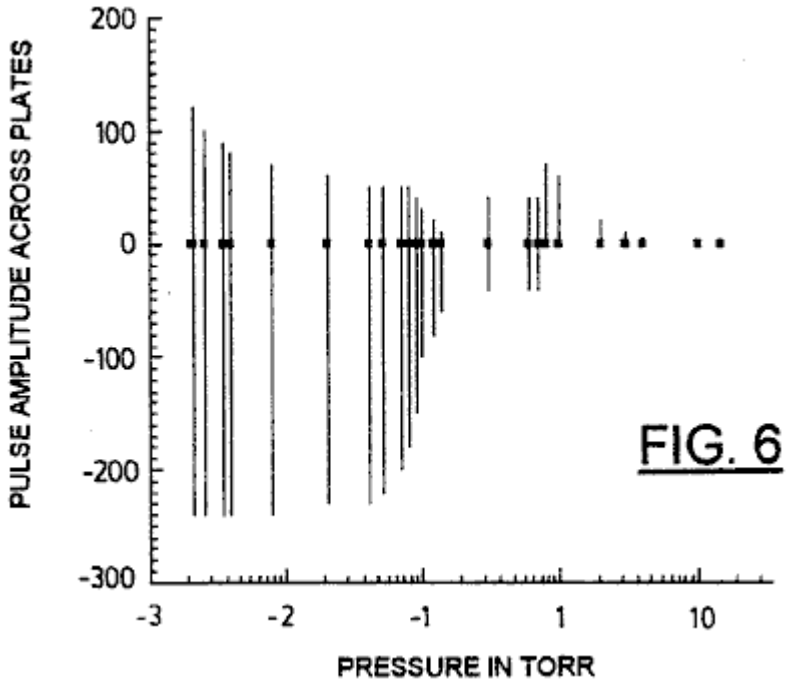

FIG. 6

Fig.6 shows volt amplitude variation of continuous PAGD at low applied current, as a function of decreasing air pressure, for a 128 cm^2 plate area device, gap length = 5 cm; (DC V at breakdown = 860).

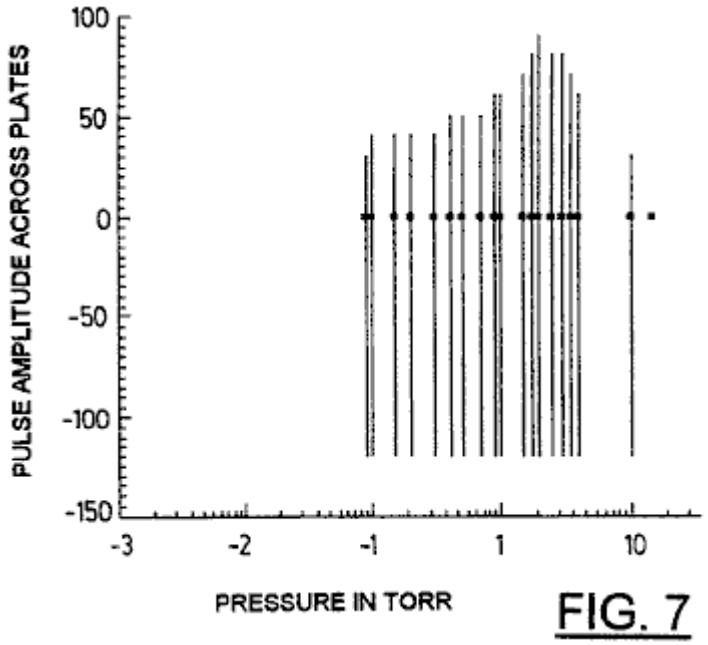

FIG. 7

Fig.7 shows volt amplitude variation of continuous PAGD at high applied current as a function of the decreasing air pressure, for a 128 cm^2 plate area device, gap length = 5 cm; (DC V at breakdown = 860).

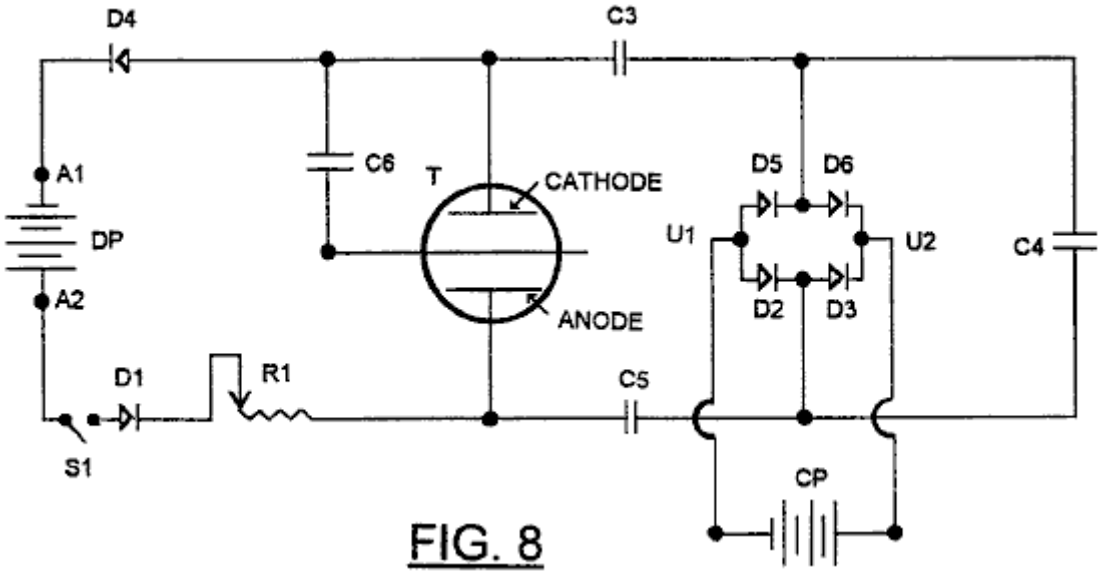

FIG. 8

Fig.8 is a schematic diagram of a first experimental diode (without C6) or triode PAGD circuit.

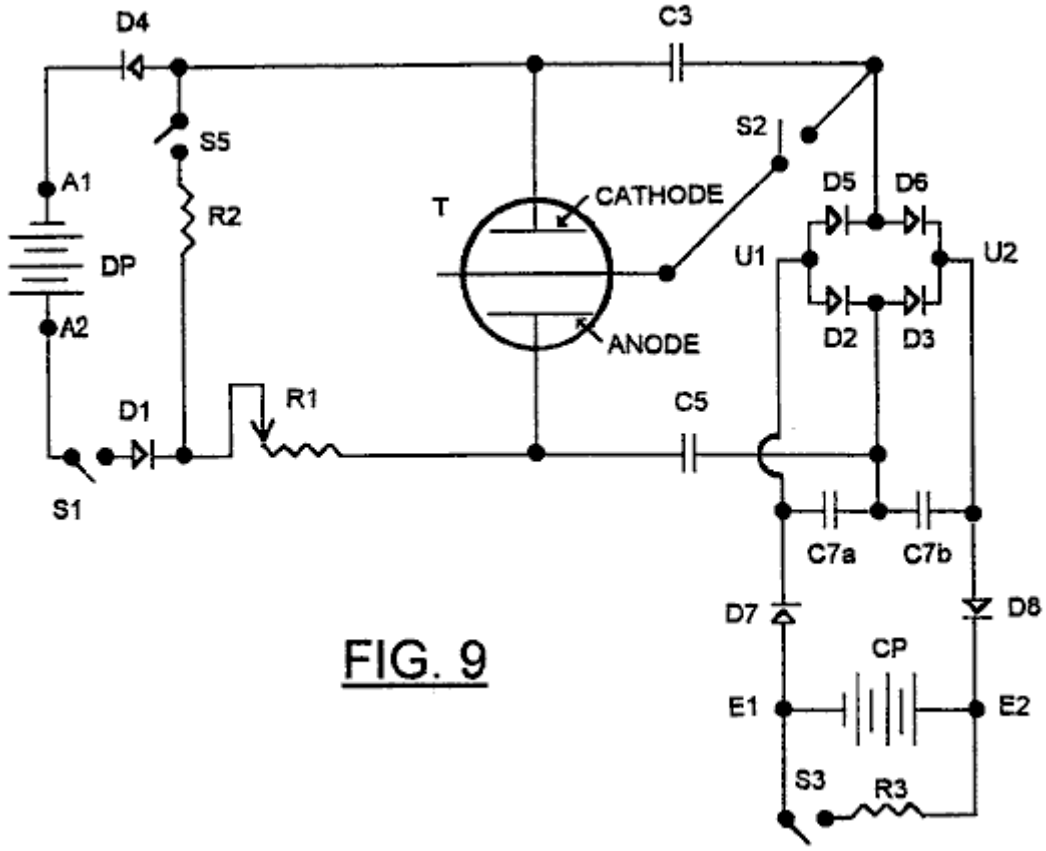

FIG. 9

Fig.9 is a schematic diagram of a preferred diode or triode PAGD circuit in accordance with the invention.

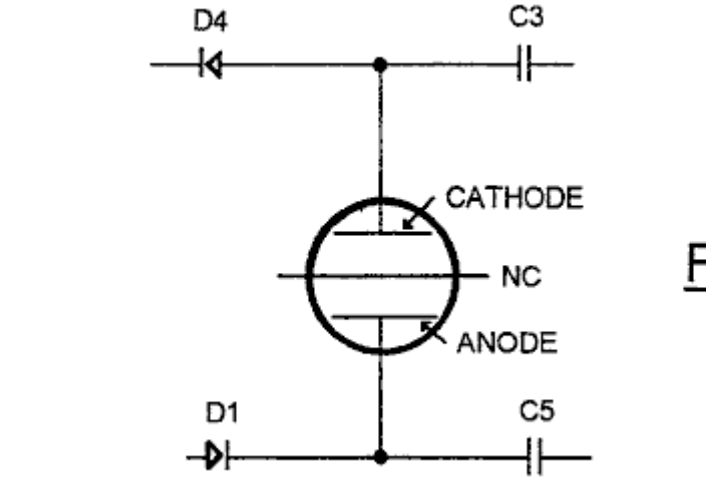

FIG. 10A

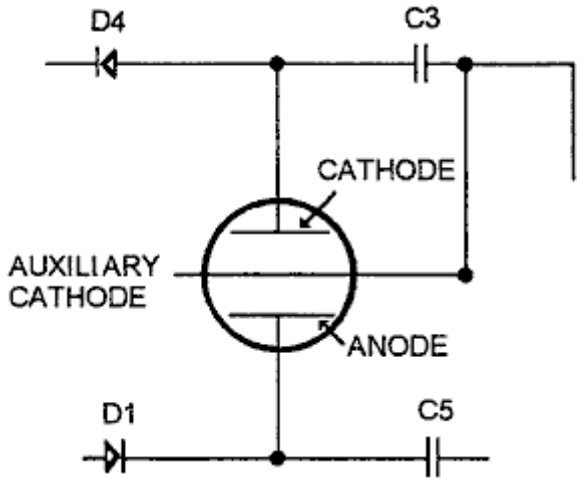

FIG. 10B

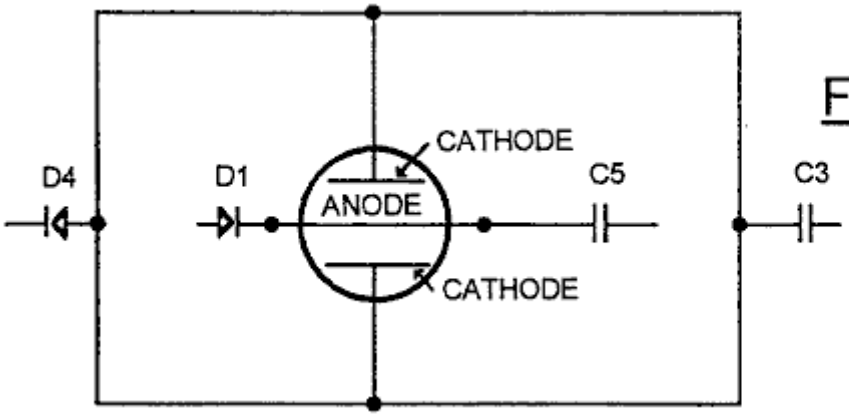

FIG. 10C

Fig.10A, **Fig.10B** and **Fig.10C** are fragmentary schematic diagrams showing variations in the configuration of the circuit of Fig.9.

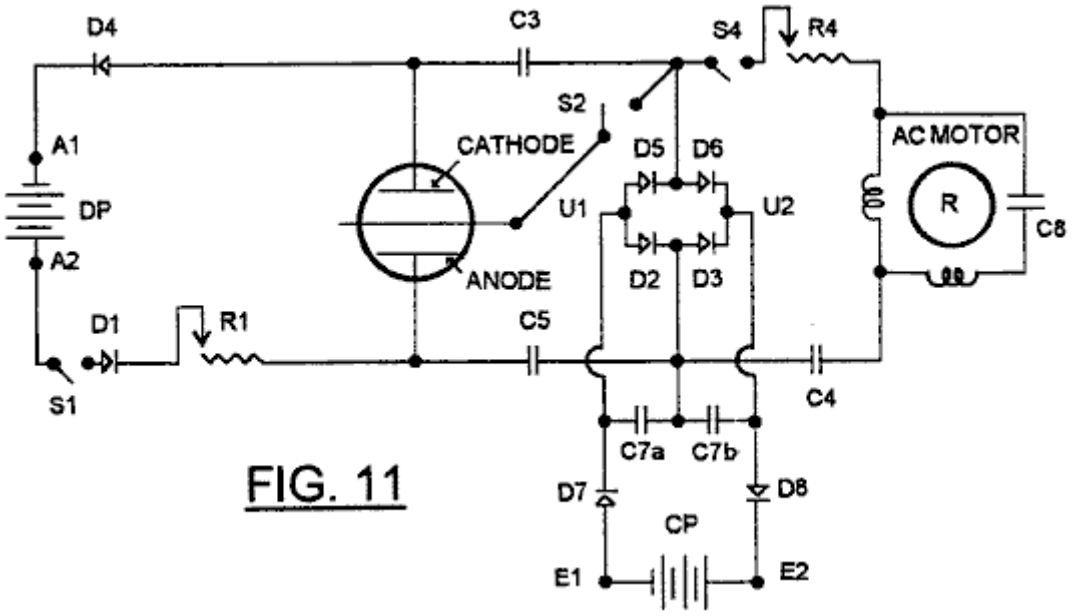

FIG. 11

Fig.11 is a modification of Fig.9, in which an electromagnetic machine, in the form of an electric motor, is connected into the circuit as an accessory electromechanical arm.

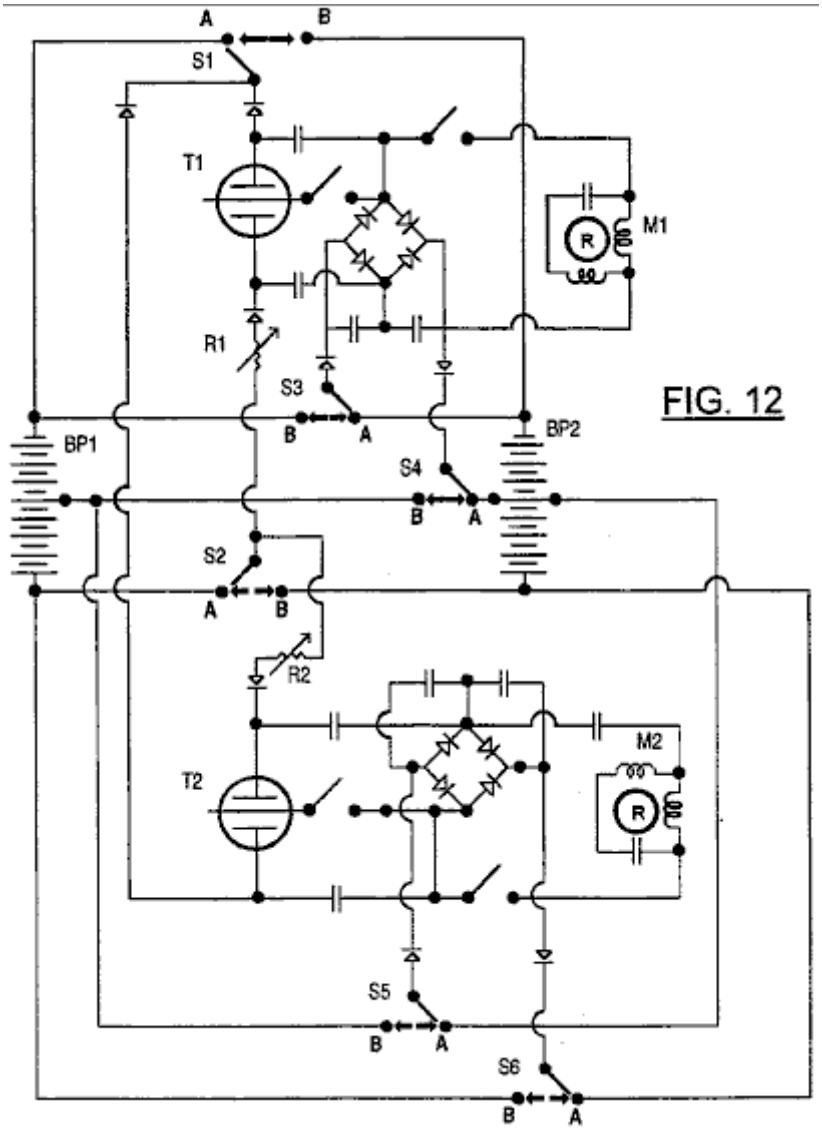

FIG. 12

Fig.12 shows a further development of the circuit of Fig.9, permitting interchange of driver pack and charge pack functions.

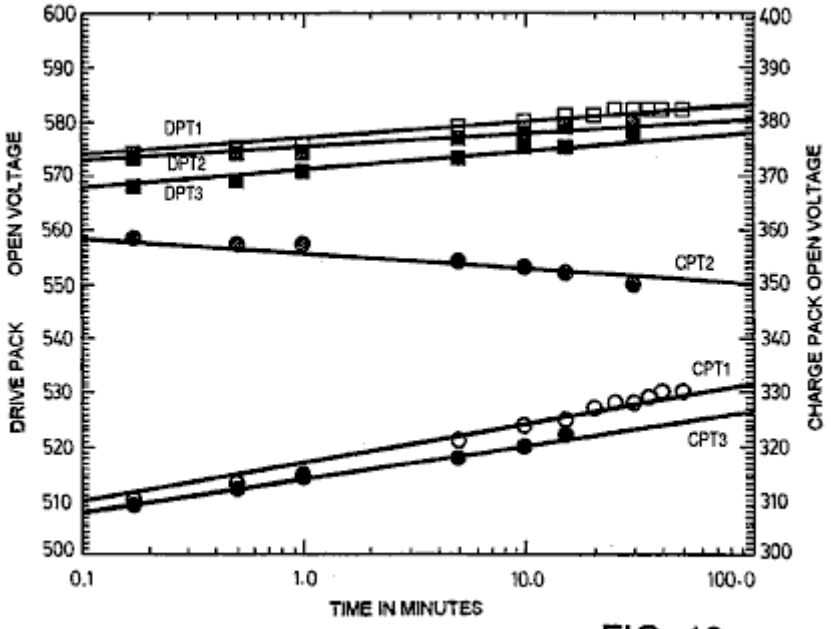

FIG. 13

Fig.13 shows open circuit voltage relaxation curves for battery packs employed in tests of the invention, respectively after pre-PAGD resistive discharge (DPT1 and CPT1), after a PAGD run (DPT2 and CPT2) and after post-PAGD resistive discharge (DPT3 and CPT3).

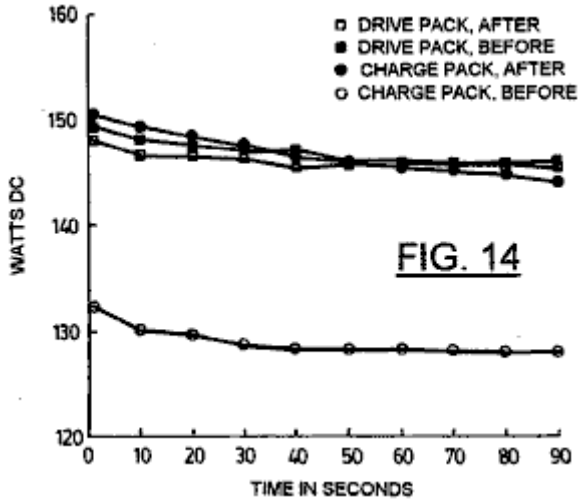

FIG. 14

Fig.14 shows an example of negligible actual power measurements taken immediately before or after a PAGD run, showing both the drive pack loss and the charge pack gain in DC Watts; DP resistance = 2083 ohms; CP resistance = 833 ohms.

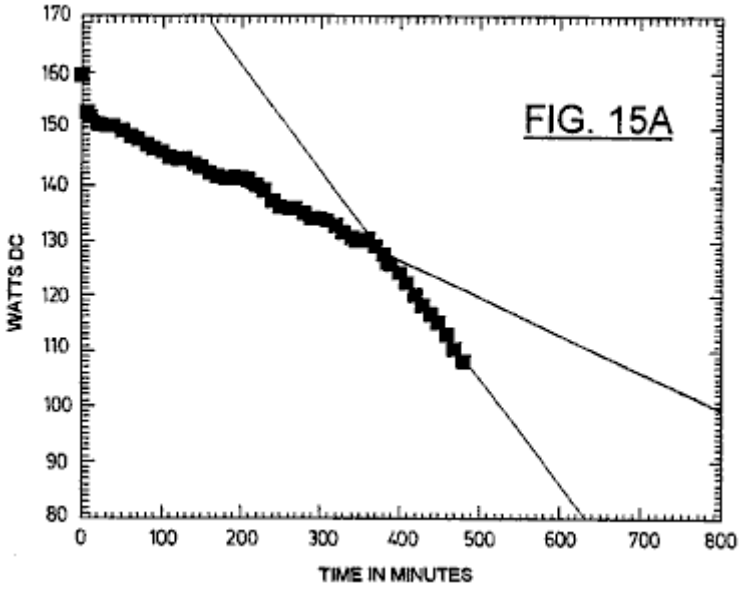

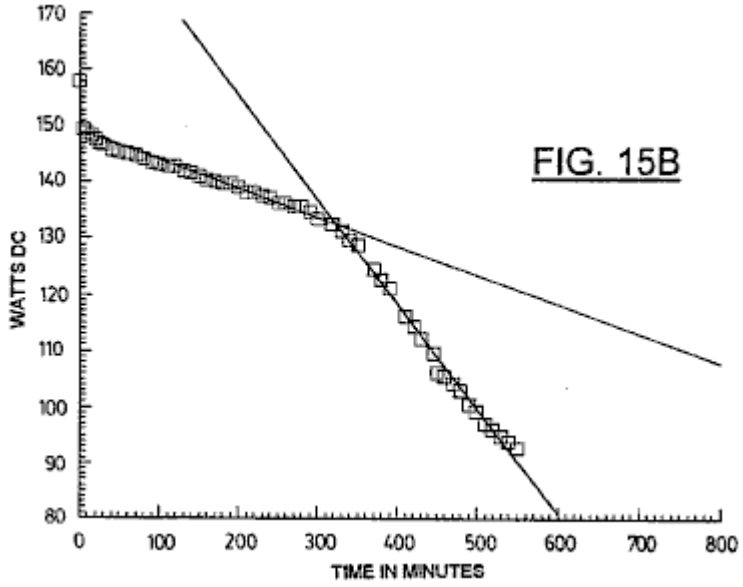

Fig.15A and **Fig.15B** show resistive voltage discharge curves for two separate lead-zero gel-cell packs utilised respectively as the drive and the charge packs; load resistances employed were 2083 ohms across the drive pack (Fig.15A) and 833 ohms across the charge pack (Fig.15B).

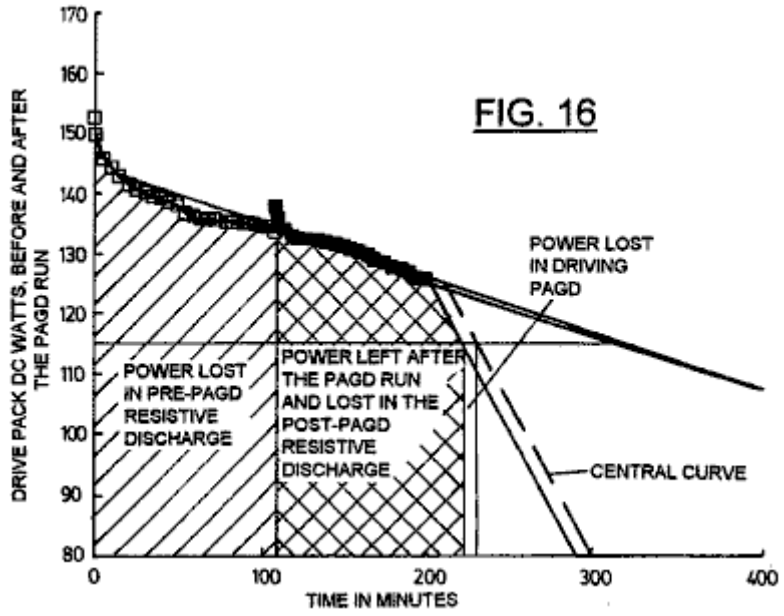

Fig.16 shows resistive discharge slopes for a drive pack before and after a very small expenditure of power in providing energy input to a PAGD run; R = 2083 ohms.

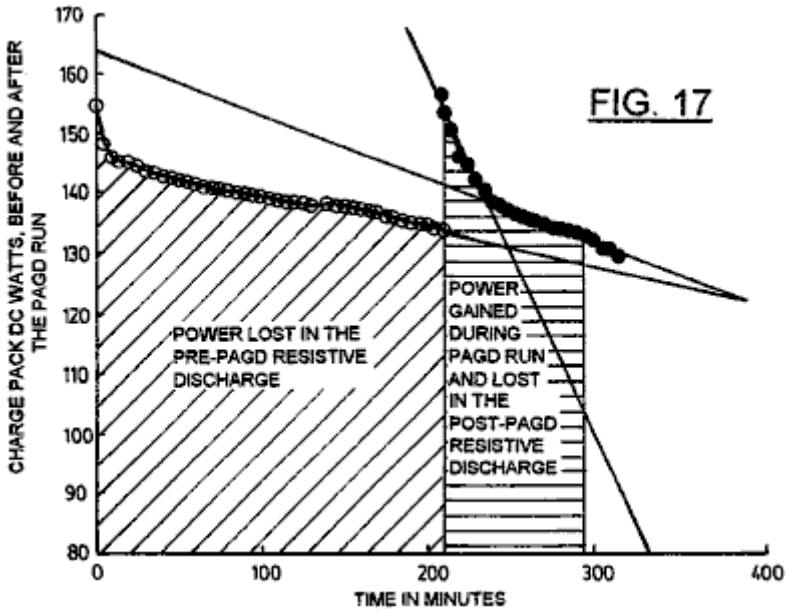

Fig.17 shows resistive discharge slopes for a charge pack before and after capturing energy from the collapse of PAGD pulses in the same test as Fig.15; R = 833 ohms.

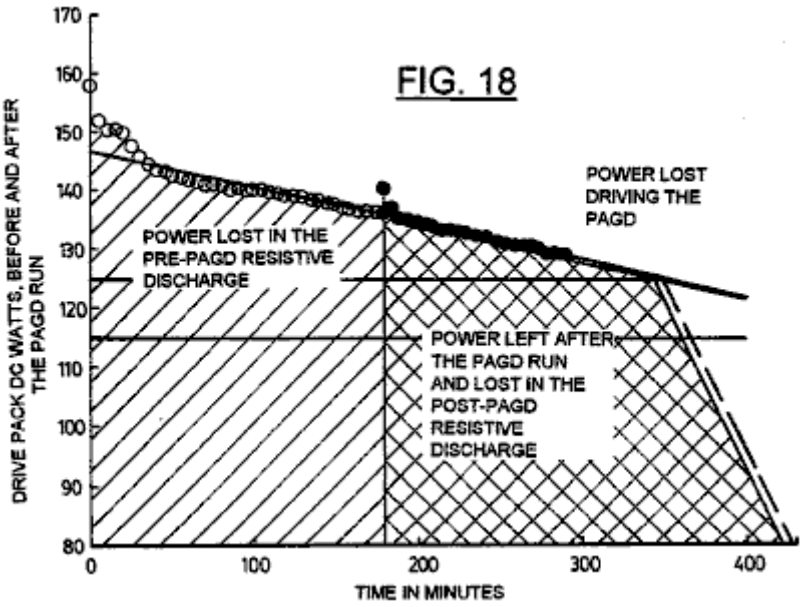

Fig.18 shows resistive discharge slopes for a drive pack before and after a very small expenditure of power in providing energy input to a PAGD run in a further experiment; R = 2083 ohms.

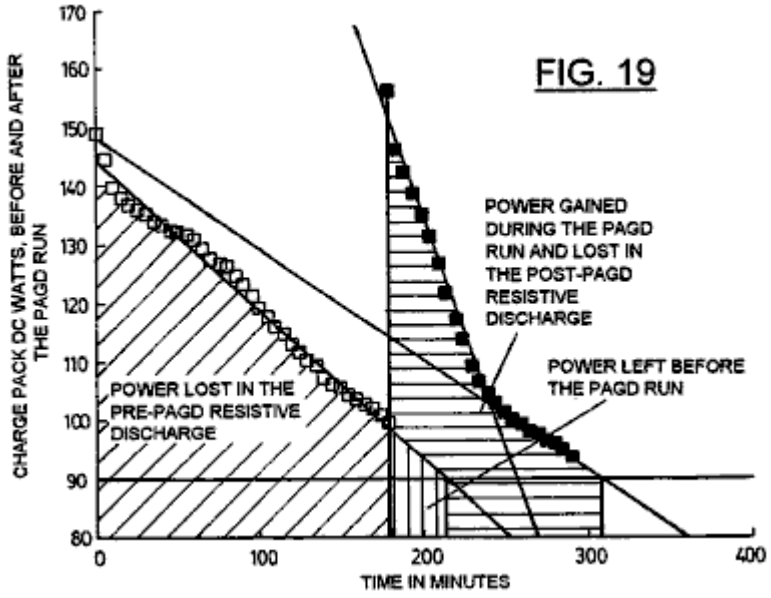

Fig.19 shows resistive discharge slopes for a charge pack before and after capturing energy from the PAGD run of Fig.18; R = 833 ohms.

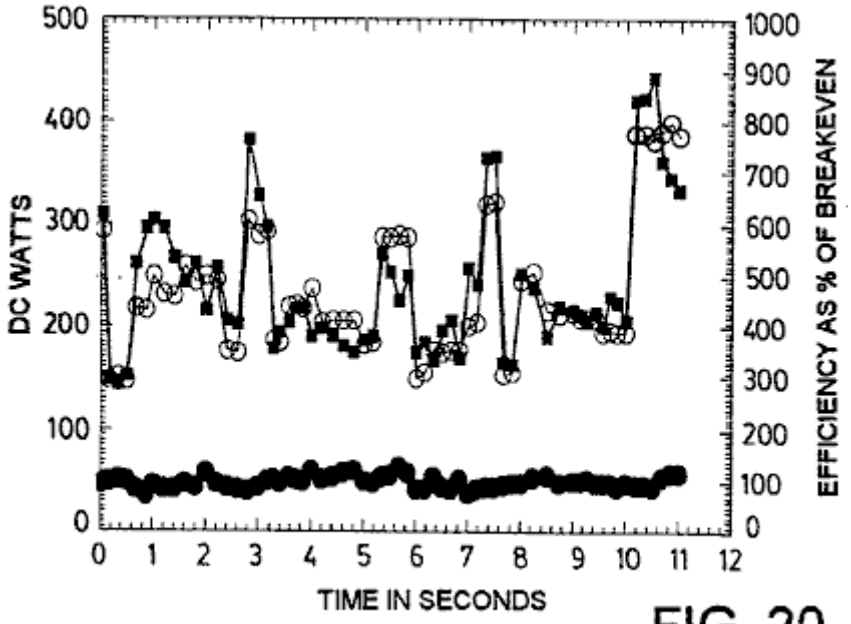

FIG. 20

Fig.20 shows an example of operational measurements taken videographically during a 10 second period for both the power consumption of the drive pack (PAGD input) and the power production captured by the charge pack (PAGD output); the two values are also related by the expression of percent break-even efficiency.

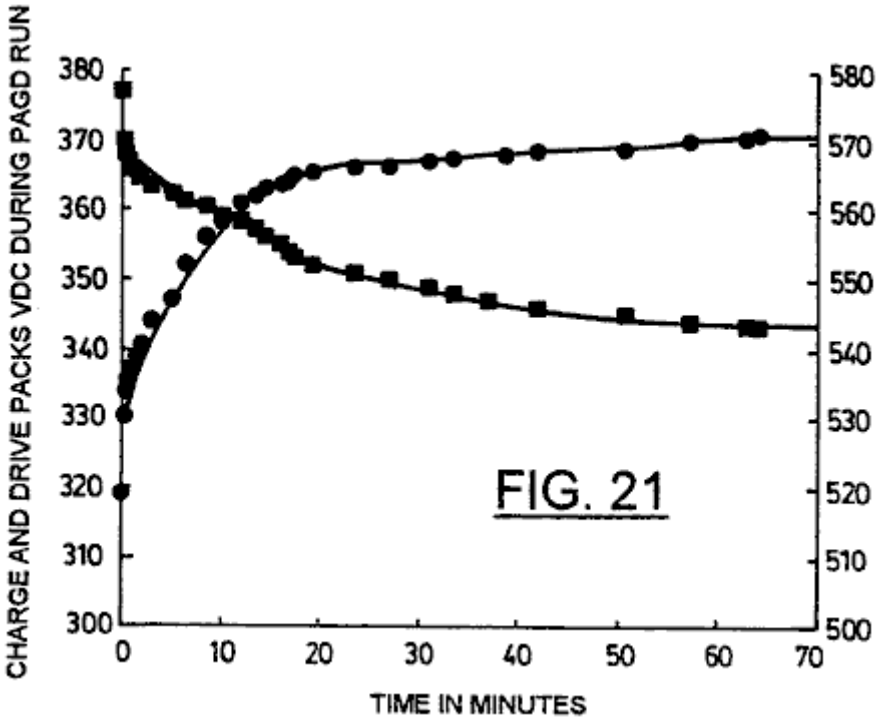

FIG. 21

Fig.21 shows variation of PAGD loaded voltage of a drive pack (in squares) compared with the PAGD charging voltage of the charge pack (in circles), during more than 1 hour of continuous PAGD operation.

DESCRIPTION OF THE PREFERRED EMBODIMENTS

The basic PAGD function and the construction of discharge tubes specifically designed for PAGD operation are described in our corresponding co-pending applications Nos. 07/922,863 (the "863" application) and 07/961,531 (the "531" application). For purposes of the experiments described below four aluminium H34 plate devices (one with 64 and three with 128 cm^2 plate areas) and three aluminium (H200) plate devices (one with 64 and two with 128 cm^2 plate areas), with inter-electrode gap lengths of 3 cm to 5.5 cm, were utilised at the indicated vacua, under pump-down conditions and with either air or argon (ultra high purity, spectroscopic grade 99.9996% pure)

constituting the residual gas mixture. The pump-down conditions were as described in the “863” application. Some experiments were performed with the tubes under active evacuation, at steady-state conditions, while others utilised sealed devices enclosing the desired residual gas pressures.

The circuit designs utilised in the various experiments to be described are set out further below, and represent further developments and extensions of the circuits set forth in the “531” application.

Test equipment utilised was as follows:

An Edwards (trade mark) thermocouple gauge (TC-7) was employed for the determination of pressure down to 1 micron of mercury (0.001 Torr).

Banks of Beckman (trade mark) rms multimeters 225 and 330 (30 and 100 kHz bandwidths, respectively) were utilised for all current measurements.

Frequency meters capable of discriminating events up to 0.1 nanosecond apart, and having adjustable amplitude windows, were used. Direct analysis on a Tektronix (trade mark) dual-trace, storage scope (Model 549) was also carried out for both parameters.

Split-phase, single-phase and two-phase motors were employed, of the synchronous, induction and universal types, as previously described in the “531” application, in the accessory electromechanical arm that may be coupled to the power producing circuit described in the present application.

Large banks of 12 V, 6 Ah lead-acid gel cells (Sonnenschein (trade mark) A212/6S) were utilised either as power sources (designated as drive packs) or as accumulators of the energy (referred to as charge packs) captured by the test circuits. Charge packs made of rechargeable 9V NiCad or of nominally non-rechargeable C-Zn or alkaline batteries were also utilised.

PAGD emission areas were determined by metallographic examination of a series of craters produced by PAGDs in clean H34 cathodes, under a metallurgical Zeiss (trade mark) standard 18 microscope equipped with an epi-fluorescent condenser, very high power apochromatic objectives and a 100 W mercury lamp. For best results a focusable oblique source of light (12V halogen) was also added to the incident light.

Following our low and high applied current studies on PAGD production as set forth in the “863” application, we noticed that the AC rms value of the component associated with each abnormal glow discharge pulse varied non-linearly with the magnitude of the applied current. We originally noted the existence of a current induced shift of the entire PAGD region upward in the pressure scale: while the PAGD regime became more clearly defined as the applied constant DC was increased, the pressure required to observe the PAGD increased two to three orders of magnitude. In the course of these rarefaction studies we found that, at applied currents of 1mA or less, the rms value of the different AC waveforms associated with the consecutive regimes of the discharge (TRD --> NGDm --> AGD+PAGD) was, by more than half log, inferior to the value of the applied DC current, during the first two regimes (TRD and NGD) and reached a value equivalent to the applied current with the onset of spontaneous PAGD, at pressures < 0.1 Torr (see **Fig.1**); however, in the downward tail of the PAGD regime (down to 3×10^{-3} Torr), the AC rms current component of each PAGD again decreased to more than half log of the intensity of the applied DC value, in a manner proportional to the log of the decreasing pressure. In stark contrast, at high applied currents of about 500 mA, and aside from the high current-induced upward shift in pressure of the PAGD regime (to the point that the compression of the previous regimes on the pressure scale results in their suppressing, as was the case in the present example), the AC rms component associated with each pulse (see closed circles, **Fig.2**) is, from onset of the discharge at about 8 Torr, greater in magnitude than the value of the applied current (open circles, **Fig.2**). Under the conditions described, the distribution of the field current associated with each pulsed abnormal glow discharge approached (on a linear Y axis; not shown) an uni-modal gaussian distribution with the pressure peak at about 1 Torr, and a corresponding observed maximum of 7.5 times. higher AC rms values than the applied DC values.

We have previously described in the “863” application how the PAGD frequency is affected by several factors, namely:
the magnitude of the parallel discharge capacitance,
the value of the negative pressure for the relevant vacuum PAGD range,
the magnitude of the applied potential, the magnitude of the applied direct current,
the inter-electrode gap distance and
the area of the parallel plate electrodes.

In the “531” application we have also described how the wiring configuration (plate diode versus triode) affects the PAGD frequency by adding tungsten auto-electronic emissions from the axial electrode, to those emissions from

the plate. There are other factors which limit the PAGD regime of discharge and have also been discussed in the “863” application. The following data indicates their specific effect upon PAGD frequency.

In the data presented in Table 1, control of the frequency parameter for the circuit shown in **Fig.9** is by a ballast resistance **R1** within a specific range of interest (about 800-150 ohms, for Table 1 experimental conditions), and this in turn increases the applied current which, at "high current" values (i.e. >100 mA, as for Table 1 conditions), will drive the PAGD frequency up, as previously reported in the “863” application.

Table 2 shows the effect of the progressive displacement of a given frequency, chosen as 200 PPS, with the cumulative pulse count of the same device, in the plate diode configuration. This displacement of the same frequency (cf. group numbers 1-3 of Table 2) on to higher pressure regions is shown to be promoted by the alteration of the work function of the PAGD emitting cathode, such as this is caused by the cumulative pulse count and resultant crater formation on the electrode surface. After the first million pulses, the anode facing cathode surface is completely turned over by emission sites, and this corresponds well to the threshold crossed by group 2 of Table 2. Once the cathode surfaces are broken in, the rates shown in groups 3 and 4 of Table 2, tend to remain constant.

Originally we wondered whether this might be caused by the alteration of the electrostatic profile of the plasma sheaths at the periphery of the envelope, due to the mirroring deposits that result from the sputter of ions and trapped neutral atoms (from air gases or metallic vapour) associated with the auto-electronic emission mechanism (and from further emissions triggered in turn, by secondary ionic bombardment of the cathode with molecular species present in the plasma ball formed over the primary emission site). However, reversal of the plate polarity (firing the ex-anode as a crater-free cathode) for over a million counts, followed by re-reversal to the original polarity, the entire operation being performed in air as the residual gas substrate, led to the partial recovery of the original work function for as long as the test was run (1.5×10^4 pulses), as shown by a comparison of groups 2, 4 and 5, of Table 2. From a metallographic examination of the surfaces of plates used solely as anodes, we have also concluded that prolonged PAGD operation has the effect, not only of cleaning the anode surface from surface films and adsorbed gases, as ionic bombardment promoted by electromagnetic induction coils does, but it also does more: it polishes the target surface and smoothes it by a molecular erosive action. Observations of the surface of reversed cathodes, shows the same smoothing and polishing effects observed in exclusive anodes. Thus the recovery of the PAGD rates promoted by polarity reversal of the plates is not a function of the sputter-promoted mirroring deposits on the envelope wall, but a function of the actual work-function of the emitting cathode.

Another variable that interacts with the PAGD frequency is the molecular nature of the residual gas: Table 3 shows the differential frequency response of air with a halogen quencher, argon, for the same pulse generator employed in the tests of Table 2. It is apparent that argon obtains much higher rates of AGD pulsation for the same range of negative pressure, for the same "broken in" cathode, than does the air mixture. All these measurements were taken at cathode support-stem temperatures of 35^0C.

Time of operation is also a variable affecting the frequency and operating characteristics of the cathode, as it becomes expressed by the passive heating of the cathode, an effect which is all the more pronounced at the higher pressures and at the higher frequencies examined. Utilising the triode circuit discussed in the next section, the pulse rate of a PAGD generator with 64 cm^2 plates can be seen (see **Fig.3**) to decrease, at a negative pressure of 0.8 Torr, from 41 PPS to the operating plateau of 6 PPS within 15 minutes of continuous operation, as the temperature of the cathode support increased from 19^0C to about 44^0C. As the temperature plateaus at about 51^0C +/- 1^0C., so does the pulse rate at 6 PPS, for the remaining 48 minutes of continuous operation.

However, in order to confirm this time-dependent heating effect and threshold, we also performed the same experiment, utilising the same circuit and the same negative air pressure, with twice as large a cathode area (128 cm^2, which should take nearly twice as long to heat), being operated for 18 one-minute long continuous periods equally spaced apart by 15 minutes of passive cooling, with the cathode stem always at 19.7^0C to 21^0C., room temperature at the start of each period. The results surprised us, inasmuch as they showed that for a larger area tube which takes longer to heat to the same temperatures at comparable rates of PAGD triggering, one could observe a much earlier frequency reduction (by half, within the first 5 minutes or periods of interrupted functioning) in the absence of any significant heating effect (< 1.5^0C) of the cathode (see **Fig.4**). Repetition of these experiments has led us to conclude that, as shown in **Fig.5**, the variable responsible for this repeatedly observed reduction in the PAGD frequency, when the PAGD operation sequence is systematically interrupted, is the state of charge/discharge of the battery pack (the charge pack) at the output of the triode circuit in question: the PPM rates in **Fig.5** decrease rapidly with the steepest rate of charging of the charge pack and the fastest recovery rate of its open circuit voltage; above a given state of charge, when the open voltage of the charge pack climbs more slowly (> 340 V), in a log fashion, the PPM rate stabilises at its plateau values.

Confirmation of the importance of the charge pack in the PAGD function of the present circuitry here considered, comes from the fact that the size (the number of cells) and the intrinsic capacitance of the charge pack affect the PAGD frequency dramatically (see Table 4): increasing the charge pack size of 29 cells to 31, by 7% leads to a 10-fold reduction in frequency; further increases in the number of charge pack cells extinguishes the phenomenon. On the upper end of the scale, this effect appears to be tied in to restrictions that it places on the ability of the larger charge packs to accept the discharge power output once the charge pack voltage exceeds the PAGD amplitude potential. All of these measurements were conducted with the same 128 cm^2 plate PAGD generator, at a pressure of 0.8 Torr and in the triode configuration (see **Fig.9**).

Other factors can also affect the frequency: the motion of external permanent magnetic fields oriented longitudinally with the inter-electrode gap, external pulsed or alternating magnetic fields, external electrostatic or electromagnetic fields, specific connections of the earth ground, and the presence of a parallel capacitative, capacitative-inductive or self-inductive arm in the circuit, such as we have described for our electromechanical PAGD transduction method as described in the “531” application.

Analysis of the modulation of PAGD amplitude is simpler than that of its frequency, because fewer factors affect this parameter:
(1) magnitude of the applied potential,
(2) inter-electrode gap distance and
(3) the negative pressure, as shown in the “863” application, for "low" applied currents.

As the magnitude of the applied potential itself is limited by the gap and the pressure, to the desired conditions of breakdown, the important control parameter for the PAGD amplitude is the pressure factor. This is shown in **Fig.6** and **Fig.7**, respectively for "low" (5 mA) and "high" (about 500 mA) applied currents and for the same plate diode configuration of a H34 Al 128 cm^2 plate PAGD generator (5 cm gap), in the simple circuit described in the “863” application; it is apparent that both positive and negative components of the amplitude of these pulses in the oscillograph, are a function of the pressure, but the maximum cut-off limit of our equipment, for the negative component (at 240 volts for the "low" current experiment and at 120 volts for the "high" current), precluded us from measuring the peak negative voltage of these pulses.

However, rms measurements of the pulse amplitude at the plates and DC measurements at the circuit output to the charge pack indicate that the negative component increases with decreasing pressure to a maximum, for a given arrangement of potential and gap distance; no pressure-dependent bell shape variation of the pulse amplitude, as that seen for the positive component at "high" applied currents (**Fig.7**) is observed with the negative amplitude component. For the typical range of 0.8 to 0.5 Torr, the rms value for pulse amplitude varies from 320 to 480 volts, for a 5.5 cm gap distance and applied DC voltages of 540 to 580 volts. PAGD amplitude is a critical factor for the design of the proper size of the charge pack to be utilised in the optimal circuit.

The development of the circuits to be described stemmed from fundamental alterations to the principles implicit in our previous methods of electromechanical transduction of AGD plasma pulses as described in the “531” application. Whereas this electromechanical coupling (capacitative and self-inductive), utilised directly, energises the AGD pulses inverted from the DC input by the vacuum generator, the purpose of the development that led to the presently described experiments was to capture efficiently, in the simplest of ways, most of the pulse energy in a closed circuit, so that power measurements for the energy transduction efficiency of the observed endogenous pulsation could be carried out. Ideally, comparative DC power measurements would be performed at both the input and output of the system, taking into account the losses generated across the components; this would overcome the measurement problems posed by the myriad of transformations implicit in the variable frequency, amplitude, crest factor and duty-cycle values of the PAGD regime, and necessitated some form of rectification of the inverted tube output.

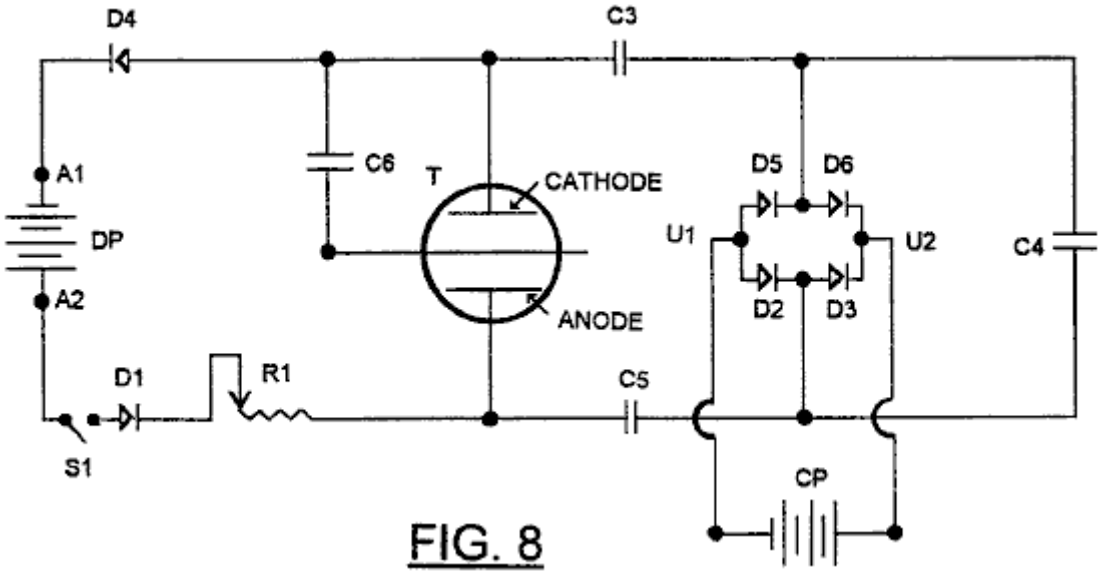

FIG. 8

From the start our objective was to do so as simply as possible. Early circuits utilising half-wave rectification methods coupled in series to a capacitative arm (for DC isolation of the two battery packs), with the charge pack also placed in series, showed marginal recoveries of the energy spent at the PAGD generator input. Attempts at inserting a polar full-wave rectification bridge led, as shown in **Fig.8**, to the splitting of the capacitor into capacitors **C3** and **C5**, at the rectification bridge input, and capacitor **C4** in series with both capacitors, all three being in a series string in parallel with the PAGD generator. Under these conditions a DC motor/generator could be run continuously in the same direction at the transversal output (**U1** and **U2**) of the bridge; but if this inductive load was replaced with a battery pack CP (charge recovery pack), either the parallel capacitor **C4** had to remain in the circuit, for the diode configuration or, less desirably, a further capacitor **C6** could replace **C4** and connect one electrode, preferably the cathode **C**, to the axial member of the discharge tube **T**, thus resulting in a first triode configuration as actually shown in **Fig.8**. Energy recovery efficiencies of the order of 15% to 60% were obtained utilising **C6** in this manner, but measurements of the potential and currents present at the output from the rectifier bridge were substantially lower than those obtained using optimal values of **C4**. Effectively, under these conditions, much of the power output from the tube was never captured by the output circuit formed by the second, right hand arm of the system and, being prevented from returning as counter-currents to the drive pack **DP** by diodes **D1** and **D4**, was dissipated and absorbed by the inter-electrode plasma, electrode heating and parasitic oscillations.

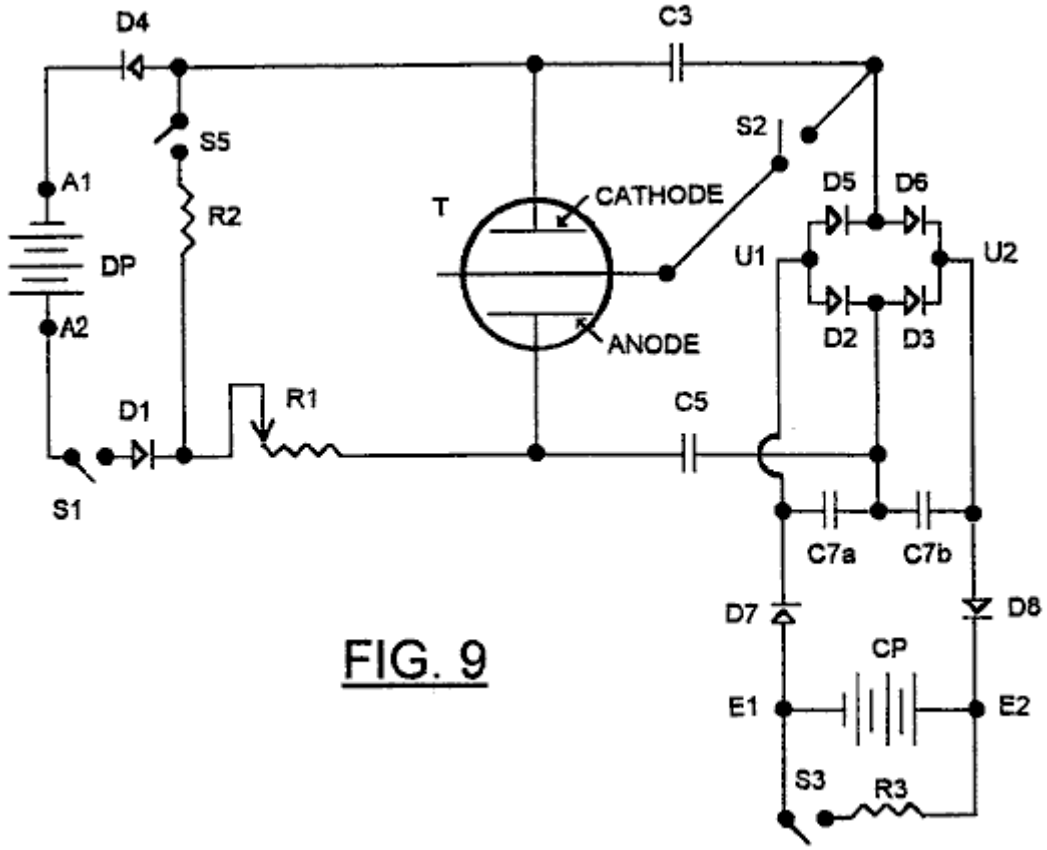

FIG. 9

Solutions to this problem were explored using the circuit shown in **Fig.9**, which still maintains the necessary communication link for the quasi-sinusoidal oscillation of the capacitatively stored charges at the input and outputs of the rectification bridge, but integrated the functions of capacitor **C4** into the single rectification circuit, in the form of an asymmetric capacitative bridge **C7a** and **C7b** placed transversally to the capacitative bridge formed by **C3** and **C5** and in parallel with the charge pack **CP** at the output from the rectification bridge **D5, D6, D2, D3**.

This second capacitative bridge is so disposed as to have its centre point connected to the anode **A** through capacitor **C5**. If the axial member of the Tube **T** were to connect to the junction of **D2** and **D3** instead of at the junction **D5-D6**, the function of bridge **C7a** and **C7b** would be connected to the cathode **C** through capacitor **C3**. The capacitative bridge is insulated from the charge pack whose voltage it stabilises, by rectifiers **D7** and **D8**, which also prevent leakage of charge across **C7a** and **C7b**.

The anode and cathode oscillations generated by the electrostatic charge transduction through **C3** and **C5** into the poles of the charge pack are trapped by the transversal transduction of the **C7** bridge, at the outputs from the rectification bridge, of which the oscillation has to become split between the bridge inputs into half-waves, for electrostatic transduction and full wave rectification to occur. In fact, under these conditions, removal of the **C7** bridge will suppress the PAGD phenomenon, unless other circuit variables are also altered. The transversal bridge is thus an essential piece of this novel circuit. Variations in the circuit as shown in **Fig.10** were then studied, the first two being selectable utilising switch **S2** (**Fig.9**).

The presence of the capacitative bridge effectively reduces the dynamic impedance of the charge pack **CP** so that the output circuit approximates to a characteristic in which it presents a very high impedance to the tube **T** at potentials below a certain level, and a very low impedance at potentials above that level.

With this modified circuit, more effective recovery of the energy produced by collapse of the PAGD pulses is possible, with more effective isolation from the input circuit utilised to trigger the pulses. Under these conditions, the energy captured by this circuit at the output, is not directly related to that utilised in triggering the pulses from the input. The attainment of this condition critically depends on the large capacitance of the transversal bridge being able to transfer the output energy from the tube **T** into the charge pack **CP**. Under these conditions, we have found, as will be shown below, that the large peak pulse currents released by collapse of the PAGD pulses released more energy than is used to trigger them, and these findings appeared to tally with other observations (abnormal volt-ampere characteristics and anomalous pulse currents, etc.) associated with the anomalous cathode reaction forces that accompany the auto-electronic emission-triggered PAGD regime. Experiments so far indicate that the power output can be increased proportionately to the series value of **C3**, **C5** and the two identical **C7** capacitors.

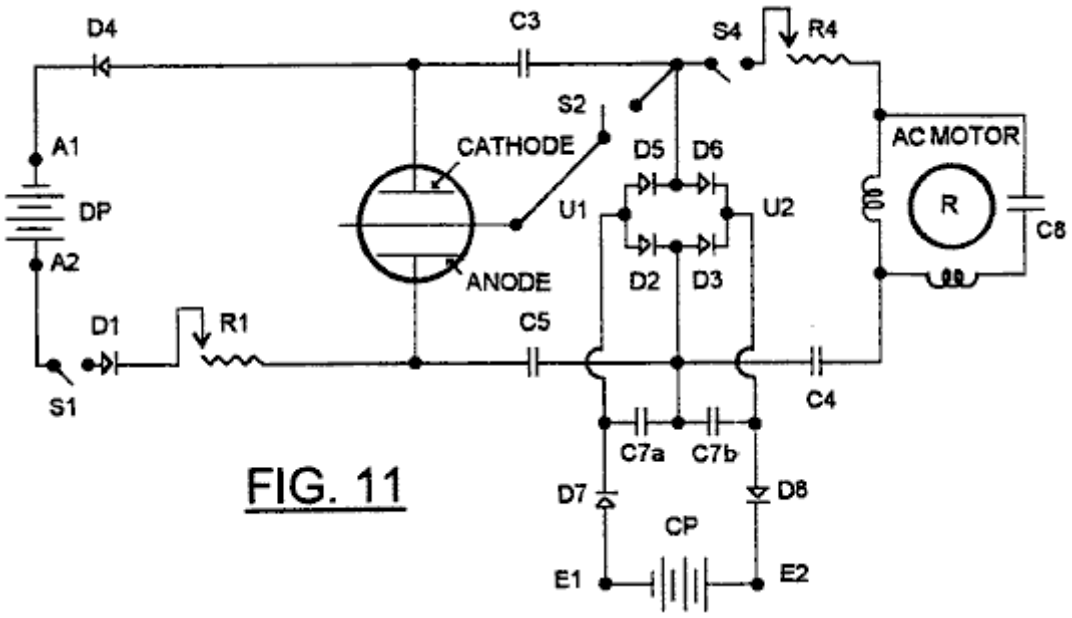

FIG. 11

The circuit of **Fig.10** can be integrated with a circuit such as that disclosed in the “863” application as shown in **Fig.11**, in which a part of the energy recovered can be shunted by the switch **S4** into an induction motor **M1** having rotor **R**, to a degree determined by the adjustment of potentiometer **R4** and the value selected for **C4**.

The circuit of **Fig.11** can be further developed as exemplified in **Fig.12** to include configurations which provide switching permitting interchange of the functions of charge packs and the drive packs, it being borne in mind that the nominal potential of the drive pack must be substantially higher than that of the charge pack, the former needing to exceed the breakdown potential of the tube at the beginning of a PAGD cycle, and the latter to be less than the extinction potential.

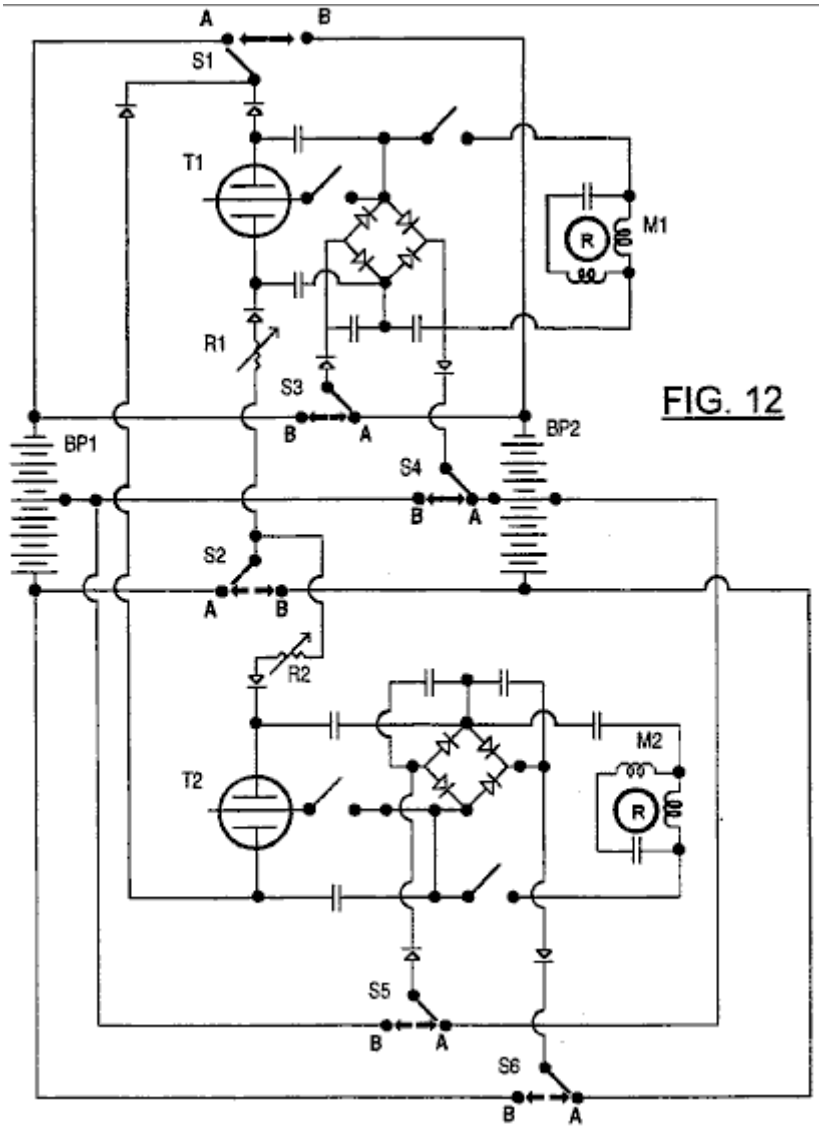

FIG. 12

Fig.12 essentially represents a duplication of the circuit of **Fig.11**, the two circuits however sharing two identical battery packs **BP1** and **BP2**, and being provided with a six pole two way switch, the contact sets of which are identified as **S1, S2, S3, S4, S5** and **S6**. When the contacts are in position **A** as shown, battery pack **BP1** acts as a drive pack for both circuits, with the upper half (as shown) of the battery pack **BP2** forming the charge pack for the upper circuit, and the lower half forming the charge pack for the lower circuit. When the pack **BP1** is at least partially discharged, the switch is thrown so that contacts move to position **B**, which reverses the function of the battery packs thus allowing extended operation of the motors in each circuit each time the switch is thrown.

Based on the manufacturer's data, and using current values within the range of our experimentation as discussed in the next sections, an optimal discharge cycle for a fully charged 6.0 AHr battery pack at 0.300 A draw is 20 hours, as claimed by the manufacturer, and this corresponds to a cycling between 100% (12.83 V/cell open circuit and load start voltage) and < 1% (10.3 V/cell load voltage) of the battery's absolute charge capacity. Even though the discharge mechanism is a time cumulative process with a log function, the discharge can, within 4 to 5 hour time segments (or periods with 20%-25% of the full range), be regarded as practically linear with time. This trait, or linearisation of the discharge slope, becomes more marked with advancing age and decreasing absolute storage capacity of the cells.

The proportionality between open circuit voltage and the percentage of residual relative capacity for these cells when new (uncycled and not yet aged) is uniform over 98% of the permissible charge capacity withdrawal. In practice this translates into a slope that becomes steeper with time, while the absolute storage capacity diminishes. In turn, this decreasing absolute capacity of the cells results in shorter load discharge times and their further linearisation.

A circuit in general accordance with **Fig.9**, employed in the studies reported in this and the following sections, utilises a drive pack of 46 12 V Lead acid gel-cells each with a 6.0 Ah rating, and a charge pack with 28 or 29 12 V identical cells. The charge pack was cycled anywhere from 11.2 V to 12.8 V/cell (open circuit voltages), within the proportional region of the relative capacity slope, to yield a capacity increment in the order of 50% (e.g. from

20% to 70%), anywhere within the range of 2% to 100% of its total charge capacity, assumed for now as invariant. The charging process, hereinafter referred to as a PAGD run, took about 20-30 minutes under optimal conditions. The drive pack typically consumed, in the same period of time, 4% to 11% of its initial total capacity , its open circuit voltage typically falling 0.1 V to 0.2 V per cell after a PAGD run, within the open circuit range of 12.8 V/cell (100% relative capacity) and 11.2 V/cell (about 2%). At the 100% capacity benchmark, the drive pack would theoretically have 20 h x 46 cells x 12.83 V/cell x 0.3 A = 3.5 kWh, and the charge pack, for example, 20 h x 29 x 12.83 V/cell x 0.3 A = 2.2 kWh. Since the capacity per cell is linear with the open circuit voltage within the proportional range, as claimed by the manufacturer, we projected the open circuit voltage intercepts on the manufacturer's proportional curve in order to determine the residual percentage of the total relative capacity and the standard hours of operation left, from any experimental open circuit voltage measurements.

Three pulse generators (one 64 cm^2 and two 128 cm^2 plate areas) were employed in these studies; they were operated in PAGD runs at 1-120 pulse/second rates, within a negative pressure range of 0.2 to 0.8 Torr and with applied direct currents of 0.2 to 0.6 A.

Both drive and charge packs utilised cells which were bought new at the same time and had initial charge values of 12.4 to 12.55 V/cell (open circuit). These batteries are capable of energy densities of 33-35 WHr/Kg. However, the experiments shown in Table 5 are selected from a series that spanned nearly 12 months, beginning 6 months after purchase; hence, loss of absolute storage capacity by the batteries had occurred in the intervening time, as a function of both age and charge/discharge cycle life.

Measurements of the open voltage of either drive (D) or charge (C) (see column 2, Table 5) packs for 8 separate experiments, all utilising the triode configuration, were performed before (b) and after (a) a PAGD run (see columns 3 and 4), at either 15 or 30 minutes (see column 26) of the open circuit voltage relaxation after a PAGD run was terminated. Corresponding open circuit voltages per cell are shown in column 5, and the percentages of the predicted total relative charge capacity resulting from the intercepts on the manufacturer's proportional curve are shown in column 6, Table 5. Equivalent maxima for the theoretical hours of operation left are shown in column 7, the percentage change in relative capacity arising as a consequence of either charge pack charge capture (capacity gained) or of drive pack output (capacity lost) is shown in column 8. Translating the intercepts into power units yields the values shown in column 9, Table 5, for total kWh left in each pack before and after PAGD production, those shown in column 10 for the actual power gained and lost during the periods of operation (presented in column 12) and those shown in column 13 for the power predicted to be gained or lost per hour of PAGD production.

On the basis of the experimental open voltage values and their intercepts, the predicted net kWh values per hour of PAGD energy production (after deduction of measured losses) and the corresponding experimental break-even efficiencies (where breakeven = 100%) are presented, respectively, in columns 14 and 15. The PAGD frequency per second is shown in column 11; the number of 12 V cells, in column 16; the tube ID, in column 17; the cathode (and anode) area (s), in column 18; the plate material, in column 19; the input ballast utilised (R1, FIG. 9), in column 20; the size of each capacitor (C3 or C5) of the tube output bridge, in column 21; the size of each capacitor (C7a or C7b) of the transversal capacitative bridge, in column 22; the status of **S4** and thus, of the parallel and auxiliary electromechanical arm (see **Fig.11**), in column 23; the negative air pressure in column 24; the gap distance between the plates, in column 25; and columns 27,28 and 29, show the status of the elements of the switched on parallel electromechanical arm of the circuit--the parallel **C4** capacitor, the motor input resistor **R4** and the motor revolutions per minute (measured stroboscopically), respectively.

From these figures of Table 5, and utilising the data for the two first examples shown, we calculated the predicted performance of the system based on the open voltage measurements. In the first example, where the system was run continuously without interruption, the charge pack increased the percentage of its total capacity by 43% (a two-fold increase in capacity) and, during the same period, the driver pack decreased the percentage of its total capacity by 7% (an approximately 10% decrease in capacity relative to the percentage of residual total capacity at the start, i.e. 77%) (cp. columns 6 and 8, Table 5). Subtracting the predicted initial total energy (0.835 kWh) available to the charge pack before the experimental run (first line of column 9, Table 5) from the predicted total energy (1.823 kWh, second line of column 9) available to the charge pack after the PAGD charge run, gives us the total energy gained by the charge pack: 0.988 kWh (column 10) in 21.5 minutes (column 12) of continuous PAGD performance.

Conversely, subtracting the predicted final total energy (2.4 kWh) available to the driver after the experimental run (fourth line of column 9, Table 5) from the predicted total energy (2.66 kWh, third line) available to the driver before the PAGD charge run, gives us the total energy lost by the drive pack: 0.26 kWh in 21.5 minutes. If we divide the total available energy gained by the charge pack, by the total energy lost by the drive pack, we obtain a surplus factor of 3.9., or 388% of the break-even point (column 15). The same values result from dividing the charge pack % of total capacity gain by the drive pack % of total capacity lost, and then down-scaling this value by multiplying it by the typical scale factor for the two packs, 29 / 46 = 0.63 times.

In an analogous fashion, we analysed the results for the second example shown in Table 5. Here, the charger increased the percentage of its total capacity by 45.5% (a 22.75 fold increase in estimated total relative capacity) and, during the same period, the driver decreased the percentage of its predicted total capacity by 7% (about a 17.5% decrease in capacity relative to the percentage of residual total capacity at the start, i.e. 40%). By dividing the predicted total available energy gained by the charge pack (0.962 kWh/18 minutes) by the expected total energy lost by the driver pack (0.246 kWh/18 minutes) we obtain a surplus factor of 3.9 times, or 391% of the break-even point. This corresponds to an interrupted, total sequential run of 18 minutes, each minute-long run being separated by a cooling and voltage relaxation period of 15 minutes before the next run is carried out, at an average PAGD frequency of 61 PPS.

Analysis of the remaining results illustrates how a number of PAGD controlling parameters interact to determine conditions for effective maintenance of a PAGD regime. The lower gain and higher loss per unit time registered for the third run of Table 5, which results in the lower break-even efficiency of 230% and a smaller net power production rate than before (power estimates of 1.396 kWh/h of PAGD operation vs 2.387 kWh/h, for the second run, Table 5) illustrate, for example, the combined effect of lowering the pressure (0.8 to 0.7 Torr) and running the PAGD continuously (the heating effect), both of which depress the PAGD frequency. The fourth run of Table 5 identifies the continuous performance of a "broken in" softer grade of aluminium (column 19), having a lower work-function (as determined from the higher PAGD frequency spectrum) than the harder H34 plates of the previous examples, and shows that, despite the series value of the total capacitance being higher (5,333 mF vs 4,030 mF for runs one through three), and despite the higher vacuum (0.2 Torr), the lower work-function results in a higher frequency; however, even though this run registers a predicted higher break-even efficiency (310%) than the previous experiments, these conditions result in a 4 / 5-fold lower estimate of net power produced, when compared to the previous three PAGD runs.

PAGD runs 5 and 6, Table 5, illustrate the effect of switching on the auxiliary electromechanical arm of the circuit shown in **Fig.11**. Increasing the amount of charge capacitatively shunted into the electromechanical arm by higher **C4** values (column 27), and increasing the current that feeds the squirrel cage induction motor utilised by lowering **R4** (column 28), results in a power capture by the charge pack that registers an energy loss (predicted to be 96% efficient, falling short 4% of break-even recovery), as most of the tube output power is spent in the electromechanical arm and its motor effect. Furthermore, under the conditions of maximum electromechanical action, the drain imposed on the drive pack becomes considerable (see loss in columns 10 and 13), even if the **C3** and **C5** values are reduced, column 21, Table 5). These runs also illustrate how the motor appears to function as an electrical induction generator having rpm values much higher than the synchronous values prescribed by the frequency of the PAGD (column 29, Table 5).

The extremely large break-even efficiency of PAGD run 5, Table 5, indicates that with selected values of **C4** and **R4**, it is possible to operate the motor in the auxiliary arm and still accumulate excess energy from the PAGD production in the charge pack.

Runs 7 and 8 illustrate results obtained for 64 cm^2 plates, and a shorter inter-electrode gap distance, for two pressures (0.8 and 0.5 Torr), the device being open to a rotary pump manifold in the first instance and sealed from the pump, in the second case. Despite the lower vacuum, the higher pulse frequency (32 vs 5 PPS) and break-even efficiency (906% vs 289%) registered by run 8 when compared to run 7, are a consequence of the method of run 8, which was interrupted systematically by 5 passive cooling periods, as in the case of run 2, whereas run 7 was continuous. This again resulted in higher average PAGD frequencies (at lower pressures), a predicted two-fold greater gain and a predicted two-fold smaller loss (columns 13 and 14) for run 8.

Fig.13 shows curves representing the slopes of the open circuit relaxation voltages, which are linear with the log of time elapsed from cessation of discharge, for both drive and charge packs, in the same run 8 set out in Table 5. The experiment in its entirety consisted of preliminary resistor-loaded measurement discharges and their corresponding open circuit voltages from the moment of cessation of the resistive discharge (illustrated, respectively, by the open squares of DPT1 for drive pack relaxation time 1, and by the open circles of CPT1 for charge pack relaxation time 1), followed by their relaxation rates in the wake of the PAGD production (the hatched squares of DPT2 for drive pack relaxation time 2, and the hatched circles of CPT2 for charge pack relaxation time 2), and finally, by the relaxation rates from the final resistor-loaded measurement discharges (the black squares of DPT3 for drive pack relaxation time 3, and the black circles of CPT3 for charge pack relaxation time 3). Discharge resistances were 833 ohms for the charge pack, and 2083 ohms for the drive pack in all cases, corresponding to resistors **R3** and **R2**, respectively, of **Fig.9**. This methodology will be examined in greater detail below. It is apparent that, after every load period, be this resistive (CPT1, DPT1, CPT3 and DPT3) or due to PAGD operation (DPT2), the relaxation slope is positive; as shown from slopes CPT1 and DPT1, the log time proportionality of the open circuit voltage relaxation, under these conditions, tends to plateau after about 30 minutes. The exception to this general behaviour lies in the voltage relaxation slope CPT2, which is negative and

reflects the charge accumulation occurring in the charge pack and obtained by capture of energy produced during PAGD operation, triggered by the energy drawn from the drive pack during load time 2.

As a first approximation of electrical power generated and consumed by the energy conversion system of the invention, the previous open circuit voltage method is of significance in showing the basic trends involved in interaction of the operating parameters. However, in all likelihood, it overestimates the actual values of electrical power consumed and generated, for a variety of reasons. First, it assumes that the relative capacity scale of the batteries in the drive and charge packs is an absolute charge capacity scale with an invariant maximal charge retention, which it is not; in fact, the absolute charge capacity is itself a variable subject to several factors, such as the cycle life, overcharging or undercharged conditions, cell age, residual memory and the rate of charge and discharge. Hence, the inference of a uniform time scale on the basis of the open circuit voltage/capacity intercepts may not be warranted. Finally, it does not integrate the open voltage decrease over time, and utilises the specification load current as the average current over time.

In order to obviate these problems, we resorted to a variety of other measurement methods. First, we proceeded to compare the closed circuit, preliminary, resistive-load discharge measurements for either charge or drive pack, under conditions of negligible loss of power, as these measurements were statistical means (n = 9) taken, at equal intervals, during the first 90 seconds of the load discharge, and obtained both just before the PAGD production runs (but separated from each PAGD run by an open circuit voltage relaxation of 30 minutes) and just after the runs (but equally separated by a relaxation of 30 minutes). As an example of the data generated by such an approach, **Fig.14** illustrates the shift of the slopes indicating marginal power loss for the drive pack (from the closed squares to the open squares) and those indicating gain of power for the charge pack (from the open circles to the closed circles), in actual total load power values.

Integration of these power measurements over the projected load discharge time, taken from the family of curves generated on the basis of the manufacturer's load voltage over discharge time specifications, led to a direct comparison of the new values, as shown in Table 6, with the values presented in Table 5, for the first three instances introduced. All values of Table 6 were obtained by resistive measurements of power that entailed a negligible power loss. Table 6 confirms the fundamental equivalence of runs 1 through 3, as already seen from their corresponding analysis using the open voltage method (see runs 1 to 3, Table 5). This new power estimation method also confirms the lower loss encountered in run 2 utilising interrupted PAGD operation. While the break-even efficiencies sensibly doubled using this method, the estimates of actual electrical power consumption recovery decreased by a 2 to 3-fold factor. Thus this direct load voltage/amperage measurement method of estimating actual power losses or gains, is a check upon the open voltage method previously utilised.

Direct, instantaneous measurements of the voltage and current characteristics of the PAGD production and capture phenomena being discussed, were also performed during PAGD runs for diverse sets of conditions, including all those described in the two previous sections. In Table 7 we show these results for two PAGD generators having an identical electrode area (128 cm^2) and connected to electrical energy capture circuits of three separate configurations as set forth in **Fig.10A, Fig.10B** and **Fig.10C** and column 2, Table 7. In the configuration of **Fig.10C**, or double diode configuration, both electrode plates act as cathodes and the axial member as the anode collector (experiments 1-4, for the H220 device and 13-14, Table 7, for the H34 device). In the configuration of **Fig.10B**, or triode configuration, one plate acts as the cathode, the axial member as an auxiliary cathode and the other plate as a collector (experiments 5-9, Table 7). In the configuration of **Fig.10A** or single (plate to plate) diode configuration, the axial member is disconnected, and the polarity of the plates remain as in the triode configuration (experiments 10-12). All measurements were taken after 1 minute of PAGD operation of the devices, which were, at the start of each run, at room temperature. All cathodes had been previously broken in with > 2×10^6 AGD pulses. The open circuit voltage of the charge pack was, for all cases, at 359 to 365 volts, before each test. The direct measurements of the PAGD input and output DC voltages and currents were obtained as statistical means of 10 second long measurements, and at no time did the standard error of the plate voltage mean exceed 35 volts.

The air pressure within the tube during these tests is shown in column 3, Table 7, the drive pack DC voltage (X), in column 5, the DC voltage across the plates (Y), in column 6, the drive pack output current (PAGD input current), in column 7, and the drive pack total watts output is shown in column 8. Columns 9 and 10 show the PAGD voltage (PAGD V = (X-Y) / I_{av}) and the value of the PAGD extinction potential in V/cm. The recovery co-ordinates (i.e. the PAGD output energy) found at the **U1-U2** output (**Fig.9**), are shown in columns 11 to 13, as the charge pack's E1-E2 input DC voltage, amperage and power watts, respectively. The calculated resistance of the entire circuit is given in column 14, the registered PAGD frequencies in column 16, and running conditions in columns 17 to 18. The break-even efficiency obtained by direct comparison of the electrical power figures for the drive and charge packs, respectively, is given in column 15. This assumes, for purposes of a generalisation of power production rates over time, that the quasi-instantaneous, direct measurements here obtained can be translated to outputs obtained per unit time, and thus into direct Watt-hour measurements.

Data from runs 1 through 4 demonstrate that, at these PAGD frequencies, there is no difference between using fast switching (32 nanoseconds) MUR 860 diodes, or regular 40HFR-120 silicon diodes, in the rectification bridge of the electrical energy capture circuit, and that the PAGD frequency varies as a function of decreasing air pressure.

Runs 5 to 14 show that, in general, for the same tube, the single and double diode configurations are the most efficient, for the same pressure, the diode configuration typically yields some 1.5 to 2 times larger break-even efficiencies (cp runs 10-11 and 13-14, with runs 5-9, Table 7). The largest accumulations of power are also registered in the diode mode(s). This trend appears to be a function of the much lower cathodic work-function of the aluminium plates, than of the tungsten of the axial member utilised as an auxiliary cathode in the triode configuration. A feature of the data from these 14 different runs is the consistent excess power outputs (column 15, Table 7) and their narrower range (218 to 563%), when compared to those observed with the previous two methods of experimental analysis.

Run 12, Table 7, shows that the switching on of the electromechanical arm can be performed without entailing a power loss in the PAGD capture circuit, as previously found for run 5, Table 5, utilising the open circuit voltage method. In fact, with **C4** = 8 microfarads and R4 = 500 ohms, the AC induction motor behaves as an electrical flywheel (e.g. 2800-3000 rpm for 10 PPS inputs), while the electrical energy capture circuit still registers a sizeable excess electrical power production (compare runs 11 and 12, Table 7). Runs 13 and 14 illustrate how the charge pack's state of charge and its inherent capacitance affects both the PAGD frequency and the power producing efficiency of the entire system: as the charge pack is reduced from 29 to 19 cells, the PAGD generator adjusts by reducing its frequency logarithmically and, while the charge pack input current is greater than before, the drive pack loss becomes still larger and the break-even efficiency much lower (by >1/2, from 563% to 228%). This is because the circuit must translate the naturally larger PAGD amplitude into a larger surplus of output current, and in this process becomes less efficient.

If the first measurement method employed (the open circuit method) had to make too many theoretical assumptions about the system's performance under load conditions and hence about its effective charge capacity, the second approach still had to suppose an invariant discharge time and thus an invariant absolute charge capacity on the part of the battery systems (charge packs) employed for capture which it approximated by an operation of integral calculus. With the third method described above, theoretical assumptions were avoided except that, in these measurements, the actual performance of a given battery in terms of time, time of delivery and time of capture, was also ignored; no account is taken of the time-dependent modulation of the PAGD frequency, as effected by certain of the parameters analysed, namely the charge pack state of charge, the method of sequencing the PAGD runs (continuous vs interrupted) and its concomitant heating effects, and the state of charge (load voltage and current capacity) of the drive pack. A simple, non-negligible, resistive measurement of power lost by the drive pack, and an identically non-negligible measurement of the power gained by the charge pack, for the same experiment and the same singular time of PAGD production, were performed repeatedly to corroborate the previous three approaches. For this purpose, all experiments were designed as a continuous series of sequential phases:

1) Before a PAGD run, a resistive discharge was measured across either pack over periods of 1 to 3 hours (utilising the DP and CP resistances previously reported in the open voltage section) and followed by a 15 to 30 minute open circuit voltage relaxation;

2) Then, the PAGD runs were performed, either continuously or as interrupted, composite sequences, and the corresponding open circuit relaxation voltage(s) were measured, after the cessation of the integral PAGD run;

3) Finally, resistive discharge measurements, obtained under identical conditions to those recorded before the PAGD run, were carried out for either pack, followed by concomitant battery voltage relaxation rate measurements.

Under these experimental conditions, exact power measurements could be taken from an analysis of the actual battery discharge curves before and after the PAGD run. Based on a comparison of the curve trends of the pre-run resistive discharge of the drive pack with those of the post-run resistive discharge, the effective power drawn ($DeltaE_c$) from the withdrawable power capacity of the drive pack incurred during a PAGD run, was ascertained. This represents the power consumption during the run, and the experimental value thus recorded constitutes the actual power figure that must be matched for break-even to occur. Hence, the break-even value equals, by definition, the electrical energy input to the system. Similarly, a comparison of the charge pack pre-run and post-run resistive discharge curve trends identified the effective power ($DeltaE_{rho}$) added to the withdrawable capacity of the charge pack. This quantity represents the electrical energy recovered during the run. The relation for the two quantities is expressed by the break-even efficiency equation:

$\% = DeltaE_{rho} / DeltaE_c \times 100$

If the break-even efficiency is less than 100%, then the apparatus registers a net loss in electrical energy in the CP with respect to the DP. Conversely, if the efficiency exceeds 100%, then there is a net gain in electrical energy in the CP, as compared to that lost in the DP. For purposes of this analysis, a limit to the minimum withdrawable capacity was placed, from experiment and in agreement with the load current curves of the manufacturer, at 115 W for the driver pack (average current of 0.250 A, minimum current of 0.230 A), and at 90 W for the charge pack (average current of 0.375 A, minimum current of 0.334 A), as a function of both their total cell size (respectively, 46:29) and the difference in the resistive loads employed for the discharge measurements. All cathodes had been broken in, as described before.

The results obtained with this fourth method, for six selected experiments with three diverse types of devices (using different electrode plate areas, gap lengths, and electrode work-functions), configured both in the triode or the (single) diode (e.g. **Fig.10B**) arrangements, at the indicated pressures, are presented in Table 8. In all cases, a net excess of combined battery pack charge, expressed as electrical watt hours, is registered (columns 8 and 10, Table 8) and the break-even efficiencies are all >100% (column 10). Experimental groups 1 and 2 again demonstrate that, for the same cathode, the interrupted PAGD sequence method of group 2 (1 minute of PAGD function, followed by a 15 minute relaxation, and so on) yields a higher break-even efficiency because of the lower losses registered with this minimal plate heating method (column 10, Table 8). Group 3 of Table 8, shows that the PAGD power production efficiency is also higher for a lower work-function cathode material (H220 vs H34), being subjected to PAGD auto-electronic conditions at a 4-fold lower pressure than the control groups 1 and 2; however, the lower pressure depresses the frequency and, together with the interrupted PAGD sequencing method, it also lowers the loss, causing an actually much larger break-even value than registered for the previous two groups. Groups 4 and 5 exemplify the dual effect of lowering both the plate area and the gap distance: the former affects the PAGD event frequency, whereas the latter affects the PAGD amplitude, and thus the capture efficiency of the charge pack. Despite a cathodic work-function practically and operationally identical to that of groups 1 and 2, these smaller plate area and shorter gap devices utilised in groups 4 and 5, yield 3- to 6-fold lower net power outputs, as well as lower break-even efficiencies, than the former groups, at the same pressure. Finally, group 6 exemplifies the results obtained for the plate diode configuration, where the frequency is lower (no triggering role for the axial member), and a higher loss leads to the lower break-even efficiency, comparable to that of the lower area and shorter gap groups 4 and 5.

In order to verify the discharge curve lengths employed in these analyses and experimentally establish the actual charge capacity of the battery packs, calibration resistive discharges, between the maximum charge state and the minimum limits chosen, were performed for each pack with their respective discharge resistances R2 and R3 (see **Fig.9**). These discharge calibration curves were plotted for half maximal charge values shown in **Fig.15A** and **Fig.15B**, and from the curve produced, we have determined the total half-charge capacities of each battery pack to be 1.033 kWh (100%=2.066 kWh) for the drive pack and 660 WHr (100%=1.320 kWh) for the charge pack. Based upon the corresponding maximal (100%) capacity values, we determined the actual percentages of the relative charge capacities shown in column 5, Table 8, which correspond to the experimental values obtained. We also noted that the curves plotted showed two quite distinct time linear slopes, the slope of the delivery of power per time unit steepening very markedly at the approach to the limits of the permissible withdrawable capacity, occurring at 115 W into **R2**, and 90 W into **R3**.

The pre-PAGD run and post-PAGD run, drive and charge pack discharge curves corresponding to groups 3 and 6, respectively for triode and plate diode configurations, in Table 8, are shown in **Fig.16** (drive pack) and 17 (charge pack), for group 3, and in **Fig.18** (drive pack) and **Fig.19** (charge pack), for group 6. In all cases, the open symbols represent the pre-PAGD run discharge curves, whereas the closed symbols represent the post-PAGD run discharge curves.

As a further check on these values, a videographic, millisecond analysis of the singular power simultaneities occurring at both ends of the system (drive and charge packs) was performed for various 10 second samples of diverse PAGD runs. A typical example is shown in **Fig.20**, which is a sample of the PAGD run designated as 6 in Table 8. While the drive pack DC wattage spent as input to PAGD production varied from 36.6 to 57.82 watts, by a factor of 1.6 times, the DC wattage entering the charge pack as captured PAGD output varied more pronouncedly by a factor of 2.7 times, from 146.4 to 399.6 watts (all meters were in the same selected ranges of voltage and current) with the semi-periodic, intermittent character of each singular emission, though within specific, ascertainable ranges for both amplitude and current outputs.

Assimilation of the singular behaviour of the PAGD in this sample, by a statistical treatment of its variation (with n = 64), indicates that the operational break-even efficiency observed during this sampled period lies at 485.2% +/- 18% with projected 48.3Wh drive pack loss and 221.7Wh charge pack gain. This matches rather closely the observed 483% break-even efficiency, and the 37.7Wh loss as well as the 182.2 kWh gain for the overall PAGD run reported in group 6 of Table 8, and indicates how close are the values obtained by the operational and extensive non-negligible resistive discharge power measurement methods employed.

Finally, an example of the correlation between the drive pack PAGD load voltage and the charge pack PAGD charging voltage, as a function of the duration of the intervening PAGD run between resistive discharge measurements, is shown in **Fig.21**, for the PAGD run corresponding to group 4 of Table 8.

Using the same pulse generator with H200 Al 128 cm^2 plates, in a double diode configuration, and the same circuit values (but with CP = 23 cells), three experiments were conducted at different PAGD frequencies, as a function of varying air pressure. Analysis of driver pack losses and charge pack gains by the extensive load discharge measurement method, as described before, led to the determination of the gross and net gains (respectively, without and with losses included) per pulse, in milliwatt-hour, for each frequency, as well as of the gross and net power gains per second of PAGD operation. The results are shown in Table 9. Even though the gross and net gains of power per pulse were observed to increase with decreasing frequency, the gross power gain per unit time increased with increasing frequency. However, this last trend does not necessarily translate into a higher net gain per unit time, because the losses in the driver pack (not shown) also increase significantly with PAGD frequency. These losses are in all probability related to more energy retention by the plasma at higher frequencies when plasma extinction becomes incomplete. We expect net gains to reach optimal thresholds for any given type of circuit configuration set of values and pulse generator dimensions.

Certain additional observations made during experiments with the double diode configuration of **Fig.10A** may assist in understanding of the invention.

1) Replacing residual air with argon gas leads to higher PAGD frequencies, as noted by us when utilising a 128 cm^2 H200 AC plate pulse generator in the double diode configuration (V = 575). At 1 Torr, the pulsation rate went from 20 PPS in air to 1300-1400 PPS in argon. With 29 12V cells in the charge pack, input currents ceased to flow into it. Under these conditions, the tube potential across the plates decreased and the drop across the input resistor increased. The value of E (= V/d) became smaller (gap size = 3 cm from plate to axial anode collector), as the extinction voltage decreased.

2) With frequencies of 400 PPS, the currents flowing into the charge pack fell to zero. Replacing a fast-recovery type HFR 120 (1200v, 40A) diode bridge by a type MUR 860 (600v, 8A) diode bridge had no effect. When the amplitude of plate potential oscillations falls below the potential of the charge pack, there is also a tendency to produce arc discharges. For output currents from the vacuum pulse generator to enter the charge pack, the number of cells must be reduced so that the potential of the charge pack is low enough to admit the transduced currents. A reduction from 29 to 23 cells allowed currents of 250 mA to enter the CP, and further reduction to 19 cells doubled these currents (per polarity arm).

3) Our observations show that it suffices under these conditions (CP of 19 cells) to increase the vacuum, so that the frequency decreases, and the plate potential and the charge pack input currents increase. At 0.1 Torr, the currents reached 1A DC per plate, and at 0.05 Torr, 2A DC

The interconnection between these factors indicates that the extinction voltage is a function of the PAGD frequency: the higher the PAGD frequency, the lower the extinction voltage, until empirical (in distinction from predicted) VAD field values are reached. As a consequence, the start voltage of the charge pack must be adjusted, by varying the number of cells composing it, so that it lies below the lowest extinction voltage of the PAGD, for any given geometry and gap distance.

Secondly, as the ion plasma is made more rarefied, the frequency of the emissions decreases, but the peak values of the output voltage and current per pulse increase. The slower the PAGD and the more rarefied the atmosphere, the higher is the output energy produced by the system relative to the input energy.

Autographic analysis of PAGD-induced cathode craters in H34 plates was performed, and their average inner diameter and maximum depth were determined. Similar studies were performed for PAGD-induced craters in Alzak (trade mark) plates. The secondary craters characteristically found in Alzak plates, along fracture lines irradiating from the main crater, are absent in H34 plates; instead, in H34 plates, one observes a roughened surface surrounding the emission crater, quite distinct from the original rough aspect of the pulled finish of these hardened aluminium plates. Also, unlike the Alzak main craters, the H34 craters often have a convex centre occupied by a cooled molten metal droplet, whereas the Alzak craters had a concave, hollowed out aspect. Eventually, as the pitting resulting from PAGD cathodic emissions covers the entire cathode, the metallic surface gains a very different rough aspect from its original appearance. In this process, craters from earlier metal layers become progressively covered and eroded by subsequent emissions from the same cathode. Altogether different is the surface deposition process occurring at the anode; here, the surface appears to become more uniform, through the mirroring and possibly abrasive actions of cathode jets. Macroscopically, with increased periods of PAGD operation, the anode surface appears cleaner and more polished.

With the data obtained by the metallographic method of crater measurement, we estimated the volume of metal ejected from the cathode, by assuming that the crater represents a concavity analogous to a spherical segment having a single base (1/6pi x H [$3r^2 + H^2$], where **H** is the height of the spherical segment and **r** the radius of the sphere), while disregarding the volume of the central droplet leftover from the emission. The following are mean +/- SEM crater diameters (D), crater depths (H) and maximum volumes (V) of extruded metallic material for two types of aluminium cathodes, Alzak and H34 hardened aluminium, subject to a high input current PAGD:

1. Alzak: D -0.028 cm +/- 0.003; H -0.002 cm +/- 0.0002; V - 6.2 x 10^{-7} cm^3

2. H34: D -0.0115 cm +/- 0.0004; H -0.0006 +/- 0.0001; V - 3.1 x 10^{-8} cm^3

Accordingly, utilising plates composed of either material with 3 mm of thickness, and thus with a volume of 38.4 cm^3 per plate and considering that only 2/3rds of the cathode shall be used (a 2 mm layer out of the 3 mm thickness), the total number of pulses per plate total (TLT) and partial (PLT) lifetimes is theoretically:

1. Alzak: TLT: 6.2 x 10^7 pulses; PLT: 4.1 x 10^7 pulses;

2. H34: TLT: 1.2 x 10^9 pulses; PLT: 8.1 x 10^8 pulses.

Typically, an H34 device can produce about 0.25 kWh per 10,000 pulses. The corresponding value for a PLT is thus a minimum of 1.0 MWh/Alzak cathode and of 20 MWh/H34 cathode. As the cathode for each combination is only 66.7% consumed, the vacuum pulse generator may continue to be used in a reverse configuration, by utilising the other plate in turn as the cathode; thus, the estimated minimal values become, respectively, 2.0 MWh/Alzak pulse generator and 40 MWh/H34 pulse generator. The same rationale applies for the double diode configuration of **Fig.10C**.

We have created a two-ported system for the production of the singular discharge events which we have previously identified in the “863” application as an endogenous pulsatory abnormal glow discharge regime where the plasma discharge is triggered by spontaneous electronic emissions from the cathode. We have examined the functioning of this two-ported system in order to determine what were the electrical power input and output characteristics of a sustained PAGD regime. Despite the wide (10-fold) variations in net power and break-even efficiencies measured by the four different methods employed (open voltage measurements, time integration of negligible power measurements, operational power measurements and real time non-negligible power measurements), all methods indicate the presence of an anomalous electrical transduction phenomenon within the vacuum pulse generator, such as can result in the production at the output port of electrical energy measured and directly captured which is greater than would be anticipated having regard to the electrical energy input at the input port. With the most accurate of the methods employed, we have found typical PAGD power production rates of 200 WHr/hour of PAGD operation, and these may reach >0.5 kWh/h values.

The discrepancies between the methods utilised have been extensively examined in the preceding section. Our systematic approach demonstrates that the most frequently employed method of measuring the charge capacity of batteries by the open voltage values is the least reliable approach for the determination of the actual net power lost or gained by the battery packs used in the system: when compared to all three other methods, it overestimates net power consumed and produced by up to 10 fold, as well as distorting the break-even efficiencies, particularly at the extremes of operation. All this results from the grossly diminished (50-60% of manufacturer's theoretical estimate) effective charge capacity of the lead acid gel cells employed, as determined experimentally from **Fig.18** and **Fig.19**, when compared to the theoretical maximal charge capacity values that serve as scale for the open voltage measurements. In other words, the effective energy density of the batteries during these experiments was in fact approximately half of the manufacturer's estimated 30 WHr/kg.

Under these actual conditions of battery performance, the third and fourth methods (respectively, operational and real-time non-negligible power measurements) of power consumption and production proved to be the best approach to measure both PAGD electrical power input and output, as the results of both methods matched each other closely, even though the former is a statistical treatment of simultaneous events and the latter is a real time integration of their cumulative effects. The second method is clearly less reliable than either the third or the fourth methods, and this stems from the fact that the power consumption slopes of negligible resistive discharges not only are very different from the quasi-steady state discharge slopes (beginning at >5 - 15 minutes) of extensive resistive discharges, but also their proportionality may not reflect the real time proportionality of equivalent prolonged resistive discharges.

The main advantage of the fourth method is that it effectively takes into account the actual time performance of the batteries comprised by the overall PAGD production and capture system we have described. As such, the method may have the main disadvantage of reflecting more the limitations of the batteries employed (their high

rate of degradation of the absolute value of total effective charge capacity, and limited efficiency in retaining charge derived from discontinuous input pulses) than indicating the actual power output. There are a number of possibilities for fine tuning of the system introduced by the present work, beginning with the utilisation of secondary batteries or other charge shortage or absorption devices that have less variable or more easily predictable actual charge capacity.

In this respect, there are two major shortcomings to the batteries used to form the drive and charge packs; (1) their significant memory effect and (
2) their design for constant, rather than discontinuous, DC charging.

Recently developed Nickel Hydride batteries are an example of an electrostatic charge-storage system that lacks a substantial charge memory effect, and their experimental batteries are being developed currently for higher efficiency intermittent charging methods. Electrostatic charge retention systems having better energy densities, better charge retentivities and insignificant memory effects will probably be more efficient at capturing and holding the energy output by the circuit. In practical embodiments of the invention, effectiveness in charge utilisation will be more important than measurability, and any device that will use the energy effectively whilst presenting an appropriate back EMF to the system may be utilised.

The effect of the performance characteristics of the drive and charge packs is only one amongst many parameters affecting operation of the invention. As shown by our extensive investigation of the diverse PAGD phenomenon the recovery of energy from it by electromechanical transduction as in the “531” application, or electrostatic capture as described above, the factors involved in modulating the frequency, amplitude and peak current characteristics of the PAGD regime are complex. Manipulation of these factors can improve electrical energy recovery, or reduce it or even suppress PAGD. We have so far noted numerous factors that affect PAGD frequency and some amongst those that also affect the PAGD amplitude. Aside from these factors, the circuit parameters of the output port portion of the circuit, in addition to the nature and chemical characteristics of the battery cells already discussed, the charge potential of the charge pack, the characteristics of the rectifiers in the recovery bridge in relation to the period of PAGD super-resonant frequencies, and the effective values of the parallel and transversal capacitance bridges can all influence the results achieved. Certain factors however have a radical effect on PAGD operation, such as the gap distance and the charge pack potential.

Too small a gap distance between the cold emitter (cathode) and the collector will result in an increasing reduction in energy recovery. The potential presented by the charge pack must be less than the voltage amplitude developed by the PAGD, as specified by a given gap distance at a given pressure. Too large a charge pack size with respect to PAGD amplitude and the gap length will preclude PAGD production or result in extremely low PAGD frequencies. In brief, the energy absorption rate and the counter potential presented by the charge pack or other energy utilisation device are important factors in the operation of the circuit as a whole, and should either be maintained reasonably constant, or changes should be compensated by changes in other operating parameters (as is typical of most power supply circuits).

Since our test results indicate that the electrical power output of the circuit can be greater than the electrical power input to the circuit, the circuit clearly draws on a further source of energy input. Whilst we do not wish to be confined to any particular theory of operation, the following discussion may be helpful in explaining our observations. These observations have been discussed in some detail so that the phenomenon observed can be reproduced, even if the principles involved are not fully understood.

In the “863” and “531” applications we have identified a novel, cold-cathode regime of vacuum electrical discharge, which we have termed the pulsed abnormal glow discharge (PAGD) regime. This regime, which occupies the abnormal glow discharge region of the volt-ampere curve of suitable discharge tubes, has the singular property of spontaneously pulsing the abnormal glow discharge in a fashion which is coming from the tube and its circuit environment that constitutes a vacuum pulse generator device, when it is operated under the conditions which we have identified. In fact, when stimulated with continuous direct current, in such conditions, such a circuit responds with spontaneous abnormal glow discharge pulses that enable effective segregation of input and output currents.

We have demonstrated electrically, metallographically, oscillographically and videographically, how the pulsed discontinuity results from a self-limiting, auto-electronic cathode emission that results in repeated plasma eruptions from the cathode under conditions of cathode saturated current input. The auto-electronic triggering of the PAGD regime is thus akin to that of the high-field emission mechanism thought to be responsible for vacuum arc discharges (VAD regime). However, under the PAGD conditions we have defined, this mechanism is found to operate in the pre-VAD region at very low field and low input average direct current values, with very large inter-electrode distances and in a self-limiting, repetitive fashion. In other words, the PAGD regime we have identified has mixed characteristics: its current versus potential (abnormal glow) discharge curve is not only distinct from that of a vacuum arc discharge, but the electrical cycle of the PAGD regime itself oscillates back and forth within the potential and current limits of the abnormal glow discharge region, as a function of the alternate

plasma generation and collapse introduced by the discontinuous sequencing of the auto-electronic emission process. Accordingly, the intermittent presence of the abnormal glow, as well as the observed segregation of the current flows, are due to the diachronic operation of these spontaneous cathode emission foci. The micro-crater and videographic analyses of the PAGD have demonstrated the presence of an emission jet at the origin of each pulse, a phenomenon which VAD theory and experiment has also identified. Metallic jets originating at the cathode spots of VADs have been known to present velocities up to, and greater than 1000 m/sec.

In light of the above, the energy graft phenomenon we have isolated would have to be operated, at the micro-event scale, by the interactions of the cathode emission jet with the vortex-formed impulse-transducing plasma in the inter-electrode space. Several aspects can be approached in terms of the complex series of events that constitute a complete cycle of operation, on a micro-scale. There are interactions within the cathode, interactions at the cathode surface, interactions between the emission jet and the plasma globule close to the cathode, and finally, interactions of the resulting electron and ion distributions in the inter-electrode plasma, within parallel boundaries.

In general, in the presence of an electrical field, the distribution of potential near the cathode forms a potential barrier to the flow of electronic charge, as this barrier is defined by the energy that the most energetic electrons within the metal (the Fermi energy electrons) must acquire before freeing themselves from the cathode surface potential, to originate an emission jet. Before any free electrons become available for conduction in the space adjoining the cathode, they must cross the boundary posed by the potential barrier. With a weak applied field, classical electron emission from a metal can only occur if an energy practically equal to the work-function of the metal is imparted in addition to the Fermi energy. Under thermionic conditions of emission, the heating of the cathode provides the needed energy input. However, the cold-cathode Fowler-Nordheim quantum-field emission theory predicted the existence of a finite probability for an electron to tunnel through the potential barrier, when the applied field is high. Cold-cathode electron emissions are thus possible, under these conditions, at practically Fermi energy levels, as the high field would catalyse the tunnelling through the potential barrier by narrowing the barrier width for the Fermi energy electrons. The exact localisation of the emission would then depend on the randomised fluctuations of high fields at the cathode, which were produced by positive space charges sweeping in proximity to it.

For most purposes, this theory has been the working hypothesis of the last 60 years of field emission studies, which have centred upon the VAD mechanism, despite the fact that observed field gradients are evidently inadequate to explain breakdown as a function of the theoretical high field mechanism. The Fowler-Nordheim theory has therefore suffered major revisions and additions, mostly to account for the fact that it postulates, as a condition for cold-cathode field emission in large area electrodes, the presence of enormous fields ($>10^9$ V/m) and extremely low work functions, neither of which are borne out by experimental VAD investigations. Some researchers have found that the breakdown responsible for the VAD field emission is promoted by Joule heating and vaporisation of microscopic emitter tips, and that this requires a critical current density (10^{12} A/cm^2), while others emphasised that this explanation and these thresholds did not hold for large area emitters and that a space charge effect of concentrating the ion distribution near the cathode promoted breakdown under these circumstances, when the field reached a critical value; large field enhancement factors (more than a thousand-fold) have been postulated to explain the discrepancy between theoretical predictions and experimental findings regarding the critical breakdown field values, and others have demonstrated how this critical field value effectively varies with work-function and electrode conditioning.

The PAGD regime and its self-extinguishing auto-electronic emission mechanism stands as an exception to the high field emission theory as it currently stands with all its modifications, especially given that in this phenomenon we are confronted with a cathode emission that spontaneously occurs across the large gaps in large plate area pulse generators, at very low field values (down to $<1 \times 10^4$ V/m), as shown above and in the “863” application. Moreover, a Fowler-Nordheim plot (in the form Log_{10} (I/V^2) versus 1/V) of the PAGD volt-ampere characteristic exhibits a positive slope, rather than the Fowler-Nordheim negative slope characteristic of VAD field emission. However, current density values obtained from correlations of autographic analysis of the cathode with an analysis of event-oscillogram (peak pulse currents), indicate that the PAGD current density J may reach values of 10^5 to 10^7 A/m^2 during the emission process (the larger Alzak craters have an associated lower J value), values which, at the upper end, do not reach the 10^9 A/m^2 current density threshold required by the Fowler-Nordheim theory. Considering these two distinct observations with regards to field strength and current density, we have to admit the existence of a low field, large area cold-cathode auto-electronic emission endowed with high current densities, which is not predicted by current field emission theory.

Unlike the typical VAD regime, the PAGD is neither a high frequency oscillation, nor does it occur in a random fashion. It constitutes a semi-regular, quasi-coherent, periodic energy transduction which cycles between cathode drop limits that are higher by a factor of 2 to 15 than typical vacuum arc cathode drops. The intermittent cathode emission responsible for the low frequency, pulsed behaviour of the abnormal glow, is also self

extinguishing and self-starting, under the conditions we have defined. Furthermore, we have also identified a novel and unexpected dependency of the periodic pulse rate upon the cathode area. This indicates the presence of field emission control parameters heretofore unsuspected. It is likely that field fluctuations of the polarised pre-breakdown field is responsible for eliciting the particular localisations of the auto-electronic emission foci, as well as what imparts, in a lens-like fashion, the distorted field energy needed for electron surface release. In this sense, external, electrical or magnetic field fluctuations (e.g. motion of static charges or of constant magnetic fields) induced by us at pre-breakdown potentials, provoked PAGD emissions and breakdown at these levels.

In general, VAD studies have shown that, for large area electrodes, microgeometry, adsorbed gas layers and gas impurity contents of the cathode play a role in modulating field emission. In our PAGD studies, the interactions at the cathode surface and across the cathode potential drop are clearly modulated by:
(1) the nature of residual gases, as shown by our air vs Argon studies;
(2) their pressure,
(3) electrode conditioning,
(4) work-function and
(5) cumulative pulse count, amongst others.

The plasma, in leak-controlled or low pressure PAGD devices, has both residual gas and metallic vapour substrates. In devices initially closed at high to very high vacua (diffusion pump pressures), the major residual substrate, whose presence increases with time of operation, is the metallic vapour released from the cathode and not impacted on to the envelope walls or the anode. It has been previously shown for externally (magnetically or electrostatically) pulsed plasma accelerators, that the amount of residual gas or vapour left in the inter-electrode space diminishes with increasing number of consecutive discharges and a growing amount of electrode-insulator absorption of gas. The effect of such removal of residual gas or vapour is to decrease the vacuum of a sealed envelope. With high vacuum sealed PAGD generators we have observed that prolonged operation and sputter-induced mirroring of the envelope causes a progressive disappearance of the discharge, as the voltage potential needed to trigger it also increases. At the thermocouple, low frequency pulsed abnormal glow discharges can also be seen to increase the vacuum significantly. These results suggest instead the presence of a pumping mechanism in the PAGD which is somewhat analogous to that of sputter ion pumps, where collision of ionised gas molecules with the cathode is responsible for the sputtering of cathode material that either combines with the gas substrate (`gettering` action) or `plasters over` the inert gas molecules on to the anode (a process known as `ion burial`). These are the two basic pressure reducing actions of sputtered getter atoms, in ion pumps.

However, in ion sputter pumps, the initiation of the cycle is a function of the presence of high velocity electrons in the high field plasma of the glow discharge, which are necessary to ionise the gas substrate molecules; also, the getter material typically has a high work-function for field emission. Hence, the sputtering is due to the secondary impact of plasma positive ions at the cathode, after plasma ionisation has occurred in the inter-electrode space. Altogether different is the mechanism of spontaneous, primary electron emission from the cathode, which is characteristic of the low field PAGD: here, the sputtering is caused by the electronic emission itself and attendant metallic vaporisation processes. By artificially confining the firing foci to a part of the cathode, we have shown in the single diode configuration how the PAGD induced sputtering is associated with the cathode auto-electronic emission mechanism, rather than with the abnormal cathode glow per se, given the localisation of sputtering on to the emission region of the plate, despite its overall cathode glow saturation.

These observations would thus seem to corroborate the hypothesis of a progressive vacuum increase with the cumulative number of emitted pulses, were it not for the fact that experiments performed with leak controlled devices (reported here and in previous studies) show that, when the negative pressure is maintained by balanced leak admission of air or argon, pulse rates still decrease with cumulative pulse count, and do so neither as a function of an increase in vacuum, nor as a function of envelope mirroring (unless this is so extensive as to establish envelope conduction), but rather as a function of processes (generally referred to as conditioning) inherent to the electrodes, specifically, to the cathode. We have further shown that, for such altered emitter states, the pressure of the vessel must be increased, not because of an increasing vacuum (precluded by the controlled gas leak), but because of the effect that residual gases may have in modulating the low field PAGD emission.

PAGD electrode conditioning is a cathode-dominant process resulting from the cumulative emission of high numbers of pulses by a cathode, and has been shown to be a factor independent of the nature and pressure of the residual gas and partially reversible only by operation with reversed plate polarity, unlike reports of copper cathode-dominant conditioning. It is thought that electrode conditioning and the accompanying increase in VAD breakdown potential are due to the progressive adsorption of residual gases, though cathode-dominant conditioning processes, such as subjecting the vacuum gap to consecutive discharges, have been shown to correlate the decrease in plasma impulse strength with electrode outgassing of absorbed or adsorbed gases. Moreover, given the pitting action of crater formation at the cathode by the PAGD regime, and, as we shall see below, the metallic plating of the anode, the PAGD cathode-dominant process of conditioning we have observed with respect to decreased pulse frequency and increase in potential, suggests that the apparent increase in

cathode work function is not due to gas adsorption or absorption. These processes are more likely to occur on the plated anode. It is likely that, given the observed PAGD pressure reducing effect caused by the cathodic jet, a certain outgassing of the cathode is in fact occurring during PAGD function.

One might also expect that the anode, if plated by sputtering atoms, would increase its gas content in the formed surface film. However, controlled leak experiments suggest instead that some other type of alteration of the cathode work function is occurring, which is, as we shall examine below, independent of the adsorbed gas state of the electrodes, as well as independent of the PAGD ion pump-like effect. Nonetheless, even at the level of the anode, the PAGD sputtering action may have contradictory effects: it may impact inter-electrode gap molecules on to the collector, as well as release, by ionic bombardment and vaporisation, gases adsorbed to, or contaminating the anode. If we assume that gas adsorption by impact on the collector is the predominant mechanism, one could explain the increase in the number of breakdown sites per unit time, as observed by us for a re-reversed cathode, if the number of PAGD breakdown sites depended on the quantity of adsorbed gases, e.g. oxygen, on the cathode being tested. Recovery of the cathode work-function would depend on the electronic charge recovery of the positively charged, adsorbed or occluded gas layer at the cathode- either by reversal or as a function of time of inactivity.

The surface film theory of “electrical double layer formation at the cathode” in fact contended that, low field flash over is a photocathodic effect dependent upon the presence of a glowingly positively polarised gaseous film at the cathode; this film would lower the cathode emissivity by decreasing the field between the cathode surface and the leading edge of the cathode glow, across the cathode drop. However, even though the surface film theory of “electrical double layer formation at the cathode” predicts the lowering of the emission breakdown potential and the increase in flash over rate when the electrodes are reversed - as the anode would have acquired a surface charge capable of affecting the breakdown potential, it acknowledges nevertheless, that the anodic surface charge hardly explains the observed intensity of the polarisation effects.

Moreover, non-reversed, conditioned cathodes retained their lower PAGD frequencies in a time-independent manner, for as long as reversal was avoided (excluding a PAGD frequency recovery effect due to plate cooling, which may be as short as 15 minutes). PAGD conditioning was independent of idle time and increased with cumulative pulse count. Moreover, the AGD pulses are not UV photocathodic Townsend discharges, liberating secondary electrons via positive ion impact at the cathode. Nor could photocathodic emissions generate currents of the magnitude observed in the PAGD. Lastly, the PAGD discharge and breakdown thresholds appear to be unaffected by UV, though they may be somewhat depressed by visible light, and the emission mechanism in the PAGD is the primary process.

Removal or flattening of protuberances and tips from the emitting cathode by the action of the discharge, is a process also thought to play a role in hardening the cathode or increasing its field emission work-function. However, this explanation may not be adequate for the PAGD emission process, if we consider our metallographic findings of a smoothing action of the discharge at the collector. In fact, it would appear that the flattened, smoother, plated, mirrored and cleaner surfaces subjected to PAGD bombardment are the explanation for the observed increased emission ability of re-reversed cathodes: mirrored Alzak surfaces emit at higher frequencies than do dull H34 and H220 surfaces; new, polished surfaces emit at a higher frequency than do pitted, broken-in surfaces; anode surfaces, never before utilised as cathodes but subjected to prolonged PAGD action, emit at higher frequencies when employed as cathodes, than do new, identical cathode surfaces; and ex-cathodes, employed for prolonged periods as anodes, regain a higher emission frequency upon re-use as cathodes. The better PAGD emission performance of smoother cathodes, compared with the worse VAD emission performance of the same, when pitted cathodes (lacking protuberances) are used, requires explanation.

Rakhovsky has put forth a VAD model for cathode spots, that distinguishes between Type I spots (quickly moving spots, far from steady state and responsible for crater formation), and Type II spots (quasi-stationary and near steady-state, but leaving an itinerant track with no sign of crater formation). Whereas the former would obey the Fowler-Nordheim requirement for high fields ($>10^9$ V/m), the latter could hardly be expected to do so with typical arc voltage drops in the order of 10 V. Once again, autographic analysis of the PAGD emission aspect indicates mixed characteristics: the PAGD cathode spot is a hybrid. It behaves as an intermittent instability that leaves single (e.g. in H34) or clustered (e.g. in Alzak) craters, which are both qualities of Type I cathode spots; and it exists under low field conditions ($<10^5$ V/m), with cathode drops of 20 to 150 V, in a quasi-coherent mode, leaving an itinerant track of successive craters when operating at the higher frequencies, all of which are properties approaching those of a VAD Type II cathode spot.

Furthermore, the macroscopically visible metal sputtering (due to the explosive action of the PAGD emission phenomenon) occurring at the upper end of the permissible DC current input scale, and the presence of large solidified molten metal droplets in and around the craters, suggest models which have been proposed for explosive electronic emission. Explosion models propose that the creation of a residual plasma ball in front of a microprotuberance provokes the large potential drop at the prospective emission focus and sufficiently high

resistive and Nottingham heating to reach $>10^7$ A/cm^2 current densities during the explosive consumption of these microemitters. Whether the explosive action associated with cathode spots is an auxiliary effect that applies solely to the vaporisation of the emitting microprotrusion, or an integral emission and vaporisation explosive process, it does not appear that it can be restricted to high-field VAD Type II cathode spots, given that it can be equally made to occur with the low field PAGD hybrid cathode spot, and be macroscopically observed. Indeed, in the plate diode configuration, it is easy to visualise the metallic particle explosions that surround and accompany the plasma jets, near to upper current limit conditions. However, if we are to assume that any of these models apply to the emission mechanism, we would, in all likelihood, have to conclude that the PAGD initial emission sites must be sub-microscopic (100 to 10 nm), rather than microscopic.

Resolution limits to our own metallographic examination of the smoothing action of the PAGD discharge on the collector would thus have precluded us from detecting formation of such sub-microscopic protrusions, as well as their presence in a “soft” cathode and thus infer their disappearance from a pitted, hardened cathode; but if the disappearance of such sub-microprotuberances were responsible for the observed alteration of cathode work function, one would also thereby have to postulate the existence of a mechanism for microroughness regeneration (e.g.. tip growth) at the anode, in order to explain the observed increased emission upon cathode re-reversal. Furthermore, this regeneration would have to be actively promoted by operation with reversed polarity, and this is problematic. Focusing of the distorted or magnified field upon alumina inclusions on pure iron electrodes has been demonstrated to degrade breakdown voltage for field emission, but the effect was greater for larger microscopic particles. If we were to apply this concept to our work, it would require the existence of unmistakably abundant microscopic heterogeneities in the quasi-homogeneous electrode surfaces employed, which we did not observe; on the contrary, their absence suggests that either the microroughness responsible for the low field PAGD emission is sub-microscopic, or that the field distortion responsible for eliciting the PAGD is independent of the presence of these protuberances. This last possibility must be taken all the more seriously, in light of the fact that PAGD functioning is able to cover the entire surface of an emitter with craters.

Whereas the discharge potentials observed in the PAGD have been shown to be relatively independent of the kind of gas present, there is a gas effect in the PAGD phenomenon, particularly in what concerns its frequency, observed when the same “run down” cathode was capable of much higher emission rates when exposed to argon, than to air. Utilising the technique of bias sputtering, it has been demonstrated that the number of charge symmetric collisions (dependent upon sheath thickness **d** and the ion mean free path) in the plasma sheath, which are responsible for lower energy secondary peaks in ion energy distribution **N**(E), at pressures of 0.2 Torr, is substantially greater in argon than in argon-nitrogen mixtures, and thus that, under these conditions, mostly Ar^+ and Ar^{++} ions impact the negatively biased electrode. In non-equilibrium RF discharges, greater ion densities have also been attained with argon, than with air. With respect to field emissions, one would expect a gas effect only with regards to changes on surface conditions, though such studies have shown contradictory effects of argon upon cathode work function.

In light of the foregoing, and given that the PAGD is an emission discharge and not a sputtering discharge per se, in the strict sense, we can conceive of the role of inert gas atoms in increasing, as compared to air or nitrogen, the ion energy density distribution at the PAGD cathode spot interface with the cathode surface emitter, and thus elicit increased emission rates from the cathode, by pulling electrons from the metal via the field effect. While this is consistent with the concept of focused distortions of space-charge field fluctuations inducing localisation of the emission foci, the argon effect can be observed in the PAGD regime over the entire range of the Paschen low vacuum curve, and into Cooke's mid to high vacuum curve, at low fields and without negative biasing. Thus, it is not simply a high pressure (nor a gas conditioning) effect, even if the gas effect in question applies to the description of a local pressure rise at the emission site/cathode spot interface, which may play a role in enhancing the local field.

Considered together, the PAGD emission-derived sputtering, the observed metallic plating of the anode and the explosive aspect of the discharge, suggest the presence of a jet of metallic vapour present in the discharge and running, contrary to the normal flow of positive ions, from the cathode to the anode. This jet appears to have properties similar to the high speed vapour ejected from the cathode in a VAD, as first detected by Tanberg with his field emission pendulum (Tanberg, R. (1930), "On the cathode of an arc drawn in vacuum", Phys. Rev., 35:1080) In fact, the VAD high field emission process is known to release, from the cathode spot, neutral atoms with energies much greater than the thermal energy of the emission discharge. This anomalous phenomenon brings into play the role of the reported cathode reaction forces detected in vacuum arc discharges (Tanberg, as above, also Kobel, E. (1930), "Pressure and high vapour jets at the cathodes of a mercury vacuum arc", Phys. Rev., 36:1636), which were thought to be due to the counterflow of neutral metallic atoms, from the cathode on to the anode (charged metallic ions are normally expected to target the cathode). In absolute units of current, this current quadrature phenomenon has been shown to reach, in the VAD regime, proportions of the order of $100 \times I^2$ (see also the Aspden papers referenced below).

Early interpretations attributed this to the cathode rebounding of <2% of gas substrate-derived plasma positive ions hitting the cathode and being charge-neutralised in the process, but having kept most of their thermal energy. Tanberg held instead that the counterflow of neutral particles responsible for the cathode reaction force was cathode derived, effectively, that it constituted a longitudinal interaction acting in the direction of the metallic arc jet. However, even though secondary high energy distributions of neutral atoms emanating from the cathode do not have thermal energies, their modal distribution does (Davis, W. D. and Miller, H. C. (1969) J. Appl. Phys., 40:2212) furthermore, the major anomalous atomic counterflow that accompanies the high-energy electron flow toward the anode, was shown mass spectrographically to consist predominantly of multiply ionised, positively charged ions of cathode metal, rather than neutral atoms. If this made it easier to abandon the primacy of the rebounding model, it was now more difficult for field emission theorists to accept and explain the observed high energies (ion voltages in excess of the discharge voltage drops) and the high ionisation multiplicity associated with these counter-flowing positive ions.

This field of investigation has indeed been one of the mounting sources of evidence suggesting that there is something amiss in the present laws of electrodynamics. The anomalous acceleration of counter-flowing ions, and the energy transfer mechanisms between high speed or “relativistic” electrons and ions in a plasma (Sethion, J. D. et al, "Anomalous Electron-Ion Energy Transfer in a Relativistic-Electron-Beam-Heated Plasma" Phys. Rev. Letters, Vol. 40, No. 7, pages 451-454), in these and other experiments, has been brilliantly addressed by the theory of the British physicist and mathematician, H. Aspden, who first proposed a novel formulation of the general law of electrodynamics capable of accounting for the effect of the mass ratio factor (M/m') in the parallel (and reverse) motion of charges with different masses, (Aspden, H. (1969) "The law of electrodynamics", J. Franklin Inst., 287:179; Aspden, H (1980) "Physics Unified", Sabberton Publications, Southampton, England). The anomalous forces acting on the counter-flowing metallic ions would stem from their out-of-balance interaction with the emitted high speed electrons, as predicated by the electrodynamic importance of their mass differential. This results in a fundamental asymmetry of the plasma flow between electrodes, localised on to the discontinuous interfaces of the plasma with the electrodes, namely, in the cathode dark space and in the anodic sheath: on the cathode side, electrons act upon ions, as the emitted electrons having less than zero initial velocities, drift against the incoming ion flux and in parallel with the ion and neutral counterflows; on the anode side of the discharge, positive ions flowing toward the cathode confront mainly the incoming counterflow of positive ions and neutral atoms, as the high speed electrons have abnormally transferred their energy to counter-flowing, high speed, cathodic metal ions. An out-of-balance reaction force thus results at the cathode, to which the leaving metallic atoms impart a force of equal momentum but opposite direction, a force which is added to the cathode momentum generated by impacting, normal flowing positive ions.

Moreover, Aspden confirmed theoretically the fundamental contention of Tanberg's experimental findings that an electrodynamic force will manifest itself along the direction of the discharge current flow, and thus, that the atomic counterflow is a metallic jet. Aspden further demonstrated that this asymmetry of plasma discharges does not imply any violation of the principles of conservation of energy and charge equivalence, given that there will be no out-of-balance force when such anomalous forces are considered in the context of the whole system of charge which must, perforce, include the local electromagnetic frame itself. Such discharges must be viewed as open-energy systems, in balance with their electromagnetic environment: their apparatuses may constitute materially closed or limited systems, but they are physically and energetically open systems. Current work on Aspden's formulation of Ampere's Law indicates that both classical electromagnetism and special relativity ignore precisely, in circuits or in plasma, the longitudinal interactions that coexist with transverse ones. Standing longitudinal pressure-waves, of a non-electromagnetic nature, have been previously shown in plasma electrons, which did not conform to the Bohm and Gross plasma oscillation mechanism (Pappas, P. T. (1983) "The original Ampere force and Bio-Savart and Lorentz forces", I1 Nuovo Cimento, 76B:189; Looney, D. H. and Brown, S. C. (1954) "The excitation of plasma oscillations" Phys. Rev. 93:965)

The present theoretical approach to the novel regime of electrical discharge which we have isolated in specially designed devices, and to its mixed glow-arc characteristics, suggests that a similar, out-of balance current quadrature phenomenon occurs in the discharge plasma during the low field, auto-electronic emission-triggered PAGD, and is responsible for the observed surplus of energy in the experimental system described in this report. Clearly, all the evidence we have adduced indicates that there is a powerful longitudinal component to the emission-triggered PAGD, i.e. that the discharge pulses characteristic of this pre-VAD regime are longitudinally propelled jets of cathode-ejected high speed electrons and high speed ions. We have performed experiments, in the PAGD regime of operation, with very thin axial members that bend easily when placed in the path of the discharge, or with Crooke radiometer-type paddle-wheels, and both show the presence of a net longitudinal force in the plasma discharge acting in the direction of the anode, which confirms the magnitude of the atomic counterflow (ionised and neutral) present during the PAGD, very much like Tanberg's pendulum did for the VAD.

These observations also tally with the explosive action of the emission mechanism, such as we have examined it above. In this context, two aspects of the PAGD are remarkable: the fact that a phenomenon akin to field emission occurs at low field values, for large area electrodes across large gaps, and the conclusion that the PAGD must deploy an excessively large counterflow of, in all probability, both ionised and neutral cathodic

particles. The observation of ion current contributions to the cathode current on the order of 8 to 10%, in VADs, can hardly apply to the PAGD mechanism responsible for the anomalous currents and counterflows observed. Hence, we should further expect that the characteristically intermittent, or chopped current regime of the PAGD, is a major factor in the generation of disproportionately high energy longitudinal pulses and in allowing our system to capture most of the electrical energy output from the device. In all probability, field collapse at the end of discharge favours the nearly integral collection of the plasma charge, and ensures the transduction of most of the plasma energy of the pulse (blocked, as it is, from flowing back through the input port to the drive pack) to the output port, through the parallel, asymmetric capacitance bridge that interfaces with the charge recovery reservoir (the charge pack). Collapse of the field of the discharge may also be a contributing factor to the anomalous acceleration of ions, and to the observed anode plating effect.

It is equally possible that such abnormally large longitudinal pulses may never be observable, for a given arrangement and scale, above threshold frequencies of the oscillation; we have, in this sense, presented data that indicates that for a given geometry, above specific PAGD frequencies, the capture of surplus energy decreases steadily in efficiency until it ceases altogether, for a given arrangement. The point at which this surplus begins to decrease coincides with the setting in of frequency-dependent irregularities in the discharge sequence and, most importantly, it coincides with a reduction of the peak pulse current for each PAGD pulse. We have further remarked that increasing the PAGD frequency above the zero surplus point, for a given arrangement, by manipulating any of the frequency control parameters, provokes the slippage of the PAGD into a full fledged VAD regime, while input currents greatly increase and output peak currents greatly decrease (to comparable peak input levels of 10 to 15A).

The transition between the two modes of emission-triggered discharge, PAGD and VAD, thus appears to be tied in to adjustable thresholds in the frequency of the emission discontinuities; in this sense, it is rather likely that the plasma field collapse plays a major role in regularising and optimising the anomalous energies of field emissions, as in the PAGD regime. At low frequencies of low field emission, the emission regime is highly discontinuous, diachronic and regular, for it has time to fully extinguish the discharge; hence the PAGD singularity, in which the phases of each discharge pulse are well defined and sequential. Above a given high frequency, when ion and electron recombination will happen more often, before each can be collected at the electrodes, the stream of emitted discontinuities merges into a noisy, randomised continuum, where simultaneous emissions become possible and the plasma field no longer has time to collapse and fully resolve the longitudinal pulses. Any anomalous energy generated is then minimised and trapped in the plasma body and, in these conditions, the VAD regime eventually sets in. Such model would easily explain why the high field VAD experiments performed to date have never detected such extraordinarily large anomalous forces.

On the other hand, the quasi-coherent aspect of the discharge suggests that the vacuum gap, in functioning during the PAGD regime both as an insulator and as a conductor with capacitative and self-inductive properties, is periodically altered by large and intense polarisations which are resolved by the discrete emission of longitudinal pulses from the cathode. It is possible that these non-linear oscillations resulting from sudden depolarisation of the vacuum gap by high-speed explosive emissions elicited at the convection focus of the distorted field, might be in resonance or near resonance with the external circuitry, but the most apparent effect of increasing the capacitance in all bridge members is to increase the jet current and the transduced current flowing into the charge pack. The PAGD amplitude variation also presents, after the large negative discontinuity, a growing oscillation at very high resonant frequencies, which are typical of inductive chopping currents in a VAD, before extinction occurs. Unlike the VAD inductive case, in the absence of any coils other than the wire wound resistors, the PAGD relaxation oscillations which follow each pulse only extinguish the discharge when the voltage potential of the amplitude curve rises above the applied voltage, just as the plasma potential drops the most.

Given the entirely non-inductive nature of the external circuit utilised in many instances, the inductive properties in evidence are those of the vacuum device itself. It also suggests that, in the absence of any need of an applied external magnetic field for the PAGD discharge to occur coherently, it is possible that the magnitude of the currents generated produces by itself a significant self-magnetic field. Thus, we cannot rule out the possibility of a self-organisation of the plasma discharge, which may, in Prigogine's sense, constitute a dissipative structure (Prigogine, I. and George, C. (1977), "New quantisation rules for dissipative systems", Int. J. Quantum Chem., 12 (Suppl.1):177). Such self-ordering of the PAGD plasma jet is suggested by the experimentally observed transition of these pulses from the current saturated limit of the normal glow discharge region, into the PAGD regime, as a function of increasing current: smaller foci of discharge can be seen to discontinuously agglutinate into larger emission cones, or into jets with a vortex-like appearance, when the input current reaches a given threshold.

It is possible that, under these conditions, the distribution of the charge carriers and their sudden fluctuations may render any steady-state plasma boundary conditions ineffective and provoke a singularity in the discharge mechanism; this non-linear behaviour, together with any self-magnetic effects, might provide radial coherence of the plasma flow along the longitudinal path of the discharge. This concept is akin to what has been proposed for periodically fading-away solution structures referred to as “instantons”, that represent self-organising transitions

between the two states of a system. The PAGD may well be an instance of an instanton type structure bridging the open, or conductive, and the closed, or insulating, states of the vacuum gap. An analytical formulation of the problem of the plasma flow from the cathode spot to the anode, which would take into account the self-magnetic and self-organising properties of the PAGD plasma channel, would be extremely difficult, given the out of balance longitudinal force, its abnormal energy transfer and associated counterflow, as well as the competition between collisional and inertial exchanges.

The plating observed at the anode most likely results from the impact of counter-flowing ions (and possibly neutral atoms), whereas the pitting of the (locally molten) cathode results from the emission of vaporised metallic material and electrons, as well as, secondarily, from bombardment by incident positive ions. The first action smoothes the surface by mirroring it (deposition of cathode-derived atoms) and abrading it, whereas the latter smoothes it in places by rounding concavities and by forming molten droplets upon local cooling, while simultaneously roughening it on the crater peripheries. One might think that this cathode roughening should lower the work function and facilitate the discharge, but the facts indicate that just the opposite must be happening in view of changes in the PAGD according to the nature and state of the cathode surface. The observed alterations of electrode work function for PAGD low field emission must thus be related to the molecular and charge effects of these different actions at the two electrodes. It appears that for large parallel plate electrodes, the PAGD low field emission is modulated by the nature and, most likely, by the molecular structure of the metallic surface layer of the emitter.

We have thus devised a system for the capture, as electricity, of the energy of anomalously energetic longitudinal pulses sequentially triggered by spontaneous emissions of high-speed electrons and ions generated from low work function cathodes, during the low field and singularly mixed PAGD regime of electrical discharge in vacuo. To confirm the above interpretation of the anomalous flux in the observed PAGD phenomenon, the cathode jet composition, as well as time-dependent and usage-dependent changes occurring in the tubes, with diverse sealed negative pressures and after submission to prolonged PAGD operation, must be analysed by mass-spectroscopy. In any event, the excess energy present in the anomalous counter-flowing force appears to stem from a discharge mechanism that effectively pulls high speed electrons and constituent atoms out of a metal surface, at low fields and with high current densities, and is modulated by a complex multiplicity of parameters.

The system described appears to transduce efficiently the observed non-linear longitudinal pulse discontinuities of the plasma field, under conditions of current saturation of the cathode, because the self-extinguishing and self-limiting properties of the discharge allows the energy from the collapse of the discharge to be captured. The particular design of the circuitry, which couples a rectification bridge to the asymmetric bridge quadrature of large capacitances, placed at the output of the PAGD generator, permits effective capture. Our findings constitute striking evidence for Aspden's contention of a need to revise our present electrodynamic concepts. The dual ported PAGD discharge tube circuits which we have described are the first electrical systems we know of which permit effective exploitation of anomalous cathode reaction forces and allow for the recovery of electrical energy from systems exhibiting this effect. Any apparent imbalance in the electrical energy input to the system and withdrawn from the system by its operator must be considered in the context of the entire continuum in which the system operates, within which it is anticipated that accepted principles of energy balance will be maintained.

Moreover, the energy conversion system of the invention has substantial utility as an electrical inverter accepting direct current, and providing one or more of a direct current output at lower voltage and higher current, variable frequency input to alternating current motors, and, by suitable combinations of discharge tube systems, more flexible DC-to-DC conversion systems.

As an alternative to the batteries used in the experiments described, a DC power supply may be utilised or, more advantageously from the viewpoint of entailing less transformation losses, a DC generator to provide the electrical energy input to the system. As a DC motor can be run directly from the rectified output of the circuit of **Fig.9** at **El-E2**, in place of a battery charge pack, DC motor/generator sets of suitable characteristics (in terms of back E.M.F. and circuit loading) can be used to charge the batteries of the drive pack, utilising the rectified PAGD output to drive the DC motor component of the set. This provides a simple, one battery pack solution, where the PAGD input and output circuits are electrically separated by the DC motor/generator interface: the drive pack is simultaneously being discharged to drive PAGD production, and charged by the DC generator output which, in turn, is being driven by the electromechanical transformation of the rectified PAGD output that would typically accrue to a charge pack in the experiments already described. The main limitations to such an arrangement lie in the efficiency of the motor and generator transformations utilised.

A pulsed DC source could be used to provide input to the circuit if suitably synchronised, but care is needed not to interfere unduly with the auto-electronic mechanism of the field induced cathode emissions.

TABLE 1

Results for the ballast resistance (and current) dependent PAGD frequency utilizing an H34 aluminum pulse generator with 128 cm^2 plates at 5.5 cm distance, in the triode configuration, at a pressure of 0.8 Torr. The circuit employed is that of the present invention, as described in the third Results Section. DCV = 560.

R in Ω	Regime of Discharge	Pulse Rate >100 V
5,000	NGD (Cold Cathode)	0
600	PAGD	10 PPS
300	PAGD	40 PPS
150	PAGD	180 PPS
100	VAD	0
50	VAD	0

TABLE 2

128 cm^2 H220 Al; 570 volts DC; 300 Ω = R1; Diode Configuration

	PPS	p(Torr)	Cumulative Pulse Count
1)	200	0.08	$\sim 2.4 \times 10^5$
2)	200	0.5	$\sim 1.5 \times 10^6$
3)	200	0.8–1	$\sim 2.5 \times 106$
4)	25	0.5	3×10^6 pulses
5)	200	0.5	1.5×10^6 (after first electrode reversal)

TABLE 3

pressure in Torr	RESIDUAL GAS EFFECT PPS in AIR	PPS in ARGON
0.45	ND	10
0.5	1.8 ± 0.3	ND
0.55	4.8 ± 0.9	16.7±1.8
1.0	11.4 ± 0.8	448 ± 27.4
1.25	214.5 ± 14.3	ND
2.0	36.2 ± 2.6	206 ± 19.6 158.7 ± 24
2.5	1.36 ± 0.3	0

TABLE 4

Charge pack No. of cells	PPS	PAGD
36	0	–
31	1	+
29	10	+
19	1	+
9	0	–

TABLE 5

1 Expt. No.	2 Battery Pack	3 Position	4 Open Voltage	5 V/cell	6 % total rel. cpty.	7 Max. hr. left	8 % rel. cpty gained	8 % rel. cpty lost	9 Total kWh	10 ΔkWh gain	10 ΔkWh loss	11 PAGD per sec
1	Charge	start	348	12.0	40	8			0.835			8
	Charge	end	366	12.62	83	16.6	43		1.823	0.988		
	Driver	start	576	12.52	77	15.4			2.660			
	Driver	end	572	12.43	70	14		7	2.402		0.258	
2	C	b	331	11.41	2	0.4			0.040			61
	C	a	351	12.1	47.5	9.5	45.5		1.002	0.962		
	D	b	553	12.02	40	8			1.327			
	D	a	546	11.9	33	6.6		7	1.081		0.246	
3	C	b	345	11.9	32.5	6.5			0.673			3
	C	a	361	12.45	72.5	14.4	40		1.559	0.886		
	D	b	559	12.15	51	10.2			1.710			
	D	a	552	12.0	40	8		11	1.324		0.386	
4	C	b	360	12.41	70	14			1.512			32
	C	a	373	12.86	103	>20	33		2.238	0.726		
	D	b	562	12.22	54.5	10.9			1.838			
	D	a	557	12.11	48	9.6		6.5	1.604		0.234	
5	C	b	340	11.7	20	4			0.408			2
	C	a	365	12.59	83	16.6	63		1.818	1.440		
	D	b	527	11.45	3.2	0.6			0.101			
	D	a	517	11.24	1.8	0.4		0.2	0.056		0.045	
6	C	b	340	11.72	21.5	4.3			0.438			8
	C	a	367	12.66	87.5	17.5	66		1.927	1.489		
	D	b	589	12.8	100	20			3.530			
	D	a	564	12.26	58.5	11.7		41.5	1.979		1.551	
7	C	b	318	10.97	1.2	0.24			0.023			5
	C	a	359	12.38	67.5	13.5	66.3		1.454	1.431		
	D	b	575	12.5	77	15.4			2.656			
	D	a	567	12.32	63.5	12.7		13.5	2.160		0.496	
8	C	b	328	11.71	20	4			0.393			32
	C	a	350	12.5	76.5	15.3	56.5		1.606	1.213		
	D	b	582	12.65	87.5	17.5			3.055			
	D	a	579.5	12.60	84	16.8		3.5	2.921		0.134	

1 Expt. No.	2 Battery Pack	3 Position	12 Exptl. time	13 rel. kWh/h gain	13 rel. kWh/h loss	14 net kWh/h production	15 Breakeven efficiency	16 Cell #/ pack	17 tube	18 Cathode Area	19 Plate
1	Charge	start	21.5'			2.071	388%	29	A26	128 cm^2	H34
	Charge	end		2.791							

TABLE 5-continued

	Driver	start						46				
	Driver	end			0.720							
2	C	b	18'			2.387	391%	29	A26	128 cm^2	H34	
	C	a		3.207								
	D	b						46				
	D	a			0.820							
3	C	b	21.5'			1.396	230%	29	A26	128 cm^2	H34	
	C	a		2.473								
	D	b						46				
	D	a			1.077							
4	C	b	63.5'			0.465	310%	29	A28	128 cm^2	H220	
	C	a		0.686								
	D	b						46				
	D	a			0.221							
5	C	b	80'			1.064	6,750%	29	A26	128 cm^2	H34	
	C	a		1.080								
	D	b						46				
	D	a			0.016							
6	C	b	21.5'			−0.173	96%	29	A26	128 cm^2	H34	
	C	a		4.155								
	D	b						46				
	D	a			4.328							
7	C	b	64.5'			0.870	289%	29	A45	64 cm^2	H34	
	C	a		1.331								
	D	b						46				
	D	a			0.461							
8	C	b	28.5'			2.272	906%	28	A45	64 cm^2	H34	
	C	a		2.554								
	D	b						46				
	D	a			0.282							

1 Expt. No.	2 Battery Pack	3 Position	20 R1 ohm	21 C3/C5 mfd	22 C7a/C7b mfd	23 Motor arm	24 Pressure	25 Gap cm	26 OV rlx. time	27 C4 mfd	28 R4 ohms	29 Motor rpm

TABLE 5-continued

1 Expt. No.	2 Battery Pack	3 Position	20 R1 ohm	21 C3/C5 mfd	22 C7a/C7b mfd	23 Motor arm	24 Pressure	25 Gap cm	26 OV rlx. time	27 C4 mfd	28 R4 ohms	29 Motor rpm
1	Charge	start	300	20,700	3,300	off	0.8 Torr	5.5	30'	NA	NA	NA
	Charge	end										
	Driver	start										
	Driver	end										
2	C	b	300	20,700	3,300	off	0.8 Torr	5.5	30'	NA	NA	NA
	C	a										
	D	b										
	D	a										
3	C	b	300	20,700	3,300	off	0.7 Torr	5.5	15'	NA	NA	NA
	C	a										
	D	b										
	D	a										
4	C	b	300	34,700	5,500	off	0.2 Torr	5.5	30'	NA	NA	NA
	C	a										
	D	b										
	D	a										
5	C	b	150	34,700	3,300	on	0.8 Torr	5.5	15'	8	500	1,200
	C	a										
	D	b										
	D	a										
6	C	b	300	20,700	3,300	on	0.8 Torr	5.5	15'	16	0	2,000
	C	a										
	D	b										
	D	a										
7	C	b	600	34,700	3,300	off	0.8 Torr	4	30'	NA	NA	NA
	C	a										
	D	b										
	D	a										
8	C	b	600	34,700	5,500	off	0.8 Torr	4	30'	NA	NA	NA
	C	a										
	D	b										
	D	a										

TABLE 6

Expt. No.	Battery Pack	Position	Load Voltage	Watts/ cell	Hr. left	Total kWh	ΔkWh gain	ΔkWh loss	rel. kWh/h gain	rel. kWh/h loss	net kWh/h	B. Eff.
1	C	s	335.7	4.445	4	0.516					3.014	776%
	C	e	357.5	5.05	12	1.757	1.241		3.46			
	D	s	568.0	3.20	13	1.766						
	D	e	564.6	3.175	11	1.606		0.16		0.446		
2	C	s	315.5	3.93	1	0.114					1.012	504%
	C	e	327.8	4.25	4.5	0.502	0.387		1.225			
	D	s	540.7	2.91	4	0.535						
	D	e	535.3	2.87	3.5	0.462		0.073		0.243		
3	C	s	328	4.23	2	0.245					1.175	703%
	C	e	351.7	4.91	7	0.737	0.492		1.370			
	D	s	546	2.95	5	0.680						
	D	s	545.5	2.90	4.5	0.610		0.070		0.195		

TABLE 7

1 Expt. No.	2 Config.	3 Pressure Torr	4 Tube	5 DP DCV	6 Plates DCV	7 DP DCA	8 DP Watts	9 PAGD Volts	10 PAGD V/cm	11 CP DCV
1	dd	0.8	A29	562	350	0.65	137.8	212	77.1	375
2	dd	0.09	A29	562	402	0.60	96	160	58.2	378
3	dd	0.8	A29	560	371	0.59	111.5	189	68.7	374
4	dd	0.09	A29	563	409	0.49	75.9	154	56	379
5	t	1.5	A28	561	439	0.41	49.9	122	22.2	377
6	t	1.5	A28	560	425	0.51	68.9	135	24.5	375
7	t	1.0	A28	556	398	0.48	75	158	28.7	376.5
8	t	0.5	A28	559.5	398	0.68	109.8	161.5	29.4	377.5
9	t	0.5	A28	563	390	0.75	112.45	173	31.5	373
10	sd	0.5	A28	565	422	0.47	67.2	143	26	376
11	sd	0.5	A28	561.5	415	0.50	73	146.5	26.6	380
12	sd	0.5	A28	562	413.5	0.55	81.7	148.5	27	380
13	dd	0.25	A28	553	438	0.35	40	115	41.8	381.5
14	dd	0.25	A28	549	325	0.70	156.8	224	81.5	263

1 Expt. No.	2 Config.	12 CP DCA	13 CP Watts	14 Total Resistance	15 Breakeven Efficiency	16 PPS	17 Bridge diode	18 Input diode	19 Motor status	20 FIG. 3
1	dd	1.25	468.8	326	340%	450	M860	HFR	off	+
2	dd	0.70	264.6	% 270	276%	92	M860	HFR	off	
3	dd	0.65	243.1	243	218%	500	HFR	HFR	off	
4	dd	0.76	288	314	379%	77	HFR	HFR	off	
5	t	0.58	219	298	439%	52	HFR	HFR	off	
6	t	0.69	259	265	376%	100	M860	HFR	off	
7	t	0.57	213.1	329	284%	355	M860	HFR	off	
8	t	0.67	252.9	238	230%	92	HFR	HFR	off	
9	t	0.65	280	266	249%	118	M860	HFR	off	+
10	sd	1.03	387.3	286	530%	25	M860	HFR	off	
11	sd	0.73	277.4	293	379%	11	HFR	HFR	off	+
12	sd	0.71	269.8	270	330%	10	HFR	HFR	on	+
13	dd	0.59	225.1	329	563%	10	HFR	HFR	off	
14	dd	1.36	257.7	320	228%	1	HFR	HFR	off	

TABLE 8

1 Expt. No.	2 Battery Pack	3 Position	4 Total Wh	5 Rel. Cap.	6 Torr	7 Limit in W	8 ΔkWh gain	8 ΔkWh loss	9 Exptl. time	10 abs. kWh/h gain	10 abs. kWh/h loss	net	11 BE
1	C	b	159	12%	0.8	90			21.5′			+664	846%
	C	a	428	32%			269			753			
	D	b	1764	85%		115							
	D	a	1732	84%				32			89		
2	C	b	118	9%	0.8	90			18′			+616	2,667%
	C	a	303.5	23%			192			640			
	D	b	542.3	26%		115							
	D	a	535	25.9%				7.3			24		
3	C	b	950.4	72%	0.2	90			70′			+186	3485%
	C	a	1,161	88%			210.9			191.7			
	D	b	660	32%		115							
	D	a	654	32%				6.5			5.6		
4	C	b	15.8	1.2%	0.8	90			64.5′			+53.7	406%
	C	a	81.9	6%			65			60			
	D	b	181	8.7%		115							
	D	a	165	8%				16			14.7		
5	C	b	34.5	2.6%	0.8	90			28.5′			+169.1	436%
	C	a	138.8	10.5%			104.3			219.6			
	D	b	1,114	54%		115							
	D	a	1,089	53%				24			50.5		
6	C	b	55.4	4.2%	0.8	90			74′			+117	483%
	C	a	237.6	18%			182.2			148			
	D	b	669.3	32%		115							
	D	a	631.7	30.6%				37.7			30.6		

1 Expt. No.	2 Battery Pack	3 Position	12 Config.	13 Tube	14 Cathode area	15 gap cm	16 PPS	17 PAGD seq. method	18 R1 ohms	19 Plate material	20	21 C3/C5 mfd	22 C7a/C7b mfd
1	C	b	Triode	A26	128 cm2	5.5	8	Continuous	300	H34		20,700	3.300
	C	a											
	D	b											
	D	a											
2	C	b	Triode	A26	128 cm2	5.5	61	Interrupted	300	H34		20,700	3,300
	C	a											
	D	b											
	D	a											
3	C	b	Triode	A28	128 cm2	5.5	32	Interrupted	300	H220		34,700	5,500
	C	a											
	D	b											
	D	a											
4	C	b	Triode	A46	64 cm2	4.0	5	Continuous	600	H34		34,700	5,500
	C	a											
	D	b											
	D	a											
5	C	b	Triode	A46	64 cm2	4.0	32	Interrupted	600	H34		34,700	5,500
	C	a											
	D	b											
	D	a											
6	C	b	Plate Diode	A29	128 cm2	5.5	8	Interrupted	300	H220		34,700	5,500
	C	a											
	D	b											
	D	a											

TABLE 9

Utilizing: Al H200, 128 cm^2 plates
DP = 46 cells
CP = 23 cells

	PPS	CP Gain per pulse in mWh	Net Gain per pulse mWh	CP Gain per second mWh	Net Gain per second mWh	Pressure in Torr
#1	1.5	22.3	11.7	33:45	17.55	0.2
#2	8	5.6	4.4	44.8	35.2	0.8
#3	110	0.78	0.27	85.8	29.7	2.0

CLAIMS

1. Apparatus comprising a discharge tube and an electrical circuit containing said discharge tube and configured to operate the latter to provide endogenous pulsatory cold cathode auto-electronic emissions, the circuit being double ported with an input port connected to a source of direct current at a potential sufficient to initiate said emissions, and an output port connected to a current sink effective to absorb at least a substantial portion of electrical energy released by collapse of said emissions.

2. Apparatus according to claim 1 configured so that the emissions occur in a pulsed abnormal glow discharge regime.

3. Apparatus according to claim 2, wherein the input port includes components ensuring that the flow of current therein is unidirectional, and incorporating impedance sufficient to limit the flow of current therein.

4. Apparatus according to claim 2, including capacitors connected to the discharge tube, the input port and the output port, which provide charge storage in the input port and direct current isolation between the input and output ports.

5. Apparatus according to claim 4, wherein the output port comprises a rectifier having an input connected to said capacitors, reservoir capacitance connected to the output of said rectifier, and reverse current blocking devices connected between said reservoir capacitance and the current sink.

6. Apparatus according to claim 5, wherein the rectifier is a bridge rectifier, and the reservoir capacitance is provided by a capacitor bridge having ends connected to outputs of the bridge rectifier, and an intermediate point connected to one input of the bridge rectifier.

7. Apparatus according to claim 4, further including an alternating current motor and a capacitor in series, connected between the connections of said capacitors to the output port.

8. Apparatus according to claim 2, wherein the current sink comprises a secondary battery.

9. Apparatus according to claim 2, wherein the current sink comprises an electric motor.

10. Apparatus according to claim 2, wherein the direct current source comprises a secondary battery.

11. Apparatus according to claim 2, wherein the direct current source is a DC generator.

12. Apparatus according to claim 9, wherein the motor is a DC motor.

13. Apparatus according to claim 10, including a circuit for charging from the output port a battery to be used as the direct current source.

14. Apparatus according to claim 2, wherein the direct current source is a rectified AC source.

15. Apparatus according to claim 2, wherein the discharge tube is connected as a single diode.

16. Apparatus according to claim 2, wherein the discharge tube is connected as a multiple diode with plates connected as cathodes and an intermediate electrode connected as an anode.

17. Apparatus according to claim 2, wherein the discharge tube is connected as a triode, with an intermediate electrode functioning as an auxiliary cathode.

18. Apparatus according to claim 2, wherein a first potential is applied to the input port by the source of direct current to induce emission, a back EMF is applied to the output port by the current sink, and an extinction potential of the emissions is greater than the back EMF.

19. A method of energy conversion, comprising initiating plasma eruptions from the cathode of a discharge tube operating in a pulsed abnormal glow discharge regime utilising electrical energy from a source in a first circuit connected to said discharge tube, and capturing electrical energy generated by the collapse of such eruptions in a second circuit connected to said discharge tube.

20. A method according to claim 19, wherein current flowing into the discharge tube during said eruptions is at least 50 ma.

21. A method according to claim 19, wherein current flowing into the discharge tube during said eruptions is at least 500 ma.

22. A method according to claim 19, in which charge carriers within plasma outputs are accelerated through at least one of an electric and magnetic field.

23. A method of energy conversion, comprising inducing endogenous pulsatory low-field, large-area cold-cathode auto-electronic emissions from the cathode of a discharge tube capable of sustaining such emissions, utilising electrical energy from a source in a first circuit connected to said discharge tube, and capturing electrical energy generated by the collapse of such emissions in a second circuit connected to said discharge tube.

FRANKLIN MEAD AND JACK NACHAMKIN

Patent US 5,590,031 31st December 1996 Inventors: Franklin Mead & Jack Nachamkin

SYSTEM FOR CONVERTING ELECTROMAGNETIC RADIATION ENERGY TO ELECTRICAL ENERGY

This patent shows a system for converting Zero-Point Energy into conventional electrical power.

ABSTRACT

A system is disclosed for converting high-frequency zero-point electromagnetic radiation energy to electrical energy. The system includes a pair of dielectric structures which are positioned near each other and which receive incident zero-point electromagnetic radiation. The volumetric sizes of the structures are selected so that they resonate at a frequency of the incident radiation. The volumetric sizes of the structures are also slightly different so that the secondary radiation emitted from them at resonance, interferes with each other producing a beat frequency radiation which is at a much lower frequency than that of the incident radiation and which is amenable to conversion to electrical energy. An antenna receives the beat frequency radiation. The beat frequency radiation from the antenna is transmitted to a converter via a conductor or waveguide and converted to electrical energy having a desired voltage and waveform.

US Patent References:

3882503	May., 1975	Gamara	343/100.
4725847	Feb., 1988	Poirier	343/840.
5008677	Apr., 1991	Trigon et al.	342/17.

DESCRIPTION

BACKGROUND OF THE INVENTION

The invention relates generally to conversion of electromagnetic radiation energy to electrical energy, and, more particularly, to conversion of high frequency bandwidths of the spectrum of a type of radiation known as ‘zero-point electromagnetic radiation’ to electrical energy.

The existence of zero-point electromagnetic radiation was discovered in 1958 by the Dutch physicist M. J. Sparnaay. Mr. Sparnaay continued the experiments carried out by Hendrik B. G. Casimir in 1948 which showed the existence of a force between two uncharged parallel plates which arose from electromagnetic radiation surrounding the plates in a vacuum. Mr. Sparnaay discovered that the forces acting on the plates arose from not only thermal radiation but also from another type of radiation now known as classical electromagnetic zero-point radiation. Mr. Sparnaay determined that not only did the zero-point electromagnetic radiation exist in a vacuum but also that it persisted even at a temperature of absolute zero. Because it exists in a vacuum, zero-point radiation is homogeneous and isotropic as well as ubiquitous. In addition, since zero-point radiation is also invariant with respect to Lorentz transformation, the zero-point radiation spectrum has the characteristic that the intensity of the radiation at any frequency is proportional to the cube of that frequency. Consequently, the intensity of the radiation increases without limit as the frequency increases resulting in an infinite energy density for the radiation spectrum. With the introduction of the zero-point radiation into the classical electron theory, a vacuum at a temperature of absolute zero is no longer considered empty of all electromagnetic fields. Instead, the vacuum is now considered as filled with randomly fluctuating fields having the zero-point radiation spectrum. The special characteristics of the zero-point radiation which are that it has a virtually infinite energy density and that it is ubiquitous (even present in outer space) make it very desirable as an energy source. However, because high energy densities exist at very high radiation frequencies and because conventional methods are only able to convert or extract energy effectively or efficiently only at lower frequencies at which zero-point radiation has relatively low energy densities, effectively tapping this energy source has been believed to be unavailable using conventional techniques for converting electromagnetic energy to electrical or other forms of easily usable energy. Consequently, zero-point electromagnetic radiation energy which may potentially be used to power interplanetary craft as well as provide for society's other needs has remained unharnessed.

There are many types of prior art systems which use a plurality of antennas to receive electromagnetic radiation and provide an electrical output from them. An example of such a prior art system is disclosed in U.S. Pat. No.

3,882,503 to Gamara. The Gamara system has two antenna structures which work in tandem and which oscillate by means of a motor attached to them in order to modulate the radiation reflected from the antenna surfaces. The reflecting surfaces of the antennas are also separated by a distance equal to a quarter wavelength of the incident radiation. However, the Gamara system does not convert the incident radiation to electrical current for the purpose of converting the incident electromagnetic radiation to another form of readily usable energy. In addition, the relatively large size of the Gamara system components make it unable to resonate at and modulate very high frequency radiation.

What is therefore needed is a system which is capable of converting high frequency electromagnetic radiation energy into another form of energy which can be more readily used to provide power for transportation, heating, cooling as well as various other needs of society. What is also needed is such a system which may be used to provide energy from any location on earth or in space.

SUMMARY OF THE INVENTION

It is a principle object of the present invention to provide a system for converting electromagnetic radiation energy to electrical energy.

It is another object of the present invention to provide a system for converting electromagnetic radiation energy having a high frequency to electrical energy.

It is another object of the present invention to provide a system for converting zero-point electromagnetic radiation energy to electrical energy.

It is another object of the present invention to provide a system for converting electromagnetic radiation energy to electrical energy which may used to provide such energy from any desired location on earth or in space.

It is another object of the present invention to provide a system for converting electromagnetic radiation energy to electrical energy having a desired waveform and voltage.

It is an object of the present invention to provide a miniaturised system for converting electromagnetic radiation energy to electrical energy in order to enhance effective utilisation of high energy densities of the electromagnetic radiation.

It is an object of the present invention to provide a system for converting electromagnetic radiation energy to electrical energy which is simple in construction for cost effectiveness and reliability of operation.

Essentially, the system of the present invention utilises a pair of structures for receiving incident electromagnetic radiation which may be propagating through a vacuum or any other medium in which the receiving structures may be suitably located. The system of the present invention is specifically designed to convert the energy of zero-point electromagnetic radiation; however, it may also be used to convert the energy of other types of electromagnetic radiation. The receiving structures are preferably composed of dielectric material in order to diffract and scatter the incident electromagnetic radiation. In addition, the receiving structures are of a volumetric size selected to enable the structures to resonate at a high frequency of the incident electromagnetic radiation based on the parameters of frequency of the incident radiation and propagation characteristics of the medium and of the receiving structures. Since zero-point radiation has the characteristic that its energy density increases as its frequency increases, greater amounts of electromagnetic energy are available at higher frequencies. Consequently, the size of the structures are preferably miniaturised in order to produce greater amounts of energy from a system located within a space or area of a given size. In this regard, the smaller the size of the receiving structures, the greater the amount of energy that can be produced by the system of the present invention.

At resonance, electromagnetically induced material deformations of the receiving structures produce secondary fields of electromagnetic energy therefrom which may have evanescent energy densities several times that of the incident radiation. The structures are of different sizes so that the secondary fields arising therefrom are of different frequencies. The difference in volumetric size is very small so that interference between the two emitted radiation fields, and the receiving structures at the two different frequencies produces a beat frequency radiation which has a much lower frequency than the incident radiation. The beat frequency radiation preferably is at a frequency which is sufficiently low that it may be relatively easily converted to usable electrical energy. In contrast, the incident zero-point radiation has its desirable high energy densities at frequencies which are so high that conventional systems for converting the radiation to electrical energy either cannot effectively or efficiently so convert the radiation energy or simply cannot be used to convert the radiation energy for other reasons.

The system of the present invention also includes an antenna which receives the beat frequency radiation. The antenna may be a conventional metallic antenna such as a loop or dipole type of antenna or a rf cavity structure

which partially encloses the receiving structures. The antenna feeds the radiation energy to an electrical conductor (in the case of a conventional dipole or comparable type of antenna) or to a waveguide (in the case of a rf cavity structure). The conductor or waveguide feeds the electrical current (in the case of the electrical conductor) or the electromagnetic radiation (in the case of the waveguide) to a converter which converts the received energy to useful electrical energy. The converter preferably includes a tuning circuit or comparable device so that it can effectively receive the beat frequency radiation. The converter may include a transformer to convert the energy to electrical current having a desired voltage. In addition, the converter may also include a rectifier to convert the energy to electrical current having a desired waveform.

BRIEF DESCRIPTION OF THE DRAWINGS

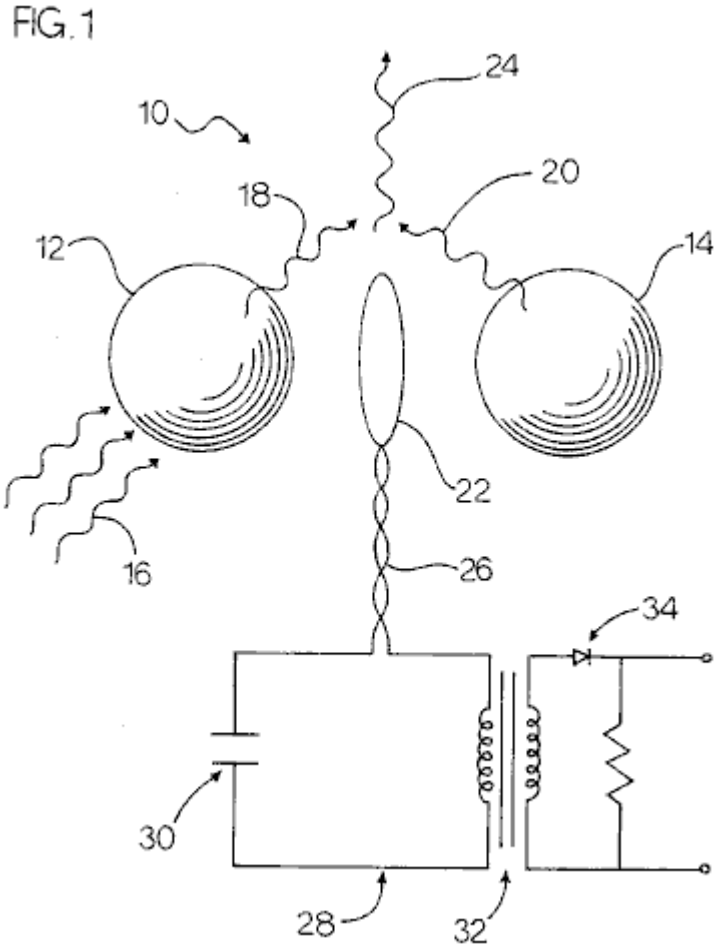

Fig.1 is a plan view of the receiving structures and antenna of a first embodiment of the system of the present invention with a schematic view of the conductor and converter thereof and also showing the incident primary and emitted secondary electromagnetic radiation.

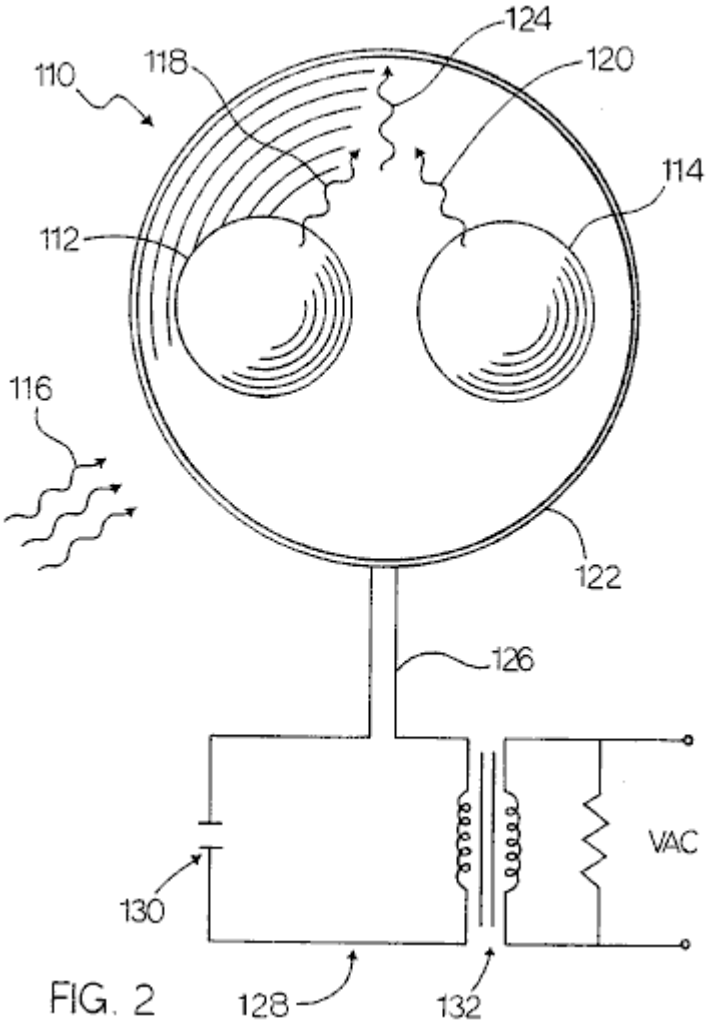

FIG. 2

Fig.2 is a front view of the receiving structures, antenna and waveguide of a second embodiment of the system of the present invention with a schematic view of the converter thereof and also showing the incident primary and emitted secondary electromagnetic radiation.

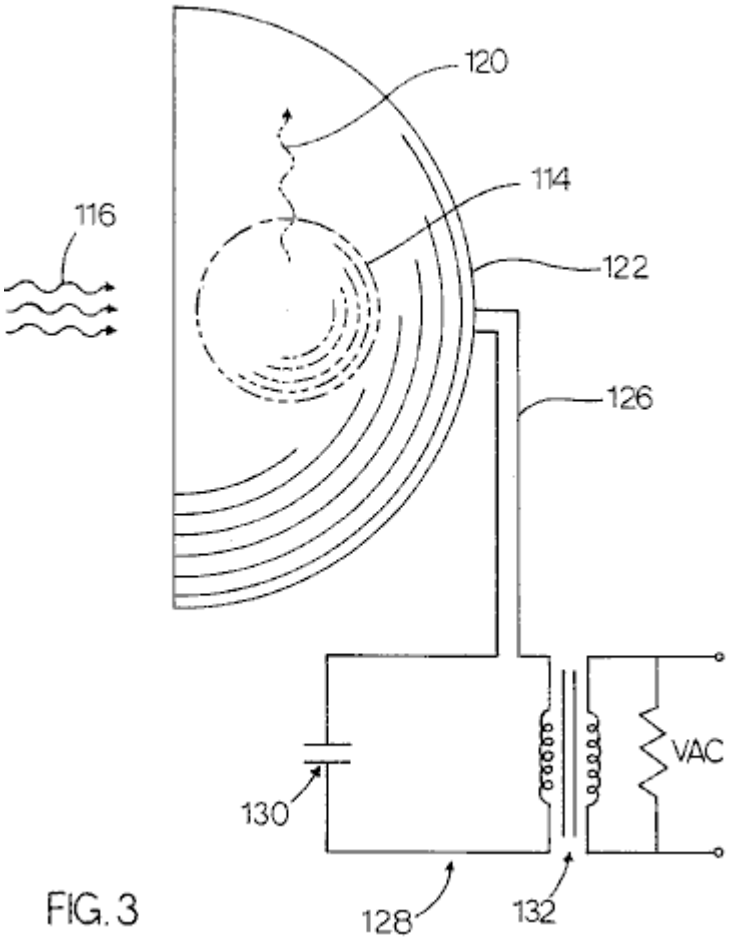

FIG. 3

Fig.3 is a perspective view of the receiving structures, antenna and waveguide of the second embodiment shown in **Fig.2** with a schematic view of the converter thereof and also showing the incident primary and emitted secondary electromagnetic radiation.

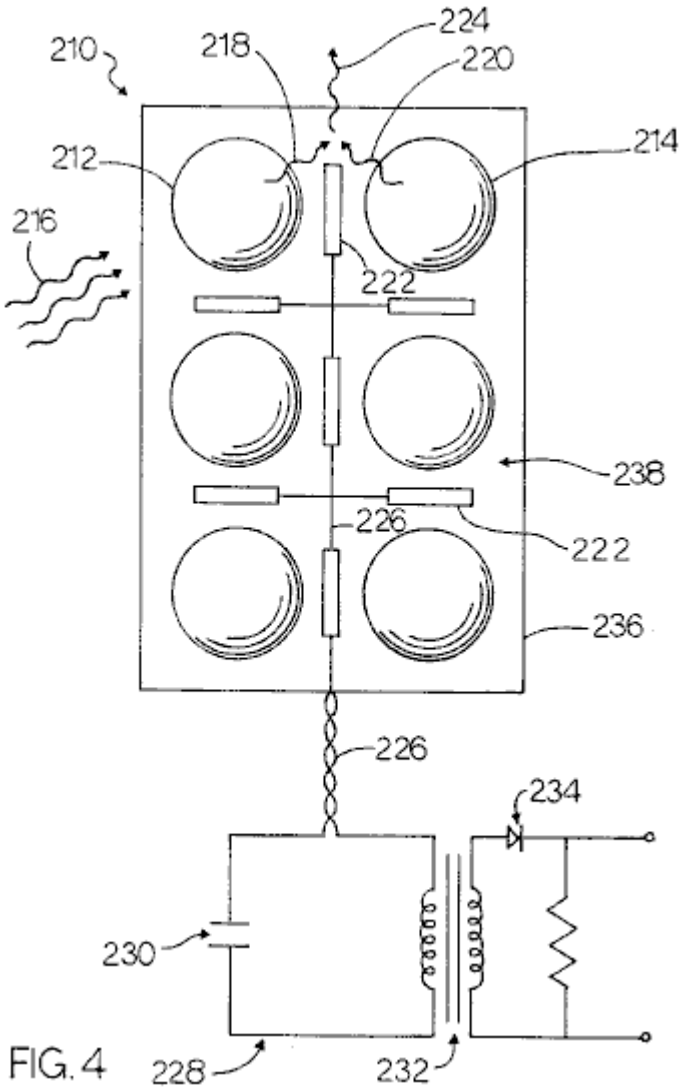

FIG. 4

Fig.4 is a front view of the substrate and a plurality of pairs of the receiving structures and a plurality of antennas of a third embodiment of the system of the present invention with a schematic view of the conductor and converter thereof and also showing the incident primary and emitted secondary electromagnetic radiation.

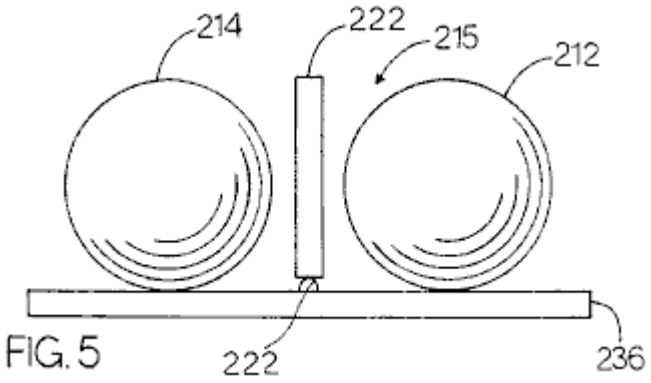

FIG. 5

Fig.5 is a top view of some of the components of the third embodiment of the system of the present invention showing two of the plurality of pairs of receiving structures and two of the plurality of antennas mounted on the substrate.

FIG. 6

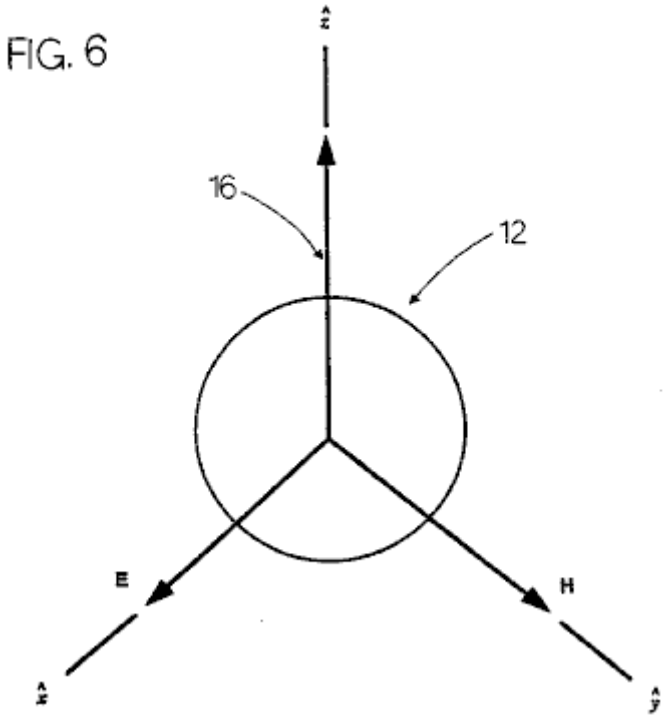

Fig.6 is a diagram of a receiving structure of the system of the present invention showing an incident electromagnetic plane wave impinging on the receiving structure and illustrating the directions of the electric and magnetic field vectors thereof.

FIG. 7

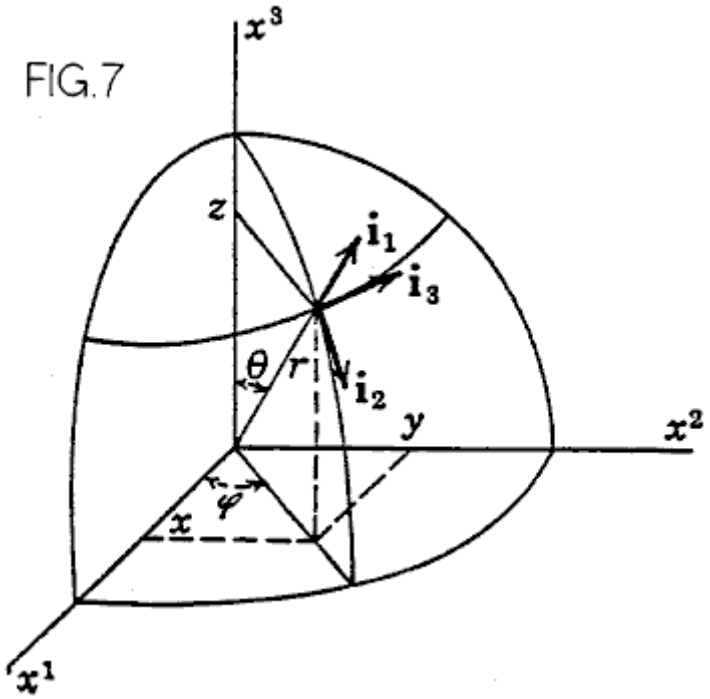

Fig.7 is a diagram of a spherical co-ordinate system as used in the formulas utilised in the system of the present invention.

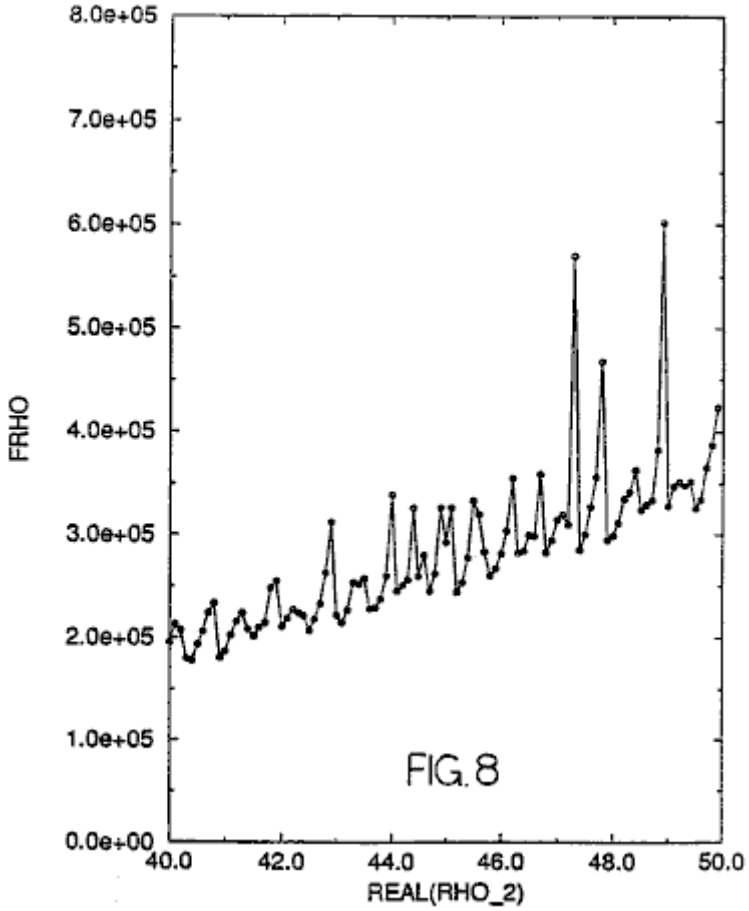

Fig.8 is a graph showing an imaginary rho parameter plotted against a real rho parameter illustrating the values thereof at resonance as well as values thereof at other than resonance.

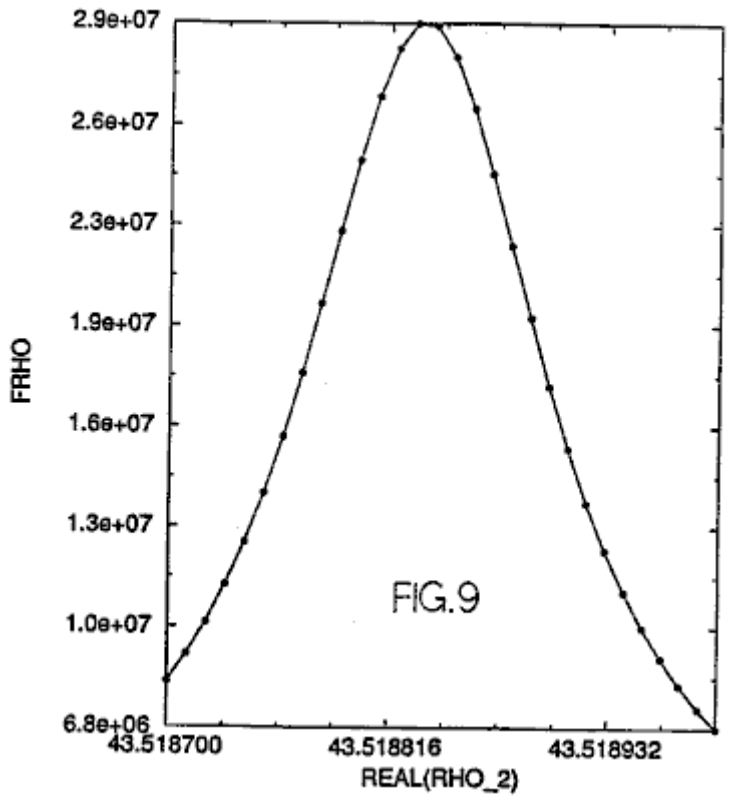

Fig.9 is a graph showing a portion of the graphical representation shown in **Fig.8** illustrating the real and imaginary rho values at or near a single resonance.

DETAILED DESCRIPTION OF THE PREFERRED EMBODIMENT

Referring to the drawings, a first embodiment of the present invention is generally designated by the numeral **10**. The system **10** includes a first and second means for receiving **12** and **14** incident electromagnetic radiation **16**. The means for receiving **12** and **14** are preferably a pair of spherical structures **12** and **14** which are preferably composed of a dielectric material. Alternatively, the spheres **12** and **14** may be cubical structures or any other suitable shape. The spheres **12** and **14** may be mounted on a suitable foundation by any suitable mounting means (not shown), or spheres **12** and **14** may be suspended from a suitable foundation by any suitable suspension means (not shown). The spheres **12** and **14** are preferably composed of a dielectric material. The dielectric spheres **12** and **14** scatter and concentrate electromagnetic waves. At very sharply defined frequencies, the spheres **12** and **14** will have resonances wherein the internal energy densities can be five orders of magnitude larger than the energy density of the incident electromagnetic field driving the spheres **12** and **14**. At resonance, the electromagnetic stresses, equivalent to pressures proportional to the energy density, can cause material deformation of the spheres **12** and **14** which produce a secondary electromagnetic field. The spheres **12** and **14** are preferably positioned proximal to each other, as shown in **Fig.1**. Although the proximity of the spheres to each other will adversely affect the resonances, the very high "Q"s of the isolated-sphere resonances results in such adverse affect being relatively small. However, the proximity of the spheres **12** and **14** allows the spheres to interact electromechanically which increases the magnitude of the secondary radiation emitted from them.

The electromagnetic radiation incident upon the spheres **12** and **14** which drives the spheres to resonance is preferably zero-point radiation **16**. However, other types of electromagnetic radiation may also be used to drive the spheres **12** and **14**, if desired.

The effect of a dielectric sphere such as **12** or **14** on an incident electromagnetic radiation such as a plane wave thereof is shown in **Fig.6**. The plane wave propagates in the z axis direction and is diffracted by the sphere **12** resulting in scattering thereof. This scattering is commonly known as Mie scattering. The incident radiation wave has an electric vector component which is linearly polarised in the x axis direction and a magnetic vector component which is linearly polarised in the y axis direction.

An electromagnetic wave incident upon a structure produces a forced oscillation of free and bound charges in synch with the primary electromagnetic field of the incident electromagnetic wave. The movements of the charges produce a secondary electromagnetic field both inside and outside the structure. The secondary electromagnetic radiation comprising this secondary electromagnetic field is shown in **Fig.1** and designated by the numerals **18** and **20**. An antenna which is shown simply as a loop antenna but may also be a dipole or any other suitable type of antenna, is also shown in **Fig.1** and designated by the numeral **22**. The non-linear mutual interactions of the spheres produces interference between the secondary electromagnetic radiation **18** and **20** produces a beat frequency radiation **24** which is preferably at a much lower frequency than the primary radiation **16**. It is this beat frequency radiation **24** which is desired for conversion into electrical energy because it preferably is within the frequency range of rf radiation which may be converted into electrical energy by generally conventional systems. Thus, the radiation **24** received by the antenna **22** is fed via an electrical conductor **26** to a means for converting the beat frequency radiation **24** to electrical energy. This means for converting is designated by the numeral **28** and preferably includes a tuning capacitor **30** and a transformer **32** and a rectifier (preferably a diode) **34**. Instead of including the capacitor **30**, transformer **32** and rectifier **34**, the converter **28** may alternatively include an rf receiver of any suitable type.

The resultant field at any point is the vector sum of the primary and secondary fields. For the equations that follow, the structure receiving the incident plane wave is a sphere of radius a having a propagation constant k_1 positioned in an infinite, homogeneous medium having a propagation constant k_2. The incident plane wave propagates in the z axis direction and is as shown in **Fig.6**. The spherical co-ordinate system used for the vector spherical wave functions is shown in **Fig.7**.

Note: As this patent contains so many non-standard keyboard characters, the remainder of this document is produced using direct images of the original text.

Expansion of the incident field provides:

$$E_i = E_o e^{-i\omega t} \sum_{n=1}^{\infty} i^n \frac{2n+1}{n(n+1)} \left(m_{01n}^{(1)} - i n_{e1n}^{(1)}\right)$$

$$H_i = -\frac{k_2}{\omega \mu_2} E_o e^{-i\omega t} \sum_{n=1}^{\infty} i^n \frac{2n+1}{n(n+1)} \left(m_{e1n}^{(1)} + i n_{01n}^{(1)}\right)$$

where E is the electric field and H is the magnetic field; and

$$m^{(1)}_{\substack{01n\\e1n}} = \pm \frac{1}{\sin\theta} j_n(k_2R)P_n^1(\cos\theta) \begin{matrix}\cos\\ \sin\end{matrix} \phi i_2 - j_n(k_2R) \frac{\partial p_n^1}{\partial\theta} \begin{matrix}\sin\\ \cos\end{matrix} \phi i_3$$

$$n^{(1)}_{\substack{01n\\e1n}} = \frac{n(n+1)}{k_2R} j_n(k_2R)P_n^1(\cos\theta) \begin{matrix}\sin\\ \cos\end{matrix} \phi i_1 + \frac{1}{k_2R} [k_2Rj_n(k_2R)]' \times$$

$$\frac{\partial P_n^1}{\partial\theta} \begin{matrix}\sin\\ \cos\end{matrix} \phi i_2 \pm \frac{1}{k_2R\sin\theta} [k_2Rj_n(k_2R)]'P_n^1(\cos\theta) \begin{matrix}\cos\\ \sin\end{matrix} \phi i_3.$$

The electric and magnetic fields of the incident wave transmitted into the sphere i.e., R<a, can be similarly expanded:

$$E_t = E_0 e^{-i\omega t} \sum_{n=1}^{\infty} i^n \frac{2n+1}{n(n+1)} \left(a_n^m {}^{(1)}_{01n} - ib_n^n {}^{(1)}_{e1n} \right)$$

$$H_t = \frac{k_2}{\phi\mu_1} E_0 e^{-i\omega t} \sum_{n=1}^{\infty} i^m \frac{2n+1}{n(n+1)} \left(b_n^m {}^{(1)}_{e1n} - ia_n^n {}^{(1)}_{01n} \right)$$

If $j_n(k_2R)$ is replaced by $h_n^{(1)}(k_2R)$ in the previous equations, the functions $m^{(1)}$ and $n^{(1)}$ become $m^{(3)}$ and $n^{(3)}$. The outgoing fields i.e., R>a, are represented by:

$$E_R = E_0 e^{-i\omega t} \sum_{n=1}^{\infty} i^n \frac{2n+1}{n(n+1)} \left(a_n^{rm} {}^{(3)}_{01n} - ib_n^n {}^{(3)}_{e1n} \right)$$

$$H_r = \frac{k_2}{\phi\mu_1} E_0 e^{-i\omega t} \sum_{n=1}^{\infty} i^m \frac{2n+1}{n(n+1)} \left(b_n^{rm} {}^{(3)}_{e1n} - ia_n^n {}^{(3)}_{01n} \right)$$

where H_r represents the resultant wave in the medium surrounding the sphere. At resonance, the values of ρ at resonance require that the a_n^t and b_n^t coefficients be infinite. In order to determine these values of a_n^t and b_n^t, the boundary conditions at the sphere radius are needed. Since there must be continuity of the E and H values at the surface, the following equations are used:

$i_1\times(E_i+E_r)=i_1\times E_t$ and

$i_1\times(H_i+H_r)=i_1\times H_t$

which lead to two pairs of inhomogeneous equations:

$$a_n{}^t j_n(N\rho) - a_n{}^r h_n^{(1)}(\rho) = j_n(\rho)$$

$$\mu_2 a_n{}^r [N\rho j_n(N\rho)]' - \mu_1 a_n{}^r [\rho h_n^{(1)}(\rho)]' = \mu_1 [\rho j_n(\rho)]' \text{ and}$$

$$\mu_2 N b_n{}^t j_n(N\rho) - \mu_1 b_n{}^r h_n^{(1)}(\rho) = \mu_1 j_n(\rho)$$

$$b_n{}^t [N\rho j_n(N\rho)]' - N b_n{}^r [\rho h_n^{(1)}(\rho)]' = N[\rho j_n(\rho)]'$$

where $k_1=Nk_2$, $\rho=k_2a$, $k_1a=N\rho$. Spherical Bessel functions of the first kind are denoted by j_n, while those of the third kind are denoted by $h_n^{(1)}$. The resulting equations are:

$$a_n' = \frac{\mu_1 j_n(\rho)[\rho h_n^{(1)}(\rho)]' - \mu_1 h_n^{(1)}\rho)[\rho j_n(\rho)]'}{\mu_1 j_n(N\rho)[\rho h_n^{(1)}(\rho)]' - \mu_2 h_n^{(1)}(\rho)[N\rho j_n(N\rho)]'}$$

and

$$b_n' = \frac{\mu_1 N j_n(\rho)[\rho h_n^{(1)}(\rho)]' - \mu_1 N h_n^{(1)}\rho)[\rho j_n(\rho)]'}{\mu_2 N^2 j_n(N\rho)[\rho h_n^{(1)}(\rho)]' - \mu_1 h_n^{(1)}(\rho)[N\rho j_n(N\rho)]'}$$

At a resonance, the denominator of either a_n' or b_n' will be zero. Thus, ρ values are found using the above equations that correspond to a resonant combination of angular frequency (ω) and radius (a) for a given sphere material and given surrounding medium. In determining such values of ρ, the following equations are also specifically used:

$$\rho = ak_2 = a\omega\sqrt{\epsilon_2\mu_2} \quad \text{and}$$

$$\rho_1 = (k_1/k_2)\rho$$

where ρ_1 corresponds to the sphere material. An iterative method is preferably used to find the desired values of ρ at resonance. In calculating ρ utilizing the above equations for purposes of example, it was assumed that $\mu_1=\mu_2=\mu_0=4\pi\times 10^{-7}$ and $\epsilon_2=\epsilon_0=8.85419\times10^{-12}$.

One major root of ρ which was found has a value of:

Real (ρ)=+66.39752607619131

Imaginary (ρ)=−0.6347867071968998.

These particular values are not shown in FIG. **8**. However, other values of ρ found using the equations set forth herein are shown in FIG. **8**. The peaks in FIG. **8** are the resonances. One of these resonances shown in FIG. **8** is shown in detail in FIG. **9**. These resonance values are shown for purposes of example. Other resonances also exist which have not been determined; thus, not all possible resonance values are shown in FIGS. **8** and **9**.

Calculation of these values also allows the determination of a possible am combination which would have these root values. For ρ, ϵ (epsilon)=ϵ_0 and μ=μ_0, and

$$\rho = a\omega\sqrt{\epsilon_0\mu_0} = a\omega/c.$$

Expressed in SI units, the speed of light $c=2.99792458\times10^{14}$ m/s. If an a value of 10^{-6} m is assumed for the examples shown herein, then:

$$\omega=\rho c/a\approx 1.9919\times10^{16} - i1.9044\times10^{14} \text{ radians/s.}$$

This is an example of the angular frequency required within the impingent EM radiation in order to create a resonant situation. Examples of other resonances were indicated, and these are shown in FIG. **8**. No complex-frequency plane waves exist. Therefore, the calculations were made by considering only the real portion of the above root and setting the imaginary portion equal to zero. However, upon

doing this, the iterative calculation procedure becomes insensitive to any root in the vicinity of the root's real portion. In the iterative calculation procedure, initially a range of ρ values is input into the equations. These ρ values are in the neighborhood of the prospective root. A range of ρ values is subsequently studied to find any imaginary ρ i.e., fρ (a function of ρ), peaks in that range. Next, once a peak has been chosen, the function order n giving the dominant fρ is determined. This also gives a clue as to whether the peak is due to a magnetic resonance (a_n approaches infinity) or an electrical resonance (b_n approaches infinity). A large number of Newton-Raphson iterations is preferably performed in order to converge upon a root ρ value.

FIGS. **2** and **3** show a second embodiment of the present invention generally designated by the numeral **110**. Embodiment **110** is essentially the same as embodiment **10** except that the antenna is a rf cavity structure **122** which feeds the received beat frequency radiation **124** to a waveguide **126**. Embodiment **110** also preferably includes two spheres **112** and **114** which receive the primary incident electromagnetic radiation **116** and emit the secondary electromagnetic radiation **118** and **120**. As with the spheres **18** and **20** of embodiment **10**, spheres **118** and **120** are preferably composed of a dielectric material. Embodiment **110** also includes converter **128**, capacitor **130**, transformer **132** and rectifier **134** which are essentially identical to the correspondingly numbered elements of embodiment **10**. Therefore, a description of these components of embodiment **110** will not be repeated in order to promote brevity. In addition, the same equations and method of calculation set forth above with regard to embodiment **10** also apply to embodiment. Therefore, their description will not be repeated in order to promote brevity.

FIGS. **4** and **5** show a third embodiment of the present invention generally designated by numeral **210**. Embodiment **210** is essentially identical to the first embodiment **10** except that the embodiment **210** includes a plurality of pairs **215** of receiving means (spheres) **212** and **214** mounted on a substrate **236**. The spheres **212** and **214** are thus in the form of an array **238**. The pairs **215** of the array **238** are preferably positioned proximal to each other in order to maximize the amount of energy extracted from a particular area or space of a given size. Since, as set forth hereinabove, the energy density of the zero point radiation increases as the frequency of the radiation increases, it is desirable that the spheres resonate at as high a bandwidth of frequencies as possible. Because the spheres **212** and **214** must be small in direct proportion to the wavelength of the high frequencies of the incident electromagnetic radiation **216** at which resonance is desirably obtained, the spheres **212** and **214** are preferably microscopic in size. Current lithographic techniques are capable of manufacturing such microscopically small spheres mounted on a suitable substrate thereby providing a suitably miniaturized system **210**. A miniaturized system enhances the energy output capability of the system by

enabling it to resonate at higher frequencies at which there are correspondingly higher energy densities. Consequently, utilization of array **238** in the system **210** enhances the maximum amount of electrical energy provided by the system **210**.

Lithographic techniques may be more amenable to manufacturing microscopically small receiving structures **212** and **214** which may be disc shaped, semispherical or have another shape other than as shown in FIGS. **4** and **5**. Consequently, the receiving means **212** and **214** may accordingly have such alternative shapes rather than the spherical shape shown in FIGS. **4** and **5**. In addition, a large number of small spheres may be manufactured by bulk chemical reactions. Packing a volume with such spheres in close proximity could enhance the output of energy.

Embodiment **210** also includes a plurality of antennas **222** positioned preferably between the spheres **212** and **214** which receive the beat frequency radiation **224** produced by the interference between the secondary radiation **218** and **220**. The antennas **222** are shown as loop antennas **222** but may be any other suitable type of antennas as well.

Embodiment **210** has a plurality of electrical conductors **226** which preferably include traces mounted on the substrate **236** which occupies a finite volume. The electrical conductors **226** feed the electrical output from the antennas **222** to a suitable converter **228** which preferably includes tuning capacitor **230**, transformer **232** and rectifier **234**, as with embodiments **10** and **110**. Except as set forth above, the components of embodiment **210** are identical to embodiment **10** so the detailed description of these components will not be repeated in order to promote brevity. In addition, the same equations and method of calculation set forth above for embodiment **10** also apply to embodiment **210**. Therefore, the description of these equations and method of calculation will not be repeated in order to promote brevity.

Accordingly, there has been provided, in accordance with the invention, a system which converts high frequency zero point electromagnetic radiation into electrical energy effectively and efficiently and thus fully satisfies the objectives set forth above. It is to be understood that all terms used herein are descriptive rather than limiting. Although the invention has been specifically described with regard to the specific embodiments set forth herein, many alternative embodiments, modifications and variations will be apparent to those skilled in the art in light of the disclosure set forth herein. Accordingly, it is intended to include all such alternatives, embodiments, modifications and variations that fall within the spirit and scope of the invention as set forth in the claims hereinbelow.

What is claimed is:

1. A system for converting incident electromagnetic radiation energy to electrical energy, comprising:

a first means for receiving incident primary electromagnetic radiation, said means for receiving producing

emitted secondary electromagnetic radiation at a first frequency, said first means for receiving having a first volumetric size selected to resonate at a frequency within the frequency spectrum of the incident primary electromagnetic radiation in order to produce the secondary electromagnetic radiation at the first frequency at an enhanced energy density;

a second means for receiving the incident primary electromagnetic radiation, said means for receiving producing emitted secondary electromagnetic radiation at a second frequency, the secondary radiation at the first frequency and the secondary radiation at the second frequency interfering to produce secondary radiation at a lower frequency than that of the incident primary radiation, said second means for receiving having a second volumetric size selected to resonate at a frequency within the frequency spectrum of the incident primary electromagnetic radiation in order to produce the emitted secondary electromagnetic radiation at the second frequency at an enhanced energy density;

an antenna for receiving the emitted secondary electromagnetic radiation at the lower frequency, said antenna providing an electrical output responsive to the secondary electromagnetic radiation received;

a converter electrically connected to said antenna for receiving electrical current output from said antenna and converting the electrical current output to electrical current having a desired voltage and waveform.

2. The system of claim **1** wherein:

said first means for receiving is composed of a dielectric material; and

said second means for receiving is composed of a dielectric material.

3. The system of claim **1** wherein:

said first means for receiving is spherical; and

said second means for receiving is spherical.

4. A system for for converting incident zero point electromagnetic radiation energy to electrical energy, comprising:

a first means for receiving incident primary zero point electromagnetic radiation, said means for receiving producing emitted secondary electromagnetic radiation at a first frequency;

a second means for receiving the incident primary zero point electromagnetic radiation, said means for receiving producing emitted secondary electromagnetic radiation at a second frequency, the secondary radiation at the first frequency and the secondary radiation at the second frequency interfering to produce secondary radiation at a beat frequency which is lower than that of the incident primary radiation;

an antenna for receiving the emitted secondary electromagnetic radiation at the lower frequency, said antenna providing an electrical output responsive to the secondary electromagnetic radiation received;

means for transmitting the emitted secondary electromagnetic radiation at the beat frequency from said antenna, said means for transmitting connected to said antenna;

a converter connected to said means for transmitting for receiving the emitted secondary electromagnetic radiation at the beat frequency from said antenna and converting the same to electrical current having a desired voltage and waveform.

5. The system of claim **4** wherein:

said first means for receiving has a first volumetric spherical size selected to resonate in response to the incident primary electromagnetic radiation in order to produce the secondary electromagnetic radiation at the first frequency at an enhanced energy density; and

said second means for receiving has a second volumetric spherical size selected to resonate in response to the incident primary electromagnetic radiation in order to produce the emitted secondary electromagnetic radiation at the second frequency at an enhanced energy density, said first and second volumetric sizes selected based on parameters of propagation constant of said first and second means for receiving, propagation constant of medium in which said first and second means for receiving are located and frequency of the incident primary electromagnetic radiation.

6. The system of claim **5** wherein the first and second volumetric sizes are selected by utilizing the formulas:

$$a_n^t = \frac{\mu_1 j_n(\rho)[\rho h_n^{(1)}(\rho)]' - \mu_1 h_n^{(1)}\rho)[\rho j_n(\rho)]'}{\mu_1 j_n(N\rho)[\rho h_n^{(1)}(\rho)]' - \mu_2 h_n^{(1)}(\rho)[N\rho j_n(N\rho)]'}$$

$$b_n^t = \frac{\mu_1 N j_n(\rho)[\rho h_n^{(1)}(\rho)]' - \mu_1 N h_n^{(1)}\rho)[\rho j_n(\rho)]'}{\mu_2 N^2 j_n(N\rho)[\rho h_n^{(1)}(\rho)]' - \mu_1 h_n^{(1)}(\rho)[N\rho j_n(N\rho)]'}$$

$$\rho = a\omega\sqrt{\epsilon_2\mu_2}$$

wherein at a resonance, the denominator of either equation for a_n^t or b_n^t will be approximately zero and wherein k_1=propagation constant of the means for receiving, k_2=propagation constant of medium through which the incident electromagnetic radiation propagates, a is the radius of either means for receiving, $N=k_1/k_2$, $\rho=k_2a$, $k_1a=N\rho$, a_n^t=magnitude of oscillations of the electric field of the nth order, b_n^t=magnitude of oscillations of the magnetic field of the nth order, ω=angular frequency of the incident electromagnetic radiation, ϵ is the permittivity of the material or medium and μ is the permeability of the material or medium.

7. The system of claim **6** wherein the radius of the first means for receiving is different from the radius of the second means for receiving, difference between the radius of said first means for receiving and the radius of said second means for receiving selected so that the beat frequency resulting from the difference is a frequency which facilitates conversion of the beat frequency electromagnetic radiation to electrical energy.

8. The system of claim **4** wherein:

said first means for receiving is composed of a dielectric material; and

said second means for receiving is composed of a dielectric material.

9. The system of claim **4** wherein:

said first means for receiving is spherical; and

said second means for receiving is spherical.

10. The system of claim **4** wherein said antenna is positioned generally between said first and second means for receiving.

11. The system of claim **4** wherein said antenna is a loop antenna.

12. The system of claim **4** wherein said antenna is a generally concave shell partially enclosing said first and second means for receiving.

13. The system of claim **4** wherein said means for transmitting is a waveguide.

14. A system for for converting incident zero point electromagnetic radiation energy to electrical energy, comprising:

a substrate;

a plurality of pairs of first means for receiving incident primary zero point electromagnetic radiation and second means for receiving incident primary zero point electromagnetic radiation, said plurality of pairs of means for receiving mounted on said substrate, said first means for receiving producing emitted secondary electromagnetic radiation at a first frequency, said second means for receiving the incident primary zero point electromagnetic radiation producing emitted secondary electromagnetic radiation at a second frequency, the secondary radiation at the first frequency and the secondary radiation at the second frequency interfering to produce secondary radiation at a beat frequency which is lower than that of the incident primary radiation, said first means for receiving having a first volumetric size selected to resonate in response to the incident primary electromagnetic radiation in

order to produce the secondary electromagnetic radiation at the first frequency at an enhanced energy density, and said second means for receiving having a second volumetric size selected to resonate in response to the incident primary electromagnetic radiation in order to produce the emitted secondary electromagnetic radiation at the second frequency at an enhanced energy density, said first and second volumetric sizes selected based on parameters of propagation constant of said first and second means for receiving, propagation constant of medium in which said first and second means for receiving are located and frequency of the incident primary electromagnetic radiation, said first and second volumetric sizes being different from each other;

a plurality of antennas for receiving the emitted secondary electromagnetic radiation at the lower frequency, said antenna providing an output responsive to the secondary electromagnetic radiation received, said plurality of antennas mounted on said substrate, each of said plurality of antennas receiving the emitted secondary electromagnetic radiation of one of said pairs of first and second means for receiving;

means for transmitting the emitted secondary electromagnetic radiation at the beat frequency from said antenna, said means for transmitting connected to said plurality of antennas;

a converter connected to said means for transmitting for receiving the emitted secondary electromagnetic radiation at the beat frequency from said antenna and converting the same to electrical current having a desired voltage and waveform.

STANLEY MEYER

US Patent 4,936,961 June 26, 1990 Inventor: Stanley A. Meyer

METHOD FOR THE PRODUCTION OF A FUEL GAS

Please note that this is a re-worded excerpt from this patent. It describes one of the methods which Stan used to split water into hydrogen and oxygen using very low levels of input power.

OBJECTS OF THE INVENTION

It is an object of the invention to provide a fuel cell and a process in which molecules of water are broken down into hydrogen and oxygen gases, and other formerly dissolved within the water is produced. As used herein the term "fuel cell" refers to a single unit of the invention comprising a water capacitor cell, as hereinafter explained, that produces the fuel gas in accordance with the method of the invention.

BRIEF DESCRIPTION OF THE DRAWINGS:

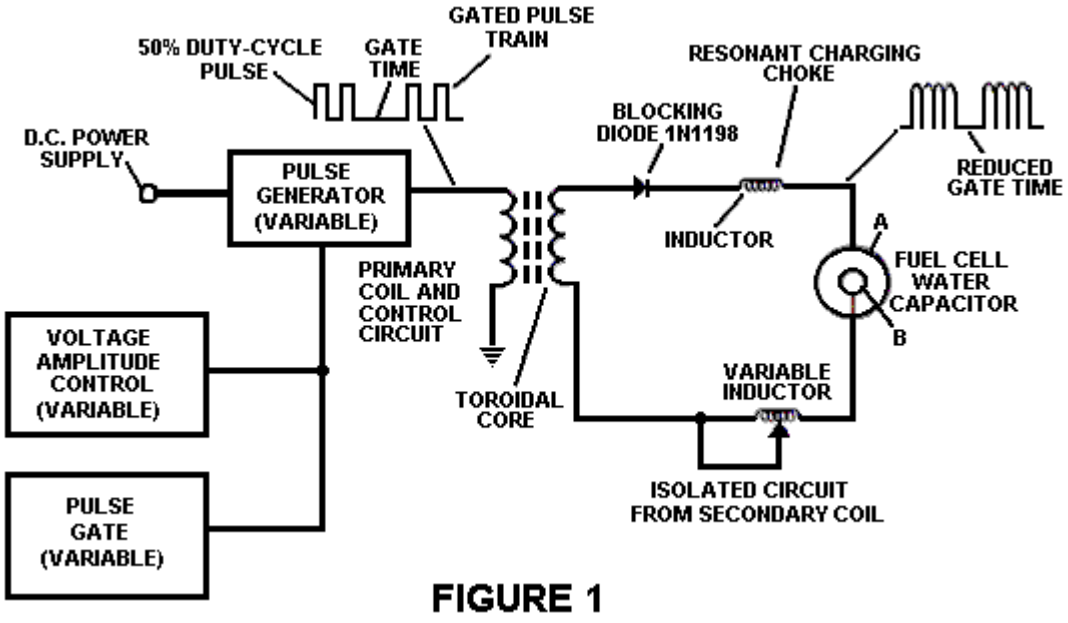

FIGURE 1

Fig.1 Illustrates a circuit useful in the process.

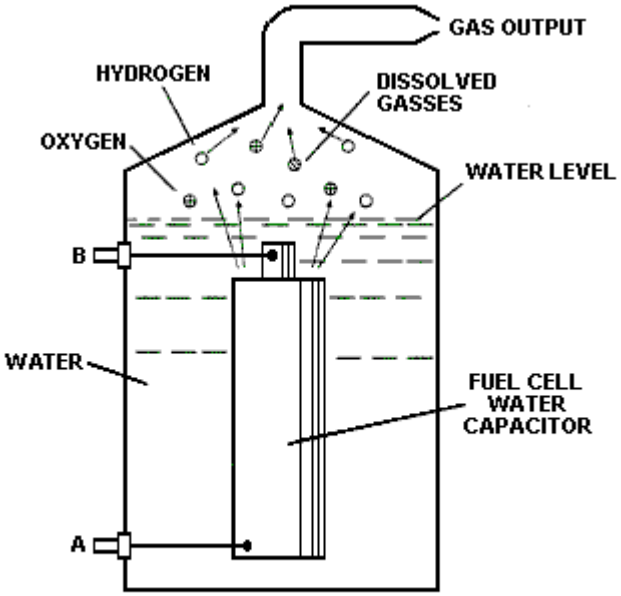

FIG 2

Fig.2 Shows a perspective of a "water capacitor" element used in the fuel cell circuit.

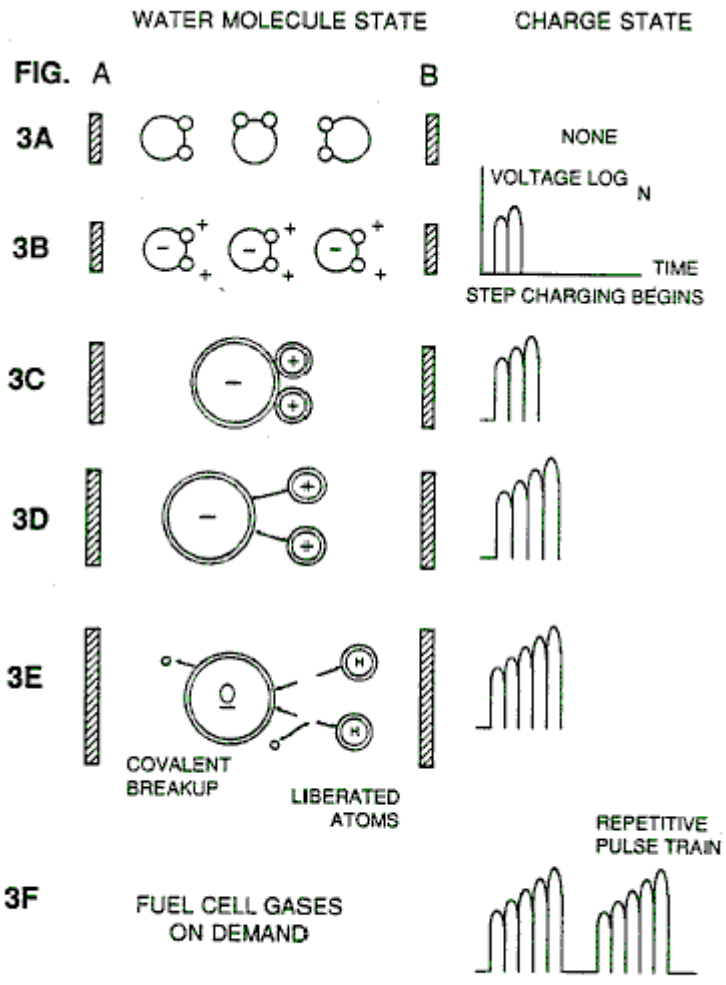

FIG. 3 (Parts A to F)

Figs. 3A through 3F are illustrations depicting the theoretical bases for the phenomena encountered during operation of the invention herein.

DESCRIPTION OF THE PREFERRED EMBODIEMENT

In brief, the invention is a method of obtaining the release of a gas mixture including hydrogen on oxygen and other dissolved gases formerly entrapped in water, from water consisting of:

(a) Providing a capacitor, in which the water is included as a dielectric liquid between capacitor plates, in a resonant charging choke circuit that includes an inductance in series with the capacitor;

(b) Subjecting the capacitor to a pulsating, unipolar electric voltage field in which the polarity does not pass beyond an arbitrary ground, whereby the water molecules within the capacitor are subjected to a charge of the same polarity and the water molecules are distended by their subjection to electrical polar forces;

(c) Further subjecting in said capacitor to said pulsating electric field to achieve a pulse frequency such that the pulsating electric field induces a resonance within the water molecule;

(d) Continuing the application of the pulsating frequency to the capacitor cell after resonance occurs so that the energy level within the molecule is increased in cascading incremental steps in proportion to the number of pulses;

(e) Maintaining the charge of said capacitor during the application of the pulsing field, whereby the co-valent electrical bonding of the hydrogen and oxygen atoms within said molecules is destabilised such that the force of the electrical field applied, as the force is effective within the molecule, exceeds the bonding force of the molecule, and hydrogen and oxygen atoms are liberated from the molecule as elemental gases; and

(f) Collecting said hydrogen and oxygen gases, and any other gases that were formerly dissolved within the water, and discharging the collected gases as a fuel gas mixture.

The process follows the sequence of steps shown in the following **Table 1** in which water molecules are subjected to increasing electrical forces. In an ambient state, randomly oriented water molecules are aligned with respect to a molecule polar orientation.

They are next, themselves polarised and "elongated" by the application of an electrical potential to the extent that covalent bonding of the water molecule is so weakened that the atoms dissociate and the molecule breaks down into hydrogen and oxygen elemental components.

Engineering design parameters based on known theoretical principles of electrical circuits determine the incremental levels of electrical and wave energy input required to produce resonance in the system whereby the fuel gas comprised of a mixture of hydrogen, oxygen, and other gases such as air were formerly dissolved within the water, is produced.

TABLE 1

Process Steps:

The sequence of the relative state of the water molecule and/or hydrogen/oxygen/other atoms:

A. (ambient state) random
B. Alignment of polar fields
C. Polarisation of molecule
D. Molecular elongation
E. Atom liberation by breakdown of covalent bond
F. Release of gases

In the process, the point of optimum gas release is reached at a circuit resonance. Water in the fuel cell is subjected to a pulsating, polar electric field produced by the electrical circuit whereby the water molecules are distended by reason of their subjection to electrical polar forces of the capacitor plates. The polar pulsating frequency applied is such that the pulsating electric field induces a resonance in the molecule. A cascade effect occurs and the overall energy level of specific water molecules is increased in cascading, incremental steps. The hydrogen and oxygen atomic gases, and other gas components formerly entrapped as dissolved gases in water, are released when the resonant energy exceeds the covalent bonding force of the water molecule. A preferred construction material for the capacitor plates is T304-grade stainless steel which is non-chemical reactive with water, hydrogen, or oxygen. An electrically conductive material which is inert in the fluid environment is a desirable material of construction for the electrical field plates of the "water capacitor" employed in the circuit.

Once triggered, the gas output is controllable by the attenuation of operational parameters. Thus, once the frequency of resonance is identified, by varying the applied pulse voltage to the water fuel cell assembly, gas output is varied. By varying the pulse shape and/or amplitude or pulse train sequence of the initial pulsing wave source, final gas output is varied. Attenuation of the voltage field frequency in the form of OFF and ON pulses likewise affects output.

The overall apparatus thus includes an electrical circuit in which a water capacitor having a known dielectric property is an element. The fuel gases are obtained from the water by the disassociation of the water molecule. The water molecules are split into component atomic elements (hydrogen and oxygen gases) by a voltage stimulation process called the electrical polarisation process which also releases dissolved gases entrapped in the water.

From the outline of physical phenomena associated with the process described in **Table 1**, the theoretical basis of the invention considers the respective states of molecules and gases and ions derived from liquid water. Before voltage stimulation, water molecules are randomly dispersed throughout water in a container. When a unipolar voltage pulse train such as shown in **Figs.3B** through **3F** is applied to positive and negative capacitor plates, an increasing voltage potential is induced in the molecules in a linear, step like charging effect. The electrical field of the particles within a volume of water including the electrical field plates increases from a low energy state to a high energy state successively is a step manner following each pulse-train as illustrated figuratively in the depictions of **Figs.3A** through **3F**. The increasing voltage potential is always positive in direct relationship to negative ground potential during each pulse. The voltage polarity on the plates which create the voltage fields remains constant although the voltage charge increases. Positive and negative voltage "zones" are thus formed simultaneously in the electrical field of the capacitor plates.

In the first stage of the process described in **Table 1**, because the water molecule naturally exhibits opposite electrical fields in a relatively polar configuration (the two hydrogen atoms are positively electrically charged relative to the negative electrically charged oxygen atom), the voltage pulse causes initially randomly oriented water molecules in the liquid state to spin and orient themselves with reference to positive and negative poles of the voltage fields applied. The positive electrically charged hydrogen atoms of said water molecule are attracted to a negative voltage field; while, at the same time, the negative electrically charged oxygen atoms of the same water molecule are attracted to a positive voltage field. Even a slight potential difference applied to inert, conductive plates of a containment chamber which forms a capacitor will initiate polar atomic orientation within the water molecule based on polarity differences.

When the potential difference applied causes the orientated water molecules to align themselves between the conductive plates, pulsing causes the voltage field intensity to be increased in accordance with **Fig.3B**. As further molecule alignment occurs, molecular movement is hindered. Because the positively charged hydrogen atoms of said aligned molecules are attracted in a direction opposite to the negatively charged oxygen atoms, a polar charge alignment or distribution occurs within the molecules between said voltage zones, as shown in **Fig.3B**. And as the energy level of the atoms subjected to resonant pulsing increases, the stationary water molecules become elongated as shown in **Fig.3C** and **Fig.3D**. Electrically charged nuclei and electrons are attracted toward opposite electrically charged equilibrium of the water molecule.

As the water molecule is further exposed to an increasing potential difference resulting from the step charging of the capacitor, the electrical force of attraction of the atoms within the molecule to the capacitor plates of the chamber also increase in strength. As a result, the covalent bonding between which form the molecule is weakened --- and ultimately terminated. The negatively charged electron is attracted toward the positively charged hydrogen atoms, while at the same time, the negatively charged oxygen atoms repel electrons.

In a more specific explanation of the "sub-atomic" action the occurs in the water fuel cell, it is known that natural water is a liquid which has a dielectric constant of 78.54 at 20 degrees C. and 1 atmosphere pressure. [Handbook of Chemistry & Physics, 68th ed., CRC Press(Boca Raton, Florida (1987-88)), Section E-50. H20(water)].

When a volume of water is isolated and electrically conductive plates, that are chemically inert in water and are separated by a distance, are immersed in water, a capacitor is formed, having a capacitance determined by the surface area of the plates, the distance of their separation and the dielectric constant of water.

When water molecules are exposed to voltage at a restricted current, water takes on an electrical charge. By the laws of electrical attraction, molecules align according to positive and negative polarity fields of the molecule and the alignment field. The plates of the capacitor constitute such as alignment field when a voltage is applied.

When a charge is applied to a capacitor, the electrical charge of the capacitor equals the applied voltage charge; in a water capacitor, the dielectric property of water resists the flow of amps in the circuit, and the water molecule itself, because it has polarity fields formed by the relationship of hydrogen and oxygen in the covalent bond, and intrinsic dielectric property, becomes part of the electrical circuit, analogous to a "microcapacitor" within the capacitor defined by the plates.

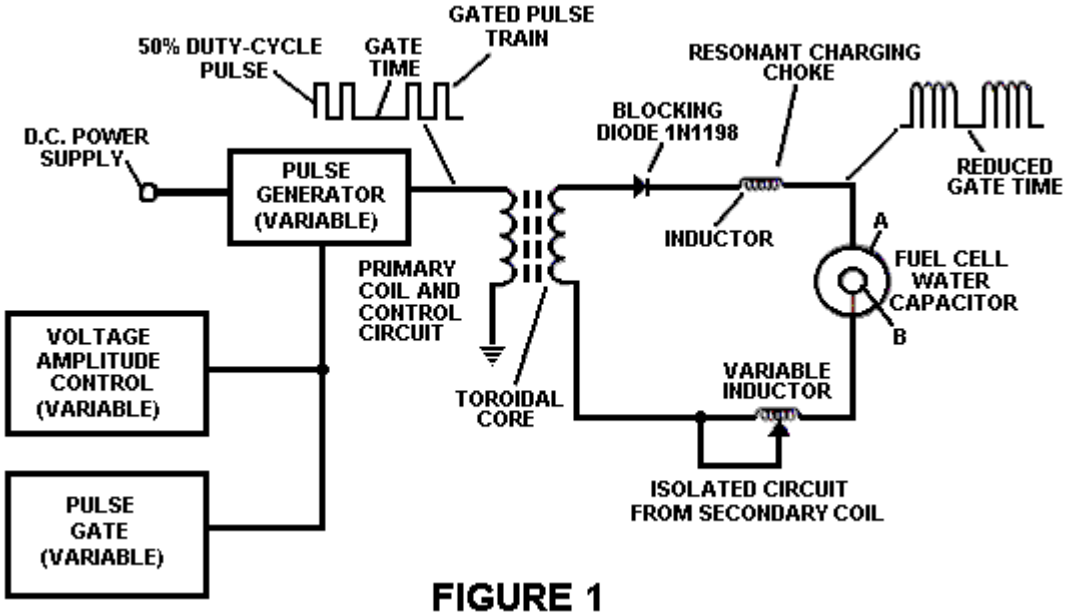

FIGURE 1

In the Example of a fuel cell circuit of **Fig.1**, a water capacitor is included. The step-up coil is formed on a conventional toroidal core formed of a compressed ferromagnetic powered material that will not itself become permanently magnetised, such as the trademarked "Ferramic 06# "Permag" powder as described in Siemens Ferrites Catalogue, CG-2000-002-121, (Cleveland, Ohio) No. F626-1205". The core is 1.50 inch in diameter and 0.25 inch in thickness. A primary coil of 200 turns of 24 gauge copper wire is provided and coil of 600 turns of 36 gauge wire comprises the secondary winding.

In the circuit of **Fig.1**, the diode is a 1N1198 diode which acts as a blocking diode and an electric switch that allows voltage flow in one direction only. Thus, the capacitor is never subjected to a pulse of reverse polarity.

The primary coil of the toroid is subject to a 50% duty cycle pulse. The toroidal pulsing coil provides a voltage step-up from the pulse generator in excess of five times, although the relative amount of step-up is determined by preselected criteria for a particular application. As the stepped-up pulse enters first inductor (formed from 100 turns of 24 gauge wire 1 inch in diameter), an electromagnetic field is formed around the inductor, voltage is switched off when the pulse ends, and the field collapses and produces another pulse of the same polarity i.e., another positive pulse is formed where the 50% duty cycle was terminated. Thus, a double pulse frequency is produced; however, in pulse train of unipolar pulses, there is a brief time when pulses are not present.

By being so subjected to electrical pulses in the circuit of **Fig.1**, water confined in the volume that includes the capacitor plates takes on an electrical charge that is increased by a step charging phenomenon occurring in the water capacitor. Voltage continually increases (to about 1000 volts and more) and the water molecules starts to elongate.

The pulse train is then switched off; the voltage across the water capacitor drops to the amount of the charge that the water molecules have taken on, i.e., voltage is maintained across the charged capacitor. The pulse train is the reapplied.

Because a voltage potential applied to a capacitor can perform work, the higher the voltage the higher the voltage potential, the more work is performed by a given capacitor. In an optimum capacitor that is wholly non-conductive, zero (0) current flow will occur across the capacitor. Thus, in view of an idealised capacitor circuit, the object of the water capacitor circuit is to prevent electron flow through the circuit, i.e. such as occurs by electron flow or leakage through a resistive element that produces heat. Electrical leakage in the water will occur, however, because of some residual conductivity and impurities or ions that may be otherwise present in the water. Thus, the water capacitor is preferably chemically inert. An electrolyte is not added to the water.

In the isolated water bath, the water molecule takes on charge, and the charge increases. The object of the process is to switch off the covalent bonding of the water molecule and interrupt the subatomic force, i.e. the electrical force or electromagnetic force, that binds the hydrogen and oxygen atoms to form a molecule so that the hydrogen and oxygen separate.

Because an electron will only occupy a certain electron shell (shells are well known) the voltage applied to the capacitor affects the electrical forces inherent in the covalent bond. As a result of the charge applied by the plates, the applied force becomes greater than the force of the covalent bonds between the atom of the water molecule;

and the water molecule becomes elongated. When this happens, the time share ratio of the electron shells is modified.

In the process, electrons are extracted from the water bath; electrons are not consumed nor are electrons introduced into the water bath by the circuit as electrons are conventionally introduced in as electrolysis process. There may nevertheless occur a leakage current through the water. Those hydrogen atoms missing electrons become neutralised; atoms are liberated from the water. The charged atoms and electrons are attracted to the opposite polarity voltage zones created between the capacitor plates. The electrons formerly shared by atoms in the water covalent bond are reallocated such that neutral elemental gases are liberated.

In the process, the electrical resonance may be reached at all levels of voltage potential. The overall circuit is characterised as a "resonant charging choke" circuit which is an inductor in series with a capacitor that produces a resonant circuit. [SAMS Modern Dictionary of Electronics, Rudolf Garff, copyright 1984, Howard W. Sams & Co. (Indianapolis, Ind.), page 859.] Such a resonant charging choke is on each side of the capacitor. In the circuit, the diode acts as a switch that allows the magnetic field produced in the inductor to collapse, thereby doubling the pulse frequency and preventing the capacitor from discharging. In this manner a continuous voltage is produced across the capacitor plates in the water bath; and the capacitor does not discharge. The water molecules are thus subjected to a continuously charged field until the breakdown of the covalent bond occurs.

As noted initially, the capacitance depends on the dielectric properties of the water and the size and separation of the conductive elements forming the water capacitor.

EXAMPLE 1

In an example of the circuit of **Fig.1** (in which other circuit element specifications are provided above), two concentric cylinders 4 inches long formed the water capacitor of the fuel cell in the volume of water. The outside cylinder was 0.75 inch in outside diameter; the inner cylinder was 0.5 inch in outside diameter. Spacing from the outside of the inner cylinder to the inner surface of the outside cylinder was 0.0625 inch. Resonance in the circuit was achieved at a 26 volt applied pulse to the primary coil of the toroid at 0 KHz (*suspected mis-typing for 10KHz*), and the water molecules disassociated into elemental hydrogen and oxygen and the gas released from the fuel cell comprised a mixture of hydrogen, oxygen from the water molecule, and gases formerly dissolved in the water such as the atmospheric gases or oxygen, nitrogen, and argon.

In achieving resonance in any circuit, as the pulse frequency is adjusted, the flow of amps is minimised and the voltage is maximised to a peak. Calculation of the resonance frequency of an overall circuit is determined by known means; different cavities have a different frequency of resonance dependant on parameters of the water dielectric, plate size, configuration and distance, circuit inductors, and the like. Control of the production of fuel gas is determined by variation of the period of time between a train of pulses, pulse amplitude and capacitor plate size and configuration, with corresponding value adjustments to other circuit components.

The wiper arm on the second conductor tunes the circuit and accommodates to contaminants in water so that the charge is always applied to the capacitor. The voltage applied determines the rate of breakdown of the molecule into its atomic components. As water in the cell is consumed, it is replaced by any appropriate means or control system.

Variations of the process and apparatus may be evident to those skilled in the art.

CLAIMS:

1. A method of obtaining the release of a gas mixture including hydrogen and oxygen and other dissolved gases formerly entrapped in water, from water, consisting of:

(a) Providing a capacitor in which water is included as a dielectric between capacitor plates, in a resonant charging choke circuit that includes an inductance in series with the capacitor;

(b) Subjecting the capacitor to a pulsating, unipolar electric charging voltage in which the polarity does not pass beyond an arbitrary ground, whereby the water molecules within the capacitor plates;

(c) Further subjecting the water in said capacitor to a pulsating electric field resulting from the subjection of the capacitor to the charging voltage such that the pulsating electric field induces a resonance within the water molecules;

(d) Continuing the application of the pulsating charging voltage to the capacitor after the resonance occurs so that the energy level within the molecules is increased in cascading incremental steps in proportion to the number of pulses;

(e) Maintaining the charge of said capacitor during the application of the pulsating charge voltage, whereby the covalent electrical bonding of the hydrogen and oxygen atoms within said molecules is destabilised, such

that the force of the electrical field applied to the molecules exceeds the bonding force within the molecules, and the hydrogen and oxygen atoms are liberated from the molecules as elemental gases.

2. The method of claim 1 including the further steps of collecting said liberated gases and any other gases that were formerly dissolved within the water and discharging said collected gases as a fuel gas mixture.

STANLEY MEYER

US Patent 4,389,981 28th June 1983 Inventor: Stanley A. Meyer

HYDROGEN GAS INJECTOR SYSTEM FOR INTERNAL COMBUSTION ENGINES

Please note that this is a re-worded excerpt from this patent. It describes one method for using hydrogen and oxygen gases to fuel a standard vehicle engine.

ABSTRACT

System and apparatus for the controlled intermixing of a volatile hydrogen gas with oxygen and other non-combustible gasses in a combustion system. In a preferred arrangement the source of volatile gas is a hydrogen source, and the non-combustible gasses are the exhaust gasses of the combustion system in a closed loop arrangement. Specific structure for the controlled mixing of the gasses, the fuel flow control, and safety are disclosed.

CROSS REFERENCES AND BACKGROUND

There is disclosed in my co-pending U.S. patent application Serial No. 802,807 filed Sept. 16, 1981 for a Hydrogen-Generator, a generating system converting water into hydrogen and oxygen gasses. In that system and method the hydrogen atoms are dissociated from a water molecule by the application of a non-regulated, non-filtered, low-power, direct current voltage electrical potential applied to two non-oxidising similar metal plates having water passing between them. The sub-atomic action is enhanced by pulsing this DC voltage. The apparatus comprises structural configurations in alternative embodiments for segregating the generated hydrogen gas from the oxygen gas.

In my co-pending patent application filed May 5, 1981, U.S. Serial No. 262,744 now abandoned for Hydrogen-Airdation Processor, non-volatile and non-combustible gasses are controlled in a mixing stage with a volatile gas. The hydrogen airdation processor system utilises a rotational mechanical gas displacement system to transfer, meter, mix, and pressurise the various gasses. In the gas transformation process, ambient air is passed through an open flame gas-burner system to eliminate gasses and other substances present. After that, the non-combustible gas-mixture is cooled, filtered to remove impurities, and mechanically mixed with a pre-determined amount of hydrogen gas. This results in a new synthetic gas.

This synthetic gas-formation stage also measures the volume and determines the proper gas-mixing ratio for establishing the desired burn-rate of hydrogen gas. The rotational mechanical gas displacement system in that process determines the volume of synthetic gas to be produced.

The above-noted hydrogen airdation processor, of my co-pending application, is a multi-stage system suited to special applications. Whereas the hydrogen generator system of my other mentioned co-pending application does disclose a very simple and unique hydrogen generator.

In my co-pending patent application Serial No. 315,945, filed Oct. 18, 1981 there is disclosed a combustion system incorporating a mechanical drive system. In one instance, this is designed to drive a piston in an automotive device. There is shown a hydrogen generator for developing hydrogen gas, and perhaps other non-volatile gasses such as oxygen and nitrogen. The hydrogen gas with the attendant non-volatile gasses is fed via a line to a controlled air intake system. The combined hydrogen, non-volatile gasses, and the air, after inter-mixing, are fed to a combustion chamber where they are ignited. The exhaust gasses of the combustion chamber are returned in a closed loop arrangement to the mixing chamber to be used again as the non-combustible gas component. Particular applications and structural embodiments of the system are disclosed.

SUMMARY OF THE INVENTION

The system of the present invention in its most preferred embodiment is for a combustion system utilising hydrogen gas; particularly to drive the pistons in an car engine. The system utilises a hydrogen generator for developing hydrogen gas. The hydrogen gas and other non-volatile gasses are then fed, along with oxygen, to a mixing chamber. The mixture is controlled in such a way as to lower the temperature of the combustion to bring it in line with that of the currently existing commercial fuels. The hydrogen gas feed line to the combustion chamber includes a fine linear control gas flow valve. An air intake is the source of oxygen and it also includes a variable

valve. The exhaust gasses from the combustion chamber are utilised in a controlled manner as the non-combustible gasses.

The hydrogen generator is improved by the inclusion of a holding tank which provides a source of start-up fuel. Also, the hydrogen gas generator includes a pressure-controlled safety switch on the combustion chamber which disconnects the input power if the gas pressure rises above the required level. The simplified structure includes a series of one-way valves, safety valves, and quenching apparatus. The result is an apparatus which comprises the complete assembly for converting a standard car engine from petrol (or other fuels) to use a hydrogen/gas mixture.

OBJECTS

It is accordingly a principal object of the present invention to provide a combustion system of gasses combined from a source of hydrogen and non-combustible gasses.

Another object of the invention is to provide such a combustion system that intermixes the hydrogen and non-combustible gasses in a controlled manner and thereby control the combustion temperature.

A further object of the invention is to provide such a combustion system that controls the fuel flow to the combustion chamber in s system and apparatus particularly adapted to hydrogen gas.

Still other objects and features of the present invention will become apparent from the following detailed description when taken in conjunction with the drawings in which:

BRIEF DESCRIPTION OF THE DRAWINGS

Fig.1 is a mechanical schematic illustration partly in block form of the present invention in its most preferred embodiment.

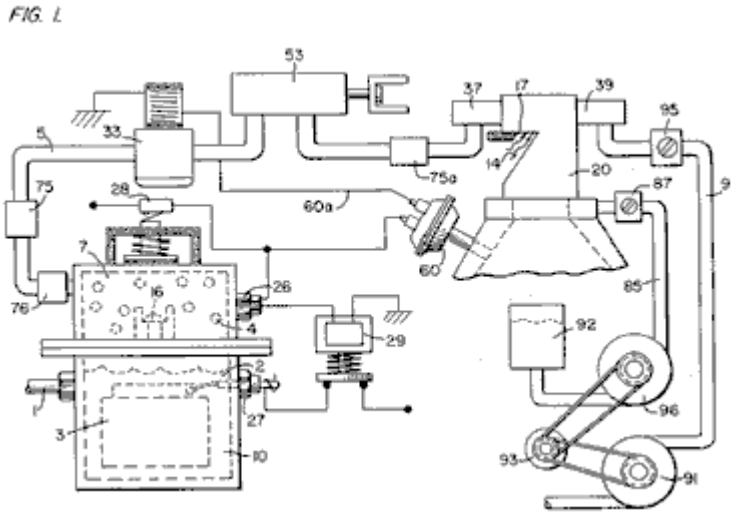

Fig.2 is a block schematic illustration of the preferred embodiment of the hydrogen injector system shown in Fig.1.

FIG. 2.

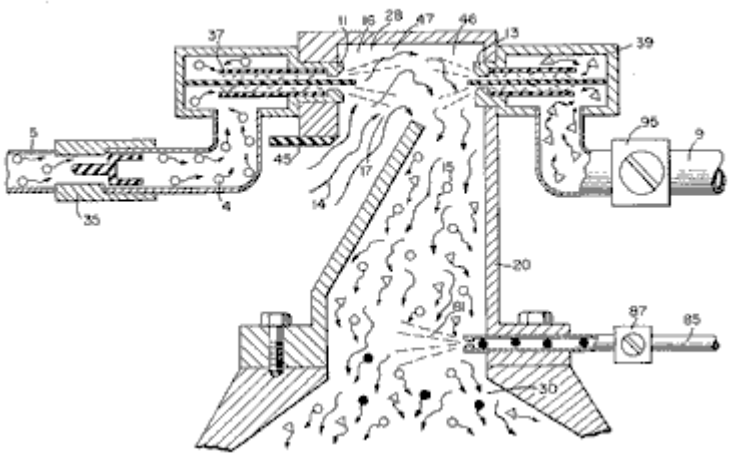

Fig.3 is the fine linear fuel flow control shown in Fig.1.

FIG. 3.

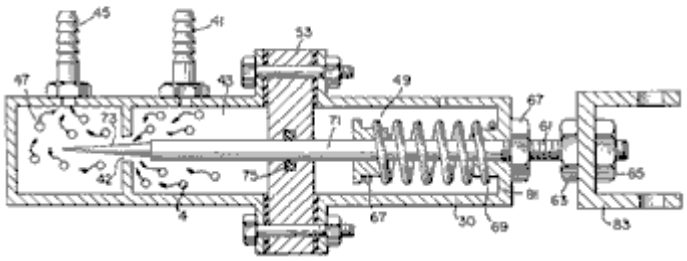

Fig.4 is cross-sectional illustration of the complete fuel injector system in an car utilising the concepts of the present invention.

FIG. 4.

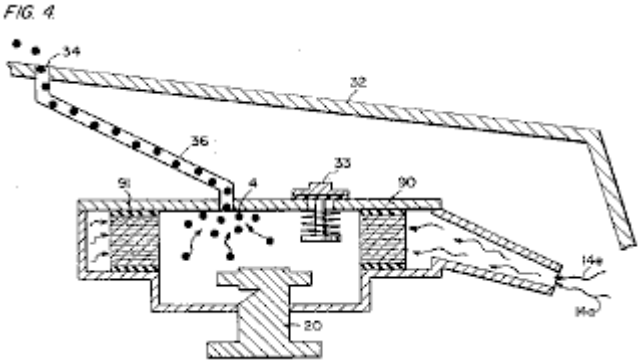

Fig.5 is a schematic drawing in a top view of the fuel injector system utilised in the preferred embodiment.

FIG. 5.

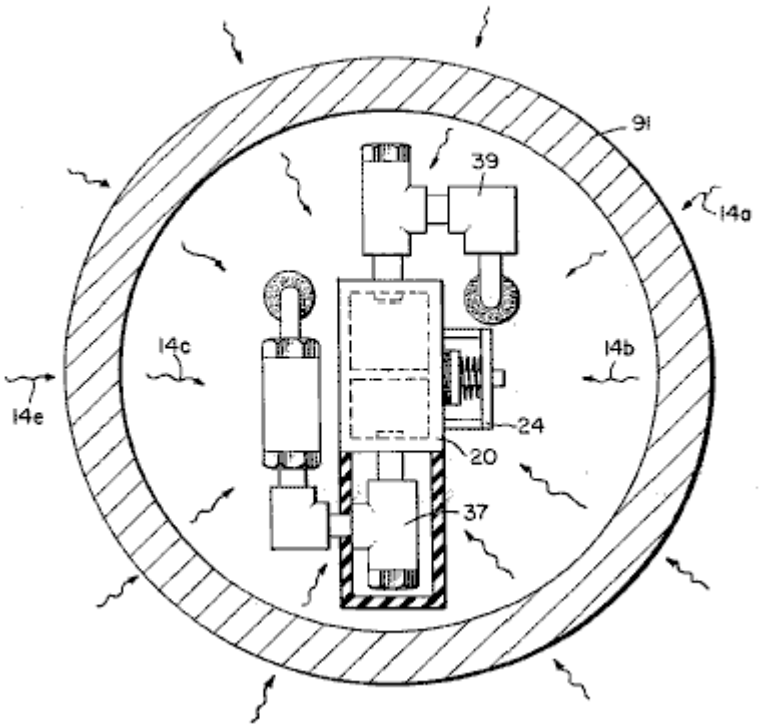

Fig.6 is a cross-sectional side view of the fuel injector system in the present invention.

FIG. 6.

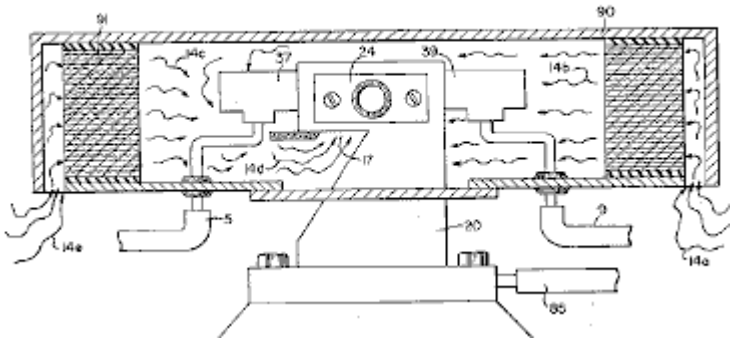

Fig.7 is a side view of the fuel mixing chamber.

FIG. 7.

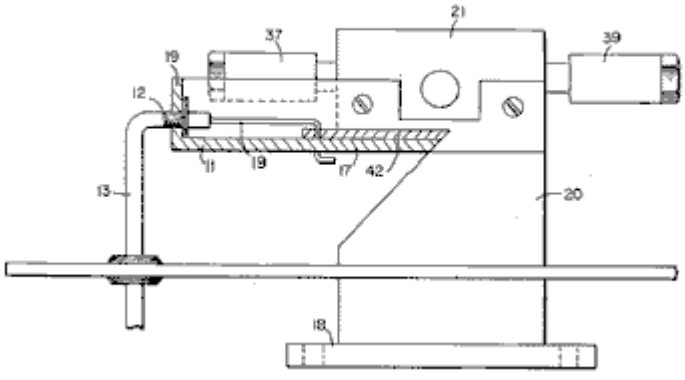

Fig.8 is a top view of the air intake valve to fuel mixing chamber.

FIG. 8.

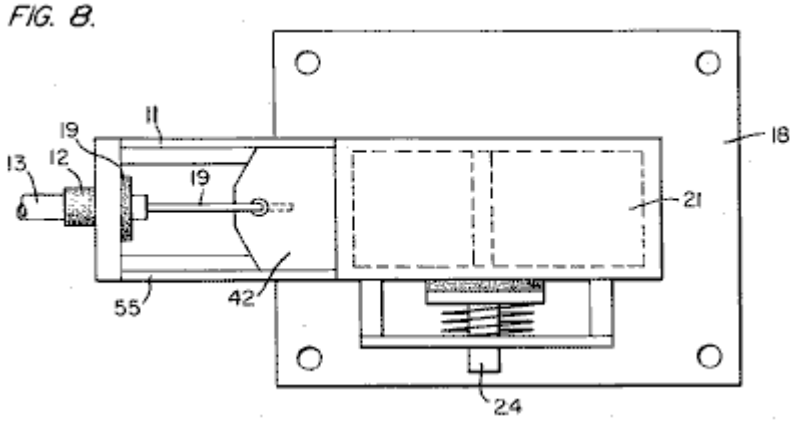

Fig.9 is a comparison of the burning velocity of hydrogen with respect to other fuels.

FIG 9

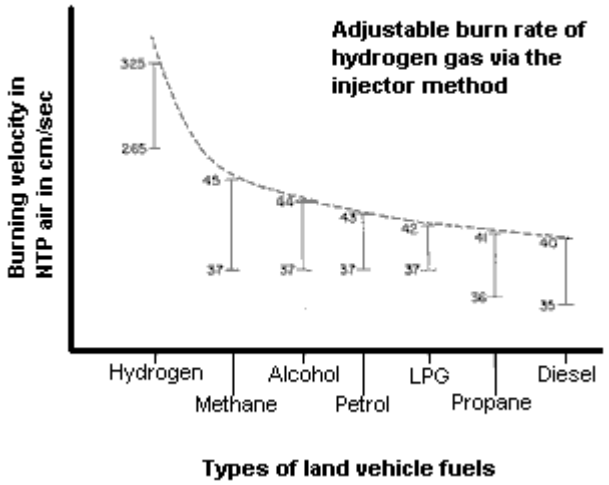

DETAILED DESCRIPTION OF INVENTION TAKEN WITH DRAWINGS:

FIG. 1

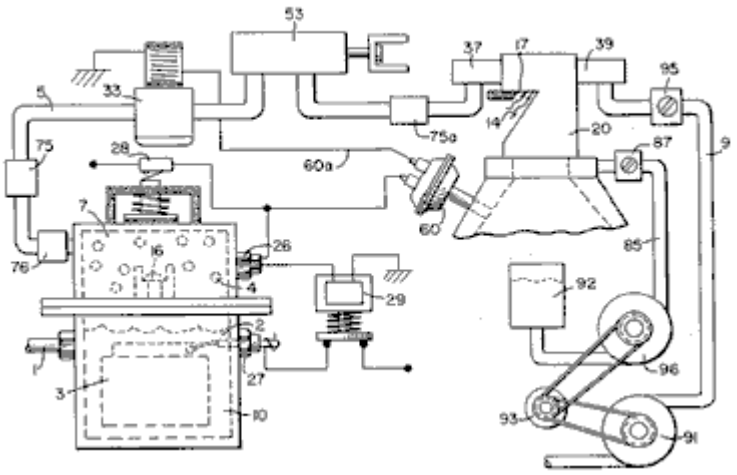

Referring to **Fig.1** the complete overall gas mixing and fuel flow system is illustrated together for utilisation in a combustion engine, particularly an engine in a car. With specific reference to **Fig.1**, the hydrogen source **10** is the hydrogen generator disclosed and described in my co-pending application, supra. The container **10** is an enclosure for a water bath **2**. Immersed in the water **2** is an array of plates **3** as further described in my co-pending application, supra. Applied to plates **3** is a source of direct current potential via electrical inlet **27**. The upper portion **7** of the container **10** is a hydrogen storage area maintaining a predetermined amount of pressure. In this way, there will be an immediate flow of hydrogen gas at start-up.

To replenish the expended water, the generator provides a continuous water source **1**. Thereafter, the generator is operable as described in the aforesaid patent application. The safety valve **28** is designed to rupture should there be an excessive build-up of gas. Switch **26** is a gas-pressure switch included to maintain a predetermined gas pressure level about a regulated low-volume.

The generated hydrogen gas **4** is fed from the one-way check valve **16** via pipe **5** to a gas-mixing chamber **20**, where the hydrogen gas is mixed with non-combustible gasses via pipe **9** from a source described later.

If the one-way valve **75** failed, there could be a return spark which could ignite the hydrogen gas **4** in the storage area **7** of the hydrogen generator **10**. To prevent this, the quenching assembly **76** has been included to prevent just such an ignition.

FIG. 2.

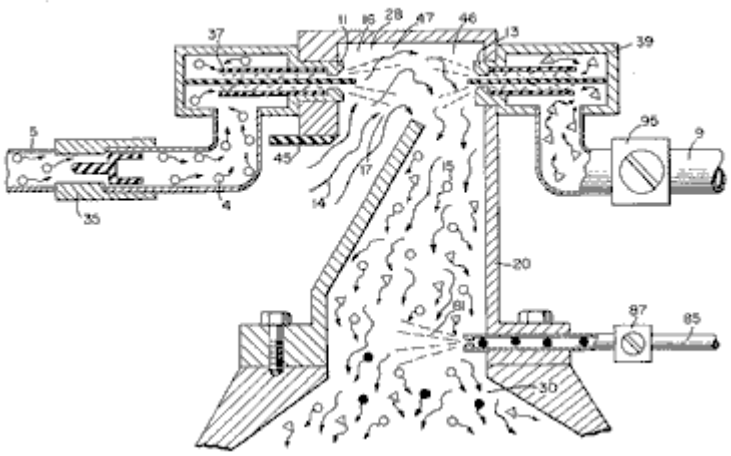

With particular reference to **Fig.2,** the hydrogen gas (via pipe **5**) and non-combustible gasses (via pipe **9**), are fed to a carburettor (air-mixture) system **20** also having an air intake **14** for ambient air.

The hydrogen gas **4** is fed via line **5** through nozzle **11** in a spray **16** in to the trap area **46** of the mixing chamber **20**. Nozzle **11** has an opening smaller than the plate openings in the quenching assembly **37**, thereby preventing flash-back in the event of sparking. The non-volatile gasses are injected into mixing chamber **20** trap area **47** in a jet spray **17** via nozzle **13**. Quenching assembly **39** is operable much in the same manner as quenching assembly **37**.

In the preferred arrangement, the ambient air is the source of oxygen necessary for the combustion of the hydrogen gas. Further, as disclosed in the aforesaid co-pending application, the non-volatile gasses are in fact, the exhaust gasses passed back via a closed loop system. It is to be understood that the oxygen and/or the non-combustible gasses might also be provided from an independent source.

With continued reference to **Fig.2** the gas trap area **47** is a predetermined size. As hydrogen is lighter than air, the hydrogen will rise and become trapped in area **47**. Area **47** is large enough to contain enough hydrogen gas to allow instant ignition upon the subsequent start-up of the combustion engine.

It will be noted that the hydrogen gas is injected in the uppermost region of the trap area **47**. Hydrogen rises at a much greater rate than oxygen or the non-combustible gasses; perhaps three times or greater. Therefore, if the hydrogen gas entered the trap area **47** (mixing area) at its lowermost region the hydrogen gas would rise so rapidly that the air could not mix with the oxygen. With the trap area **47** shown in **Fig.2**, the hydrogen is forced downwards into the air intake **15**. That is, the hydrogen gas is forced downwards into the upwardly forced air and this causes adequate mixing of the gasses.

The ratio of the ambient air (oxygen) **14** and the non-combustible gas via line **9** is a controlled ratio which is tailored to the particular engine. Once the proper combustion rate has been determined by the adjustment of valve **95** (for varying the amount of the non-combustible gas) and the adjustment of valve **45** (for varying the amount of the ambient air), the ratio is maintained thereafter.

In a system where the non-combustible gasses are the exhaust gasses of the engine itself, passed back through a closed loop-arrangement, and where the air intake is controlled by the engine, the flow velocity and hence the air/non-combustible mixture, is maintained by the acceleration of the engine.

The mixture of air with non-combustible gasses becomes the carrier for the hydrogen gas. That is, the hydrogen gas is mixed with the air/non-combustible gas mixture. By varying the amount of hydrogen gas added to the air/non-combustible mixture, the engine speed is controlled.

FIG. 3.

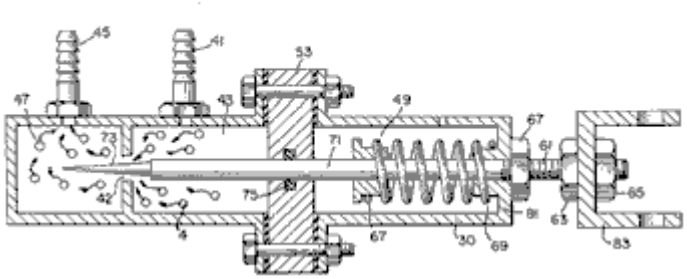

Reference is made to **Fig.3** which shows in a side view cross-section, the fine linear fuel flow control **53**. The hydrogen gas **4** enters chamber **43** via gas inlet **41**. The hydrogen gas passes from chamber **43** to chamber **47** via port or opening **42**. The amount of gas passing form chamber **43** to chamber **47** is dictated by the setting of the port opening **42**.

The port opening is controlled by inserting the linearly tapered pin **73** into it. The blunt end of pin **73** is fixed to rod **71**. Rod **71** is passed, (via supporting O-ring **75**), through opening **81** in housing **30**, to the manual adjustment mechanism **83**.

Spring **49** retains the rod **71** in a fixed position relative to pin **73** and opening **42**. When mechanism **83** is operated, pin **73** moves back from the opening **42**. As pin **73** is tapered, this backward movement increases the free area of opening **42**, thereby increasing the amount of gas passing from chamber **43** to chamber **47**.

The stops **67** and **69** maintain spring **49** in its stable position. The nuts **63** and **67** on threaded rod **61** are used to set the minimum open area of opening **42** by the correct positioning of pin **73**. This minimum opening setting, controls the idle speed of the engine, so pin **73** is locked in its correct position by nuts **63** and **67**. This adjustment controls the minimum rate of gas flow from chamber **43** to chamber **47** which will allow continuous operation of the combustion engine.

Referring now to **Fig.8** which illustrates the air adjustment control for manipulating the amount of air passing into the mixing chamber **20**. The closure **21** mounted on plate **18** has an opening **17** on end **11**. A plate-control **42** is mounted so as to slide over opening **17**. The position of this plate, relative to opening **17**, is controlled by the position of the control rod **19** which passes through grommet **12** to control line **13**. Release valve **24** is designed to rupture should any malfunction occur which causes the combustion of the gasses in mixing chamber **20**.

FIG. 4.

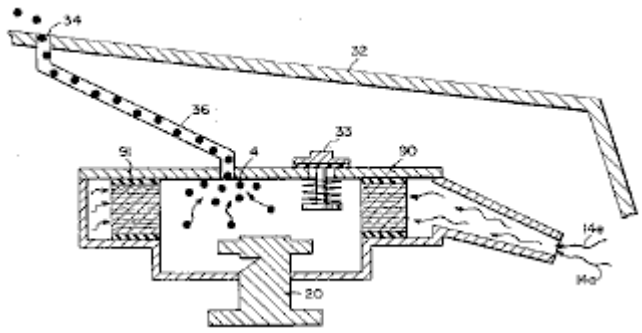

With reference now to **Fig.4**, if hydrogen gas **4** were to accumulate in mixing chamber **20** and reach an excessive pressure, the escape tube **36** which is connected to port **34** (located on the car bonnet **32**), permits the excess hydrogen gas to escape safely to the atmosphere. In the event of a malfunction which causes the combustion of the gasses in mixing chamber **20**, the pressure relief valve **33** will rupture, expelling the hydrogen gas without combustion.

In the constructed arrangement of **Fig.1**, there is illustrated a gas control system which may be fitted to an existing car's internal combustion engine without changing or modifying the car's design parameters or characteristics. The flow of the volatile hydrogen gas is, of course, critical; therefore, there is incorporated in line **5** a gas-flow valve **53**, and this is used to adjust the hydrogen flow. This gas-flow valve is shown in detail in **Fig.3**.

FIG. 8.

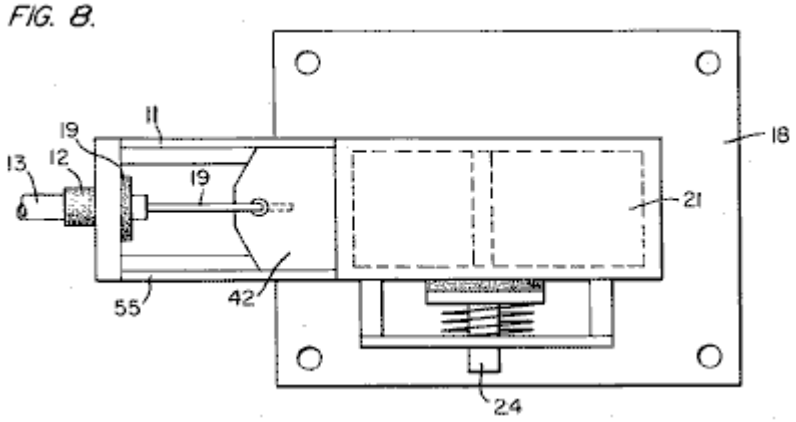

The intake air **14** may be in a carburettor arrangement with an intake adjustment **55** which adjusts the plate **42** opening. This is shown more fully in **Fig.8**. To maintain constant pressure in hydrogen gas storage **7** in the on-off operation of the engine, the gas flow control valve is responsive to the electrical shut-off control **33**. The constant pressure permits an abundant supply of gas on start-up and during certain periods of running time in re-supply.

The switch **33** is in turn responsive to the vacuum control switch **60**. During running of the engine vacuum will be built up which in turn leaves switch **33** open by contact with vacuum switch **60** through lead **60a**. When the engine is not running the vacuum will decrease to zero and through switch **60** will cause electrical switch **33** to shut off cutting off the flow of hydrogen gas to the control valve **53**.

As low-voltage direct current is applied to safety valve **28**, solenoid **29** is activated. The solenoid applies a control voltage to the hydrogen generator exciter **3** via terminal **27** through pressure switch **26**. As the electrical power activates solenoid **29**, hydrogen gas is caused to pass through flow adjustment valve **16** and then outlet pipe **5** for utilisation. The pressure differential hydrogen gas output to gas mixing chamber **20** is for example 30 lbs. to 15 lbs. Once hydrogen generator **10** reaches an optimum gas pressure level, pressure switch **26** shuts off the electrical power to the hydrogen excitors. If the chamber pressure exceeds a predetermined level, the safety release valve **28** is activated disconnecting the electrical current and thereby shutting down the entire system for safety inspection.

FIG. 6.

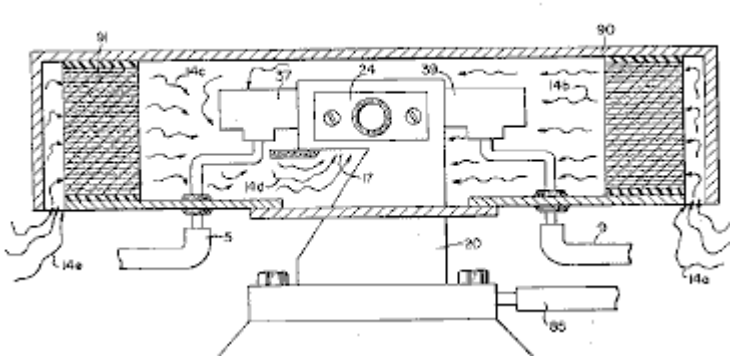

With particular reference now to **Fig.6** which illustrates the fuel injector system in a side cross-sectional view and to **Fig.5** the top view. The structural apparatus incorporated in the preferred embodiment comprises housing **90** which has air intakes **14a** and **14e**. The air passes through filter **91** around the components **14b** and **14c** and then to intake **14d** of the mixing chamber **20**. The hydrogen enters via line **5** via quenching plates **37** and into the mixing chamber **20**. The non-volatile gasses pass via line **9** to the quenching plates **39** and into the mixing chamber **20**.

FIG. 7

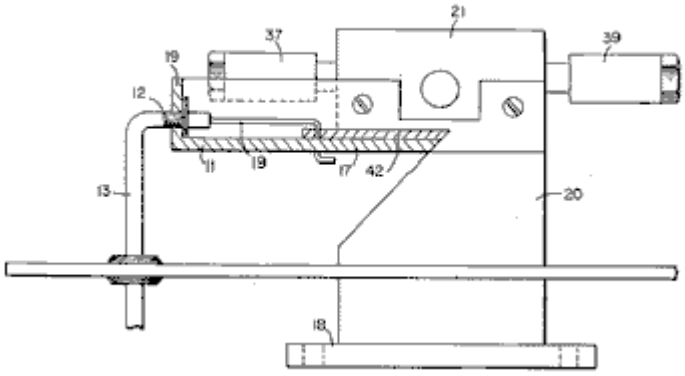

Fig.7 illustrates the mechanical arrangement of the components which make up the overall structure of mixing chamber **20** (shown independently in the other figures).

FIG. 1

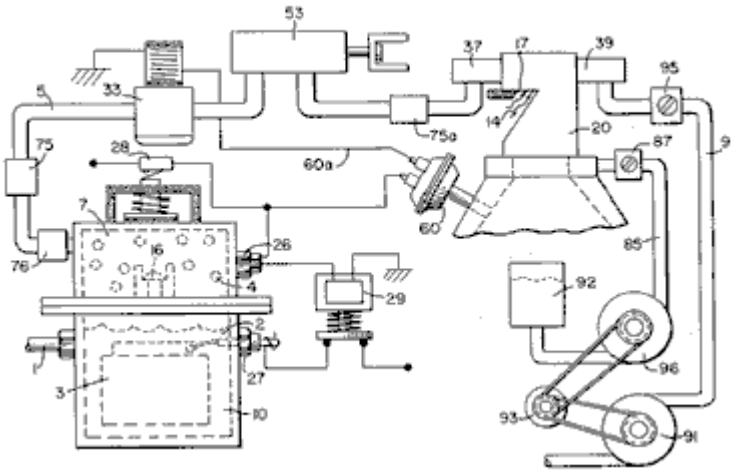

Returning to **Fig.1** there is illustrated the non-volatile gas line **9** passing through mixture pump **91** by engine pulley **93**. Valve **95** controls the rate of flow. Also driven by pulley **93** is pump **96** having line **85** connected to an oil reservoir **92** and valve **87** and finally to mixing chamber **20**. As a practical matter, such as in a non-oil lubricated engine, lubricating fluid such as oil **81** is sprayed in the chamber **20**, via oil supply line **85** for lubrication.

There have been several publications in the past year or so, delving into the properties of Hydrogen gas, its potential use, generating systems, and safety. One such publication is "Selected Properties of Hydrogen" (Engineering Design Data) issued February 1981 by the National Bureau of Standards.

These publications are primarily concerned with the elaborate and costly processes for generating hydrogen. Equally so, they are concerned with the very limited use of hydrogen gas because of its extremely high burning velocities. This in turn reflects the danger in the practical use of hydrogen.

With reference to the graph of the Appendix A, it is seen that the burning velocities of alcohol, propane, methane, petrol, Liquid Petroleum Gas, and diesel oil are in the range of minimum 35 to maximum 45. Further, the graph illustrates that the burning velocity of hydrogen gas is in the range of 265 minimum to 325 maximum. In simple terms, the burning velocity of hydrogen is of the order of 7.5 times the burning velocity of ordinary commercial fuels.

Because of the unusually high burning velocity of hydrogen gas, it has been ruled out as a substitute fuel, by these prior investigators. Further, even if an engine could be designed to accommodate such high burning velocities, the danger of explosion would eliminate any thoughts of commercial use.

The present invention, as above described, has resolved the above-noted criteria for the use of hydrogen gas in a standard commercial engine. Primarily, the cost in the generation of hydrogen gas, as noted in the aforementioned co-pending patent applications, is minimal. Water with no chemicals or metals is used. Also, as noted in the aforementioned co-pending patent applications, the reduction in the hydrogen gas burn velocity has

been achieved. These co-pending applications not only teach the reduction in velocity, but teach the control of the velocity of the hydrogen gas.

In the preferred embodiment, practical apparatus adapting the hydrogen generator to a combustion engine is described. The apparatus linearly controls the hydrogen gas flow to a mixing chamber mixing with a controlled amount of non-combustible gas oxygen, hence, the reduction in the hydrogen gas velocity. The reduction in the hydrogen gas velocity makes the use of hydrogen as safe as other fuels.

In more practical terms the ordinary internal combustion engine of any size or type of fuel, is retrofitted to be operable with only water as a fuel source. Hydrogen gas is generated from the water without the use of chemicals or metals and at a very low voltage. The burning velocity of the hydrogen gas has been reduced to that of conventional fuels. Finally, every component or step in the process has one or more safety valves or features thereby making the hydrogen gas system safer than that of conventional cars.

In the above description the terms ‘non-volatile’ and ‘non-combustible’ were used. It is to be understood they are intended to be the same; that is, simply, gas which will not burn.

Again, the term ‘storage’ has been used, primarily with respect to the hydrogen storage area 7. It is not intended that the term ‘storage’ be taken literally - in fact, it is not storage, but a temporary holding area. With respect to area 7, this area retains a sufficient amount of hydrogen for immediate start-up.

Other terms, features, apparatus, and the such have been described with reference to a preferred embodiment. It is to be understood modifications and alternatives can be had without departing from the spirit and scope of the invention.

STANLEY MEYER

US Patent 4,421,474 December 1983 Inventor: Stanley A. Meyer

HYDROGEN GAS BURNER

Please note that this is a re-worded excerpt from this patent. It describes how to burn the hydrogen and oxygen gas mix produced by electrolysis of water. Normally, the flame produced is too hot for practical use other than cutting metal or welding. This patent shows a method of reducing the flame temperature to levels suitable for general use in boilers, stoves, heaters, etc.

ABSTRACT

A hydrogen gas burner for the mixture of hydrogen gas with ambient air and non-combustible gasses. The mixture of gasses when ignited provides a flame of extremely high, but controlled intensity and temperature.

The structure comprises a housing and a hydrogen gas inlet directed to a combustion chamber positioned within the housing. Air intake ports are provided for adding ambient air to the combustion chamber for ignition of the hydrogen gas by an ignitor therein. At the other end of the housing there is positioned adjacent to the outlet of the burner (flame) a barrier/heating element. The heating element uniformly disperses the flame and in turn absorbs the heat. The opposite side to the flame, the heating element uniformly disperses the extremely hot air. A non-combustible gas trap adjacent to the heating element captures a small portion of the non-combustible gas (burned air). A return line from the trap returns the captured non-combustible gas in a controlled ratio to the burning chamber for mixture with the hydrogen gas and the ambient air.

CROSS REFERENCE

The hydrogen/oxygen generator utilised in the present invention is that disclosed and claimed in my co-pending patent application, Serial. No.: 302,807, filed: Sept. 16, 1981, for: HYDROGEN GENERATOR SYSTEM. In that process for separating hydrogen and oxygen atoms from water having impurities, the water is passed between two plates of similar non-oxidising metal. No electrolyte is added to the water. The one plate has placed thereon a positive potential and the other a negative potential from a very low amperage direct-current power source. The sub-atomic action of the direct current voltage on the non-electrolytic water causes the hydrogen and oxygen atoms to be separated--and similarly other gasses entrapped in the water such as nitrogen. The contaminants in the water that are not released are forced to disassociate themselves and may be collected or utilised and disposed of in a known manner.

The direct current acts as a static force on the water molecules; whereas the non-regulated rippling direct current acts as a dynamic force. Pulsating the direct current further enhances the release of the hydrogen and oxygen atoms from the water molecules.

In my co-pending patent application, Serial. No. 262,744, filed: May 11, 1981, for: HYDROGEN AERATION PROCESSOR, there is disclosed and claimed the utilisation of the hydrogen/oxygen gas generator. In that system, the burn rate of the hydrogen gas is controlled by the controlled addition of non-combustible gasses to the mixture of hydrogen and oxygen gasses.

SUMMARY OF INVENTION

The present invention is for a hydrogen gas burner and comprises a combustion chamber for the mixture of hydrogen gas, ambient air, and non-combustible gasses. The mixture of gasses is ignited and burns at a retarded velocity rate and temperature from that of hydrogen gas, but at a higher temperature rate than other gasses.

The extremely narrow hydrogen gas mixture flame of very high temperature is restricted from the utilisation means by a heat absorbing barrier. The flame strikes the barrier which in turn disperses the flame and absorbs the heat therefrom and thereafter radiates the heat as extremely hot air into the utilisation means.

Positioned on the opposite side of the heat radiator/barrier is a hot air trap. A small portion of the radiated heat is captured and returned to the combustion chamber as non-combustible gasses. Valve means in the return line regulates the return of the non-combustible gas in a controlled amount to control the mixture.

The present invention is principally intended for use with the hydrogen generator of my co-pending patent application, supra; but it is not to be so limited and may be utilised with any other source of hydrogen gas.

OBJECTS

It is accordingly a principal object of the present application to provide a hydrogen gas burner that has a temperature controlled flame and a heat radiator/barrier.

Another object of the present invention is to provide a hydrogen gas burner that is capable of utilising the heat from a confined high temperature flame.

Another object of the present invention is to provide a hydrogen gas burner that is retarded from that of hydrogen gas, but above that of other gasses.

Another object of the present invention is to provide a hydrogen gas burner that utilises the exhaust air as non-combustible gas for mixture with the hydrogen gas.

Another object of the present invention is to provide a hydrogen gas burner that is simple but rugged and most importantly safe for all intended purposes.

Other objects and features of the present invention will become apparent from the following detailed description when taken in conjunction with the drawings in which:

BRIEF DESCRIPTION OF THE DRAWINGS

Fig.1 is an overall cross-sectional view of the present invention in its most preferred embodiment.

Fig. 1

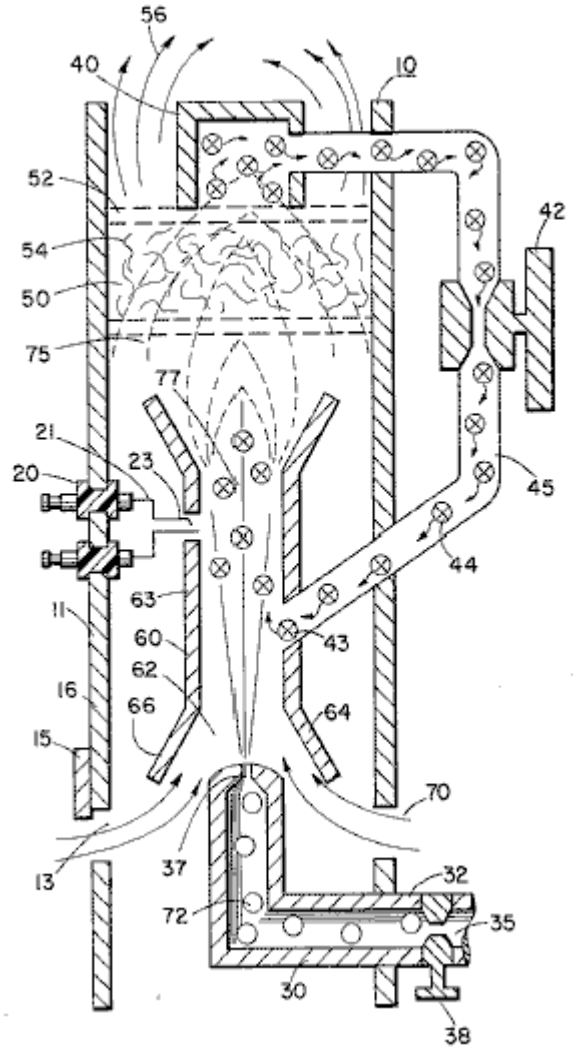

Fig.2 is a graphical illustration of the burning of various standard fuels with that of hydrogen velocities.

Fig. 2

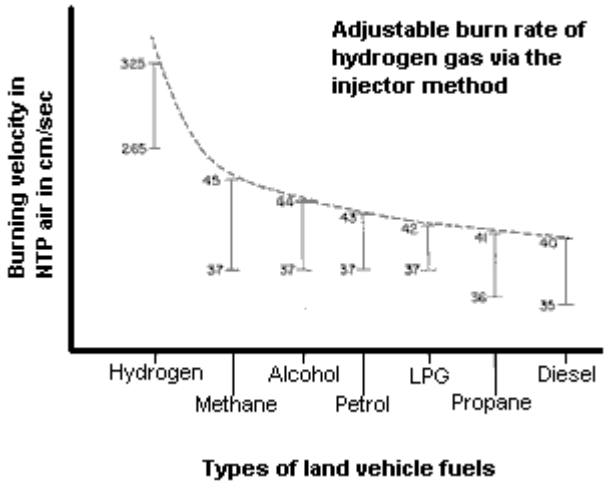

DETAILED DESCRIPTION OF INVENTION

Fig. 1

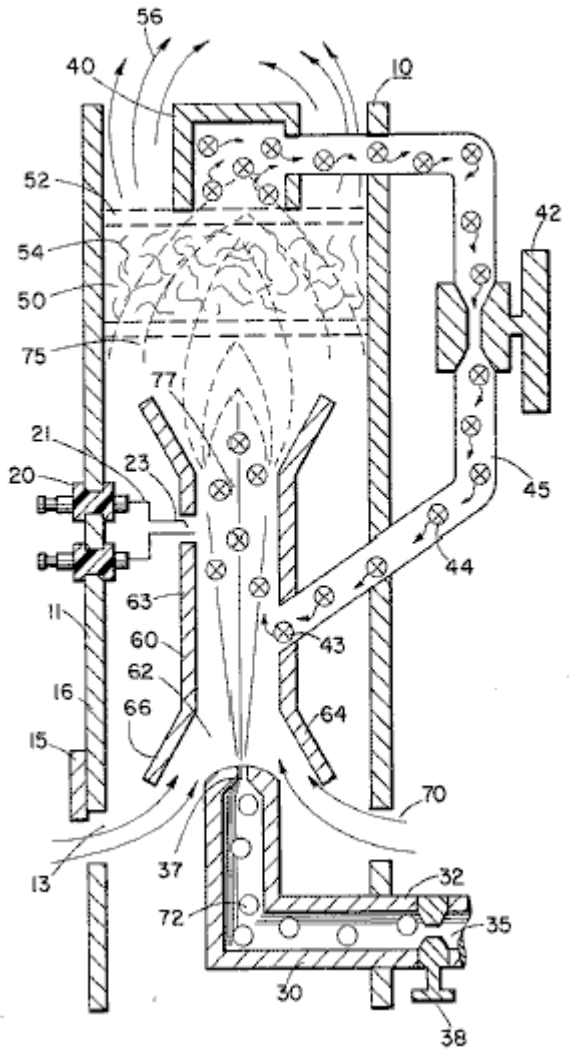

With particular reference **Fig.1** there is illustrated in a schematic cross-section the principals of the present invention. The structure of the preferred embodiment comprises a housing **10**, having an igniter **20** extending through the wall **11** thereof. A combustion chamber **60** positioned within the housing **10** has a first open end **62**. A hydrogen gas **72** inlet **30** directs hydrogen gas via port **37** from a source **35** to the inlet **62** of the combustion chamber **68**. Also directed to the same inlet **62**, and assisted by flanges **64** and **66**, is ambient air **70** entering through ports **13** in the housing **10**.

Adjacent the opposite end of the combustion chamber **60** the gas mixture **75** is ignited by the ignitor **20** to produce flame **77**. The velocity of the flame **77** causes it to strike and penetrate the barrier/radiator **50**. The barrier **50** is of a material, such as metallic mesh or ceramic material, to disperse therein the flame and in turn become saturated with heat. The flame **77** is of a size sufficient to be dispersed throughout the barrier **50**, but yet, not penetrate through the barrier **50**.

Radiated from the surface **52** of the barrier **50** is superheated air **56** (gasses) to be passed on to a utilisation device. Adjacent to surface **52** of barrier/radiator **50** is a hot air trap **40** with closed loop line **45** returning non-combustible gas **44** to the combustion chamber **60**. Control valve **42** is intermediate the line **45**.

In operation of the preferred embodiment hydrogen gas, **72**, emitted from the nozzle **37** is directed to the combustion chamber **60**. The flanges **64** and **66** on the open end of housing **63** of the combustion chamber **60** enlarges the open end of **62**. In the enlargement ambient air from the opening **13** in the housing **10** is also directed to the combustion chamber **60**.

The ambient air and hydrogen traverses the opening **43** and further mixes with the non-combustible gas **44** from the closed loop line **45** with the hot air trap **40**. The mixture of hydrogen gas **72**, ambient air **70**, and non-combustible gas **44**, is ignited by the ignitor **20** having electrical electrodes **21** and **23**. Upon ignition flame **77** ensues. The mixture is controlled with each of three gasses. That is, the line **32** from the hydrogen source **35** has a valve **38** therein for controlling the amount of hydrogen **72** emitted from the nozzle **37**. The opening **13** has a

plate adjustment **15** for controlling the amount of ambient air **60** directed to the combustion chamber **60**, and the closed-loop line has valve **42**, as aforesaid, for controlling the amount of non-combustible gasses in the mixture.

It can be appreciated that the temperature of the flame **77** and the velocity of the flame **77** is a function of the percentage of the various gasses in the mixture. In a practical embodiment, the flame **70** temperature and velocity was substantially retarded from that of a hydrogen flame per se; but yet, much greater than the temperature and velocity of the flame from the gasses utilised in a conventional heating system.

To maintain a sufficient pressure for combustion of the hydrogen gas mixture with a minimum of pressure (for safety) and to limit blow-out, the nozzle **37** opening **39** is extremely small. As a consequence, if the hydrogen gas were burned directly from the nozzle **37**, the flame would be finite in diameter. Further, its velocity would be so great it is questionable whether a flame could be sustained. The mixing of ambient air and non-combustible gas does enlarge the flame size and reduce its velocity. However, to maintain a flame higher in temperature and velocity than the conventional gasses, the size and temperature of the flame is controlled by the mixture mentioned earlier.

Therefore, to utilise the flame **77** in a present day utilisation means, the flame is barred by the barrier **50**. The barrier **50** is of a material that can absorb safely the intense flame **77** and thereafter radiate heat from its entire surface **52**. The material **54** can be a ceramic, metallic mesh or other heat absorbing material known in the art. The radiated heat **56** is directed to the utilisation means.

As stated earlier, the mixture of gasses which are burned include non-combustible gasses. As indicated in the above-noted co-pending patent applications, an excellent source of non-combustible gasses is exhaust gasses. In this embodiment, the trap **50** entraps the hot air **74** and returns the same, through valve **42**, to the combustion chamber **60** as non-combustible gas.

With reference to **Fig.2** there is illustrated the burning velocity of various standard fuels. It can be seen the common type of fuel burns at a velocity substantially less than hydrogen gas. The ratio of hydrogen with non-combustible oxygen gasses is varied to obtain optimum burning velocity and temperature for the particular utilisation. Once this is attained, the ratio, under normal conditions, will not be altered. Other uses having different fuel burn temperature and velocity will be adjusted in ratio of hydrogen/oxygen to non-combustible gasses in the same manner as exemplified above.

Further, perhaps due to the hydrogen gas velocity, there will occur unburned gas at the flame **77** output. The barrier **50**, because of its material makeup will retard the movement and trap the unburned hydrogen gas. As the superheated air **77** is dispersed within the material **54**, the unburned hydrogen gas is ignited and burns therein. In this way the barrier **50** performs somewhat in the nature of an after-burner.

US Patent 5,149,407 22nd September 1992 Inventor: Stanley Meyer

PROCESS AND APPARATUS FOR THE PRODUCTION OF FUEL GAS AND THE ENHANCED RELEASE OF THERMAL ENERGY FROM SUCH GAS

Please note that this is a re-worded excerpt from this patent. It describes in considerable detail, one of Stan's methods for splitting water into hydrogen and oxygen gasses and the subsequent methods for using those gasses.

ABSTRACT

Water molecules are broken down into hydrogen and oxygen gas atoms in a capacitive cell by a polarisation and resonance process dependent on the dielectric properties of water and water molecules. The gas atoms are then ionised or otherwise energised and thermally combusted to release a degree of energy greater than that of combustion of the gas in air.

OBJECTS OF THE INVENTION

A first object of the invention is to provide a fuel cell and a process in which molecules of water are broken down into hydrogen and oxygen gasses, and a fuel gas mixture comprised of hydrogen, oxygen and other gasses formerly dissolved in the water, is produced. A further object of the invention is to realise significant energy-yield from a fuel gas derived from water molecules. Molecules of water are broken down into hydrogen and oxygen gasses. Electrically charged hydrogen and oxygen ions of opposite electrical polarity are activated by electromagnetic wave energy and exposed to a high temperature thermal zone. Significant amounts of thermal energy with explosive force beyond the gas burning stage are released.

An explosive thermal energy under a controlled state is produced. The process and apparatus provide a heat energy source useful for power generation, aircraft rocket engines or space stations.

BRIEF DESCRIPTION OF THE DRAWINGS

Figs.1A through **1F** are illustrations depicting the theoretical bases for phenomena encountered during operation of the fuel gas production stage of the invention.

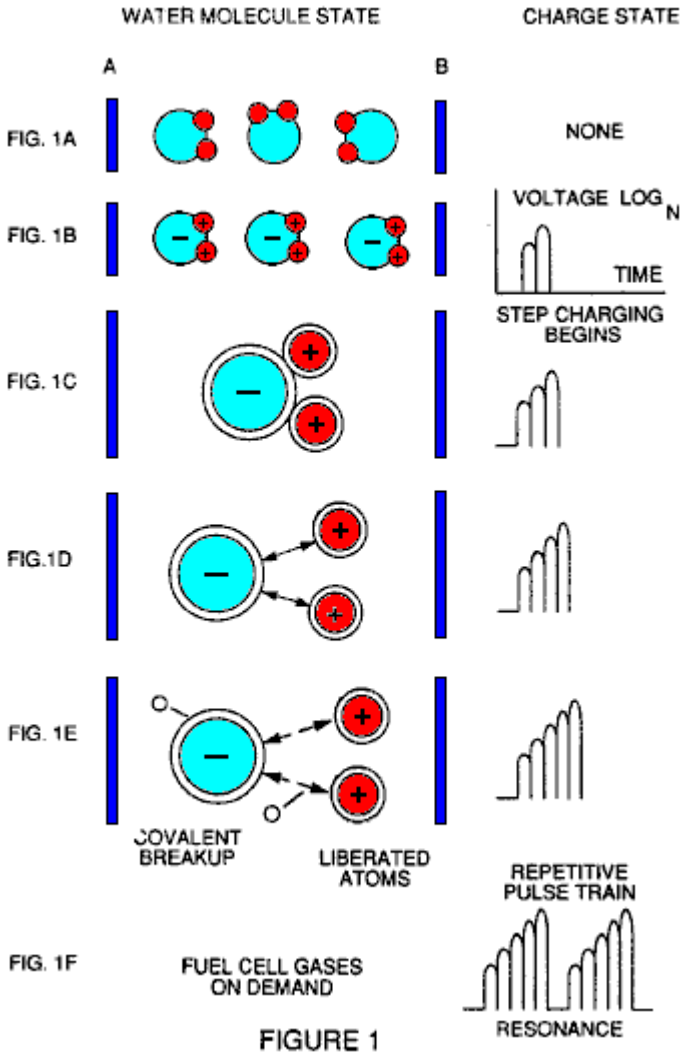

FIGURE 1

Fig.2 illustrates a circuit which is useful in the fuel gas generation process.

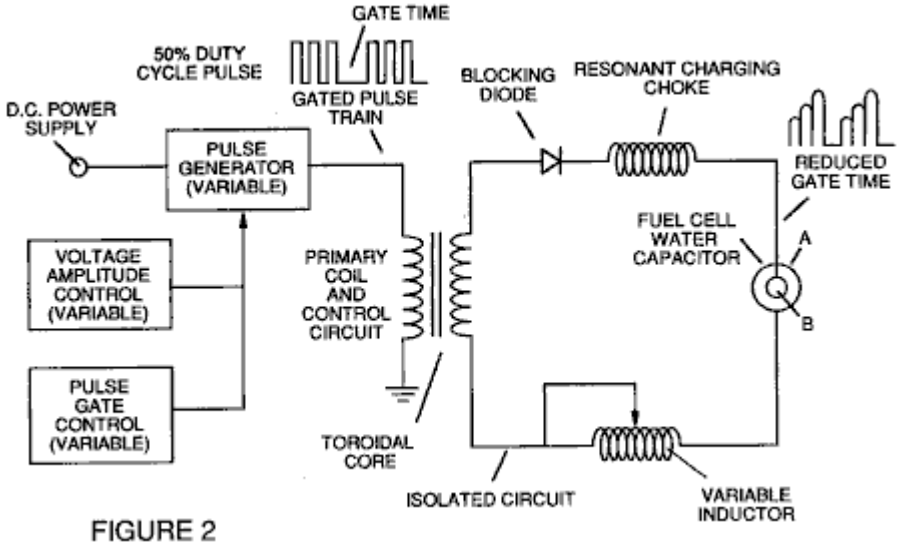

FIGURE 2

Fig.3 shows a perspective of a “water capacitor” element used in the fuel cell circuit.

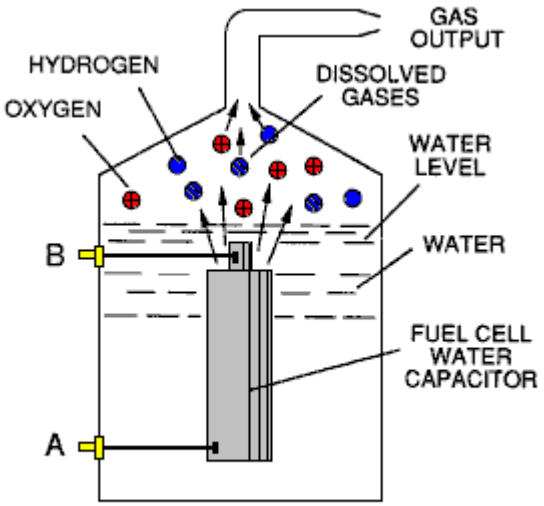

FIGURE 3

Fig.4 illustrates a staged arrangement of apparatus useful in the process, beginning with a water inlet and culminating in the production of thermal explosive energy.

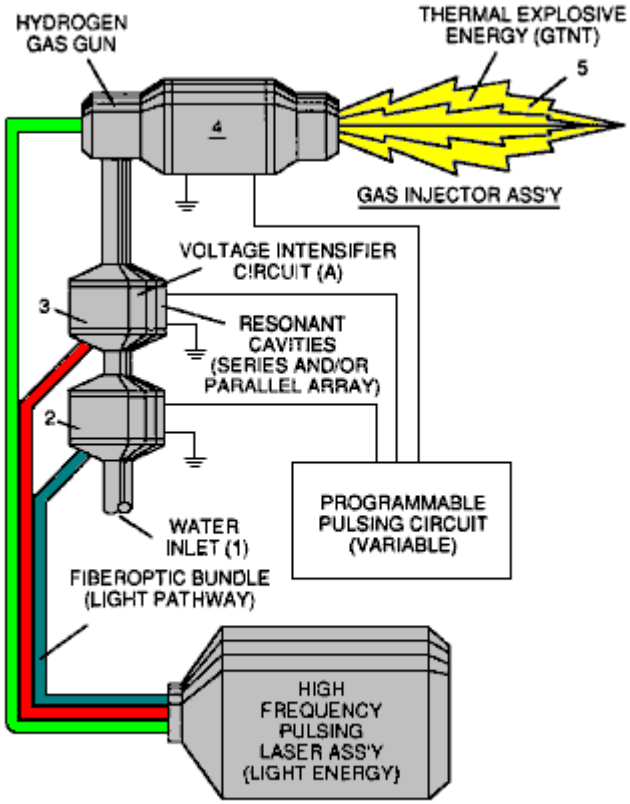

FIGURE 4

Fig.5A shows a cross-section of a circular gas resonant cavity used in the final stage assembly of **Fig.4**

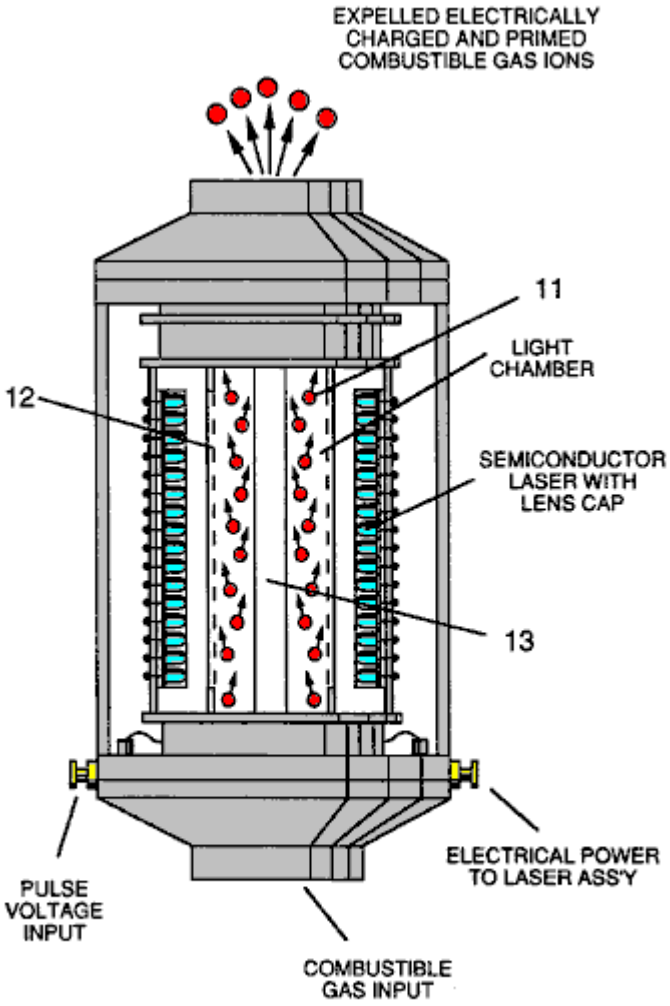

FIGURE 5A

Fig.5B shows an alternative final stage injection system useful in the apparatus of **Fig.4**

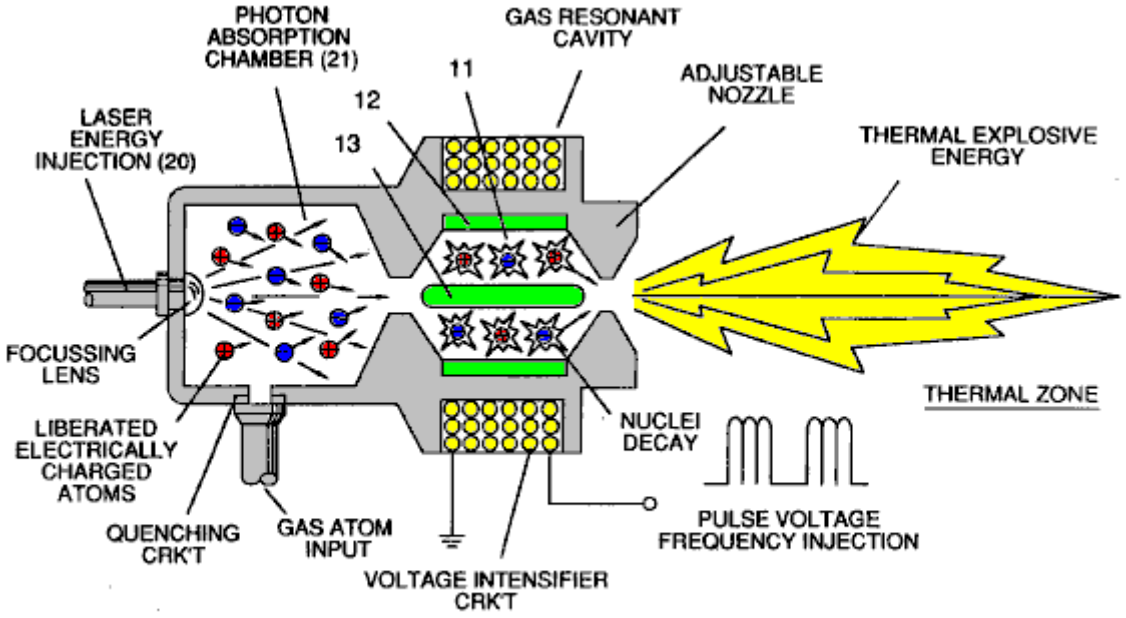

FIGURE 5B

Fig.5C shows an optical thermal lens assembly for use with either final stage of **Fig.5A** or **Fig.5B**.

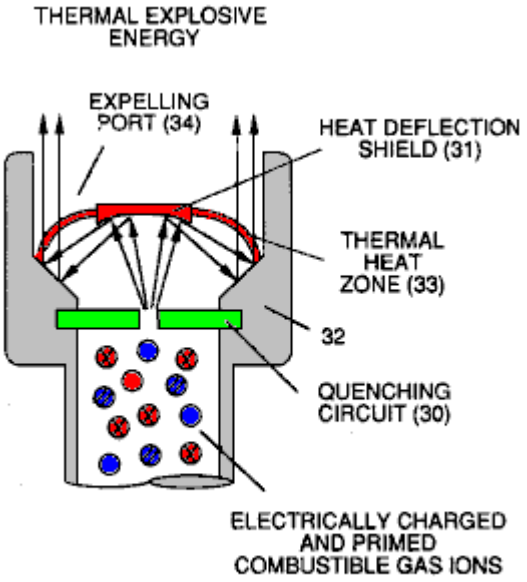

FIGURE 5C

Figs.6A, 6B, 6C and **6D** are illustrations depicting various theoretical bases for atomic phenomena expected to occur during operation of this invention.

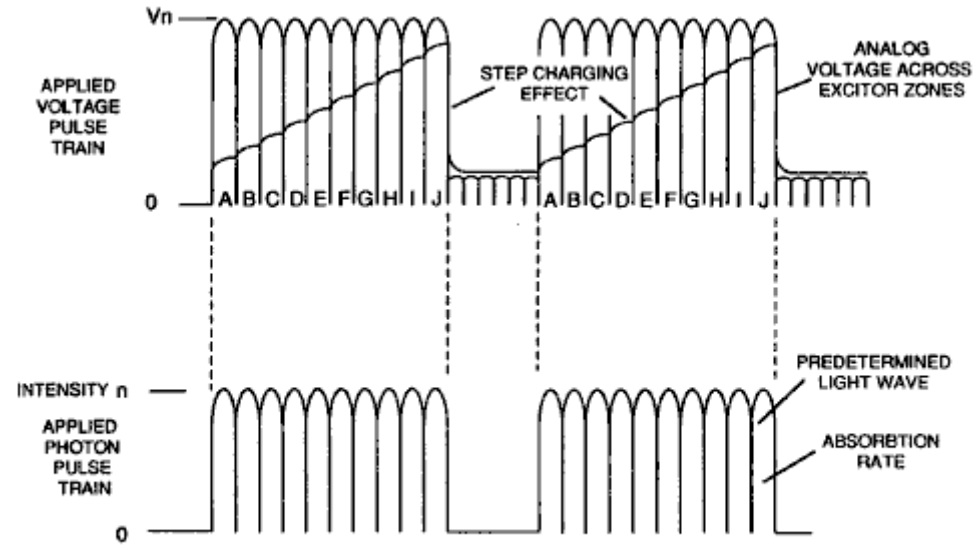

FIGURE 6A

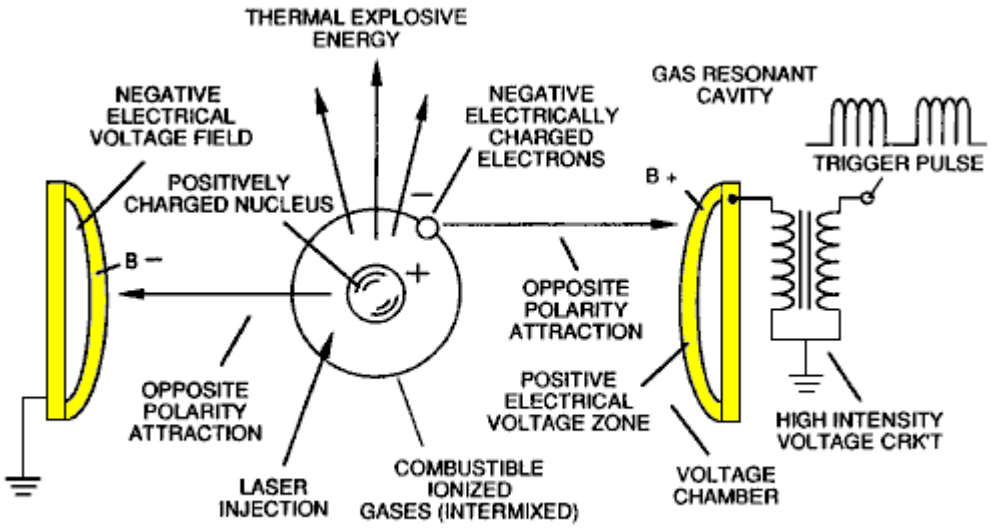

FIGURE 6B

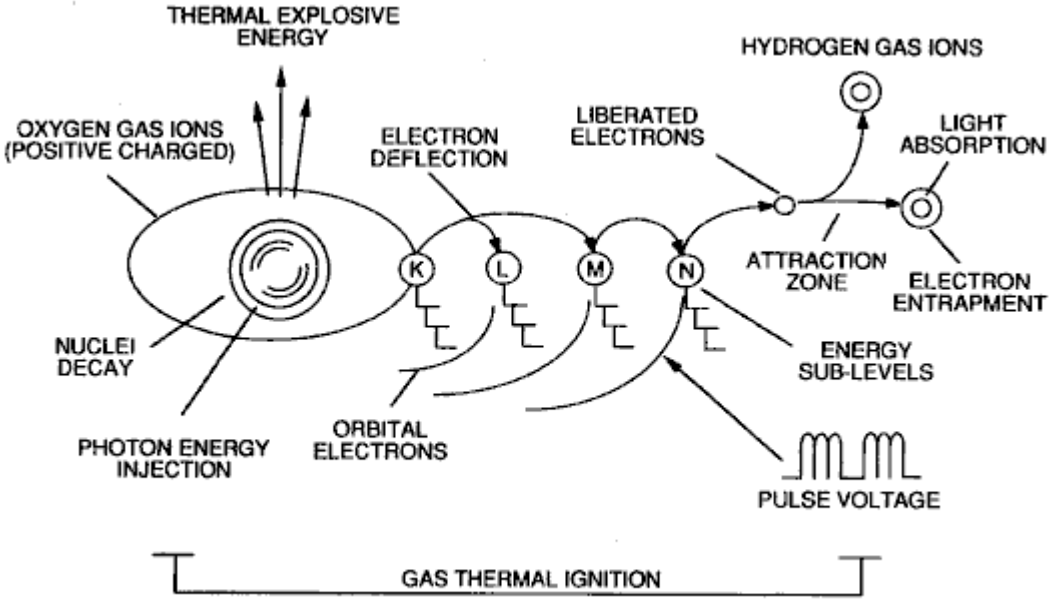

FIGURE 6C

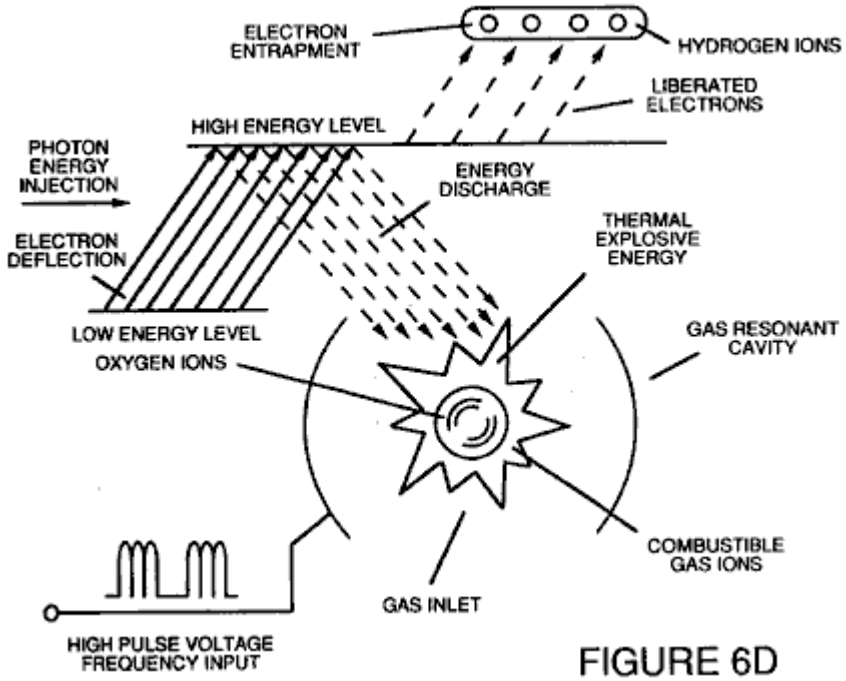

FIGURE 6D

Fig.7 is an electrical schematic of the voltage source for the gas resonant cavity.

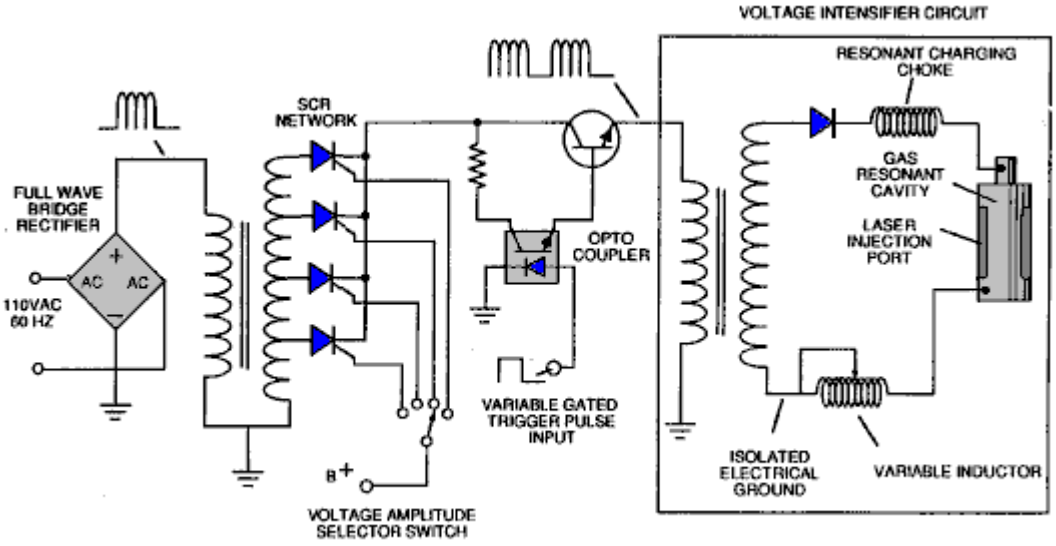

FIGURE 7

Figs.8A and **8B** respectively, show (A) an electron extractor grid used in the injector assemblies of **Fig.5A** and **Fig.5B**, and (B) the electronic control circuit for the extractor grid.

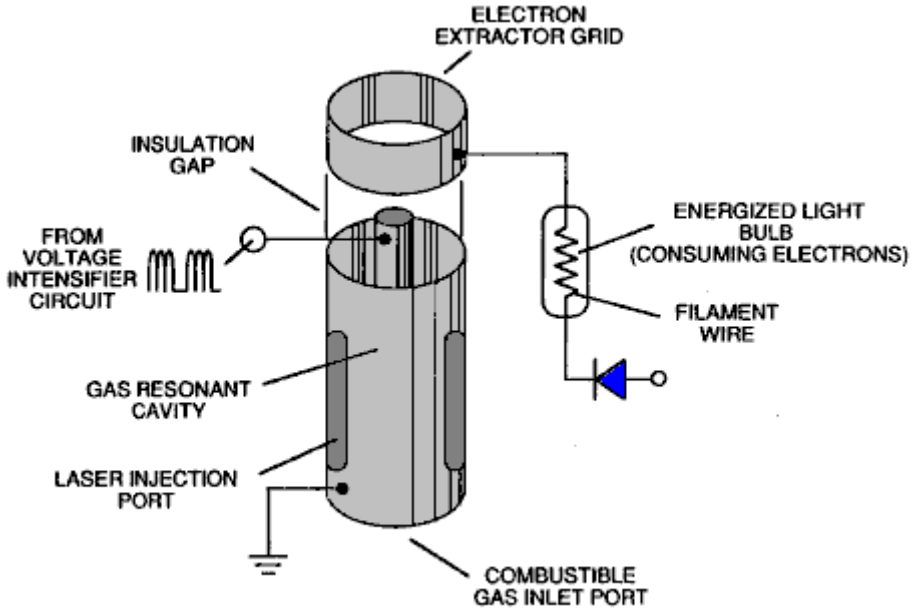

FIGURE 8A

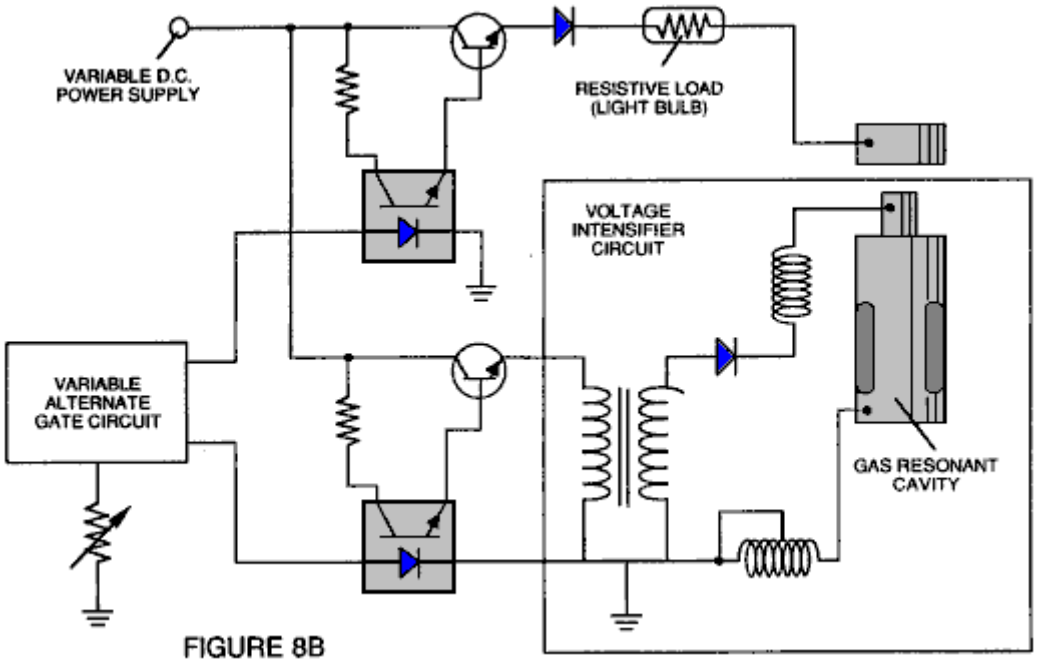

FIGURE 8B

Fig.9 shows an alternative electrical circuit useful in providing a pulsating waveform to the apparatus.

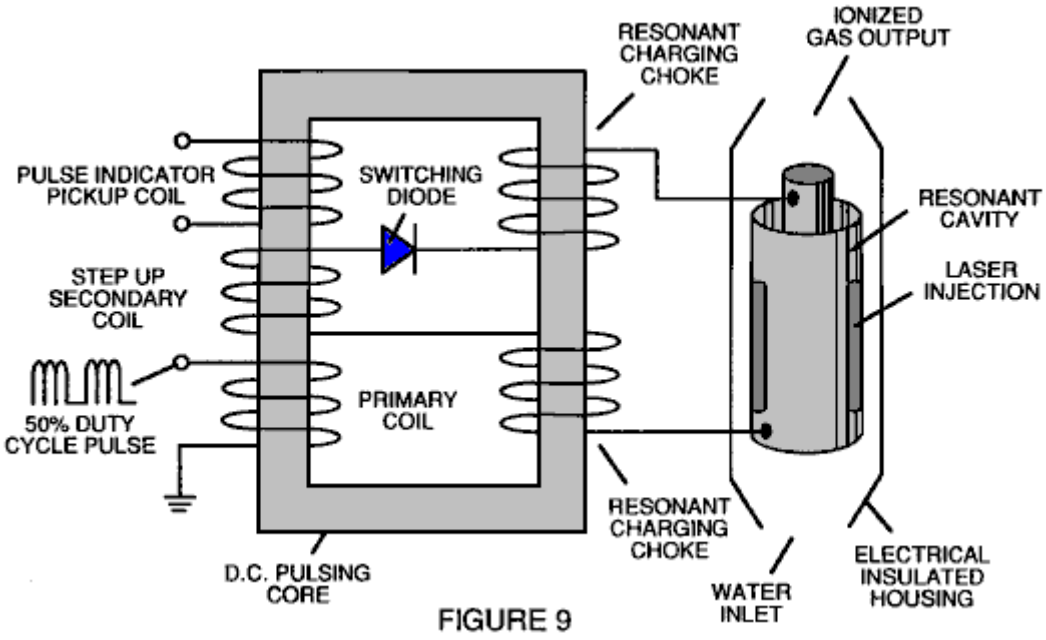

FIGURE 9

TABLE 1: PROCESS STEPS LEADING TO IGNITION

Relative State of Water Molecule and/or Hydrogen/Oxygen/Other Atoms	Stage
Random (ambient state) alignment of polar fields, polarisation of molecules. Molecular elongation. Atom liberation by breakdown of covalent bond	1st Stage: Water to Gas
Release of gasses, Liquid to gas ionisation, Electrical charging effect, Particle Impact	2nd Stage: Gas Ionisation
Electromagnetic Wave, Laser or photon injection, Electron extraction, Atomic destabilisation	3rd Stage: Priming
Thermal Ignition	Final Stage: Ignition

DESCRIPTION OF THE PREFERRED EMBODIMENT

A fuel gas is produced by a hydrogen fracturing process which follows the sequence of steps shown in Table 1. Beginning with water molecules, the molecule is subjected to successively increasing electrical wave energy and thermal forces. In the succession of forces, randomly orientated water molecules are aligned with respect to molecular polar orientation and themselves polarised and "elongated" by the application of an electric potential, to the extent that the co-valent bonding of the water molecules is so weakened that the atoms disassociate and the molecule breaks down into hydrogen and oxygen elemental components. Next, the released atomic gasses are ionised and electrically charged in a vessel while being subjected to a further energy source which promotes inter-particle impact in the gas at an increased overall energy level. Finally, the atomic particles in the excited gas, having achieved successively higher energy levels, are subjected to a laser or electromagnetic wave energy source which produces atomic destabilisation and the final release of thermal explosive energy.

Engineering design parameters based on known theoretical principles of atomic physics, determine the incremental levels of electrical and wave energy input required to produce resonance in each stage of the system. Instead of a dampening effect, a resonant energisation of the molecule, atom or ion provides a compounding energy interaction resulting in the final energy release.

In brief, in the first stage, a gas mixture including hydrogen, oxygen and other gasses formerly dissolved in the water, is obtained from water. In general, the method used in the first stage consists of:

(A) Providing a capacitor, in which the water is included as a dielectric liquid between capacitor plates, in a resonant charging choke circuit, which includes an inductor in series with the capacitor.
(B) Subjecting the capacitor to a pulsating, unipolar electric voltage field in which the polarity does not pass beyond an arbitrary ground, whereby the water molecules within the capacitor are subjected to a charge of the same polarity, and the water molecules are distended by the electrical polar forces.
(C) Further subjecting the water in the capacitor to the pulsating electric field to achieve a pulse frequency which induces a resonance within the water molecule.
(D) Continuing the application of the pulsing frequency to the capacitor cell after resonance occurs so that the energy level within the molecule is increased in cascading incremental steps in proportion to the number of pulses.
(E) Maintaining the charge of the capacitor during the application of the pulsating field, whereby the co-valent electrical bonding of the hydrogen and oxygen atoms within the water molecules is destabilised to such a degree that the force of the electrical field within the molecule exceeds the bonding force of the molecule, causing the molecule to break apart into the elemental gasses of hydrogen and oxygen.
(F) Collecting the hydrogen and oxygen gasses, along with any other gasses formerly dissolved in the water, and discharging the collected gasses as a fuel gas mixture.

The water molecules are subjected to increasing electrical forces. In an ambient state, randomly orientated water molecules are aligned with respect to a molecular polar orientation. Next, they themselves are polarised and "elongated" by the application of an electrical potential to the extent that co-valent bonding of the water molecules is so weakened that the atoms disassociate and the molecule breaks down into hydrogen and oxygen elemental components. In this process, the point of optimum gas release is reached when the circuit is at resonant frequency. Water in the cell is subjected to a pulsating, polar electric field produced by the electrical circuit, whereby the water molecules are distended by the electrical force on the plates of the capacitor. The polar pulsating frequency applied is such that the pulsating electric field induces a resonance in the molecules. A cascade effect occurs, and the overall energy of specific water molecules is increased in cascading incremental steps. The hydrogen and oxygen are released when the resonant energy exceeds the co-valent bonding force of the water molecules.

A preferred construction material for the capacitor plates is stainless steel T-304 which does not react chemically with water, hydrogen or oxygen. An electrically conductive material which is inert in the fluid environment, is a desirable material of construction for the electric field plates of the "water capacitor" employed in the circuit.

Once triggered, the gas output is controllable by the attenuation of operational parameters. Thus, once the frequency of resonance is identified, by varying the applied pulse voltage to the water fuel cell assembly, gas output is varied. By varying the pulse shape, pulse amplitude or pulse train sequence, the gas output can be varied. Attenuation of the voltage field's mark/space ratio of OFF/ON periods also affects the rate of gas production.

The overall apparatus thus includes and electrical circuit in which a water capacitor is an element. The water capacitor has a known dielectric property. The fuel gasses are obtained from the water by the disassociation of the water molecules. The water molecules are split into component atomic elements by a voltage stimulation process called the 'electrical Polarisation process' which also releases dissolved gasses trapped in the water.

From the outline of physical phenomena associated with the first stage of the process described in Table 1, the theoretical basis of the invention considers the respective states of molecules, gasses and ions derived from liquid water. Before voltage stimulation, water molecules are randomly dispersed throughout water in a container.

When a unipolar voltage pulse train such as that shown in **Figs.1B** through **1F** is applied to positive and negative capacitor plates, and increasing voltage potential is induced in the molecules in a linear, step-like charging effect. The electrical field of the particles within a volume of water including the electrical field plates, increases from a low energy state to a high energy state in a step manner following each pulse train as illustrated figuratively in **Figs.1A** through **1F**. The increasing voltage potential is always positive in direct relationship to negative ground potential during each pulse. The voltage polarity on the plates which create the voltage fields remains constant although the voltage charge increases. Positive and negative voltage "zones" are thus formed simultaneously in the electrical field of the capacitor plates.

In the first stage of the process described in Table 1, because the water molecule naturally exhibits opposite electrical fields in a relatively polar configuration (the two hydrogen atoms have a positive charge while the oxygen atom has a negative charge), the voltage pulse causes the water molecules which were initially orientated in random directions, to spin and align themselves with the electrical field applied to the cell. The positively charged hydrogen atoms are attracted to the negative field while the negatively charged oxygen atoms, of the same water molecule, are attracted to the positive voltage field. Even a slight potential difference between the plates of a containment chamber capacitor will initiate the alignment of each water molecule within the cell.

When the voltage applied to the plates causes the water molecules to align themselves, then the pulsing causes the voltage field intensity to be increased in accordance with **Fig.1B**. As further molecular alignment occurs, molecular movement is hindered. Because the positively charged hydrogen atoms of the aligned molecules are attracted in a direction opposite to the negatively charged oxygen atoms, a polar charge alignment or distribution occurs within the molecules between the voltage zones as shown in **Fig.1B**, and as the energy level of the atoms, subjected to resonant pulsing, increases, the stationary water molecules become elongated as shown in **Figs.1C** and **1D**. Electrically charged nuceli and electrons are attracted towards opposite electrically charged voltage zones - disrupting the mass and charge equilibrium of the water molecule.

As the water molecule is further exposed to an increasing potential difference resulting from the step charging of the capacitor, the electrical force of attraction of the atoms within the molecule to the capacitor plates of the chamber also increases in strength. As a result, the co-valent bonding between the atoms of the molecule is weakened and ultimately, terminated. The negatively charged electron is attracted toward the positively charged hydrogen atoms, while at the same time, the negatively charged oxygen atoms repel electrons.

In a more specific explanation of the "sub-atomic action which occurs in the water cell, it is known that natural water is a liquid which has a dielectric constant of 78.54 at 20 degrees Centigrade and 1 atmosphere of pressure [Handbook of Chemistry and Physics, Section E-50].

When a volume of water is isolated and electrically conductive plates that are chemically inert in water and which are separated by a distance, are immersed in the water, a capacitor is formed, having a capacitance determined by the surface area of the plates, the distance of their separation and the dielectric constant of the water.

When water molecules are exposed to voltage at a restricted current, water takes on an electrical charge. By the laws of electrical attraction, molecules align according to positive and negative polarity fields of the molecule and the alignment field. The plates of a capacitor constitute such an alignment field when a voltage is applied across them.

When a charge is applied to a capacitor, the electrical charge of the capacitor equals the applied voltage charge. In a water capacitor, the dielectric property of water resists the flow of current in the circuit, and the water molecule itself, because it has polarity fields formed by the relationship of hydrogen and oxygen in the co-valent bond, and an intrinsic dielectric property, becomes part of the electrical circuit, analogous to a "microcapacitor" within the capacitor defined by the plates.

In the Example of a fuel cell circuit of **Fig.2**, a water capacitor is included. The step-up coil is formed on a conventional torroidal core formed of a compressed ferromagnetic powered material that will not itself become permanently magnetised, such as the trademarked "Ferramic 06# 'Permag'" powder as described in *Siemens Ferrites Catalogue*, CG-2000-002-121, (Cleveland, Ohio) No. F626-1205. The core is 1.50 inch in diameter and 0.25 inch in thickness. A primary coil of 200 turns of 24 AWG gauge copper wire is provided and a coil of 600 turns of 36 AWG gauge wire comprises the secondary winding. Other primary/secondary coil winding ratios may be conveniently determined.

An alternate coil arrangement using a conventional M27 iron transformer core is shown in **Fig.9**. The coil wrap is always in one direction only.

In the circuit of **Fig.2**, the diode is a 1N1198 diode which acts as a blocking diode and an electric switch which allows current flow in one direction only. Thus, the capacitor is never subjected to a pulse of reverse polarity.

The primary coil of the torroid is subject to a 50% duty-cycle pulse. The torroidal pulsing coil provides a voltage step-up from the pulse generator in excess of five times, although the relative amount of step-up is determined by pre-selected criteria for a particular application. As the stepped-up pulse enters the first inductor (formed of 100 turns of 24 gauge wire, 1 inch in diameter), an electromagnetic field is formed around the inductor. Voltage is switched off when the pulse ends, and the field collapses and produces another pulse of the same polarity; i.e. another positive pulse is formed where the 50% duty-cycle was terminated. Thus, a double pulse frequency is produced; however, in a pulse train of unipolar pulses, there is a brief time when pulses are not present.

By being so subjected to electrical pulses in the circuit of **Fig.2**, the water between the capacitor plates takes on an electrical charge which is increased by a step-charging phenomenon occurring in the water capacitor.. Voltage continually increases (to about 1000 volts and more) and the water molecules start to elongate.

The pulse train is then switched off; the voltage across the water capacitor drops to the amount of charge that the water molecules have taken on, i.e. voltage is maintained across the charged capacitor. The pulse train is then applied again.

Because a voltage potential applied to a capacitor can perform work, the higher the voltage potential, the more work is performed by a given capacitor. In an optimum capacitor which is wholly non-conductive, zero current flow will occur across the capacitor. Thus, in view of an idealised capacitor circuit, the object of the water capacitor circuit is to prevent electron flow through the circuit, i.e. such as occurs by electron flow or leakage through a resistive element that produces heat. Electrical leakage in water will occur, however, because of some residual conductivity and impurities, or ions that may otherwise be present in the water. thus, the water capacitor is preferably chemically inert. An electrolyte is not added to the water.

In the isolated water bath, the water molecule takes on charge, and the charge increases. The object of the process is to switch off the co-valent bonding of the water molecule and interrupt the sub-atomic force that binds the hydrogen and oxygen atoms together to form a molecule, thus causing the hydrogen and oxygen to separate.

Because an electron will only occupy a certain electron shell, the voltage applied to the capacitor affects the electrical forces inherent in the co-valent bond. As a result of the charge applied by the plates, the applied force becomes greater than the force of the co-valent bonds between the atoms of the water molecule, and the water molecule becomes elongated. When this happens, the time share ratio of the electrons between the atoms and the electron shells, is modified.

In the process, electrons are extracted from the water bath; electrons are not consumed nor are electrons introduced into the water bath by the circuit, as electrons would be during conventional electrolysis. Nevertheless, a leakage current through the water may occur. Those hydrogen atoms missing electrons become neutralised and atoms are liberated from the water. The charged atoms and electrons are attracted to opposite polarity voltage zones created between the capacitor plates. The electrons formerly shared by atoms in the water co-valent bond are re-allocated so that neutral elemental gasses are liberated.

In the process, the electrical resonance may be reached at all levels of voltage potential. The overall circuit is characterised as a “resonant charging choke” circuit which is an inductor in series with a capacitor [*SAMS Modern Dictionary of Electronics*, 1984 p.859]. Such a resonant charging choke is on each side of the capacitor. In the circuit, the diode acts as a switch which allows the magnetic field produced in the inductor to collapse, thereby doubling the pulse frequency and preventing the capacitor from discharging. In this manner, a continuous voltage is produced across the capacitor plates in the water bath and the capacitor does not discharge. The water molecules are thus subjected to a continuously charged field until the breakdown of the co-valent bond occurs.

As noted initially, the capacitance depends on the dielectric properties of the water and the size and separation of the conductive elements forming the water capacitor.

Example 1

In an example of the circuit of **Fig.2** (in which other circuit element specifications are provided above), two concentric cylinders 4 inches long, formed the water capacitor of the fuel cell in the volume of water. The outside cylinder was o.75 in outside diameter; the inner cylinder was 0.5 inch in outside diameter. Spacing between the inside cylinder and the outside cylinder was 0.0625 inch (1.59 mm). Resonance in the circuit was achieved at a 26 volt pulse applied to the primary coil of the torroid at 10khz and a gas mixture of hydrogen, oxygen and dissolved gasses was given off. The additional gasses included nitrogen and argon from air dissolved in the water.

In achieving resonance in any circuit, as the pulse frequency is adjusted, the current flow is minimised and the voltage on the capacitor plates is maximised. Calculation of the resonant frequency of an overall circuit is determined by known means; different cavities have a different resonant frequency. The gas production rate is varied by the period of time between trains of pulses, pulse amplitude, capacitor plate size and plate separation.

The wiper arm on the second inductor tunes the circuit and allows for contaminants in the water so that the charge is always applied to the capacitor. The voltage applied , determines the rate of breakdown of the molecule into its atomic components. As water in the cell is consumed, it is replaced by any appropriate means or control system.

Thus, in the first stage, which is of itself independently useful, a fuel gas mixture is produced having, in general, the components of elemental hydrogen and oxygen and some additional atmospheric gasses. The fuel gas is itself combustible in a conventional manner.

After the first stage, the gas atoms become elongated during electron removal as the atoms are ionised. Laser or light wave energy of a predetermined frequency is injected into a containment vessel in a gas ionisation process. The light energy absorbed by voltage-stimulated gas nuclei, causes destabilisation of gas ions still further. The absorbed laser energy causes the gas nuclei to increase in energy state, which in turn, causes electron deflection to a higher orbital shell.

The electrically charged and laser-primed combustible gas ions from a gas resonant cavity, may be directed into a an optical thermal lens assembly for triggering. Before entry into the optimal thermal lens, electrons are stripped from the ions and the atom is destabilised. The destabilised gas ions which are electrically and mass unbalanced atoms having highly energised nuclei, are pressurised during spark ignition. The unbalanced, destabilised atomic components interact thermally; the energised and unstable hydrogen gas nuclei collide with highly energised and unstable oxygen gas nuclei, causing and producing thermal explosive energy beyond the gas burning stage. The ambient air gas components in the initial mixture aid the thermal explosive process under a controlled state.

In the process, the point of optimum energy yield is reached when the electron-deficient oxygen atoms (having less than a normal number of electrons) lock on to an capture a hydrogen atom electron, prior to, or during, thermal combustion of the hydrogen/oxygen mixture. Atomic decay results in the release of energy.

After the first stage, the gas mixture is subjected to a pulsating, polar electric field which causes the orbits of the electrons of the gas atoms to become distended . The pulsating electrical field is applied at a frequency which resonates with the electrons of the gas atoms. This results in the energy levels of the electrons increasing in cascading incremental steps.

Next, the gas atoms are ionised and subjected to electromagnetic wave energy of the correct frequency to induce further electron resonance in the ion, whereby the energy level of the electron is successively increased. Electrons are extracted from the resonating ions while they are in this increased energy state, and this destabilises the nuclear electron configuration of the ions. This gas mixture of destabilised ions is thermally ignited.

In the apparatus shown in **Fig.4**, water is introduced at inlet **1** into a first stage water fracturing module **2**, such as the water fuel cell described above, in which water molecules are broken down into hydrogen, oxygen and released gasses which were trapped in the water. These gasses may be introduced to a successive stage **3** or other number of like resonant cavities, which are arranged in either a series or parallel combined array. The successive energisation of the gas atoms, provides a cascading effect, successively increasing the voltage stimulation level of the released gasses as they pass sequentially through cavities **2**, **3**, etc. In a final stage, and injector system **4**, of a configuration of the type shown in **Fig.5A** or **Fig.5B**, receives energised atomic and gas particles where the particles are subjected to further energy input, electrical excitation and thermal stimulation, which produces thermal explosive energy **5**, which may be directed through a lens assembly of the type shown in **Fig.5C** to provide a controlled thermal energy output.

A single cell, or battery of cells such as shown in **Fig.3**, provides a fuel gas source for the stages following the first stage. The fuel gas is activated by electromagnetic waves, and electrically charged gas ions of hydrogen and oxygen (of opposite polarity) are expelled from the cascaded cells **2**, **3**, etc. shown in **Fig.4**. The circuit of **Fig.9** may be utilised as a source of ionising energy for the gasses. The effect of cascading, successively increases the voltage stimulation level of the released gasses, which are then directed to the final injector assembly **4**. In the injector assembly, gas ions are stimulated to an even greater energy level. The gasses are continually exposed to a pulsating laser or other electromagnetic wave energy source together with a high-intensity oscillating voltage field which occurs within the cell between electrodes or conductive plates of opposite electrical polarity. A preferred construction material for the plates is a stainless steel T-304 which is non-chemically reactive with water, hydrogen or oxygen. An electrically conductive material inserted in the fluid environment, is a desirable

material of construction for the electrical field producing plates, through which field, the stream of activated gas particles passes.

Gas ions of opposite electrical charges reach and maintain a critical energy level state. The gas ions have opposite electrical charges and are subjected to oscillating voltage fields of opposite polarity. They are also subjected to a pulsating electromagnetic wave energy source. Immediately after reaching critical energy, the excited gas ions are exposed to a high temperature thermal zone in the injection cell **4**, which causes the excited gas ions to undergo gas combustion. The gas ignition triggers atomic decay and releases thermal energy **5**, with explosive force.

Once triggered, the explosive thermal energy output is controllable by the attenuation of operational parameters. With reference to **Fig.6A**, for example, once the frequency of resonance is identified, by varying applied pulse voltage to the initial water fuel cell assemblies **2**, **3**, the ultimate explosive energy output is likewise varied. By varying the pulse shape and/or amplitude, or pulse train sequence of the electromagnetic wave energy source, final output is varied. Attenuation of the voltage field frequency in the form of OFF and ON pulses, likewise affects the output of the staged apparatus. Each control mechanism can be used separately, grouped in sections, or systematically arranged in a sequential manner.

A complete system in accordance with the present application thus includes:

1. A water fuel cell for providing a first fuel gas mixture consisting of at least a portion of hydrogen and oxygen gas.
2. An electrical circuit of the type shown in **Fig.7** providing a pulsating, polar electric field to the gas mixture as illustrated in **Fig.6A**, whereby electron orbits of the gas atoms are distended by being subjected to electrical polar forces, changing from the state shown conceptually in **Fig.6B** to that of **Fig.6C**, at a frequency such that the pulsating electric field induces a resonance with respect to electrons of the gas atoms. The energy level of the resonant electrons is thereby increased in cascading incremental steps.
3. A further electric field to ionise the gas atoms and
4. An electromagnetic wave energy source for subjecting the ionised gas atoms to wave energy of a predetermined frequency to induce further electron resonance in the ions, whereby the energy level of the electron is successively increased, as shown in **Fig.6D**.
5. An electron sink, which may be in the form of the grid element shown in **Fig.8A**, extracts further electrons from the resonating ions while such ions are in an increased energy state and destabilises the nuclear electron configuration of the ions. The “extraction” of electrons by the sink is co-ordinated with the pulsating electrical field of the resonant cavity produced by the circuit of **Fig.7**, by means of
6. An interconnected synchronisation circuit, such as shown in **Fig.8B**.
7. A nozzle, **10** in **Fig.5B**, or thermal lens assembly, **Fig.5C**, provides the means to direct the destabilised ions, and in which they are finally thermally ignited.

As previously noted, to reach and trigger the ultimate atomic decay of the fuel cell gasses at the final stage, sequential steps are taken. First, water molecules are slit into hydrogen and oxygen gasses by a voltage stimulation process. In the injector assembly, a laser produced coherent light wave is absorbed by the gasses. At this point, as shown in **Fig.6B**, the individual atoms are subjected to an electric field to begin an ionisation process. The laser energy is absorbed and causes gas atoms to lose electrons and form positively charged gas ions. The energised, positively charged hydrogen atoms now accept electrons liberated from the heavier gasses and attract other negatively charged gas ions as conceptually illustrated in **Fig.6C**. Positively and negatively charged gas ions are re-exposed to further pulsating energy sources to maintain random distribution of ionised gas particles.

The gas ions within the wave energy chamber are subjected to an oscillating high-intensity voltage field in a chamber **11** in **Fig.5A** and **Fig.5B** formed within electrodes **12** and **13** in **Fig.5A** and **Fig.5B** of opposite electrical polarity, to produce a resonant cavity. The gas ions reach a critical energy state at the point of resonance.

At this point, within the chamber, additional electrons are attracted to the positive electrode; while positively charged ions or atomic nuclei are attracted to the negative electrode. The positive and negative attraction forces are co-ordinated and act on the gas ions simultaneously; the attraction forces are non-reversible. The gas ions experience atomic component deflection approaching the point of electron separation. At this point electrons are extracted from the chamber by a grid system such as shown in **Fig.5A**. The extracted electrons are consumed and prevented from re-entering the chamber by a circuit such as shown in **Fig.8B**. The elongated gas ions are subjected to a thermal heat zone to cause gas ignition, releasing thermal energy with explosive force. During ionic gas combustion, highly energised and stimulated atoms and atom nuclei collide and explode during thermal excitation. The hydrogen fracturing process occurring, sustains and maintains a thermal zone, at a temperature in excess of normal oxygen/hydrogen combustion temperature, that is, in excess of 2,500 degrees Fahrenheit. To cause and maintain the atomic elongation depicted in **Fig.6C** before gas ignition, a voltage intensifier circuit such

as shown in **Fig.7** is utilised as a current-restricting voltage source to provide the excitation voltage applied to the resonant cavity. At the same time, the interconnected electron extractor circuit shown in **Fig.8B**, prevents the reintroduction of electrons back into the system. depending on calculated design parameters, a predetermined voltage and frequency range may be designed for any particular application or physical configuration of the apparatus.

In the operation of the assembly, the pulse train source for the gas resonant cavity shown at **2** and **3** in **Fig.4** may be derived from a circuit such as shown in Figs. **2**, **7** or **9**, and such cavity circuits may be in sequence to provide a cascading energy input. It is necessary in the final electron extraction, that the frequency with which electrons are removed from the system be sequenced and synchronised with the pulsing of the gas resonant cavity. In the circuit of **Fig.8B**, the co-ordination of synchronisation of the circuit with the circuit of **Fig.7** may be achieved by interconnecting point **"A"** of the gate circuit of **Fig.8B** to point **"A"** of the pulsing circuit of **Fig.7**.

The circuit shown in **Fig.9** enhances the voltage potential across the resonant charging choke coils during pulsing operations and restricts current flow by allowing an external electromagnetic pulsing field **F**, derived from the primary coil **A** being energised to traverse the coil windings **D** and **E** being energised by the incoming pulse train **Ha xxx Hn**, through switching diode **G**. The external pulse field **F**, and the incoming pulse train **Ha xxx Hn**, are sequentially the same, allowing resonant action to occur, restricting current flow while allowing voltage intensity to increase to stimulated the electrical polarisation process, the gas ionisation process and the electron extraction process. The voltage intensifier circuit of **Fig.9** prevents electrons from entering into those processes.

Together, the hydrogen injector assembly **4**, and the resonant cavity **2** and **3**, form a gas injector fuel cell which is compact, low in weight and whose design can be varied. For example, the hydrogen injector system is suited for cars and jet engines. Industrial applications require larger systems. For rocket engine applications, the hydrogen gas injector system is positioned at the top of each resonant cavity arranged in a parallel cluster array. If resonant cavities are sequentially combined in a parallel/series array, the hydrogen injection assembly is positioned after the exits of the resonant cavities have been combined.

From the outline of the physical phenomena associated with the process described in **Table 1**, the theoretical basis of the invention considers the respective states of molecules, gasses and ions derived from liquid water. Before voltage stimulation, water molecules are randomly dispersed throughout water within a container. When a unipolar voltage pulse train such as shown in **Fig.6A (53a xxx 53n)** is applied, an increasing voltage potential is induced in the molecules, gasses and/or ions in a linear, step-like charging effect. The electrical field of the particles within a chamber including the electrical field plates increases from a low-energy state (**A**) to a high-energy state (**J**) in a step manner, following each pulse train as illustrated in **Fig.6A**. The increasing voltage potential is always positive in direct relationship to negative ground potential during each pulse. The voltage polarity on the plates which create the voltage fields, remains constant. Positive and negative voltage "zones" are thus formed simultaneously.

In the first stage of the process described in **Table 1**, because the water molecule naturally exhibits opposite electric fields in a relatively polar configuration (the two hydrogen atoms are positively electrically charged relative to the negatively electrically charged oxygen atom), the voltage pulse causes initially randomly orientated water molecules in the liquid state to spin and orientate themselves with reference to the voltage fields applied.

When the potential difference applied causes the oriented water molecules to align themselves between the conductive plates, pulsing causes the voltage field intensity to be increased in accordance with **Fig.6A**. As further molecular alignment occurs, molecular movement is hindered. Because the positively charged hydrogen atoms are attracted in the opposite direction to the negatively charged oxygen atoms, a polar charge alignment or distribution occurs as shown in **Fig.6B**. As the energy level of the atoms subjected to resonant pulsing increases, the stationary water molecules become elongated as shown in **Fig.6C**. Electrically charged nuceli and electrons are attracted towards opposite voltage zones, disrupting the mass equilibrium of the water molecule.

In the first stage, as the water molecule is further exposed to a potential difference, the electrical force of attraction of the atoms to the chamber electrodes also increases in intensity. As a result, the co-valent bonding between the atoms is weakened and ultimately, terminated. The negatively charged electron is attracted towards the positively charged hydrogen atoms, while at the same time, the negatively charged oxygen atoms repel electrons.

Once the applied resonant energy caused by pulsation of the electrical field in the cavities reaches a threshold level, the disassociated water molecules, now in the form of liberated hydrogen, oxygen and ambient air gasses, begin to ionise and lose or gain electrons during the final stage in the injector assembly. Atom destabilisation occurs and the electrical and mass equilibrium of the atoms is disrupted. Again, the positive field produced within the chamber or cavity that the encompasses the gas stream, attracts negatively charged ions while the positively charged ions are attracted to the negative field. Atom stabilisation does not occur because the pulsing voltage

applied is repetitive without polarity change. A potential of approximately several thousand volts, triggers the ionisation state.

As the ionised particles accumulate within the chamber, the electrical charging effect is again an incremental stepping effect that produces an accumulative increased potential, while, at the same time, resonance occurs. The components of the atom begin to "vibrate" at a resonant frequency such that an atomic instability is created. As shown in **Fig.6D**, a high energy level is achieved, which then collapses, resulting in the release of thermal explosive energy. Particle impact occurs when liberated ions in a gas are subjected to further voltage. A longitudinal cross-section of a gas resonant cavity is shown in **Fig.5A**. To promote gas ionisation, electromagnetic wave energy such as a laser or photon energy source of a predetermined wavelength and pulse intensity is directed to, and absorbed by, the ions of the gas. In the device of **Fig.5A**, semiconductor optical lasers **20a - 20p, 20xxx** surround the gas flow path. In the device of **Fig.5B**, photo energy **20** is injected into a separate absorption chamber **21**. The incremental stimulation of nuclei to a more highly energised state by electromagnetic wave energy causes electron deflection to a higher orbital state. The pulse rate as well as intensity of the electromagnetic wave source is varied to match the absorption rate of ionised particles to produce the stepped incremental increase in energy. A single laser coupled by means of fibre optic light guides is an alternative to the plurality of lasers shown in **Fig.5B**. Continued exposure of the gas ions to different forms of wave energy during voltage stimulation, maintain individual atoms in a destabilised state and prevents atomic stabilisation.

The highly energised gas ions are thermally ignited when they pass from injector **4** and enter into and pass through a nozzle **10** in **Fig.5B**, or an optical thermal lens assembly as shown in **Fig.5C**. In **Fig.5C**, the combustible gas ions are expelled through and beyond a quenching circuit **30**, and reflected by lenses **31** and **32**, back and forth through a thermal heat zone **33**, prior to atomic breakdown and then exiting through a final port **34**. A quenching circuit is a restricted orifice through which the particle stream passes, such that flashback does not occur. The deflection shield or lens **31**, superheats beyond 3000 degrees Fahrenheit and the combustible gas ions passing through the exiting ports are regulated to allow a gas pressure to form inside the thermal zone. The energy yield is controlled by varying the applied voltage or pulse-train since the thermal-lens assembly is self-adjusting to the flow rate of the ionised and primed gasses. The combustible ionic gas mixture is composed of hydrogen, oxygen and ambient air gasses. The hydrogen gas provides the thermal explosive force, the oxygen atoms aid the gas thermal ignition, and the ambient air gasses retard the gas thermal ignition process to a controllable state.

As the combustible gas mixture is exposed to a voltage pulse train, the stepped increasing voltage potential causes the moving gas atoms to become ionised (losing or gaining electrons) and changes the electrical and mass equilibrium of the atoms. Gasses which do not undergo the gas ionisation process may accept the liberated electrons (electron entrapment) when exposed to light or photon stimulation. The electron extractor grid circuit shown in **Fig.8A** and **Fig.8B**, is applied to the assembly of **Fig.5A** or **Fig.5B**, and restricts electron replacement. The extractor grid **56**, is applied adjacent to electric field producing components **44** and **45**, within the resonant cavity. The gas ions incrementally reach a critical state which occurs after a high energy resonant state. At this point, the atoms no longer tolerate the missing electrons, the unbalanced electrical field and the energy stored in the nucleus. Immediate collapse of the system occurs and energy is released as the atoms decay into thermal explosive energy.

The repetitive application of a voltage pulse train (**A** through **J** of **Fig.6A**) incrementally achieves the critical state of the gas ions. As the gas atoms or ions (**1a xxx 1n**) shown in **Fig.6C**, become elongated during electron removal, electromagnetic wave energy of a predetermined frequency and intensity is injected. The wave energy absorbed by the stimulated gas nuclei and electrons, causes further destabilisation of the ionic gas. The absorbed energy from all sources, causes the gas nuclei to increase in energy state and induces the ejection of electrons from the nuclei.

To further stimulate the electron entrapment process beyond the atomic level (capturing the liberated electrons during the hydrogen fracturing process), the electron extractor grid (as shown in **Fig.8A**) is placed in spaced relationship to the gas resonant cavity structure shown in **Fig.5A**. The electron extractor grid is attached to an electrical circuit (such as that shown in **Fig.8B**) which allows electrons to flow to an electrical load **55**, when a positive electrical potential is placed on the opposite side of the electrical load. The electrical load may be a typical power-consuming device such as a light bulb or resistive heat-producing device. As the positive electrical potential is switched on, or pulse-applied, the negatively charged electrons liberated in the gas resonant cavity, are drawn away and enter into the resistive load where they are released as heat or light energy. The consuming electrical circuit may be connected directly to the gas resonant cavity positive electrical voltage zone. The incoming positive wave form applied to the resonant cavity voltage zone through a blocking diode, is synchronised with the pulse train applied to the gas resonant cavity by the circuit of **Fig.7** via an alternate gate circuit. As one pulse train is gated "ON", the other pulse train is switched "OFF". A blocking diode directs the electron flow to the electrical load, while resistive wire prevents voltage leakage during the pulse train "ON" time.

The electron extraction process is maintained during gas-flow change by varying the trigger pulse rate in relationship to the applied voltage. The electron extraction process also prevents spark-ignition of the combustible gasses travelling through the gas resonant cavity because electron build-up and potential sparking is prevented.

In an optical thermal lens assembly or thrust-nozzle, such as shown in **Fig.5C**, destabilised gas ions (electrically and mass unbalanced gas atoms having highly energised nuclei) can be pressurised during spark ignition. During thermal interaction, the highly energised and unstable hydrogen gas nuclei collide with the highly energised and unstable oxygen gas nuclei and produce thermal explosive energy beyond the gas-burning stage. Other ambient air gasses and ions not otherwise consumed, limit the thermal explosive process.

STANLEY MEYER

Canadian Patent 2,067,735 16th May 1991 Inventor: Stanley Meyer

WATER FUEL INJECTION SYSTEM

ABSTRACT

An injector system comprising an improved method and apparatus useful in the production of a hydrogen containing fuel gas from water in a process in which the dielectric property of water and/or a mixture of water and other components determines a resonant condition that produces a breakdown of the atomic bonding of atoms in the water molecule. The injector delivers a mixture of water mist, ionised gases and non-combustible gas to a zone within which the breakdown process leading to the release of elemental hydrogen from the water molecules occurs.

DESCRIPTION

This invention relates to a method and apparatus useful in producing thermal combustive energy from the hydrogen component of water.

In my patent no. 4,936,961 “Method for the Production of a Fuel Gas”, I describe a water fuel cell which produces a gas energy source by a method which utilises water as a dielectric component of a resonant electrical circuit.

In my patent no. 4,826,581 “Controlled Process for the Production of Thermal Energy From Gasses and Apparatus Useful Therefore”, I describe a method and apparatus for obtaining the enhanced release of thermal energy from a gas mixture including hydrogen and oxygen in which the gas is subjected to various electrical, ionising and electromagnetic fields.

In my co-pending application serial no. 07/460,859 “Process and Apparatus for the Production of Fuel Gas and the Enhanced Release of Thermal Energy from Fuel Gas”, I describe various means and methods for obtaining the release of thermal/combustive energy from the hydrogen (H) component of a fuel gas obtained from the disassociation of a water (H_2O) molecule by a process which utilises the dielectric properties of water in a resonant circuit; and in that application I more thoroughly describe the physical dynamics and chemical aspects of the water-to-fuel conversion process.

The invention of this present application represents generational improvement in methods and apparatus useful in the utilisation of water as a fuel source. In brief, the present invention is a microminiaturised water fuel cell which permits the direct injection of water, and its simultaneous transformation into a hydrogen-containing fuel, in a combustion zone, such as a cylinder in an internal combustion engine, a jet engine or a furnace. Alternatively, the injection system of the present invention may be utilised in any non-engine application in which a concentrated flame or heat source is desired, for example: welding.

The present injection system eliminates the need for an enclosed gas pressure vessel in a hydrogen fuel system and thereby reduces a potential physical hazard heretofore associated with the use of hydrogen-based fuels. The system produces fuel-on-demand in real-time operation and sets up an integrated environment of optimum parameters so that a water-to-fuel conversion process works at high efficiency.

The preferred embodiment of the invention is more fully explained below with reference to the drawings in which:

Fig.1 figuratively illustrates the sections and operating zones included in a single injector of the invention.

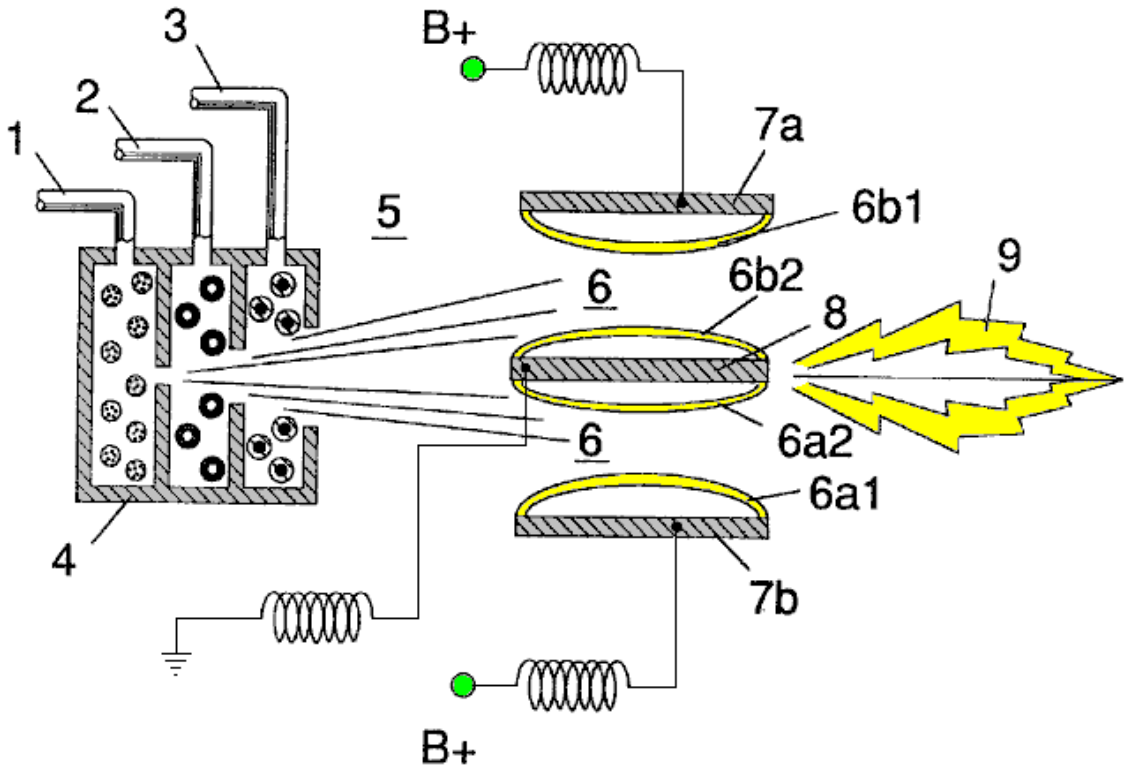

Fig.2A is a side cross-sectional view.

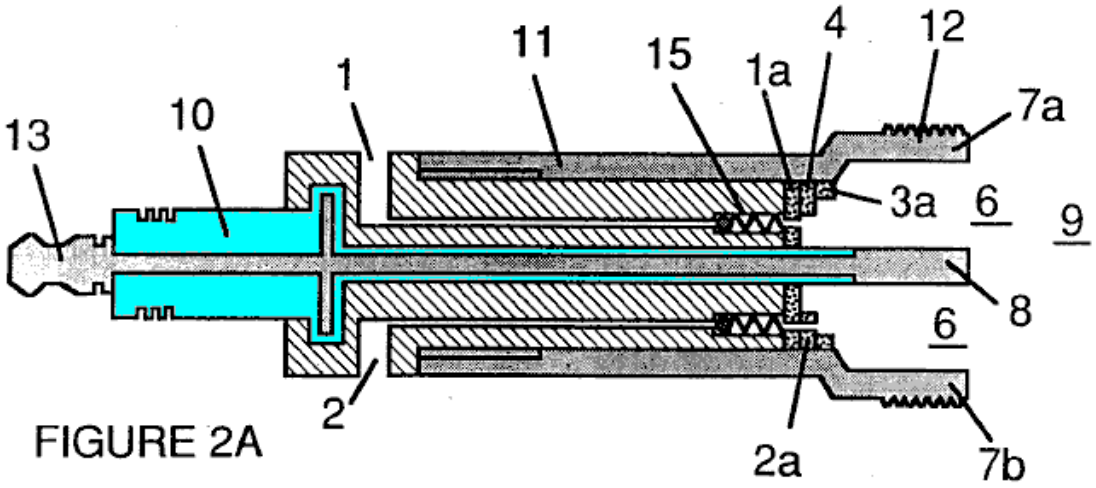

FIGURE 2A

Fig.2B is a frontal view from the operative end.

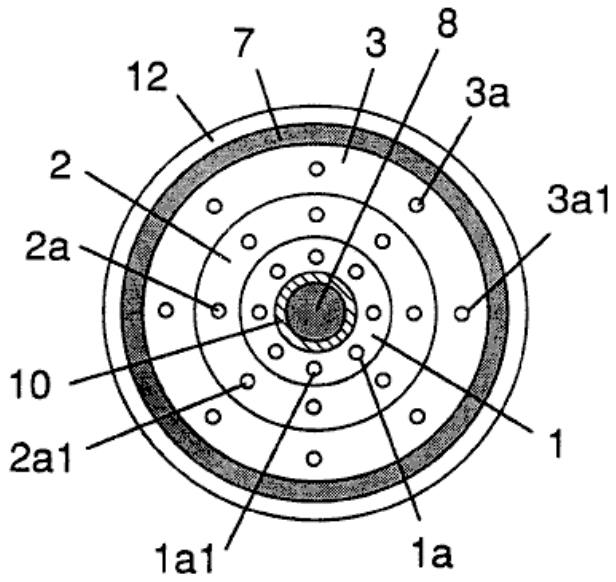

FIGURE 2B

Fig.2C is an exploded view of an individual injector.

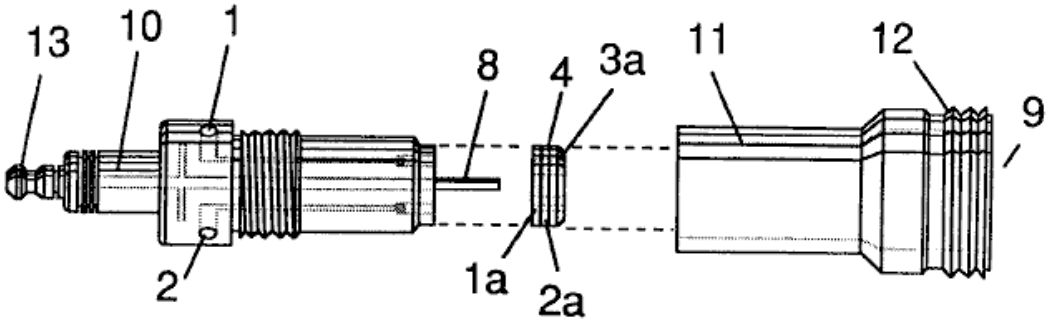

FIGURE 2C

Fig.3 and **Fig.3A** show the side and frontal cross-sectional views of an alternatively configured injector.

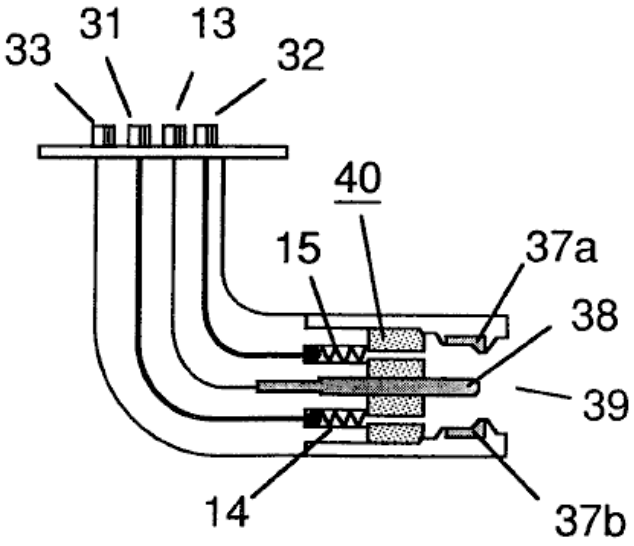

FIGURE 3

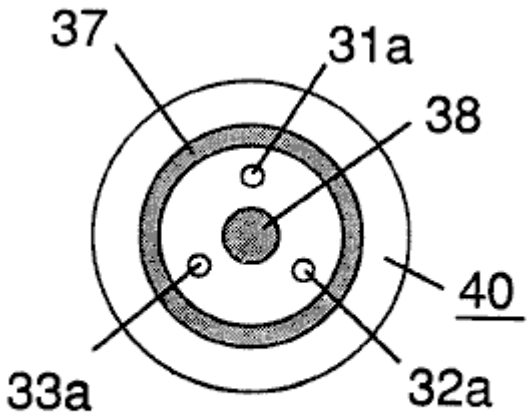

FIGURE 3A

Fig.4 shows a disk array of injectors.

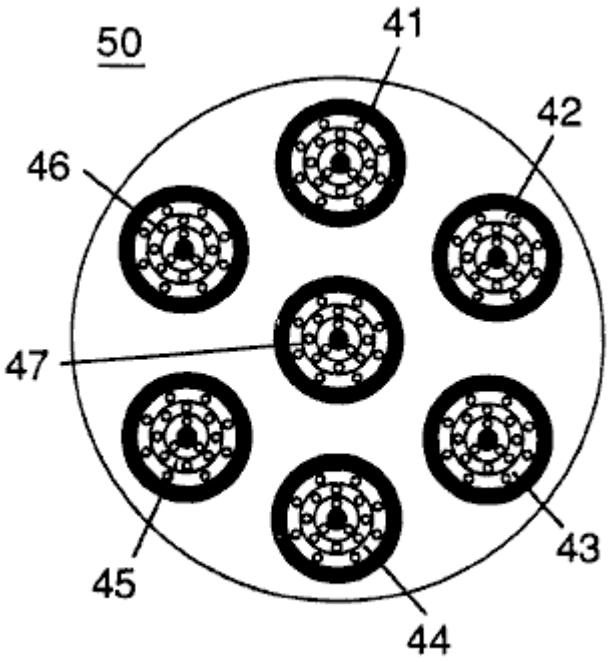

FIGURE 4

Fig.5 shows the resonance electrical circuit including the injector.

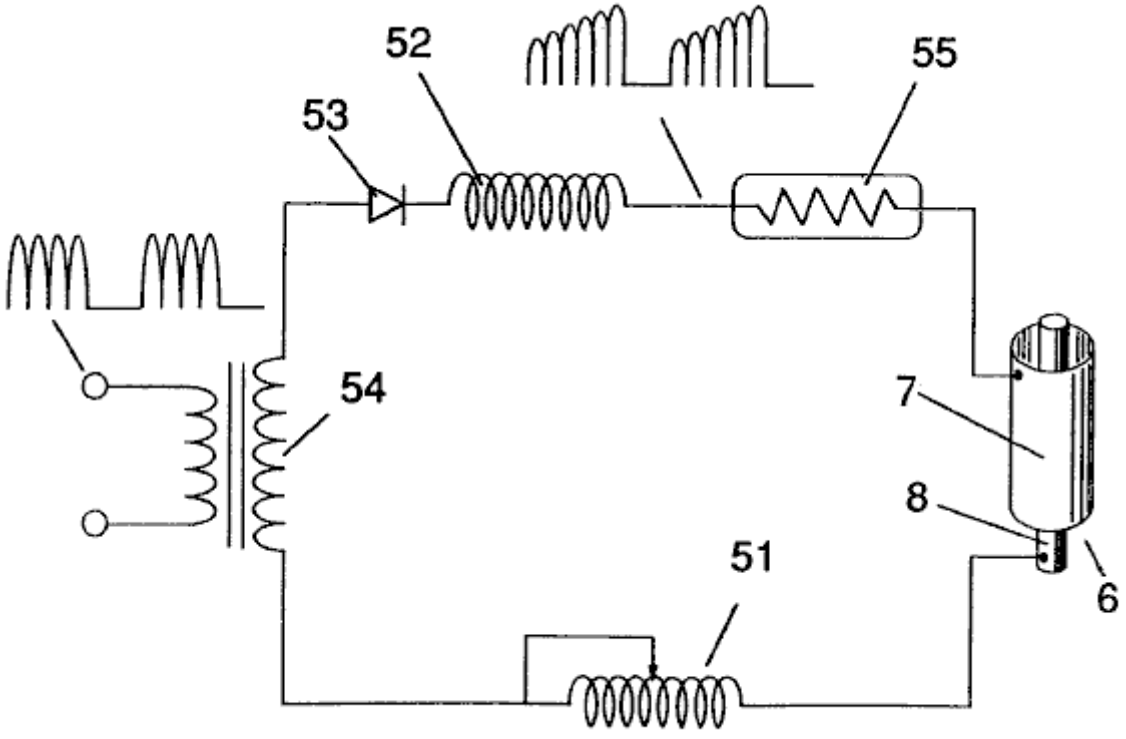

FIGURE 5

Fig.6 depicts the inter-relationship of the electrical and fuel distribution components of an injector system.

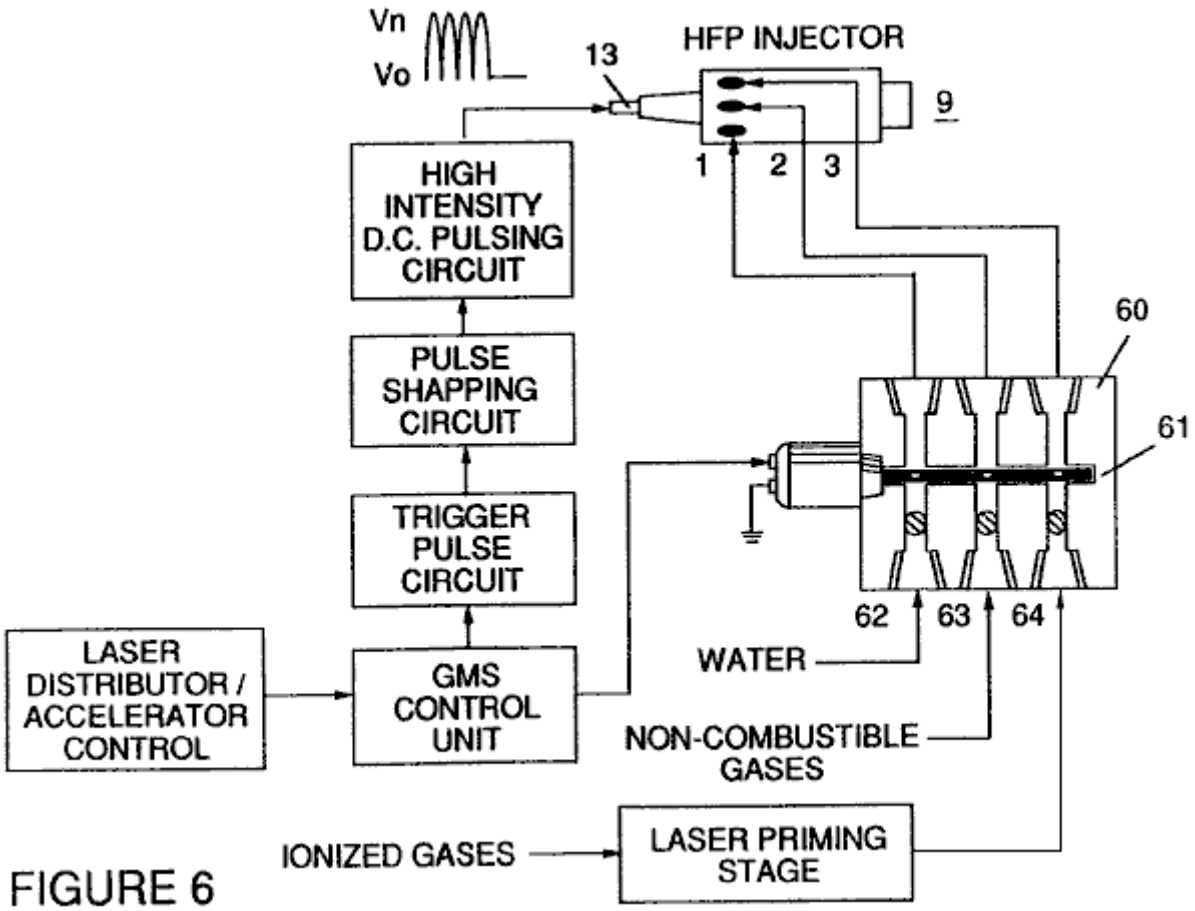

FIGURE 6

Although I refer to an "injector" in this document, the invention relates not only to the physical configuration of an injector apparatus, but also to the overall process and system parameters determined in the apparatus to achieve the release of thermal energy. In a basic outline, an injector regulates the introduction of process constituents into a combustion zone and sets up a fuel mixture condition permitting combustion. That combustion condition is triggered simultaneously with injector operation in real-time correspondence with control parameters for the process constituents.

In the fuel mixture condition which is created by the injector, water (H_20) is atomised into a fine spray and mixed with **1** ionised ambient air gasses and **2** other non-combustible gasses such as nitrogen, argon and other rare gasses, and water vapour. (Exhaust gas produced by the combustion of hydrogen with oxygen is a non-combustible water vapour. This water vapour and other inert gasses resulting from combustion may be recycled from an exhaust outlet in the injector system, back into the input mixture of non-combustible gasses.) The fuel mix is introduced at a consistent flow rate maintained under a predetermined pressure. In the triggering of the condition created by the injector, the conversion process described in my patent no. 4,936,961 and co-pending application serial no. 07/460,859 is set off spontaneously on a "micro" level in a predetermined reaction zone. The injector creates a mixture, under pressure in a defined zone of water, ionised gasses and non-combustible gasses. Pressure is an important factor in the maintenance of the reaction condition and causes the water/gas mixture to become intimately mixed, compressed and destabilised to produce combustion when activated under resonance conditions of ignition. In accordance with the earlier mentioned conversion process of my patent and application, when water is subjected to a resonance condition water molecules expand and distend; electrons are ejected from the water molecule and absorbed by ionised gasses and the water molecule, thus destabilised, breaks down into its elemental components of hydrogen (H_2) and oxygen (O) in the combustion zone. The hydrogen atoms released from the molecule provide the fuel source in the mixture for combustion with oxygen. The present invention is an application of that process and is outlined in Table 1:

Table 1

Injector Mixture	+	Process conditions	=	Thermal Energy
(1) Water Mist		(1) Release Under pressure into Combustion Zone		(1) Heat
and		and		or
(2) Ionised Gas		(2) Resonance utilising the dielectric property of water as a capacitor		(2) Internal Combustion Engine (Explosive force)
and		and		or
(3) Non-combustible Gas		(3) Unipolar pulsing at high voltage		(3) Jet Engine
				or
				(4) Other application

The process occurs as water mist and gasses under pressure are injected into, and intimately mixed in the combustion zone and an electrically polarised zone. In the electrically polarised zone, the water mixture is subjected to a unipolar pulsed direct current voltage which is tuned to achieve resonance in accordance with the electrical, mass and other characteristics of the mixture as a dielectric in the environment of the combustion zone. The resonant frequency will vary according to the injector configuration and depends upon the physical characteristics, such as the mass and volume of the water and gasses in the zone. As my prior patents and application point out, the resonant condition in the capacitative circuit is determined by the dielectric properties of water: (1) as the dielectric in a capacitor formed by adjacent conductive surfaces, and (2) as the water molecule itself is a polar dielectric material. At resonance, current flow in the resonant electrical circuit will be minimised and voltage will peak.

The injector system provides a pressurised fuel mixture for subjection to the resonant environment of the voltage combustion zone as the mixture is injected into the zone. In a preferred embodiment, the injector includes concentrically nested serial orifices, one for each of the three constituent elements of the fuel mixture. (It may be feasible to combine and process non-combustible and ionised gasses in advance of the injector. In this event, only two orifices are required, one for the water and the other for the combined gasses.) The orifices disperse the water mist and gasses under pressure into a conically shaped activation and combustion zone.

Fig1A shows a transverse cross-section of an injector, in which, supply lines for water **1**, ionised gas **2**, and non-combustible gas **3**, feed into a distribution disk assembly **4** which has concentrically nested orifices. The fuel mixture passes through a mixing zone **5**, and a voltage zone **6**, created by electrodes **7a** and **7b** (positive) and **8** (negative or ground). Electrical field lines are shown as **6a1** and **6a2** and **6b1** and **6b2**. Combustion (i.e. the oxidation of hydrogen) occurs in the zone **9**. Ignition of the hydrogen can be primed by a spark or may occur spontaneously as a result of the exceptionally high volatility of hydrogen and its presence in a high-voltage field.

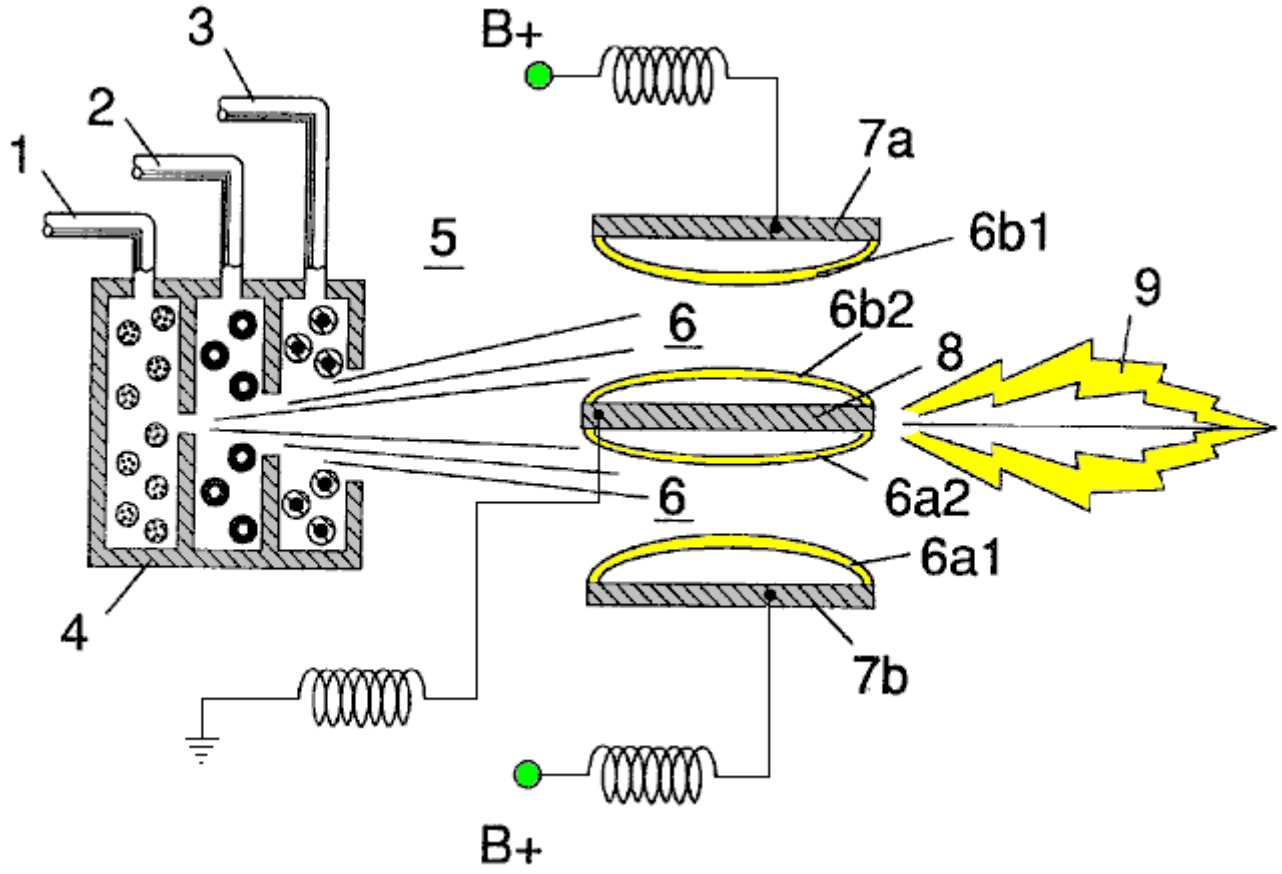

Although the mixing zone, the voltage zone and the combustion zone are mentioned separately in this explanation, they are not in fact physically separated, as can be seen from **Fig.1**. In the zone(s), there is produced an “excited” mixture of vaporised water mist, ionised gasses and other non-combustible gasses, all of which have been instantaneously released from under high pressure. Simultaneously, the released mixture in the zone, is exposed to a pulsed voltage at a frequency corresponding to electrical resonance. Under these conditions, outer-shell electrons of atoms in the water molecule are de-stabilised and molecular time-share is interrupted. Thus, the gas mixture in the injector zone is subjected to physical, electrical and chemical interactive forces which cause a breakdown of the atomic bonding forces of the water molecule.

Process parameters are determined, based on the size of a particular injector. In an injector sized appropriately for use to provide a fuel mixture to a conventional cylinder in a passenger vehicle car engine, the injector may resemble a conventional spark plug. In such an injector, the water orifice is 0.1 to 0.15 inch in diameter; the ionised gas orifice is 0.15 to 0.2 inch in diameter, and the non-combustible gas orifice is 0.2 to 0.25 inch in diameter. In such a configuration, the serial orifices increase in size from the innermost orifice, as appropriate in a concentric configuration. As noted above, it is desirable to maintain the introduction of the fuel components at a constant rate. Maintaining a back-pressure of about 125 pounds per square inch for each of the three fuel gas constituents appears to be satisfactory for a “spark-plug” injector. In the pressurised environment of the injector, spring-loaded one-way check valves in each supply line, such as **14** and **15**, maintain pressure during pulse off times.

Voltage zone **6** surrounds the pressurised fuel mixture and provides an electrically charged environment of pulsed direct current in the range from about 500 to 20,000 volts and more, at a frequency tuned into the resonant characteristic of the mixture. this frequency will typically lie within the range from about 20 KHz to about 50 KHz, dependent, as noted above, on the mass flow of the mixture from the injector and the dielectric property of the mixture. In a spark-plug sized injector, the voltage zone will typically extend longitudinally about 0.25 to 1.0 inch to permit sufficient dwell time of the water mist and gas mixture between the conductive surfaces **7** and **8** which form a capacitor so that resonance occurs at a high-voltage pulsed frequency, and combustion is triggered. In the zone, an energy wave which is related to the resonant pulse frequency, is formed. The wave continues to pulse through the flame in the combustion zone. The thermal energy produced is released as heat energy. In a confined zone such as a piston/cylinder engine, gas detonation under resonant conditions, produces explosive physical power.

In the voltage zone, the time-share ratio of the hydrogen and oxygen atoms comprising the individual water molecules in the water mist, is upset in accordance with the process explained in my patent no. 4,936,961 and application serial no. 07/460,859. Namely, the water molecule, which is itself a polar structure, is distended or

distorted in shape by being subjected to the polar electric field in the voltage zone. The resonant condition induced in the molecule by the unipolar pulses, upsets the molecular bonding of shell electrons such that the water molecule, at resonance, breaks apart into its constituent atoms. In the voltage zone, the water molecules are excited into an ionised state, and the pre-ionised gas component of the fuel mixture, captures the electrons released from the water molecule. In this manner, at the resonant condition, the water molecule is destabilised and the constituent atomic elements of the molecule 2H and O, are released and the released hydrogen atoms are available for combustion. the non-combustible gasses in the fuel mixture, reduce the burn rate of hydrogen to that of a hydrocarbon fuel such as gasoline (petrol) or kerosene (paraffin), from its normal burn rate which is about 2.5 times that of gasoline. Hence the presence of non-combustible gasses in the fuel mixture, moderates the energy release and the rate at which the free hydrogen and oxygen molecules combine in the combustion process.

The combustion process does not occur spontaneously so the conditions in the zone must be fine-tuned carefully to achieve an optimum input flow rate for water and the gasses corresponding to the maintenance of a resonant condition. The input water mist and gasses may likewise be injected into the zone in a physically pulsed (on/off) manner corresponding to the resonance achieved. In an internal combustion engine, the resonance of the electrical circuit and the physical pulsing of the input mixture may be required to be related to the combustion cycle of the reciprocating engine. In this regard, one or two conventional spark plugs may require a spark cycle tuned in correspondence to the conversion cycle resonance, so that combustion of the mixture will occur. Thus, the input flow, conversion rate and combustion rate are interrelated and optimally, each should be tuned in accordance with the circuit resonance at which conversion occurs.

The injection system of the present invention is suited to retrofit applications in conventionally fuelled gasoline and diesel internal combustion engines and conventionally fuelled jet aircraft engines.

Example 1

Figs 2A, 2B and **2C** illustrate a type of injector useful, among other things, as a fuel source for a conventional internal combustion engine. In the cross-section of **Fig.2A**, reference numerals corresponding to the identifying numerals used in **Fig.1** show a supply line for water **1**, leading to first distribution disc **1a** and supply line for ionised gas **2**, leading to second distribution disc **2a**. In the cross-section, the supply line for non-combustible gas **3** leading to distribution disc **3a**, is not illustrated, however, its location as a third line should be self evident. The three discs comprise distribution disc assembly 4. The supply lines are formed in an electrically insulating body **10**, surrounded by electrically conductive sheath/housing **11** having a threaded end segment **12**.

A central electrode **8**, extends the length of the injector. Conductive elements **7a** and **7b** (**7a** and **7b** depict opposite sides of the diameter in the cross-section of a circular body), adjacent threaded section **12** and electrode **8**, form the electrical polarisation zone **6** adjacent to combustion zone **9**. An electrical connector **13** may be provided at the other end of the injector. (In this document, the term “electrode” refers to the conductive surface of an element forming one side of a capacitor.) In the frontal view of **Fig.2B**, it is seen that each disc making up the distribution disc assembly **9**, includes a plurality of micro-nozzles **1a1, 2a1, 3a1**, etc. for the injection of the water and gasses into the polarisation/voltage and combustion zones. The exploded view of **Fig.2C** shows another view of the injector and additionally depicts two supply line inlets **1** and **2**, the third not being shown because of the inability of representing the uniform 120^0 separation of three lines in a two-dimensional drawing.

In the injector, water mist (forming droplets in the range, for example, of from 10 to 250 microns and above, with size being related to voltage intensity) is injected into the fuel-mixing and polarising zone by way of water spray nozzles **1a1**. The tendency of water to form a “bead” or droplet is a parameter related to droplet mist size and voltage intensity. ionised air gasses and non-combustible gasses, introduced through nozzles **2a1** and **3a1**, are intermixed with the expelling water mist to form a fuel-mixture which enters into voltage zone **6** where the mixture is exposed to a pulsating, unipolar, high-intensity voltage field (typically 20,000 volts at 50 Hz or above, at the resonant condition in which current flow in the circuit (amps) is reduced to a minimum) created between electrodes **7** and **8**.

Laser energy prevents discharge of the ionised gasses and provides additional energy input into the molecular destabilisation process which occurs at resonance. It is preferable that the ionised gasses be subjected to laser (photonic energy) activation prior to their introduction into the zone(s); although, for example, a fibre optic conduit may be useful to channel photonic energy directly into the zone. However, heat generated in the zone may affect the operability of such an alternate configuration. The electrical polarisation of the water molecule and a resonant condition occurs to destabilise the molecular bonding of the hydrogen and oxygen atoms. Combustion energy is then released by spark ignition.

To ensure proper flame projection and subsequent flame stability, pumps for the ambient air, non-combustible gas and water, introduce these components to the injector under static pressure up to and beyond 125 pounds per square inch.

Flame temperature is regulated by controlling the volume flow-rate of each fluid-media in direct relationship to applied voltage intensity. To elevate flame temperature, fluid displacement is increased while the volume flow rate of non-combustible gasses is maintained or reduced and the applied voltage amplitude is increased. To lower flame temperature, the fluid flow rate of non-combustible gasses is increased and pulse voltage amplitude is lowered. To establish a predetermined flame temperature, the fluid media and applied voltage are adjusted independently. The flame-pattern is further maintained as the ignited, compressed, and moving gasses are projected under pressure from the nozzle ports in distribution disc assembly **4** and the gas expands in the zone and is ignited.

In the voltage zone, several functions occur simultaneously to initiate and trigger thermal energy yield. Water mist droplets are exposed to high intensity pulsating voltage fields in accordance with an electrical polarisation process which separates the atoms of the water molecule and causes the atoms to experience electron ejection. The polar nature of the water molecule which facilitates the formation of minute droplets in the mist, appears to cause a relationship between the droplet size and the voltage required to effect the process, i.e. the greater the droplet size, the higher the voltage required. The liberated atoms of the water molecule interact with laser-primed ionised ambient air gasses to cause a highly energised and destabilised mass of combustible gas atoms to ignite thermally. Incoming ambient air gasses are laser primed and ionised when passing through a gas processor, and an electron extraction circuit (**Fig.5**) captures and consumes in sink **55**, ejected electrons, and prevents electron flow into the resonant circuit.

In terms of performance, reliability and safety, ionised air gasses and water fuel liquid do not become volatile until the fuel mixture reaches the voltage and combustion zones. Injected non-combustible gasses retard and control the combustion rate of hydrogen during gas ignition.

In alternate applications, laser-primed ionised liquid oxygen and laser-primed liquid hydrogen stored in separate fuel tanks, can be used in place of the fuel mixture, or liquefied ambient air gasses alone with water can be substituted as a fuel source.

The injector assembly is design variable and is retro-fittable to fossil fuel injector ports conventionally used in jet/rocket engines, grain dryers, blast furnaces, heating systems, internal combustion engines and the like.

Example 2

A flange-mounted injector is shown in cross-section in **Fig.3** which shows the fuel mixture inlets and illustrates an alternative three-nozzle configuration leading to the polarisation (voltage) and combustion zones in which one nozzle **31a**, **32a** and **33a** is provided for each of the three gas mixtures, and connected to supply lines **31** and **32** (**33** is not shown). Electrical polarisation zone **36** is formed between electrode **38** and surrounding conductive shell **37**. The capacitative element of the resonant circuit is formed when the fuel mixture, acting as a dielectric, is introduced between the conductive surfaces of **37** and **38**. **Fig.3A** is a frontal view of the operative end of the injector.

Example 3

Multiple injectors may be arranged in a gang as shown in **Fig.4** in which injectors **40, 41, 42, 43, 44, 45, 46, 47, 48** and **49** are arranged concentrically in an assembly **50**. Such a ganged array is useful in applications having intensive energy requirements such as jet aircraft engines and blast furnaces.

Example 4

The basic electrical system utilised in the invention is depicted in **Fig.5** showing the electrical polarisation zone **6** which receives and processes the water and gas mixture as a capacitive circuit element in a resonant charging circuit formed by inductors **51** and **52** connected in series with diode **53**, pulsed voltage source **54**, electron sink **55** and zone **6** formed from conductive elements **7** and **8**. In this manner, electrodes **7** and **8** in the injector, form a capacitor which has electrical characteristics dependent on the dielectric media (e.g. the water mist, ionised gasses and non-combustible gasses) introduced between the conductive elements. Within the macro-dielectric media, however, the water molecules themselves, because of their polar nature, can be considered micro-capacitors.

Example 5

Fuel distribution and management systems useful with the injector of this application are described in my co-pending applications for patent; PCT/US90/6513 and PCT/US90/6407.

A distribution block for the assembly is shown in **Fig.6**. In **Fig.6** the distribution block pulses and synchronises the input of the fuel components in sequence with the electrical pulsing circuit. The fuel components are injected into the injector ports in synchronisation with the resonant frequency, to enhance the energy wave pulse extending from the voltage zone through the flame. In the configuration of **Fig.6**, the electrical system is interrelated to distribution block **60**, gate valve **61** and separate passageways **62, 63** and **64** for fuel components. The distributor produces a trigger pulse which activates a pulse-shaping circuit that forms a pulse having a width and amplitude determined by resonance of the mixture and establishes a dwell time for the mixture in the zone to produce combustion..

As in my referenced application regarding control and management and distribution systems for a hydrogen-containing fuel gas produced from water, the production of hydrogen gas is related to pulse frequency on/off time. In the system shown in **Fig.6**, the distributor block pulses the fluid media introduced to the injector in relationship to the resonant pulse frequency of the circuit and to the operational on/off gate pulse frequency. In this manner, the rate of water conversion (i.e. the rate of fuel produced by the injector) can be regulated and the pattern of resonance in the flame controlled.

STANLEY MEYER

Patent WO 92/07861 2nd November 1990 Inventor: Stanley A. Meyer

CONTROL AND DRIVER CIRCUITS FOR A HYDROGEN GAS FUEL PRODUCING CELL

The major difficulty in using Stan's low-current Water Fuel Cell (recently reproduced by Dave Lawton and shown in Chapter 10) is the issue of keeping the cell continuously at the resonant frequency point. This patent application shows the Stan's circuitry for doing exactly that, and consequently, it is of major importance.

ABSTRACT

A control circuit for a capacitive resonant cavity water capacitor cell (**7**) for the production of a hydrogen containing fuel has a resonant scanning circuit co-operating with a resonance detector and PLL circuit to produce pulses. The pulses are fed into the primary transformer (**TX1**). The secondary transformer (**TX2**) is connected to the resonant cavity water capacitor cell (**7**) via a diode and resonant charging chokes (**TX4**, **TX5**).

This invention relates to electrical circuit systems useful in the operation of a Water Fuel Cell including a water capacitor/resonant cavity for the production of a hydrogen containing fuel gas, such as that described in my United States Letter Patent No. 4,936,961 "Method for the Production of a Fuel Gas" issued on 26th June 1990.

In my Letters Patent for a "Method for the Production of a Fuel Gas", voltage pulses applied to the plates of a water capacitor tune into the dielectric properties of the water and attenuate the electrical forces between the hydrogen and oxygen atoms of the molecule. The attenuation of the electrical forces results in a change in the molecular electrical field and the covalent atomic bonding forces of the hydrogen and oxygen atoms. When resonance is achieved, the atomic bond of the molecule is broken, and the atoms of the molecule disassociate. At resonance, the current (amp) draw from a power source to the water capacitor is minimised and voltage across the water capacitor increases. Electron flow is not permitted (except at the minimum, corresponding to leakage resulting from the residual conductive properties of water). For the process to continue, however, a resonant condition must be maintained.

Because of the electrical polarity of the water molecule, the fields produced in the water capacitor respectively attract and repel the opposite and like charges in the molecule, and the forces eventually achieved at resonance are such that the strength of the covalent bonding force in the water molecule (which are normally in an electron-sharing mode) disassociate. Upon disassociation, the formerly shared bonding electrons migrate to the hydrogen nuclei, and both the hydrogen and oxygen revert to net zero electrical charge. The atoms are released from the water as a gas mixture.

In the invention herein, a control circuit for a resonant cavity water capacitor cell utilised for the production of a hydrogen-containing fuel gas is provided.

The circuit includes an isolation means such as a transformer having a ferromagnetic, ceramic or other electromagnetic material core and having one side of a secondary coil connected in series with a high speed switching diode to one plate of the water capacitor of the resonant cavity and the other side of the secondary coil connected to the other plate of the water capacitor to form a closed loop electronic circuit utilising the dielectric properties of water as part of the electronic resonant circuit. The primary coil of the isolation transformer is connected to a pulse generation means. The secondary coil of the transformer may include segments which form resonant charging choke circuits in series with the water capacitor plates.

In the pulse generation means, an adjustable resonant frequency generator and a gated pulse frequency generator are provided. A gate pulse controls the number of the pulses produced by the resonant frequency generator sent to the primary coil during a period determined by the gate frequency of the second pulse generator.

The invention also includes a means for sensing the occurrence of a resonant condition in the water capacitor / resonant cavity, which when a ferromagnetic or electromagnetic core is used, may be a pickup coil on the transformer core. The sensing means is interconnected to a scanning circuit and a phase lock loop circuit, whereby the pulsing frequency to the primary coil of the transformer is maintained at a sensed frequency corresponding to a resonant condition in the water capacitor.

Control means are provided in the circuit for adjusting the amplitude of a pulsing cycle sent to the primary coil and for maintaining the frequency of the pulsing cycle at a constant frequency regardless of pulse amplitude. In

addition, the gated pulse frequency generator may be connected to a sensor which monitors the rate of gas production in the cell and controls the number of pulses from the resonant frequency generator sent to the cell in a gated frequency in correspondence with the rate of gas production. The sensor may be a gas pressure sensor in an enclosed water capacitor resonant cavity which also includes a gas outlet. The gas pressure sensor is connected to the circuit to determine the rate of gas production with respect to ambient gas pressure in the water capacitor enclosure.

Thus, a comprehensive control circuit and it's individual components for maintaining and controlling the resonance and other aspects of the release of gas from a resonant cavity water cell is described here and illustrated in the drawings which depict the following:

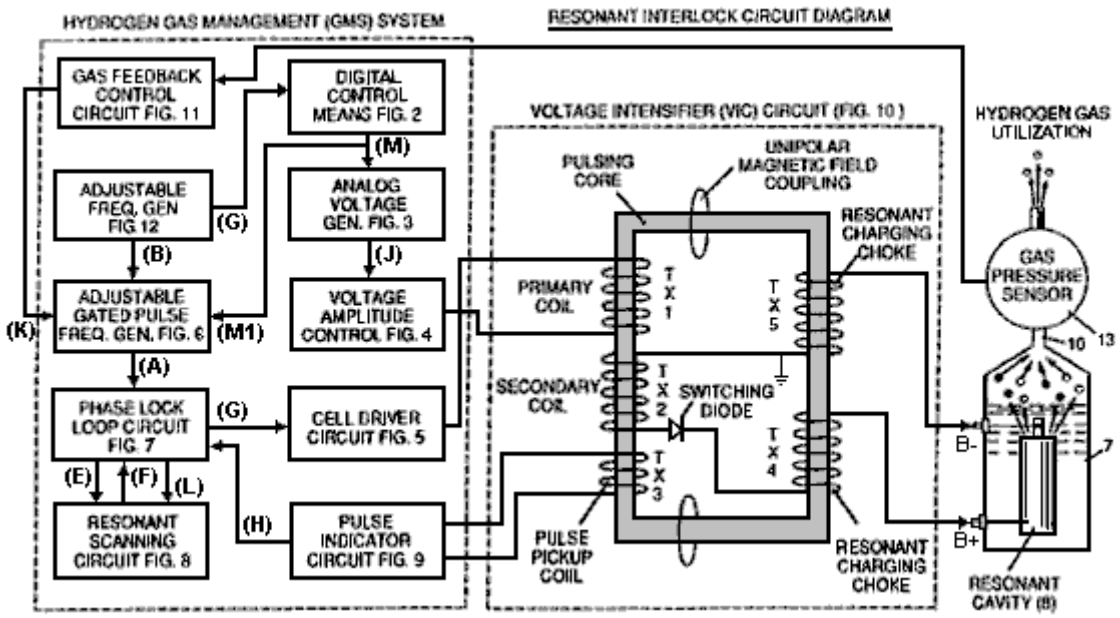

Fig.1 is a block diagram of an overall control circuit showing the interrelationship of sub-circuits, the pulsing core / resonant circuit and the water capacitor resonant cavity.

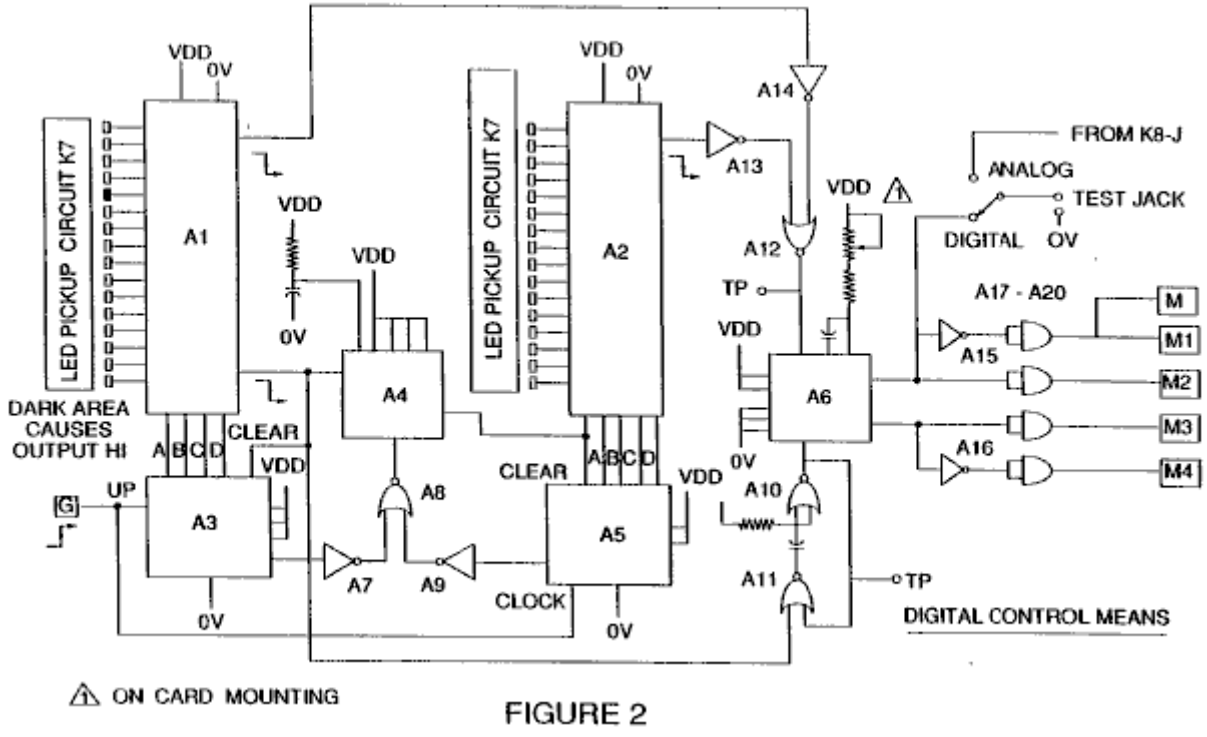

FIGURE 2

Fig.2 shows a type of digital control circuit for regulating the ultimate rate of gas production as determined by an external input. (Such a control circuit would correspond, for example, to the accelerator in a car, or the thermostat control in a building).

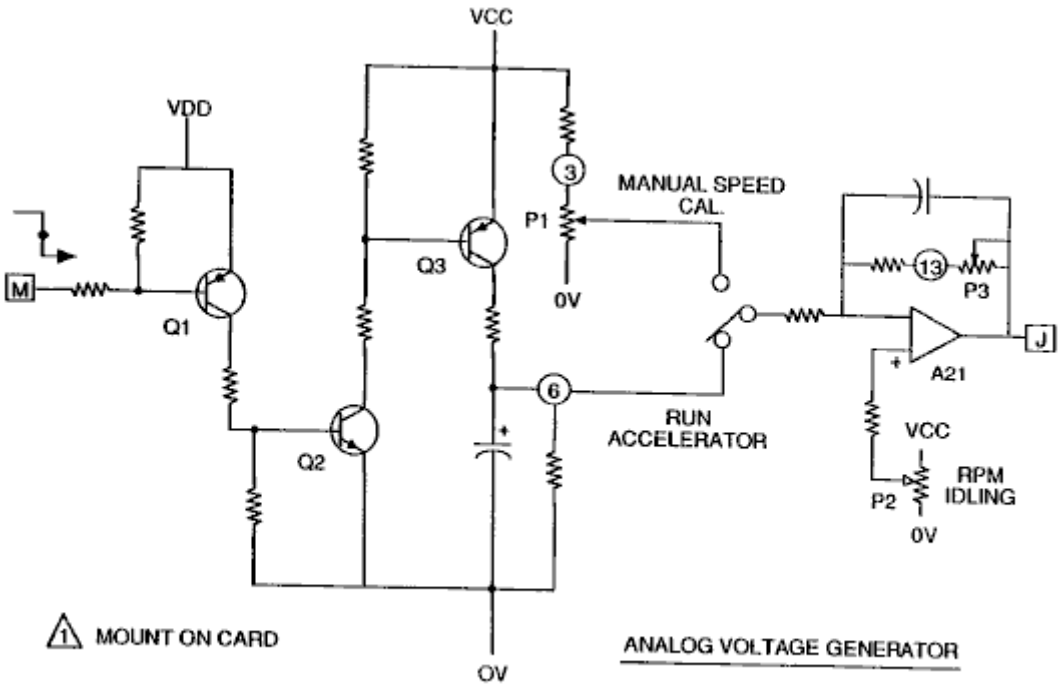

FIGURE 3

Fig.3 shows an analog voltage generator.

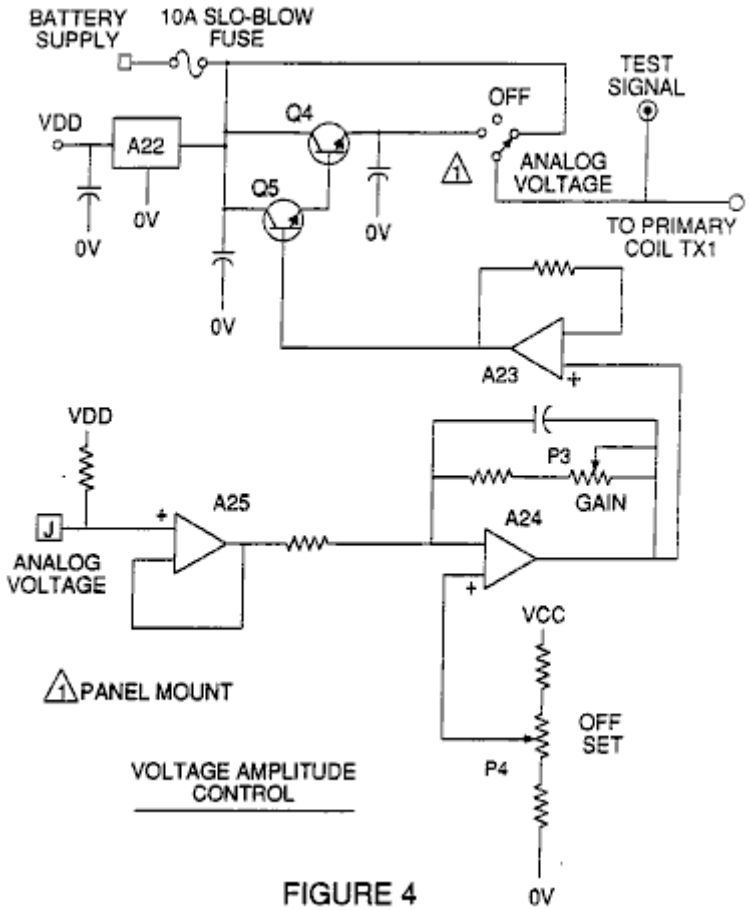

FIGURE 4

Fig.4 is a voltage amplitude control circuit interconnected with the voltage generator and one side of the primary coil of the pulsing core.

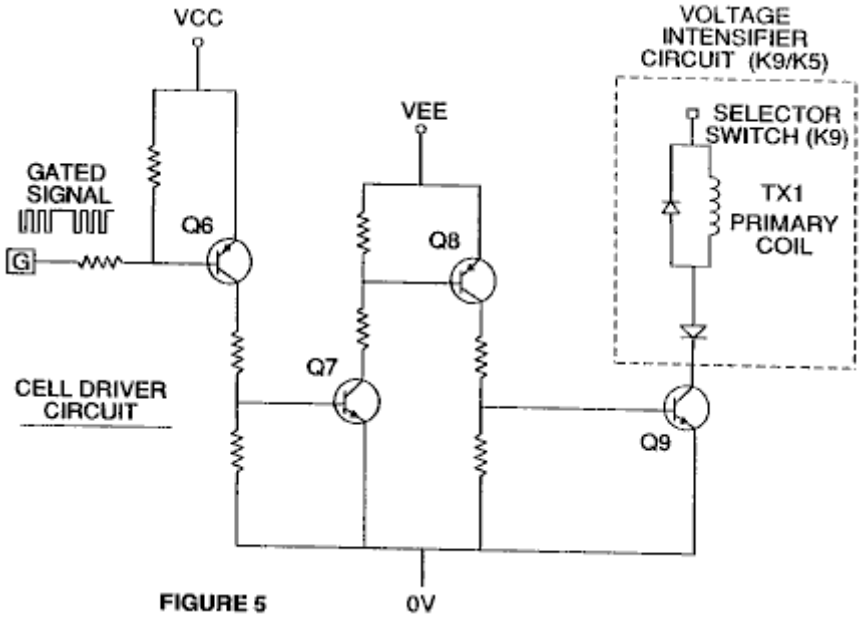

Fig.5 is the cell driver circuit that is connected with the opposite side of the primary coil of the pulsing core. **Figures 6 to 9** form the pulsing control circuitry:

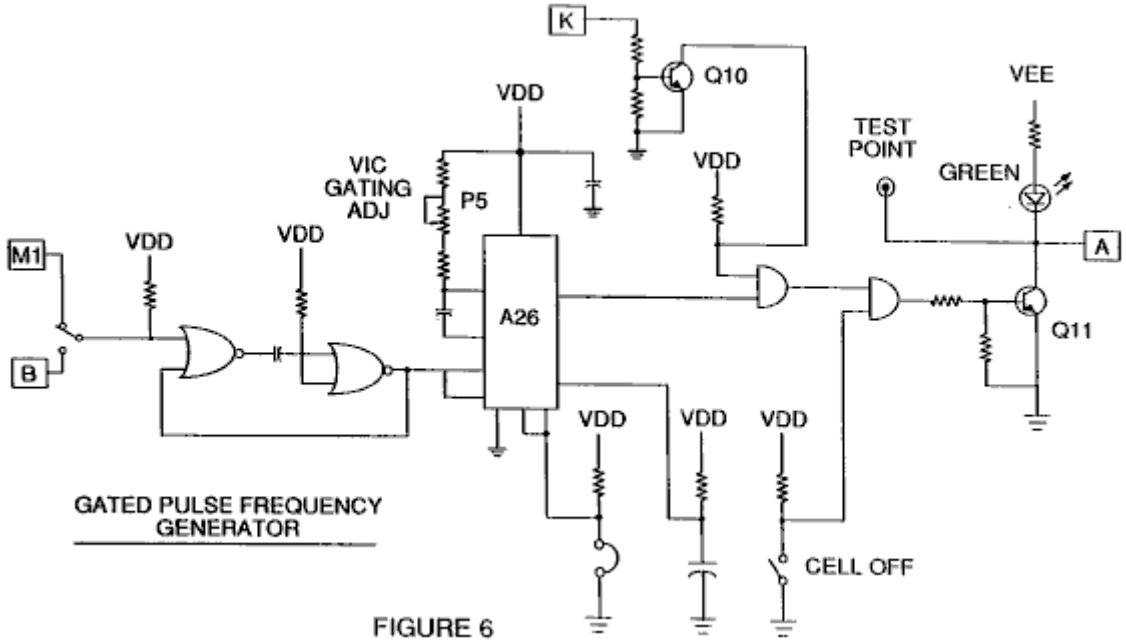

Fig.6 is a gated pulse frequency generator.

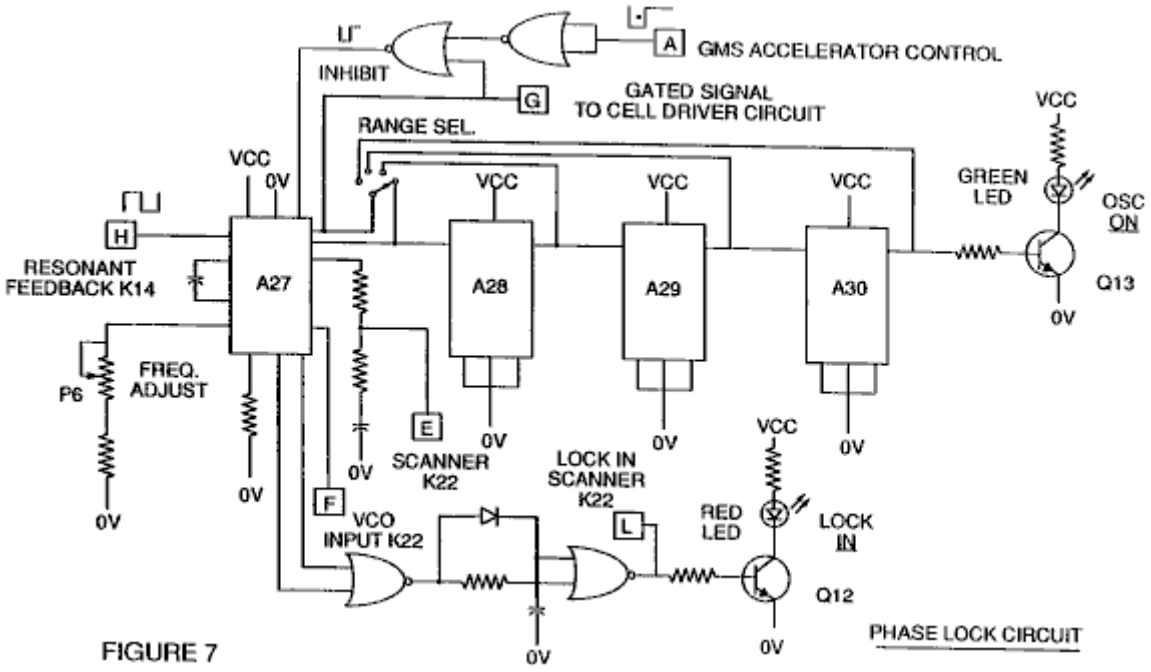

FIGURE 7

Fig.7 is a phase lock circuit.

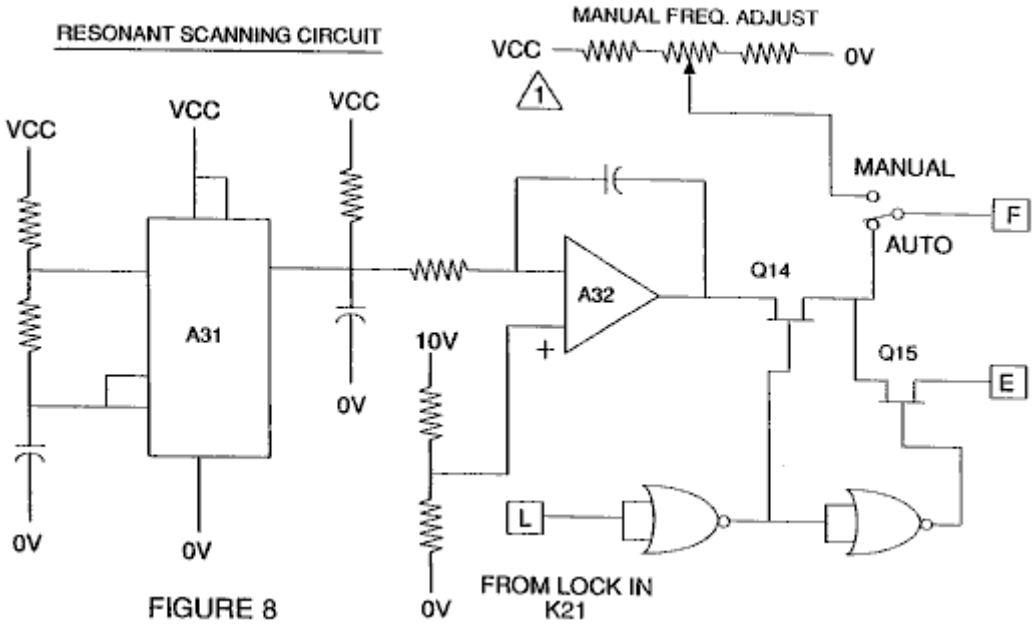

FIGURE 8

Fig.8 is a resonant scanning circuit

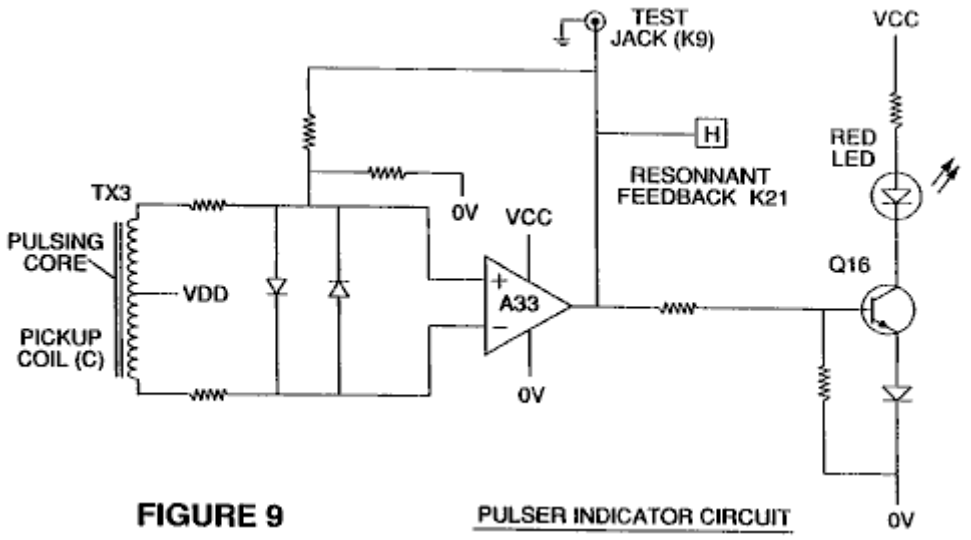

FIGURE 9 PULSER INDICATOR CIRCUIT

Fig.9 is the pulse indicator circuit.

These four circuits control the pulses transmitted to the resonant-cavity / Water Fuel Cell capacitor.

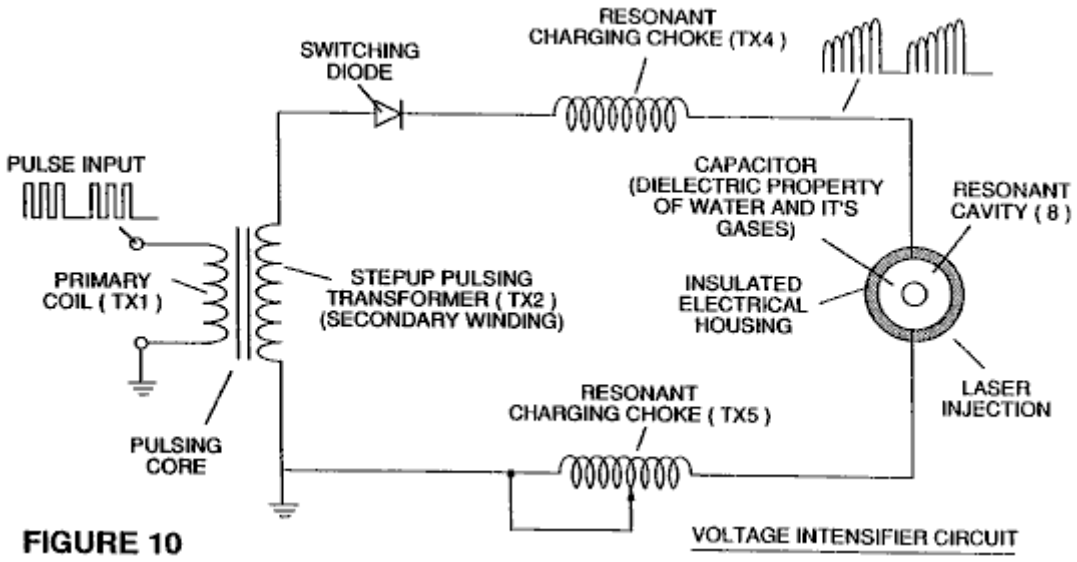

FIGURE 10 VOLTAGE INTENSIFIER CIRCUIT

Fig.10 shows the pulsing core and the voltage intensifier circuit which forms the interface between the control circuit and the resonant cavity.

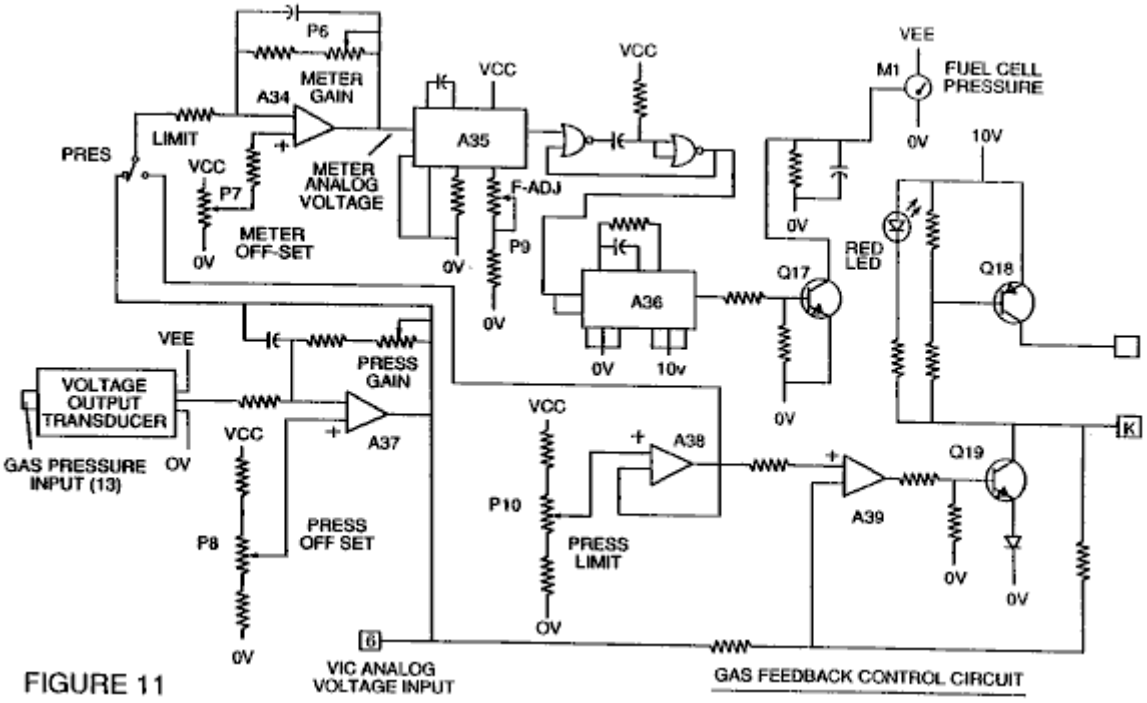

FIGURE 11

Fig.11 is a gas feedback control circuit

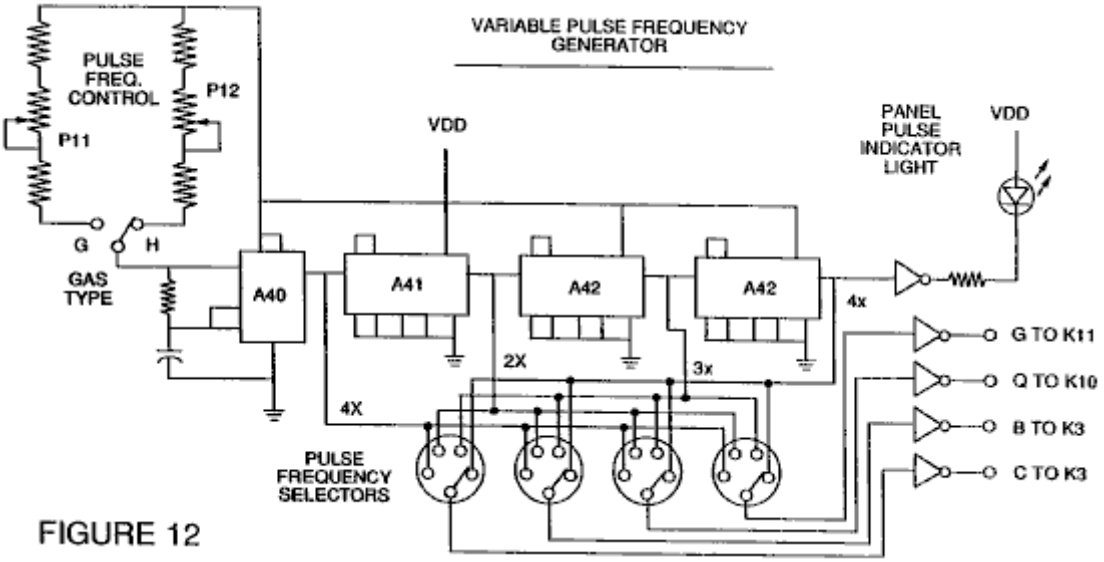

FIGURE 12

Fig.12 is an adjustable frequency generator circuit.

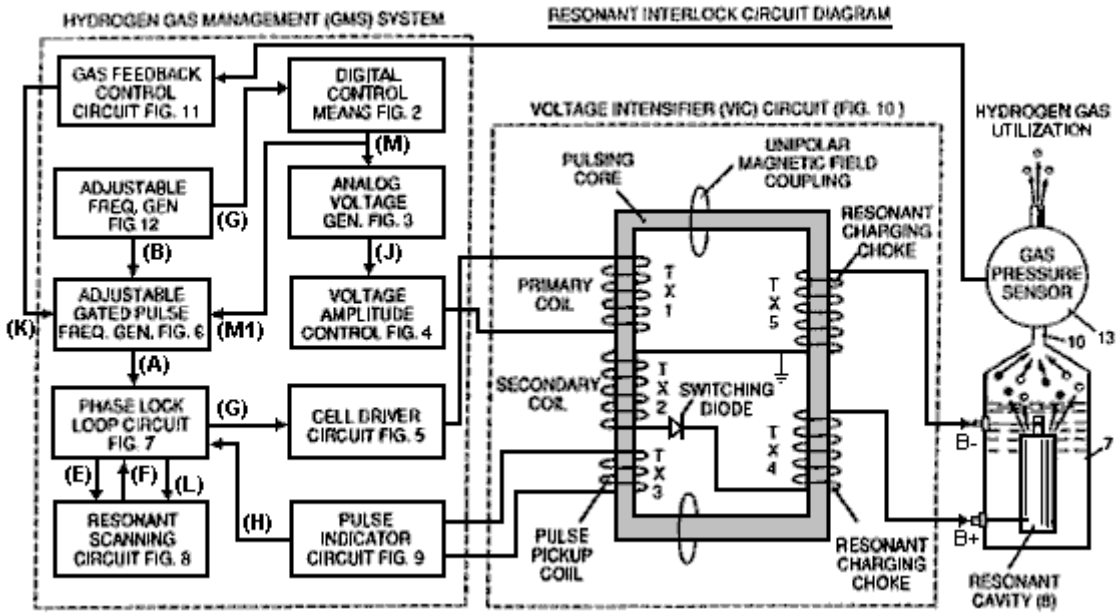

The circuits are interconnected as shown in **Fig.1** and to the pulsing core voltage intensifier circuit of **Fig.10**, which, among other things, isolates the water capacitor electrically so that it becomes an electrically isolated cavity for the processing of water in accordance with it's dielectric resonance properties. By reason of this isolation, power consumption in the control and driving circuits is minimised when resonance occurs, and current demand is minimised as voltage is maximised in the gas production mode of the water capacitor / Fuel Cell.

The reference letters "**A**" through "**M**" and "**M1**" show, with respect to each separate circuit shown, the point at which a connection in that circuit is made to another of the circuits shown.

In the invention, the water capacitor is subjected to a duty pulse which builds up in the resonant charging choke coil and then collapses. This occurrence allows a unipolar pulse to be applied to the Fuel Cell capacitor. When a resonant condition of the circuit is locked-in by the circuit, current leakage is held to a minimum as the voltage which creates the dielectric field tends to infinity. Thus, when high voltage is detected upon resonance, the phase-lock-loop circuit, which controls the cell driver circuit, maintains the resonance at the detected (or sensed) frequency.

The resonance of the water capacitor cell is affected by the volume of water in the cell. The resonance of any given volume of water contained in the water capacitor cell is also affected by "contaminants" in the water which act as a damper. For example, with a potential difference of 2,000 to 5,000 volts applied to the cell, a current spike or surge may be caused by inconsistencies in the water characteristics which cause an out-of-resonance condition which is remedied instantaneously by the control circuits.

In the invention, the adjustable frequency generator, shown in **Fig.12**, tunes in to the resonant condition of the circuit which includes the water cell and the water inside it. The generator has a frequency capability of 0 to 10 KHz and tunes into resonance typically at a frequency of 5 KHz in a typical 3-inch long water capacitor formed from a 0.5 inch rod inside a 0.75 inch inside-diameter cylinder. At start up, in this example, current draw through the water cell will measure about 25 milliamps; however, when the circuit finds a tuned resonant condition, the current drops down to a 1 to 2 milliamp leakage condition.

The voltage to the capacitor water cell increases according to the turns of the winding and the size of the coils, as in a typical transformer circuit. For example, if 12 volts is sent to the primary coil of the pulsing core and the secondary coil resonant charging choke ratio is 30 to 1, then 360 volts is sent to the capacitor water cell. The number of turns is a design variable which controls the voltage of the unipolar pulses sent to the capacitor.

The high-speed switching diode, shown in **Fig.10**, prevents charge leaking from the charged water in the water capacitor cavity, and the water capacitor as an overall capacitor circuit element, i.e. the pulse and charge status of the water/capacitor never pass through an arbitrary ground. the pulse to the water capacitor is always unipolar. The water capacitor is electrically isolated from the control, input and driver circuits by the electromagnetic coupling through the core. The switching diode in the Voltage Intensifier Circuit (**Fig.10**) performs several functions in the pulsing. The diode is an electronic switch which determines the generation and collapse of an electromagnetic field to permit the resonant charging choke(s) to double the applied frequency and it also allows the pulse to be sent to the resonant cavity without discharging the "capacitor" therein. The diode is, of course,

selected in accordance with the maximum voltage encountered in the pulsing circuit. A 600 PIV ("Peak Inverse Volts") fast switching diode, such as an NVR 1550, has been found to be useful in this circuit.

The Voltage Intensifier Circuit of **Fig.10** also includes a ferromagnetic or ceramic ferromagnetic pulsing core capable of producing electromagnetic flux lines in response to an electrical pulse input. The flux lines affect both the secondary coil and the resonant charging choke windings equally. Preferably, the core is of a closed loop construction. The effect of the core is to isolate the water capacitor and to prevent the pulsing signal from going below an arbitrary ground and to maintain the charge of the already charged water and water capacitor.

In the pulsing core, the coils are preferably wound in the same direction to maximise the additive effect of the electromagnetic field in them. The magnetic field of the pulsing core is synchronised with the pulse input to the primary coil. The potential from the secondary coil is introduced to the resonant charging choke(s) series circuit elements which are subjected to the same synchronous applied electromagnetic field, simultaneously with the primary pulse.

When resonance occurs, control of the gas output is achieved by varying the time of duty gate cycle. The transformer core is a pulse frequency doubler. In a figurative explanation of the workings of the fuel gas generator water capacitor cell, when a water molecule is "hit" by a pulse, electron time-share is effected and the molecule is charged. When the time of the duty cycle is changed, the number of pulses that "hit" the molecules in the fuel cell is modified correspondingly. More "hits" result in a greater rate of molecular disassociation.

With reference to the overall circuit of **Fig.1**, **Fig.3** receives a digital input signal, and **Fig.4** shows the control circuit which applies 0 to 12 volts across the primary coil of the pulsing core. Depending on design parameters of primary coil voltage and other factors relevant to core design, the secondary coil of the pulsing core can be set up for a predetermined maximum, such as 2,000 volts.

The cell driver circuit shown in **Fig.5**, allows a gated pulse to be varied in direct relation to voltage amplitude. As noted above, the circuit of **Fig.6** produces a gate pulse frequency. The gate pulse is superimposed on the resonant frequency pulse, to create a duty cycle that determines the number of discrete pulses sent to the primary coil. For example, assuming a resonant pulse of 5 KHz, a 0.5 KHz gating pulse with a 50% duty cycle, will allow 2,500 discrete pulses to be sent to the primary coil, followed by an equal time interval in which no pulses are passed through. The relationship of resonant pulse to the gate pulse is determined by conventional signal addition/subtraction techniques.

The phase lock loop circuit shown in **Fig.7** allows the pulse frequency to be maintained at a predetermined resonant condition sensed by the circuit. Together, the circuits of **Fig.7** and **Fig.8**, determine an output signal to the pulsing core until the peak voltage signal sensed at resonance is achieved.

A resonant condition occurs when the pulse frequency and the voltage input attenuates the covalent bonding forces of the hydrogen and oxygen atoms of the water molecule. When this occurs, current leakage through the water capacitor is minimised. The tendency of voltage to maximise at resonance, increases the force of the electric potential applied to the water molecules, which ultimately disassociate into atoms.

Because resonances of different waters, water volumes and capacitor cells vary, the resonant scanning circuit of **Fig.8** scans frequency from high to low and back to high, until a signal lock is achieved. The ferromagnetic core of the voltage intensifier circuit transformer, suppresses electron surge in an out-of-resonance condition of the fuel cell. In an example, the circuit scans at frequencies from 0 Hz to 10 KHz and back to 0 Hz. In water having contaminants in the range of 1 part per million to 20 parts per million, a 20% variation in resonant frequency is encountered. depending on water flow rate into the fuel cell, the normal variation range is about 8% to 10%. For example, iron in well water affects the status of molecular disassociation. Also, at a resonant condition, harmonic effects occur. In a typical operation of the cell with a representative water capacitor described below, at a frequency of about 5 KHz, with unipolar pulses from 0 to 650 volts, at a sensed resonant condition in the resonant cavity, on average, the conversion into gas occurs at a rate of about 5 US gallons (19 litres) of water per hour. To increase the rate, multiple resonant cavities can be used and/or the surfaces of the water capacitor can be increased, however, the water capacitor cell is preferably small in size. A typical water capacitor may be formed from a 0.5 inch diameter stainless steel rod and a 0.75 inch inside-diameter cylinder which extends over the rod for a length of 3 inches.

The shape and size of the resonant cavity may vary. Larger resonant cavities and higher rates of consumption of water in the conversion process require higher frequencies up to 50 KHz and above. The pulsing rate, to sustain such high rates of conversion, must be increased correspondingly.

From the above description of the preferred embodiment, other variations and modifications of the system disclosed will be evident to those skilled in the art.

CLAIMS

1. A control circuit for a resonant cavity water capacitor cell utilised for the production of a hydrogen- containing fuel gas, including an isolation transformer with a ferromagnetic core, and having one side of a secondary coil connected in series with a high-speed switching diode to one plate of the water capacitor of the resonant cavity, and the other side of the secondary coil connected to the other plate of the water capacitor, to form a closed-loop electronic circuit utilising the dielectric properties of water as part of the electronic circuit, and a primary coil connected to a pulse generator.

2. The circuit of Claim 1. in which the secondary coil includes segments which form a resonant charging choke circuit in series with the water capacitor.

3. The circuit of Claim 1. in which the pulse generator includes an adjustable first frequency generator and a second gated pulse frequency generator which controls the number of pulses produced by the first frequency generator, sent to the primary coil during a period determined by the gate frequency of the second pulse generator.

4. The circuit of Claim 1. further including a means for sensing the occurrence of a resonant condition in the water capacitor of the resonant cavity.

5. The circuit of Claim 4. in which the means for sensing is a pickup coil on the ferromagnetic core of the transformer.

6. The circuit of Claim 4. or Claim 5. in which the sensing means is interconnected to a scanning circuit and a phase-lock-loop circuit, by which the pulsing frequency sent to the primary coil of the transformer is maintained at a sensed frequency corresponding to a resonant condition in the water capacitor.

7. The circuit of Claim 1. including means for adjusting the amplitude of a pulsing cycle sent to the primary coil.

8. The circuit of Claim 6. including further means for maintaining the frequency of the pulsing cycle at a constant frequency regardless of pulse amplitude.

9. the circuit of Claim 3. in which the gated pulse frequency generator is connected to a sensor which monitors the rate of gas production from the cell and controls the number of pulses sent to the cell in a gated frequency, corresponding to the rate of gas production.

10. The circuit of Claim 7. or Claim 8. or Claim 9. further including a gas-pressure sensor in an enclosed water capacitor resonant cavity which also includes a gas outlet, where the gas-pressure sensor is connected to the circuit to determine the rate of gas production with respect to ambient gas pressure in the water capacitor enclosure.

11. The methods and apparatus as substantially described herein.

STEPHEN MEYER

Patent application US 2005/0246059 3rd November 2005 Inventor: Stephen F. Meyer

MLS-HYDROXYL FILLING STATION

This is a patent application from Stephen Meyer, brother of the late Stan Meyer. While this application mentions filling stations, it is clear that the design is aimed at use in vehicles with internal combustion engines. I believe that the impedance-matching interface between the alternator and the cell electrodes is particularly important. The water-splitter cell uses sets of three pipes in a concentric array which results in small gaps between the innermost, middle and outer pipe. Stephen refers to these three electrode pipes as a "wave-guide", so please bear that in mind when reading this patent application. Stephen uses the word "hydroxyl" to refer to the mixture of hydrogen and oxygen gases produced by electrolysis of water. Other people use the word "hydroxy" to describe this mixture, so they should be considered interchangeable.

The operation of this system as described here, calls for the generating power to be removed when the gas pressure in the generating chambers reaches 5 psi. The gas is then pumped into a pressure chamber where the pressure ranges from 40 psi to 80 psi, at which point the compressor is powered down and the excess gas vented to some external storage or using device. It is not until this is completed that the power is applied again to the generating chambers. May I remark that, in my opinion, there is no need to remove the power from at generating chambers at any time when this system is in operation, since all that that does is to lower the generating capacity, unless of course, the production rate is so high that it exceeds the level of demand.

ABSTRACT

The usefullness of this system, it's configuration, design and operation, are the keystone of a new type of automation: the production of hydroxyl gases from renewable sources.

BACKGROUND OF THE INVENTION

Fuel Cell and auto industries have been looking for methods and apparatus that can supply a source of hydrogen and oxygen for its new hybrid industry. This invention is such a device.

SUMMARY OF THE INVENTION

The invention is a computerised, automatic, on-site/mobile hydroxyl gas producing filling station which allows the products being produced to be used, either by the hydrogen fuel cells installed in automobiles, trucks, buses, boats and land-based generating applications, or in any internal combustion engine.

BRIEF DESCRIPTION OF THE DRAWINGS

Fig.1 shows the configuration of the components which go to make up the MLS-hydroxyl Filling Station.

Fig.2 shows the software display which the operator uses to monitor and control the production of hydroxy gases and heat.

Fig.3 shows the methods, configuration, and apparatus used in the hydroxyl producing cell system **120**.

Fig.4 shows the electronic impedance-matching circuits **102**, connected between the dual three-phase synchronised generators (**110A** and **110B** in **Fig.3**) and each of the electrodes or "waveguide" arrays **132** in cell **120** of **Fig.3**. Note that only generator **A** is depicted in **Fig.4** as being connected to arrays **A**, **B** and **C** using PC cards **1 to 3**. generator **B** is connected to arrays **D**, **E** and **F** using cards **4 to 6**.

Fig.5 Shows the signals emitted by each of the impedance-matching circuits (**102** in **Fig.4** mounted on cards **1 to 6**) which are applied to each of the cylinder arrays (**132** in **Fig.3**) installed in hydroxyl cell **120**. These sets of signals with their offset phase relationship, frequencies and amplitudes, are the driving forces producing the hydroxy gases in cell **120** of **Fig.3**.

Fig.6 shows the high-frequency ringing signal which is produced between points **T1** and **T2** in the impedance-matching circuit **102** in **Fig.4**. It is this ringing which enhances the production of the hydroxyl gas in cell **120** of **Fig.3**.

DETAILED DESCRIPTION OF THE DRAWINGS

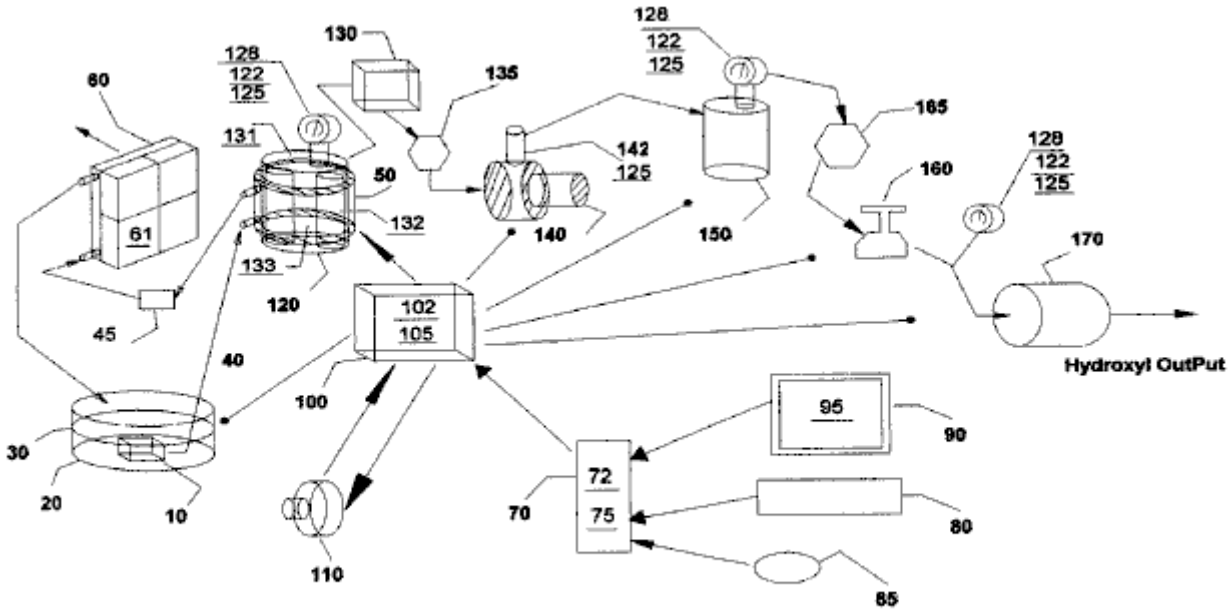

MLS- Hydroxyl Filling Station (MLS-HFS)

Fig 1

The heat-removing section in **Fig.1** consists of a liquid bath **30** and its container **20**, a liquid circulating pump **10**, conveying-conduits **40**, cooling chamber 50 attached to hydroxyl generating cell **120**, filter **45**, radiator **60** and cooling fans **61** attached to it.

The automatic-control section in **Fig.1** consists of a computer **70**, software program **75**, video monitor **90** and it's graphic operator display **95** (**Fig.2**), pointer **85**, keyboard **80**, interface card **72**, and Input/Output controller **100** with it's driver electronics cards **102** and **105**.

Dual three-phase power sources **110** and impedance-matching circuits **102**, provide the power needed to drive the hydroxyl cell **120**.

The remaining apparatus is used to convey the gases from cells **120**, through liquid trap **130**, through gas flow restriction valve **135**, elevate its gas pressures through compressor **140**, transfer them to storage tank **150**, then deliver the gases through safety cut off **165**, regulators **160** and through flash-back arrestor **170** for external delivery.

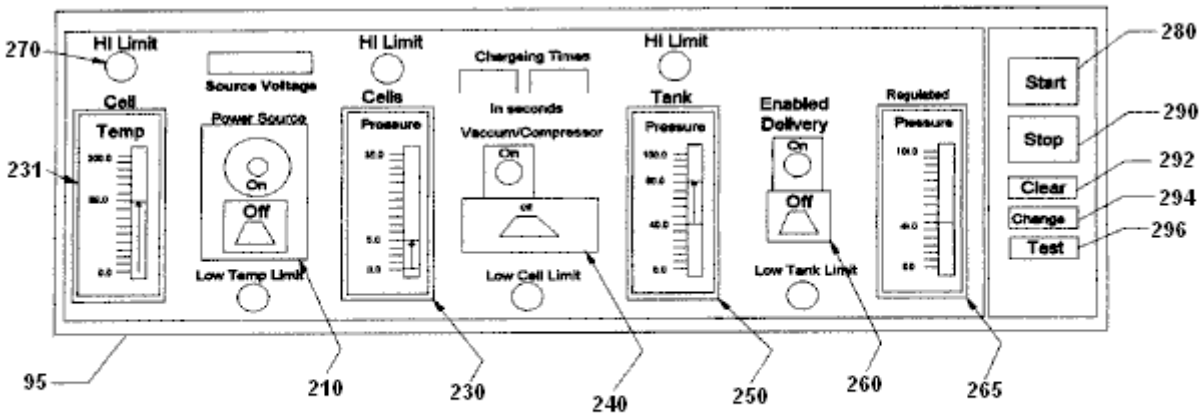

MLS-Hydroxyl Filling Station (MLS-HFS) Graph Display and Operator Control

Fig-2

Fig.2 shows the layout and functions of the operator control display **95** of program **75** in **Fig.1**. It consists of cell temperature indicator **230**, vacuum controller **240**, high-pressure tank indicator **250**, delivery controller **260**, delivery regulated-pressure indicator **265** and related alarm/status indicators **270**. Also, software control buttons

are provided to start **280**, stop **290**, clear data **292**, change setting **294** and the testing of equipment and their sequences **296**.

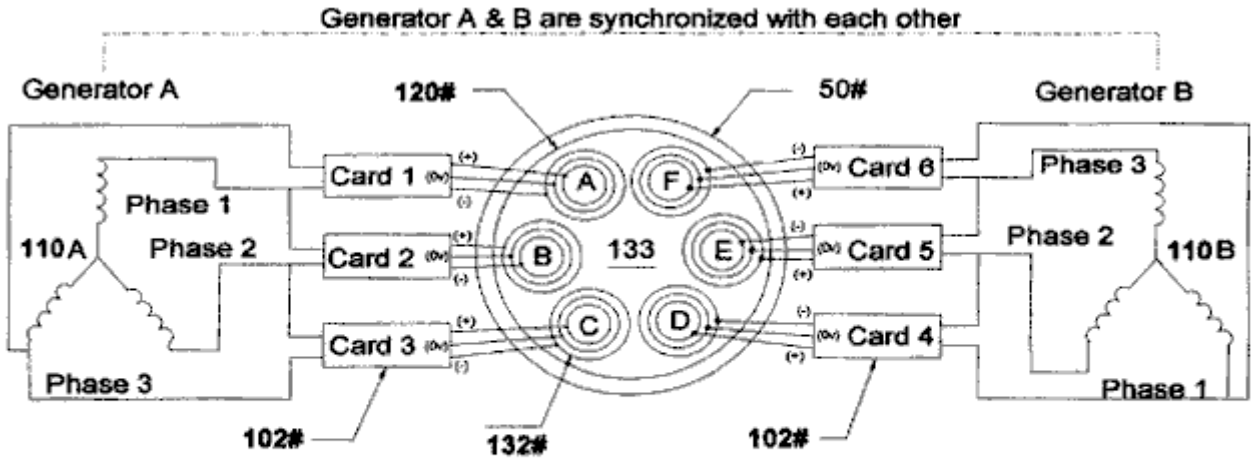

Configuration of Hydroxyl gas producting appartuses

Fig-3

Fig.3 shows the configuration of our proprietary hydroxyl-producing apparatus **120** consisting of dual three-phase power source **110**, impedance matching electronic circuits **102** and gas converter devices **132** submerged in a bath of water **133** in cell **120**. The drawing also shows the water jacket **50** surrounding the cell **120** that helps lower its temperature and allows more production of the hydroxyl gases at higher voltage signals as shown in **Fig.5**.

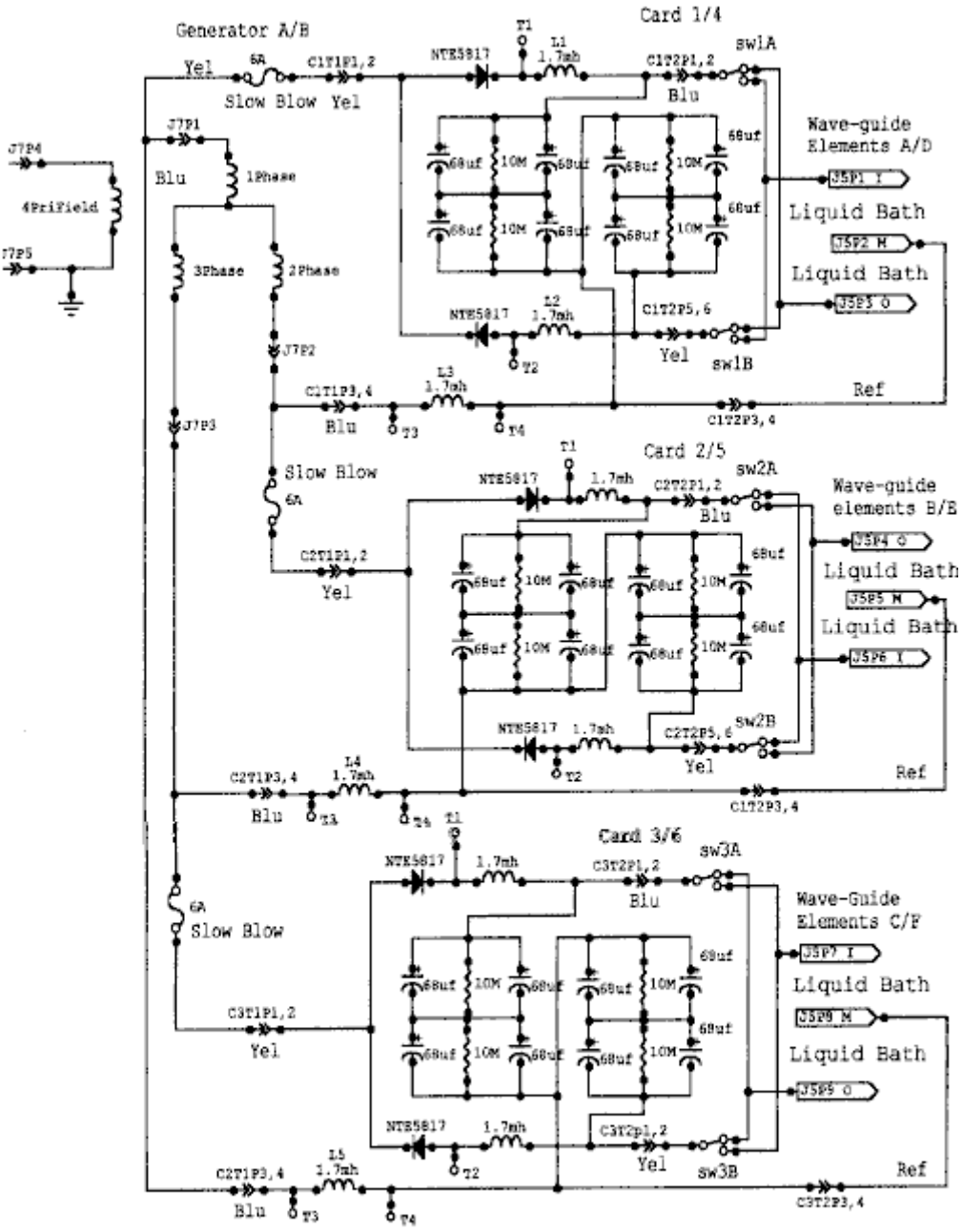

Impedance matching circuits 102

Fig-4

Fig.4 shows the electrical circuits **102**, used to drive the gas converting arrays (**132** in **Fig.3**) submerged in a bath of water **133** in cell **120**. **Fig.4** shows three identical circuits connected to each of the three-phase signals from one half of the dual three-phase generator **110A** in **Fig.3**. The circuits **102,** convert the AC signal from each phase of **110** into a modulated signal as depicted by **Fig.5**. These signals are then coupled to the triple array elements **132**, (Inside, Middle and Outside) by alternating the connection between the Inside and Outside elements of the arrays (**132** in **Fig.3**).

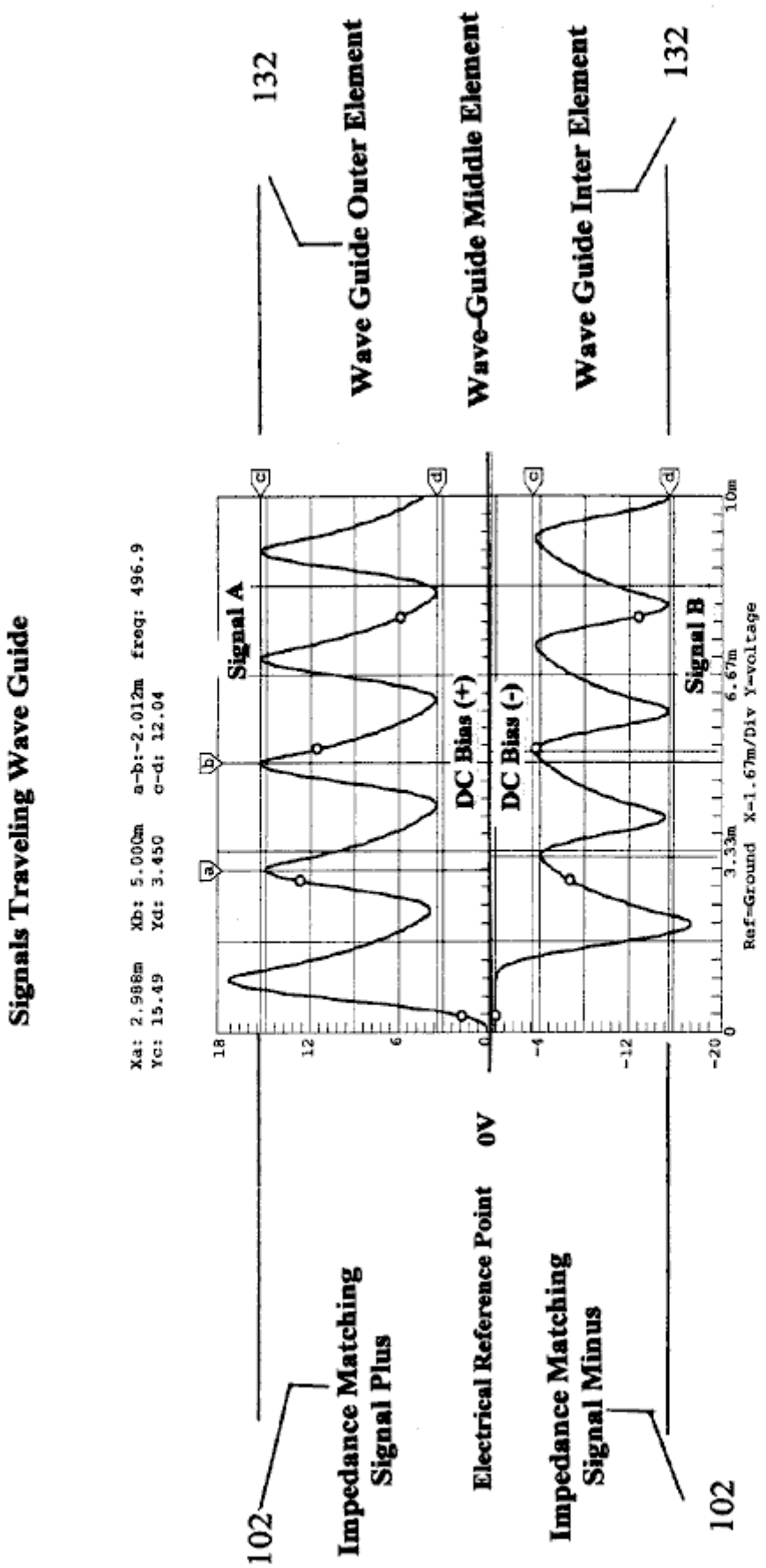

FIG-5

Fig.5 shows the composite signals applied to each of the arrays (**132** in **Fig.3**) submerged in the water bath **133** in cell **120**, and indicates the differential voltages used in the hydroxyl producing process. Note that the Middle wave-guide element is used as the electrical reference point for both the Outside and Inside elements of array **132**. It is this composite signal applied to the surface of the stainless steel elements in array **132** submerged in water bath **133**, heat allows the ions from the elements in array **132** to cross its water surface barriers **133** and contribute to the hy-droxyl production. Note the DC bias voltage +,- on either side of the centre electrical

reference point 0V. It is this bias voltage being modulated by multi-polarity differential signals from **102**, that contributes to the wave-guide action of arrays **132**. Also, the frequency of the waveform shown in **Fig.5** is adjusted to match the electrical wavelength of the arrays **132** of **Fig.3** and the impedance of water bath **133**.

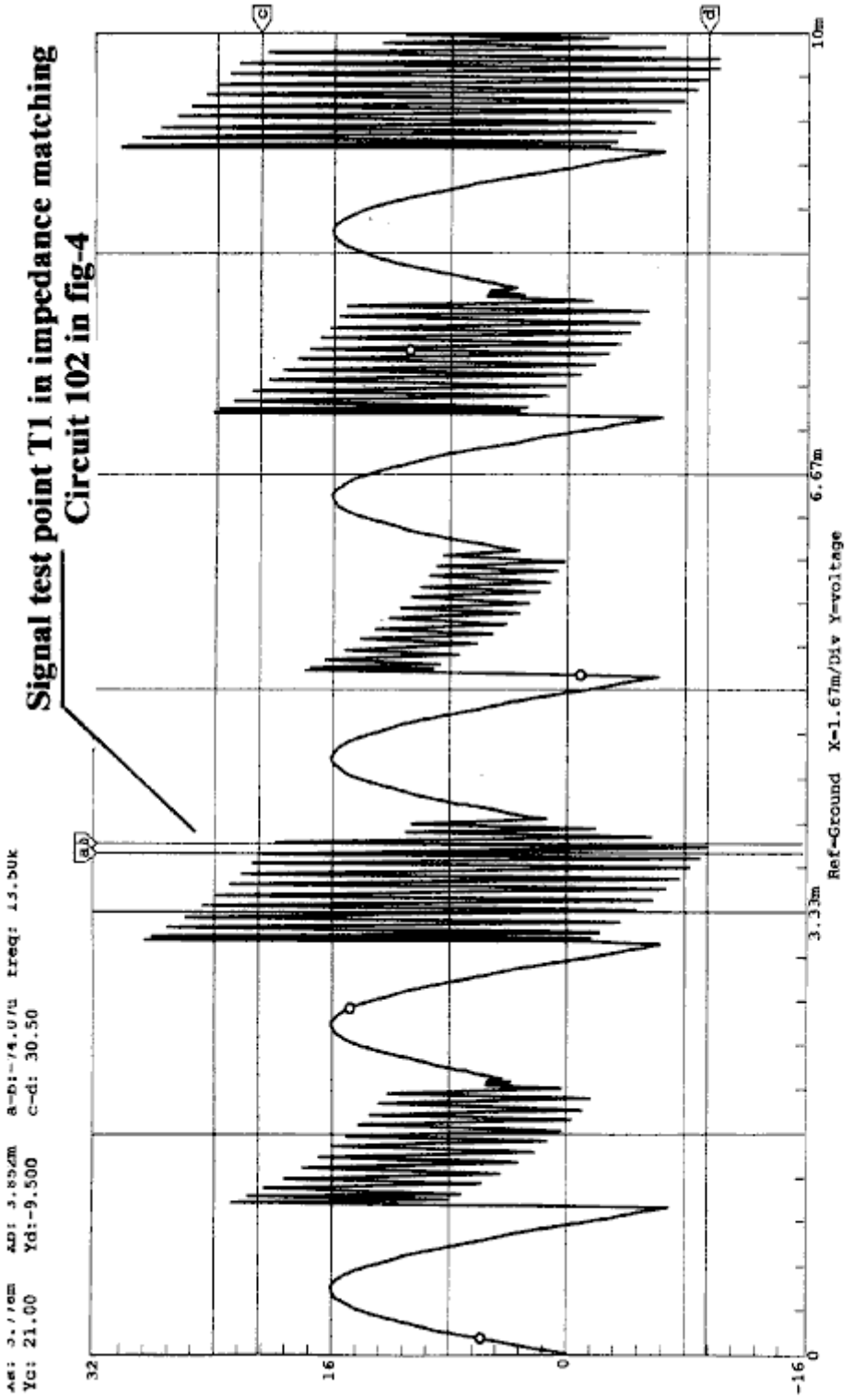

FIG-6

Fig.6 shows the high-frequency ringing signals which contribute to the operation of the hydroxyl production. just as a tuning fork rings when struck by a hammer, so do the wave-guide elements in array **132** immersed in the hydroxyl-generating liquid **133** when struck by the electrical signals shown in **Fig.5** and **Fig.6**, coming from the impedance-matching circuits **102** shown in **Fig.4**.

Brief Description of Sequences

This invention is a computerised Hydroxyl Gas producing filling station "**MLS-HFS**" designed to provide automatic control of its on-site gas production and delivery.

The MLS-HFS shown in **Fig.1**, is a hydroxyl gas and heat generating system which uses a renewable source of liquid supply **30** such as water. It uses a computer control program **75** with display interface **95**, for the monitoring, adjusting and controlling of the electronic and hardware apparatus and process logic. The electronic circuits **102** mounted in driver **100**, control the production of the gases and heating while circuit **105** controls the process and routeing of the hydroxyl gas.

The system consists of a low-pressure hydrolyser cell **120** in **Fig.1**, a liquid trap **130**, an adjustable flow-restriction valve **135**, high-pressure vacuum pump **140**, and check valve **142** installed in **140**. It also contains a high-pressure storage tank **150**, an alarm/low-pressure cut-off valve **165**, gas regulator **160**, flashback arrestor **170**, over-pressure safety release valves **125**, pressure gauges **128**, analogue pressure-sending units **122** installed on cell **120**, and tank **150** at the regulating side of regulator **160**. Also, **125** is installed on Compressor **140** high-pressure output. The computer controller **70**, monitor **90**, keyboard **80**, interface I/O card **72** and software position pointer **85**, are used to control the production process, using electronic driver **100** through it's PC boards **105** and their attached control devices. The power to the cell-driving circuits **102**, installed in driver **100**, is supplied from a dual three-phase isolated power source **110**. The amplitude, signal phases and frequency from this power source is controlled by signal adjustments coming from the computer **70**.

Detailed Description

Sequence of Operation

The system shown in **Fig.1** is monitored and controlled by the software program **75**, computer **70**, monitor **90**, keyboard **80**, pointer **85**, and display interface **95** in **Fig.2**.

The software program has five main functions, namely: to purge the system of ambient air, check and test for any equipment malfunctions, prepare the system for production, monitor and control the current activities of the production process, and the safety shutdown of the system if alarms are detected.

During the initial installation, and again after any repairs, the total system is purged using the vacuum pump **140**, using manual procedures to ensure that all ambient air has been removed from the system. Before the system is put into service, the operator can test the operation of the system by using the graphic display. The main functions of the testing is to ensure that the temperature electronics **131** attached to the hydroxyl cells **120**, transferring compressor **140** and analogue pressure sensors **122** mounted on cells **120**, high-pressure tank **150** and the discharge side of regulator **160** used for control and monitoring, are working properly. the operator can then activate the Run Sequence of the program **75** via the start software button **280** in **Fig.2** on graphic display **95**.

During the initial startup phase of the system, the computer program will configure the system for the purge sequence. this sequence allows the vacuum pump **140** to draw down the hydroxyl cells **120** liquid trap **130** coupled to flow-restriction valve **135**, to remove all ambient air from them. Once the program has done this and detected no leaks in the system, it then prepares the system for gas production by switching the gas flow from cells **120** to high-pressure tank **150** and on to the output flashback protector **170**.

The program starts it's production sequence by turning on the cooling system pump **10** which is submerged in the liquid bath **30**, contained in vessel **20**. The cooling liquid is pumped through the cooling jacket **50** which is attached to the outside of cells **120**, through filter **45** and then through an air-cooled radiator **60**. Fans attached to the radiator are turned on for cooling.

Next, the computer turns on the dual three-phase power source **110**, which supplies operating power to the frequency, phase-shifting, signal amplitude and impedance-matching circuits coupled to the hydroxyl generating cells.

The result of this is just like the operation of a radio transmitter matching it's signal to the air via the antenna impedance. **Fig.3** shows the relationship of this configuration to arrays **132**, water bath **133** and Signals (**Fig.5** and **Fig.6**).

While the power source **110** is operating, the computer **70** is monitoring the pressure **122** and temperature **131** of hydroxyl cells **120**. When the cell pressure reaches a typical level of **5** pounds per square inch, the power source is turned off and compressor **140** is turned on the pump the gas into pressure tank **150**. When the pressure in the hydroxyl cells **120** is drawn down to near zero, the compressor is turned off and the power to the gas generating cells is turned back on again, to repeat the cycle.

The production cycle is repeated until tank **150** reaches a pressure of, typically, 80 psi, at which time the computer enables the output pressure regulator **160** which is typically set to operate at 40 psi, for the delivery of the hydroxyl gas to some external storage system or device. During this operation, the computer program handles all switching and displays the current status and any alerts or warning messages for the operator on the graphical display **95**.

Impedance-Matching Circuit 102:

The impedance-matching circuits **102** in **Fig.4**, convert the sinewave signals coming from the three-phase power source (**110** in **Fig.3**) into multi-polarity differential signals (**Fig.5**) which are applied to the triple wave-guide cluster arrays **132 A, 132B, 132C, 132D, 132E** and **132F** installed in cell **120**.

It is this converted signal, along with the phase relationship of the power source **110** and the triple wave-guide elements in cluster **132** submerged in water bath **133**, which produce the hydroxyl gases. It is important to note that not only is the gas produced between the elements in the array, but also between each array installed in the cell - see the phase relationship of array **A-B-C** shown in **Fig.3**. Also note that the array elements themselves are supplying many of the ions needed for the production of the gases.

Sequence of Hydroxyl Gas Generation:

Once the hydroxyl-generating cell **120** has been purged of ambient air and the production routing completed (**Fig.1**), the dual three-phase power source **110** is activated, supplying frequency, amplitude and phase signals to the impedance-matching circuitry **102**. The converted signals from **102** are then applied to cell array **132** for processing. It is the combination of the impedance-matching circuits signal transformations (as shown in **Fig.5** and **Fig.6**), the cell configuration and materials used in arrays **132**, and the rotational phase relationship between arrays **AD**, **BE** and **CF** and the submersion of these arrays in a bath of water **133**, that allows this system to produce large amounts of hydroxyl gases. The computer program 75 and it's graphic display **95**, is used by the operator to adjust the rate of gas production and set the upper limit to which the low-pressure cell **120** will charge.

After the cell **120** has reached its upper pressure cut-off limit (typically 5 psi), the power source **110** is turned off, enabling the compressor **140** to start its draw-down and transfer of the gases to the high-pressure tank **150**. When the pressure in the cell **120** reaches a low-level limit (near zero psi), **140** stops its charging cycle of **150**. Check valve **142** which is installed in **140**, prevents any back flow of gases to **120** from high-pressure tank **150**. The power source **110** is then turned back on to repeat the cycle. These charging cycles continue until the high-pressure tank **150** reaches it's upper pressure limit (typically 80 psi), at which point the hydroxyl production is stopped. As the gases in the high-pressure tank are being used or transferred to some external storage system, the pressure in **150** is monitored at the output of pressure-regulator **160**, until the low-pressure limit for this tank is reached (typically 40 psi). When this pressure level is reached, the hydroxyl gas production is started again.

During the operation of cell **120**, it's temperature is monitored to ensure that it does not exceed the "out of limits" conditions set by control **231** and monitored via the graphics display **95**. If the temperature exceed the limit set, then the gas production is stopped and the computer program alerts the operator, indicating the problem. The cooling system **30** which uses water jacket **50** surrounding cell **120**, helps to reduce the temperature and allows higher rates of gas production.

After extended running times, the water in cell **120** is replenished from bath **30** and filtered by **45**, to help control the operating impedance of the cell.

CLAIMS

1. The MLS-HFS information in this specification is the embodiment of the claims.

2. The system according to Claim 1 further enhances the production of hydroxyls based on the configuration of the hydroxyl gas-producing apparatuses of **Fig.3**.

3. The system according to Claim 1 further enhances the production of hydroxyls based on the configuration of the impedance-matching circuits of **Fig.4**.

4. The system according to Claim 1 further enhances the production of hydroxyls based on the application of the electrical signals shown in **Fig.5** applied to signal travelling wave-guides **132** submerged in a bath of water **133** installed in cell **120** and configured as depicted in **Fig.3**.

5. The system according to Claim 1 further enhances the production of hydroxyls based on the resonating action of the electrical signals depicted in **Fig.6**.

6. The system according to Claim 1 further enhances the production of hydroxyls based on the software program's ability to control the production of hydroxyl gases; controlling it's process limits, controlling it's storage and controlling it's delivery via operator controller **Fig.2**.

7. The software program **75** according to Claim 6, further enhances the safety of the production of hydroxyls based on the monitoring of high and low limits and either alerting the operator of the conditions and/or stopping the production on device failures via operator controller **Fig.2**.

8. The software according to Claim 6 further enhances the safety of the hydroxyls based on its ability to purge the system of ambient air before starting the production of hydroxyl gases.

Dr HENRY PUHARICH

Dr Andrija Puharich (who later changed his name to Henry Puharich) reportedly drove his motor home for hundreds of thousands of miles around North America in the 1970s using only water as fuel. At a mountain pass in Mexico, he collected snow for water. Here is an article which he wrote:

Cutting The Gordian Knot of the Great Energy Bind

by Andrija Puharich

Introduction

It is hardly necessary to weigh the value of the World Energy bank account for any sophisticated person, these days. It is grim. The oil reserves will dwindle away in a score of years or so, and the coal reserves will be gone in some twelve score years. This is not to say that the outlook is hopeless. There is an abundance of alternative energy sources, but the economics of development and exploitation present an enormous short-term strain on the world political and banking resources.

Visionary scientists tell us that the ideal fuel in the future will be as cheap as water, that it will be non-toxic both in its short-term, and in its long-term, effects, that it will be renewable in that it can be used over and over again, that it will be safe to handle, and present minimal storage and transportation problems and costs. And finally that it will be universally available anywhere on earth. What is this magical fuel, and why is it not being used? The fuel is water. It can be used in its fresh water form. It can be used in its salt water form. It can be used in its brackish form. It can be used in its snow and ice form. When such water is decomposed by electrolytic fission into hydrogen and oxygen gases, it becomes a high energy fuel with three times the energy output which is available from an equivalent weight of high grade gasoline.

Then why is water not being used as a fuel? The answer is simple - it costs too much with existing technology to convert water into hydrogen and oxygen gases. The basic cycle of using water for fuel is described in the following two equations, familiar to every high school student of Chemistry:

$$H_2O \text{ Electrolysis} + 249.68 \text{ BTU } \Delta G \rightarrow H_2 + (1/2)O_2 \text{ per mole of water.....(1)}$$

(1 mole = 18 gm). This means that it requires 249.688 BTU of energy (from electricity) to break water by electrolysis into the gases hydrogen and oxygen.

$$H_2 + (1/2)O_2 + \text{catalyst} \rightarrow H_2O - \Delta H \text{ 302.375 BTU per mole of water.....(2)}$$

This means that 302.375 BTU of energy (heat or electricity) will be released when the gases, hydrogen and oxygen, combine. The end product (the exhaust) from this reaction is water. Note that more energy (under ideal conditions) is released from combining the gases than is used to free them from water. It is know that under ideal conditions it is possible to get some 20% more energy out of reaction (2) above, then it takes to produce the gases of reaction (1) above. Therefore, if reaction (1) could be carried out at 100% efficiency, the release of energy from reaction (2) in an optimally efficient engine (such as a low temperature fuel cell), there would be a net energy profit which would make the use of water as a fuel an economically feasible source of energy .

The cost of producing hydrogen is directly related to the cost of producing electricity. Hydrogen as produced today is generally a by-product of off-peak-hour electrical production in either nuclear or hydroelectric plants. The electricity thus produced is the cheapest way of making hydrogen. We can compare the cost of production of electricity and the cost of producing hydrogen. The following table is adapted from Penner whose data source is based on Federal Power Commission, and American Gas Association Figures of 1970 and on a 1973 price evaluation (just before the OPEC oil price escalation.)

Table 1: Relative Prices in Dollars per 106 BTU

Cost Component	Electricity	Electrolytically-Produced H
Production	2.67 (b)	2.95 to 3.23 (b)
Transmission	0.61	0.52 (c)
Distribution	1.61	0.34
Total Cost	$4.89	$3.81 to $4.09

If we compare only the unit cost of production of electricity vs Hydrogen from the above table:

106 BTU H_2 / 106 BTU El = $3.23 / $2.67, or 20.9% higher cost, H_2

It must also be noted that the price of natural gas is much cheaper than either electricity or hydrogen, but because of the price fluctuations due to recent deregulation of gas it is not possible to present a realistic figure. In the opinion of Penner, if the hydrogen production cost component of its total cost could be reduced three fold, it would become a viable alternate energy source. In order to achieve such a three-fold reduction in production costs, several major breakthroughs would have to occur.

1. **Endergonic Reaction** A technological breakthrough which permits 100% conversion efficiency of water by electrolysis fission into the two gases, Hydrogen as fuel and Oxygen as oxidant.

2. **Hydrogen Production in Situ** A technological breakthrough which eliminates the need and cost of hydrogen liquefaction and storage, transmission, and distribution, by producing the fuel in situ, when and where needed.

3. **Exergonic Reaction** A technological breakthrough which yields a 100% efficient energy release from the combination of hydrogen and oxygen into water in an engine that can utilize the heat, steam, or electricity thus produced.

4. **Engine Efficiency** By a combination of the breakthroughs outlined above, 1, 2, and 3 utilized in a highly efficient engine to do work, it is theoretically possible to achieve a 15% to 20% surplus of energy return over energy input.

It is of interest to record that a new invention is now being developed to realise the above outlined goal of cheap, clean renewable and high grade energy. A Thermodynamic Device has been invented which produces hydrogen as fuel, and oxygen as oxidant, from ordinary water or from sea water, eliminating the cost and hazard of liquefaction, storage, transmission, and distribution. The saving of this aspect of the invention alone reduces the total cost of hydrogen by about 25%.

This Thermodynamic Device is based on a new discovery - the efficient electrolytic fission of water into hydrogen gas and oxygen gas by the use of low frequency alternating currents as opposed to the conventional use of direct current, or ultra-high frequency current today. Such gas production from water by electrolytic fission approaches 100% efficiency under laboratory conditions and measurements. No laws of physics are violated in this process.

This Thermodynamic Device has already been tested at ambient pressures and temperatures from sea level to an altitude of 10,000 feet above sea level without any loss of its peak efficiency. The device produces two types of gas bubbles; one type of bubble contains hydrogen gas; the other type contains oxygen gas. The two gases are thereafter easily separable by passive membrane filters to yield pure hydrogen gas, and pure oxygen gas.

The separate gases are now ready to be combined in a chemical fusion with a small activation energy such as that from a catalyst or an electrical spark, and yield energy in the form of heat, or steam, or electricity as needed. When the energy is released by the chemical fusion of hydrogen and oxygen, the exhaust product is clean water. The water exhaust can be released into nature and then renewed in its energy content by natural processes of evaporation, solar irradiation in cloud form, an subsequent precipitation as rain on land or sea, and then collected again as a fuel source. Or, the exhaust water can have its energy content pumped up by artificial processes such as through solar energy acting through photocells. Hence, the exhaust product is both clean and renewable. The fuel hydrogen, and the oxidant oxygen, can be used in any form of heat engine as an energy source if economy is not an important factor. But the practical considerations of maximum efficiency, dictate that a low temperature fuel cell with its direct chemical fusion conversion from gases to electricity offers the greatest economy and efficiency from small power plants of less than 5 kilowatts.

For large power plants, steam and gas turbines are the ideal heat engines for economy and efficiency. With the proper engineering effort, automobiles could be converted rather easily to use water as the main fuel source.

The Thermodynamic Device (“TD”) is made up of three principal components:
Component 1: An electrical function generator which energizes a water cell.
Component 2: The Thermodynamic Device
Component 3: A weak electrolyte.

Component 1: The Electrical Function Generator:

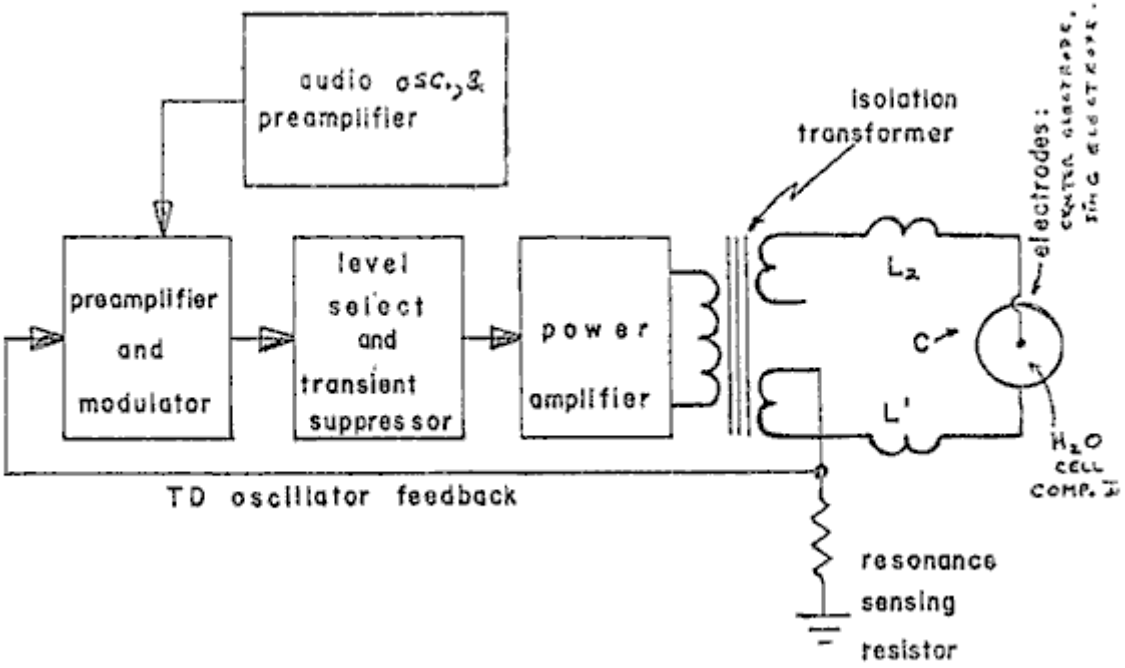

Figure 1: Signal Generator Component Block

This electronic device has a complex alternating current output consisting of an audio frequency (range 20 to 200 Hz) amplitude modulation of a carrier wave (range: 200 to 100,000 Hz). The output is connected by two wires to Component II at the center electrode, and at the ring electrode. See Fig.1. The impedance of this output signal is continuously being matched to the load which is the water solution in Component II.

Component 2: The Thermodynamic Device:

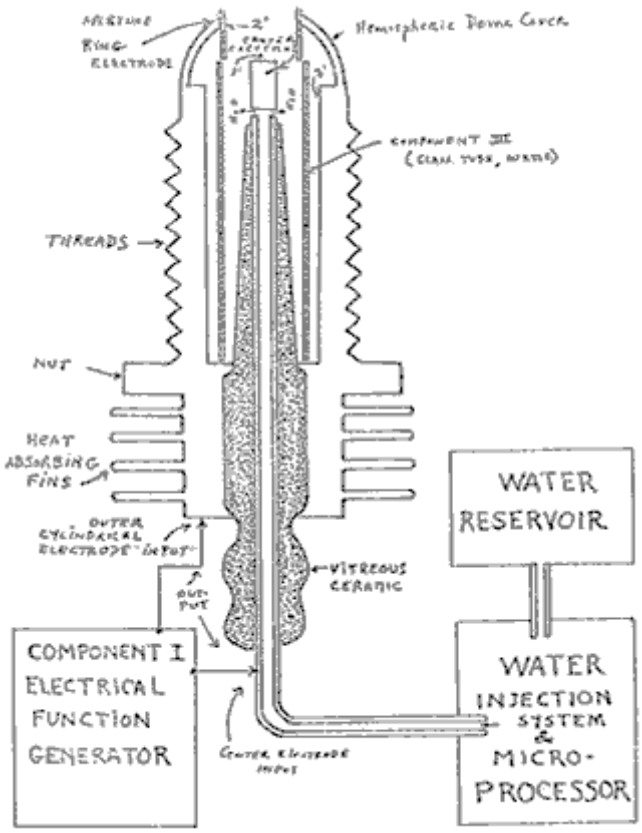

Figure 2: Thermodynamic Device

The TD is fabricated of metals and ceramic in the geometric form of a coaxial cylinder made up of a centered hollow tubular electrode which is surrounded by a larger tubular steel cylinder. These two electrodes comprise the coaxial electrode system energised by Component I. The space between the two electrodes is, properly speaking, Component III which contains the water solution to be electrolysed. The center hollow tubular electrode carries water into the cell, and is further separated from the outer cylindrical electrode by a porous ceramic vitreous material. The space between the two electrodes contains two lengths of tubular Pyrex glass, shown in Figures 2 and 3. The metal electrode surface in contact with the water solution are coated with a nickel alloy.

Component 3: The weak electrolyte water solution:

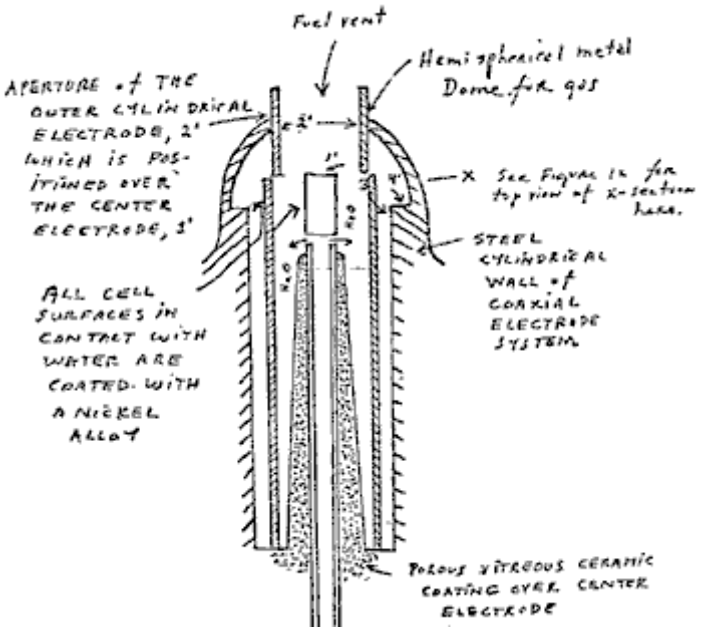

Figure 3: The Water Cell Section of Component 2

This consists of the water solution, the two glass tubes, and the geometry of the containing wall of Component 2. It is the true load for Component 1, and its electrode of Component 2.

The Component 3 water solution is more properly speaking, ideally a 0.1540 M Sodium Chloride solution, and as such, it is a weak electrolyte. In Figure 4 we show the hypothetical tetrahedral structure of water molecule, probably in the form in which the complex electromagnetic waves of Component 1 to see it. The center of mass of this tetrahedral form is the oxygen atom. The geometric arrangement of the p electrons of oxygen probably determine the vectors i (L1) and i (L2) and i (H1) and i (H2) which in turn probably determine the tetrahedral architecture of the water molecule. The p electron configuration of oxygen is shown in Figure 5. Reference to Figure 4, shows that the diagonal of the right side of the cube has at its corner terminations, the positive charge hydrogen (H+) atoms; and that the left side of the cube diagonal has at its corners, the lone pair electrons, (e-). It is to be further noted that this diagonal pair has an orthonormal relationship.

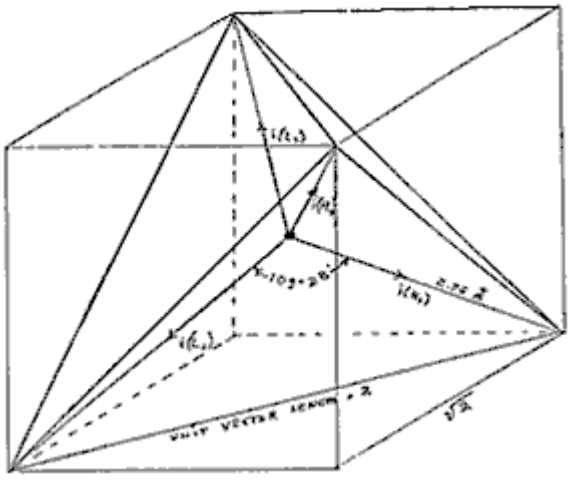

Figure 4: The Water Molecule in Tetrahedral Form:

Hydrogen bonding occurs only along the four vectors pointing to the four vertices of a regular tetrahedron, and in the above drawing we show the four unit vectors along these directions originating from the oxygen atoms at the center. i(H1) and i(H2) are the vectors of the hydrogen bonds formed by the molecule i as a donor molecule. These are assigned to the lone pair electrons. Molecules i are the neighboring oxygen atoms at each vertex of the tetrahedron.

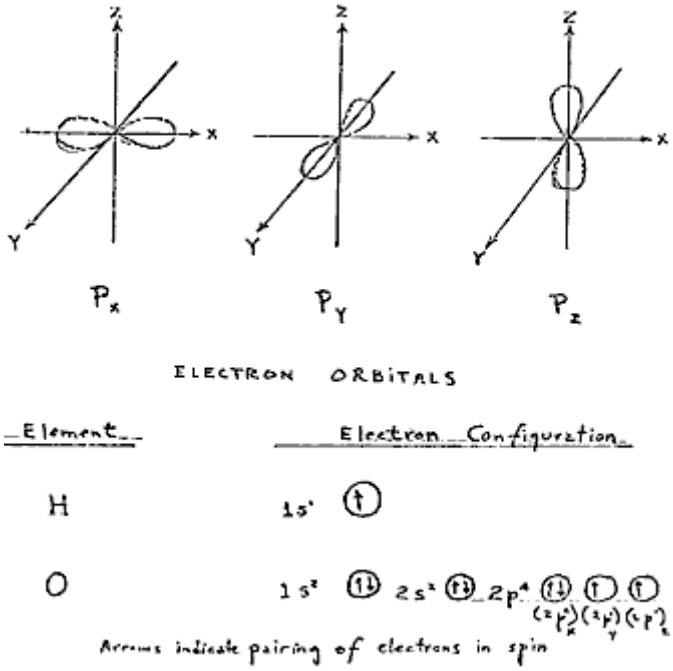

Figure 5: Electron Orbitals

3. Electrothermodynamics

We will now portray the complex electromagnetic wave as the tetrahedral water molecule sees it. The first effect felt by the water molecule is in the protons of the vectors, i (H1) and i (H2). These protons feel the 3-second cycling of the amplitude of the carrier frequency and its associated side bands as generated by Component 1. This sets up a rotation moment of the proton magnetic moment which one can clearly see on the XY plot of an oscilloscope, as an hysteresis loop figure. However, it is noted that this hysteresis loop does not appear in the liquid water sample until all the parameters of the three components have been adjusted to the configuration which is the novel basis of this device. The hysteresis loop gives us a vivid portrayal of the nuclear magnetic relaxation cycle of the proton in water.

The next effect felt by the water molecule is the Component 1 carrier resonant frequency, Fo. At the peak efficiency for electrolysis the value of Fo is 600 Hz +/- 5 Hz.

This resonance however is achieved through control of two other factors. The first is the molal concentration of salt in the water. This is controlled by measuring the conductivity of the water through the built-in current meter of Component 1. There is maintained an idea ratio of current to voltage where I/E = 0.01870 which is an index to the optimum salt concentration of 0.1540 Molal.

The second factor which helps to hold the resonant which helps to hold the resonant frequency at 600 Hz is the gap distance of Y, between the centre electrode, and the ring electrode of Component 2.

This gap distance will vary depending on the size scale of Component 2, but again, the current flow I, is used to set it to the optimal distance when the voltage reads between 2.30 (rms) volts, at resonance Fo, and at molal concentration, 0.1540. The molal concentration of the water is thus seen to represent the electric term of the water molecule and hence its conductivity.

The amplitude modulation of the carrier gives rise to side bands in the power spectrum of the carrier frequency distribution. It is these side bands which give rise to an acoustic vibration of the liquid water, and it is believed, also to the tetrahedral water molecule. The importance of the phonon effect - the acoustic vibration of water in electrolysis - was discovered in a roundabout way. Research work with Component 1 had earlier established that it could be used for the electro-stimulation of hearing in humans. When the output of Component 1 is comprised of flat circular metal plates applied to the head of normal hearing humans, it was found that they could hear pure tones and speech. Simultaneously, acoustic vibration could also be heard by an outside observer with a stethoscope placed near one of the electrodes on the skin. It was observed that the absolute threshold of hearing could be obtained at 0.16 mW (rms), and by calculation that there was an amplitude of displacement of the eardrum of the order of 10^{-11} meter and a corresponding amplitude of the cochlear basilar membrane of 10^{-13}

meter. Corollary to this finding, I was able to achieve the absolute reversible threshold of electrolysis at a power level of 0.16 mW (rms). By carrying out new calculations, I was able to show that the water was being vibrated with a displacement of the order of 1 Angstrom unit (= 10^{-10} meters). This displacement is of the order of the diameter of the hydrogen atom. Thus it is possible that the acoustic phonons generated by audio side bands of the carrier are able to vibrate particle structures within the unit water tetrahedron.

We now turn to the measurement problem with respect to efficiency of electrolysis. There are four means which can be used to measure the reactant product of water electrolysis. For simple volume measurements, one can use a precision nitrometer such as the Pregl type. For both volume and quantitative analysis one can use the gas chromatography with thermal conductivity detector. For a continuous flow analysis of both volume and gas species the mass spectrometer is very useful. For pure thermodynamic measurements the calorimeter is useful. In our measurements, all four methods were examined, and it was found that the mass spectrometer gave the most flexibility and the greatest precision. In the next section we will describe our measurement using the mass spectrometer.

Protocol

4. Methodology for the Evaluation of the Efficiency of Water Decomposition by Means of Alternating Current Electrolysis

Introduction

All systems used today for the electrolysis of water into hydrogen as fuel, and oxygen as oxidant apply direct current to a strong electrolyte solution. These systems range in efficiency from 50% to 71%. The calculation of energy efficiency in electrolysis is defined as follows:

"The energy efficiency is the ratio of the energy released from the electrolysis products formed (when they are subsequently used) to the energy required to effect electrolysis."

The energy released by the exergonic process under standard conditions is

$H_2(g) + (1/2)\ O_2(g) \rightarrow H_2O = 3\ 02.375$ BTU

which is 68.315 Kcal/mol. or, 286,021 Joules/mol, and is numerically equal to the enthalphy charge (ΔH) for the indicated process. On the other hand, the minimum energy (or useful work input) required at constant temperature and pressure for electrolysis equals the Gibbs free energy change (ΔG).

Penner shows that there is a basic relation derivable from the first and second laws of thermodynamics for isothermal changes which shows that

$\Delta G = \Delta H - T\ \Delta S$ ..... (2)

where ΔS represents the entropy change for the chemical reaction and T is the absolute temperature.

The Gibbs free energy change (ΔG) is also related to the voltage (e) required to implement electrolysis by Faraday's equation:

$e = (\Delta G / 23.06\ n)$ volts ..... (3)

where ΔG is in Kcal/mol, and n is the number of electrons (or equivalents) per mole of water electrolysed and has the numerical value 2 in the equation (endergonic process),

$H_2O \rightarrow H_2\ (g) + (1/2)O_2\ (g) + 56.620$ kcal or + 249.68 BTU ..... (4)

Therefore, according to equation (2) at atmospheric pressure, and $300^{O}K$:
$\Delta H = 68.315$ kcal/mol of H_2O, and
$\Delta G = 56.620$ kcal / mol of $H_2O = 236{,}954$ J/mol H_2O for the electrolysis of liquid water.

In view of these thermodynamic parameters for the electrolysis of water into gases, hydrogen and oxygen, we can establish by Eq.(2) numeric values where,

$\Delta G = 236.954$ J/mol H_2O under standard conditions. Thus

$n = \Delta G\ (J/mol) / \Delta Ge\ (J/mol) = <1$ ..... (5)

where ΔGe is the electrical energy input to H_2O (1) in Joules, and ΔG is the Gibbs free energy of H_2O. The conversion between the two quantities is one Watt second (Ws) = one Joule.

Or, in terms of gas volume, as hydrogen, produced and measured,

$n =$ Measured H_2 (cc) / Ideal H_2 (cc) = <1 ..... (6)

In accordance with these general principles we present the methodology followed in evaluating the electrolytic of alternating current on H_2O in producing the gases, hydrogen and oxygen. No attempt has been made to utilize these gases according to the process of Eq.(1). It is to be noted that the process

$H_2\ (g) + (1/2)O_2\ (g) \rightarrow H_2O\ (g)$ ..... (7)

yields only 57.796 kcal /mol. Eq.(7) shows that per mole of gases water formed at 300^OK, the heat released is reduced from the 68.315 kcal/mol at Eq. (1) by the molar heat of evaporation of water at 300^OK (10.5 kcal) and the overall heat release is 57.796 kcal/mol if H_2O (g) is formed at 300^OK.

In the following sections we describe the new method of electrolysis by means of alternating current, and the exact method and means used to measure the endergonic process of Eq.(4) and the governing Eq.(2) and Eq.(5).

5. Thermodynamic Measurement

In order to properly couple Component 2 to a mass spectrometer, one requires a special housing around Component 2 which will capture the gases produced, and permit these to be drawn under low vacuum into the mass spectrometer. Therefore a stainless steel and glass chamber was built to contain Component 2, and provision made to couple it directly through a CO_2 water-trap to the mass spectrometer with the appropriate stainless steel tubing. This chamber is designated as Component 4. Both the mass spectrometer and Component 4 were purged with helium and evacuated for a two hour period before any gas samples were drawn. In this way, contamination was minimized. The definitive measurement were done at Gollob Analytical Services in Berkeley Heights, New Jersey.

We now describe the use of Component 1 and how its energy output to Component 2 is measured. The energy output of Component 1 is an amplitude-modulated alternating current looking into a highly non-linear load, i.e., the water solution. Component 1 is so designed that at peak load it is in resonance across the system (Components 1, 2, and 3) and the vector diagrams show that the capacitive reactance, and the inductance reactance are almost exactly 180^O out of phase with each other, and so the net power output is reactive (the dissipative power is very small). This design ensures minimum power losses across the entire output system. In the experiments to be described, the entire emphasis is placed on achieving the maximum gas yield (credit) in exchange for the minimum applied electrical energy.

The most precise way to measure the applied energy from Component 1 to Component 2 and Component 3, is to measure the power, P, in watts, W. Ideally this should be done with a precision wattmeter, but since we were interested in following the voltage and current separately, it was decided not to use the watt meter. Separate meters were used to continuously monitor the current and the volts.

This is done by precision measurement of the volts across Component 3 as root mean square (rms) volts; and the current flowing in the system as rms amperes. Precisely calibrated instruments were used to take these two measurements. A typical set of experiments using water in the form of 0.9% saline solution 0.1540 molar to obtain high efficiency hydrolysis gave the following results:

rms Current = I = 25mA to 38 mA (0.025 A to 0.038 A.)

rms Volts = E = 4.0 Volts to 2.6 Volts

The resultant ration between current and voltage is dependent on many factors such as the gap distance between the center and ring electrodes, dielectric properties of the water, conductivity properties of the water, equilibrium states, isothermal conditions, materials used, and even the pressure of clathrates. The above current and voltage values reflect the net effect of various combinations of such parameters. When one takes the product of rms current, and rms volts, one has a measure of the power, P in watts.

P = I x E = 25 mA x 4.0 volts =100 mW (0.1 W)

and P = I x E =38 mA x 2.6 volts = 98.8 mW (0.0988 W)

At these power levels (with load), the resonant frequency of the system is 600 Hz (plus or minus 5 Hz) as measured on a precision frequency counter. The waveform was monitored for harmonic content on an oscilloscope, and the nuclear magnetic relaxation cycle was monitored on an XY plotting oscilloscope in order to maintain the proper hysteresis loop figure. All experiments were run so that the power in watts, applied through Components 1, 2, and 3 ranged between 98.8 mW to 100 mW.

Since by the International System of Units 1971 (ST), one Watt-second (Ws) is exactly equal to one Joule (J), our measurements of efficiency used these two yardsticks (1 Ws = 1J) from the debit side of the measurement.

The energy output of the system is, of course, the two gases, Hydrogen (H_2) and Oxygen, $(1/2)O_2$, and this credit side was measured in two laboratories, on two kinds of calibrated instruments, namely gas chromatography machine, and mass spectrometer machine.

The volume of gases H_2 and $(1/2)O_2$ was measured as produced under standard conditions of temperature and pressure in unit time, i.e., in cubic centimeters per minute (cc/min), as well as the possibility contaminating gases, such as air oxygen, nitrogen and argon, carbon monoxide, carbon dioxide, water vapor, etc.

The electrical and gas measurements were reduced to the common denominator of Joules of energy so that the efficiency accounting could all be handled in one currency. We now present the averaged results from many experiments. The standard error between different samples, machines, and locations is at +/- 10%, and we only use the mean for all the following calculations.

2. Thermodynamic Efficiency for the Endergonic Decomposition of Liquid Water (Salininized) to Gases Under Standard Atmosphere (754 to 750 mm. Hg) and Standard Isothermal Conditions @ $25^{O}C = 77^{O}F = 298.16^{O}K$, According to the Following Reaction:

$H_20\ (1) \rightarrow H_2(g) + (1/2)O_2(1) + \Delta G = 56.620$ Kcal /mole ..... (10)

As already described, ΔG is the Gibbs function. We convert Kcal to our common currency of Joules by the formula, One Calorie = 4.1868 Joules

$\Delta G = 56.620$ Kcal x 4.1868 J = 236,954/J/mol of H_2O where 1 mole = 18 gr. ..... (11)

ΔGe = the electrical energy required to yield an equivalent amount of energy from H_2O in the form of gases H_2 and $(1/2)O_2$.

To simplify our calculation we wish to find out how much energy is required to produce the 1.0 cc of H_2O as the gases H_2 and $(1/2)O_2$. There are (under standard conditions) 22,400 cc = V of gas in one mole of H_2O. Therefore

$\Delta G / V =$ 236,954 J / 22,400 cc = 10.5783 J/cc. ..... (12)

We now calculate how much electrical energy is required to liberate 1.0 cc of the H_2O gases (where H_2 = 0.666 parts, and $(1/2)O_2$ = 0.333 parts by volume) from liquid water. Since P = 1 Ws = 1 Joule , and V = 1.0 cc of gas = 10.5783 Joules, then

PV = 1 Js x 10.5783 J = 10.5783 Js, or, = 10.5783 Ws ..... (13)

Since our experiments were run at 100 mW (0.1 W) applied to the water sample in Component II, III, for 30 minutes, we wish to calculate the ideal (100% efficient) gas production at this total applied power level. This is,

0.1 Ws x 60 sec x 30 min = 180,00 Joules (for 30 min.). The total gas production at ideal 100% efficiency is 180 J/10.5783 J/cc = 17.01 cc H_2O (g)

We further wish to calculate how much hydrogen is present in the 17.01 cc H_2O (g).

17.01 cc H_2O (g) x 0.666 H_2 (g) = 11.329 cc H_2 (g) ..... (14)

17.01 cc H_2O (g) x 0.333 $(1/2)O_2$ (g) = 5.681 cc $(1/2)O_2$ (g)

Against this ideal standard of efficiency of expected gas production, we must measure the actual amount of gas produced under: (1) Standard conditions as defined above, and (2) 0.1 Ws power applied over 30 minutes. In our experiments, the mean amount of H_2 and (1/2)O_2 produced, as measured on precision calibrated GC, and MS machines in two different laboratories, where SE is +/- 10%, is,

Measured Mean = 10.80 cc H_2 (g)
Measured Mean = 5.40 cc (1/2) cc (1/2)O_2 (g)
Total Mean = 16.20 cc H_2O (g)

The ratio, n, between the ideal yield, and measured yield,

Measured H_2 (g) / Ideal H_2 (g) = 10.80 cc / 11.33 cc = 91.30%

6. Alternative Method for Calculating Efficiency Based on the Faraday Law of Electrochemistry

This method is based on the number of electrons that must be removed, or added to decompose, or form one mole of, a substance of valence one. In water (H_2O), one mole has the following weight:

H = 1.008 gr /mol
H = 1.008 gr /mol
O = 15.999 gr/mol
Thus, 1 mol H_2O = 18.015 gr/mol

For a univalent substance, one gram/mole contains 6.022 x 10-23 electrons = N = Avogadro's Number. If the substance is divalent, trivalent, etc., N is multiplied by the number of the valence. Water is generally considered to be of valence two.

At standard temperature and pressure ("STP") one mole of a substance contains 22.414 cc, where Standard temperature is 273.15^{O}K = 0^{O}C = T . Standard Pressure (one atmosphere) = 760 mm Hg = P.

One Faraday ("F") is 96,485 Coulombs per mole (univalent).

One Coulomb ("C") is defined as:

1 N / 1 F = 6.122 x 10^{23} Electrons / 96,485 C = one C

The flow of one C/second = one Ampere.
One C x one volt = one Joule second (Js).
One Ampere per second @ one volt = one Watt = one Joule.

In alternating current, when amps (I) and Volts (E) are expressed in root mean squares (rms), their product is Power in watts.

P = IE watts (Watts = Amps x Volts).

With these basic definitions we can now calculate efficiency of electrolysis of water by the method of Faraday's electrochemistry.

The two-electron model of water requires 2 moles of electrons for electrolysis (2 x 6.022 x 10^{23}), or two Faraday quantities (2 x 96,485 = 192,970 Coulombs).

The amount of gas produced will be:

H_2 = 22,414 cc /mol at STP
(1/2)O_2 = 11,207 cc / mol at STP
Gases = 33.621 cc / mol H_2O (g)

The number of coulombs required to produce one cc of gases by electrolysis of water:

193,970 C / 33621 C = 5.739567 C per cc gases.

Then, 5,739 C /cc /sec = 5.739 amp/sec/cc. How many cc of total gases will be produced by 1 A/sec?

0.1742291709 cc.

How many cc of total gases will be produced by 1 A/min ?

10.45375 cc/min

What does this represent as the gases H_2 and O_2 ?

$(1/2)O_2$ = 3.136438721 cc/Amp/min.
H_2 = 6.2728 cc/Amp /min.

We can now develop a Table for values of current used in some of our experiments, and disregarding the voltage as is done conventionally.

1. Calculations for 100 mA per minute:
Total Gases = 1.04537 cc/min
H_2 = 0.6968 cc/min
$(1/2)O_2$ = 0.3484 cc/min
30 min. H_2 = 20.9054 cc/ 30 minutes

2. Calculations for 38 mA per minute:
Total Gases = 0.3972 cc/ 30 minutes
H_2 = 0.2645 cc/min
$(1/2)O_2$ = 0.1323 cc/min
30 min. H_2 = 7.9369 cc/min

3. Calculations for 25mA per minute:
30 min. H_2 = 5.2263 cc/ minute

7. Conclusion

Fig.6 and Fig.7 [not available] show two of the many energy production systems that may be configured to include renewable sources and the present electrolysis technique. Figure 6 shows a proposed photovoltaic powered system using a fuel cell as the primary battery. Assuming optimum operating conditions using 0.25 watt seconds of energy from the photovoltaic array would enable 0.15 watt-seconds to be load.

Figure 7 depicts several renewable sources operating in conjunction with the electrolysis device to provide motive power for an automobile.

****

US Patent 4,394,230 DATE 19th July 1983 INVENTOR: HENRY K. PUHARICH

METHOD AND APPARATUS FOR SPLITTING WATER MOLECULES

This is a re-worded extract from the United States Patent number 4,394,230. It describes how Henry Puharich was able to split water into hydrogen and oxygen gasses by a process which used very little input power.

ABSTRACT

Disclosed herein is a new and improved thermodynamic device to produce hydrogen gas and oxygen gas from ordinary water molecules or from seawater at normal temperatures and pressure. Also disclosed is a new and improved method for electrically treating water molecules to decompose them into hydrogen gas and oxygen gas at efficiency levels ranging between approximately 80-100%. The evolved hydrogen gas may be used as a fuel; and the evolved oxygen gas may be used as an oxidant.

Inventors: Puharich; Henry K. (Rte. 1, Box 97, Delaplane, VA 22025)

BACKGROUND OF THE INVENTION

The scientific community has long realised that water is an enormous natural energy resource, indeed an inexhaustible source, since there are over 300 million cubic miles of water on the earth's surface, all of it a potential source of hydrogen for use as fuel. In fact, more than 100 years ago Jules Verne prophesied that water eventually would be employed as a fuel and that the hydrogen and oxygen which constitute it would furnish an inexhaustible source of heat and light.

Water has been split into its constituent elements of hydrogen and oxygen by electrolytic methods, which have been extremely inefficient, by thermochemical extraction processes called thermochemical water-splitting, which have likewise been inefficient and have also been inordinately expensive, and by other processes including some employing solar energy. In addition, artificial chloroplasts imitating the natural process of photosynthesis have been used to separate hydrogen from water utilising complicated membranes and sophisticated artificial catalysts. However, these artificial chloroplasts have yet to produce hydrogen at an efficient and economical rate.

These and other proposed water splitting techniques are all part of a massive effort by the scientific community to find a plentiful, clean, and inexpensive source of fuel. While none of the methods have yet proved to be commercially feasible, they all share in common the known acceptability of hydrogen gas as a clean fuel, one that can be transmitted easily and economically over long distances and one which when burned forms water.

SUMMARY OF THE PRESENT INVENTION

In classical quantum physical chemistry, the water molecule has two basic bond angles, one angle being 104°, and the other angle being 109°28'. The present invention involves a method by which a water molecule can be energised by electrical means so as to shift the bond angle from the 104° degree. configuration to the 109° degree 28' tetrahedral geometrical configuration.

An electrical function generator (Component 1) is used to produce complex electrical wave form frequencies which are applied to, and match the complex resonant frequencies of the tetrahedral geometrical form of water. It is this complex electrical wave form applied to water which is contained in a special thermodynamic device (Component II) which shatters the water molecule by resonance into its component molecules --- hydrogen and oxygen.

The hydrogen, in gas form, may then be used as fuel; and oxygen, in gas form is used as oxidant. For example, the thermodynamic device of the present invention may be used as a hydrogen fuel source for any existing heat engine --- such as, internal combustion engines of all types, turbines, fuel cell, space heaters, water heaters, heat exchange systems, and other such devices. It can also be used for the desalination of sea water, and other water purification purposes. It can also be applied to the development of new closed cycle heat engines where water goes in as fuel, and water comes out as a clean exhaust.

For a more complete understanding of the present invention and for a greater appreciation of its attendant advantages, reference should be made to the following detailed description taken in conjunction with the accompanying drawings.

DESCRIPTION OF THE DRAWINGS:

Fig.1 is a schematic block diagram illustrating the electrical function generator, Component I, employed in the practice of the present invention:

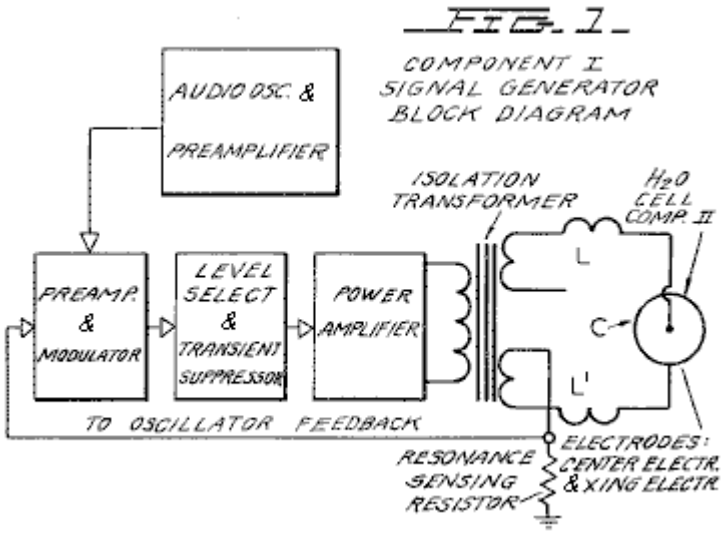

Fig.2 is a schematic illustration of the apparatus of the present invention, including a cross sectional representation of the thermodynamic device, Component II:

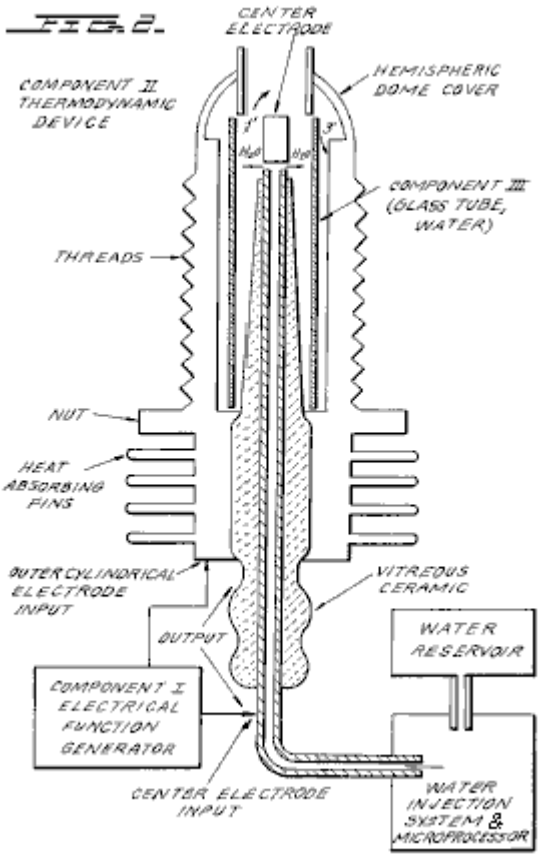

Fig.3 is a cross-sectional view of Component III of the present invention, the water cell section of Component II:

FIG. 3.

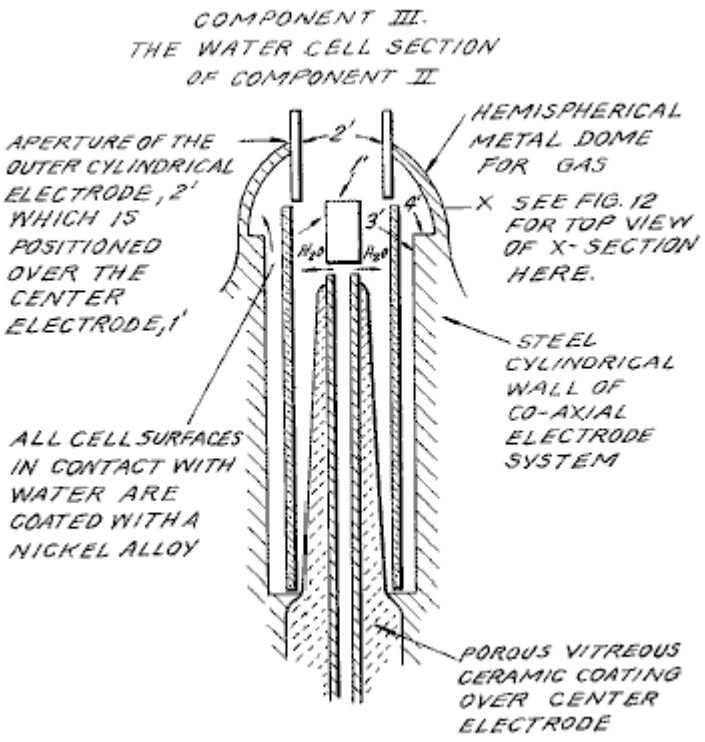

Fig.4 is an illustration of the hydrogen covalent bond:

FIG. 4.

Fig.4A is an illustration of the hydrogen bond angle:

FIG. 4A.

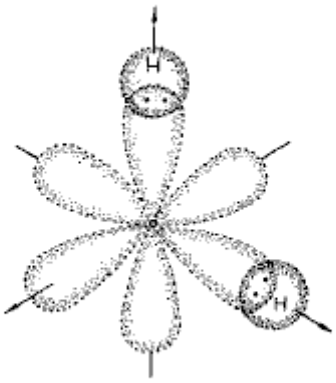

UNHYBRIDIZED ORBITAL INTERACTION IN WATER BOND ANGLE IS 104° RATHER THAN 90° AS PREDICTED

Fig.4B is an illustration of hybridised and un-hybridised orbitals:

FIG. 4B.

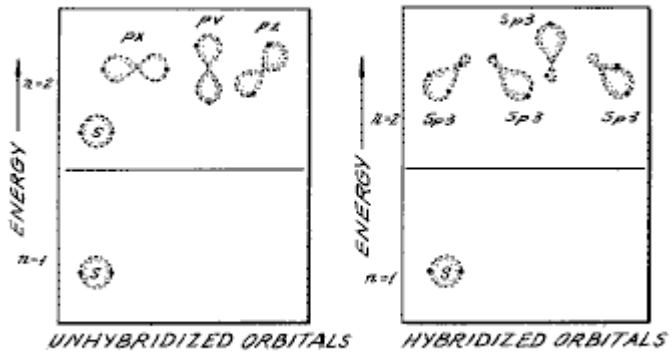

FORMATION OF sp3 HYBRID ORBITALS

Fig.4C is an illustration of the geometry of methane ammonia and water molecules:

FIG. 4C.

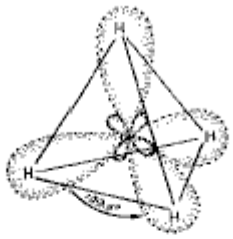

HYBRIDIZED METHANE MOLECULE CH_4

HYBRIDIZED AMMONIA MOLECULE NH_3

HYBRIDIZED WATER MOLECULE H_2O

GEOMETRY OF METHANE,
AMMONIA, AND WATER MOLECULES

Fig.5 is an illustration of an amplitude modulated carrier wave:

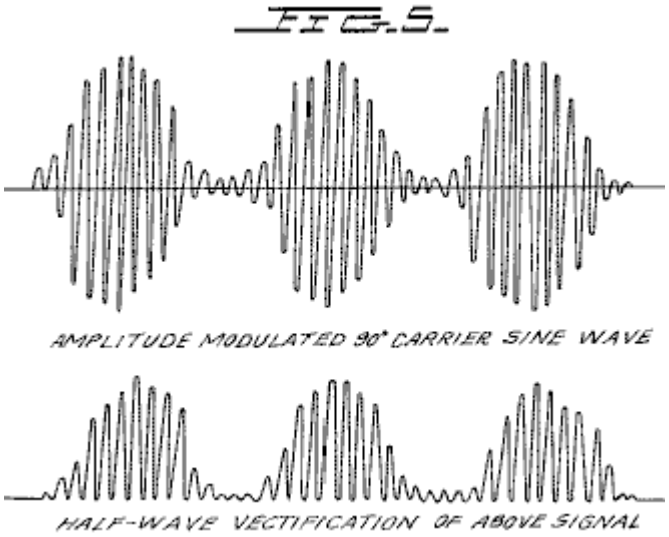

Fig.6 is an illustration of a ripple square wave:

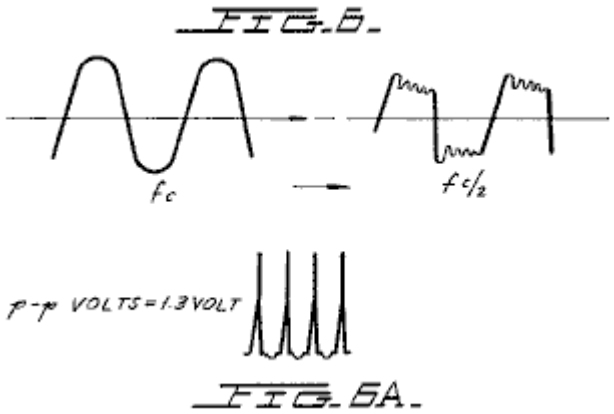

Fig.6A is an illustration of unipolar pulses.

Fig.7 is a diagram showing ion distribution at the negative electrode:

FIG. 7

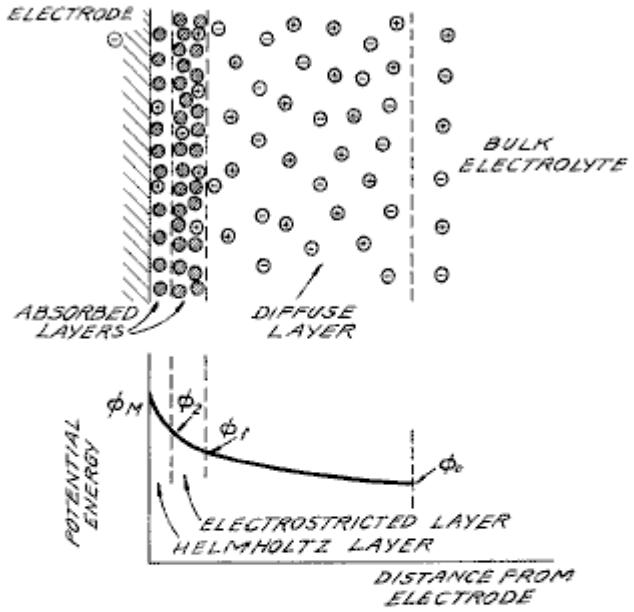

DIAGRAM OF THE DOUBLE LAYER CLOSE TO A NEGATIVE ELECTRODE. THE POTENTIAL ENERGY OF POSITIVE IONS IN THIS REGION WHEN NO CURRENT IS FLOWING IS SHOWN IN THE LOWER DIAGRAM. $\phi_M - \phi_2$ IS THE ELECTRON TRANSFER POTENTIAL: $\phi_2 - \phi_1$ IS RELATED TO THE ACTIVATION OVERPOTENTIAL: AND $\phi_1 - \phi_o$ IS RELATED TO THE DIFFUSION OVERPOTENTIAL.

KEY
- SOLVENT MOLECULE = H_2O
- POSITIVE ION = H^+
- NEGATIVE ION = O^-

Fig.8 is an illustration of tetrahedral bonding orbitals:

FIG.8.

EQUIVALENT TETRAHEDRAL
BONDING ORBITALS OF WATER

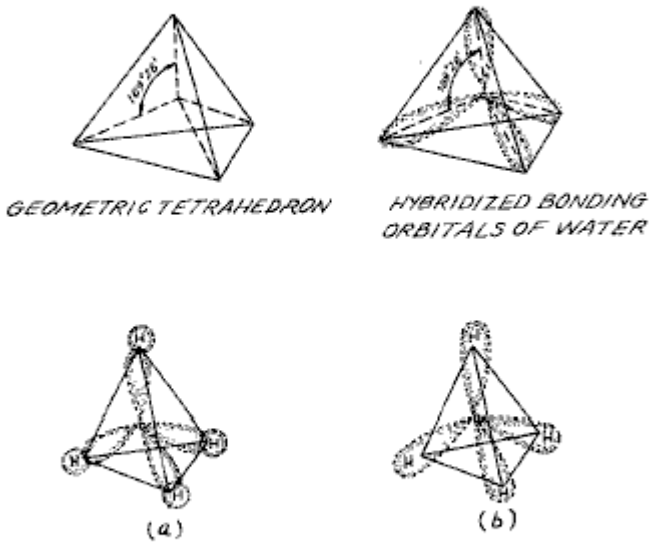

METHANE OVERLAP OF SPHERICAL
1s ORBITAL OF HYDROGEN WITH
sp3 BONDING ORBITALS OF CARBON
(a) RESULTS IN EQUIVALENT SIGMA
BONDS, THE MOLECULAR ORBITALS
OF (b).

Fig.9 is an illustration of water molecules:

FIG.9.

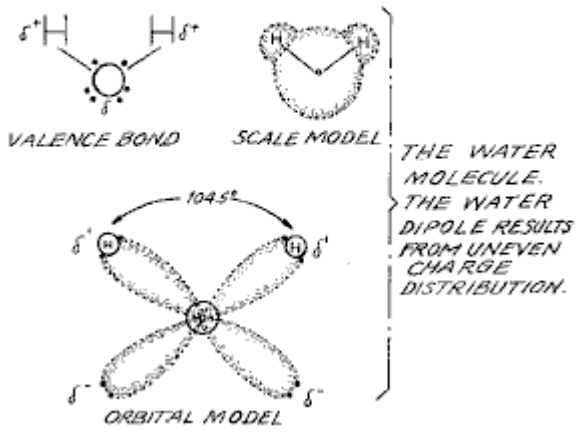

Fig.10 is an illustration of productive and non-productive collisions of hydrogen with iodine:

FIG. 10.

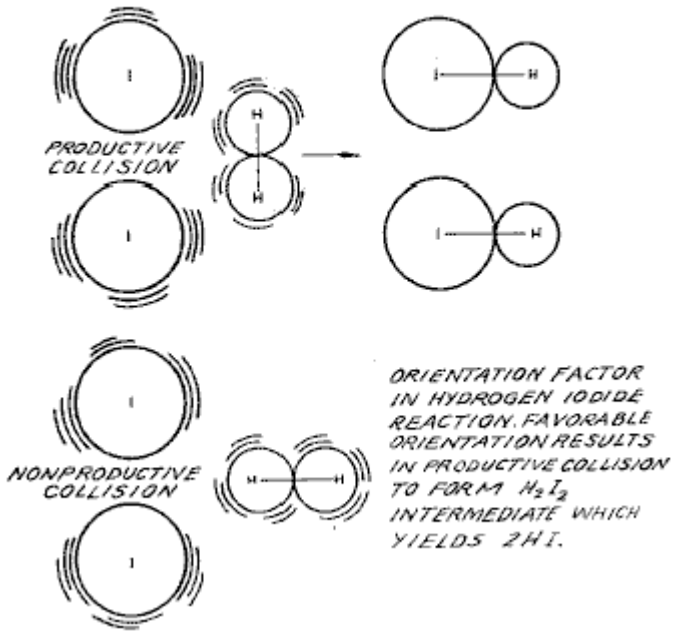

Fig.11 is a wave form found to be the prime characteristic for optimum efficiency:

FIG. 11.

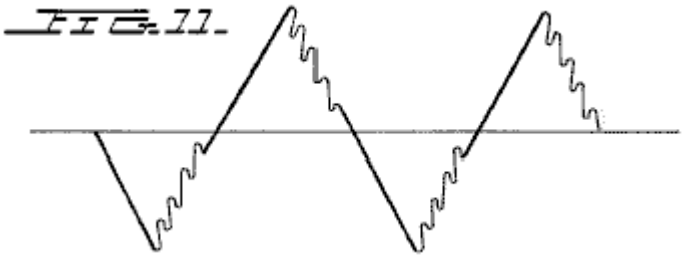

Fig.12 is an illustration of pearl chain formation:

FIG. 12.

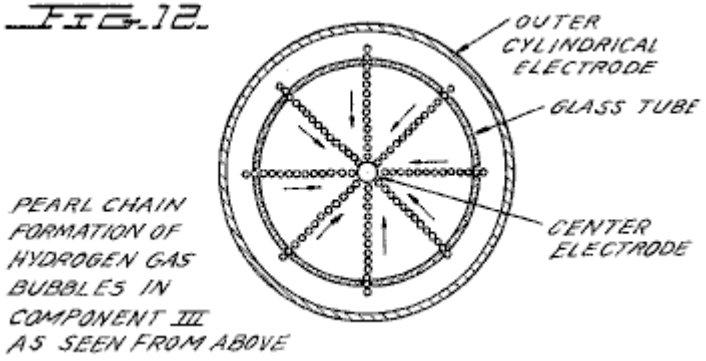

Fig.13 is a plot of the course of the onset of the barrier effect and the unblocking of the barrier effect:

FIG. 13.

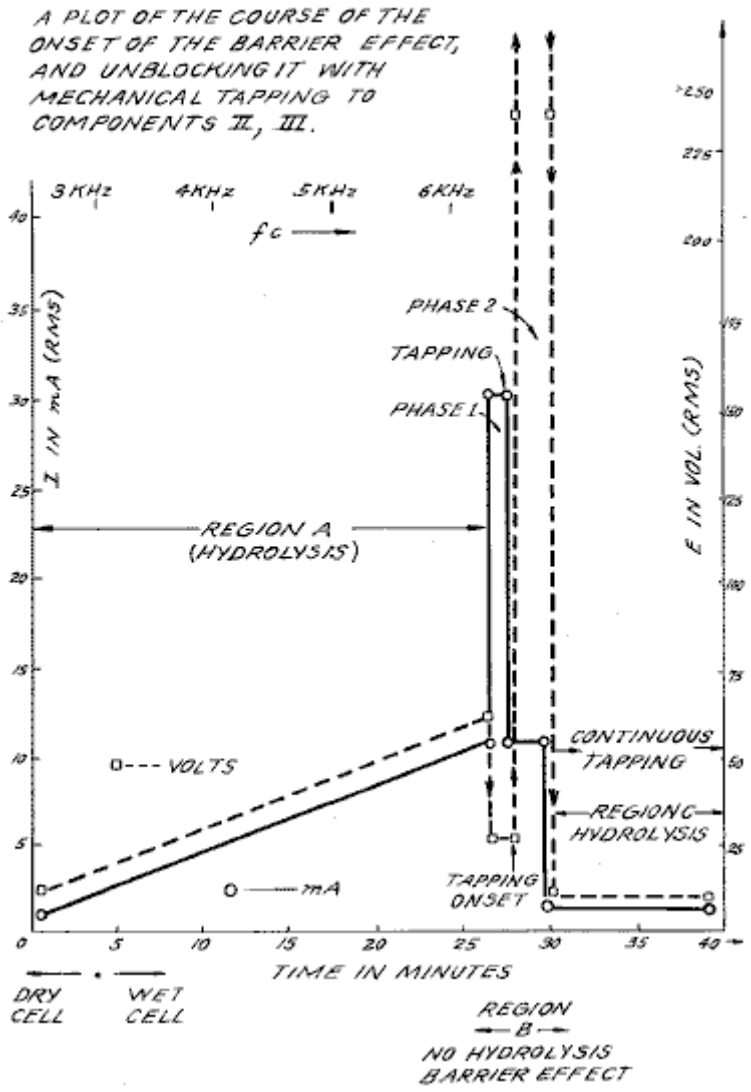

Figs.14A, B, and C are energy diagrams for exergonic reactions:

FIG. 14A.

(a) AN EXERGONIC REACTION. PRODUCTS HAVE A LOWER POTENTIAL ENERGY THAN REACTANTS, THEREFORE, ENERGY IS RELEASED.

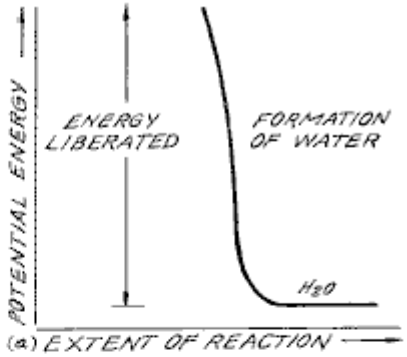

FIG. 14B.

(b) AN ENDERGONIC REACTION PRODUCTS HAVE A HIGHER POTENTIAL ENERGY THAN REACTANTS, CAUSING ENERGY TO BE CONSUMED.

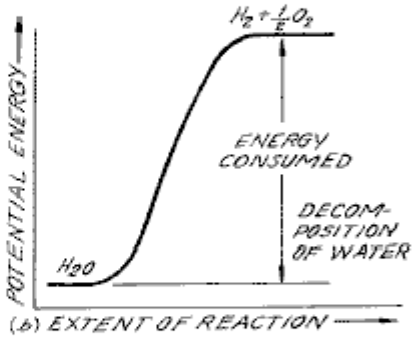

FIG. 14C.

ENERGY DIAGRAM FOR EXERGONIC REACTION. ACTIVATION ENERGY IS BARRIER TO BE OVERCOME FOR REACTION TO PROCEED, ℰ IS SUPPLIED AS A "SPARK" TO THE GASES TO GET IGNITION.

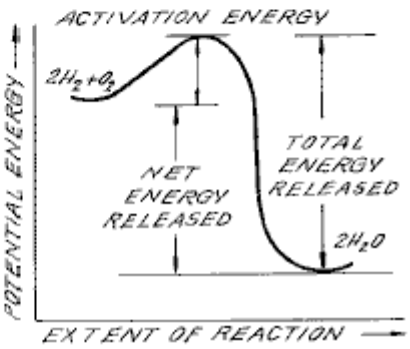

DETAILED DESCRIPTION OF INVENTION:

Section 1:
Apparatus of Invention;
The apparatus of the invention consists of three components, the Electrical Function Generator, the Thermodynamic Device, and the Water Cell.

Component I: The Electrical Function Generator;
This device has an output consisting of an audio frequency (range 20 to 200 Hz) amplitude modulation of a carrier wave (range 200 Hz to 100,000 Hz). The impedance of this output signal is continuously being matched to the load which is the second component, the thermodynamic device. The electrical function generator represents a novel application of circuitry disclosed in my earlier U.S. Pat. Nos. 3,629,521; 3,563,246; and 3,726,762, which are incorporated by reference herein. See **Fig.1** for the block diagram of Component I.

Component II: The Thermodynamic Device;
The thermodynamic device is fabricated of metals and ceramic in the geometric form of coaxial cylinder made up of a central hollow tubular electrode which is surrounded by a larger tubular steel cylinder, said two electrodes comprising the coaxial electrode system which forms the load of the output of the electrical function generator, Component I. Said central hollow tubular electrode carries water, and is separated from the outer cylindrical electrode by a porous ceramic vitreous material. Between the outer surface of the insulating ceramic vitreous material, and the inner surface of the outer cylindrical electrode exists a space to contain the water to be electrolysed. This water cell space comprises the third component (Component III) of the invention. It contains two lengths of tubular Pyrex glass, shown in **Fig.2** and **Fig.3**. The metal electrode surfaces of the two electrodes which are in contact with the water are coated with a nickel alloy.

The coaxial electrode system is specifically designed in materials and geometry to energise the water molecule to the end that it might be electrolysed. The central electrode is a hollow tube and also serves as a conductor of water to the Component III cell. The central tubular electrode is coated with a nickel alloy, and surrounded with a porous vitreous ceramic and a glass tube with the exception of the tip that faces the second electrode. The outer cylindrical electrode is made of a heat conducting steel alloy with fins on the outside, and coated on the inside with a nickel alloy. The central electrode, and the cylindrical electrode are electrically connected by an arching dome extension of the outer electrode which brings the two electrodes at one point to a critical gap distance which is determined by the known quenching distance for hydrogen. See **Fig.2** for an illustration of Component II.

Component III: The Water Cell;
The water cell is a part of the upper end of Component II, and has been described. An enlarged schematic illustration of the cell is presented in FIG. 3. The Component III consists of the water and glass tubes contained in the geometrical form of the walls of cell in Component II, the thermodynamic device. The elements of a practical device for the practice of the invention will include:
(A) Water reservoir; and salt reservoir; and/or salt

(B) Water injection system with microprocessor or other controls which sense and regulate (in accordance with the parameters set forth here:
a. Carrier frequency
b. Current
c. Voltage
d. RC relaxation time constant of water in the cell
e. Nuclear magnetic relaxation constant of water
f. Temperature of hydrogen combustion
g. Carrier wave form
h. RPM of an internal combustion engine (if used)
i. Ignition control system
j. Temperature of region to be heated;

(C) An electrical ignition system to ignite the evolved hydrogen gas fuel.
The important aspects of Component III are the tubular vitreous material, the geometry of the containing walls of the cell, and the geometrical forms of the water molecules that are contained in the cell. A further important aspect of the invention is the manipulation of the tetrahedral geometry of the water molecule by the novel methods and means which will be more fully described in the succeeding sections of this specification.

The different parts of a molecule are bound together by electrons. One of the electron configurations which can exist is the covalent bond which is achieved by the sharing of electrons. A molecule of hydrogen gas, H_2 is the smallest representative unit of covalent bonding, as can be seen in **Fig.4**. The molecule of hydrogen gas is formed by the overlap and pairing of 1s orbital electrons. A new molecular orbit is formed in which the shared electron pair orbits both nuclei as shown in **Fig.4**. The attraction of the nuclei for the shared electrons holds the atoms together in a covalent bond.

Covalent bonds have direction. The electronic orbitals of an uncombined atom can change shape and direction when that atom becomes part of a molecule. In a molecule in which two or more covalent bonds are present the molecular geometry is dictated by the bond angles about the central atom. The outermost lone pair (non-bonding) electrons profoundly affect the molecular geometry.

The geometry of water illustrates this concept. In the ground state, oxygen has the outer shell configuration:
$$\mathbf{1s^2\ 2s^2\ 2p^2_x\ 2p^1_y\ 2p^1_z}$$
In water the 1s electrons from two hydrogen atoms bond with the $2p_y$ and $2p_z$ electrons of oxygen. Since p orbitals lie at right angles to each other (see **Fig.4A**), a bond angle of 90° might be expected. However, the bond angle is found experimentally to be approximately 104°. Theoretically this is explained by the effect of lone pair electrons on hybridised orbitals.

Combined or hybrid orbitals are formed when the excitement of 2s electrons results in their promotion from the ground state to a state energetically equivalent to the 2p orbitals. The new hybrids are termed sp^3 from the combination of one s and three p orbitals (See **Fig.4B**). Hybrid sp^3 orbitals are directed in space from the centre of a regular tetrahedron toward the four corners. If the orbitals are equivalent the bond angle will be 109°28' (See **Fig.15**) consistent with the geometry of a tetrahedron. In the case of water two of the orbitals are occupied by non-bonding electrons (See **Fig.4C**). There is greater repulsion of these lone pair electrons which orbit only one nucleus, compared to the repulsion of electrons in bonding orbitals which orbit two nuclei. This tends to increase the angle between non-bonding orbitals so that it is greater than 109°, which pushes the bonding orbitals together, reducing the bond angle to 104°. In the case of ammonia, NH_3 where there is only one lone pair, the repulsion is

not so great and the bond angle is 107°. Carbon forms typical tetrahedral forms and components the simplest being the gas methane, CH_4 (See **Fig.4C** and **Fig.8**). The repulsion of lone pair electrons affects charge distribution and contributes to the polarity of a covalent bond. (See **Fig.16**)

As demonstrated in succeeding sections of this patent specification, a significant and novel aspect of this invention is the manipulation, by electronic methods and means, of the energy level of the water molecule, and the transformation of the water molecule into, and out of, the geometrical form of the tetrahedron. This is made possible only by certain subtle dynamic interactions among the Components I, II, and III of the present invention.

Section 2:
Electrodynamics (Pure Water);
The electrodynamics of Components I, II, and III, will be described individually and in interaction during the progress of pure water reaction rate in time. The reactions of saline water will be described in Section 3. It is to be noted that the output of Component I automatically follows the seven stages (hereinafter Stages A-F) of the reaction rate by varying its parameters of resonant carrier frequency, wave form, current voltage and impedance. All the seven states of the reaction herein described are not necessary for the practical operation of the system, but are included in order to explicate the dynamics and novel aspects of the invention. The seven stages are applicable only to the electrolysis of pure water.

Stage A:
Dry Charging of Component II by Component I;
To make the new system operational, the Component I output electrodes are connected to component II, but no water is placed in the cell of Component III. When Component I output is across the load of Component II we observe the following electrical parameters are observed:

Range of current (I) output with (dry) load: 0 to 25 mA (milliamps) rms.
Range of voltage (E) output with (dry) load: 0 to 250 Volts (AC) rms.
There is no distortion of the amplitude modulated (AM), or of the sine wave carrier whose central frequency, f_c' ranges between 59,748 Hz to 66, 221 Hz, with f_c average = 62, 985 Hz

The carrier frequency varies with the power output in that f_c goes down with an increase in amperes (current). The AM wave form is shown in **Fig.5**. It is to be noted here that the electrical function generator, Component I, has an automatic amplitude modulation volume control which cycles the degree of Amplitude Modulation from 0% to 100%, and then from 100% to 0% every 3.0 seconds. This cycle rate of 3.0 seconds corresponds to the nuclear spin relaxation time, tau/sec, of the water in Component III. The meaning of this effect will be discussed in greater detail in a later section.

In summary, the principal effects to be noted during Stage A -dry charging of Component II are as follows:

a. Tests the integrity of Component I circuitry.
b. Tests the integrity of the coaxial electrodes, and the vitreous ceramic materials of Component II and Component III.
c. Electrostatic cleaning of electrode and ceramic surfaces.

Stage B:
Initial operation of Component I, Component II, and with Component III containing pure water. There is no significant electrolysis of water during Stage B. However, in Stage B the sine wave output of Component I is shaped to a rippled square wave by the changing RC constant of the water as it is treated;

There is an `Open Circuit` reversible threshold effect that occurs in Component III due to water polarisation effects that lead to half wave rectification and the appearance of positive unipolar pulses; and
There are electrode polarisation effects in Component II which are a prelude to true electrolysis of water as evidenced by oxygen and hydrogen gas bubble formation.

Appearance of Rippled Square Waves:
Phase 1: At the end of the Stage A dry charging, the output of Component I is lowered to typical values of: I = 1 ma. E = 24V AC. f_c .congruent.66,234 Hz.

Phase 2: Then water is added to the Component III water cell drop by drop until the top of the centre electrode, 1', in **Fig.3** is covered, and when this water just makes contact with the inner surface of the top outer electrode at 2'. As this coupling of the two electrodes by water happens, the following series of events occur:

Phase 3: The f_c drops from 66,234 Hz, to a range from 1272 Hz to 1848 Hz. The current and voltage both drop, and begin to pulse in entrainment with the water nuclear spin relaxation constant, tau =3.0 sec. The presence of

the nuclear spin relaxation oscillation is proven by a characteristic hysteresis loop on the X-Y axes of an oscilloscope.
I = 0 to 0.2 mA surging at .tau. cycle
E = 4.3 to 4.8V AC surging at .tau. cycle
The sine wave carrier converts to a rippled square wave pulse which reflects the RC time constant of water, and it is observed that the square wave contains higher order harmonics. See **Fig.6**:
With the appearance of the rippled square wave, the threshold of hydrolysis may be detected (just barely) as a vapour precipitation on a cover glass slip placed over the Component III cell and viewed under a low power microscope.

The 'Open Circuit' Reversible Threshold Effect:
Phase 4 A secondary effect of the change in the RC constant of water on the wave form shows up as a full half wave rectification of the carrier wave indicating a high level of polarisation of the water molecule in tetrahedral form at the outer electrode.

With the already noted appearance of the rippled square wave, and the signs of faint vapour precipitation which indicate the earliest stage of electrolysis, it is possible to test for the presence of a reversible hydrolysis threshold. This test is carried out by creating an open circuit between Components I and II, i.e., no current flows. This is done by lowering the water level between the two electrodes in the region --- 1' and 2' shown in **Fig.3**; or by interrupting the circuit between Component I and II, while the Component I signal generator is on and oscillating.

Immediately, with the creation of an `open circuit` condition, the following effects occur:
(a) The carrier frequency, f_c, shifts from Phase 4 valve 1272 Hz to 1848 Hz to 6128 Hz.
(b) The current and voltage drop to zero on the meters which record I and E, but the oscilloscope continues to show the presence of the peak-to-peak (p-p) voltage, and the waveform shows a remarkable effect. The rippled square wave has disappeared, and in its place there appear unipolar (positive) pulses as follows in **Fig.6A**.

The unipolar pulse frequency stabilises to ca. 5000 Hz. The unipolar pulses undergo a 0 to 1.3 volt pulsing amplitude modulation with .tau. at 3.0 seconds. Thus, there exists a pure open circuit reversible threshold for water electrolysis in which the water molecules are capacitor charging and discharging at their characteristic low frequency RC time constant of 0.0002 seconds. It is to be noted that pure water has a very high dielectric constant which makes such an effect possible.

The pulsing amplitude modulation of the voltage is determined by the Hydrogen Nuclear Spin Relaxation constant of 3.0 seconds. It is to be noted that the positive pulse spikes are followed by a negative after-potential. These pulse wave forms are identical to the classic nerve action potential spikes found in the nervous system of all of the living species which have a nervous system. The fact that these unipolar pulses were observed arising in water under the conditions of reversible threshold hydrolysis has a profound significance. These findings illuminate and confirm the Warren McCulloch Theory of water "crystal" dynamics as being the foundation of neural dynamics; and the converse theory of Linus Pauling which holds that water clathrate formation is the mechanism of neural anesthesia.

Phase 5: The effects associated with reversible threshold electrolysis are noted only in passing, since they reflect events which are occurring on the electrode surfaces of Component II, the Thermodynamic Device.

A principal effect which occurs in Stage B, Phase 3, in Component II, (the thermodynamic device), is that the two electrodes undergo stages of polarisation. It has been observed in extensive experiments with different kinds of fluids in the cell of Component II , i.e., distilled water, sea water, tap water, Ringers solution, dilute suspensions of animal and human blood cells, etc. that the inner surface of the outer ring electrode at 3' in **Fig.3** (the electrode that is in contact with the fluid) becomes negatively charged. Referring to **Fig.7**, this corresponds to the left hand columnar area marked, "Electrode .crclbar.".

Electrode Polarisation Effects at the Interface Between Components II and III:
Concurrently with the driver pulsing of Component I at the .tau. constant cycle which leads to electrode polarisation effects in Component II, there is an action on Component III which energises and entrains the water molecule to a higher energy level which shifts the bond angle from 104° to the tetrahedral form with angle 109°28' as shown in **Fig.8** and **Fig.15**.

This electronic pumping action is most important, and represents a significant part of the novel method of this invention for several reasons. First, the shift to the tetrahedral form of water increases the structural stability of the water molecule, thereby making it more susceptible to breakage at the correct resonant frequency, or frequencies. Second, increasing the polarisation of the water molecule makes the lone pair electrons, S- connected with the oxygen molecule more electronegative; and the weakly positive hydrogen atoms, S+ more positive. See **Fig.9** and **Fig.22**.

As the outer electrode becomes more electrically negative, the central electrode becomes more electrically positive as will be shown. As the polarity of the water molecule tetrahedron increases, a repulsive force occurs between the two S+ apices of the water tetrahedron and the negatively charged electrode surface within the region of the Helmholtz layer, as shown in **Fig.7**. This effect "orients" the water molecule in the field, and is the well-known "orientation factor" of electrochemistry which serves to catalyse the rate of oxygen dissociation from the water molecule, and thereby causes the reaction rate to proceed at the lowest energy levels. See **Fig.10** for an example of how the orientation factor works. Near the end of Stage B, the conditions are established for the beginning of the next stage, the stage of high efficiency electrolysis of water.

Stage C:
Generation of the complex wave form frequencies from Component I to match the complex wave form resonant frequencies of the energised and highly polarised water molecule in tetrahedral form with angles, 109°28' are carried out in Stage C. In the operation of the invention active bubble electrolysis of water is initiated following Stage B, phase 3 by setting (automatically) the output of Component I to:
I = 1 mA., E = 22V AC-rms, causing the rippled square wave pulses to disappear with the appearance of a rippled sawtooth wave. The basic frequency of the carrier now becomes, f_c = 3980 Hz.

The wave form now automatically shifts to a form found to be the prime characteristic necessary for optimum efficiency in the electrolysis of water and illustrated in **Fig.11**. In the wave form of **Fig.11**, the fundamental carrier frequency, f_c = 3980 Hz., and a harmonic modulation of the carrier is as follows:

1st Order Harmonic Modulation (OHM) = 7960 Hz.
2nd Order Harmonic Modulation (II OHM) = 15,920 Hz.
3rd Order Harmonic Modulation (III OHM) = 31,840 Hz.
4th Order Harmonic Modulation (IV OHM) = 63,690 Hz.

What is believed to be happening in this IV OHM effect is that each of the four apices of the tetrahedron water molecule is resonant to one of the four harmonics observed. It is believed that the combination of negative repulsive forces at the outer electrode with the resonant frequencies just described work together to shatter the water molecule into its component hydrogen and oxygen atoms (as gases). This deduction is based on the following observations of the process through a low power microscope. The hydrogen bubbles were seen to originate at the electrode rim, 4', of **Fig.3**. The bubbles then moved in a very orderly `pearl chain` formation centripetally (like the spokes of a wheel) toward the central electrode, 1' of **Fig.3**, (**Fig.12** shows a top view of this effect).

Thereafter, upon lowering the output of Component I, the threshold for electrolysis of water as evidenced by vapour deposition of water droplets on a glass cover plate over the cell of Component III, is:

I = 1 mA, E = 10V so, Power = 10 mW

with all other conditions and waveforms as described under Stage C, supra. Occasionally, this threshold can be lowered to:

I = 1 ma, E = 2.6V so, Power = 2.6 mW

This Stage C vapour hydrolysis threshold effect cannot be directly observed as taking place in the fluid because no bubbles are formed --- only invisible gas molecules which become visible when they strike a glass plate and combine into water molecules and form droplets which appear as vapour.

Stage D:
Production of hydrogen and oxygen gas at an efficient rate of water electrolysis is slowed in Stage D when a barrier potential is formed, which blocks electrolysis, irrespective of the amount of power applied to Components II and III.

A typical experiment will illustrate the problems of barrier potential formation. Components I, II, and III are set to operate with the following parameters:

I = 1 ma, E = 11.2V so, Power = 11.2 mW (at the start, rising to 100 mW later)

This input to Component III yields, by electrolysis of water, approximately 0.1 cm^3 of hydrogen gas per minute at one atmosphere and 289^{O}K. It is observed that as a function of time the f_c crept up from 2978 Hz to 6474 Hz over 27 minutes. The current and the voltage also rose with time. At the 27th minute a barrier effect blocked the electrolysis of water, and one can best appreciate the cycle of events by reference to **Fig.13**.

Stage E:
The Anatomy of the Barrier Effect:
Region A: Shows active and efficient hydrolysis
Region B: The barrier region effect can be initiated with taps of the finger, or it can spontaneously occur as a function of time.
Phase a: The current rose from 1 mA to 30 mA. The voltage fell from 22 volts to 2.5 V.
Phase b: If component II is tapped mechanically during Phase a supra --- it can be reversed as follows: The current dropped from 30 mA to 10 mA. The voltage shot up from 5 volts to over 250 volts (off scale).

Throughout 'Phase a' and 'Phase b', all hydrolysis has ceased. It was observed under the microscope that the inner surface of the outer electrode was thickly covered with hydrogen gas bubbles. It was reasoned that the hydrogen gas bubbles had become trapped in the electrostricted layer, because the water molecule tetrahedrons had flipped so that the S+ hydrogen apices had entered the Helmholtz layer and were absorbed to the electronegative charge of the electrode. This left the S- lone pair apices facing the electrostricted layer. This process bound the newly forming H^+ ions which blocked the reaction
$H^+ + H^+ + 2e \rightarrow H_2$ (gas)

Stage F:
Region C: It was found that the barrier effect could be unblocked by some relatively simple procedures:
(a) Reversing the output electrodes from Component I to Component II, and/or:
(b) Mechanically tapping the Component III cell at a frequency T/2 = 1.5 seconds per tap.
These effects are shown in FIG. 12 and induce the drop in barrier potential from:

I = 10 mA to 1 ma, E = 250V to 4V so, Power fell from 2.5W to 4 mW

Upon unblocking of the barrier effect, electrolysis of water resumed with renewed bubble formation of hydrogen gas.

The barrier potential problem has been solved for practical application by lowering the high dielectric constant of pure water, by adding salts (NaCl, KOH, etc.) to the pure water thereby increasing its conductivity characteristics. For optimum efficiency the salt concentration need not exceed that of sea water (0.9% salinity) in Section 3, "Thermodynamics of the Invention", it is to be understood that all water solutions described are not "pure" water as in Section B, but refer only to saline water.

Section 3:
The Thermodynamics of the Invention (Saline Water);

Introduction: (water, hereinafter refers to saline water);
The thermodynamic considerations in the normal operations of Components I, II, and III in producing hydrogen as fuel, and oxygen as oxidant during the electrolysis of water, and the combustion of the hydrogen fuel to do work in various heat engines is discussed in this section.

In chemical reactions the participating atoms form new bonds resulting in compounds with different electronic configurations. Chemical reactions which release energy are said to be exergonic and result in products whose chemical bonds have a lower energy content than the reactants. The energy released most frequently appears as heat. Energy, like matter, can neither be created nor destroyed according to the Law of Conservation of Energy. The energy released in a chemical reaction, plus the lower energy state of the products, is equal to the original energy content of the reactants. The burning of hydrogen occurs rather violently to produce water as follows:

$2H_2 + O_2 \rightarrow 2H_2O - \Delta H$ 68.315 Kcal/mol (this is the enthalpy, or heat of combustion at constant pressure) where 18 gms = 1 mol.

The chemical bonds of the water molecules have a lower energy content than the hydrogen and oxygen gases which serve at the reactants. Low energy molecules are characterised by their stability. High energy molecules are inherently unstable. These relations are summarised in the two graphs of **Fig.14**. It is to be noted that **Fig.14B** shows the endergonic reaction aspect of the invention when water is decomposed by electrolysis into hydrogen and oxygen.

Fig.14A shows the reaction when the hydrogen and oxygen gases combine, liberate energy, and re-form into water. Note that there is a difference in the potential energy of the two reactions. **Fig.14C** shows that there are two components to this potential energy. The net energy released, or the energy that yields net work is labelled in the diagram as "Net Energy Released", and is more properly called the free energy change denoted by the Gibbs function, $-.\Delta.G$.

The energy which must be supplied for a reaction to achieve (burning) spontaneity is called the “Activation Energy”. The sum of the two is the total energy released. A first thermodynamic subtlety of the thermodynamic device of the invention is noted in Angus McDougall's Fuel Cells, Energy Alternative Series, The MacMillan Press Ltd., London, 1976, where on page 15 it is stated:

"The Gibbs function is defined in terms of the enthalpy H, and the entropy S of the system:

G = H-T S (where .tau. is the thermodynamic temperature) . A particularly important result is that for an electrochemical cell working reversibly at constant temperature and pressure, the electrical work done is the net work and hence,

. Δ.G = -w_e

For this to be a reversible process, it is necessary for the cell to be on `open circuit`, that is, no current flows and the potential difference across the electrodes is the EMF, E. Thus,

. Δ.G = -zFE

(where F is the Faraday constant --- the product of the Avogadro Constant + N_A = 6.022045 x 10^{23} $mole^{-1}$, and the charge on the electron, e = 1.602 189 x 10^{-19} C --- both in SI units; and z is the number of electrons transported.) when the cell reaction proceeds from left to right."

It is to be noted that the Activation Energy is directly related to the controlling reaction rate process, and thus is related to the Gibbs free energy changes. The other thermodynamic subtlety is described by S. S. Penner in his work: Penner, S. S. and L. Icerman, Energy, Vol, II, Non-Nuclear Energy Technologies. Addison-Wesley Publishing Company, Inc. Revised Edition, 1977. Reading, Mass. where on page 140 it is stated that:

"It should be possible to improve the efficiency achieved in practical electrolysis to about 100% because, under optimal operating conditions, the theoretically-attainable energy conversion by electrolysis is about 120% of the electrical energy input. The physical basis for this last statement will now be considered:

"A useful definition for energy efficiency in electrolysis is the following: the energy efficiency is the ratio of the energy released from the electrolysis products formed (when they are subsequently used) to the energy required to effect electrolysis. The energy released by the process

H_2 (gas) + (1/2)O_2 (gas) $\rightarrow$ H_2O (liquid)

under standard conditions (standard conditions in this example are: (1) atmospheric pressure = 760 mm Hg and (2) temperature = 298.16^{O}K. = 25^{O}C. = 77^{O}F.) is 68.315 Kcal and is numerically equal to the enthalph change (.Δ.H) for the indicated process. On the other hand, the minimum energy (or useful work input) required at constant temperature and pressure for electrolysis equals the Gibbs free energy change (.Δ.G). There is a basic relation derivable from the first and second laws of thermodynamics for isothermal changes, which shows that:

.Δ.G = . Δ.H - T. Δ.S

where .Δ.S represents the entropy change for the chemical reaction. The Gibbs free energy change (.Δ.G) is also related to the voltage (E) required to implement electrolysis by Faraday's equation, viz.

E = (.Δ.G/23.06n) volts

where . Δ.G is in Kcal/mol and n is the number of electrons (or equivalents) per mol of water electrolysed and has the numerical value 2.

At atmospheric pressure and 300^{O}K., .Δ.H = 68.315 Kcal/mol of H_2O (i) and .Δ.G = 56.62 Kcal/mole of H_2O (i) for the electrolysis of liquid water. Hence, the energy efficiency of electrolysis at 300^{O}K. is about 120%.

(When) H_2 (gas) and O_2 (gas) are generated by electrolysis, the electrolysis cell must absorb heat from the surroundings, in order to remain at constant temperature. It is this ability to produce gaseous electrolysis products with heat absorption from the surroundings that is ultimately responsible for energy-conversion efficiencies during electrolysis greater than unity."

Using the criteria of these two authorities, it is possible to make a rough calculation of the efficiency of the present invention.

Section 4:
Thermodynamic Efficiency of the Invention;

Efficiency is deduced on the grounds of scientific accounting principles which are based on accurate measurements of total energy input to a system (debit), and accurate measurements of total energy (or work) obtained out of the system (credit). In principle, this is followed by drawing up a balance sheet of energy debits and credits, and expressing them as an efficiency ration, ε.

$$\eta = \frac{\text{Credit}}{\text{Debit}} = \frac{\text{Energy Out}}{\text{Energy In}} < 1$$

The energy output of Component I is an alternating current passing into a highly non-linear load, i.e., the water solution. This alternating current generator (Component I) is so designed that at peak load it is in resonance (Components I, II, III), and the vector diagrams show that the capacitive reactance, and the inductive reactance are almost exactly 180° out of phase, so that the net power output is reactive, and the dissipative power is very small. This design insures minimum power losses across the entire output system. In the experiments which are now to be described the entire emphasis was placed on achieving the maximum gas yield (credit) in exchange for the minimum applied energy (debit).

The most precise way to measure the applied energy to Components II and III is to measure the Power, P, in Watts, W. This was done by precision measurements of the volts across Component II as root mean square (rms) volts; and the current flowing in the system as rms amperes. Precisely calibrated instruments were used to take these two measurements. A typical set of experiments (using water in the form of 0.9% saline solution = 0.1540 molar concentration) to obtain high efficiency hydrolysis gave the following results:

ms Current = 25 mA to 38 mA (0.025 A to 0.038 A)
rms Volts = 4 Volts to 2.6 Volts

The resultant ratio between current and voltage is dependent on many factors, such as the gap distance between the central and ring electrodes, dielectric properties of the water, conductivity properties of the water, equilibrium states, isothermal conditions, materials used, and even the presence of clathrates. The above current and voltage values reflect the net effect of various combinations of such parameters. The product of rms current, and rms volts is a measure of the power, P in watts:

P = I x E = 25 mA x 4.0 volts = 100 mW (0.1 W)
P = I x E = 38 mA x 2.6 volts = 98.8 mW (0.0988 W)

At these power levels (with load), the resonant frequency of the system is 600 Hz (plus or minus 5 Hz) as measured on a precision frequency counter. The wave form was monitored for harmonic content on an oscilloscope, and the nuclear magnetic relaxation cycle was monitored on an X-Y plotting oscilloscope in order to maintain the proper hysteresis loop figure. All experiments were run so that the power in Watts, applied through Components I, II, and III ranged between 98.8 mW to 100 mW. Since, by the International System of Units --- 1971 (SI), One-Watt-second (Ws) is exactly equal to One Joule (J), the measurements of efficiency used these two yardsticks (1 Ws = 1 J) for the debit side of the measurement.

The energy output of the system is, of course, the two gases, hydrogen (H_2) and oxygen ($1/2O_2$), and this credit side was measured in two laboratories, on two kinds of calibrated instruments, namely, a Gas Chromatography Machine, and, a Mass Spectrometer Machine.

The volume of gases, H_2 and $(1/2)O_2$, was measured as produced under standard conditions of temperature and pressure in unit time, i.e., in ccs per minute (cc/min), as well as the possibly contaminating gases, such as air oxygen, nitrogen and argon; carbon monoxide, carbon dioxide, water vapour, etc.

The electrical, and gas, measurements were reduced to the common denominator of Joules of energy so that the efficiency accounting could all be handled in common units. The averaged results from many experiments follow. The Standard Error between different samples, machines, and locations is plus or minus 10%, and only the mean was used for all the following calculations.

Section 5:
Endergonic Decomposition of Liquid Water;

Thermodynamic efficiency for the endergonic decomposition of saline liquid water into gases under standard atmosphere (754 to 750 m.m. Hg), and standard isothermal conditions @ 25^{O}C. = 77^{O}F. = 298.16^{O}K., according to the following reaction:

$$H_2O(1) \rightarrow H_2\,(g) + (1/2)O_2\,(g) + .\Delta.G\ 56.620\ KCal/mole$$

As already described, $.\Delta.G$ is the Gibbs function (**Fig.14B**). A conversion of Kcal to the common units, Joules, by the formula, One Calorie = 4.1868 Joules was made.

$.\Delta.G$ = 56.620 Kcal x 4.1868 J = 236,954 J/mol of H_2O (1) where, 1 mole is 18 gms.

$.\Delta.G$ = the free energy required to yield an equivalent amount of energy from H_2O in the form of the gases, H_2 and $(1/2)O_2$.

To simplify the calculations, the energy required to produce 1.0 cc of H_2O as the gases, H_2 and $(1/2)O_2$ was determined. There are (under standard conditions) 22,400 cc = V, of gas in one mole of H_2O. Therefore:

$$\frac{\Delta G}{V} = \frac{236{,}954\ J}{22{,}400\ cc} = 10.5783\ J/cc$$

The electrical energy required to liberate 1.0 cc of the H_2O gases (where H_2 = 0.666 parts, and $(1/2)O_2$ = 0.333 parts, by volume) from liquid water is then determined. Since P = 1 Ws = 1 Joule, and V=1.0 cc of gas = 10.5783 Joules, then:

PV = 1 x 10.5783 J = 10.5783 Ws

Since the experiments were run at 100 mW (0.1 W) applied to the water sample in Component II, III, for 30 minutes, the ideal (100% efficient) gas production at this total applied power level was calculated.
0.1 Ws x 60 sec x 30 min = 180.00 Joules (for 30 min)
The total gas production at Ideal 100% efficiency is,
180.00 J / 10.5783 J/cc = 17.01 cc H_2O (g)
The amount of hydrogen present in the 17.01 cc H_2O (g) was then calculated.
17.01 cc H_2O (gas) x 0.666 H_2 (g) = 11.329 cc H_2 (g)
17.01 cc H_2O (g) x 0.333 $(1/2)O_2$ (g) = 5.681 cc $(1/2)O_2$ (g)
Against this ideal standard of efficiency of expected gas production, the actual amount of gas produced was measured under: (1) standard conditions as defined above (2) 0.1 Ws power applied over 30 minutes. In the experiments, the mean amount of H_2 and $(1/2)O_2$ produced, as measured on precision calibrated GC, and MS machines in two different laboratories, where the S.E. is +/-10%, was,

---

Measured Mean = 10.80 cc H_2 (g)
Measured Mean = 5.40 cc $(1/2)O_2$ (g)
Total Mean = 16.20 cc H_2O(g)

The ratio, ε, between the ideal yield, and measured yield is:

$$\eta = \frac{\text{Measured } H_2(g)}{\text{Ideal } H_2(g)} = \frac{10.80 \text{ cc}}{11.33 \text{ cc}} = 91.30\%$$

Section 6:
Energy Release;
The total energy release (as heat, or electricity) from an exergonic reaction of the gases, H_2 and O_2, is given by:

$$H_2(g) + (\tfrac{1}{2})O_2(g) \rightarrow H_2O(P) - \Delta H\ 68.315\ \text{Kcal/mol} = (-\Delta H\ 286{,}021\ \text{Joules})/\text{mol}$$

It is possible (Penner, Op. Cit., p.128) to get a total heat release, or total conversion to electricity in a fuel cell, in the above reaction when the reactants are initially near room temperature (298.16^{O}K.), and the reactant product (H_2O) is finally returned to room temperature. With this authoritative opinion in mind, it is desirable to determine the amount of energy released (ideal) from the exergonic experiment. The total energy of 1.0 cc of H_2O (1), as above is:

$$1.0 \text{ cc } \Delta H = \frac{286{,}021 \text{ J/mol}}{22{,}400 \text{ cc/mol}} = 12.7687 \text{ J/cc } H_2O$$

for H_2 = 12.7687 x 0.666 = 8.509 J/0.66 cc H_2 for O_2 = 12.7687 x 0.333 = 4.259 J/0.33 cc $(1/2)O_2$ The energy produced from the gases produced in the experiments in an exergonic reaction was:

16.20 cc H_2O (g) x 12.7687 J/cc H_2O = 206,8544 J.

The overall energy transaction can be written as:

$$\frac{\text{EXERGONIC}}{\text{ENDERGONIC}} - \eta - \frac{-\Delta H}{+\Delta G} = \frac{206{,}854.4 \text{ J}}{180{,}000 \text{ J}} = 114.92\%$$

In practical bookkeeping terms the balance of debits and credits, n = (-.Δ.H) - (+.Δ.G), so:

n = 206.8544 J - 180.0 = + 26.8544 J (surplus).

Since, in the invention, the gas is produced where and when needed, there is no additional cost accounting for liquefaction, storage, or transportation of the hydrogen fuel, and the oxygen oxidant. Therefore, the practical efficiency, is:

$$\eta P = \frac{26.8544\ J}{180.0000\ J} = 14.919\%\ \text{(as net return on the original energy investment)}$$

In practical applications, the energy output (exergonic) of the Component II System can be parsed between the electrical energy required to power the Component I System, as an isothermal closed loop; while the surplus of approximately 15% can be shunted to an engine (heat, electrical, battery, etc.) that has a work load. Although this energy cost accounting represents an ideal model, it is believed that there is enough return (approximately 15%) on the capital energy investment to yield a net energy profit that can be used to do useful work.

CONCLUSION:

From the foregoing disclosure it will be appreciated that the achievement of efficient water splitting through the application of complex electrical waveforms to energised water molecules, i.e. tetrahedral molecules having bonding angles of 109°28', in the special apparatus described and illustrated, will provide ample and economical production of hydrogen gas and oxygen gas from readily available sources of water. It is to be understood, that the specific forms of the invention disclosed and discussed herein are intended to be representative and by way of illustrative example only, since various changes may be made therein without departing from the clear and specific teachings of the disclosure. Accordingly, reference should be made to the following appended claims in determining the full scope of the method and apparatus of the present invention.

SHIGETA HASEBE

US Patent 4,105,528 8th August 1978 Inventor: Shigeta Hasebe

APPARATUS FOR DECOMPOSITION OF AQUEOUS LIQUID

Please note that this is a re-worded excerpt from this patent. This patent describes an electrolysis system which it is claimed has demonstrated ten times the efficiency that Faraday considered to be the maximum possible.

ABSTRACT

An apparatus for decomposition of liquid, in which spiral negative and positive electrodes are arranged close together but not touching. These two electrodes are supplied with power through external terminals and the electrolyte is caused to flow between the negative and positive electrodes for the electrolysis between two electrodes under the function of the potential magnetic field formed by the coil current which is generated by the electrodes with active movement of an electrolytic ion so that the electrolysis of water takes place smoothly under the spin functions of the atom and electron.

BACKGROUND AND SUMMARY OF THE INVENTION

This invention relates to an apparatus for decomposition of liquid where a flowing electrolyte is subjected to electrolysis for the production of gases.

As is well known, water is composed of hydrogen atoms and oxygen atoms. When water is sufficiently magnetised, each constitutive atom is also weakly magnetised to rotate the elementary particle in a regular direction. This rotation of the elementary particle is generally called "spin". That is, the spin function is caused by an electron, atomic nucleus, atom and even by the molecule. When a negative electrode is immersed in the electrolyte - Sodium Hydroxide (“lye”) solution - with a view to applying a voltage to it in order to cause the elementary particle to react with the electric field, the coupling state of the hydrogen with the oxygen is varied and the electrolysis is facilitated by the spin.

In the present invention, spiral negative and positive electrodes are arranged close together but not touching and these two electrodes are supplied with power through external terminals and the electrolyte is caused to flow between the negative and positive electrodes. Thus, the electrolyte is subjected to the electrolysis between two electrodes while within a magnetic field formed by the coil current which is generated by the electrodes with active movement of an electrolytic ion (Na^+, OH^-) so that the electrolysis of water takes place smoothly under the spin functions of the atom and electron.

It has been confirmed that the rate of the electrolysis of water using this invention is approximately 10 or more times (approximately 20 times when calculated) than that produced by conventional electrolysis.

The design of the electrolytic cell of this invention is such that the electrolyte flowing through the supply ports provided at the lower portion of the electrolytic cell is subjected to the magnetic field produced by a permanent magnet and the electrodes cause it to be further subjected to magnetic and electric fields which cause it to obtain a sufficient spin effect.

It is, therefore, a general object of the invention to provide a novel apparatus for decomposition of liquid in which an electrolyte (NaOH) solution is subjected to magnetic fields to cause electrolysis assisted by the spin of the water molecules which produces a great amount of gas with less consumption of electrical energy.

A principal object of the invention is to provide an apparatus for decomposition of liquid which has a liquid circulating system for the separation of gas and liquid in which positive and negative spiral electrodes are arranged across the flow path of the liquid and the opposite ends of the electrodes being provided with magnetic materials to augment the effect caused by the applied voltage across a liquid passing through a magnetic field caused by the positive and negative spiral electrodes, thereby to promote generation and separation of cat-ions and an-ions with a high efficiency in production of a large quantity of gases.

Other objects and advantages of the present invention will become apparent through the detailed description which follows.

BRIEF DESCRIPTION OF THE DRAWINGS

The invention will be described more in detail in the following with reference to the accompanying drawings, wherein:

Fig.1 is a partially cross-sectional schematic elevation of an apparatus in accordance with the invention;

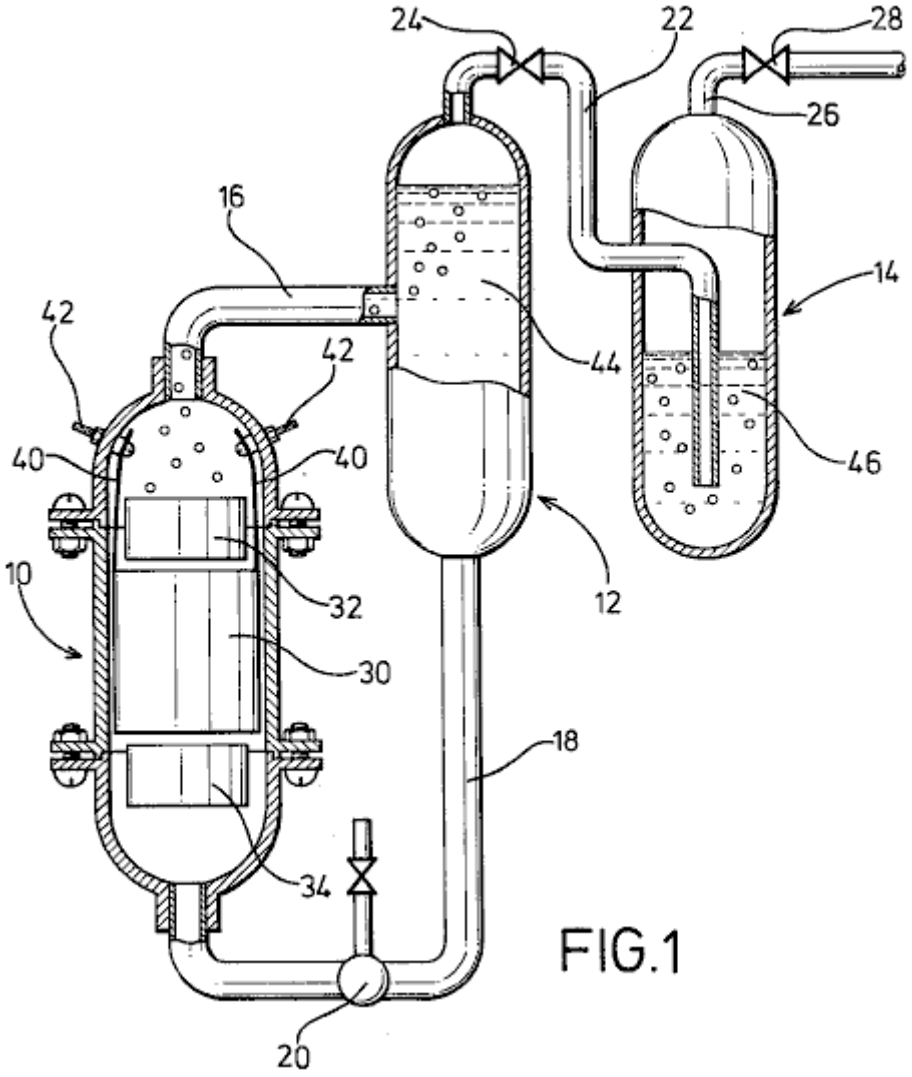

FIG.1

Fig.2 is a perspective view of electrodes arranged in accordance with the invention;

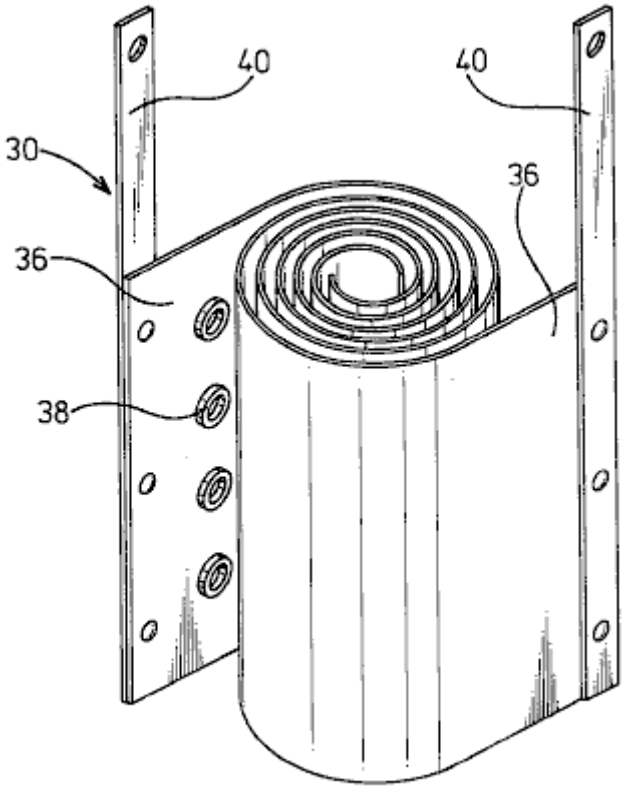

FIG.2

Fig.3 is a plan view of electrodes with magnetic materials.

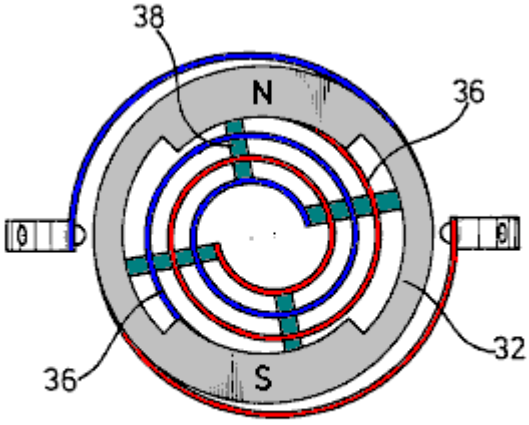

FIG.3

DESCRIPTION OF THE PREFERRED EMBODIMENT

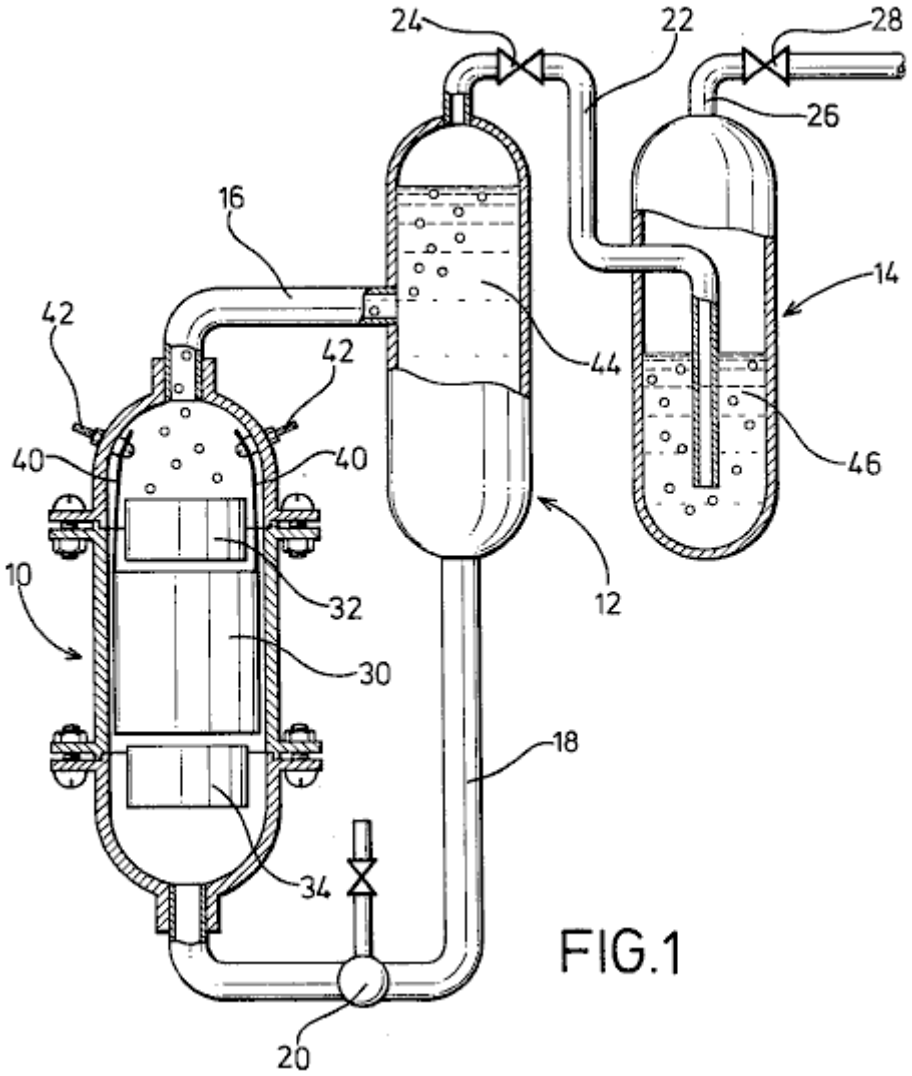

FIG.1

In **Fig.1**, an electrolysis cell **10**, a gas-liquid separation tank **12** and a gas-washing tank **14** are vertically arranged as shown with the electrolytic cell **10** being positioned a little lower than the tanks.

Cell **10** and tanks **12** and **14** are connected together by a delivery pipe **16** which connects the top of the electrolytic cell **10** with the middle of the gas-liquid separation tank **12**. A feed-back pipe **18** containing a pump **20**, is provided to connect the bottom of the gas-liquid separation tank **12,** with the bottom of the electrolytic cell **10**. Also provided is pipe **22**, which runs from the top of the gas-liquid separation tank **12** through a valve **24** to the bottom of the gas-washing tank **14**. A drain pipe **26**, provided with a valve **28**, is taken from the top of the gas-washing tank **14**.

In the electrolytic cell **10**, positive and negative spiral electrodes **30** of diameters suited to the internal diameter of the electrolytic cell **10** are arranged coaxially. At the upper and lower parts of the spiral electrodes **30** are arranged magnet rings **32** and **34** made from ferrite or similar material, positioned so that North and South poles are opposite one another to create a magnetic field which is at right angles to the axis of the electrolytic cell.

Electrodes **30** are composed of two metal strips **36** which are wound into spiral shapes with cylindrical insulating spacers **38** made of rubber or a similar material, placed between them and attached to the surface of the metal strips **36**. From the metal strips **36,** wires **40**, are taken to the positive and negative power supply terminals, via connectors provided in the inner wall of the electrolytic cell.

The electrolytic cell **10** and the gas-liquid separation tank **12** are filled with a electrolyte **44** which is circulated by the pump **20**, while the gas-washing tank **14** is filled with a washing liquid **46** to such a level that gases gushing out of the conduit **22** are thoroughly washed.

The apparatus of the present invention may be well be used for the electrolysis of flowing water for the production of hydrogen gas and oxygen gas at a high efficiency. That is to say, the electrolytic cell **10** and the gas-liquid separation tank **12** are filled with the electrolyte **44** which is caused by pump **20** to flow through a magnetic field in an vortex path in which positive and negative magnetic poles N, S of the magnets **32** and **34** face each other to

produce a transverse field, and through the metal plates **36** of the vortical electrodes **30** to generate an orientation for the electrical migration of cat-ions and an-ions, causing an increased gas separation rate and enhancement of the electrolysis.

In particular, the flowing oxygen gas serves to facilitate an aeration of the electrolyte since it has varying magnetic effects as it passes through the magnetic field. The spiral electrodes **30** of this invention, create a remarkable increase in the rate of electrolysis. This is caused by the continuously decreasing space between the electrodes **30** which causes the flow velocity to increase as the flow progresses along its path. This causes turbulence which instantly removes bubbles of gas from the surface of the electrodes, allowing fresh ions full contact with the metal surfaces, thus raising the efficiency of the cell.

The spiral coiling of the electrodes also enables a very desirable reduction in the size of the cell, while increasing the electrode area and improving its contact with the electrolyte **44**. There is also a relatively short migration distance of ions which also promotes rapid gas production. On the other hand, insulating spacers **38** interposed between the metal strips **36** serves to create the desired turbulence of the electrolyte passing through the cell.

The liquid circulating system for separation of gas and liquid requires no other driving unit except the circulation pump **20** to achieve separation of gas and liquid by utilising differences in water heads between cell **10** and tanks **12** and **14**. In other words, a flow of gas-liquid mixture supplied from electrolytic cell **10** is fed into the gas-liquid separation tank **12** where, due to the difference in buoyancy of gases and liquid, the gas rises and is fed into the gas-washing tank **14** while the liquid moves down and is returned to the electrolytic cell **10**. The washing tank **14** is filled with any convenient washing liquid **46** so that the gases gushing out of conduit **22** are thoroughly washed and fed into the drain pipe **26**. Thus, the apparatus may be constructed at reduced cost and without any complexity.

As described earlier, the magnets **32** and **34** provide positive and negative magnetic poles N, S which are confronted in the annular wall for facilitating an alignment between the cross section of the flow-path of the liquid and the annular portion of the magnets **32** and **34** and a generation of a magnetic field in a direction perpendicular to that of the liquid flow, so that the liquid is forced to flow through the magnetic field.

Experimental data	Value
Room temperature	20^0 Centigrade
Atmospheric pressure	1003 millibars
Electrolyte temperature	25^0 Centigrade
Humidity	43%
Voltage	2.8 Volts
Current	30 Amps
Hydroxy gas production rate	116 cc/sec.
Hydrogen production per Coulomb (1A x 1 sec.)	2.6 cc.
Oxygen production per Coulomb	1.3 cc.

The rate of generation shown by these figures is over 20 times that which could be obtained by standard Faraday electrolysis.

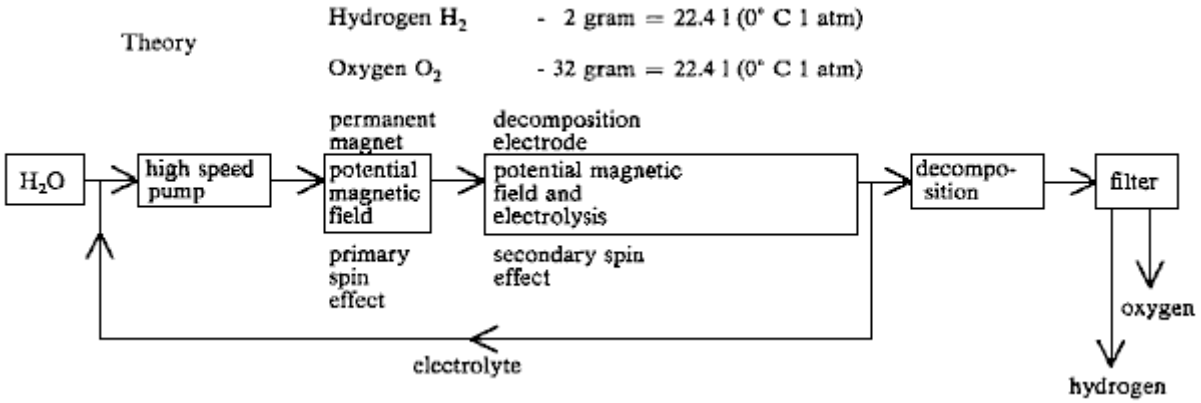

While a preferred embodiment of the invention has been illustrated by way of example in the drawings and particularly described, it will be understood that various modifications may be made in the construction and that the invention is no way limited to the embodiments shown.

STEPHEN CHAMBERS (Xogen Power Inc.)

US Patent 6,126,794 16th July 2002 Inventor: Stephen Chambers

AN APPARATUS FOR PRODUCING ORTHOHYDROGEN AND/OR PARAHYDROGEN

This patent describes an electrolyser system capable of running a small internal combustion engine directly from water alone.

ABSTRACT

An apparatus for producing orthohydrogen and/or parahydrogen. The apparatus includes a container holding water and at least one pair of closely-spaced electrodes arranged within the container and submerged in the water. A first power supply provides a particular first pulsed signal to the electrodes. A coil may also be arranged within the container and submerged in the water if the production of parahydrogen is also required. A second power supply provides a second pulsed signal to the coil through a switch to apply energy to the water. When the second power supply is disconnected from the coil by the switch and only the electrodes receive a pulsed signal, then orthohydrogen can be produced. When the second power supply is connected to the coil and both the electrodes and coil receive pulsed signals, then the first and second pulsed signals can be controlled to produce parahydrogen. The container is self-pressurised and the water within the container requires no chemical catalyst and yet can produce the orthohydrogen and/or parahydrogen efficiently. Heat is not generated, and bubbles do not form on the electrodes.

BACKGROUND OF THE INVENTION

Conventional electrolysis cells are capable of producing hydrogen and oxygen from water. These conventional cells generally include two electrodes arranged within the cell which apply energy to the water to thereby produce hydrogen and oxygen. The two electrodes are conventionally made of two different materials.

However, the hydrogen and oxygen generated in the conventional cells are generally produced in an inefficient manner. That is, a large amount of electrical power has to be applied to the electrodes in order to produce the hydrogen and oxygen. Moreover, a chemical catalyst such as sodium hydroxide or potassium hydroxide must be added to the water to separate hydrogen or oxygen bubbles from the electrodes. Also, the produced gas must often be transported to a pressurised container for storage, because conventional cells produce the gases slowly. Also, conventional cells tend to heat up, creating a variety of problems, including boiling of the water. In addition, conventional cells tend to form gas bubbles on the electrodes which act as electrical insulators and reduce the efficiency of the cell.

Accordingly, it is extremely desirable to produce a large amount of hydrogen and oxygen with only a modest amount of input power. Furthermore, it is desirable to produce the hydrogen and oxygen with "regular" tap water and without any additional chemical catalyst, and to operate the cell without the need for an additional pump to pressurise it. It is also desirable to construct both of the electrodes from the same material. It is also desirable to produce the gases quickly, and without heat, and without bubbles forming on the electrodes.

Orthohydrogen and parahydrogen are two different isomers of hydrogen. Orthohydrogen is that state of hydrogen molecules in which the spins of the two nuclei are parallel. Parahydrogen is that state of hydrogen molecules in which the spins of the two nuclei are antiparallel. The different characteristics of orthohydrogen and parahydrogen lead to different physical properties. For example, orthohydrogen is highly combustible whereas parahydrogen is a slower burning form of hydrogen. Thus, orthohydrogen and parahydrogen can be used for different applications. Conventional electrolytic cells make only orthohydrogen and parahydrogen. Parahydrogen is difficult and expensive to make by conventional means.

Accordingly, it is desirable to produce orthohydrogen and/or parahydrogen cheaply within a cell and to be able to control the amount of either produced by that cell. It is also desirable to direct the produced orthohydrogen or parahydrogen to a coupled machine in order to provide a source of energy for it.

SUMMARY OF THE INVENTION

It is therefore an object of the present invention to provide a cell having electrodes and containing water which produces a large amount of hydrogen and oxygen in a relatively small amount of time, and with a modest amount of input power, and without generating heat.

It is another object of the present invention for the cell to produce bubbles of hydrogen and oxygen which do not bunch around or on the electrodes.

It is also an object of the present invention for the cell to operate properly without a chemical catalyst. Thus, the cell can be run using ordinary tap water. This has the advantage of avoiding the additional costs required for producing the chemical catalyst.

It is another object of the present invention for the cell to be self-pressurising. Thus avoiding the need for an additional pump.

It is another object of the present invention to provide a cell having electrodes made of the same material. This material can, for example, be stainless steel. Thus, the construction of the cell can be simplified and construction costs reduced.

It is another object of the present invention to provide a cell which is capable of producing orthohydrogen, parahydrogen or a mixture thereof and can be set so as to produce any relative amount of orthohydrogen and parahydrogen desired by the user.

It is another object of the invention to couple the gaseous output of the cell to a device, such as an internal combustion engine, so that the device may be powered from the gas supplied to it.

These and other objects, features, and characteristics of the present invention will be more apparent upon consideration of the following detailed description and appended claims with reference to the accompanying drawings, wherein the same reference numbers have been used to indicate corresponding parts in the various figures.

Accordingly, the present invention includes a container for holding water. At least one pair of closely-spaced electrodes are positioned within the container and submerged under the water. A first power supply provides a particular pulsed signal to the electrodes. A coil is also arranged in the container and submerged under the water. A second power supply provides a particular pulsed signal through a switch to the electrodes.

When only the electrodes receive a pulsed signal, then orthohydrogen can be produced. When both the electrodes and coil receive pulsed signals, then parahydrogen or a mixture of parahydrogen and orthohydrogen can be produced. The container is self pressurised and the water within the container requires no chemical catalyst to produce the orthohydrogen and/or parahydrogen efficiently.

BRIEF DESCRIPTION OF THE DRAWINGS

Fig.1 is a side view of a cell for producing orthohydrogen including a pair of electrodes according to a first embodiment of the present invention;

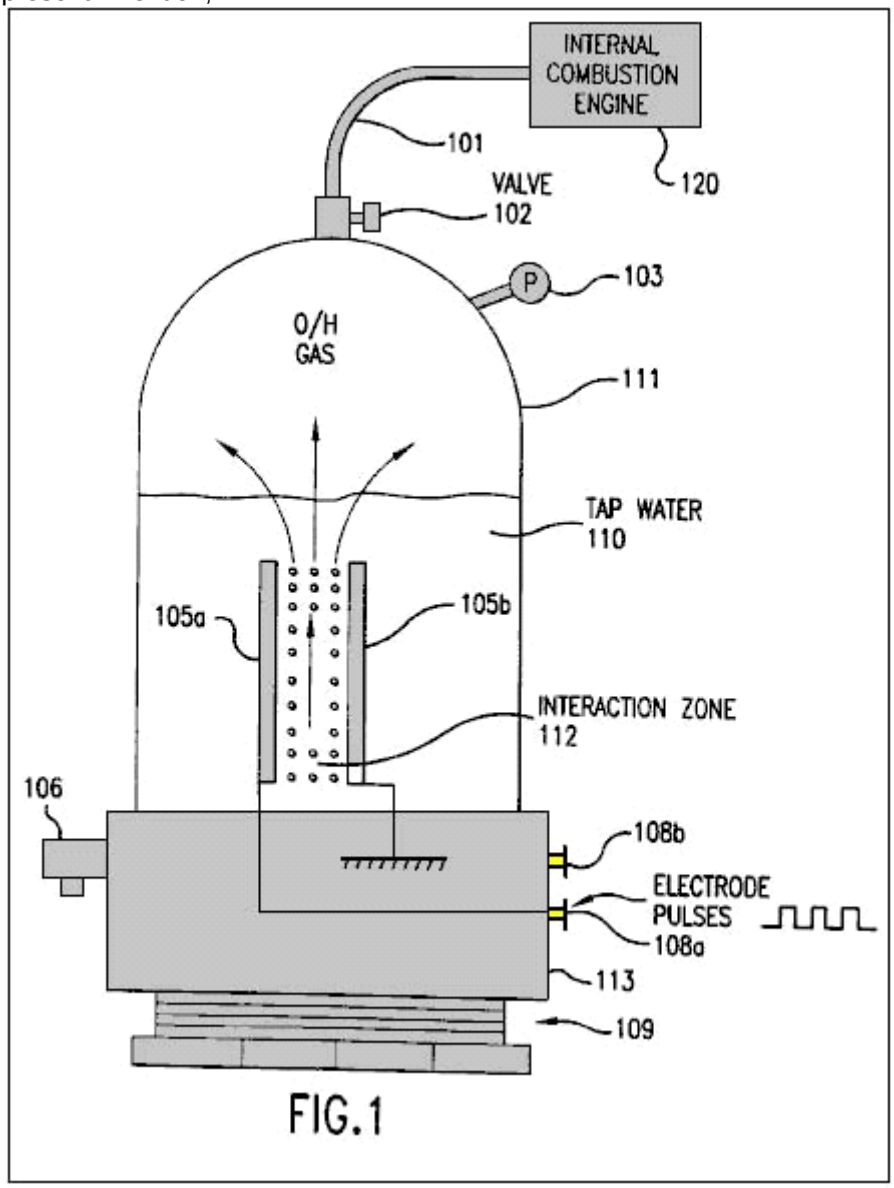

FIG.1

Fig.2 is a side view of a cell for producing orthohydrogen including two pairs of electrodes according to a second embodiment of the present invention;

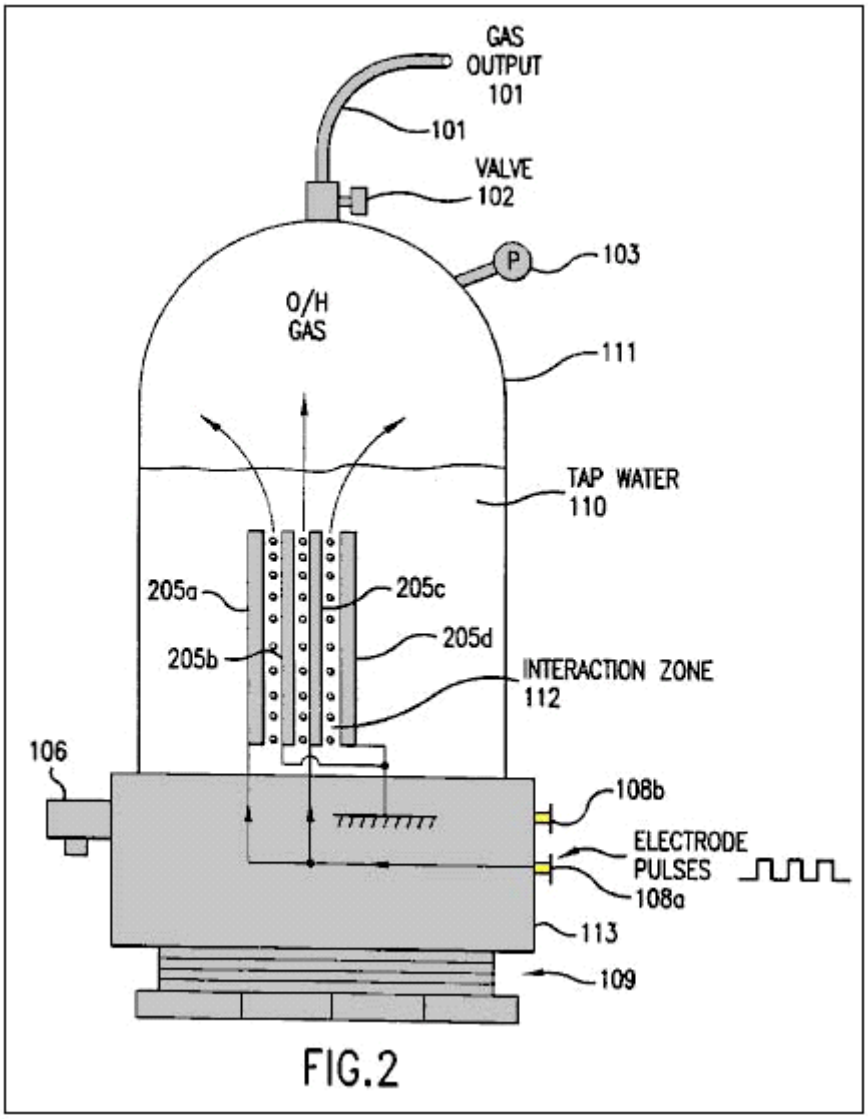

FIG.2

Fig.3 is a side view of a cell for producing orthohydrogen including a pair of cylindrical-shaped electrodes according to a third embodiment of the present invention;

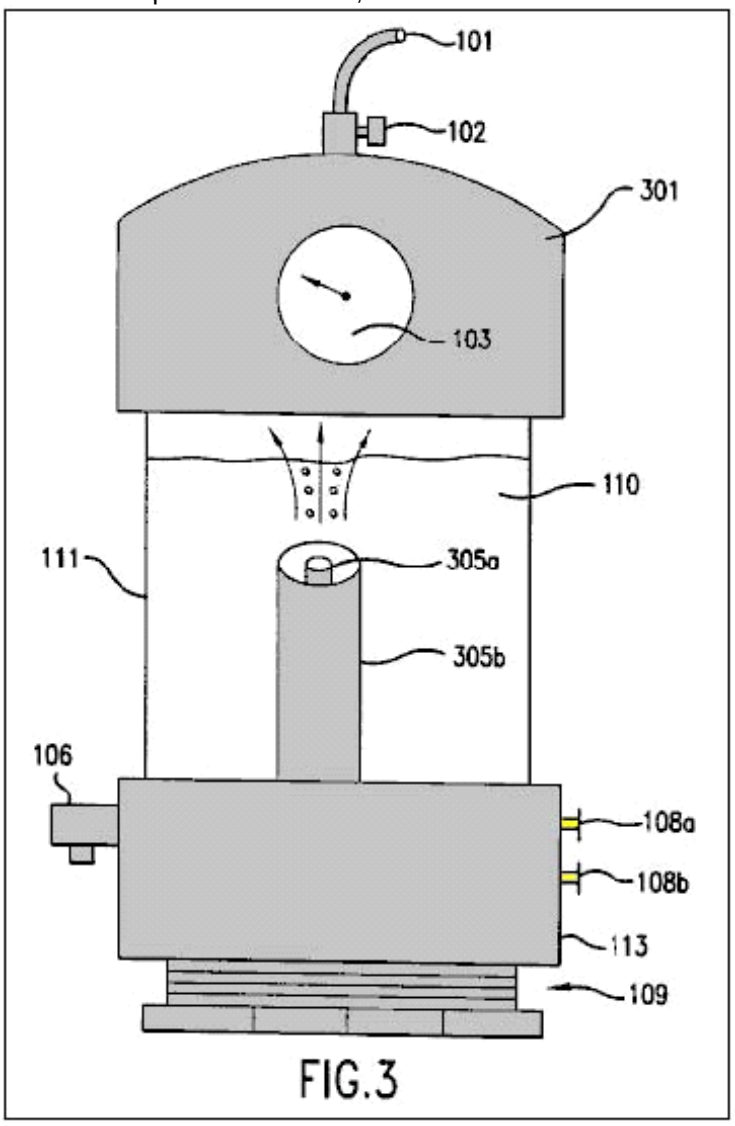

FIG.3

Fig.4a is a diagram illustrating a square wave pulsed signal which can be produced by the circuit of **Fig.5** and applied to the electrodes of **Fig.1** through **Fig.3**;

Fig.4b is a diagram illustrating a saw tooth wave pulsed signal which can be produced by the circuit of **Fig.5** and applied to the electrodes of **Fig.1** through **Fig.3**;

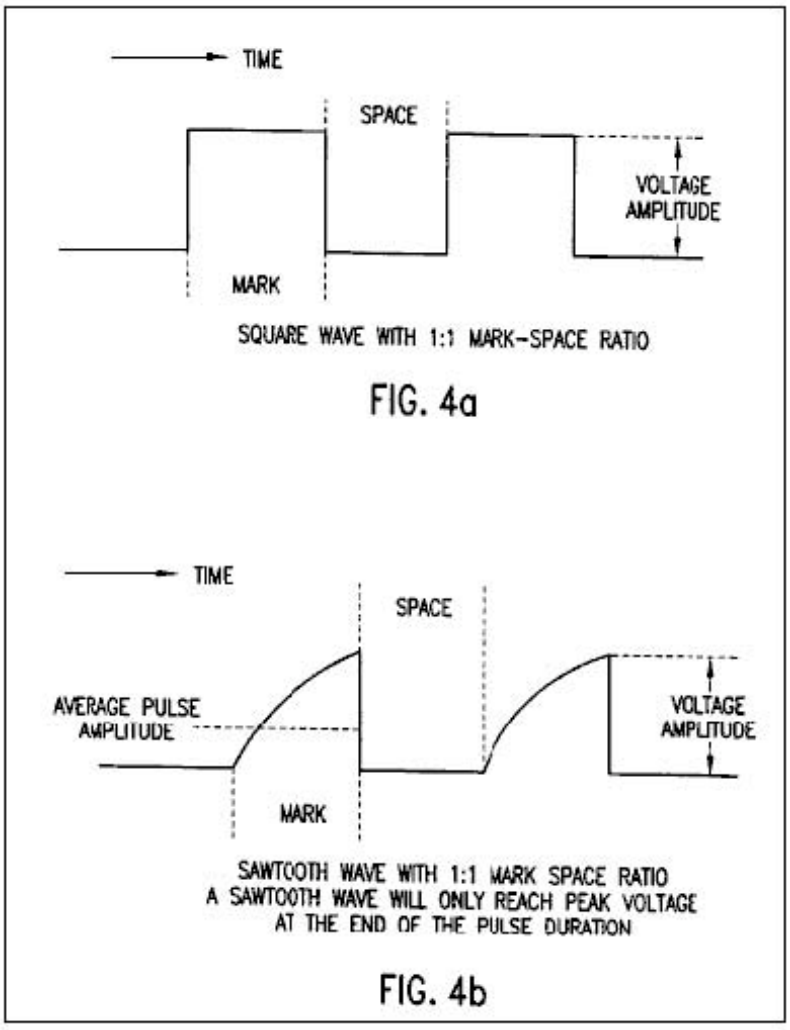

FIG. 4a

FIG. 4b

Fig.4c is a diagram illustrating a triangular wave pulsed signal which can be produced by the circuit of **Fig.5** and applied to the electrodes of **Fig.1** through **Fig.3**;

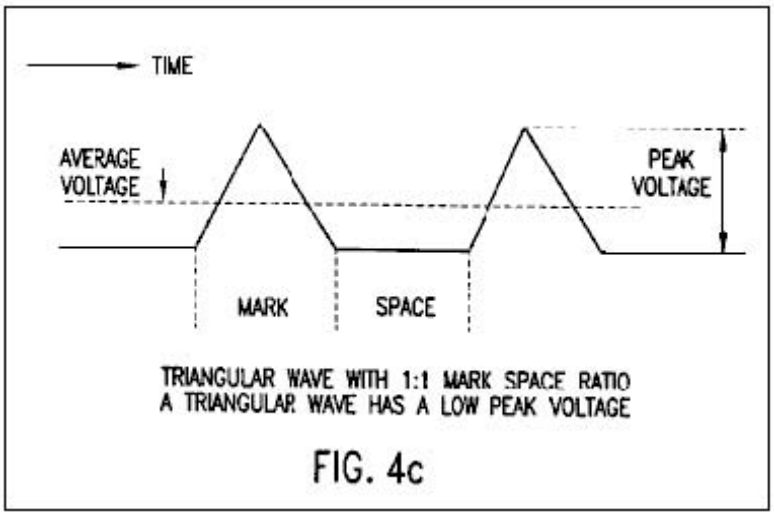

FIG. 4c

Fig.5 is an electronic circuit diagram illustrating a power supply which is connected to the electrodes of **Fig.1** through **Fig.3**;

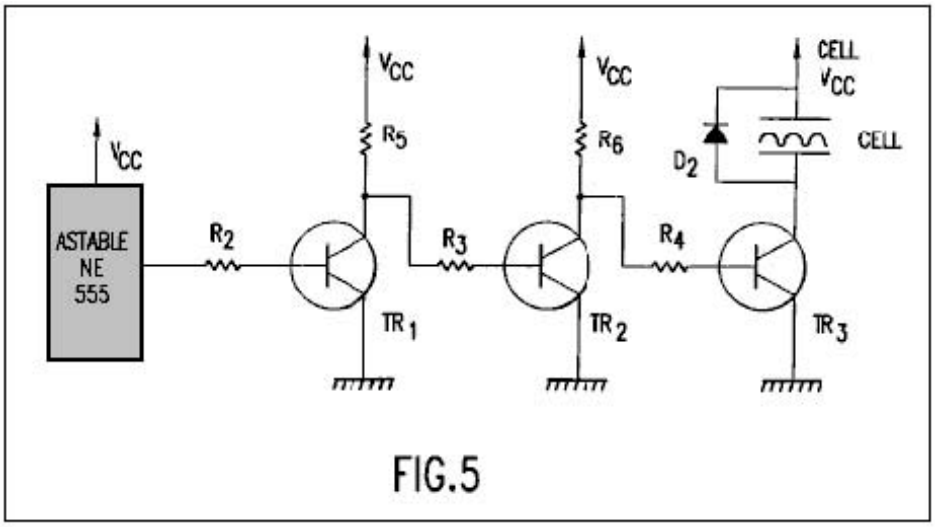

FIG.5

Fig.6 is a side view of a cell for producing at least parahydrogen including a coil and a pair of electrodes according to a fourth embodiment of the present invention;

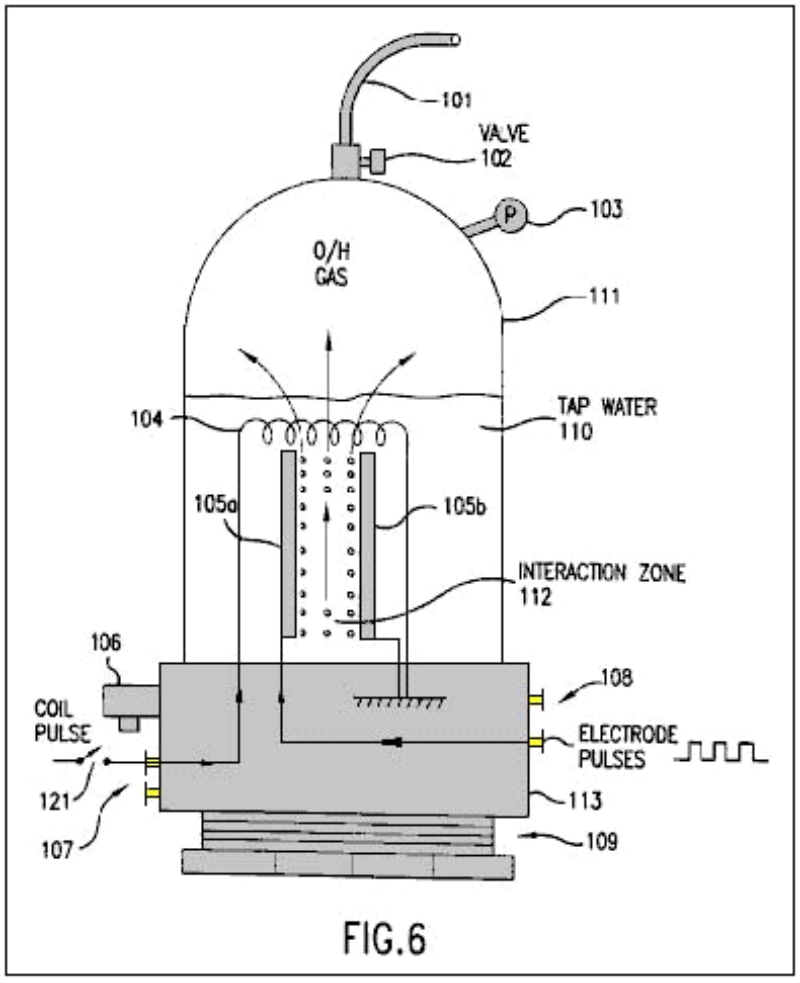

FIG.6

Fig.7 is a side view of a cell for producing at least parahydrogen including a coil and two pairs of electrodes according to a fifth embodiment of the present invention;

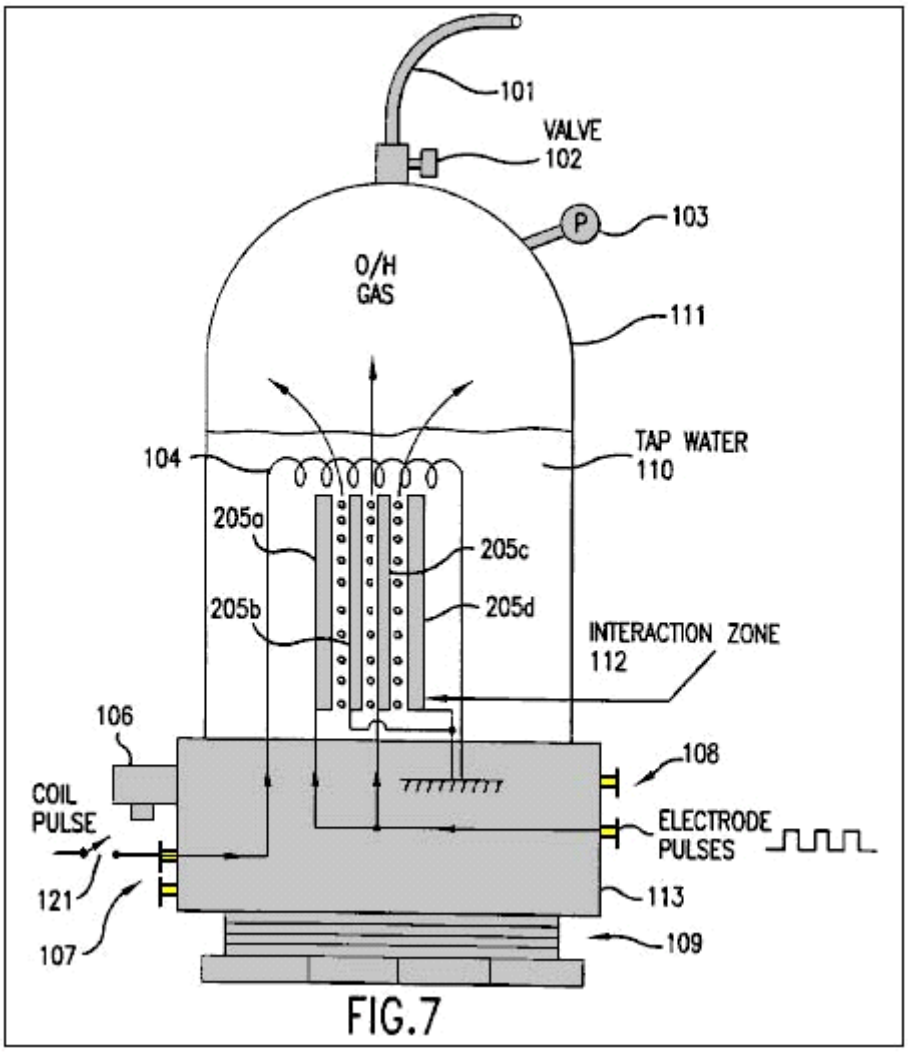

FIG.7

Fig.8 is a side view of a cell for producing at least parahydrogen including a coil and a pair of cylindrical-shaped electrodes according to a sixth embodiment of the present invention; and

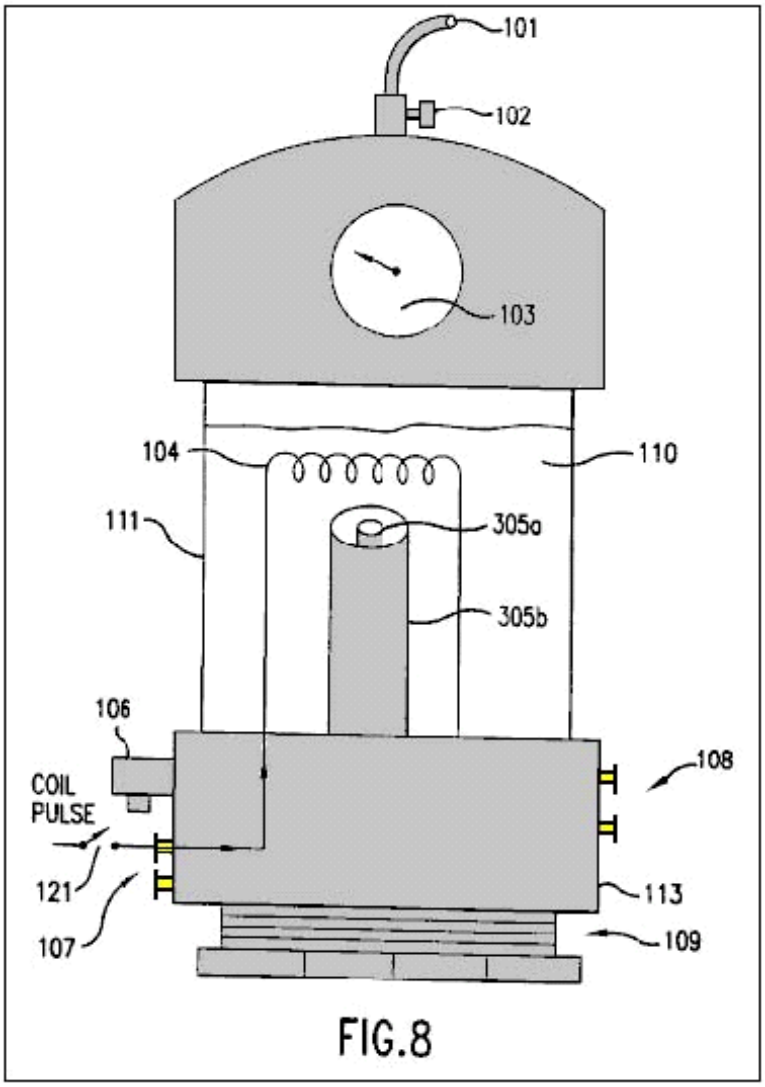

FIG.8

Fig.9 is as electronic circuit diagram illustrating a power supply which is connected to the coil and electrodes of **Fig.6** through **Fig.8**.

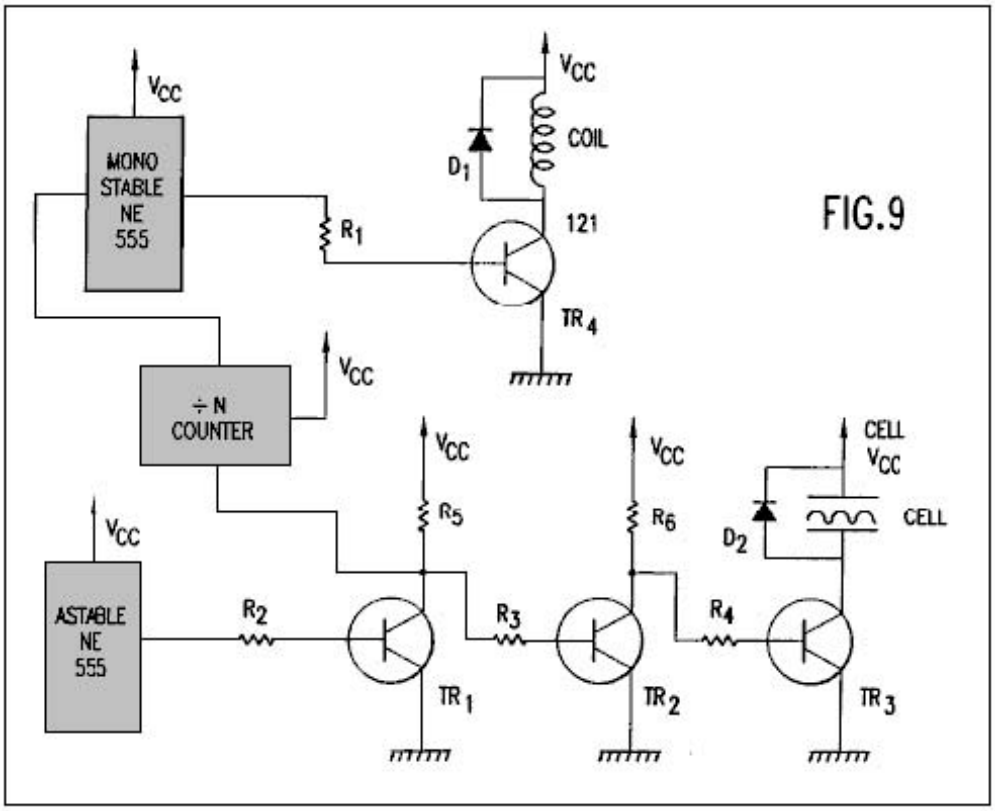

DETAILED DESCRIPTION OF THE PREFERRED EMBODIMENT

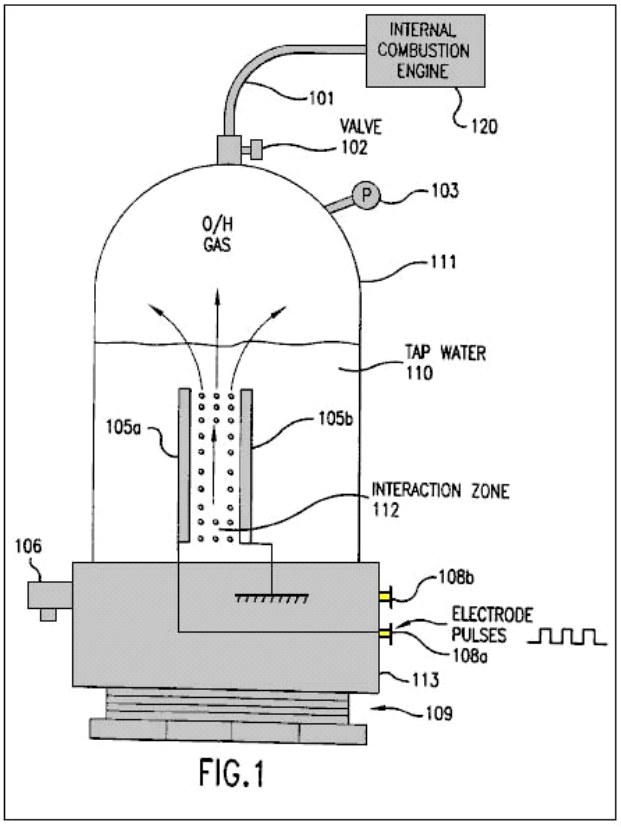

Fig.1 shows a first embodiment of the present invention including a cell for producing hydrogen and oxygen. As will be discussed below in conjunction with **Figs.6-8**, the production of parahydrogen requires an additional coil not shown in **Fig.1**. Thus, the hydrogen produced by the first embodiment of **Fig.1** is orthohydrogen.

The cell includes a closed container **111** which is closed at its bottom portion by threaded plastic base **113** and screw thread base **109**. The container **111** can be made of, for example, Plexiglas and might have a height of 430 mm and a width of 90 mm. The container **111** holds tap water **110**.

The cell also includes a pressure gauge **103** to measure the pressure within the container **111**. An outlet valve **102** is connected to the top of the container **111** to permit any gas within the container to escape into an output tube **101**.

The cell also includes an over-pressure valve **106** connected to a base **113**. The valve **106** provides a safety function by automatically releasing the pressure within the container **111** if the pressure exceeds a predetermined threshold. For example, the valve **106** may be set so that it will open if the pressure in the container exceeds 75 p.s.i. Since the container **111** is built to withstand a pressure of about 200 p.s.i., the cell is provided with a large safety margin.

A pair of electrodes **105a** and **105b** are arranged within the container **111**. These electrodes are submerged under the top level of the water **110** and define an interaction zone **112** between them. The electrodes are preferably made from the same material, such as stainless steel.

In order to produce an optimum amount of hydrogen and oxygen, an equal spacing between the electrodes **105a** and **105b** must be maintained. Moreover, it is preferable to minimise the spacing between the electrodes. However, the electrodes cannot be positioned excessively close together, because arcing between the electrodes would occur. It has been determined that a spacing of 1 mm is the optimum spacing for producing hydrogen and oxygen. Spacing up to 5 mm can work effectively, but spacing above 5 mm has not worked well, except with excessive power.

Hydrogen and oxygen gas may be output through tube **101** to a device **120** which can use those gases, for example an internal combustion engine, such as shown in **Fig.1**. Instead of an internal combustion engine, device **120** may be any device using hydrogen and oxygen, including a reciprocating piston engine, a gas turbine engine, a stove, a heater, a furnace, a distillation unit, a water purification unit, a hydrogen/oxygen jet, or other device using the gases. With an adequately productive example of the present invention, any such device **120** using the output gases can be run continuously without the need for storing dangerous hydrogen and oxygen gases.

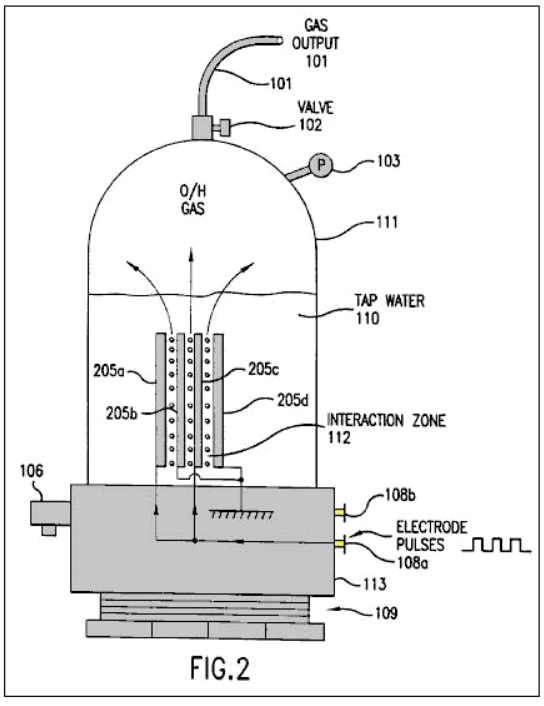

FIG.2

Fig.2 shows a second embodiment of the present invention which includes more than one pair of electrodes **205a-d**. The spacing between the electrodes is less than 5 mm as in the embodiment of **Fig.1**. While **Fig.2** shows only one additional pair of electrodes, it is possible to include many more pairs (e.g., as many as 40 pairs of electrodes) within the cell. The rest of the cell illustrated in **Fig.2** remains the same as that illustrated in **Fig.1**. The multiple electrodes are preferably flat plates closely spaced, parallel to each other.

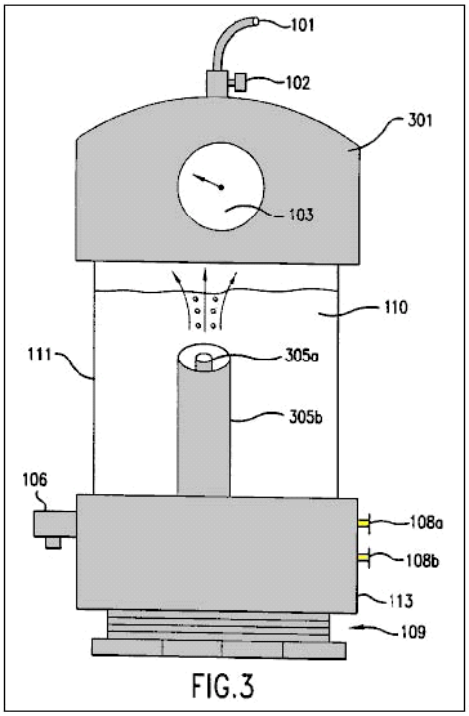

FIG.3

Fig.3 illustrates a cell having a cylindrically shaped electrodes **305a** and **305b**. The outer electrode **305b** surrounds the coaxially aligned inner electrode **305a**. The equal spacing of the electrodes **305a** and **305b** is less than 5 mm and the interactive zone is coaxially arranged between the two electrodes. While **Fig.3** illustrates the top portion of the container **111** being formed by a plastic cap **301**, it will be appreciated by those skilled in the art, that the cap **301** may be used in the embodiments of **Fig.1** and **Fig.2** and the embodiment of **Fig.3** can utilise the same container **111** illustrated in **Figs.1-2**. As suggested by **Fig.3**, the electrodes can be almost any shape such as flat plates, rods, tubes or coaxial cylinders.

The electrodes **105a** and **105b** of **Fig.1** (or electrodes **205a-d** of **Fig.2** or electrodes **305a** and **305b** of **Fig.3**) are respectively connected to power supply terminals **108a** and **108b** so that they can receive a pulsed electrical signal from a power supply. The pulsed signal can be almost any waveform and have a variable current level, voltage level, frequency and mark-space ratio (i.e., a ratio of the duration of a single pulse to the interval between two successive pulses). For example, the power supply providing power to the electrodes can be a mains 110 volts to a 12 volt supply or a car battery.

Fig.4a, **Fig.4b** and **Fig.4c** illustrate a square wave, a saw tooth wave and a triangular wave, respectively which can be applied to the electrodes **105a** and **105b** (or **205a-d** or **305a**, **305b**) in accordance with the present invention. Each of the waveforms illustrated in **Figs.4a-4c** has a 1:1 mark-space ratio. As shown in **Fig.4b**, the saw tooth wave will only reach a peak voltage at the end of the pulse duration. As shown in **Fig.4c**, the triangular wave has a low peak voltage. It has been found that optimal results for producing hydrogen and oxygen in the present invention are obtained using a square wave.

After initiation of the pulsed signal from the power supply, the electrodes **105a** and **105b** continuously and almost instantaneously generate hydrogen and oxygen bubbles from the water **110** in the interaction zone **112**. Moreover, the bubbles can be generated with only minimal heating of the water or any other part of the cell. These bubbles rise through the water and collect in the upper portion of the container **111**.

The generated bubbles are not bunched around or on the electrodes **105a** and **105b** and thus readily float to the surface of the water. Therefore, there is no need to add a chemical catalyst to assist the conduction of the solution or reduce the bubble bunching around or on the electrodes. Thus, only tap water is needed for generation of the hydrogen and oxygen in the present invention.

The gases produced within the container are self-pressurising (i.e., pressure builds in the container by the production of gas, without an air pump). Thus, no additional pump is needed to be coupled to the container **111** and the produced gases do no need to be transported into a pressurised container.

The power supply in the present invention is required to provide a pulsed signal having only 12 volts at 300 mA (3.6 watts). It has been found that an optimal amount of hydrogen and oxygen has been produced when the pulsed signal has mark-space ratio of 10:1 and a frequency of 10-250 KHz. Using these parameters, the prototype cell of the present invention is capable of producing gas at the rate of 1 p.s.i. per minute. Accordingly,

the cell of the present invention is capable of producing hydrogen and oxygen in a highly efficient manner, quickly and with low power requirements.

As noted above, the hydrogen produced by the embodiments of **Figs.1-3** is orthohydrogen. As is well understood by those skilled in the art, orthohydrogen is highly combustible. Therefore, any orthohydrogen produced can be transported from the container **111** through valve **102** and outlet tube **101** to be used by a device such as an internal combustion engine.

The present invention, with sufficient electrodes, can generate hydrogen and oxygen fast enough to feed the gases directly into an internal combustion engine or turbine engine, and run the engine continuously without accumulation and storage of the gases. Hence, this provides for the first time a hydrogen/oxygen driven engine that is safe because it requires no storage of hydrogen or oxygen gas.

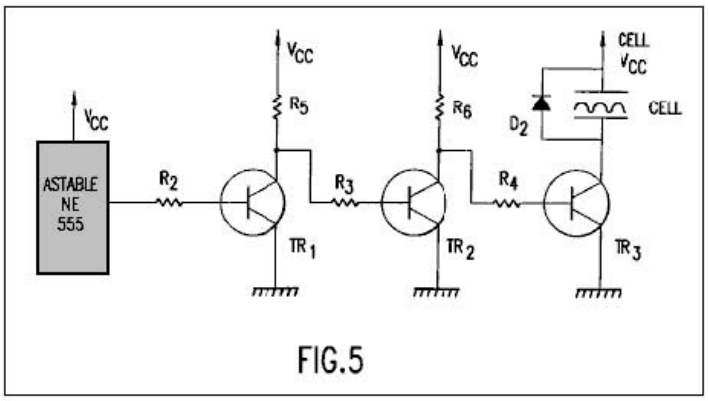

FIG.5

Fig.5 illustrates an exemplary power supply for providing D.C. pulsed signals such as those illustrated in **Figs.4a-4c** to the electrodes illustrated in **Figs.1-3**. As will be readily understood by those skilled in the art, any other power supply which is capable of providing the pulsed signals discussed above can be substituted.
The power supply illustrated in **Fig.5** includes the following parts, components and values:

The astable circuit is connected to the base of transistor **TR1** through resistor **R2**. The collector of transistor **TR1** is connected to voltage supply **Vcc** through resistor **R5** and the base of transistor **TR2** through resistor **R3**. The collector of transistor **TR2** is connected to voltage supply **Vcc** through resistor **R6** and the base of transistor **TR3** through resistor **R4**. The collector of transistor **TR3** is connect to one of the electrodes of the cell and diode **D2**. The emitters of transistors **TR1, TR2** and **TR3** are connected to ground. Resistors **R5** and **R6** serve as collector loads for transistors **TR1** and **TR2**, respectively. The cell serves as the collector load for transistor **TR3**. Resistors **R2, R3** and **R4** ensure that transistors **TR1**, **TR2** and **TR3** are saturated. Diode **D2** protects the rest of the circuit from any induced back emf within the cell.

The astable circuit is used to generate a pulse train at a specific time and with a specific mark-space ratio. This pulse train is provided to the base of transistor **TR1** through resistor **R2**. Transistor **TR1** operates as an invert switch. Thus, when the a stable circuit produces an output pulse, the base voltage of the transistor **TR1** goes high (i.e. close to **Vcc** or logic 1). Hence, the voltage level of the collector of transistor **TR1** goes low (i.e., close to ground or logic 0).

Transistor **TR2** also operates as an inverter. When the collector voltage of transistor **TR1** goes low, the base voltage of transistor **TR2** also goes low and transistor **TR2** turns off. Hence, the collector voltage of transistor **TR2** and the base voltage of Transistor **TR3** go high. Therefore, transistor **TR3** turns on with the same mark-space ratio as the astable circuit. When the transistor **TR3** is on, one electrode of the cell is connected to **Vcc** and the other is connected to ground through transistor **TR3**. Thus, the transistor **TR3** can be turned on (and off) and therefore the transistor **TR3** effectively serves as a power switch for the electrodes of the cell.

Figs.6-8 illustrate additional embodiments of the cell which are similar to the embodiments of **Figs.1-3**, respectively. However, each of embodiments of **Figs.6-8** further includes a coil **104** arranged above the electrodes and power supply terminals **107** connected to the coil **104**. The dimensions of coil **104** can be, for example, 5 x 7 cm and have, for example, 1500 turns. The coil **104** is submerged under the surface of the water **110**.

The embodiments of **Figs.6-8** further include an optional switch **121** which can be switched on or off by the user. When the switch **121** is not closed, then the cell forms basically the same structure as **Figs.1-3** and thus can be operated in the same manner described in **Figs.1-3** to produce orthohydrogen and oxygen. When the switch **121** is closed, the additional coil **104** makes the cell capable of producing oxygen and either (1) parahydrogen or (2) a

mixture of parahydrogen and orthohydrogen.

When the switch **121** is closed (or not included), the coil **104** is connected through terminals **106** and the switch **121** (or directly connected only through terminals **106**) to a power supply so that the coil **104** can a receive a pulsed signal. As will be discussed below, this power supply can be formed by the circuit illustrated in **Fig.9**.

When the coil **104** and the electrodes **105a** and **105b** receive pulses, it is possible to produce bubbles of parahydrogen or a mixture of parahydrogen and orthohydrogen. The bubbles are formed and float to the surface of the water **110** as discussed in **Figs.1-3**. When the coil is pulsed with a higher current, a greater amount of parahydrogen is produced. Moreover, by varying the voltage of the coil **104**, a greater/lesser percentage of orthohydrogen/parahydrogen can be produced. Thus, by controlling the voltage level, current level and frequency (discussed below) provided to the coil **104** (and the parameters such as voltage level, current level, frequency, mark-space ratio and waveform provided to the electrodes **105a** and **105b** as discussed above) the composition of the gas produced by the cell can be controlled. For example, it is possible to produce only oxygen and orthohydrogen by simply disconnecting the coil **104**. It is also possible to produce only oxygen and parahydrogen by providing the appropriate pulsed signals to the coil **104** and the electrodes **105a** and **105b**. All of the benefits and results discussed in connection with the embodiments of **Figs.1-3** are equally derived from the embodiments of **Figs.6-8**. For example, the cells of **Figs.6-8** are self-pressurising, require no-chemical catalyst, do not greatly heat the water **110** or cell, and produce a large amount of hydrogen and oxygen gases from a modest amount of input power, without bubbles on the electrodes.

A considerable amount of time must pass before the next pulse provides current to the coil **104**. Hence, the frequency of the pulsed signal is much lower than that provided to the electrodes **105a** and **105b**. Accordingly, with the type of coil **104** having the dimensions described above, the frequency of pulsed signals can be as high as 30 Hz, but is preferably 17-22 Hz to obtain optimum results.

Parahydrogen is not as highly combustible as orthohydrogen and hence is a slower burning form of hydrogen. Thus, if parahydrogen is produced by the cell, the parahydrogen can be coupled to a suitable device such as a cooker or a furnace to provide a source of power or heat with a slower flame.

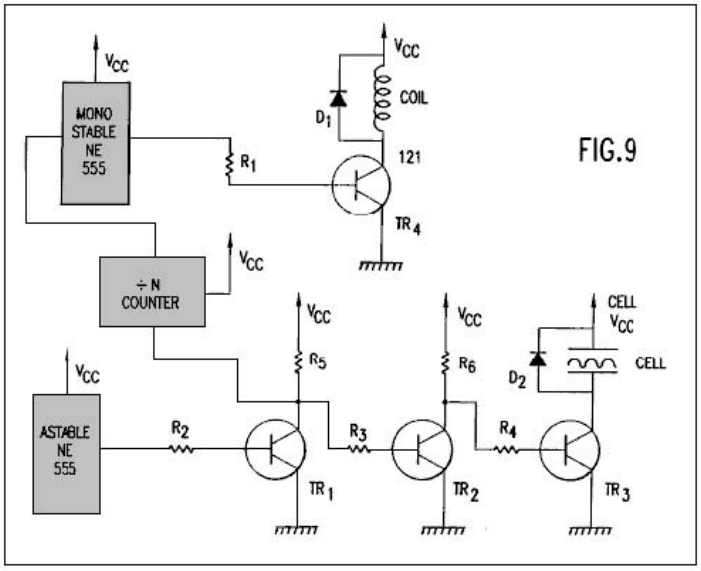

Fig.9 illustrates an exemplary power supply for providing D.C. pulsed signals such as those illustrated in **Figs.4a-4c** to the electrodes illustrated in **Figs.6-8**. Additionally, the power supply can provide another pulsed signal to the coil. As will be readily understood by those skilled in the art, any other power supply which is capable of providing the pulsed signals discussed above to the electrodes of the cell and the coil can be substituted. Alternatively, the pulsed signals provided to the electrodes and the coil can be provided by two separate power supplies.

The portion of the power supply (astable circuit, **R2-R6**, **TR1-TR3**, **D2**) providing a pulsed signal to the electrodes of the cell is identical to that illustrated in **Fig.5**. The power supply illustrated in **Fig.9** further includes the following parts and their respective exemplary values:

The input of the ‘divide-by-N’ counter (hereinafter "the divider") is connected to the collector of transistor **TR1**. The output of the divider is connected to the monostable circuit and the output of the monostable circuit is connected to the base of transistor **TR4** through resistor **R1**. The collector of transistor **TR4** is connected to one end of the coil and a diode **D1**. The other end of the coil and the diode **D1** are connected to the voltage supply

Vcc. Resistor **R1** ensures that **TR4** is fully saturated. Diode **D2** prevents any induced back emf generated within the coil from damaging the rest of the circuit. As illustrated in **Figs.6-8**, a switch **121** can also incorporated into the circuit to allow the user to switch between (1) a cell which produces orthohydrogen and oxygen, and (2) a cell which produces at least parahydrogen and oxygen.

The high/low switching of the collector voltage of transistor **TR1** provides a pulsed signal to the divider. The divider divides this pulsed signal by N (where N is a positive integer) to produce a pulsed output signal. This output signal is used to trigger the monostable circuit. The monostable circuit restores the pulse length so that it has a suitable timing. The output signal from the monostable circuit is connected to the base of transistor **TR4** through resistor **R1** to switch transistor **TR4** on/off. When transistor **TR4** is switched on, the coil is placed between **Vcc** and ground. When the transistor **TR4** is switched off, the coil is disconnected from the rest of the circuit. As discussed in conjunction with **Figs.6-8**, the frequency of pulse signal provided to the coil is switched at a rate preferably between 17-22 Hz; i.e., much lower than the frequency of the pulsed signal provided to the electrodes.

As indicated above, it is not required that the circuit (divider, monostable circuit, **R1, TR4** and **D1**) providing the pulsed signal to the coil be connected to the circuit (astable circuit, **R2-R6**, **TR1-TR3, D2**) providing the pulsed signal to the electrodes. However, connecting the circuits in this manner provides an easy way to initiate the pulsed signal to the coil.

A working prototype of the present invention has been successfully built and operated with the exemplary and optimal parameters indicated above to generate orthohydrogen, parahydrogen and oxygen from water. The output gas from the prototype has been connected by a tube to the manifold inlet of a small one cylinder gasoline engine, with the carburettor removed, and has thus successfully run such engine without any gasoline:

CHARLES GARRETT

US Patent 2,006,676 2nd July 1935 Inventor: Charles H. Garrett

ELECTROLYTIC CARBURETTOR

Please note that this is a re-worded excerpt from this patent. It describes an electrolyser which Charles claimed was able to generate enough gas from hydrolysis of water, to be able to run a car engine without the use of any other fuel. It should be remembered that in Garrett's day, car electrics were all 6-volt systems.

DESCRIPTION

This invention relates to carburettors and it has particular reference to an electrolytic carburettor by means of which water may be broken up into its hydrogen and oxygen constituents and the gases so formed suitably mixed with each other and with air.

Another object of the invention is to provide a means whereby the electrolyte level in the carburettor may be maintained at a more or less constant level regardless of fluctuations in water pressure at the water inlet of the carburettor.

Another object of the invention is to provide a means whereby the relative amount of air mixed with the hydrogen and oxygen may be regulated as desired.

Still another object of the invention is the provision of a means to prevent the loss of hydrogen and oxygen gases during periods in which these gases are not being drawn from the carburettor.

Still another object of the invention is the provision of a means whereby the hydrogen and oxygen resulting from electrolysis may be formed in separate compartments, and a further object of the invention is the provision of a means to periodically reverse the direction of current flow and thereby alternate the evolution of the gases in the separate compartments, to be intermingled at a later time.

With reference to the accompanying drawings: -

Figure 1 is a view in vertical section of one form of carburettor.

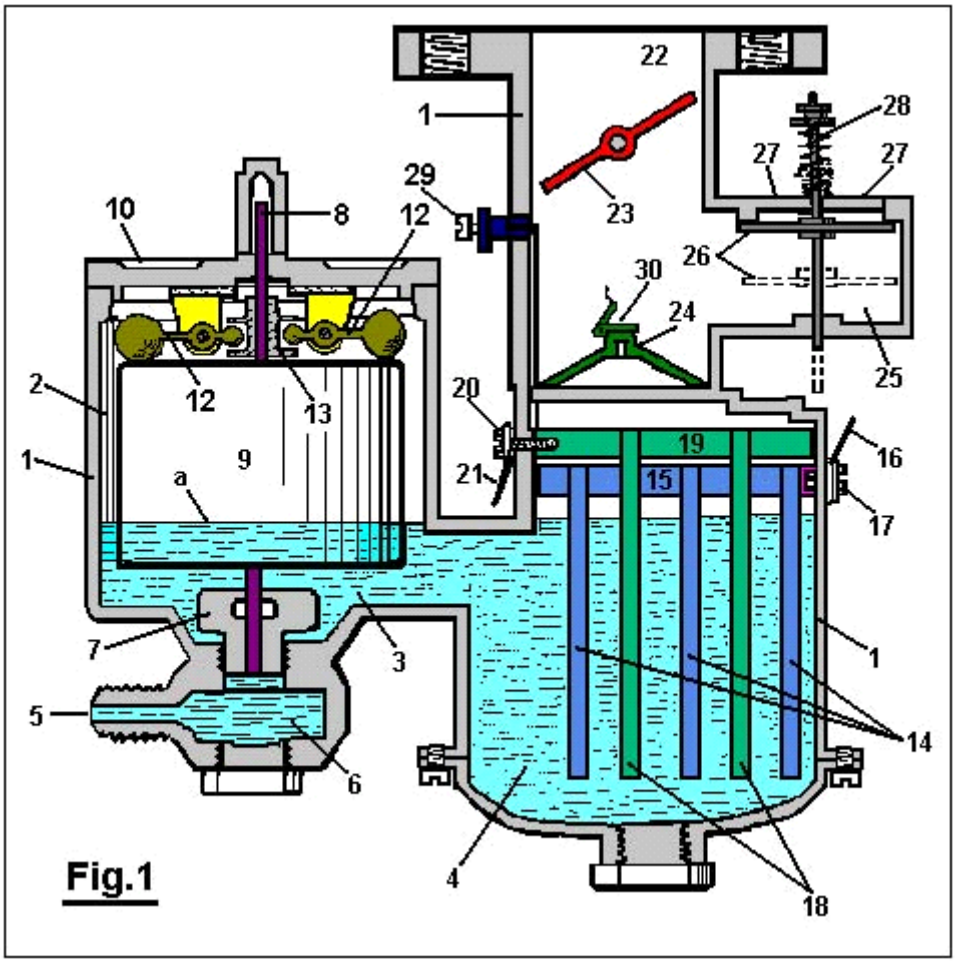

Fig.1

Figure 2 is a modified form.

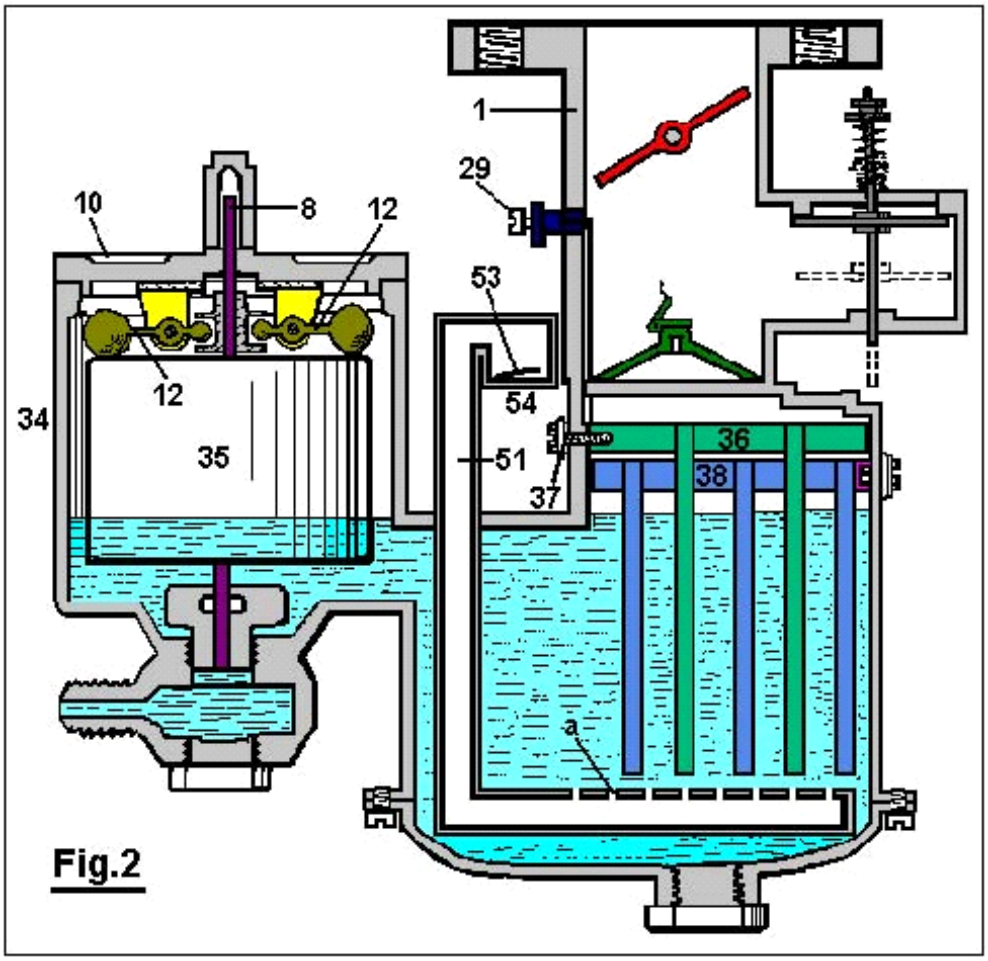

Fig.2

Figure 3 is a diagrammatic view of a pole changer, showing its actuating mechanism, and

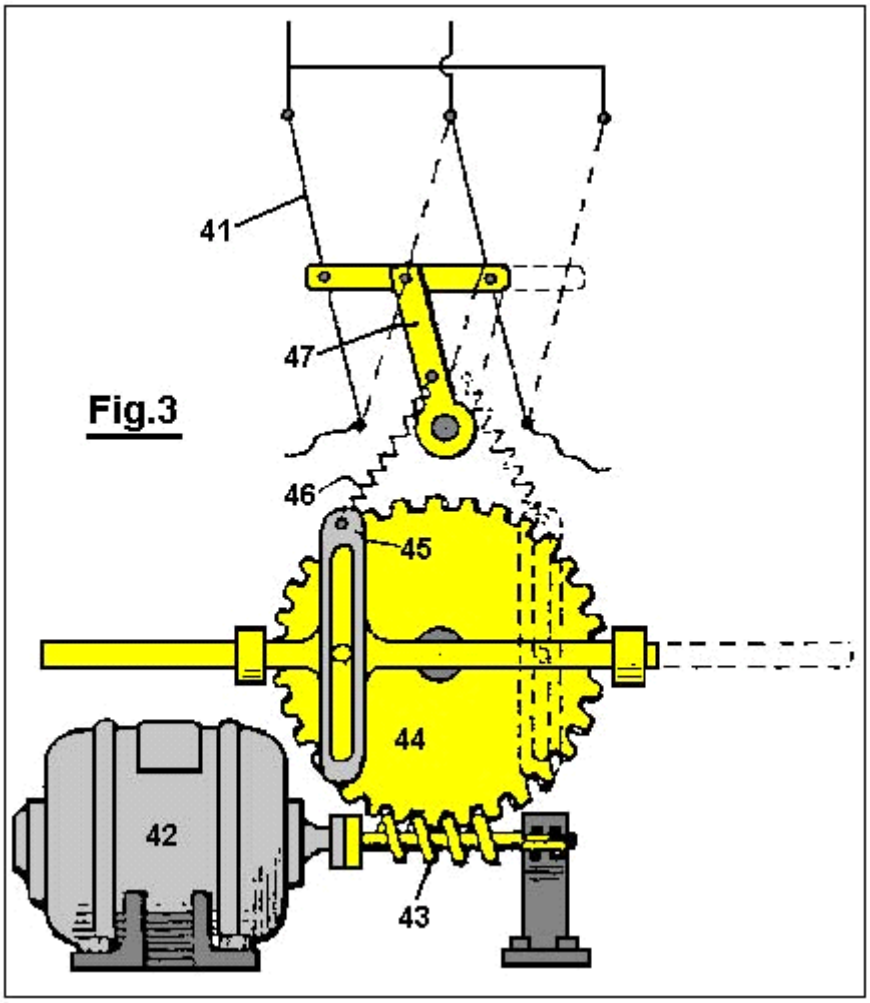

Figure 4 is a wiring diagram for the modified form of carburettor shown in Figure 2.

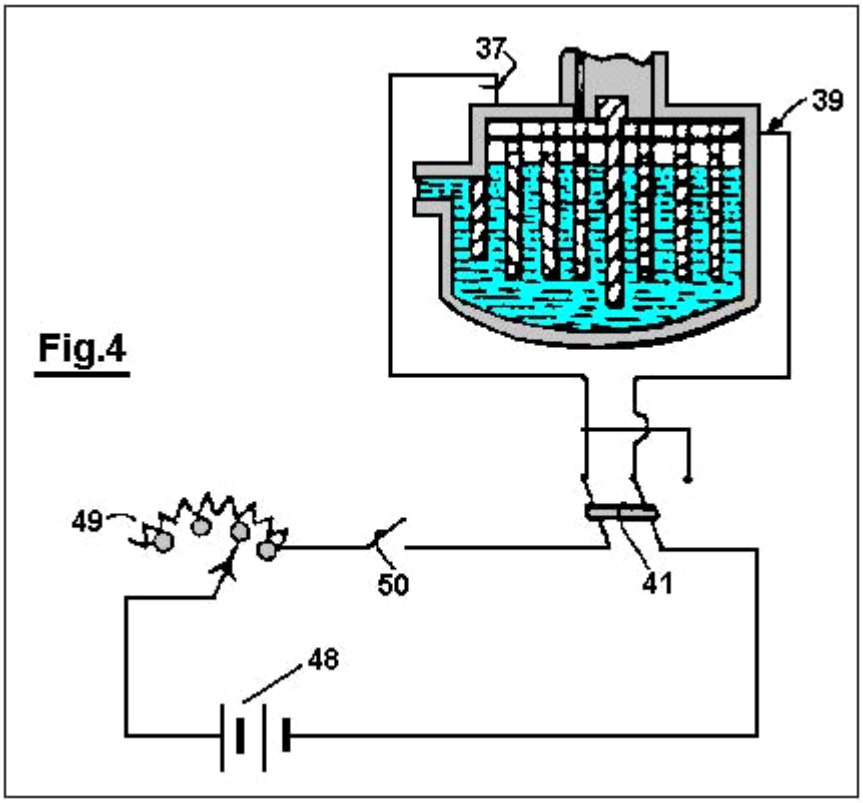

Fig.4

With reference to **Fig.1**: The reference numeral **1** designates the carburettor housing, which is preferably constructed of bakelite or other suitable insulating material. This housing is designed so as to divide the carburettor into a float chamber **2** and gas generating chamber **4**, connected by a fluid passage **3**.

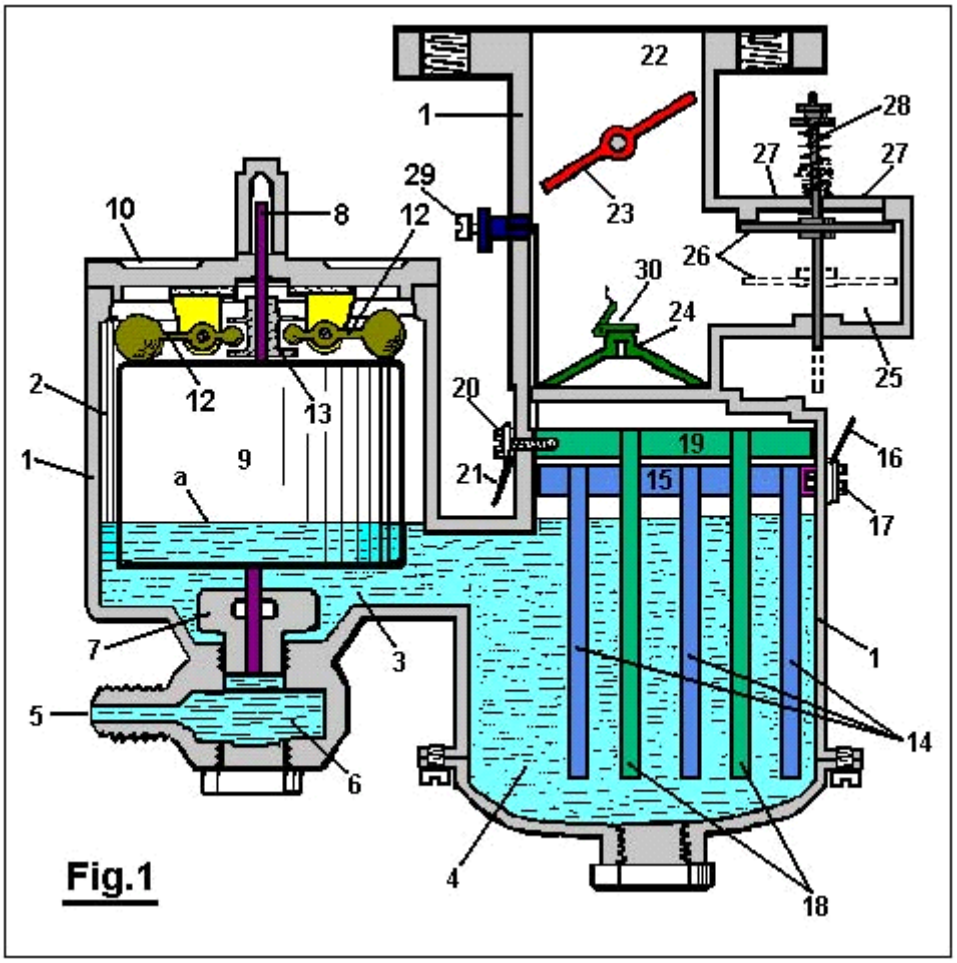

Fig.1

Water under pressure is forced into the carburettor through an opening **5** which communicates with the float chamber **2** through the medium of the sediment chamber **6** and the needle valve orifice **7**, which is closed by a needle valve **8** when the device is not in operation. A float **9** surrounds the needle valve **8** and is free to move vertically relative thereto. Descending from the cover **10** to the float chamber **2** are two ears **11**, located at spaced intervals on opposite sides of the needle valve **8**. The members **12** are pivoted to the ears **11**, as shown. The weighted outer ends of the members **12** rest on top of the float **9**, and their inner ends are received in an annular groove in the collar **13** which is rigidly attached to the needle valve **8**.

Within the gas generating chamber **4**, a series of spaced, descending plates **14** are suspended from a horizontal member **15** to which a wire **16** has electrical contact through the medium of the bolt **17**, which extends inwards through housing **1** and is threaded into the horizontal member **15**.

A second series of plates **18** is located between the plates **14** and attached to the horizontal member **19**, and has electrical contact with the wire **20** through the bolt **21**.

A gas passageway **22**, in which a butterfly valve **23** is located, communicates with the gas generating chamber **4** through an orifice **24**. An air inlet chamber **25** has communication with the gas passageway **22** above the orifice **24**. A check valve **26** which opens downwards, controls the openings **27**, and is held closed and inoperative by means of light spring **28**.

An adjustable auxiliary air valve **29** is provided in the wall of the gas passageway **22**, which air valve is closed by the butterfly valve **23** when the butterfly valve is closed, but communicates with the outside air when the butterfly valve is open.

The operation of the device is as follows :

The chambers **2** and **4** are first filled to the level **'a'** with a solution of weak sulphuric acid (or other electrolyte not changed by the passage of current through it), and the opening **5** is connected to a tank of water (not shown).

The wire **16** is next connected to the positive pole of a storage battery or other source of direct current and the wire **20** to the negative pole. Since the solution within the carburettor is a conductor of electricity, current will flow through it and hydrogen will be given off from the negative or cathode plates **18** and oxygen from the positive or anode plates **14**.

The butterfly valve **23** is opened and the gas passageway **22** brought into communication with a partial vacuum. Atmospheric pressure acting on the top of the check valve **26** causes it to be forced downwards as shown in dotted lines. The hydrogen and oxygen liberated from the water at the plates **18** and **14** are drawn upwards through the orifice **24** covered by the check valve **30** where they are mixed with air entering through the openings **27** and through the auxiliary air valve **29**.

When it is desired to reduce the flow of hydrogen and oxygen from the plates **18** and **14**, the current flowing through the device is reduced, and when the current is interrupted the flow ceases. When the butterfly valve **23** is moved to its ‘closed’ position, the check-valve **26** is automatically closed by the spring **28**. Any excess given off during these operations is stored in the space above the fluid where it is ready for subsequent use.

Water is converted into its gaseous constituents by the device herein described, but the dilute sulphuric acid or other suitable electrolyte in the carburettor remains unchanged, since it is not destroyed by electrolysis, and the parts in contact therewith are made of bakelite and lead or other material not attacked by the electrolyte.

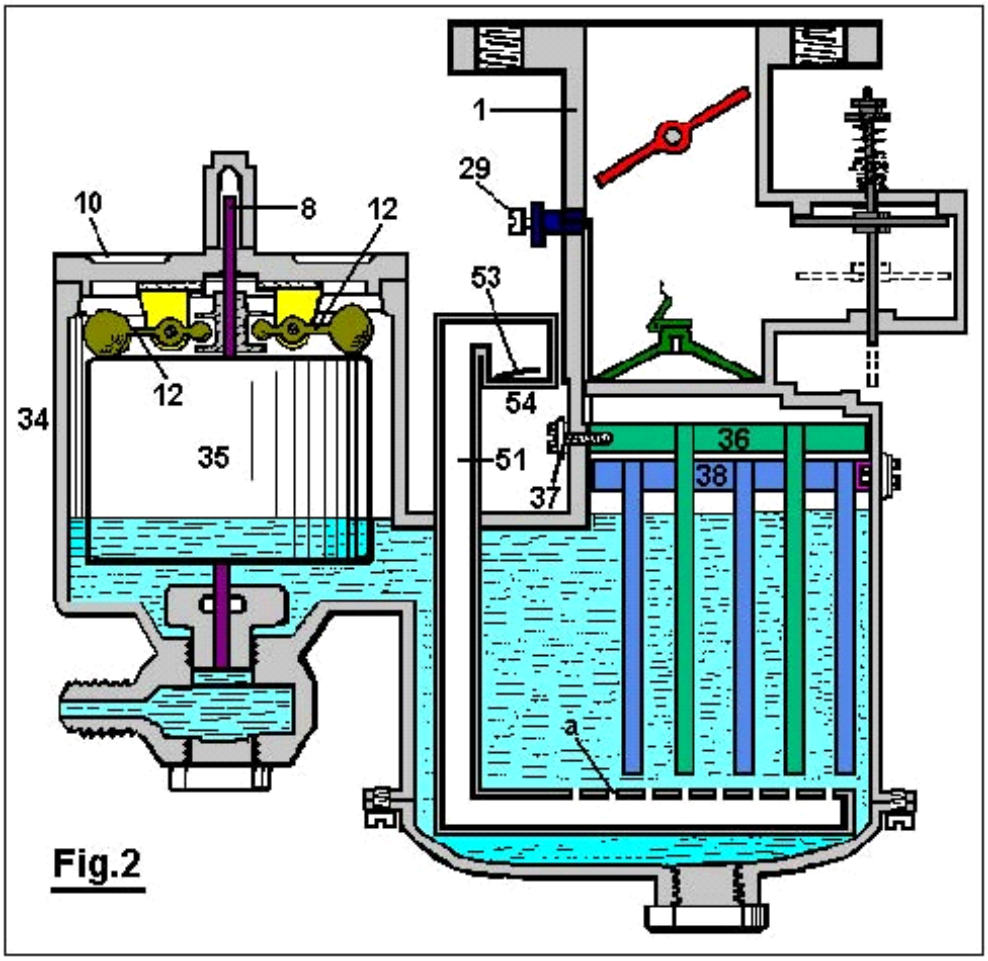

Fig.2

The structure shown in **Fig.2** is substantially the same as that shown in **Fig.1** with the exception that the modified structure embraces a larger gas generating chamber which is divided by means of an insulating plate **31** and is further provided with a depending baffle plate **32** which separates the gas generating chamber **33** from the float chamber **34** in which the float **35** operates in the same manner as in **Fig.1**. Moreover, the structure shown in **Fig.2** provides a series of spaced depending plates **36** which are electrically connected to the wire **37**, and a second series of similar plates **38** which are electrically connected to the wire **39** and are kept apart from the plates **36** by the insulating plate **31**.

Gases generated on the surfaces of the plates **36** and **38** pass upward through the orifice **39a** into the gas passageway **40** where they are mixed with air as explained in the description of **Fig.1**.

A pipe **51,** bent as shown in **Fig.2**, passes downwards through the housing of the carburettor and has a series of spaced apertures **'a'** in its horizontal portion beneath the plates **36** and **38**. Check valve **53**, with opens upwards, controls air inlet **54**. When a partial vacuum exists in the chamber **33**, air is drawn in through the opening **54** and then passes upwards through the apertures **'a'**. This air tends to remove any bubbles of gas collecting on the plates **36** and **38** and also tends to cool the electrolyte. The check valve **53** automatically closes when a gas pressure exists within the carburettor and thereby prevents the electrolyte from being forced out of the opening **54**.

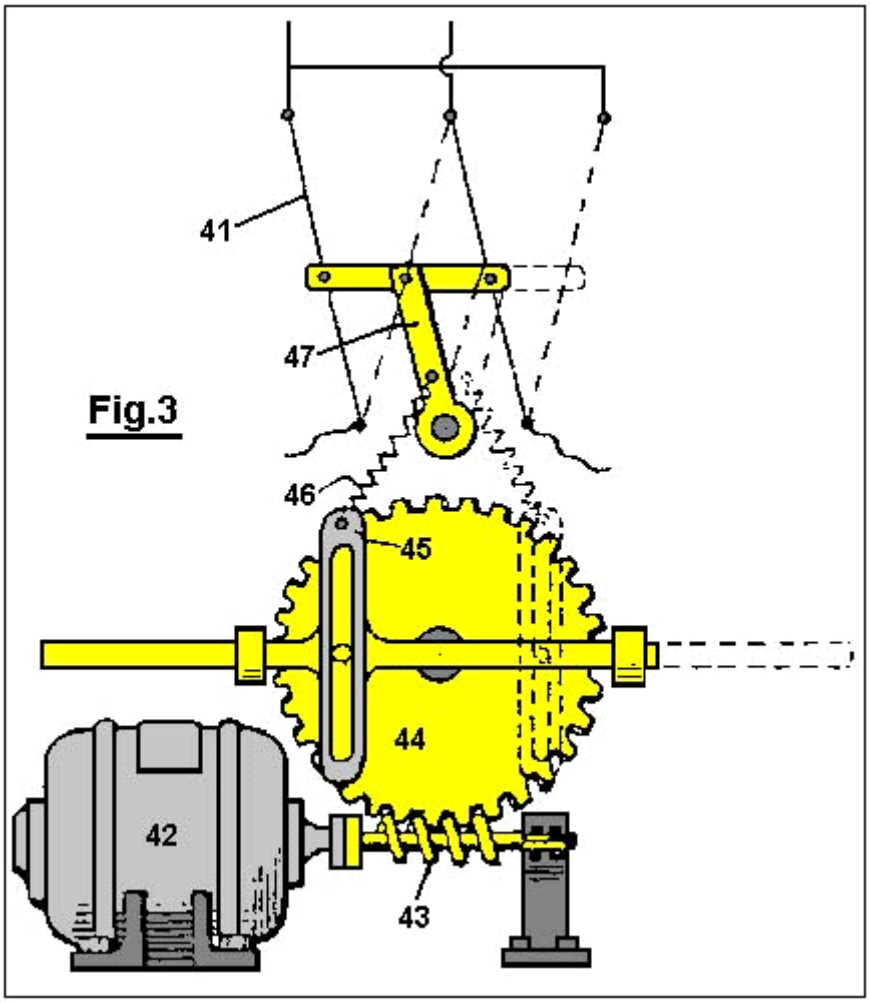

Fig.3

In order to provide for alternate evolution of the gases from the plates **36** and **38**, a pole changer **41**, shown in **Fig.3**, is actuated periodically by the motor **42** which drives the worm **43** and the gear **44** and causes oscillations of the member **45** which is connected by a spring **46** to the arm **47**, thereby causing the pole changer to snap from one position to the other.

In operation, the carburettor shown in **Fig.2** is connected as shown in the wiring diagram of **Fig.4**. A storage battery **48** or other suitable source of direct current is connected to a variable rheostat **49**, switch **50**, pole changer **41** and to the carburettor as shown. Thus the rate of evolution of the gases can be controlled by the setting of the rheostat **49** and the desired alternate evolution of the gases in the compartments of the carburettor is accomplished by means of the periodically operated pole changer **41**.

Manifestly, the construction shown is capable of considerable modification and such modification as is considered within the scope and meaning of the appended claims is also considered within the spirit and intent of the invention.

ARCHIE BLUE

US Patent 4,124,463 7th November 1978 Inventor: Archie H. Blue

ELECTROLYTIC CELL

Please note that this is a re-worded excerpt from this patent. It describes an electrolyser system where air is drawn through the electrolyte to dislodge bubbles from the electrodes.

ABSTRACT

In the electrolytic production of hydrogen and oxygen, air is pumped through the cell while the electrolysis is in progress so as to obtain a mixture of air, hydrogen and oxygen.

BACKGROUND AND BRIEF DESCRIPTION OF THE INVENTION

This invention relates to the production of gases which can be utilised primarily, but not necessarily, as a fuel.

To decompose water electrically, it is necessary to pass direct current between a pair of electrodes which are immersed in a suitable electrolyte. During such electrolysis, it is normal to place some form of gas barrier between the two electrodes, in order to prevent the gases produced forming an explosive mixture. However provided suitable precautions are taken, it has been found that the gases can be allowed to mix and can be fed into a storage tank for subsequent use. Because the gases when mixed form an explosive mixture, it is possible for the mixture to be utilised, for instance, as a fuel for an internal combustion engine. In such circumstances it is desirable that the gases should also be mixed with a certain proportion of air in order to control the explosive force which results when the gases are ignited.

One of the difficulties encountered with electrolysis is that bubbles of gas are liable to remain on the electrodes during the electrolysis thus effectively limiting the area of electrode which is in contact with the electrolyte and preventing optimum current flow between the electrodes. Because it is desirable that the gases evolved during the electrolysis be mixed with air, it is possible for air to be passed through the cell while electrolysis is in progress. The passage of air through the cell can be directed past the electrodes so as to pick up any gas bubbles on the electrodes.

Accordingly, the invention comprises an electrolytic cell with a gas tight casing, several electrodes supported on a central post within the cell, spaced apart and electrically insulated from each other, each alternative electrode being connected to a positive direct current source or a negative direct current source respectively and wherein the central post is in the form of a tube, one end of which is extended out of the cell and connected to a source of air under pressure, with the other end of the central post terminating in an air outlet below the electrodes. The cell also includes a gas outlet to carry the air forced into the cell through the central post and to exhaust the gases produced by electrolysis.

DETAILED DESCRIPTION OF THE INVENTION

Various forms of the invention will now be described with the aid of the accompanying drawings wherein:

Fig.1 is a diagrammatic elevational view partly in section of one form of the invention,

FIG. 1

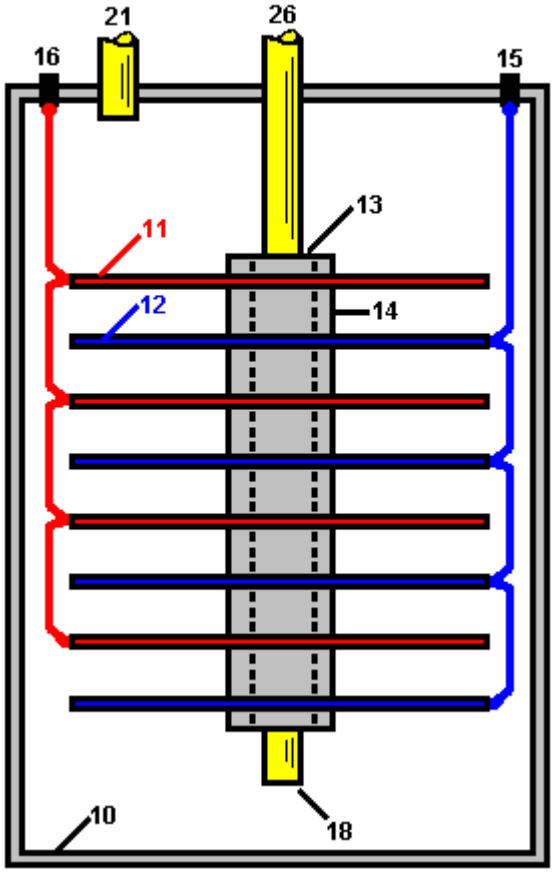

Fig.2 is a diagrammatic elevational view partly in section of a modified form of the invention,

FIG. 2

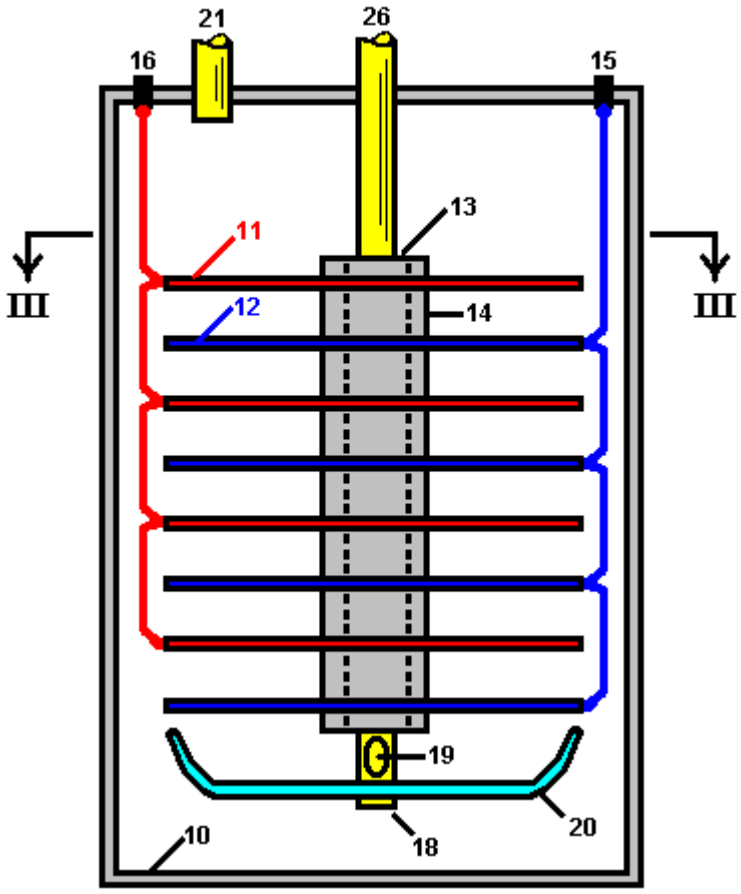

Fig.3 is a section along the line **III--III** of **Fig.2**.

FIG. 3

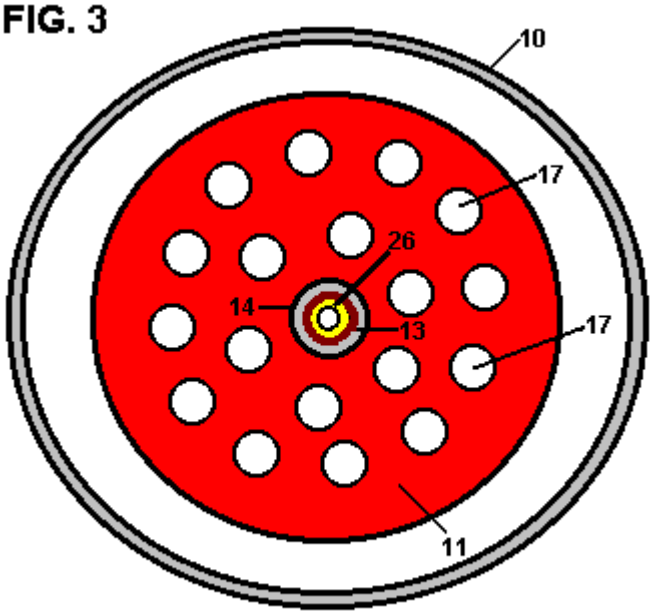

Section III - III

FIG. 1

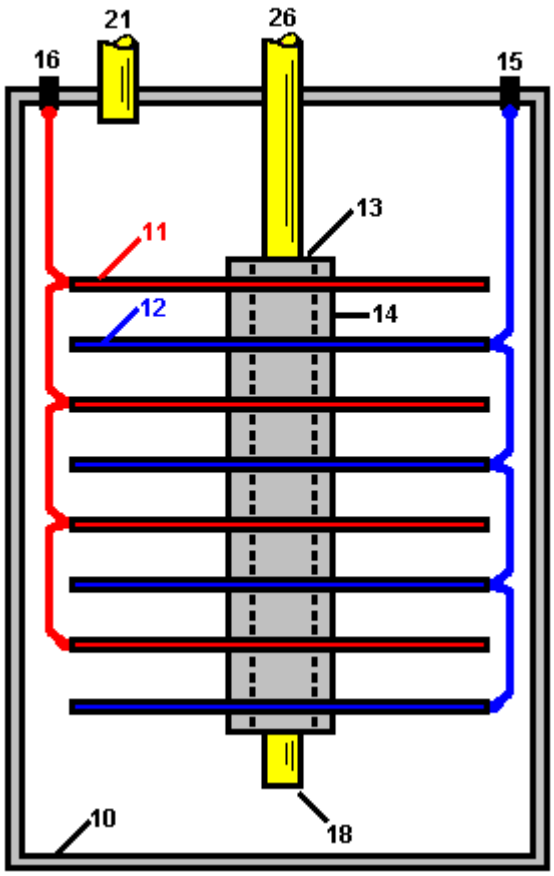

The cell as shown in **Fig.1** comprises a gas-tight casing **10** which is formed from a material incapable of corrosion, such as plastic. Several cathode plates **11** and several anode plates **12** are supported within the cell on an electrically insulating central post **13**, with the cathode plates and anode plates being spaced apart by means of insulating spacers **14**. The anode plates **12** are all connected in parallel to a positive terminal post **15** while the cathode plates are all connected in parallel to the negative terminal post **16**, these connections being indicated in dotted lines in the drawings. The cathode and anode plates are preferably in the form of discs made from a metal suited to the electrolyte, thus ensuring a satisfactory cell life. These plates may be shaped to conform with the shape of the walls of the cell which may be circular in cross section as indicated or any other desired shape.

The central post **26** is preferably in the form of a tube which extends out of the cell. The lower end of the tube **18** is open so that air can be pumped into the cell through the central post **26** and enter the cell via the lower end **18** where it will pass up through the electrolyte. This keeps the electrolyte in constant motion which assists in the rapid removal of any gas bubbles which may be adhering to the electrode plates.

FIG. 2

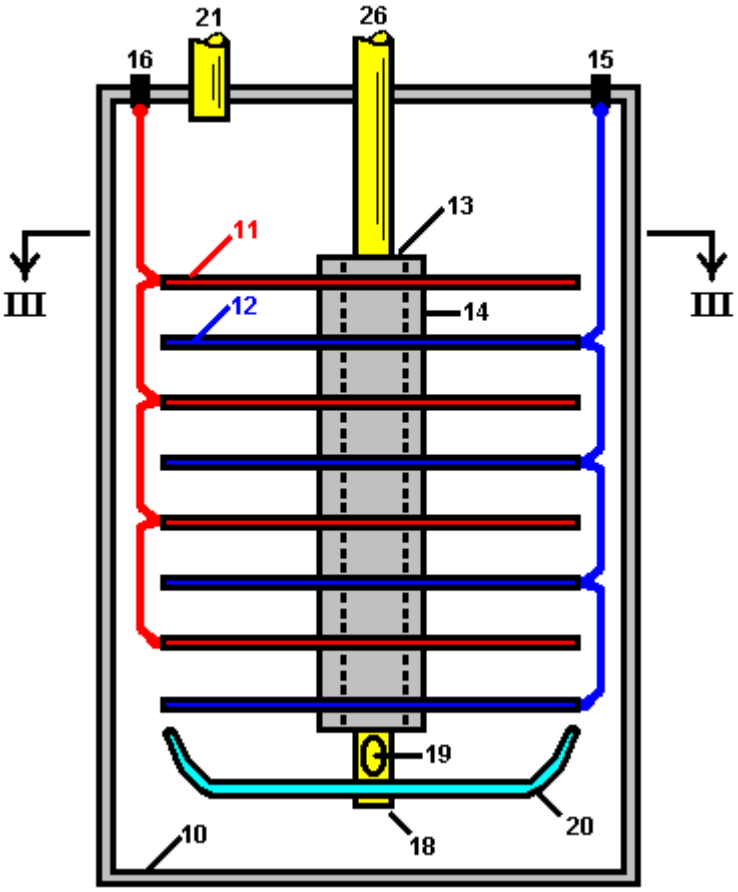

In the modification shown in **Fig.2** and **Fig.3**, each electrode plate is provided with holes **17.** The central post **26** is also provided with at least one air hole **19** adjacent to its the lower end. A deflector plate **20** is also supported by the central post **26**, this plate being dish shaped so as to deflect air issuing out of the air hole **19** up through the holes **17** in the electrodes. This further assists in dislodging any bubbles of gas clinging to the electrode plates.

The cell also includes a gas outlet **21** so that the air which enters the cell, together with the gases produced by electrolysis, can be taken out of the cell into a suitable storage tank (not shown in the drawings). If desired, such storage tank can be arranged to accept the gases under pressure and for this purpose the air pumped into the cell will be pumped in under the required pressure. A gas drier (not shown in the drawings) can also be interposed between the gas outlet **21** and the storage tank.

Although the electrolysis will naturally produce considerable heat, nevertheless it can be found advantageous to install a heater in the cell, preferably in the bottom of the cell, to assist and facilitate the warming up of the electrolyte so that the cell reaches its most efficient operating conditions as quickly as possible.

Preferably also, a current-control device should be employed so that the intensity of the electrolytic action can be controlled.

A mechanism may also be provided for the automatic replenishment of water within the cell as the level of the electrolytic drops during use.

While it is recognised that the mixing of hydrogen and oxygen will create a dangerous explosive mixture, nevertheless by carrying out the invention as described above, the risk of explosion is minimised. The gases produced can be utilised, for instance, as a fuel to power an internal combustion engine and for this purpose it is desirable, as already mentioned, to mix a proportion of air with the gases produced during electrolysis, so that when the mixture is ignited within the cylinder or cylinders of the engine, the explosive force so created can be of the desired amount.

While in the foregoing description reference is made to the utilisation of the mixed gases as a fuel, it will of course be understood that the gases can be separated for individual use.

CLAIMS

1. A process for producing, Through the electrolysis of an aqueous liquid, a combustible mixture of hydrogen, oxygen and air. This is achieved in an electrolytic cell having a gas-tight casing, a substantially central tubular post mounted in the casing and having an air inlet at its upper end, and a several electrodes supported on the post and axially spaced along it, alternate electrodes being connected to a first electrical terminal and to a second electrical terminal respectively connected to a respective poles of a current source and being mutually insulated, the post having an air outlet below the electrodes out of which flows air from the air inlet into the cell and over the electrodes; and a source of air under pressure connected to the said air inlet forcing a flow of air through the aqueous liquid contained in the cell; the cell having in its upper region a common outlet exhausting the combustible mixture comprising air forced through the cell, along with hydrogen and oxygen produced by electrolysis in the cell.

2. The process according to claim 1 wherein the electrodes are discs each having a several holes through them.

3. The process according to claim 1 further including a dish-shaped air deflector plate supported on the post below the air outlet.

4. Apparatus for producing by electrolysis of an aqueous liquid, a combustible mixture of hydrogen and oxygen, comprising: an electrolytic cell having a gas-tight casing, a substantially central tubular post mounted in the casing and having an air inlet at its upper end, and a plurality of electrodes supported on the post and axially spaced along it, alternate electrodes being connected to a first electrical terminal and to a second electrical terminal respectively for connection to respective poles of a current source and being mutually insulated, the post having an air outlet below the electrodes for flow of air from the air inlet into the cell and over the electrodes; a dish-shaped air deflector supported on said post below said air outlet; and a source of air under pressure connected to the said air inlet for forcing a flow of air through the aqueous liquid contained in the cell in operation thereof; the cell having in its upper region a common outlet for exhausting the combustible mixture comprising air forced through the cell and hydrogen and oxygen produced by electrolysis of the liquid in the cell.

5. The apparatus according to claim 4 wherein the electrodes are discs each having a several holes through them.

RUGGERO SANTILLI

US Patent 6,183,604 6th February 2001 Inventor: Ruggero M. Santilli

Durable and Efficient Equipment for the Production of a Combustible and Non-Pollutant Gas from Underwater Arcs and Method therefor

Please note that this is a re-worded excerpt from this patent. It shows how electrolysis of water can be carried out on a large scale as a continuous process.

ABSTRACT

A system for producing a clean burning combustible gas comprising an electrically conductive first electrode and an electrically conductive second electrode. A motor coupled to the first electrode is adapted to move the first electrode with respect to the second electrode to continuously move the arc away from the plasma created by the arc. A water-tight container for the electrodes is provided with a quantity of water within the tank sufficient to submerge the electrodes.

BACKGROUND OF THE INVENTION

1. Field of the Invention

The present invention relates to durable and efficient equipment for the production of a combustible and non-polluting gas from underwater arcs and the method for doing this and more particularly, the invention pertains to producing a combustible gas from the underwater arcing of electrodes which move with respect to each other.

2. Description of the Prior Art

The combustible nature of the gas bubbling to the surface from an underwater welding arc between carbon electrodes was discovered and patented in the last century. Various improved equipment for the production of said combustible gas have been patented during this century. Nevertheless, the technology has not yet reached sufficient maturity for regular industrial and consumer production and sales because of numerous insufficiencies, including excessively short duration of the carbon electrodes which requires prohibitive replacement and service, as well as low efficiency and high content of carbon dioxide responsible for the greenhouse effect. As a result of numerous experiments, this invention deals with new equipment for the production of a combustible gas from underwater arcs between carbon electrodes which resolves the previous problems, and achieves the first known practical equipment for industrial production and sales.

The technology of underwater electric welding via the use of an arc between carbon electrodes to repair ships, was established in the last century. It was then discovered that the gas bubbling to the surface from underwater arcs is combustible. In fact, one of the first U.S. patents on the production of a combustible gas via an underwater electric arc between carbon electrodes dates back to 1898 (U.S. Pat. No. 603,058 by H. Eldridge).

Subsequently, various other patents were obtained in this century on improved equipment for the production of this combustible gas, among which are:

US Pat. No. 5,159,900 (W.A. Dammann abd D. Wallman, 1992); U.S.Pat. No. 5,435,274 (W. H. Richardson, Jr., 1995); U.S. Pat. No. 5,417,817 (W. A. Dammann and D. Wallman, 1995); U.S. Pat. No. 5,692,459 (W. H. Richardson, Jr., 1997); U.S. Pat. No. 5,792,325 (W. H. Richardson, Jr., 1998); and U.S. Pat. No. 5,826,548 (W. H. Richardson, Jr., 1998).

The main process in these inventions is essentially the following. The arc is generally produced by a DC power unit, such as a welder, operating at low voltage (25-35 V) and high current (300 A to 3,000 A) depending on the available Kwh input power. The high value of the current brings the tip of the carbon electrode in the cathode to incandescence, with the consequential disintegration of the carbon crystal, and release of highly ionised carbon atoms to the arc. Jointly, the arc separates the water into highly ionised atoms of Hydrogen and Oxygen. This causes a high temperature plasma in the immediate surrounding of the arc, of about 7,000^{o}F, which is composed of highly ionised H, O and C atoms.

A number of chemical reactions then occur within or near the plasma, such as: the formation of the H_2O_2 molecule; the burning of H and O into H_2O; the burning of C and O into CO; the burning of CO and O into CO_2, and other reactions. Since all these reactions are highly exothermic, they result in the typical, very intense glow of the arc within water, which is bigger than that of the same arc in air. The resulting gases cool down in the water surrounding the discharge, and bubble to the surface, where they are collected with various means. According to numerous measurements conducted at various independent laboratories, the combustible gas produced with the above process essentially consists of 45%-48% H_2, 36%-38% CO, 8%-10% CO_2, and 1%-2% O_2, the remaining gas consisting of parts per million of more complex molecules composed by H, O and C.

This process produces an excellent combustible gas because the combustion exhausts meet all current EPA requirement without any catalytic converter at all, and without the highly harmful carcinogenic pollutants which are contained in the combustion exhausts of gasoline, diesel, natural gas and other fuels of current use.

Despite the indicated excellent combustion characteristics, and despite research and development conducted by inventors for decades, the technology of the combustible gas produced by an underwater arc between carbon electrodes has not reached industrial maturity until now, and no equipment producing said combustible gas for actual practical usages is currently sold to the public in the U.S.A. or abroad, the only equipment currently available for sale being limited to research and testing. The sole equipment currently sold for public use produce different gases, such as Brown's gas which is not suitable for use in internal combustion engines because it implodes, rather than explodes, during combustion.

The main reason for lack of industrial and consumer maturity is the excessively short duration of the carbon electrodes, which requires prohibitive replacement and services. According to extensive, independently supervised, and certified measurements, the electrodes are typically composed of solid carbon rods of about 3/8 inch (9 mm) in diameter and about 1 foot length. Under 14 Kwh power input, said electrodes consume at the rate of about one and one quarter inch (32 mm) length per minute, requiring the halting of the operation, and replacement of the electrodes every ten minutes.

The same tests have shown that, for 100 Kwh power input, said electrodes are generally constituted by solid carbon rod of about 1 inch diameter and of the approximate length of one foot, and are consumed under a continuous underwater arc at the rate of about 3 inch length per minute, thus requiring servicing after 3 to 4 minutes of operation. In either case, current equipment requires servicing after only a few minutes of usage, which is unacceptable on industrial and consumer grounds for evident reasons, including increased risks of accidents for very frequent manual operations in a piece of high current equipment.

An additional insufficiency of existing equipment is the low efficiency in the production of said combustible gas, which efficiency will from now on be referred to as the ratio between the volume of combustible gas produced in cubic feet per hour (cfh) and the real input power per hour (Kwh). For instance extensive measurements have established that pre-existing equipment has an efficiency of 2-3 cfh/Kwh. Yet another insufficiency of existing equipment is the high carbon dioxide content in the gas produced. Carbon dioxide is the gas responsible for the greenhouse effect. In fact, prior to combustion the gas has a CO_2 content of 8%-10% with a corresponding content after combustion of about 15% CO_2, thus causing evident environmental problems.

SUMMARY OF THE INVENTION

In view of the foregoing disadvantages inherent in the known types of traditional equipment for the production of combustible and non-polluting gases now present in the prior art, the present invention provides improved durable and efficient equipment for the production of a combustible and non-polluting gas from underwater arcs and the method of production.

As such, the general purpose of the present invention, which will be described later in greater detail, is to provide new, improved, durable and efficient equipment for the production of a combustible and non-polluting gas from underwater arcs and the method for achieving this, a method which has all the advantages of the prior art and none of the disadvantages.

To attain this, the present invention essentially comprises of a new and improved system for producing a clean burning combustible gas from an electric arc generating plasma under water. First provided is an electrically conductive anode fabricated of tungsten. The anode is solid in a generally cylindrical configuration with a diameter of about one inch and a length of about three inches. Next provided is a generally Z-shaped crank of a electrically conductive material. The crank has a linear output end supporting the anode. The crank also has a linear input end essentially parallel with the output end. A transverse connecting portion is located between the input and output ends.

An electrically conductive cathode is next provided. The cathode is fabricated of carbon. The carbon is in a hollow tubular configuration with an axis. The cathode has a supported end and a free end. The cathode has a length of about 12 inches and an internal diameter of about 11.5 inches and an external diameter of about 12.5 inches. A motor is next provided. The motor has a rotatable drive shaft. The drive shaft has a fixed axis of rotation. The motor is coupled to the input end of the crank and is adapted to rotate the crank to move the output end and anode in a circular path of travel. The circular path of travel has a diameter of about twelve inches with the anode located adjacent to the free end of the cathode. In this manner the anode and the arc are continuously moved around the cathode and away from the plasma created by the arc.

Next provided is an axially shifted support. The support is in a circular configuration to receive the supported end of the cathode and to move the cathode axially toward the anode as the carbon of the cathode is consumed during operation and use. Next provided is a water tight container for the anode, cathode, crank and support. A quantity of water is provided within the tank, sufficient to submerge the anode and the cathode. Next provided is an entrance port in the container. The entrance port functions to feed water and a carbon enriched fluid into the container to supplement the carbon and water lost from the container during operation and use. Next provided is a source of potential. The source of potential couples the anode and the cathode. In this manner an electrical arc is created between the anode and the cathode with a surrounding plasma for the production of gas within the water. The gas will then bubble upwards and collect above the water. Last provided is an exit port for removing the gas which results from the application of current from the source of potential to the anode and the cathode while the anode is rotating and the cathode is shifting axially.

This broad outline indicates the more important features of the invention in order that the detailed description which follows may be better understood and in order that the present contribution to the art may be better appreciated. There are, of course, additional features of the invention that will be described and which will form the subject matter of the claims made.

In this respect, before explaining at least one embodiment of the invention in detail, it is to be understood that the invention is not limited in its application to the details of construction and to the arrangements of the components set forth in the following description or illustrated in the drawings. The invention is capable of other embodiments and of being practised and carried out in various ways. Also, it is to be understood that the phraseology and terminology employed here are for the purpose of descriptions and should not be regarded as limiting the scope of this invention.

It is another object of the present invention to provide new and improved durable and efficient equipment for the production of a combustible and non-polluting gas from underwater arcs and method therefor which may be easily and efficiently manufactured and marketed on a commercial basis.

Lastly, it is an object of the present invention to provide a new and improved system for producing a clean burning combustible gas comprising an electrically conductive first electrode, an electrically conductive second electrode, a motor coupled to the first electrode and adapted to move the first electrode with respect to the second electrode to continuously move the arc away from the plasma created by the arc, and a water-tight container for the electrodes with a quantity of water within the tank sufficient to submerge the electrodes.

These together with other objects of the invention, along with the various novel features which characterise the invention, are pointed out particularly in the claims section of this disclosure. For a better understanding of the invention, its operating advantages and the specific objects attained by its uses, reference should be made to the accompanying drawings and descriptive matter in which there is illustrated preferred embodiments of the invention.

BRIEF DESCRIPTION OF THE DRAWINGS

The invention will be better understood and objects other than those set forth above will become apparent when consideration is given to the following detailed description thereof. Such description makes reference to the annexed drawings wherein:

Fig.1 and **Fig.2** are illustrations of prior art equipment for the fabrication of a pollutant-free combustible gas produced by an electric arc under water constructed with prior art techniques.

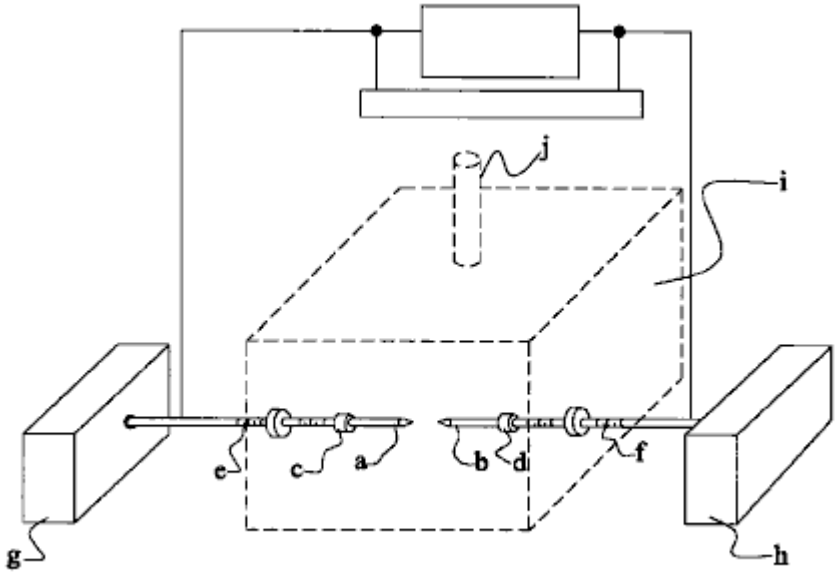

FIG. 1

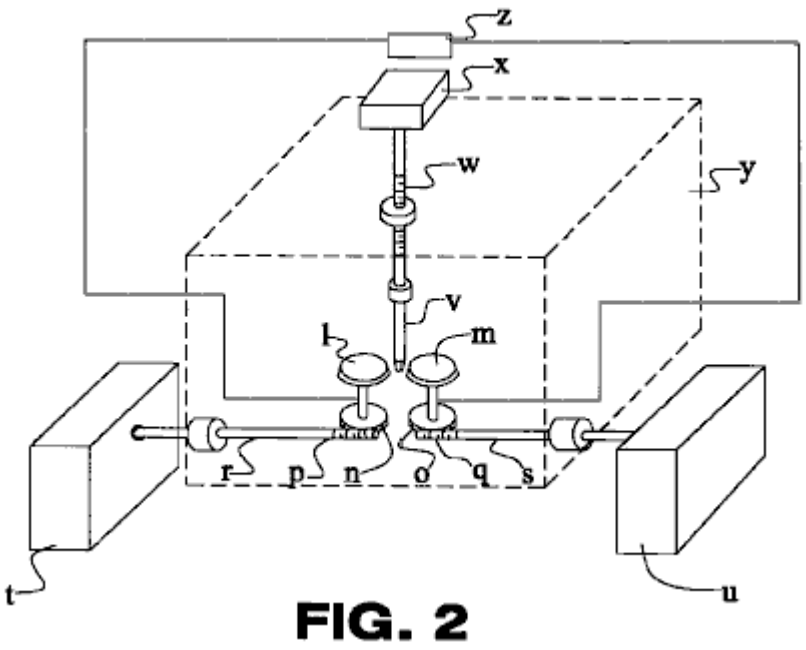

FIG. 2

Fig.3 is a schematic diagram depicting the principles of the present invention.

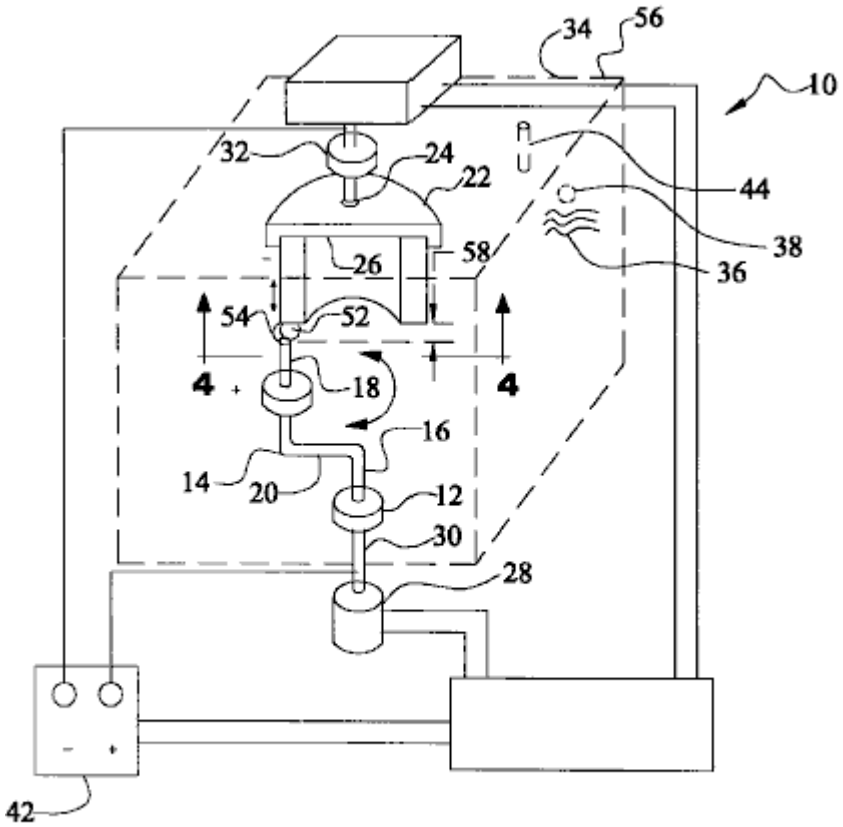

FIG. 3

Fig.4 is a schematic diagram of a partial sectional view taken along line 4--4 of Fig.3, depicting an additional embodiment of the present invention.

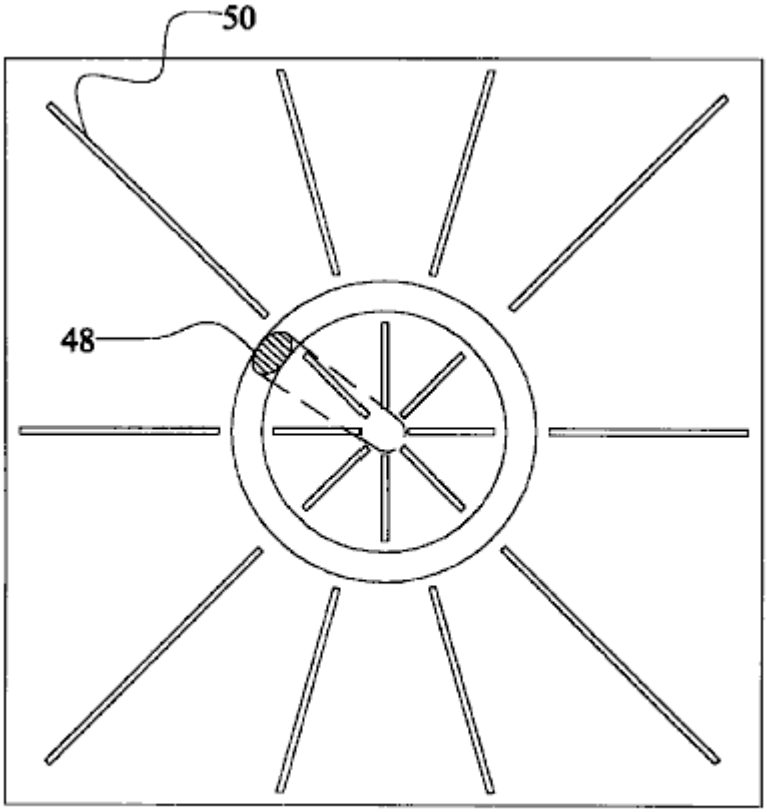

FIG. 4

The same reference numerals refer to the same parts throughout the various Figures.

DESCRIPTION OF THE PREFERRED EMBODIMENT

With reference to **Fig.1**, a typical embodiment of the electrodes of current use for the production of a combustible gas from underwater arcs is that in which one or more pairs of solid carbon rods are immersed within the selected liquid head-on along their cylindrical symmetry axis. The activation of the arc first requires the physical contact of the tips of the two rods, with consequential large surge of electricity due to shorting, followed by a retraction of the electrodes up to the arc gap, which is typically of the order of 1/16 inch (1.5 mm) depending on the input power. The components of such embodiment include:

a, b: carbon electrodes
c, d: holder of a & b
e, f: screws for advancement of a & b
g, h: mechanism for the advancement of a & b
i: reaction chamber
j: exit of combustible gas from chamber

Numerous alternatives to the above typical embodiment have been invented. For instance, in the U.S. Pat. No. 603,058 (H. Eldridge, 1898) one can see a variety of configurations of the electrodes, including rod shaped anodes and disk-shaped cathodes. As a further example also with reference to Fig.1, the embodiment of U.S. Pat. No. 5,159,900 (W. A. Dammann and D. Wallman, 1992) and U.S. Pat. No. 5,417,817 (W. A. Dammann and D. Wallman, 1995), essentially consists of the preceding geometric configuration of the electrodes, complemented by a mechanism for the inversion of polarity between the electrodes, because the cathode experiences the highest consumption under a DC arc, while the anode experiences a much reduced consumption. Even though innovative, this second embodiment also remains manifestly insufficient to achieve the duration of the electrodes needed for industrial maturity, while adding other insufficiencies, such as the interruption of the arc at each time the polarities are inverted, with consequential loss of time and efficiency due to the indicated electrical surges each time the arc is initiated.

As an additional example, and with reference to **Fig.2**, the mechanism of the U.S. Pat. No. 5,792,325 (W. H. Richardson, Jr., 1998), has a different preferred embodiment consisting of one or more pairs of electrodes in

the shape of carbon disks rotating at a distance along their peripheral edges, in between which an electrically neutral carbon rod is inserted. This rod causes the shorting necessary to activate the arc, and then the maintenance of the arc itself. This latter mechanism also does not resolve the main problem considered here. In fact, the neutral carbon rod is consumed at essentially the same rate as that of the preceding embodiments. In addition, the mechanism has the disadvantage of breaking down the single arc between two cylindrical electrodes into two separate arcs, one per each the two couplings of the conducting disk and the neutral rod, with consequential reduction of efficiency due to the drop of voltage and other factors. Numerous means can be envisaged to improve the life of carbon electrodes, such as mechanisms based on barrel-type rapid replacements of the carbon rods. These mechanisms are not preferred here because the arc has to be reactivated every time a rod is replaced, thus requiring the re-establishing of the arc with physical contact, and consequential shortcomings indicated earlier. The components of such embodiment include:

l, m: carbon disk electrodes
n, O: gear rotating l & m
p, q: side gear for rotating n & o
r, s: shaft of gears p & q
t, u: mechanism for rotating shafts r & s
v: electrodes neutral vertical rod
w: advancement of v
x: mechanism for advancement of v
y: reactor chamber
z: electrical power mechanism

This inventor believes that the primary origin of the insufficiency considered here, rests with the carbon rods themselves, which are indeed effective for underwater welding, but are not adequate for the different scope of producing a combustible gas from underwater arcs.

With reference to **Fig.3**, this invention specifically deals with equipment which solves the insufficiency considered here, by achieving the duration of operation desired by the manufacturer, while sustaining a continuous arc without interruptions for the entire desired duration. For the case of large industrial production of this combustible gas with electrical energy input of the order of 100 Kwh, a representative equipment of this invention essentially consists of:

1) One or more arcs produced by a DC current as typically available in commercially sold power units;
2) One or more anodes made of solid rods of about 1 inch in diameter and about 2 inches in length and composed of a high temperature conductor, such as Tungsten or ceramic. Extensive and diversified experiments have established that the consumption of an anode composed of ordinary Tungsten is minimal, and definitely of the order of several weeks of operation.
3) One or more carbon-based cathodes in the configuration of a large hollow rod geometrically defined as a cylinder with the same thickness of the anode, but with a radius and length selected to provide the desired duration. This cathode performs the vital function of becoming incandescent in the immediate vicinity of the arc, thus releasing carbon to the plasma.

More specifically, and with reference to **Fig.3** and **Fig.4**, the present invention essentially comprises a new and improved system **10** for producing a clean burning combustible gas from an electric arc generating plasma under water. First provided is an electrically conductive anode **12** fabricated of tungsten. The anode is solid in a generally cylindrical configuration with a diameter of about one inch and a length of about three inches.

Next provided is a generally Z-shaped crank **14** of a electrically conductive material. The crank has a linear output end **16** supporting the anode. The crank also has a linear input end **18** essentially parallel with the output end. A transverse connecting portion **20** is located between the input and output ends.
An electrically conductive cathode **22** is next provided. The cathode is fabricated of carbon. The carbon is in a hollow tubular configuration with an axis. The cathode has a supported end **24** and a free end **26**. The cathode has a length of about 12 inches and an internal diameter of about 11.5 inches and an external diameter of about 12.5 inches.

A motor **28** is next provided. The motor has a rotatable drive shaft **30**. The drive shaft has a fixed axis of rotation. The motor is coupled to the input end of the crank and is positioned so as to rotate the crank and move the output end and anode in a circular path of travel. The circular path of travel has a diameter of about twelve inches with the anode located adjacent to the free end of the cathode. In this manner the anode and the arc are continuously moved around the cathode and away from the plasma created by the arc.

Next provided is an axially shifted support **32**. The support is in a circular configuration to receive the supported end of the cathode and to move the cathode axially toward the anode as the carbon of the cathode is consumed during operation and use.

A water-tight container **34** for the anode, cathode, crank and support is next provided. A quantity of water **36** is provided within the tank sufficient to submerge the anode and the cathode.

An entrance port **38** is provided in the container. The entrance port functions to feed water and a carbon enriched fluid into the container to supplement the carbon and water lost from the container during operation and use.

Next provided is a source of potential **42**. The source of potential couples the anode and the cathode. In this manner an electrical arc is created between the anode and the cathode with a surrounding plasma for the production of gas within the water. The gas will then bubble upwardly to above the water.

Lastly provided is an exit port **44** for the gas resulting from the application of current from the source of potential to the anode and the cathode while the anode is rotating and the cathode is shifting axially.

Fig.4 is a cross-sectional view taken along line 4--4 of Fig.3, but is directed to an alternate embodiment. In such an embodiment, the anode **48** is wing shaped to cause less turbulence in the water when moving. In addition, various supports **50** are provided for abating turbulence and for providing rigidity.

Again with reference to **Fig.3**, the anode rod is placed head-on on the edge of the cylindrical cathode and is permitted to rotate around the entire periphery of the cylindrical edge via an electric motor or other means. (The inverse case of the rotation of the cathode cylinder on a fixed anode rod or the simultaneous rotation of both, are equally acceptable, although more expensive for engineering production). Extensive tests have established, that under a sufficient rotational speed of the anode rod on the cylindrical cathode of the order of 100 r.p.m. or thereabouts, the consumption of the edge of the cathode tube is uniform, thus permitting the desired continuous underwater arc without the interruptions necessary for the frequent cathode rod replacements in the pre-existing configurations.

For the case of smaller electrical power input the above equipment remains essentially the same, except for the reduction of the diameter of the non-carbon based anode and of the corresponding thickness of the carbon-based cylindrical cathode. For instance, for 14 Kwh power input, the anode diameter and related thickness of the cylindrical cathode can be reduced to about 3/8 inch.

The above new equipment does indeed permit the achievement of the desired duration of the electrodes prior to servicing. As a first illustration for industrial usage, suppose that the manufacturer desires an equipment for the high volume industrial production of said combustible gas from about 100 Kwh energy input with the duration of four hours, thus requiring the servicing twice a day, once for lunch break and the other at the end of the working day, as compared to the servicing only after a few minutes of use for the pre-existing equipment.

This invention readily permits the achievement of this duration with this power input. Recall that carbon rods of about 1 inch in diameter are consumed by the underwater arc from 100 Kwh at the speed of about 3 inches in length per minute. Numerous experiments have established that a cylindrical carbon cathode of 1 inch thickness, approximately one foot radius and approximately two feet in length, permits the achievement of the desired duration of 4 hours of continuous use prior to service. In fact, such a geometry implies that each 1 inch section of the cylindrical cathode is consumed in 6 minutes. Since 4 hours correspond to 240 minutes, the duration of four hours of continuous use requires forty 1 inch sections of the cylindrical cathode. Then, the desired 4 hours duration of said cathode requires the radius R = 40/3.14 or 12.7 inches, as indicated. It is evident that a cylindrical carbon cathode of about two feet in radius and about one foot in length has essentially the same duration as the preceding configuration of one foot radius and two feet in length. As a second example for consumer units with smaller power input than the above, the same duration of 4 hours prior to servicing can be reached with proportionately smaller dimensions of said electrodes which can be easily computed via the above calculations.

It is important to show that the same equipment described above also permits the increase of the efficiency as defined earlier. In-depth studies conducted by this inventor at the particle, atomic and molecular levels, here omitted for brevity, have established that the arc is very efficient in decomposing water molecules into hydrogen and oxygen gases. The low efficiency in the production of a combustible gas under the additional presence of carbon as in pre-existing patents is due to the fact that, when said H and O gases are formed in the plasma surrounding the discharge, most of these gases burn, by returning to form water molecules again. In turn, the loss due to re-creation of water molecules is the evident main reason for the low efficiency of pre-

existing equipment. The very reason for this poor efficiency is the stationary nature of the arc itself within the plasma, because under these conditions the arc triggers the combustion of hydrogen and oxygen originally created from the separation of the water.

The above described new equipment of this invention also improves the efficiency. In fact, the efficiency can be improved by removing the arc from the plasma immediately after its formation. In turn, an effective way for achieving such an objective without extinguishing the arc itself is to keep the liquid and plasma in stationary conditions, and instead, rapidly move the arc away from the plasma. This function is precisely fulfilled by the new equipment of this invention because the arc rotates continuously, therefore exiting the plasma immediately after its formation. Extensive experiments which were conducted, have established that the new equipment of this invention can increase the efficiency from the 2-3 cu. ft. per kWh of current embodiments to 4-6 cu. ft. per kWh.

It is easy to see that the same equipment of this invention also decreases the content of carbon dioxide. In fact, CO_2 is formed by burning CO and O, thus originating from a secondary chemical reaction in the arc plasma following the creation of CO. But the latter reaction is triggered precisely by the stationary arc within the plasma. Therefore, the removal of the arc from the plasma after its formation via the fast rotation of the anode on the cylindrical edge of the cathode while the liquid is stationary implies a decrease of CO_2 content because of the decrease of the ignition of CO and O.

Extensive experimentation has established that a rotation of 100 r.p.m of the anode over the edge of the cylindrical cathode of radius one foot decreases the content of carbon dioxide in the combustible gas at least by half, thus permitting a significant environmental advantage. The decrease of the CO_2 content also implies an increase of the efficiency, alternatively defined as energy content of the gas produced per hour (BTU/hr) divided by the real electric energy absorbed per hour (kWh). In fact, CO_2 is a non-combustible gas, thus having no meaningful BTU content. It is then evident that, since the total carbon content in the gas remains the same, the decrease of the non-combustible CO_2 is replaced in the gas by a corresponding increase of the combustible CO with the same carbon content, thus increasing the energy content of the gas for the same production volume of pre-existing inventions and for the same real power absorbed.

With reference to **Fig.3**, among various possible alternatives, a preferred embodiment of this invention for the high volume industrial production of a combustible gas from underwater arcs with about 100 Kwh real electrical energy essentially comprises:

A) An enclosed reactor chamber **56** of the approximate dimensions 4 feet high, 3 feet wide and 3 feet long fabricated out of steel sheets or other metal of about 1/4 inch thickness, comprising in its interior the electrodes for the creation of the arc and having some means for the exiting of the gas produced in its interior as well as some means for the rapid access or servicing of the internal electrodes;
B) The filling up of said chamber with a liquid generally consisting of water and/or water saturated with carbon rich water soluble substances;
C) One or more anodes consisting of rods of about 1 inch in diameter and about 2 inches in length made of Tungsten or other temperature resistant conductor;
D) One or more cylindrical shaped carbon cathodes with essentially the same thickness as that of the anodes and with radius and length selected for the desired duration;
E) Electromechanical means for the rotation of the anode rod head-wise on the edge of the cylindrical cathode, or the rotation of the edge of the cylindrical cathode on a stationary anode rod, or the simultaneous rotation of both;
F) Automation for the initiation of the arc and its maintenance via the automatic advancement of the carbon cathode, and/or the anode rod and/or both, in such a way to maintain constant the arc gap **58**.
G) Fastenings of the cylindrical carbon cathode so as to permit its rapid replacement; various gauges for the remote monitoring of the power unit, combustible gas, liquid and electrodes; tank for the storage of the gas produced and miscellaneous other items.

An improved version of the above embodiment is conceived to minimise the rotation of the liquid because of drag due to the submerged rotation of the anode, with consequential return to the stationary character of the plasma **54** and the arc, consequential loss of efficiency and increase of CO_2 content for the reasons indicated above.

With reference to **Fig.4**, and among a variety of embodiments, this objective can be achieved by shaping the rotating anode in the form of a wing with minimal possible drag resistance while rotating within said liquid, and by inserting in the interior of the enclosed reactor chamber panels fabricated out of metal or other strong material with the approximate thickness of 1/8 inch, said panels being placed not in contact with yet close to the cathode and the anode in a radially distributed with respect to the cylindrical symmetry axis of the equipment and placed both inside as well as outside said cylindrical cathode. The latter panels perform the

evident function of minimising the rotational motion of said liquid due to drag created by the submerged rotation of the anode.

The remote operation of the equipment is essentially as follows:

1) The equipment is switched on with electric current automatically set at minimum, the anode rod automatically initiating its rotation on the edge of the cylindrical cathode, and the arc being open;
2) The automation decreases the distance between anode and cathode until the arc is initiated, while the amps are released automatically to the desired value per each given Kwh, and the gap distance is automatically kept to the optimal value of the selected liquid and Kwh via mechanical and/or optical and/or electrical sensors;
3) The above equipment produces the combustible gas under pressure inside the metal vessel, which is then transferred to the storage tank via pressure difference or a pump; production of said combustible gas then continues automatically until the complete consumption of said cylindrical carbon cathode.

As to the manner of usage and operation of the present invention, the same should be apparent from the above description. Accordingly, no further discussion relating to the manner of usage and operation will be provided.

With respect to the above description then, it is to be realised that the optimum dimensional relationships for the parts of the invention, to include variations in size, materials, shape, form, function and manner of operation, assembly and use, are deemed readily apparent and obvious to one skilled in the art, and all equivalent relationships to those illustrated in the drawings and described in the specification are intended to be encompassed by the present invention.

Therefore, the foregoing is considered as illustrative only of the principles of the invention. Further, since numerous modifications and changes will readily occur to those skilled in the art, it is not desired to limit the invention to the exact construction and operation shown and described, and accordingly, all suitable modifications and equivalents may be resorted to, falling within the scope of the invention

CHAK CHANG

Patent Application US 2006/060464 23rd March 2006 Inventor: Chak Chang

A METHOD AND APPARATUS FOR GENERATING PLASMA IN A FLUID

This patent application is for a most unusual system which produces a plasma discharge at room temperature and ambient pressure, using voltages as low as 350 volts and currents as low as 50 milliamps and among other things, it is capable of promoting the production of pharmaceuticals, production of nano-particles, the extraction of metals from liquids, low temperature sterilisation of liquid food, use in paper industries to decontaminate the effluent discharge, fragmentation or de-lignifications of cellulose; the removal of odour from discharging liquid in the food industries, and the treatment of fluid effluent. It is also a method of producing hydrogen gas at low cost.

ABSTRACT

A method and apparatus for generating plasma in a fluid. The fluid **3** is placed in a bath **2** having a pair of spaced electrodes **4, 6** forming a cathode and an anode. A stream of bubbles is introduced or generated within the fluid adjacent to the cathode. A potential difference is applied across the cathode and anode such that a glow discharge is formed in the bubble region and a plasma of ionised gas molecules is formed within the bubbles. The plasma may then be used in electrolysis, gas production, effluent treatment or sterilisation, mineral extraction, production of nanoparticles or material enhancement. The method can be carried out at atmospheric pressure and room temperature. The electrodes may carry means to trap the bubbles in close proximity. Partitions may be present between the electrodes.

DESCRIPTION

The invention relates to the provision and utilisation of a plasma formed in a fluid, and in particular to the provision and utility of a plasma formed within bubbles contained in an aqueous medium.

BACKGROUND

Plasma is an electrically conductive gas containing highly reactive particles such as radicals, atoms, plasma electrons, ions and the like. For example plasma may be formed when atoms of a gas are excited to high energy levels whereby the gas atoms lose hold of some of their electrons and become ionised to produce plasma.

Thermal plasma, including plasma arc is known. However plasma arc is associated with high power consumption, the rapid erosion of electrodes when used in electrolysis, the need for catalysts and high-energy loss due to the associated high temperatures.

Clearly therefore, it would be advantageous if a non-thermal plasma could be devised. This would enable the plasma to be used for a number of applications for which plasma is useful without the disadvantages associated with using a high temperature plasma arc.

SUMMARY OF THE INVENTION

According to a first aspect of the present invention, there is provided a method for generating plasma in a fluid, comprising the steps of providing a fluid, introducing and/or generating one or more gas chambers or bubbles within the fluid, whereby the chambers or bubbles are contained by the fluid, and treating the fluid such that a plasma is generated within the chambers or bubbles.

The fluid may be a liquid that is contained within liquid containment means.

The applicant has discovered that a plasma can be generated relatively easily within bubbles within an aqueous medium. This plasma causes dissociation of molecules and/or atoms which can then be treated and/or reacted to obtain beneficial reaction products and/or molecules and/or atoms.

The liquid container may be open to the atmosphere and the process may therefore be carried out at substantially atmospheric pressure. Alternatively the container may be placed inside a sealed reaction chamber, e.g. under

partial vacuum. This reduction in pressure can reduce the energy required to achieve a glow discharge within the bubbles passing over a cathode.

Importantly the process is not required to be carried out in a vacuum.

The plasma may be formed, for example, by applying a potential difference across electrodes which are immersed in the liquid.

Upon passing electricity of sufficient potential between two electrodes, the dielectric barrier associated with the bubble/chamber surface breaks down, with the accompanying formation of a glow discharge and plasma inside the gas bubbles or chambers. This enables plasma formation to be effected at very low voltages, current, temperature and pressure, as compared with known methods of plasma formation.

For example, typical voltages and currents associated with plasma arc are in the region of 5 KV and 200 A respectively, whilst in the present invention, a plasma may be provided with a voltage as low as 350 V and a current as low as 50 mA.

The formation of a glow discharge region adjacent said one electrode is caused by a dielectric breakdown in the bubbles surrounding the electrode. The bubbles have a low electrical conductivity and as a result there is a large voltage drop between the electrodes across this bubble region. This voltage drop accounts for a large portion of the overall voltage drop across the electrodes. The plasma is generated within the bubbles contained within the electrolyte. The liquid electrolyte acts as containment for the plasma within the bubbles.

When plasma discharge occurs, any water vapour inside the bubbles will experience plasma dissociation whereby H+, OH^-, O^-, H, H_3, and other oxidative, reductive and radicals species are formed. The formation of charged plasma species will of course also depend on the chemical composition of the electrolyte.

In the present invention, the voltage needed for plasma generation is much lower than plasma glow discharge generated under gas only conditions. For example experiments have demonstrated that plasma begins to occur at voltages as low as 350 V and the maximum voltage required should not exceed 3,000 V. This requirement is based on a current density of 1 to 3 Amp/cm^2 which can be achieved at the point of discharge whereby the current input ranges from 50 mA to about 900 mA.

Plasma can be created, according to the present invention, in a steady manner with a low voltage and current supply, which leads to an economy in power consumption.

The bubbles may contain precursor materials originating in the fluid, which is preferably a liquid, more preferably being an aqueous electrolyte. This material may have been transferred from the liquid to the bubbles by diffusion or evaporation.

Alternatively the precursor may be introduced directly into the bubbles from outside the system.

The step of generating bubbles within the aqueous medium may be accomplished by one or more of the following: electrolysis, ebullition, ultrasonic cavitations, entrainment, scattering, chemical reaction, dissociation by electrons and ion collisions or local heating or ebullition, hydraulic impingement, ultrasonic waves, laser heating, or electrochemical reaction, electrode heating, releasing of trapped gases in the liquid, and externally introduced gases or a combination of them.

Electrolysis bubbles may be generated by the electrode as a result of the potential differences applied across them, e.g. hydrogen bubbles liberated by the cathode or oxygen bubbles liberated by the anode. Ebullition bubbles may be generated by electrical heating in the region of the electrodes. The bubbles may be generated by direct electrical heating or by heating in proximity to the electrode by a moving wire or grid. Microwave heating and heating using lasers may also be used to generate ebullition bubbles.

Cavitation bubbles may be generated by using an ultrasonic bubble generator or a jet of fluid or a jet of a mixture of gas and liquid injected into the electrolyte in proximity to the electrode. Cavitation bubbles may also be generated by hydrodynamic flow of the electrolyte in proximity to the electrode. Scattering of gas in proximity to the electrode may also be used to generate bubbles.

Bubbles may also be generated by a chemical reaction which evolves gas as a reaction product. Typically such reactions involve thermal decomposition of compounds in the electrolyte or acid based reactions in the electrolyte. Bubbles may also be formed in the electrolyte by adding a frother to it.

Typically the generation of bubbles forms a bubble sheath around one electrode. The bubble sheath may have a thickness of anything from a few nanometres to say, 50 millimetres. Typically the bubble sheath may have a thickness of 1 mm to 5 mm. Further, it should be understood that the bubbles may not be homogeneous throughout the sheath.

Gas or vapour formed external to the container may be pumped or blown into the aqueous medium near the cathode.

Thus the composition of the plasma that is generated within the bubbles may be tailored to suit the application to which the plasma is being put and the bubbles may either be generated within the liquid from components within the liquid or introduced into the liquid from outside the containment means.

The bubbles can assume various sizes and shapes including a sheet form air gap or air pocket covering shrouding the electrodes or spread across the liquid medium in micro bubbles.

Liquid foam may also be considered to be bubbles or gas chambers for the purposes of the present invention. This is a highly concentrated dispersion of gas within a continuous interconnecting thin film of liquid. The gas volume can reach up to 80% of a contained area. Gas generated within or introduced to the reactor externally can also be encapsulated within a foaming agent to enable it to undergo plasma discharge treatment.

Gases trapped inside a thick liquid mist in a confined space are also considered to be gas containing bubbles, which contain the gases, and liquid vapours that provide the condition for generation of non-thermal plasma. The liquid may contribute one or more source materials for dissociation during the plasma discharge.

In practise, gas bubbles evolving near and shrouding an electrode in an electrolysis process create a dielectric barrier which prevents and slows down the flow of current. At the same time the dissolved gas or micro bubbles spread and diffuse in the liquid volume thereby creating a high percentage of void fractions (micro gas bubbles) which in turn increase the electric resistance whereby the voltage across the liquid medium is raised. When the voltage has increased sufficiently, gas trapped inside the bubbles undergoes non-equilibrium plasma transformation. At this point, di-electric breakdown occurs enabling resumption of current flow through the bubbles sheath or air pocket layer.

Any water molecules and atoms lining the gas and liquid interface of a bubble shell will also be subjected to the influence of the plasma to produce H^+ and OH^- and other radical species. Some of these neutralised atoms and molecules will transpose into the gas bubbles as additional gas that increases the size of the bubble. As such the bubbles pick up more liquid vapours before a next succession of plasma discharge. Such a cycle of such repetitive discharge can take place in a fraction of a second to several seconds depending on the make up of the electrode and reactor.

The step of generating bubbles within the aqueous medium may include adding a foaming agent to the aqueous medium such that bubbles are formed within foam. The foam bubbles are confined by an aqueous medium that is electrically conductive. The foam bubbles can vary widely in size down to a fraction of a millimetre.

The step of generating bubbles may include forming an aerosol mist. The gas within the aerosol mist broadly defines bubbles in the sense that there are volumes of gas between liquid droplets. These bubbles in the form of spaces between liquid drops function in a similar way to conventional bubbles within a liquid and a plasma is formed in this gas in the same way as described above.

An advantage of foam and aerosol mist is that it provides for good mixing of gaseous components within the mist and foam. The plasma is generated in the bubbles of the foam and aerosol mist in the same way that they are formed in an aqueous liquid, e.g. by passing electrical current between spaced electrodes within the foam or mist.

The step of forming a glow discharge in the bubble region may be achieved by increasing the potential difference across the electrodes above a certain threshold point.

The formation of a glow discharge and generation of plasma within the bubbles may be assisted by a pulsed or steady power supply, a magnetron field, ultrasonic radiation, a hot filament capable of electron emission, laser radiation, radio radiation or microwave radiation. The energy requirements may also be assisted by a combination of any two or more of the above features. These factors may have the effect of lowering the energy input required to reach the threshold potential difference at which glow discharge is formed.

In conventional electrochemical processes bubbles are regarded as undesirable. As a result concerted efforts are made to avoid the generation of bubbles during the operation of electrochemical cells. By contrast the process of the current invention deliberately fosters the formation of bubbles and utilises bubbles in proximity to the electrode

as an essential feature of the invention. The bubble sheath surrounding the electrode is essential to establishing a plasma region which then gives rise to the plasma deposition on the article.

Thus the plasma is formed within bubbles and the molecules and/or atoms that are ionised are surrounded by liquid which effectively provides a containment structure within which the plasma is contained. The liquid in turn generally opens to the atmosphere.

Plasma glow discharge can be fairly easily accomplished within the cell because the sheath of bubbles has the effect of causing a substantial proportion of the voltage drop to occur across the bubble sheath. It is concentrated in this area rather than a linear drop across the electrode space. This provides the driving force to generate plasma glow discharge and from there deposition of the ionic species.

The electrical charge is preferably applied in pulses, since this enables plasma production at lower voltages.

The fluid is preferably a liquid electrolyte, for example an aqueous medium, whereby in one preferred embodiment, the medium is water.

The electrolyte may comprise a carrier liquid and /or a source or precursor of the material to be ionised by the plasma.

When the liquid is water, charged plasma particles include species such as OH radicals, O^- and H^+, -OH, O_2 and O_3, which will react with the surrounding liquid.

Distilled water is known to be dielectric and non-conductive. It is however when water contains impurities such as dissolved minerals, salts and colloids of particles, whereby water becomes conductive, that ionisation and electrolysis can occur.

The method may further include adding an additive, such as an acidic or alkaline conductivity enhancing agent, to the aqueous medium to enhance this electrical conductivity such as organic salts or inorganic salts, e.g. KCl, $MgCl_2$, NaOH, Na_2CO_3, K_2CO_3, H_2SO_4, HCl.

The method may include adding a surfactant to the aqueous medium for lowering the surface tension of the medium and enhancing the formation of bubbles, e.g. to stabilise bubble formation.

The electrolyte may further include additives in the form of catalysts for increasing the reaction of molecules and/or atoms produced in the plasma, additives for assisting the formation of bubbles, and additives for buffering the pH.

The method may further include cooling the electrolyte to remove excess heat generated by the plasma reaction and regulating the concentration of one or more components within the electrolyte.

The cooling may comprise drawing electrolyte from the bath pumping it through a heat exchanger, and then returning it to the bath.

Plasma creation, according to the present invention can be effected in the absence of extreme conditions, for example plasma according to the present invention may be provide under atmospheric pressure and at room temperature.

During plasma production according to the present invention, a shroud of bubbles preferably builds up and smothers around at least one of the electrodes, whereby electrical charge builds up in the bubble shroud thereby creating a dielectric barrier which impedes current flow, whereby electrical resistance in the fluid medium builds up so that voltage through the medium is raised to a degree such that gas within the bubbles is excited to an energy level at which a plasma is produced.

The method according to the present invention preferably comprises the further step of exposing the plasma to a material, which on contact with the plasma undergoes a chemical and/or physical change.

For example the plasma can be used to cause dissociation of toxic compounds and then break down the compounds and/or cause them to undergo reactions leading to innocuous reaction products.

The plasma produced according to the present invention, which will be referred to as 'under-liquid' plasma has the same physical and chemical properties as plasma produced according to known methods and accordingly also has the utility of such plasma.

The under-liquid plasma according to the present invention can create an active catalytic condition which facilitates gas and liquid interaction. As such, the plasma according to the present invention, may promote any reaction which takes place in a liquid medium, for example chemical reactions, the production of pharmaceuticals, production of nano-particles, the extraction of metals from liquid, low temperature sterilisation of liquid food, use in paper industries to decontaminate the effluent discharge, fragmentation or de-lignifications of cellulose; the removal of odour from discharging liquid in the food industries, and the treatment of fluid effluent. Material may be chemically modified by means comprising one or more of the following: ionisation, reduction, oxidation, association, dissociation, free radical addition/removal, whereby, optionally, following chemical modification, the material is removed.

The invention may be used to tackle existing problems. For example, water that has been used in industrial processes or used in some other way has to be treated to remove harmful components before it is returned to ground water. This is typically achieved by reacting the harmful components with other chemical components introduced to the water to form relatively harmless products. Many undesirable components are treated fairly effectively in this way.

However some harmful components within water are not capable of being treated in this fashion. This poses a problem as these harmful components, e.g. contaminants, need to be removed from the water before it is returned to ground water. One known way of treating some of these components is to use an electric arc process to break down these toxic chemicals. However an electric arc process requires a substantial amount of energy to arc between electrodes within the liquid and is therefore costly. In addition the number of chemicals that are able to be treated in this way is limited. A further limitation of these processes is that they often cause rapid consumption and degradation of electrode material. Applicant believes that this water could be better treated by the method of this invention.

Moreover, the electric arc method of providing plasma, applies a high voltage across closely spaced electrodes causing the break down and ionisation of molecules, and then a surge of electrical current between the electrodes.

Further, many metals or mineral occur naturally in the ground in the form of ores as mineral oxides. The minerals need to be reduced to useful minerals. Typically the reduction is carried out using pyrometallurgical techniques, e.g. such as are used in electric arc furnaces. These treatments are very aggressive and utilise enormous amounts of electrical energy. Clearly it would be advantageous if a simpler more streamlined and more energy efficient method of reducing a mineral oxide to a mineral could be devised. Applicant believes that this could be done by the method of this invention.

Yet further, the generation of electrical energy with fuel cells is seen as an exciting new area of technology. Such fuel cells utilise hydrogen as a fuel. Accordingly a relatively inexpensive source of this hydrogen as a fuel is required. Currently hydrogen is produced by solar cells. However the present invention could be used to provide such a source of hydrogen.

In one form of the current invention, the undesirable compounds may be deposited on an electrode, e.g. the cathode, as a layer or coating. The compound can then be removed from the liquid by simply removing it from the aqueous medium.

In another form, the undesirable component can be reacted with a chemical compound, e.g. within the plasma, to form a solid compound, e.g. a salt in the form of a precipitate, that settles out of the aqueous medium and can then be removed from the aqueous medium.

Typically the undesirable component will be toxic to animals or harmful to the environment. However components that are undesirable in other ways are also included within the scope of the invention.

Applicant envisages that this will be particularly useful for the removal of harmful heavy metals from waste water. It will probably also be useful for the treatment of contaminated gases. Such gases will be introduced to the aqueous medium in such a way that they form part of the bubbles passing over the cathode and then be treated as described above.

Another example is the extraction of a mineral, e.g. a metal, from its metal oxide, the method including: dissolving the mineral oxide in an aqueous medium and then subjecting it to the method described above according to the first aspect of the invention whereby a plasma is generated within bubbles passing over the cathode, and the plasma reduces the mineral oxide to the mineral per se.

The ozone which is formed in the plasma can then be reacted with hydrogen to form an innocuous compound such as water. The reduced mineral which is formed in the plasma, e.g. a metal, may be deposited on the cathode or else may be precipitated out as a solid in the container.

In the case of water, hydrogen and oxygen produced, travel to the anode and cathode and are preferably then removed. As such, the process according to the present invention is an economical, simple and effective way of producing hydrogen.

The hydrogen produced in this fashion may be used as fuel, e.g. in fuel cells for the generation of electricity. Applicant believes that hydrogen can be produced relatively inexpensively in this fashion. Fuel cell technology is currently receiving an increased level of acceptance looking for a cheap source of the supply of hydrogen.

According to another aspect of the present invention, there is provided the use of this 'under-liquid' plasma in one or more of the following: chemical and/or physical treatments of matter, electrolysis, gas production, in particular hydrogen gas production; water, fluid and/or effluent treatment; mineral extraction; sterilisation of drinking water and/or liquid food, production of nano-particles, the enhancement of material chemical and physical properties.

According to a further related aspect of the present invention there is provided an apparatus for providing a plasma comprising; a container in which a plasma is provideable, bubble trapping means, arranged within the container, for trapping gas bubbles at a predetermined location in the container and, plasma creation means, in association with the container, for creating a plasma from the gas within the bubbles.

The plasma creation means preferably comprise electrical discharge means which most preferably comprise a cathode and/or an anode.

The apparatus, in one preferred embodiment being an electrolysis cell, further preferably comprises bubble introduction and/or generating means, for introducing and/or generating bubbles in the container.

Furthermore, the apparatus preferably comprises one or more of the following: enhancing means for enhancing plasma formation and one or more non-conductive partitions arranged between the electrodes, whereby the enhancing means preferably comprise bubble trapping means most preferably associated with the electrodes and wherein the enhancing means may also comprise current concentrating means for concentrating the electrical current at a predetermined position in the container which can take the form of one or more channels arranged through one or more of the electrodes.

The electrodes may take any suitable form, for example the electrodes may be so profiled as to entrap/attract bubbles, in order to help gas bubbles being created or introduced to the discharging electrode to form a dielectric barrier by which the voltage can be raised whereby a suitable current density is provided directly by high input of current or passively created by a current concentrating arrangement, for example, by conducting the current through small holes on the electrodes or by reducing the discharge surface area of the electrodes whereby in the latter case, the electrodes may take the form of pins, wires, rods and the like.

For example, the cathode may be formed by a hollow tube with perforated holes therein, e.g. small perforated holes. The holes allow bubbles introduced into the tube to pass out of the tube into the aqueous medium. Alternatively a cathode may be made of wire mesh or have a roughened surface, e.g. to encourage the attachment of bubbles thereto to slow down the movement of the bubbles.

In one embodiment there are a plurality of cathodes spaced apart from each other and in parallel with each other, and a single rod-like anode, e.g. centrally positioned relative to the cathode.

The other electrode (non discharging) preferably has a larger surface area such than the discharging electrode.

The discharging electrode can either be cathode or anode depending on the application necessity.

In an experimental reactor the separating membrane, non-conductive partition, was nylon cleaning cloth having a tight matrix 0.5 mm thick. This semi-permeable membrane is capable of resisting the passage of oxygen and hydrogen ions through it in the aqueous medium, intermediate the anodes and cathodes thereby to maintain separation of oxygen and hydrogen produced in the plasma.

Most preferably, the apparatus according to the present invention is an electrolytic cell.

A known problem with carrying out electrolysis is that any gas/bubble build up in the electrolytic cell creates a barrier to the flow of current through the electrolyte, thereby impeding electrolysis, which increase in resistance in turn forces the required voltage up. As such, electrolytic cells require a great deal of energy and are often very large in order to effect dispersion of such gas/bubbles. However the present invention actively promotes such bubble build up, in order to effect plasma creation which the inventors have shown is effective in carrying out electrolysis.

DETAILED DESCRIPTION OF PREFERRED EMBODIMENTS OF THE INVENTION

A plasma formed in a fluid in accordance with this invention may manifest itself in a variety of forms. It will be convenient to provide a detailed description of embodiments of the invention with reference to the accompanying drawings. The purpose of providing this detailed description is to instruct persons having an interest in the subject matter of the invention how to put the invention into practice. It is to be clearly understood however that the specific nature of this detailed description does not supersede the generality of the preceding statements. In the drawings:

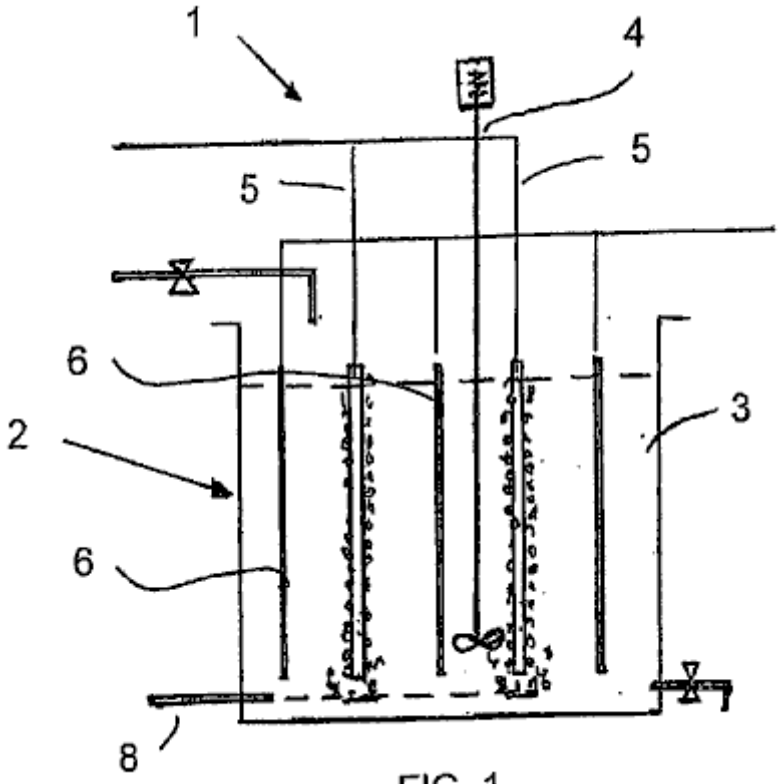

FIG. 1

Fig.1 is a schematic sectional front view of apparatus for carrying out a method in accordance with the invention.

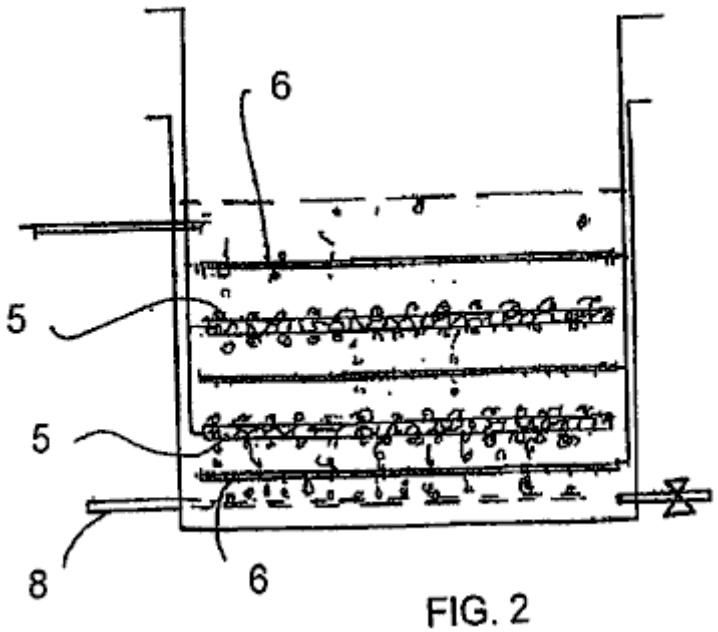

FIG. 2

Fig.2 is a schematic sectional front view of a variation on the apparatus of Fig.1.

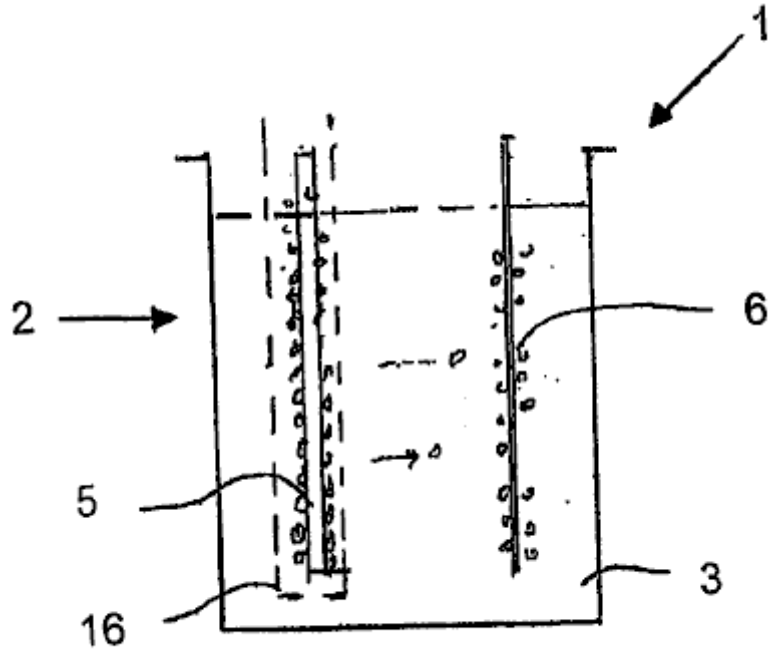

FIG. 3

Fig.3 is a schematic sectional front view of an apparatus in accordance with the invention suitable for producing hydrogen gas.

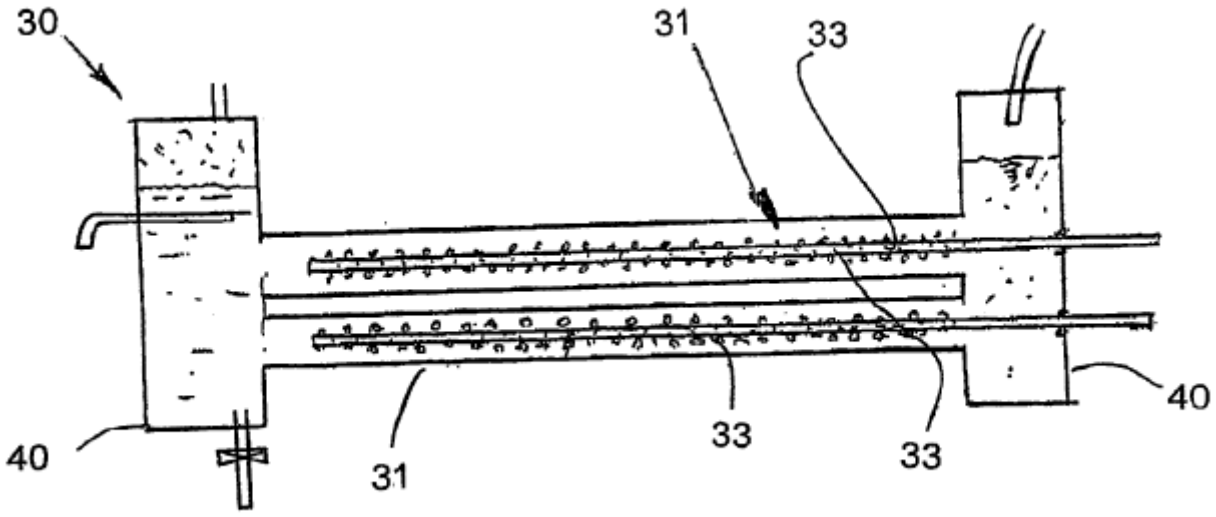

FIG. 4

Fig.4 is a schematic sectional front view of a tubular reactor carrying out a method in accordance with another embodiment of the invention.

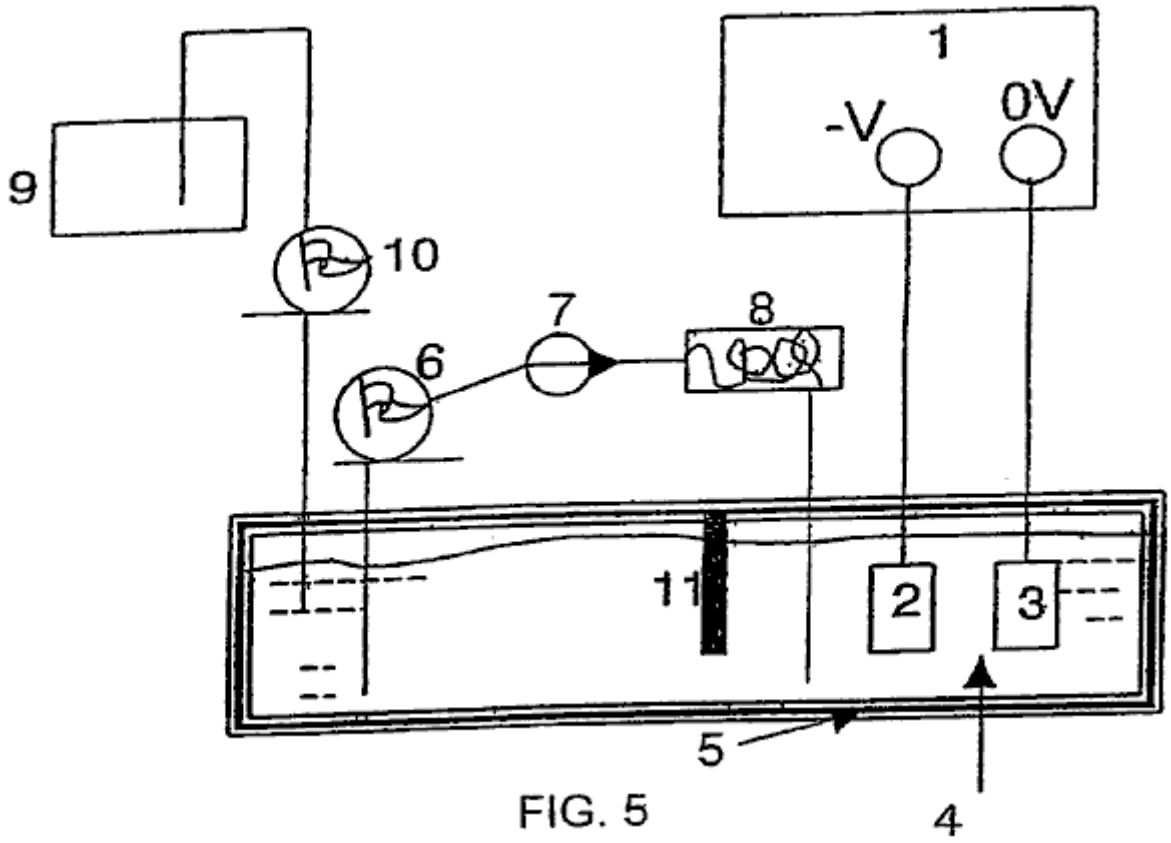

FIG. 5

Fig.5 is a schematic flow sheet of apparatus in the form of a cell for carrying out the invention.

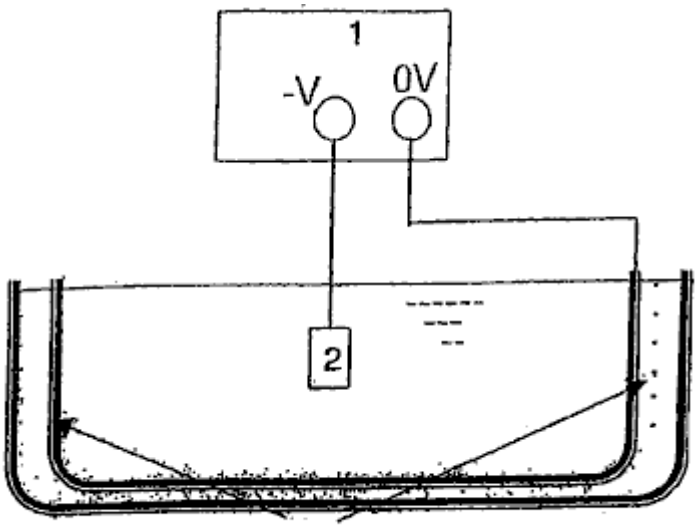

FIG. 6

Fig.6 is a schematic view of a bath for the cell of Fig.5 having an ultrasonic generator for generating bubbles.

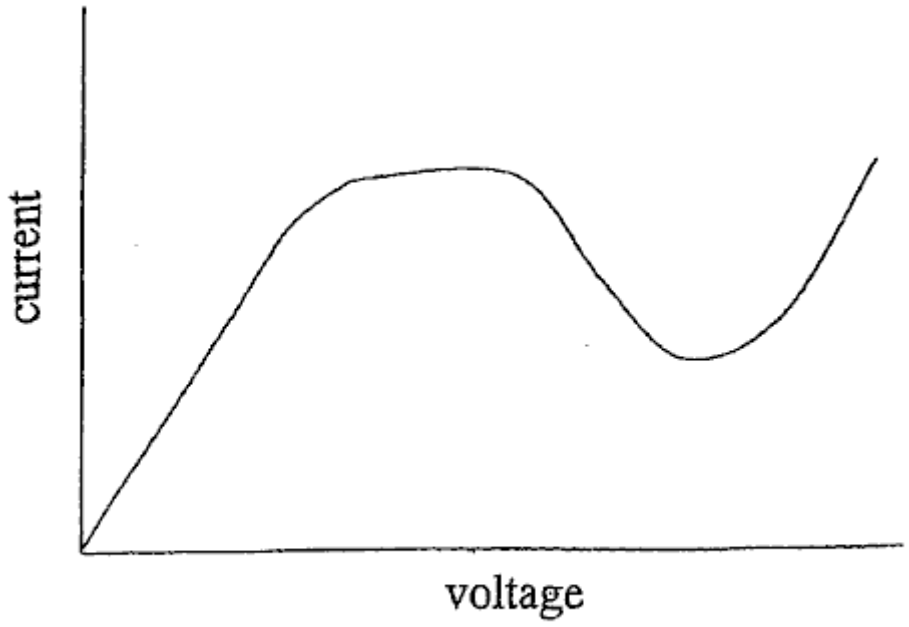

FIG. 7

Fig.7 is a schematic graph of current against voltage in an electrolytic cell.

FIG. 8

Fig.8 shows the initial formation of a bubble sheath around the cathode due to the application of voltage across the electrodes.

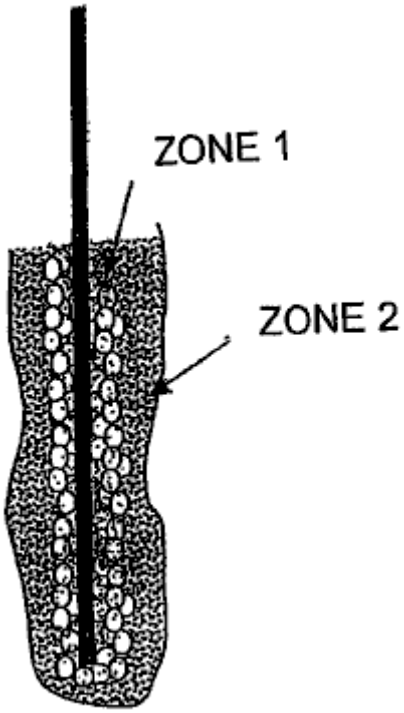

FIG. 9

Fig.9 shows the bubble sheath around the cathode during stable glow discharge within the cell, and

Figs.10-53 refer to further embodiments and experimental results in respect of the present invention.

The present invention relates to the production of non-thermal plasma contained in a liquid by generating corona discharge and or glow plasma discharge inside the bubbles or air pockets present in the liquid.

Upon passing electricity of sufficient potential through the liquid, electric breakdown of the dielectric bubble barrier results in the formation of plasma discharge inside the gas bubbles or pockets present in the liquid. In most cases glow discharge occurs near the electrodes but occasionally glow discharge is also observed away from the electrode.

The bubbles can be produced either by electrolysis, electrochemical reaction, heating of electrodes, releasing of trapped gases in the liquid, ultrasonic cavitations, laser heating, and externally introduced gases.

Bubbles produced by electrolysis of water contain hydrogen gas at the cathode and oxygen gas at the anode. Such bubbles can also contain other chemical vapours originating from the electrolyte or additives.

The liquid serves as an electrolyte which provides conductivity of electricity, the source material from which gases and vapour are produced for plasma dissociation to form, for example, reduction and oxidation, radicals and neutral species. The liquid also provides an active catalytic chemical environment for forming new compounds. It also serves as containment of gases in the form of bubbles or air pockets in which the non-thermal plasma discharge takes place.

In practise, gas bubbles evolving and shrouding the electrodes during electrolysis create a dielectric barrier which inhibits the flow of current.

At the same time the dissolved gas or micro bubbles spread and diffuse in the liquid volume create a high percentage of void fractions (micro gas bubbles) which also increase the electric resistance and so raise the voltage across the liquid medium.

When the voltage between two electrodes reaches a critical level, the gas trapped inside the bubbles undergoes non-equilibrium plasma transformation. This is also known as electric breakdown which enables the resumption of current flow through the bubble sheath or air pocket layer. In the case of water electrolysis, the production of hydrogen will then resume.

During plasma discharge, light emission may be observed in the bubbles in a sporadic or steady manner in short and continuous flashes near the surface of the electrodes and in the liquid medium.

Continuous light spots may also be observed in areas distanced from the electrodes where suspected small air bubbles are trapped and yet remain under the influence of strong electrical field.

The temperature in the electrolyte near the electrodes has been measured to be in the region of $50^{O}C$ to about $90^{O}C$ with an experiment running in water for 30 minutes, which indicates that the plasma is non-thermal plasma.

The temperature variation may be influenced by electrode geometry, electrolyte concentration, level of inception voltage and current density for the glow discharge. The temperature measured directly over the discharging electrode can reach over $200^{O}C$ during reformation of methanol for example.

Configurations of electrodes, size, spacing, dielectric barrier coating, electrolyte temperature, current density, voltage and reactor geometry are factors influencing plasma formation.

A special structure and arrangement to retain gas or gas bubbles close to the electrodes provide favourable circumstances for the ready formation of a steady and cyclical plasma glow discharge with lower voltage and current input.

Electrode configurations can be in following forms: plate to plate, plate to pinned plate, dielectric coated plate to plate or pinned plate or both, wire mesh to plate, wire mesh to wire mesh or to perforated plate, wire or groups of wires in perforated cylinder tube, and tube in tube.

The electrode material may be sponge porous metal electrode, electrode covered with honeycomb non-conductive materials and porous ceramic filter to entrench gas or using non-conductive plate with drilled holes and gas traps that retain gas bubbles and concentrate the current density next to the electrode surface.

In general keeping the bubbles close to the surface of the electrodes can also be achieved by attaching a porous non-conductive nylon foam mattress and/or a honeycomb or porous ceramics slab of suitable thickness, so that the mobility of the bubbles is slowed down and at the same time the conduit for current flow is narrowed by a shading effect of the dielectric materials which in turn raises the current density locally.

For the same reason glass beads, plastic beads and beads of catalytic material i.e. TiO_2, graphite of suitable size can be placed between the electrodes in order to slow down the flow of bubbles.

A non-conductive, heat and corrosion electrode covering material, structured to retain and trap gas bubbles which also concentrates current density through small openings arranged through it whilst providing an adequate exposed electrode surface for electro-chemical and electrolysis reactions, improves the generation of steady and short cyclical reactions under-liquid plasma discharge.

Multiple layers of very fine stainless mesh, sandwiched between two plastic cover plates with small perforated holes, have produced a steady glow plasma. The void space created by the layered wire mesh provides a trap for air bubbles as well as enlarging the contact surface for electrochemical and electrolysis reaction.

In an experiment both vertical or horizontal electrodes were covered and bonded with non-conductive materials (plastic) with patterned perforations to trap gas bubbles while at the same time allowing for electrical contact of the electrodes through the perforations.

The electrode contact surface was enlarged underneath the shielding to increase gas production during electrolysis or heating. Current flow was concentrated through small holes of 1 to 3 mm leading to the trapped gas and bubbles, which underwent plasma transformation. Cyclical and steady plasma was observed with an input DC voltage ranging from 350V to 1900V and current ranging from 50 mA to 800 mA.

A non-conductive diaphragm, which does not restrict the free flow of ions and electrolyte, is placed between two opposite electrodes to prevent crossing of bubbles between two half electrolytic cells avoids re-mixing of the gases which have been separated by electrolysis.

A reactor may be so structured that the electrolyte is able to enter into the reactor through the separating membrane or opening form in the reactor to replenish the loss of electrolyte within the enclosed reactor.

There are other techniques which can be incorporated into the proposed invention for the enhancement of plasma generation such as pulsed power supply, RF power, microwaves, ultrasonic waves, magnetron field, and laser. Some of the above techniques may also be applied in pulsed form.

Ultrasonic cavitations in liquid (sonic-technology) will enhance the plasma formation and the catalytic reactions that benefit a number of under-liquid plasma applications.

The under-liquid plasma requires an input of DC or AC voltage in the range from 350V up to 3000V and current density ranging from 1 Amp to 3 Amp per cm^2 in dealing with a large range of liquid media. The specific voltage and current requirement for a given application depends very much on the chemical and physical properties of electrolytic liquid as well as those factors mentioned above.

The under-liquid plasma method according to the current invention, can operate at atmospheric pressure and ambient temperature. However, an external pressure less than one atmosphere or over one atmosphere with higher temperatures does not deter the generation of plasma in the bubbles. A higher temperature in the liquid also means more active gas molecules within the bubbles, which can benefit plasma formation.

Non-thermal plasma generated in a liquid according to the present invention, has advantages over known types of plasma discharge, for example in gas, under water plasma arc and pulse power electric discharge, these being:

It requires only simple electrolytic cells to be the reactor to perform such discharge. There is little erosion to the electrodes and wider range of electrode materials can be chosen such as stainless steel, graphite, aluminium and good conductive materials which are resistance to chemical erosion. The polarity of the electrode can be reverted if necessary to compensate the lost of electrode materials if so desired.

It works under one atmospheric pressure and ambient temperature. The liquid electrolyte will be primary source of materials for the chemical and physical reaction take part in the process. There are number of ways that bubbles can be produced within the electrolytic cell. Gas can also be introduced to the reactor where plasma catalytic and dissociation is taking place.

It is a low-temperature system as the plasma discharge is non-thermal. Any excessive or undesirable high temperature can be lowered by increasing the circulation rate of the liquid which can lose its temperature through heat exchange. Heat generated can be recovered as secondary energy.

The electrolyte (liquid) will serve as extension of the conducting electrodes in contact with the gases or vapour trapped inside the bubbles. The air gap between two electrodes is reduced to the thickness of the gas bubbles or air pocket which thus enables plasma discharge at a much lower voltage and current compared with other plasma discharge systems. Plasma glow discharge, according to the present invention, can be initiated under conditions of a voltage as low as 350V and the current ranging from 50 mA to 800 mA. Extra energy is not required in splitting the water molecules to transient bubbles as in the other underwater electrical discharge system which requires voltage not less than 5 to 6 KV, and very high current over 200 A in pulsed supply. Plasma discharge will also take place in gas pockets or bubbles away from the electrode as long as the electric field strength is sufficient to cause such discharge.

The electrolyte also serves as a confinement of gas generated within the system, or purposely introduced gas of known properties, instead of ordinary air which may lead to production of unwanted NOx for example. Noble gas such as argon is not necessary to enhance the initiation of glow discharge sometime required in the air discharge system.

The electrolyte also serves as a conductor and passage for the transportation of ionised species and transmission of electrons. The ionised atoms and molecules deriving from the electrolyte will be collected in their respective electrodes in the form of gas or material deposit. These ionised species are either serving as a reduction or oxidation agent in their respective half-cell. Since the gas ions produced during the discharge migrate to their respective poles to be collected individually, hydrogen gas and oxygen gas can be collected separately.

The gas and vapour molecules and atoms inside the bubble which undergo plasma glow discharge are ionised, excited or dissociated to produce the very active species for reduction, oxidation, and the forming of neutral or radical species which in turn react with the chemical elements present in the gas and liquid interface aligning bubbles wall. The large number of bubbles generated near the electrodes and in the nearby liquid, come into contact with a much larger volume of liquid nad so provides effective treatment, breakdown, transformation of chemicals, organic matter or elements which have been targeted.

Liquid is a good medium for transmitting ultrasonic waves. Sonic-excitation is beneficial for the dissociation of materials and extermination of microbes and it aids the breakdown and local melting of colloidal solids during impact which also enhances the plasma oxide reduction process. The generated ultrasonic cavitations may be fully utilised to work in conjunction with the under-liquid plasma discharge. An ultrasonic cavity is micro in size and uniformly distributed in the entire liquid volume. The cavities are a high vacuum which contain liquid vapour and gas, and these favour plasma discharge. The high temperature and pressure reaching $10{,}000^{O}K$ and a

thousand times atmospheric pressure, produced on the collapsing phase of these cavities work is complementary to that of the electro discharge plasma. This enables under-liquid plasma discharge to spread further from the electrodes and be well distributed in the liquid volume which increases its overall effectiveness.

The electrolyte may also be in the form of a mixture, an emulsified liquid, a colloid, or foams encapsulating gas emissions either coming from the liquid or introduced externally. The emulsified liquid of an oil/water mixture and encapsulating gas of hydrocarbon fuel with the ultrasonic irradiation, will facilitate their reformation for hydrogen production.

Fine granular insoluble particles of mineral oxide such as aluminium, titanium, iron, silica etc. can be suspended in the form of colloid with the liquid which is than subjected to reduction with active ionic hydrogen atoms in a highly reactive plasma catalytic environment to become deoxidised and refined. This will be more so, with the assistance of sonic impedance. The Plasma glow discharge has also demonstrated the ability to dissociate soluble ionic metal compounds, whereby subsequently the positively charged metal ions will be segregated near the cathode electrode in the form of precipitation and plasma electroplating deposition.

The electrolyte may be a source of materials for thin-film deposition with the assistance of plasma glow discharge. In addition, nano size particles of certain compounds and elements i.e. metal hydride, oxide, pure metals, semi metals, organic, ceramic etc. can also be produced with the assistance of the under-liquid plasma discharge in conjunction with the ultrasonic cavitations mechanism, to cause breakdown and reformation of certain compounds. The highly catalytic, reactive and dissociation capacity of the glow discharge plasma, reforms and reconstitutes chemical elements and compounds from basic atoms or molecules to form nano particles. These include organic, inorganic, metallic and non-metallic materials such as silica, titanium carbon etc. This is also a very effective way to extract or remove heavy metals from a liquid by oxidising such as Hg to HgO; Cu, Zn, Cr etc. to form hydroxide precipitation and ionic metal solute to be deposited by the plasma electroplating process.

The under-liquid plasma creates a highly catalytic and reactive environment for chemical reactions which would not take place under normal circumstances. The reductive species i.e. H+ and oxidative radicals i.e. O-, O_3, H_2O_2, OH- and other radical species produced in the electrolysis and plasma dissociation derived from the liquid itself. The sonic excitation action which enhances the effectiveness of plasma discharge can only be conducted spontaneously under and within liquid.

The under-liquid plasma technique, coupled with the sonic-excitation and electro-chemical action, creates an environment of localised high temperature up to $10{,}000^{O}K$ and pressure up to thousands of atmospheres which favour the generation of cold-fusion phenomena.

It is a low-energy system. Generally high voltage from 0.35 KV up to 3 KV with low current density rarely required more than 3 Amp/cm^2 will be needed to deal with a vast number of different types of the under-liquid plasma process. If other enhancement method is applied, the high voltage and current requirement will be further reduced.

It is a method for producing hydrogen, oxygen with water or other gases and material deposition with liquid containing chemical solute, other than the conventional exchange of ions. The molecules and atoms are being ionised, excited and subjected to dissociation to form ionised, radicals and neutral species by the influence of plasma discharge. The dissociated species can be produced near either anode or cathode electrodes. The ionised species are then attracted to their respective polarity to be neutralised to produce gas or deposition of materials. The dissociation of atoms or molecules are the result of electron collisions and a wide variety of dissociated species is produced which creates the reactive elements for reduction, oxidation, and highly catalytic environments that facilitate chemical reaction of those relatively stable compounds and elements.

No chemicals are needed as an additive in a decontamination process, of which chemicals, i.e. chlorine and ozone, could become a secondary source of pollution.

EXPERIMENTAL OBSERVATIONS

When sufficient micro bubbles originating from the electrode surface block the current flow, the voltage rises steadily until a point of voltage inception is reached whereby some micro bubbles begin experiencing glow discharge. This precedes an avalanche effect which spreads through other micro bubbles close by.

A massive light is then emitted in a flash with a sound of bursting bubbles. The light is yellow to orange in colour indicating plasma discharge in hydrogen gas at the cathode electrode. Soon after switching on the reactor, temperature in the electrode rises which contributes to the formation of vapour bubbles which in turn creates a large bubble environment full of water vapour whereby the next succession of plasma discharge takes place within a fraction of a second.

The features which enable the trapping of gas, the concentration of current density within a small region, and the continued replenishment of gas, are steady and a self-regulating voltage and current power supply, electrode spacing, electrode configuration and electrolyte concentration, all of which have a bearing on generating desirable steady, and short cycle plasma glow discharges.

The invention has a number of applications including:

Plasma assisted electrolysis for hydrogen generation.
Non-thermal plasma reformation of hydrocarbon and hydrogen rich compounds for the production of hydrogen.
Treatment of polluted and contaminated liquid waste containing chemical and heavy metal pollutants.
Treatment of polluted gas emission and removal of odours.
Sterilisation of drinking water and liquid foods.
Extraction and refinement of mineral from its oxide or oxide ores.
Production of nano particles.
Enhancement of a material's chemical and physical properties by plasma discharge irradiation in under- liquid conditions. This also favours the need of any plasma reaction and treatment under-liquid.

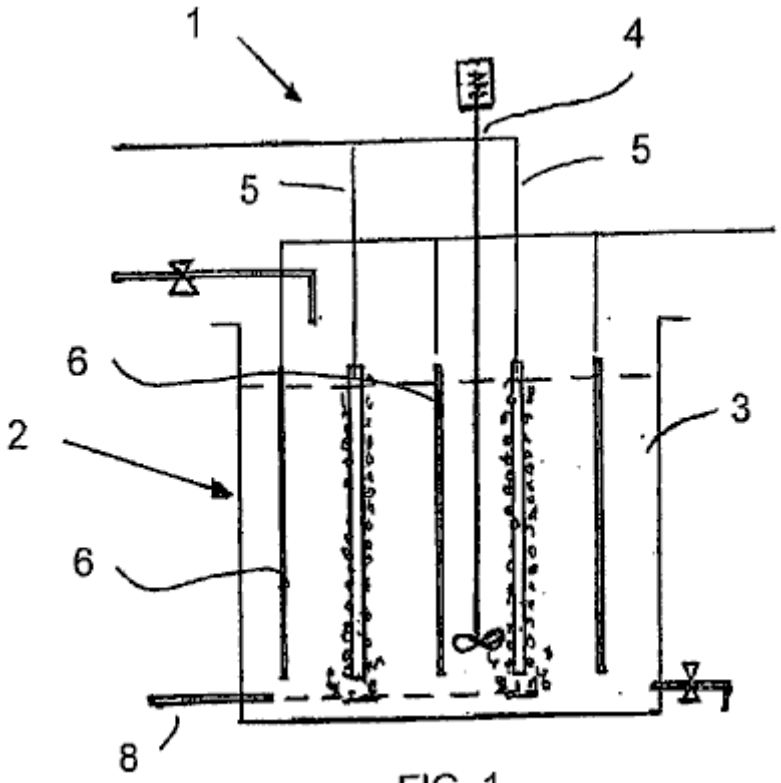

FIG. 1

Fig.1 illustrates a basic apparatus **1** for carrying out the method of the invention, namely, generating a plasma within bubbles formed adjacent to a cathode within an aqueous medium. The apparatus **1** comprises a liquid containment means in the form of an open rectangular tank **2** opening to the atmosphere and containing an aqueous liquid **3**. A stirrer **4** for agitating the aqueous liquids in the tank **2**.

Two spaced cathodes **5** are positioned in the tank **2** alternating with three anodes **6** projecting into the tank **2** and extending generally parallel to the cathodes **5**. A bubble pipe **8** is positioned at the bottom of the tank **2** for introducing bubbles into the aqueous medium in proximity to each of the cathodes **5**.

The application of a suitable potential difference across the anodes and cathodes leads to a glow discharge being formed and a plasma within the bubbles adjacent the cathode. This ionises the atoms and/or molecules within the bubbles and can be used to achieve a number of industrially and commercially useful objectives. For example, it can be used to generate hydrogen gas, one of its uses includes placement in a fuel cell to generate electricity. It can also be used to neutralise harmful compounds within the aqueous medium, e.g. originating in a liquid source or a contaminated gas and treating these harmful compounds. Finally, it can also be used to coat the surface of an article with a particular material.

Each of the cathodes is in the form of a perforated tube. At least one end of the tube is open and typically gas is introduced through such an open end. The side wall of the tube is perforated such that gas issues from the tube into the aqueous medium around the cathode. Alternatively, each of the anodes may be rod-like.

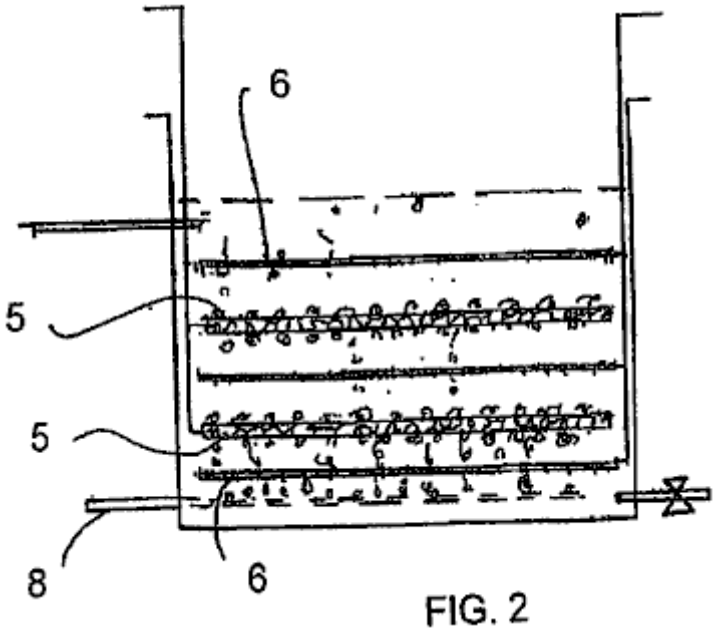

FIG. 2

Fig.2 illustrates a variation on the apparatus of **Fig.1**. This description will be confined to the difference between the **Fig,1** and **Fig.2** apparatuses. In **Fig.2** the electrodes extend horizontally with each cathode positioned between two vertically spaced anodes.

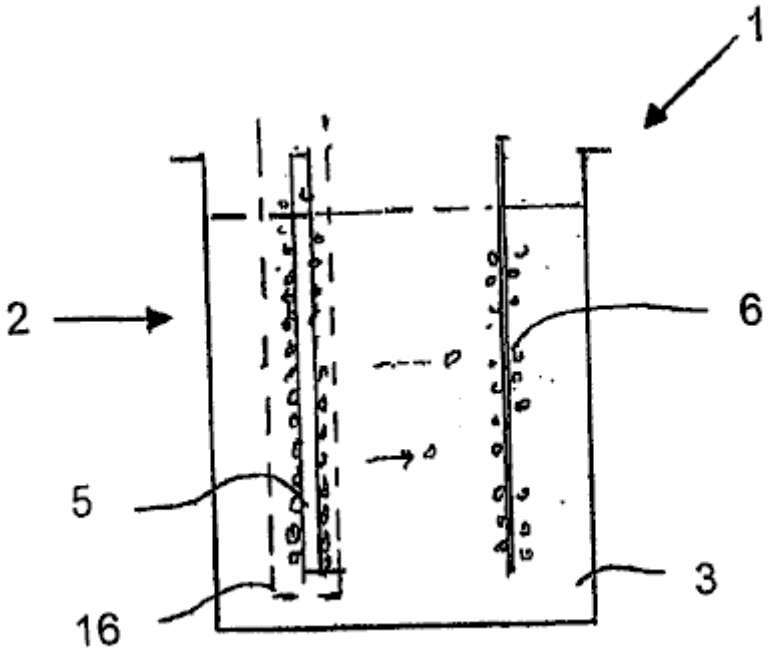

FIG. 3

Fig.3 illustrates an apparatus suitable for the generation of hydrogen. The tank contains an anode and a cathode spaced apart from each other. The electrodes are generally the same as those described above with reference to **Fig.1**. The cathode is surrounded by a semi-permeable membrane. Specifically the membrane is designed to resist the passage of hydrogen and oxygen bubbles through it. Hydrogen gas is formed from the combining the two neutralised hydrogen ions adjacent to the cathode and then is drawn off from the aqueous medium above the cathode and collected for use.

Similarly, oxygen gas is formed adjacent to the anode and this is also drawn off separately and collected for use. An advantage of this method for the formation of hydrogen fuel is that it consumes essentially less energy than other known methods, and as a result, will be a very attractive source of hydrogen for use in fuel cells.

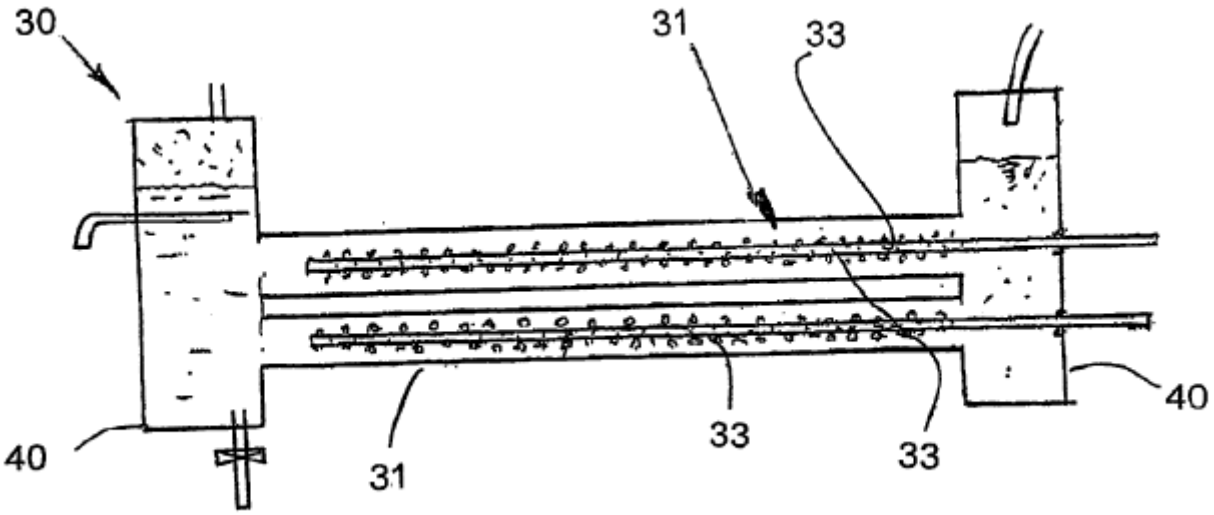

FIG. 4

Fig.4 illustrates a tubular reactor which is quite different to the tank **2** shown in the previous embodiment. The reactor **30** comprises a circular cylindrical body **31** with its longitudinal axis extending horizontally. A pair of electrodes **32**, **33** extend longitudinally through the body, spaced in from the wall of the body **31**. Each cathode **33** is formed by a perforated tube. By contrast, the anode is formed by the body **31**. Thus the single anode **31** extends concentrically around the cathodes **33**, positioned radially inwards from them. A gas, which ultimately forms the bubbles, is pumped into the cathodes, e.g. through their open ends, and then issues through the openings along the length of the cathodes **33**.

Settling tanks are located at each end of the body **31**. The settling tanks **40** permit gas to be separated from the liquid. The gas rises to the top of the tanks **40** from where it can be drawn off. The aqueous liquid can be drawn off through a drain point positioned below this level of aqueous medium in the tank **40**. An aqueous medium can also be introduced into the apparatus, by passing it through an inlet into one of the tanks **40**. Otherwise, the method of generating plasma in bubbles adjacent to the cathodes is very similar to that described above with reference to **Fig.1** to **Fig.3**.

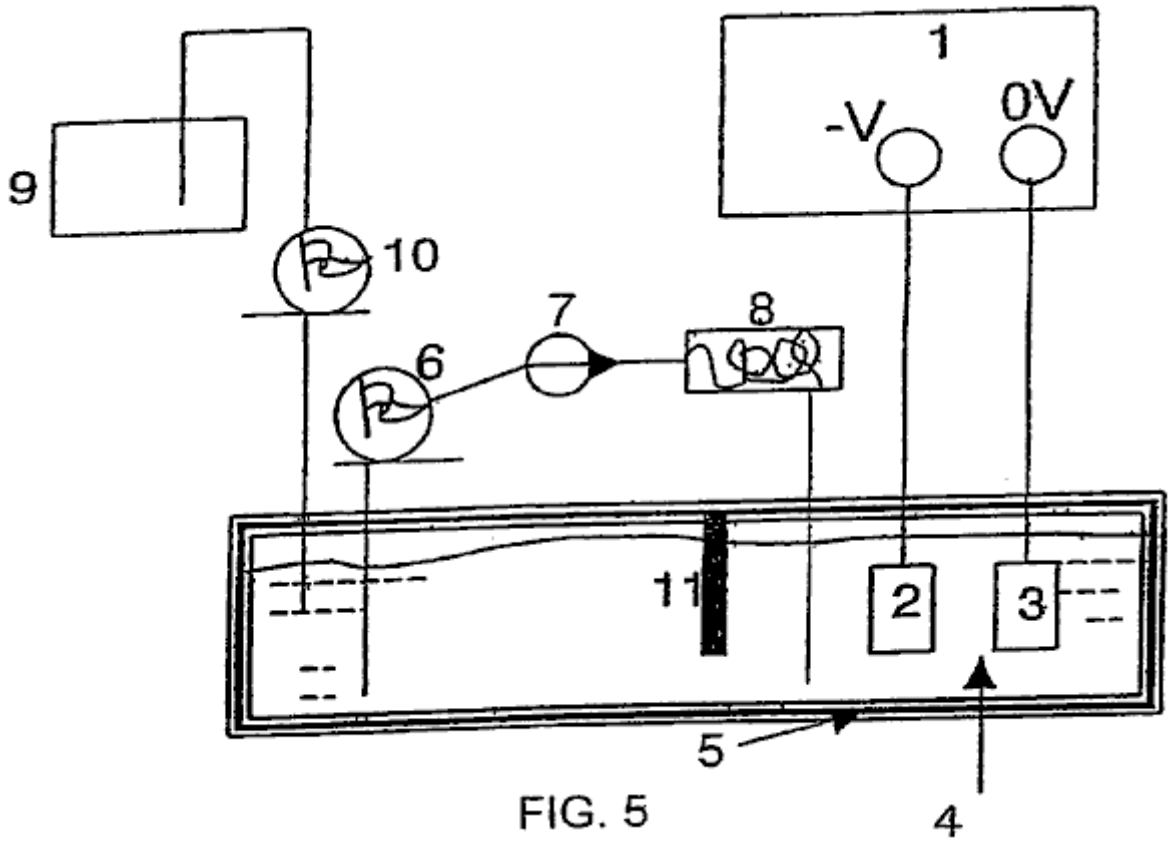

FIG. 5

In **Fig.5**, reference number **1** refers generally to apparatus in the form of a cell and associated components for carrying out a plasma electroplating process (PEP) in accordance with the invention. The cell **1** comprises

broadly, a liquid container in the form of a bath which is filled with an electrolyte which also forms part of the apparatus or cell. A pair of spaced electrodes are positioned in the bath, one being a cathode and the other being an anode. An electrical circuit is formed by electrically connecting up the anode and cathode to a power supply, e.g. a mains power supply. When the bath is being used, a potential difference is applied across the electrodes. A partition divides the bath into an electrode compartment and a circulating compartment. Electrolyte is drawn off the circulating compartment and pumped through a heat exchanger to cool it and then return it to the bath. This helps to keep the temperature of the electrolyte within a suitable range during operation. In addition a make-up tank is positioned adjacent the circulating compartment to replenish the level of electrolyte within the bath as and when required.

The apparatus also includes the means for producing a bubble sheath around the cathode. The bubbles can be generated by gas evolved at the cathode as a result of a cathodic electrochemical reaction. This is one of the ways in which the bubbles were generated in the experiments conducted by the applicant. There are however, alternative ways of generating the bubbles for the bubble sheath. One alternative way, is by boiling the solution (ebullition bubbles). Other ways of producing the bubbles are by cavitation generated by ultrasonic waves or by hydrodynamic flow. Entrainment bubbles can also be produced by a mixture of gas and liquids.

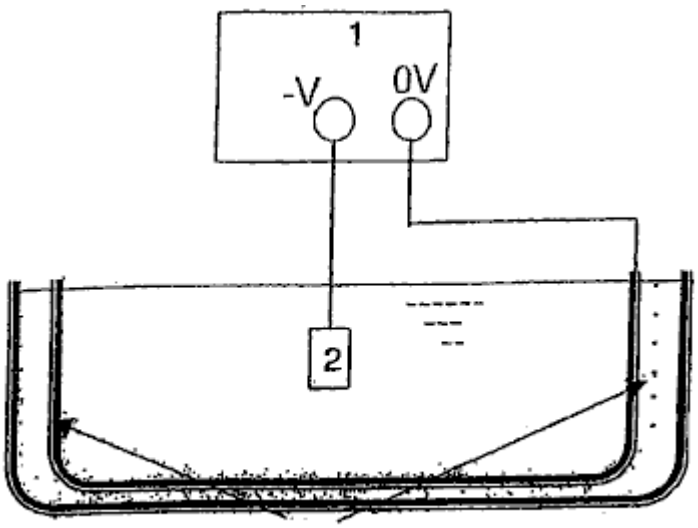

FIG. 6

Fig.6 illustrates an ultrasonic generator surrounding a bath similar to that in **Fig.5**. The generator generates ultrasonic waves which are transmitted into the electrolyte liquid and act to generate bubbles in the electrolyte which then surround the cathode. The cathode, which typically provides the surface for deposition, can be formed of a conductive material, a semi-conductive material or a non-conductive material, coated with a conductive coating. Cathodic materials that have been successfully used in this method are nickel, mild steel, stainless steel, tungsten and aluminium. The cathode can be in the form of either a plate, a mesh, a rod or wire. There may be any number of cathodes and the cathodes can be any shape or size. Any conductive material can be used for the anodes. Graphite, aluminium and stainless steel have all been successfully used to practise this method by the applicant. Generally, aluminium is preferred for the anodes. There may be any number of anodes and the anodes can be any shape.

In use, the bath is filled with an appropriate electrolyte. Broadly speaking, the electrolyte contains a solvent or carrier which provides a liquid environment, within which, electrolysis can occur and which also provides a support for plasma generation in the sense that it provides containment for the plasma generation. The electrolyte also contains a source of the material to be deposited in the form of a precursor. The electrolyte may also include additives for example for enhancing the electrical conductivity of the electrolyte and for assisting in bubble formation and a buffer to maintain a suitable pH in the cell.

In use, the article to be coated is placed in the bath where it typically forms the cathode. In some instances however, it may also form the anode. A voltage or potential difference is then applied across the electrodes and this voltage is set at a level that is higher than the firing point at which the system or cell achieves a stable glow discharge in which glow clusters envelope the cathode surface.

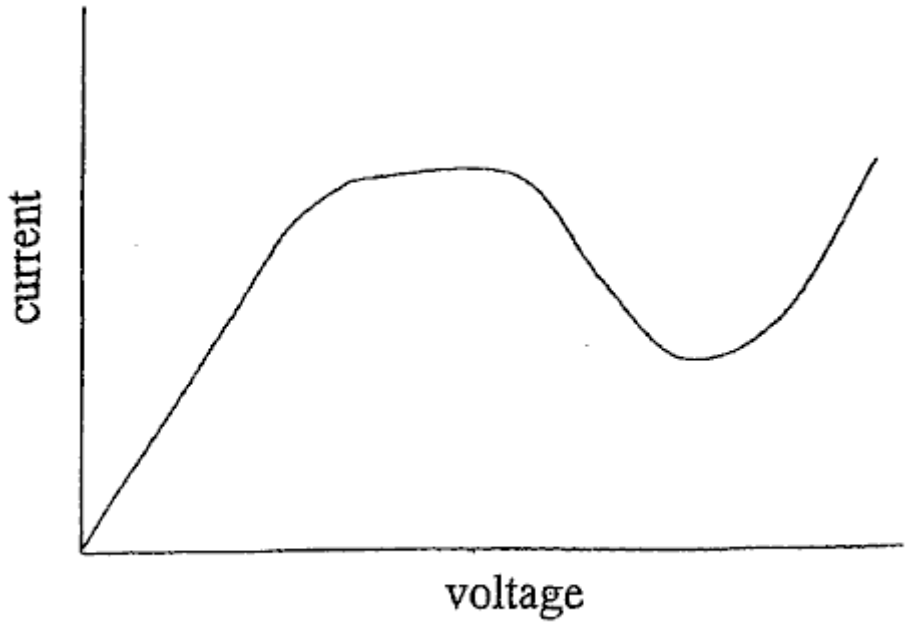

FIG. 7

Fig.7 illustrates a typical current against voltage profile for such a cell as the voltage is progressively increased. Initially there is an ohmic zone where the current increases proportionally with the voltage. After that the curve enters an oscillation zone where the current starts to oscillate. Applicant believes that this condition may be due to the fact that bubbles are evolving out of the solution and partly obscuring the electrodes. The bubbles form plasma, grow and then burst forming a shield shrouding the electrode. These bubbles block the conducting part of the cathode and this might lead to a decrease in apparent current density.

At the cathode, the evolved bubbles include hydrogen generated by the electrolysis of water in the electrolyte and by evaporation of liquid within the electrolyte. The bubbles may also be generated by other means as described above, for example ultrasonic generation. After some time, the number and density of bubbles increases until the entire cathode surface is sheathed in bubbles. At a critical voltage that is constant for a given system, known as the fire point, a glow discharge is formed. Experimental observation shows that this occurs when there is a near continuous bubble sheath around the cathode.

With a wire cathode, a tiny fireball or cluster of fireballs usually appears at the tip of the wire at the fire point. With further increases in voltage a glow discharge is established across the entire cathode. The glow discharge is dynamic and usually shows evidence of glow clusters and/or flashing through the bubble region. The glow discharge is caused by a dielectric breakdown in the bubbles. This is caused mainly by a high electrical field strength. Due to the presence of the bubbles the majority of the voltage drop from the anode to the cathode occurs in the near cathode region occupied by the bubbles. The electric field strength in this region may be of the order of 10,000 to 100,000 V/m. The voltage is set at a setting of 50 to 100 volts higher than the ignition point. This may typically mean a setting of 250 to 1500 volts. A preferred voltage setting would be at the low point of the graph in **Fig.4** within the glow discharge region.

FIG. 8

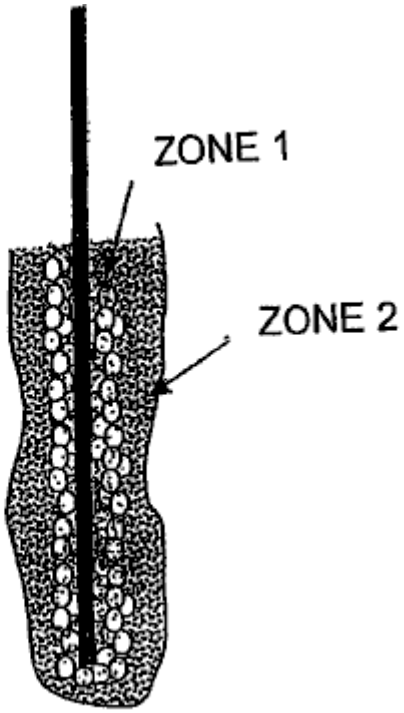

FIG. 9

The glow discharge causes the generation of a plasma in the bubble. **Fig.8** shows the formation of a bubble sheath around the cathode. **Fig.9** shows the cathode during stable glow discharge. As shown in the drawings, applicant has observed the formation of two distinct zones during stable glow discharge. In zone 1 where the glow discharge clusters are present, there is a plasma envelope that directly shrouds the cathode surface. This envelope is where plasma deposition takes place. The plasma interacts with the cathode surface in a process similar to ion plating and deposition occurs. A film is progressively formed through nucleation and growth on the cathode surface. Zone 2 is a plasma-chemical reaction zone, which forms the interface between the electrolyte and zone 1. This zone envelopes the plasma deposition zone and is often clearly visible as a separate region with a milky appearance.

Dissociation, and possibly also ionisation of the electrolyte components, including the precursor, occur in the outer zone, zone 2. This gives rise to the species that are deposited on the cathode. The species is transferred from the outer zone 2 to the inner zone 1 by the electric field strength, diffusion, and convection. Deposition on the cathode then occurs for as long as these conditions are maintained and the precursor material is available in the electrolyte. After the glow discharge commences the temperature of the electrodes increases in a short space of time. The temperature of the electrolyte must be maintained within acceptable limits for certain type of application. To do this, electrolyte is drawn off from the bath and pumped through a cooling system as shown in **Fig.5**. The cooled electrolyte is then re-introduced into the bath. This cooling is required for both stability and safety reasons. Some of the electrolyte components are flammable. In addition electrolyte is consumed during the deposition reaction. Accordingly, it is necessary to top up the bath with additional electrolyte from time to time. A replenishment tank containing electrolytes is provided to perform this purpose.

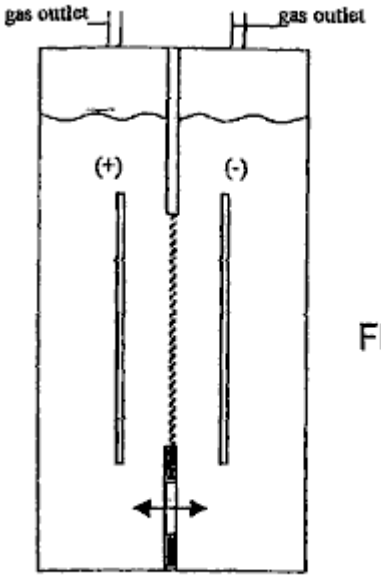

FIG. 10

BASIC TWO ELECTRODE REACTOR
WITH GAS SEPARATOR DIAPHRAGM

As shown in **Fig.10**, the reactor may include a pair of metal electrodes spaced apart and separated by an ion-conducting diaphragm. The electrodes can also be positioned horizontally or vertically.

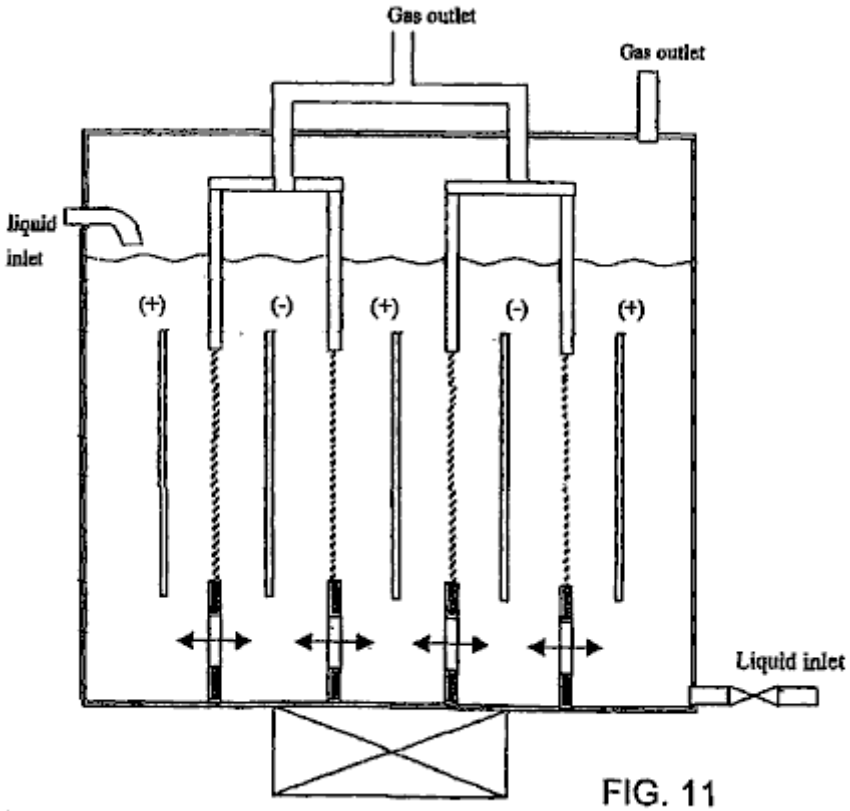

FIG. 11

Multiple Cell Reactors with common bath

As shown in **Fig.11**, the reactor may also include multiple pairs of alternating anodes and cathodes with a diaphragm. The diaphragm can be removed for decontamination and partial oxidation reformation process (**Fig.12**). In the case of reduction process, the hydrogen atoms produced on the side of cathode electrode are kept well separated from mixing back with oxygen by a diaphragm (**Fig.13**). It is possible to increase the throughput capacity of the reactor in treating contaminants with transverse flow through multitudes of alternating electrodes of anode and cathode (**Fig.14**). Wires or rods in tube reactors are suitable to adopt for hydrogen production and reduction process with the metal oxide confined within the narrow space within the cathode half cell and subjecting it to ultrasonic irradiation (**Fig.15** and **Fig.16**).

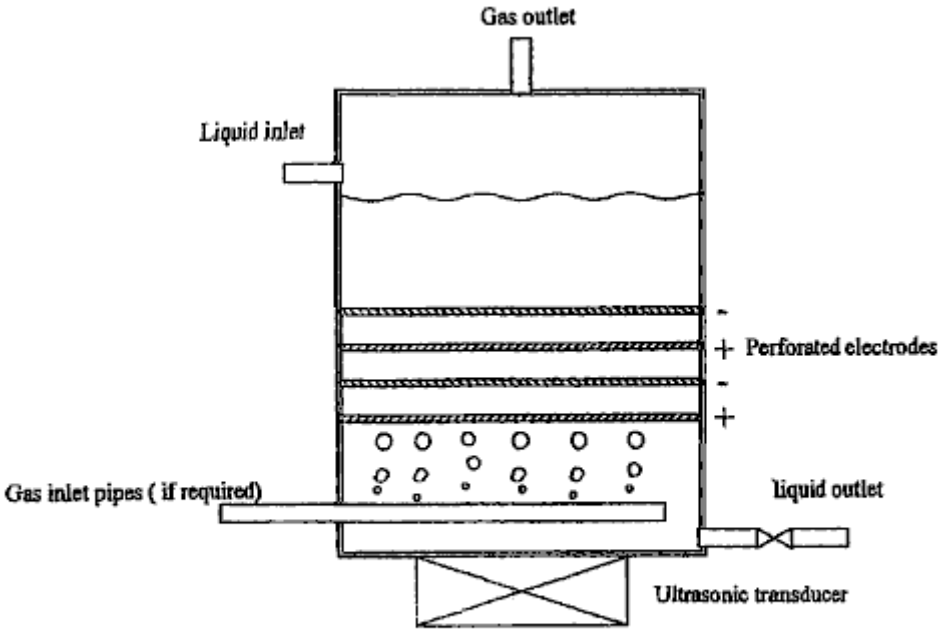

FIG. 12

Tower Reactor with Perforated Electrodes

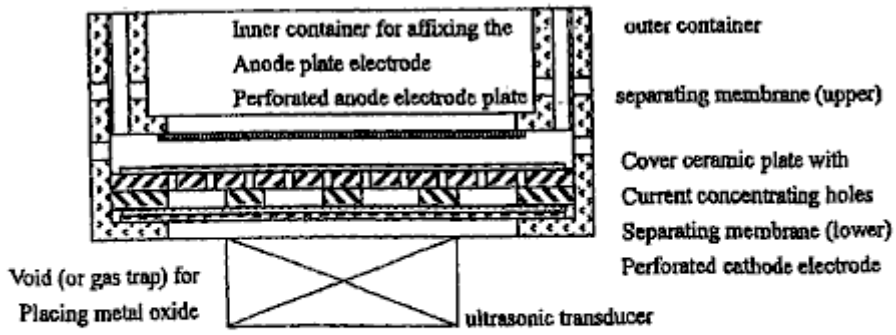

FIG. 13

Reactor for Metal Oxide Reducing Process
(which is to be placed inside an electrolytic bath)

FIG. 14

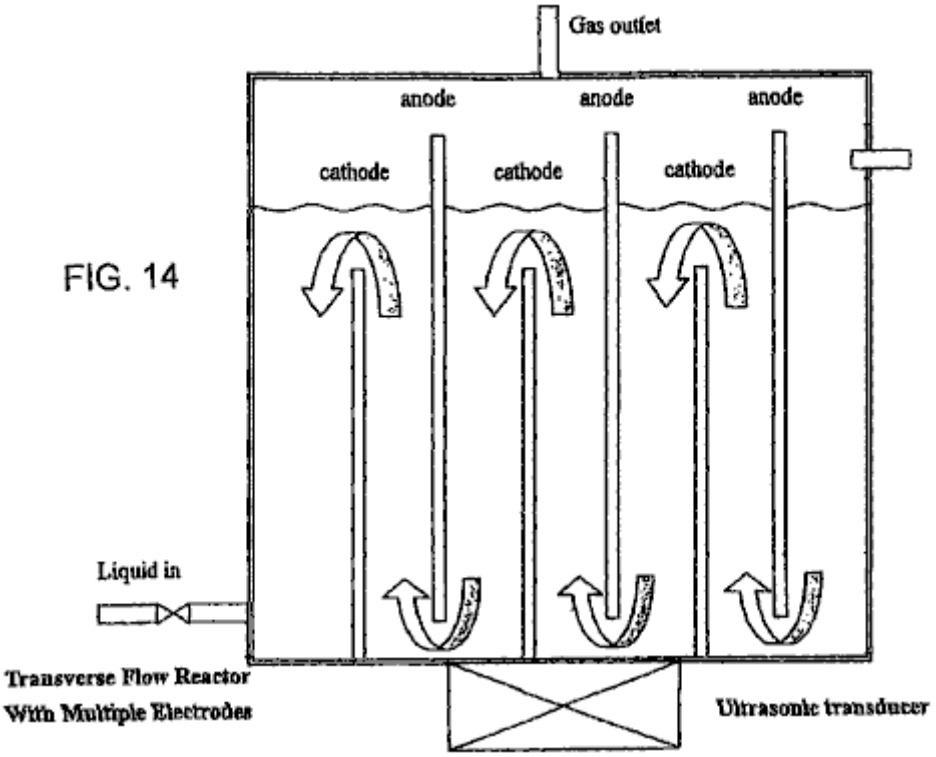

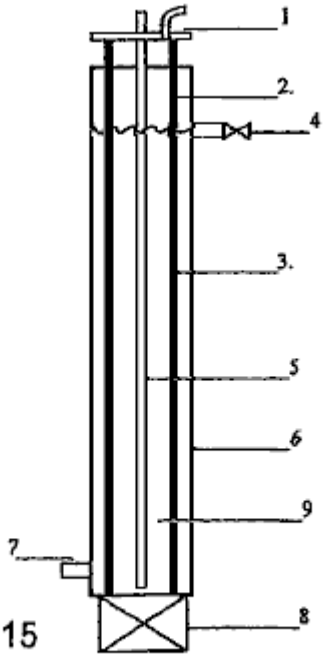

FIG. 15

WIRES OR RODE IN TUBE REACTOR
THE OUTER ELECTRODE SERVING AS BATH

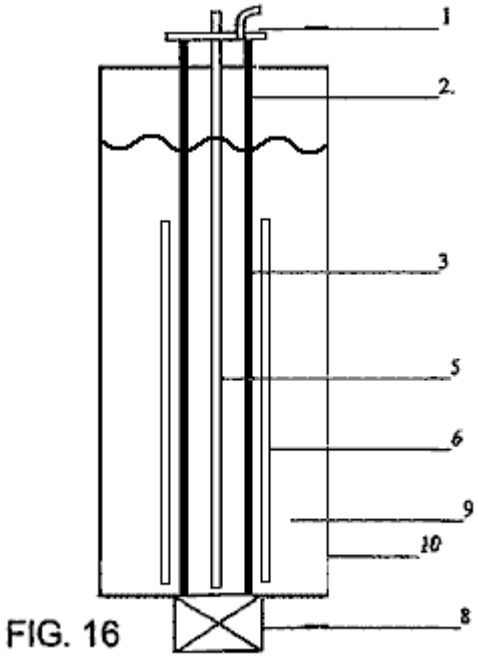

FIG. 16

WIRES OR RODE IN TUBE REACTOR

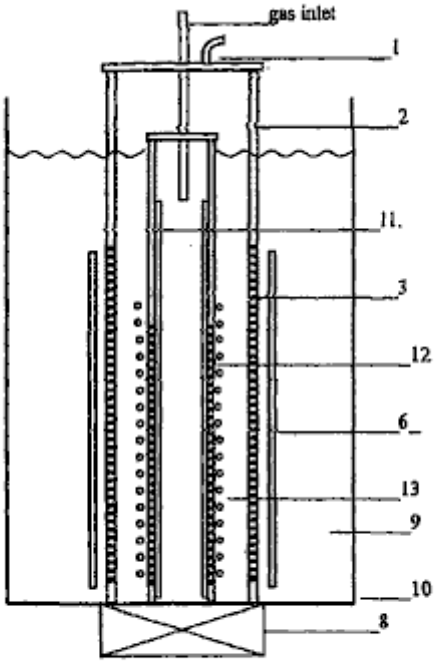

FIG. 17

TUBE IN TUBE REACTOR WITH PERFORATED INNER TUBE COVERED WITH GAS-TRAPPING COVER LAYER

Tube in tube reactor (**Fig.17**) has a tube electrode within the outer tube electrode instead of wire or rod. The inner tube is covered with non-conductive materials of suitable thickness with small diameter holes and gas trap forming in between the inner metal tube which also have small holes formed correspondingly. The gap between the outer electrode and inner electrode is kept close but giving a minimum 3 mm to 5 mm space between the separation diaphragm and the dielectric cover of the inner electrode, to allow free flow of electrolyte and gas. Bubbles of gas will be discharged into the plasma discharging zone with hydrocarbon rich gas i.e. methane, natural gas, H_2S to undergo reformation for the production of hydrogen gas. It can also be adopted for decontamination of polluted gas laden with NOx, SOx and particulates; and reduction process where the metal oxide will flow through the space between the electrodes with the ultrasonic irradiation keeping the fine powder in colloidal and at the same time hydrogen gas or methane gas may also bubble in to provide the extra H_2, H+ and CO to enhance the reduction process.

Configuration of Electrode with Gas Trapping and Current Concentrating Cover Arrangements

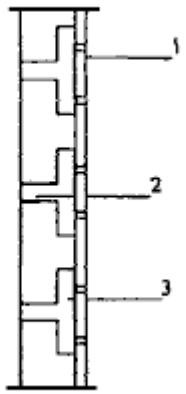

FIG. 18A

Type 1

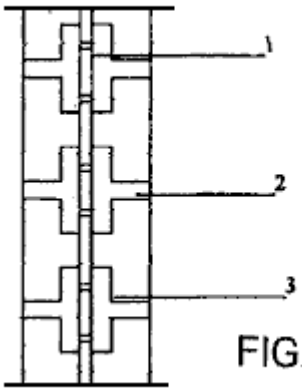

FIG. 18B

Type 2

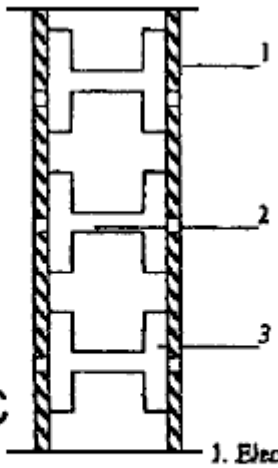

FIG. 18C

Type 3

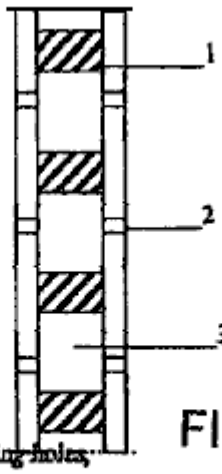

FIG. 18D

Type 4

1. Electrode, 2. Current concentrating holes, 3. Gas traps

Cross Section of Electrodes showing the Gas Trap and Current Concentrating holes

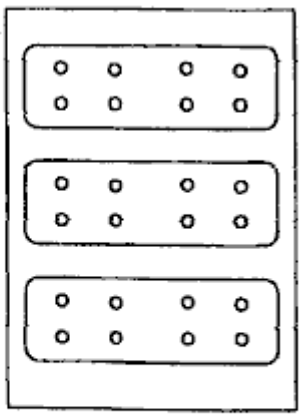

FIG. 18E

Type 5

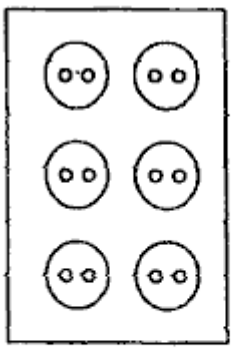

FIG. 18F

Type 6

Plan or Elevation of Gas Trap Cover Plate (with perforated current concentrating holes)

A number of gas trap and bubble retaining arrangements are shown in **Fig.18A** to **Fig.18F**.

The under-liquid plasma discharge, in order to produce various reductive, oxidative, radicals and neutrals species through excitation, ionisation and dissociation of the liquid molecules and atoms, requires high voltage input DC or AC, normally within 3 KV and current density under 3 Amp/cm^2. The electrodes cathode and anode have to be kept as close as possible but not close enough to cause arcing. The electrode surface is preferably flat, even and smooth with no pronounced irregularities. Because of the need of placing diaphragm and complementary gas trapping and retaining construction on the discharging electrode, a minimum distance of 6 mm to 15 mm has been experimented with and shown to produce steady glow plasma under-liquid. With better material choice and engineering capability, there is no reason why the electrode space distant cannot be further reduced. The size, shape and arrangement of the electrodes is not restricted, but the electrodes will usually be somewhat smaller than those required for conventional electrolysis, for the same gas production volume. Both the electrodes, anode and cathode, can be at work at the same time as the plasma discharging electrodes especially if a gas-trapping dielectric cover construction is provided.

Experiments have been conducted to establish the basic criteria to generate steady and rapid cyclical non-thermal plasma glow discharge under-liquid with basic DC high voltage and low current input at atmospheric pressure and ambient temperature leading to the proposal of a phenomenal model of reactor structure and electrode configuration which demonstrate the usefulness of bubbles or gas pocket that creates the under-liquid environment for plasma discharge and it also provides the back ground of further improvement and construction of reactor unite which verify the inventive idea of under-liquid plasma and it subsequent practical applications.

A reactor according to the present invention can basically follow that of a simple water electrolysis cell with one anode electrode separated from the cathode electrode with an ion conducting membrane and yet has the capability to prevent re-mixing of the produced gas on each half-cell. The electrolyte allows moving across the membrane or replenish through the opening in the reactor. In order to increase the proficiency of the reactor the cathode electrode is placed inbetween two anode electrodes and separated from them by a membrane. The hydrogen gas produced is isolated and collected independently. The polarity of the electrode can be reversed with the anode electrode in the middle when oxidative species are needed for the decontamination process. Most importantly, the simple electrode and reactor unit will form the basic module, placed inside a common bath and linked together to form a lage production unit, and these modules can be replaced individually.

Despite the apparent success of the simple perforated plate-to-plate electrode arrangement, it does not preclude other electrode configurations and arrangements such as tube in tube, wire in tube and other flat surface electrodes having different surface structure e.g. wire mesh, expanded metals, pinned plate, sponge porous metal, corrugated plate etc. as long as it is a good electric conductor, corrosion resistant, heat-tolerant material, i.e. stainless steel, aluminium, graphite, platinum etc. The shape and size of the electrode piece is not restricted and sometime it may form the object article which is to undergo plasma surface enhancement treatment.

In practice, a reactor with vertical electrodes, suits plasma-assisted water electrolysis, reformation of hydrocarbon liquid fuel, production of nano materials and decontamination process, while the reactor with horizontal electrodes suits reformation of hydrocarbon gas such as natural gas, methane, hydrogen sulphurs and the like.

This ability to generate steady plasma discharge, can well be adopted for other useful purposes such as thin and thick-film deposition and additional method in the creating of cold fusion.

There have been a series of experiments conducted to generate non-thermal plasma under-liquid by utilising the gas bubbles self generated during electrolysis, electrochemical reaction, heating and releasing of dissolved air or gases in the liquid. Bubbles can also be produce with the influence such as transient bubbles created by shock waves resulted from pulsed power input, ultrasonic cavitations, laser heating and hydraulic impingement. External introduced gas (e.g. air & fuel gas) is found to work well in providing bubbles environment for ready plasma discharge in a steady manner. A number of experiments have also been conducted to test the applicability of under-liquid plasma in the field of hydrogen generation, hydrocarbon fuel reformation, sterilisation and decontamination and reduction of metal oxide. Because of the restriction of the power converter that some result is less than ideal but it all indicate the potential of the under-liquid plasma which is in the first place having the same physical/chemical capability as its counter part operating in gases environment in exciting, ionisation and dissociation, but with some distinctive advantage which has well been described in the foregoing text.

Generation of steady plasma discharge under-liquid has been one of the primary objectives in the research. In general the generation of steady plasma glow discharge are influenced by a number of factors, such as physical and chemical properties of the liquid, its conductivity, temperature, electrode type, electrode spacing, gas retaining or trapping arrangement, current density, voltage input, reactor construction, liquid circulation, influence of ultrasonic irradiation, pulsed power input etc.

There are of course a number of electrode shapes, size and configuration one could choose. In order to find out the how important is the supply of bubbles or gas pocket affects the generation of plasma, a gas retaining or

trapping covering with current concentrating conducting holes over perforated plate electrode is formulated, which has proved effective producing steady glow plasma discharge within the range of 350 V to 2 KV (2,000 V) and current up to 850 mA, but most the time around 100 to 300 mA range. This is considered low in compare with other under-liquid plasma system (i.e. Plasma arc, pulsed high voltage and current electric discharge). Throughout the experiments, a horizontal reactor was used. However an alternative reactor is a vertical reactor.

INTRODUCTION TO THE EXPERIMENTS

Several groups of experiments have been conducted:

1. Preliminary trial experiments
2. Plasma assisted water electrolysis
3. Reformation of methanol
4. Reformation of emulsified diesel
5. Reformation of LPG as hydrocarbon gas (methane is not available in the market)
6. Decontamination or sterilisation of food drink
7. Reduction experiment of TiO_2.

In the preliminary trial experiments a number of electrode types have been adopted and have eventually select the wire to plate configuration and perforated plate to perforated plate or wire mesh as the most suitable under the limiting power supply condition where max. voltage available is 2,000 V and the maximum current is 1,200 mA. In reality, the current input is voluntarily restricted to work below 900 mA for durations not exceeding 30 minutes, to avoid damage to the converter which has happen in a number of occasion which caused stoppage of the experiments for weeks.

To overcome the power supply limitation, and to achieve steady plasma glow discharge, a gas-retaining or trapping cover or layer with current concentration holes has been devised to cover the discharging electrode surface (perforated electrode plate) which is the basic features adopted in the construction of reactor.

In the trial experiments, it has been demonstrated that infrequent visual plasma discharge begins with a voltage of 350 V and steady plasma can be achieved in around 550 V. The initial current input reaches 850 mA and begins to fluctuating in the range of 150 to 650 mA. On many occasions the current fluctuated at 100 mA to 350 mA.

Through these experiments, the mechanism of generating bubbles or gas pocket dielectric barrier which impedes the current flow, leading to an increase of voltage until a threshold voltage is reached which causes the electric breakdown and the formation of plasma inside the bubble, at which point the current immediately returns to its normal level and then another cycle of discharge is established. When the discharge is infrequent it resembles a corona streamer discharge but as the voltage increases, the glow discharge becomes a continuous glow over an extend electrode surface resembling a glow plasma discharge. The colour of the discharge appears as an orange-yellow or red colour in the electrolysis of water and the temperature of the discharging electrode ranges from $50^{O}C$ to about $90^{O}C$ and the temperature of the bath liquid ranges from $40^{O}C$ to $70^{O}C$. No sign of any damage to the electrode or its covering plastic gas trapping plate was observed even after prolong experimentation. When the voltage is allowed to increase beyond the glow plasma region, a plasma arc begin to occurs and becomes an intensive bright blue discharge when voltage is further increased and this causes damage to the metal electrode and plastic covering plate which is easily seen.

On two occasions, hydrogen production was recorded which produced a gas volume with an equivalent energy conversion efficiency up to 56%. Due to damage to the reactor by the plasma arc, that particular experiment cannot be repeated as new model of reactor is designed to achieve low current input and early high voltage response. However with the apparent success of the trial experiment, it shows that a more suitable reactor can be designed specifically for the purpose of hydrogen production by plasma assisted water electrolysis and a higher energy efficiency figure can be achieved with a small reactor.

PLASMA ASSISTED WATER ELECTROLYSIS

Experiments to check the behaviour of plasma discharge at different voltage input levels were carried out. Despite the apparently large volume of bubbles boiling inside the reactor, the total volume of gas produced was unexpectedly low. This may have been caused by the horizontal reactor design adopted throughout the experiments. This may have allowed the hydrogen gas recombine with the hydroxyl ions and convert back into water again. A vertical reactor would be more suited for the plasma assisted water electrolysis where the produced hydrogen gas will rise quickly to the top of the reactor and can be channeled away from the area filled with OH ions.

In this experiments plasma discharge begin to occur at 1,350 V with current fluctuating around 100 mA to 200 mA. At about 1,550 V the reactor produced highest volume of gas. Plasma arc discharge occurs at 1,900 V and is

becoming vigorous when the voltage is increased further. KOH of 0.02% concentration has been used as electrolyte additive throughout the experiment.

The production of gas appears to have a linear relation with time but various substantially with different voltage input. The rate of energy consumption is increasing slowly with time in a constant rate which various with the voltage input and its corresponding energy consumption per unit gas volume produced is having a peak at the first 10 minutes of the experiments and level off with time. The temperature in the electrode rise sharply to from 50^{O}C to 90^{O}C and is maintained more or less at that level throughout the test. The temperature in the bath liquid within the reactor rises slowly from its ambient temperature to around 50^{O}C to 55^{O}C.

EXPERIMENTS WITH METHANOL

Several sets of tests have been conducted with the aim of finding out how different hydrocarbon fuels will be affected by the non-thermal plasma under-liquid system. A methanol / water mixture with methanol concentrations of 5%, 10%, 15%, 20%, 25%, 30% and 40% were tested using the same method and equipment set-up already used for the plasma-assisted water electrolysis. There are three independent tests for each methanol concentration. It has been observed that the gas production is peaked at 25% methanol concentration and the energy consumption per unit gas volume produced is also lower than the others and is nearly at constant rate around 0.0225 Kw.h/L. The voltage input for each test is kept at 1,850 V and the current fluctuating in the range of 100 mA to 200 mA. The temperature measured at the cathode electrode started at 80^{O}C and rose quickly to reach over 200^{O}C at the end of a 30 minute experiment. The temperature recorded in other tests stayed within the range of 60^{O}C to 80^{O}C. The temperature of bath liquid at 25% concentration stayed in the range of 50^{O}C to 60^{O}C, which is typical for each of these tests.

The greatest surprise coming out of the experiments is that the produced gas is composed of two gases. One is hydrogen gas and the other is oxygen gas and no trace of carbon dioxide is found. Repeated examination of the gases produced shows the same result and the hydrogen is having an average value of 51.3% and oxygen 48.7%. This is later found out that the presence of oxygen in the gas is the result of the removal of the separating diaphragm. An acidic electrolyte is preferable in order to increase the hydrogen gas percentage in the output gas mix. This is shown in the latest experiments using sulphuric acid of 0.02% concentration.

A set of experiments with the use of 40 KHz ultrasonic bath having methanol concentration of 10%, 15%, 20% and 25% with the same reactor and equipment arrangement have been conducted to find out the influence of ultrasonic radiation. It has been observed that gas production at 25% is substantially higher than the others and yet the energy consumption per unit gas volume produced is around 0.015 Kw.h/L throughout the 30 minute experiment, which is lower than that without ultrasonic radiation.

The chromatographic analysis of the output gas having an average value of 97.56% hydrogen and 2.4039% of carbon monoxide. Chromatographic analysis of gas produced by reformation of methanol with ultrasonic radiation. Methanol concentration at 25%, and conductive reagent 0.02% sulphuric acid.

TABLE 1

Test	Resident time minutes	Composition V/V %	Gas type
First Test	0.364	98.9937	H_2
	1.047	1.0063	CO
Second Test	0.364	96.7418	H_2
	1.047	3.2582	CO
Third Test	0.354	96.9719	H_2
	1.048	3.0281	CO
Average		97.5691	H_2
		2.4309	CO

EXPERIMENTS WITH LPG

Decomposition of LPG by under-liquid plasma has been conducted (methane or natural gas is preferred but none is available in the market). The LPG is allowed to pass through the horizontal reactor through the perforated anode plate and enter the reactor and trapped at the cathode plate where plasma is taking place at voltage 1980V and current at 100 to 130 mA input. C_3H_8 and C_4H_{10} are the two main components of LPG, it is expected that the volume output having been subjected to plasma dissociation should be larger than the original input volume. This is found to be so that the output gas volume increases by about 50%. The experiment is conducted together with ultrasonic radiation. It is regrettable that the chromatogram is incapable of undertaking analysis of the output gas composition. The next set of experiments should be conducted with methane or natural gas so that more definitive result could be obtained. Rudimentary analysis of the produced gas has shown the presence of H_2, CO_2 and C_3H_6 etc.

REFORMATION OF EMULSIFIED DIESEL AND WATER WITH ULTRASONIC IRRADIATION

Decomposition of emulsified diesel with distilled water has also been carried out. Diesel oil in 25% and 50% by volume has been emulsified by adding 1.25% emulsified agent inside the ultrasonic bath. Since the diesel oil is dielectric, a KOH additive is needed. The emulsified liquid is subjected to plasma discharge at a voltage of 1,850 V and a current fluctuating from 100 mA to 200 mA for a period of 30 minutes. The temperature of the cathode electrode increased from 70^{O}C to about 94^{O}C during the experiment. The gas volume produced was 160 ml with 25% diesel and 1,740 ml with 50% diesel, which is substantially higher and its energy consumption is 0.1213 KWh/L. It is clearly indicated, that gas production is proportional to the diesel contend in the emulsion. Because of the limited power supply capability, the voltage of 1,850 V is merely adequate to produce some plasma discharge but it is far from establishing extensive vigorous plasma with higher current and voltage input, which would produce more gas.

STERILISATION (DECONTAMINATION) OF MULBERRY FRUIT DRINK

The ability of non-thermal plasma to decontaminate noxious chemicals and gases has already established. This experiment is conducted to find out how well the under-liquid plasma may apply in the field of beverage sterilisation with low levels of plasma radiation and keeping the treated liquid within an acceptable temperature.

Two litters of 15% concentrated fruit drink is placed in the bath where a horizontal reactor is submerged. The bacteria count and mold colony count is obtained before the forty minute test. A sample of the fruit drink is extracted at 20 minutes and 40 minutes. The mulberry drink has good natural conductivity so no additive is required. The applied voltage is kept at 1,200 V and the current fluctuates around 200 mA. The temperature at the electrode is maintained at around 62^{O}C and the bath liquid (fruit drink) is kept at around 50^{O}C.

TABLE 2 - The micro-organism count

Time (minutes)	Bacteria count/ml	Mold colony count/ml
0	3,400	37,000
20	1,300	17,000
40	90	10

The favour and colour of the fruit drink had not changed after the test. The bacteria sterilisation is 97.5% and that of mold colony has been sterilised more than 99%. This has given proof that the under-liquid plasma has the same capability as those operated in a gaseous environment.

The time for the treatment could be reduced by providing forced circulation of the liquid and increasing the electrode size. Sterilisation of drinking water imposes no limit on the temperature. Higher voltage input for better plasma glow discharge spreading over larger and multiple electrodes should be able to remove all harmful chemical substance, bacteria, biological matter and microbial matter, thus meeting the municipal requirement for drinking water.

REDUCTION OF METAL OXIDE

One trial experiment to reduce TiO_2 back to Titanium metal has been attempted with little success. It was found that in the X-ray diffraction test, minor traces of titanium nitride and titanium monoxide (TiO) were found. In the experiment, only a minor electrolyte of 0.05% KOH with 25% methanol added to the distilled water was used to increase the production of hydrogen. The applied voltage was fixed at 1,850 V and the current fluctuated in the range of 200 mA to 500 mA. Ultrasonic radiation up to 40 KHz was also provided through an ultrasonic bath. The temperature recorded in the bath liquid rose from $46^{O}C$ to $75^{O}C$ at the end of the 60 minute test. The fine TiO_2 with was suspended with ultrasonic radiation, in the bath liquid in colloidal form, showing as a milky white colour, which gradually became a milky yellow colour towards the end of the experiment. The bath liquid also became viscous.

The X-ray refractive "d" value of TiO_2 were:

Before the experiment: 3.512, 1.892, 2.376 but after the experiment there were two new groups of "d" measurements not seen before the experiment:
a: 2.089, 1.480, 2.400
b: 2.400, 2.329, 2.213
This indicates a new material, positioned between TiO and n-Ti_3N_2-x.

This experiment indicates that a change did happen to the TiO_2, possibly because of the limited voltage and current available as input, which could not provide the intensity of plasma discharge needed to effect the reduction process properly. Higher concentration of either HCl or H_2SO_4 should be use as reagent demonstrated in the following chemical reaction and in the same time serving as electrolyte. The horizontal reactor is not a suitable piece of equipment to undertake such experiment; it is adopted merely for convenience. A wire-in-tube and tube-in-tube reactor would be a suitable candidate, which would keep the metal oxide exposed to plasma discharge throughout the whole of the duration of the experiment. Further, more hydrogen or CO gases produced during the process may be passed back to the reactor to enhance the reaction. (Methane is a suitable gas for this type of reduction process, as both hydrogen and CO gas will be produced to enhance the reaction). The following are the chemical formula, which suggested by transforming TiO_2 to either $TiCl_4$ or $TiOSO_4$ as a soluble ionic compound, will facilitate its reduction with prolong exposure to active atomic hydrogen under the influence of a plasma catalytic environment.

$TiO_2 + 4HCl \rightarrow TiCl_4 + 2H_2O$,
$TiCl_4 + 4H \rightarrow Ti + 4HCl$.
$TiO_2 + H_2SO_4 \rightarrow TiO(SO_4) + H_2O$,
$TiO(SO_4) + 4H \rightarrow Ti + H_2SO_4 + H_2O$
Where $TiCl_4$ is readily produced by an established process from ilmenite.

Similarly, aluminium oxide Al_2O_3 can first be transformed to $AlCl_3$, which is soluble ionic compound, ready to be extracted by electro-deposition enhanced with plasma-reduction and plasma-electroplating process:

$Al_2O_3 + 6HCl \rightarrow 2AlCl_3 + 3H_2O$,

$2AlCl_3 + 6H \rightarrow 2Al + 6HCl$.

In the case of electrode positive oxide such as Fe_2O_3, it can be reduced in the presence of ionised atomic hydrogen and the presence of carbon monoxide with catalytic reactive plasma irradiation.

Fine metal oxide powder irradiated with ultrasonic waves will maintain in colloidal form allowing it to be exposed to the reduction agent atomic hydrogen and/or carbon monoxide. The process of ultrasonic cavitations and collapse is also known to create extreme localised high temperature up to 10,000^{O}K and thousands of atmospheres of pressure together with the high temperature at the impact point of the fine powder particles which is beneficial to the entire reduction process.

DETAILS OF THE EXPERIMENTS CARRIED OUT

Establishing Generation of Under-Liquid Plasma:

Distilled water is used in the experiments with 0.05% KOH as a conducting reagent. The voltage is controlled at 1,250 V & 1,850 V. The current is raised in steps of 100 mA until it reaches 850 mA. In the beginning the voltage remains low and gradually builds up as more gas bubbles are generated. Once it reaches a certain high level the current drops immediately. The self-regulating current and voltage input of the power unit automatically switches from current input control to voltage input control. At 45 seconds after switching the experiment on, the voltage rose to 470 V and the current dropped below 500 mA. From 3 min. 10 sec to 5 min 20 sec, the voltage rose to a relatively high level while the current kept on fluctuating. After a period of unstable voltage and current movement they become stabilised at 20 min with the characteristic high voltage and low current. At this instant prominent glow is observed at the perforated cover plate (current concentrating holes). The temperature of the cathode electrode has risen and stays steady at around 70^{O}C.

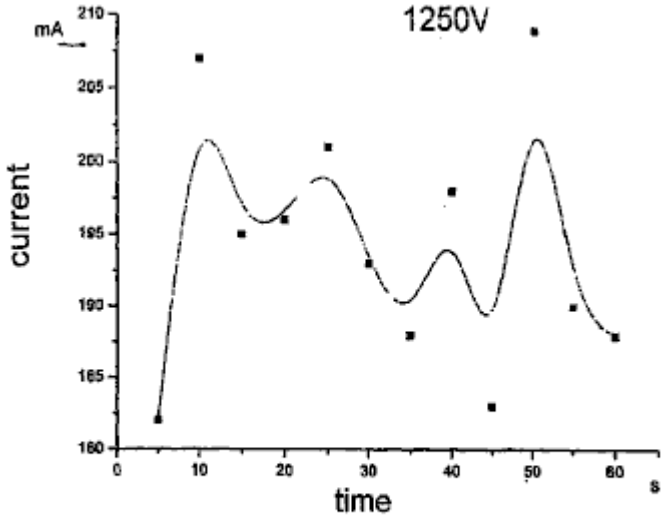

Glow discharge at stable 1250V input

FIG. 25

Fig.25 shows the current fluctuating with stable 1,250 V voltage input and a steady plasma glow discharge. The temperature of the cathode increases rapidly in the early stages and then becomes steady at the 5 min mark, and then rising slowly to it's highest temperature of about 96^{O}C.

OBSERVATION

Generating Under-Liquid Plasma:

In accordance with the experimental results, it is possible to generate non-thermal plasma under-liquid providing that certain conditions are met: a suitable power supply, electrolytic liquid, reactor and other supplementary equipment.

The design of the reactor, with relatively low voltage and limited power rating (restricted current input) requires special construction to trap or retain gas and at the same time to raise the current density at the discharge area.

The gas trap or chamber should be of a suitable size. If the gas trap or chamber is too big, then the trapped gas is too thick which requires a much higher voltage for discharge breakdown and prolongs the time of each cycle of discharge. It becomes difficult to maintain rapid cyclical steady glow discharge. The perforated covering plate, is also an important part of the electrode structure, concentrating the current density. The thickness of the perforated plate and the size of the gas trapping chamber should be carefully controlled so that the electrode spacing gap is not unduly wide as that also influences the voltage requirement. The size and disposition of perforated holes can be determined by trial and error. Wide electrode spacing increase the voltage input requirement and unsuitably close electrode spacing will cause early occurrence of plasma arcing with high current surge and generation of temperatures which will damage the electrodes and their attachments.

The power unit should be of adequate power rating. The electric breakdown is highly dependent on the high voltage supply. If the rating of the power supply unit is inadequate, it could easily be damaged during sudden the high current surge caused at cyclical electric breakdown. There will be no plasma discharge if the power input is inadequate.

The electrolytic liquid should have suitable conductivity, not too low nor too high. Voltage cannot be easily raised between two electrodes the liquid has high conductivity and no plasma discharge will be generated unless there is a high voltage input. The discharging electrode may be fully encapsulated inside a bubble barrier, but high conductivity liquid allows the current to pass through the bubble-liquid interface which in turn, also prevents the voltage rising high enough. If the conductivity of the liquid is too low, then the bubble barrier forms a complete dielectric barrier which requires a much higher inception voltage to cause electric breakdown or discharge and at the same time, the passage of current becomes too low which results in a low current density which also influences the occurrence of discharge. A much higher breakdown voltage (discharging voltage) creates electric arcing in gaseous condition which is no longer considered non-thermal under-liquid plasma discharge.

CONCLUSIONS

1. Gas layer or bubbles form the dielectric barrier that provide the environment for building up the discharge voltage and gaseous space for plasma discharge to take place. High voltage and relatively low current input is characteristic of under-liquid plasma.

2. With the characteristic high voltage and low current requirement, the under-liquid plasma can be generated over a wide range of liquids. The electrolyte liquid can be acidic, alkaline or a solution of salts. Liquids containing conducting impurities or a mixture of organic compounds may also serve as electrolyte such as the case of tape water and fruit drinks.

3. There are a number of factors which would affect the generating of under-liquid plasma such as voltage, current density, configuration of electrodes, area of electrode surface, electrode gap spacing, electrolytic physical and chemical properties, gas retaining and trapping arrangement, provision of plasma enhancement, ultrasonic cavitations, pulsed power supply, ambient temperature and reactor construction. This appears complicated, but the experiments undertaken have demonstrated that all the mentioned factors can be manipulated to achieve generation of stable non-thermal plasma at one atmosphere of pressure.

4. Plasma is the fourth state of matter. It has been widely employed in the field of chemical, electronic, materials and energy industries. Plasma generated under-liquid plasma has its own intrinsic characteristics and advantages, which have already proved to be a useful tool for plasma electroplating or deposition of both metallic and non-metallic materials. It will find its application in the plasma-assisted water electrolysis for hydrogen production; reformation of hydrogen rich compounds or hydrocarbon fuel (gas and liquid); decontamination of both liquid and gas pollution discharges containing persistent harmful chemicals, dissolved heavy metals and organic and biological contaminants; sterilisation of fruit drinks, potable water supply; and reduction of material oxide such as oxide ores, metal oxide as an alternative method metal refinement. It is probable that the proposed under-liquid plasma generation, and this established basic scientific information, would form the basis for further refinements leading to the practical new applications put forward in this patent application.

PLASMA ASSISTED ELECTROLYTES FOR HYDROGEN PRODUCTION

Water electrolysis is still used for the production of pure hydrogen. This hydrogen production is restricted because of it's relatively low energy conversion efficiency. In order to achieve higher energy efficiency, the electric voltage must be kept low to avoid energy loss through heat conversion. There are also claims that the energy efficiency can be improved by better electrode configuration, an increase in the reactive surface area, reduction of the electrode gap and increasing the operatingpressure. The PEM solid electrode system is in its early development and its efficiency remains similar to that of water electrolysis system. In any case the basic principle of water electrolysis has not changed since it was first put to use. Electrolysis as a whole, is considered to be non-competitive with the competing production process of reforming hydrocarbon fuel, but electrolysis has the advantage of being a clean process producing high gas purity and CO_2 is not produced.

The hydrogen bubbles evolving from the electrode surface slow down with time when tiny bubbles gradually built up and smother the electrode surface. These are not easily dislodged and the rate of hydrogen production is reduced further as those tiny bubbles become a barrier to current flow between the two electrodes.

The proposed invention is closely related to the water electrolysis process but the mechanism of separating hydrogen from water molecules is different. Generating non-equilibrium plasma within the bubbles that smother the electrodes will break down the dielectric barrier bubble layer and cause the normal flow of current to be resumed. At the same time, water molecules contained in the bubbles coming into contact with the plasma discharge, will be dissociated to produce extra hydrogen. In addition, the vigorous plasma discharge near the electrode surface will also create an hydrodynamic condition, which will wash away the fine bubbles which block the current flow. The mechanism of producing hydrogen by plasma discharge is different from the conventional electrolysis which splits the ionic water molecules by electro-polarity attraction, while in the plasma discharge the water molecule is broken down as the result of electron collisions. The water molecules under the plasma discharge irradiation would lose one electron due to electron collision to yield $H_2O + e \rightarrow OH + H^+ + e$

The hydrogen produced is of high purity. Ordinary potable water or rainwater with a very low concentration of electrolyte can be used as the main source of material, instead of distilled water, as they contain sufficient impurity to be slightly electro-conductive.

The experiment has demonstrated that hydrogen gas can be produced with plasma glow discharge as a supplementary process to the conventional method. The energy required to produce 1 cubic meter of hydrogen with plasma glow discharge with a very rudimentary reactor has achieved an efficiency of 56% which can be further improved with better engineering, by closing the electrode gap distance, selecting the right concentration of electrolyte, reactor construction and better means of trapping and retaining gas near the discharge electrode.

High temperatures of up to $90^{O}C$ is recorded in the electrolyte, which increases within very short time of the reaction. This may in part due exothermic reaction of recombining H and OH to water. The excessive heat can well be utilised as secondary source of energy. The gas or vapour bubbles by heating assuming greater importance as source materials for plasma dissociation leading to the production of Hydrogen. The high purity oxygen co-produce is also a valuable by-product with many applications.

Since high voltage with moderate current is needed in the plasma process, the production rate per unite area of electrode surface is high, and so only a small reactor is needed for the production of hydrogen, especially when other plasma enhancement methods are employed, such as ultrasonic cavitations, pulsed powers and RF input.

The electrodes could be of any conductive materials such as aluminium, stainless steel, graphite, tungsten, platinum, palladium etc. The size of the electrode for the plasma discharge is much smaller than that required by the conventional electrolysis to produce the same quantity of gas. As a result of this, a smaller reactor is possible.

Sponge porous electrodes will increase the reactive surface area available to produce electrolysis gases. In the experiment, several layers of fine wire mesh were packed tightly together to mimic a sponge porous electrode plate.

Some of the basic electrode configuration is: plate to plate; perforated plate to perforated plate; plate or perforated plate to wire mesh; wire mesh to wire mesh; plate to pinned plate; dielectric coating on one or both electrodes plate or mesh or pinned plate, tube in tube and wire in tube arrangement. It is noted that electrode configuration including any lining or covering materials that help to concentrate the current density and having the ability in retaining gas around the electrode would be adopted which will help to lower the voltage and current requirement to generate steady plasma discharge.

In order to create an environment for steady and short cyclical plasma glow discharge as already mention in the previous text, the electrode configuration should be so structured to retain the bubbles and concentrate the current density and yet keeping the true electrode gap distance to a minimum. This creates a suitable voided

space either in the metal electrode or in the covering materials, capable of retaining gas while at the same time having the mechanism to concentrate the current density to a localised discharge point. This leads to a wide variety of designs and choice of materials to satisfy plasma discharge requirement.

In order to avoid recombination of H^+ and H_2 with OH ions and reverting back to water, the hydrogen atoms after regaining their lost electrons through contacting the cathode should be allowed to escape quickly from the area which abounds with other oxidation species and radicals. This has greatly influenced the productivity of hydrogen gas. If H^+ and OH is allowed to recombined, despite of the apparent bubble boiling in the reactor very little gas can be collected and the temperature in the reactor rises quickly which could well be the exothermic effect of recombination of H^+ and OH.

The hydrogen produced is collected separately from the oxygen. Since the produced hydrogen gas contains a fair amount of water vapour, the hydrogen gas is collected by passing it through a water chiller or other known method, so that the measured gas volume is at room temperature with minimum water vapour content.

The basic plasma assisted electrolysis cell or reactor can be produced in modular form which can be mounted side by side and placed inside a single electrolytic tank with their respective power and output gas collected to form a major production unit. Several reactor types can be employed for the production of hydrogen. Rod or wire in tube reactor, tube in tube reactor, single or multiple cell reactors are also suitable for the plasma assisted water electrolysis. The gas retaining and current concentrating cover will be affixed on the cathode electrode facing the anode electrode. A horizontal reactor whose cathode has a gas-retaining cover can be placed on top of an anode which is separated by a diaphragm and the hydrogen gas will then collect in isolation.

The introduction of ultrasonic cavitations into the electrolytic liquid is easy since the electrolysis bath is also the ultrasonic bath and ultrasonic transducers can be attached to the bath externally. A mixture of sonic frequency should be used to avoid any occurrence of a dead sonic zone. The introduction of sonic excitation through cavitations enhances the production performance of plasma-assisted electrolysis.

Pulsed high-voltage DC supply with single polarity square wave from 5 KHz up to 100 KHz has been found to be beneficial for generating plasma at a much reduced voltage.

The distinct advantage of the under-liquid plasma enables ionised species migrate to the respective half cell and electrodes which will avoid and minimise re-mixing of the produced hydrogen and oxygen causing a reversion to water again and creating a hazardous, explosive condition. The oxygen is considered as a by- product which can be collected for use or it can be channelled to the combustion chamber if hydrogen is used as direct fuel for a combustion engine.

Water is the primary source material for hydrogen production, being economically available and of unlimited supply. It is a completely clean source material that produces no unwanted by-products.

The anode may be gradually losing its materials due to electro transportation, but if so, it will be a very slow process. In practice the polarity of electrodes can be reversed which reverses the materials transportation and deposition. Conductor materials which are inert to electro-chemical corrosion are a good choice to serve as electrodes.

A chemically conductive reagent may be added to water to increase its conductivity and a foaming agent added to enhance generation of bubbles. The electrolyte can be of acidic or alkaline base. The concentration of the electrolyte should be maintained at a steady level for best results. High electrolyte concentration increases liquid conductivity as well as productivity of gas bubbles but it might prevent the rising voltage required for discharge as the current flow between electrode will not be inhibited by the presence of bubbles. However, a very low concentration of electrolyte will favour dielectric breakdown of bubbles, as a lesser current will be carried by the liquid medium inbetween the bubbles. It has been found that either acidic or alkaline electrolyte with 0.02% concentration work extremely well in maintaining steady glow discharge with DC voltage ranging from 350 V to 1,800 V and a current from 100 mA to 800 mA.

Tap water has been used without adding any conducting reagent and it often works unexpected well, most likely due to present of impurity and high pH, in the plasma-assisted electrolysis where steady glow discharge occurs at around 450 V to 900 V and current around 200 mA to 350 mA. The power input requirement varies in accordance to electrode spacing, electrode and reactor configuration, electrolyte concentration and the structure of gas retaining arrangement. Again other plasma assisted method such as pulsed power input and ultrasonic cavitations etc. also help to lower the power input requirement.

The process is in general, conducted at one atmosphere pressure. An increase of pressure will slow down upward movement of the bubbles and raise the temperature of the electrolyte. Some increase in temperature in

the electrolyte is not detrimental to the generation of plasma. Water vapour bubbles provide the source materials and active environment for plasma discharge. In general, electrolyte temperature is well below boiling point as non-thermal plasma produces little heat. The temperature sometime rises quickly in the electrolyte due to occurrence of infrequent plasma arc and exothermic in the recombination of H+ and OH- in quantity.

During the steady glow discharge, vigorous bubbles with yellow/orange/red colour light spots appear all over the plastic perforation. The light spots also appear widely on the electrode surface when the voltage is increased. On examination of the electrode and plastic cover sheet, no burn marks were observed. This proves that the plasma glow is non-thermal after an hour of glow discharge. The temperature in the electrode plate recorded with a thermal couple was around 50^{O}C to about 90^{O}C. The gas produced is composed mainly of hydrogen with some water vapour, which condenses quickly on cooling. The rate of hydrogen production is variable and energy conversion rate also fluctuated throughout the test. This is suspected to cause by the recombination of H and OH, which is affected by the electrode and reactor structure and configuration.

Hydrogen can now be produced with high voltage and low current, which is contrary to the conventional electrolysis system where a small reactor with a high rate of production is becoming possible. This has clearly demonstrated that the mechanism of producing hydrogen with plasma discharge is different from conventional water electrolysis in a number of ways. Steam and gas vapour produced due to heating of the electrodes (cathode) in short space of time are becoming an importance source of materials for plasma dissociation that also influence the productivity of hydrogen.

1.3 Experimental Procedure

1.3.1 A flow diagram for carrying out experiments in relation to this invention is shown in **Fig.28**.

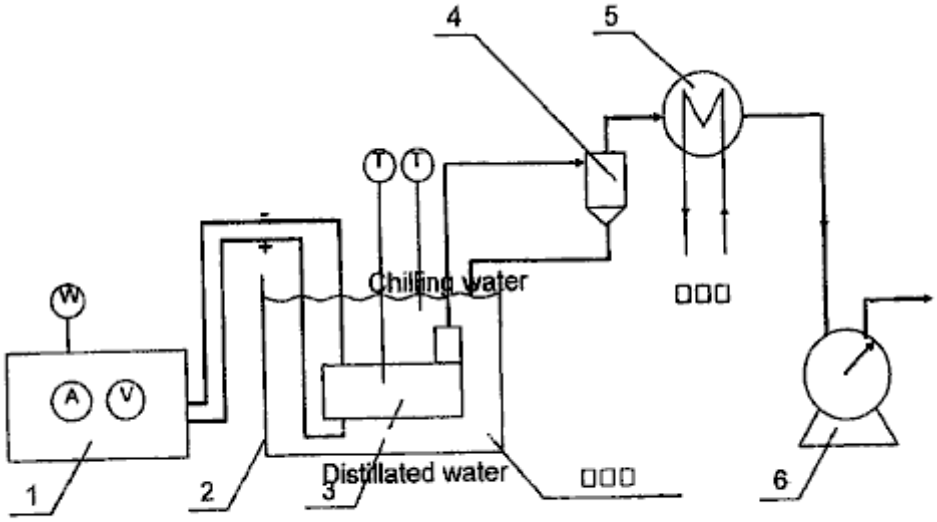

FIG. 28

The apparatus comprises broadly, a DC power source **1**, liquid bath **2**, reactor **3**, gas and liquid separator **4**, water chiller **5**, and gas-volume measuring meter **6**. Gas was produced by electrolysis which was catalysed by the plasma. Hydrogen gas was produced at the cathode and oxygen gas at the anode.

1.3.2 Equipment Function:

DC power source: provides high voltage DC.
Horizontal reactor: generation of non-thermal under-liquid plasma.
Gas and liquid separator: to separate liquid from gas and return as chilled liquid.
Chiller: to condense any liquid vapour admixed in the gas and return to reactor.
Gas-volume measuring meter: to measure the volume of gas flow.

1.4 Method and Operation of the Experiments

(1) The experiment is conducted in according to the occurrence of plasma discharge. Six different levels of voltage are selected to produce under-liquid plasma with same reactor for the generation of hydrogen. They are: 1350 V, 1450 V, 1550 V, 1650 V, 1750 V, and 1850 V. Each experiment lasts 30 minutes and the experiment is repeated three times under the same set of conditions. The data obtained are than averaged out.

1.5 Experimental Observations

Plasma discharge at 1,350 V is observed to have few and limited lighting illumination on the electrode in comparing with those vigorous, steady discharging over a much larger electrode surface at voltage 1,850 V. The corresponding current input is also very much reduced. It has been recorded that the temperature at the cathode electrode rises with time until it reaches about $90^{O}C$ and gradually becomes steady. The colour of the plasma discharge appears to be orange and red and it's colour is greatly different from that of electric arc (plasma arc discharge) which appears to be sharp bright blue in colour.

Applicant also conducted experiments with the same equipment utilising the under-liquid plasma to transform methanol for use in hydrogen production. Applicant found that the plasma was efficacious in producing hydrogen gas from the methanol. CO and CO_2 gases were completely absent from the gas produced. This was unexpected. Without being bound thereby, Applicant believes that CO and CO_2 may have been absorbed by KOH which was added as a conductive agent to the electrolyte. Some oxygen gases were recorded before methanol was added to the electrolyte.

Applicant also conducted experiments with the same equipment utilising the under-liquid plasma to reform hydrocarbons for hydrogen production. Applicant found that the plasma was efficacious in reforming the hydrocarbons and producing amongst other things hydrogen gas.

Applicant also conducted experiments with the same equipment utilising the under-liquid plasma to treat diesel oil. The diesel oil was emulsified in water to disperse it through the body of liquid. After being subjected to plasma conditions near the cathode, a gas was produced that was smoky and resembled an exhaust gas emission that did not easily burn. Applicant established by means of these experiments that diesel oil could be reformed and also dissociated by the in liquid plasma with this equipment.

Reformation of hydrocarbon liquid and gas fuel, and hydrogen rich compounds for hydrogen production:

Water is one of the primary source materials, which serves as carrier, conductor and confinement to the bubbles space where plasma corona and glow discharge would take place when adequate electro-potentials apply across single, or multiple electrodes pairs. The hydrocarbon fuel methane (gas), methanol, diesel, gasoline, kerosene (paraffin), ethane, natural gas, LPG gas, bio-diesel etc. and hydrogen sulphur (H_2S) are also good source material for hydrogen production.

The majority world-wide of hydrogen production conventionally is by high-pressure steam reformation of methane. This requires high pressure and high temperature. The production plant is large and costly to set up. Storage and delivery in association with the production are an added cost for the supply of hydrogen gas. The importance of hydrogen as an alternative environmentally clean fuel is well understood. The upcoming fuel cell technology demands an economic and ready supply of pure hydrogen gas. To produce hydrogen with a small processor to enrich fuels for combustion engines and gas turbines will not only be reducing fuel consumption but it also reduces polluting emissions.

The proposed plasma reformation process can deal with both gaseous fuel and liquid fuel. The gas fuel will be bubbled into the reactor along with an inhibitor to slow down the upward flow of the fuel gas. Since the dissociation of the hydrocarbon fuel will be mainly achieved by plasma dissociation which is similar to the plasma-assisted electrolysis process, but with electrolytic liquid containing hydrogen rich compounds. In the case of liquid fuel, it can either form a mixture with water or be emulsified with water. The percentage of fuel in the mix depends on the type of fuel, its conductivity, boiling point, flammability and electrochemical reaction. The reformation is mainly due to partial oxidation either with the active OH^-, O^-, O_2, O_3 created by the plasma dissociation. At the same time, the hydrogen-rich compound such as CH_4 or CH_3OH will be dissociated directly with electron

collisions. Since carbon dioxide is a major by-product together with some other minor gases coming out from the impurity of the fuel, they will be separated by the conventional absorption method or the membrane separation method.

Transformation of hydrocarbon fuel by corona and glow plasma has been attempted by passing the hydrocarbon gas such as methane, natural gas, LPG and vaporised liquid fuel sometime mixed with water vapours through the plasma reactor. They have all been successful in producing hydrogen-rich gas through corona discharge at atmospheric pressure by subjecting methane, vaporised methanol, diesel fuel mixed with water vapour, by passing it through a plasma gild arc reactor, wire in tube reactor and reactor proposed by MIT plasmatron or other gas phase corona streamer reactor.

The proposed under-liquid plasma reactor has many advantage over the gas-phase plasma reactor as it is able to generate a steady plasma-glow discharge at a very much lower voltage, i.e. from 350 V to (rarely) 1,800 V with current in the range of 100 mA to 800 mA in water. The liquid medium will also permit the application of ultrasonic waves producing an effect which will enhance the generation of glow plasma and thereby increase the overall transformation process. Again, no external air or gas is need be introduced for the reaction. However, the hydrocarbon gas such as methane, natural, LPG or hydrogen sulphurs gas can be introduced to work in conjunction, and complementing the liquid fuel in the reformation process. The fuel gases will enhance plasma-discharge reformation and allow it to take place without having to rely on gas produced by electrolysis.

Those hydrocarbon fuel molecules which come in contact with the plasma-discharge, will be subjected to dissociation and partial oxidation depicted in the following:

$H_2O + e \rightarrow +OH + H^+ + e$ dissociation
$CH_4 + e \rightarrow CH_3 + H^+ + e$ direct plasma dissociation
$CH_4 + H \rightarrow CH_3 + H_2$ reacting with H radicals
$CH_4 + H_2O \rightarrow CO + 3H_2$ partial oxidation
$CO + H_2O \rightarrow CO_2 + H_2$ water shifting
$CH_3OH + H_2O \rightarrow CO_2 + 3H_2$ electrolysis and partial oxidation
$H_2S \rightarrow S + 2H$ without experiencing oxidation
$H_2S + 2H_2O \rightarrow SO_2 + 3H_2$ partial oxidation
$SO_2 + 2H_2O \rightarrow H_2SO_4 + H_2$

Endothermic catalytic conversion of light hydro-carbon (methane to gasoline):

$CnHm + nH_2O \rightarrow nCO + (n + m/2)H_2$

With heavy hydro-carbon:

$CH1{,}4 + 0{,}3H_2O + 0{,}4O_2 \rightarrow 0{,}9CO + 0{,}1CO_2 + H_2$
$C_8H_{18} + H_2O + 9/2O_2 \rightarrow 6CO + 2CO_2 + 10H_2$

The hydrogen gas and carbon dioxide are collected. The CO_2 is separated by establish absorption or the membrane separation method.

The OH radical produced by the plasma dissociation will play an important role in oxidising the CH_4 to produce CO which would further be oxidised to become CO_2. The same applied to methanol CH_3OH and H_2S. The S is being oxidised to form SO_2 and further oxidising to become SO_3 and subsequently reacting with H_2O to produce H_2SO_4. This type of chemical reaction will be possible only with the encouragement of the highly chemical reactive and plasma catalytic environment. Not every CO will become CO_2 and sulphur particles may be observed in the precipitation.

REACTOR

There are number of reactors which can be used for the reformation of hydrogen-rich compounds. Reactors such as the wire in tube, tube in tube; single cell and multiple cell reactors; and the multi-electrodes without diaphragm separation. The tube in tube reactor and tower reactor with horizontal electrodes are suitable for treating both liquid and gas hydrocarbons and both at the same time. The anode and cathode are closely spaced with a gap distance ranging from 6 mm to 12 mm and are covered with dielectric gas-retaining and current-concentrating

construction on one side or both sides of the electrode. One important aspect of the reactor is having the construction, which will accommodate the ultrasonic transducer, which would induce proper sonic cavitations uniformly distributed throughout the reacting volume. The size, shape and arrangement of the electrodes can vary but its size would be restricted by the electric power available. A small reactor electrode plate is quite adequate for good uniform discharge and high productivity. The size of reactor plate use in most of the experiments is in the range of 16 cm^2 to 30 cm^2. It is preferable that the non-discharging electrode has an electrode area larger than the discharging electrode with the dielectric gas-retaining construction. With sufficient power available, both the anode and the cathode electrode can be functioning as plasma discharging electrodes at the same time. This is particularly useful in the partial oxidation process.

In the case of an emulsified oil/water mixture, it is best maintained with ultrasonic excitation which at the same time generates transient micro bubbles which enhance the whole reactive process. Hydrocarbon gas may also introduce to the reactor to form air bubbles or trapped gas pockets for the ready formation of the plasma glow discharge. Since the oily hydrocarbon fuel is highly dielectric this would require a higher concentration of conducting reagent than that required for the plasma-assisted water electrolysis, in order to maintain a suitable level of current density for the discharge to occur.

Reformation of methane gas by the under-liquid non-thermal plasma is by bubbling the gas through the perforated horizontal electrodes of tower a reactor or a tube-in-tube reactor. Since the methane gas is to be oxidised by the plasma dissociated water molecule (OH- + H+) to form carbon monoxide and hydrogen gas ($CH_4 + H_2O \rightarrow CO + 3H_2$). The CO will be further oxidised to form CO_2 with oxygen derived from the plasma dissociated water molecule, releasing two more hydrogen atoms (H_2). The resultant gas is either H_2 or CO_2 with perhaps small amount of CO. The hydrogen gas will be collected with reasonable purity after the CO_2 or CO is removed by absorption or membrane separation. Since the methane gas may not thoroughly reform with one past through the reactor, it is important to regulate the gas flow rate to ensure suitable resident time for the reformation or to have the methane gas recovered by the next round of reformation or to have the gas going through a series of reactors to made sure that the methane gas is fully utilised. The later case may not be energy efficient.

Reformation of methanol for hydrogen production can be achieved in the first place, by ordinary electrolysis or by partial oxidation. When CH_3OH is subjected to plasma discharge irradiation, it will react with the oxidising species and radicals dissociated from the water molecules. Conventional electrolysis will also contribute to the overall production of hydrogen gas. Reformation of methanol/water mixture will achieve better efficiency when plasma discharges is used in conjunction with ultrasonic excitation and cavitation. Several types of reactor can be adopted for the methanol reformation such as a tower reactor with horizontal electrodes, a tube-in-tube reactor, a transverse flow reactor, etc. These types of reactor offer very active oxidising species and hydroxyl radicals needed in the reformation.

Reformation of heavy oil such as diesel by under-liquid plasma discharge will be with emulsified liquid. The best way to maintain a thorough emulsification of diesel fuel and water is by ultrasonic excitation. Micro droplets of diesel will be encapsulated in the water. It is again observed that the conductivity of the emulsified liquid is very low as diesel oil is dielectric and current can only be conducted through the water film inbetween. This has rendered the need of more electrolytes added, especially as the diesel content increases. Bubbles are not easily produced by electrolysis due to its low current flow. It is therefore an advantage to either introduce gas to the reactor from outside or to produce ultrasonic cavitations in the liquid at the same time as the emulsification of the water/oil mixture. The tower reactor, tube-in-tube reactor and the transverse-flow reactor are all suitable for heavy hydrocarbon fuel reformation provided that an adequate ultrasonic transducer is properly located to ensure effective excitation and cavitations distributed throughout the liquid volume. A pulsed power supply will enhance the plasma generation and electrode heating will assist the generation of bubbles at the discharging electrode.

REDUCTION OF METAL AND MINERAL OXIDE PROCESS

Mineral refinment is an expensive and polluting process. To remove oxygen from the oxide, is either by reacting with higher electro-positive elements, which is uneconomic, or by exposing the metal oxide to C, CO, and hydrogen inside a high-temperature furnace such as the case in iron production. The electrolysis of a molten melt of Al_2O_3 or TiO_2 to extract pure metals Al or Ti respectively, consumes a large quantity of electricity, and requires the use of expensive refractory and electrode materials along with polluting emissions, render these two useful metals very expensive and inhibit their common application.

An under-liquid plasma reductive process to reduce oxide of ore or metals is proposed. The plasma discharge irradiation of the metal oxides in a highly catalytic environment, will cause interaction with the active hydrogen atoms produced by the plasma dissociation of water or methane or a methanol/water mix and introduced hydrogen gas together with the assistance of ultrasonic excitation would be sufficient in many instances to dislodge the most stubborn oxide.

It is reported that research is underway to extract Al from Al_2O_3 by electrolysis. Aluminium is electrode wired to cathode from porous Alumina anode electrode. The reduction of TiO_2 and Al_2O_3 by hydrogen plasma discharge is also being actively researched elsewhere with the aim of economically refining these two useful metals. A tube-in-tube reactor, or a wire-in-tube reactor can be used for this reduction process. These two reactors can be easily modified for continuous processing of either the granular form of the mineral or the metal oxide. The metal oxide will be exposed to the influence of highly active hydrogen atoms and subsequently the oxygen in the metal will be removed. This would not be a problem for those electro-positive elements but would present some difficulty for oxides such as Al and Ti.

The oxygen is strongly bonded with the parent metals such as Al_2O_3 and TiO_2 which cannot be reduced easily. This rudimentary horizontal reactor serves to demonstrate that metal oxide can be refined by exposing it in granular form to plasma discharge irradiation, ultrasonic excitation and in a highly reactive environment containing active hydrogen atoms. Additional hydrogen can be derived from the plasma dissociation of methane gas introduced to the reaction chamber where CO and atomic H are produced. Similarly by plasma dissociation of the methane water mixture that active hydrogen and CO_2 are also produced to supplement the reductive atomic hydrogen. Hydrogen gas can also bubble into the reactor and any excess will be collected and passed back to the reactor.

Reduction of Al_2O_3, TiO_2, TiF_3, TiO, $AlCl_3$ will be taking place in the following manner, where:

$TiO_2 + 4H(2H_2) \rightarrow Ti + 2H_2O$
$Al_2O3 + 6H(3H_2) \rightarrow Al + 3H_2O$
$TiF_3 + 3H(3/2H_2) \rightarrow Ti + 3HF$

The alternative is to have:

$TiO_2 + H_2SO_4 \rightarrow TiOSO4 + H_2O$
$TiOSO_4 + 2H \rightarrow TiO + H_2SO_4$
or $TiO + 2H \rightarrow Ti + H_2O$
and
$TiO_2 + 4HCL \rightarrow TiCl4 + 2H2O$
$TiCl_4 + 4H \rightarrow Ti + 4HCl$
where $TiCl_4$ is ionic and is soluble in water

The above reaction is under the influence of a non-thermal plasma so that the oxide of ores or metal is subjected to a highly catalytic environment and comes into contact with the reactive atomic hydrogen whereby the oxygen will be taken out. To enhance the matter further, the whole reaction process is also subjected to sonic excitation. The fine particles in the colloidal suspension of the granular oxide will collide with each other and at the point of impact, the temperature will rise over 1,500^{O}C to 3,000^{O}C and local melting is reported. The high temperature and pressure of a collapsing sonic bubble will work in conjunction with the plasma glow discharge irradiating the oxide particles with atomic hydrogen with localised high temperature due to collision and cavitations implosion which in the end remove the oxygen. The refined metals will be in powder form down to nano size.

The other method of extracting and refining metals from their oxides is to subject the ionic solution of the metal such as $AlCl_3$ to an electrolysis process which is reported to have achieved efficiency of 3 KWh/Kg of Al. The whole process can be further improved with the plasma electroplating technique with the proposed under-liquid glow plasma discharge. The Al will be deposited on the cathode electrode. Part of the chlorine gas will come out from the anode side and will react with the active hydrogen to form Hcl.

The fine granular metal oxide is placed inside a horizontal reactor on top of cathode electrode. A close matrix separator membrane, used to prevent the metal oxide from crossing over, placed above and below the anode electrode is used to separate it from the cathode. The whole reactor is submerged inside an ultrasonic bath. Ultrasonic waves will penetrate the membrane separator to cause the granular metal oxide in colloidal suspension. The oxide will be subjected to the under-liquid plasma glow discharge irradiation and atomic hydrogen reduction. The percentage of metal oxide being reduced after a period of time is evaluated. Metal oxide of TiO_2 will be put to test. A methane/water mixture will be employed as the liquid medium which will produce larger amount of active atomic hydrogen serving as reduction agents.

DECONTAMINATION OF LIQUID

The problem of pollution is a major issue affecting every living being on this planet. A lot of effort has been expended by Governments, universities and private enterprises, seeking a comprehensive process to deal with a vast variety of pollution issues. Polluting gas emissions from industries and motor vehicles produce large quantities of CO_2 causing global warming; NOx, VOC, and particulates causes cancer and smog; SO_2 causes acid rain. Decontamination of the gases discharged from industries is costly to achieve and what is urgently needed is a comprehensive and economical treatment process to reduce the overall trestment cost. Water contamination is another major issue. Contaminated water unfit for human consumption, enters the sea and kills marine life near the shore. Governments worldwide are passing stringent laws setting a pollution standard, which demands the development of efficient and economic ways to control pollutants. The present proposed invention is put forward as a versatile process, which can treat a variety of contaminants either separately or together.

Corona discharge and glow plasma discharge as non-equilibrium plasma has been developed for applications in the decontamination of a wide range of noxious chemical compounds and recalcitrant chlorinated organic compounds such as dichloro-ethane, pentachlorophenol, perchloroethylene, chlorom, carbon tectrachloride, organochlorine presiticides, endocrine disrupter, dioxin etc. It is also capable of sterilising tough microbial, bacteria and biological contaminants present in ground water such as cryptosporidia parvum. Noxious gas emissions such as NOx and SOx can also be neutralised by passing them through the wet reactor, which includes the removal of particulates as well as the pollution emissions. This is mainly due to the ability of plasma to create a very reactive catalytic environment for those normally very stable and inactive compounds to be reduced, oxidised or neutralised by reacting with the OH* radicals, atomic hydrogen H+ and other oxidative species such as O^-, O_2, O_3, H_2O_2 etc. present and is reported to have high efficiency especially in dealing with diluted contaminants.

Microbial bacteria is removed by both oxidations when they come in contact with the oxidative species such as O_3, O_2^-, O^-, H_2O_2, and OH*. At the same time, they are subjected to the electromechanical stretching of the cell wall, which weakens its oxidative resistance, especially when ultrasonic cavitations, implosions and shock waves created by pulse power, are incorporated into the reactive process. Again reports of over 99% sterilisation are not uncommon.

At the present, most of the treatment work is conducted in a gaseous environment, by spraying or vaporising the contaminated liquid over the plasma discharging electrodes, or by producing plasma discharge irradiating over the surface of a liquid which contains the undesirable contaminants, or by passing the polluted gas through a dry reactor sometimes mixed with water vapour or using plasma torch irradiation of the polluted object.

A surface water contact plasma glow discharge system has also been developed as a decontamination process under the name “Plasmate”. Under water plasma by pulsed high voltage electric discharge with high current input to dissociate the water to produce H and OH* radicals to treat bacterial and microbial decontamination has also been reported as being successful.

The proposed under-liquid plasma is a low energy consumption system, which produces steady plasma by utilising the present of bubbles. The voltage required for dealing with a wide range of liquids having variable electrolytic properties, ranges from 350 V to 3,000 V and current intensity ranging from 1 to 2 Amp/cm^2. It produces a highly reactive environment with a supply of oxidative radicals and reductive atomic hydrogen spread over a large volume of liquid, making it highly effective as a decontaminatinf process, and one which is also both economic and easy to operate.

The under-liquid plasma has the advantage of being able to decontaminate several pollutants at the same time and it also has a very active gas and liquid interaction which makes it highly effective as a treatment process. Liquid waste, containing harmful chemical, bacteria, microbial, heavy metals, noxious gas, polluted air and odour can be treated in the same reactor simultaneously.

Recalcitrant organic chlorinated materials in water, which include dichloromethane, pentachlorophenol, chloroform and carbon tetrachloride, will either be oxidised or degraded to CO_2 and chlorine. While the pathogens in drinking water such as cryptosporidia with thick phospholipids wall protecting the trophs is in the first place being stretched and weakened and subsequently broken down by the oxidising species. Some of the oxidative species such as OH radicals, O^-, O_2^-, and O_3 are present in quantity and are more active than chlorine and other mild oxidants. It has the advantage that no chemical is needed as an oxidation agent, which can sometimes result in secondary pollution.

Heavy metals in dilute solution, can be extracted or removed through a simple electrolysis process by turning the metal to hydroxide which could than be removed by filter. Soluble metal ions can also be extracted by deposition on to the cathode electrode, which can be further facilitated by the plasma electroplating process owned by the inventor, and which uses the same under-liquid bubble plasma process.

The treatment of NO, SO_2 and particulates is to pass the polluted gas through the reactor where the particulate will be removed and the NO is either oxidised to become NO_2 or NO_3 by O^-, or O_3. It can also be reduced to N by the active hydrogen. NO_3 will react with water to become nitric acid. NO_2 is not considered to be a noxious gas. SO_2 reacting with O_3 or oxygen radical to form SO_3 can be easily oxidised and then react with water to become H_2SO_4 (sulpheric acid). When the said gas is introduced to the reactor it can be utilised as a gas bubble for plasma discharge especially when this gas bubble is collected or retained near the electrodes.

The effectiveness of non-thermal plasma discharge in treating carcinogenic organic compounds and pollutant gases is well established. Removal or reduction of the amount of heavy metals, arsenic and mercury to an acceptable safe low concentration level from or in water, have been successfully carried out by a simple electrolysis process. The extraction efficiency is further improved by the presence of an under-liquid plasma discharge where some of them will readily react with the OH radicals to become metal hydroxide or to be deposited by the very active plasma electroplating (deposition) method which has been adequately proven as a useful technique.

Further experiments in this area are unnecessary. Adequate information can be drawn upon from much research work which already been carried out. Concentrated effort has already been used to search for a better way of generating steady plasma glow discharge under-liquid by utilising the bubbles which will enable the manufacturing of a simple and economic reactor which requires only low power input and wich will work well in treating a wide scope of contaminants.

Sterilisation of drinking water at municipal scale can be simplified by adopting the under-liquid plasma discharge which will effectively neutralise and degrade carcinogen organic compounds in the water by creating the dissociation and active catalytic environment which encourages the breakdown of the inert chemicals and at the same time subject it to the active reductive and oxidative radicals. The heavy metals dissolved in the water will also be removed or reduced in the same time through the plasma electrolysis and electroplating as described previously. The biological contaminants will be sterilised by the highly oxidative environment existing during the glow discharge. The effectiveness of the combined treatment to produce potable water fit for human consumption is further enhanced by the adoption of ultrasonic cavitation and shock waves with a pulsed power supply.

The entire sterilisation process does not require any added chemicals such as ozone, chlorine or any electrolytic additive. The impurity in the pre-treated liquid will be adequate to serve as conductor for the under-water plasma discharge to take place. Any excessive ozone, which has not been used up in the oxidation process during the plasma discharge, will be easily neutralised by the presence of active hydrogen atoms. Hydroxyl radicals (OH) are one of the most aggressive oxidising agents, which being produced in quantity will do most of the useful work. There will be no chlorine remnant left in the water, as it is unnecessary.

The under-liquid plasma technique will be useful in food industries for low temperature sterilisation and removal of odour. The same method may also find its use in the paper-making industry in fragmentation and de-lignification of the fluidised pulps, treating the highly polluted discharge, and treating fabrics and dyes in the textiles industry.

There are several types of reactors which can be employed in the decontamination process. The separation membrane diaphragm in the wire-in-tube and tube-in-tube reactor is no longer required. Other reactors such as the transverse-flow reactor and the tower reactor can also be adopted.

The reactor can be arrange in such way that the plasma discharge occurs either at the cathode or at the anode provided that a good gas-trapping cover is provided on the electrode. Since much of the decontamination action relies on the presence of strong oxidation agents such as hydroxyl radicals, atomic oxygen, ozone, singlet oxygen and hydroperoxyl radicals, plasma discharge on the side of anode electrode enhanced with the gas retaining cover will cause the formation of said species represented by the following equations:

$H_2O + e \rightarrow +OH + H + e$	dissociation
$H_2O + e \rightarrow + H_2O_+ + 2e$	ionisation
$H_2O_+ + H_2O \rightarrow H_3O_+ + OH$	dissociation
$O_2 + e \rightarrow O_2^* + e$	excitation
$O_2 + e \rightarrow +2O + e$	dissociation
$O_2 + e \rightarrow O^- + O$	dissociation
$O_2 + O \rightarrow O_3$	association
$OH + OH \rightarrow H_2 O_2$	association

Some chemical contaminants can only be broken down by reduction with active atomic hydrogen, which would require plasma discharge at the cathode electrode. In the tower reactor (**Fig.7**) and transverse-flow reactor (**Fig.6**) it is possible to have the gas-retaining cover on one side of electrode facing the side of the opposite electrode with the gas-retaining covers, so that an alternating zone of oxidation and reduction is created in the reactors to deal with a variety of contaminants.

Production of hydrogen by plasma dissociation of water molecules is the result of electron collisions, which is different from the conventional electrolysis, which separates the dipole water molecules by electro-induction. They also have different sets of requirements to dissociate water molecules for the production of hydrogen:

Conventional electrolysis	Plasma glow discharge under water, according to the present invention
1. Low voltage and high current density	High voltage and relatively low current density
2. High concentration of electrolyte (up to 25% KOH)	Low concentration electrolyte (0.01% KOH) low electrolytic requirement
3. Avoid bubble attachment to the electrodes	Bubbles smothering the electrodes is welcome to create a dielectric barrier.
4. Electrode space distance is not restricted.	Electrode space distance has to keep close as far as possible.
5. Water molecules is split by induction	Water molecules are dissociated by electron collision.
6. Large production unit is required for efficiency and productivity	Small production unit favours the decentralisation of production.

The reactors and gas-trapping and retaining structures enclosing the electrode is made of perspex plastic. No sign of burning is observed in the plastic covering plate directly over the discharging electrode and the light emission is an orange/red colour (burning of hydrogen) which is distinctively different from the plasma arc which is bright blue colour when the voltage is brought beyond the glow discharge voltage level. A burn mark will be observed after plasma arc discharge. This proves that the plasma glow discharge with it's orange yellow colour, is non-thermal in nature.

Applicant also conducted experiments with the same equipment utilising the under-liquid plasma to sterilise mulberry juice. Applicant found that the plasma was effective in reducing the bacterial count and the mold colony count in the juice. After 40 minutes the counts of both bacteria and mold had been reduced substantially to less than 100 per ml. This demonstrates that the invention could be used to sterilise potable water, waste water, food, and liquid food and others.

CONCLUSION

A further advantage of the method described above is that plasma can be generated with relative ease within bubbles in the aqueous medium. It does not require excessive amounts of energy and can be done at atmospheric pressure. It certainly does not require a vacuum chamber.

A further advantage of the invention is that it provides a method of treating aqueous waste which contains components that cannot be neutralised or otherwise rendered harmless by the addition of chemicals to the liquid.

It will of course be realised that the above has been given only by way of illustrative example of the invention and that all such modifications and variations thereto as would be apparent to persons skilled in the art are deemed to fall within the broad scope and ambit of the invention as herein set forth.

Figures which are included in the patent application but which are not directly referenced in it:

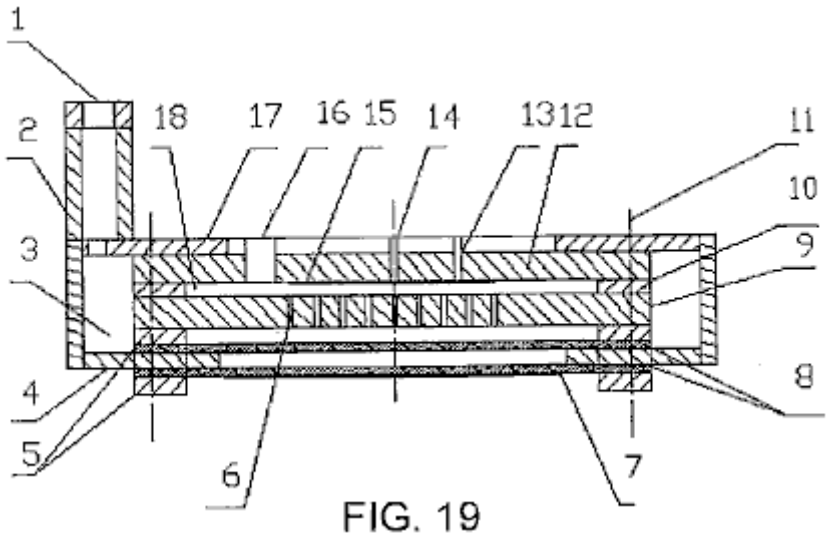

FIG. 19

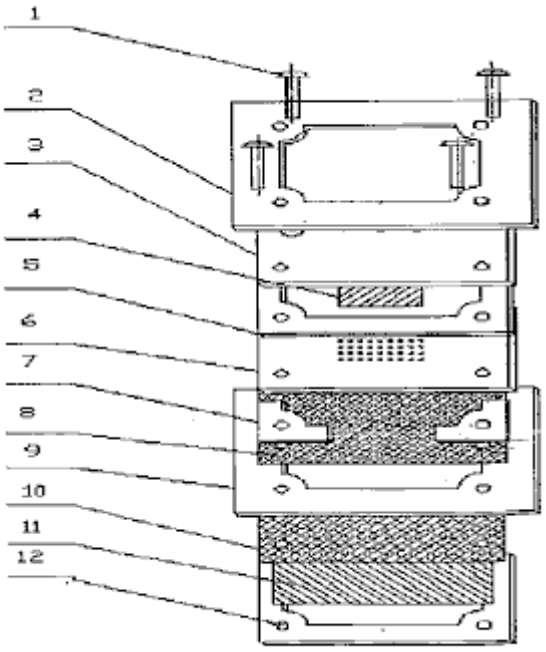

FIG. 20

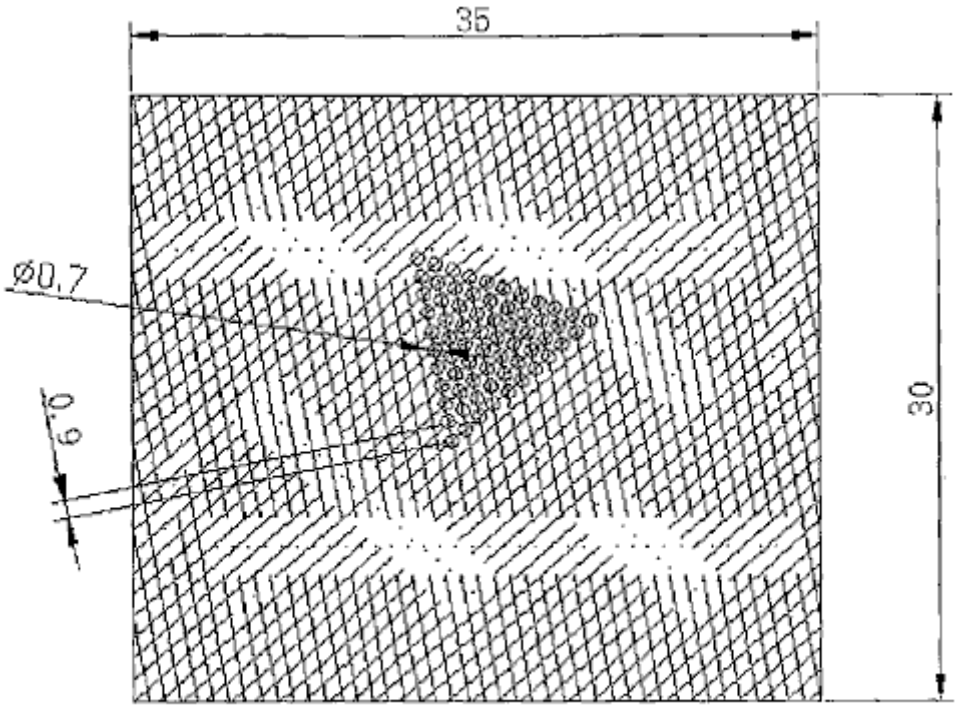

FIG. 21

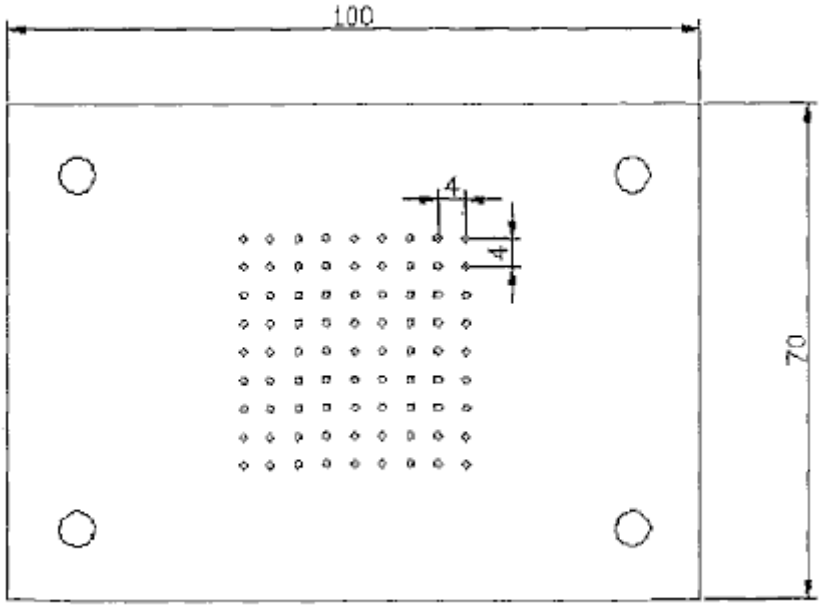

FIG. 22

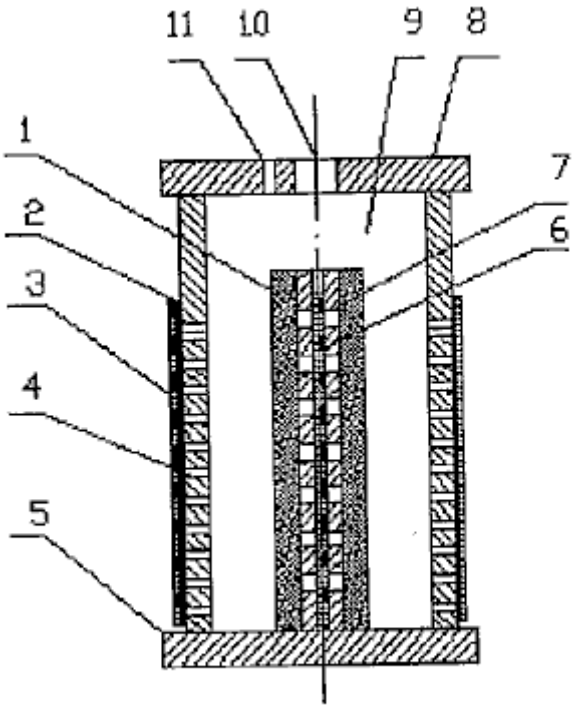

FIG. 23

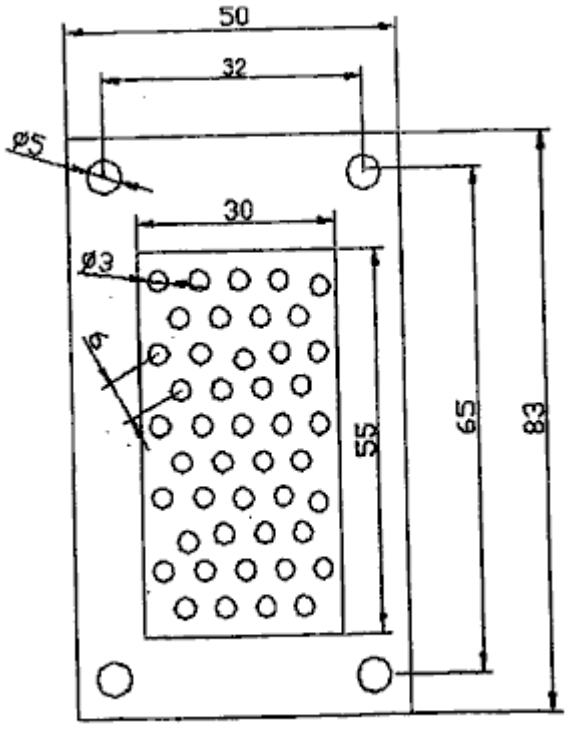

FIG. 24

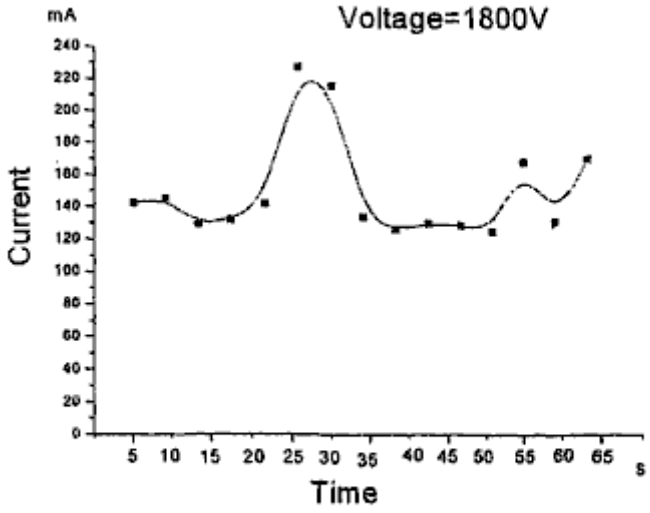

Glow discharge at stable 1800V voltage input

FIG. 26

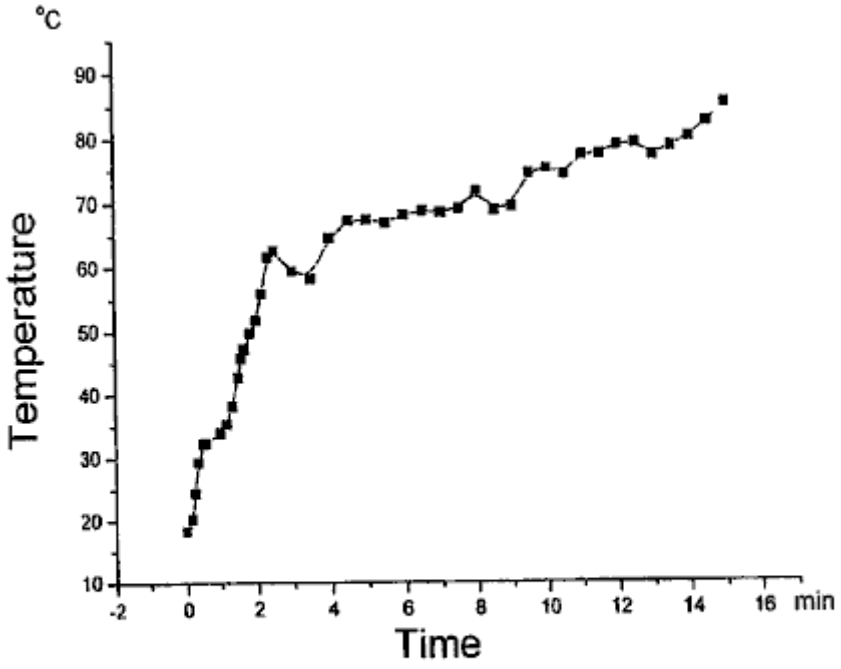

Temperature measured in the cathode electrodes

FIG. 27

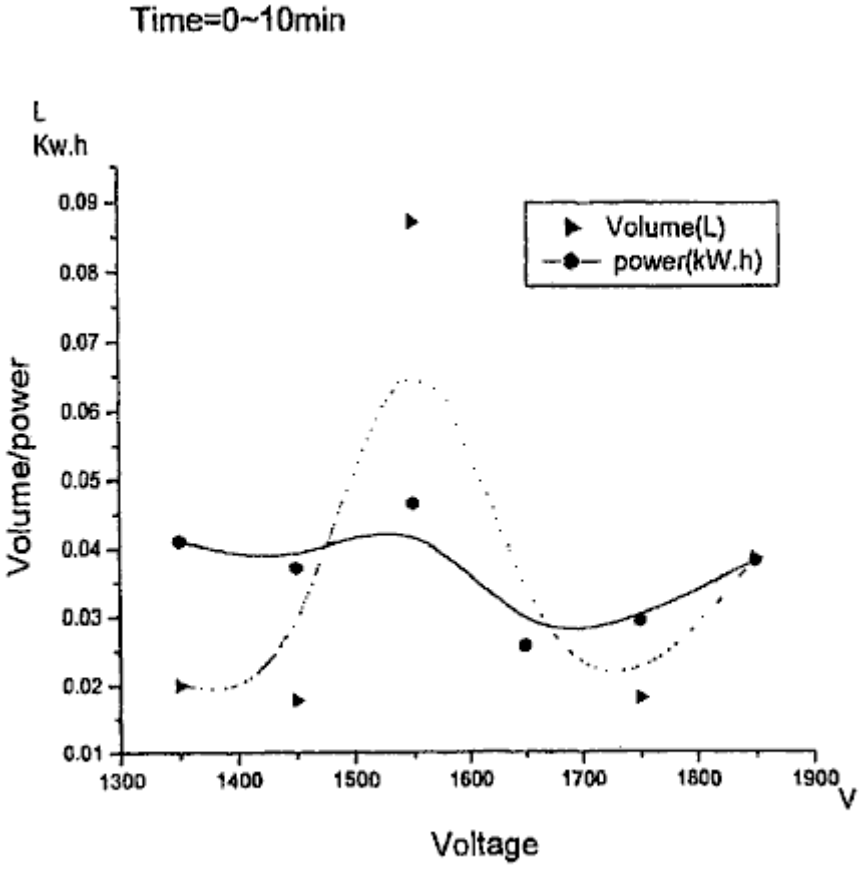
Time=0~10min
L
Kw.h
Volume(L)
power(kW.h)
Volume/power
0.09
0.08
0.07
0.06
0.05
0.04
0.03
0.02
0.01
1300
1400
1500
1600
1700
1800
1900
V
Voltage

FIG. 29

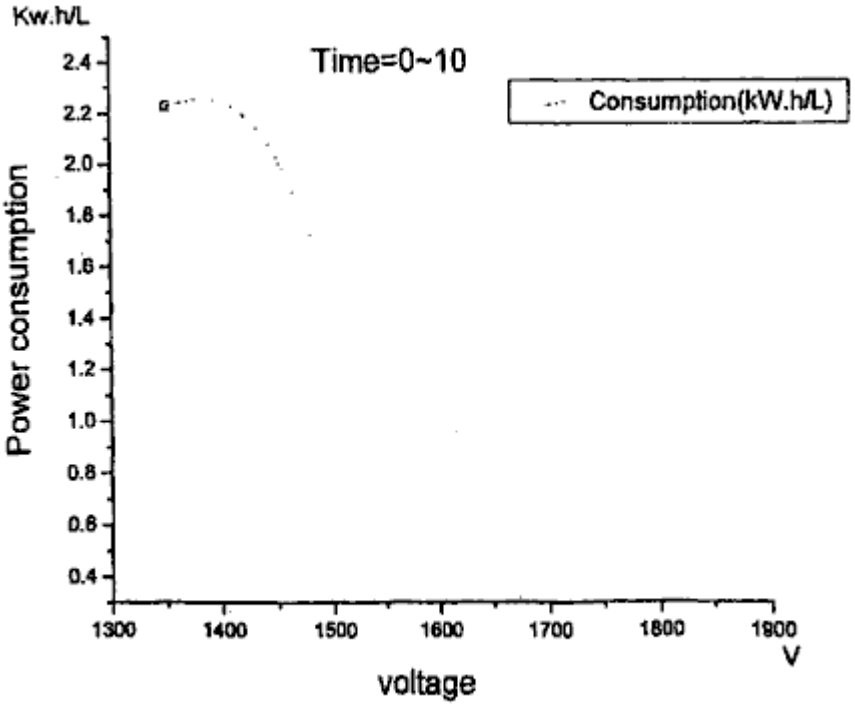
Kw.h/L
Time=0~10
Consumption(kW.h/L)
Power consumption
2.4
2.2
2.0
1.8
1.6
1.4
1.2
1.0
0.8
0.6
0.4
1300
1400
1500
1600
1700
1800
1900
V
voltage

FIG. 30

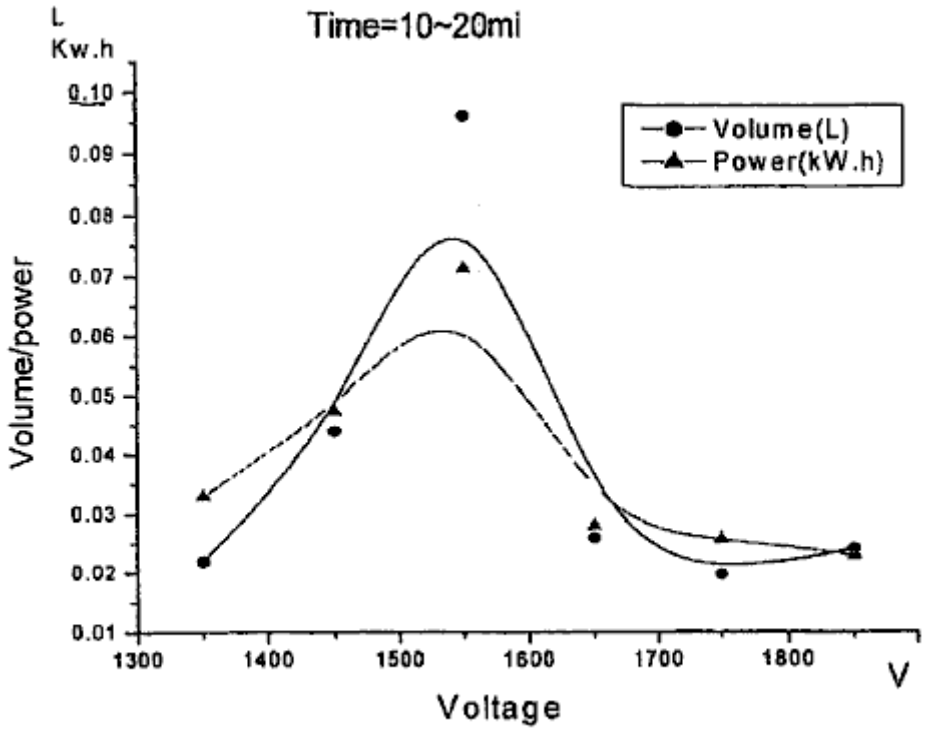
L
Kw.h
Time=10~20mi
Volume(L)
Power(kW.h)
Volume/power
0.10
0.09
0.08
0.07
0.06
0.05
0.04
0.03
0.02
0.01
1300
1400
1500
1600
1700
1800
V
Voltage

FIG. 31

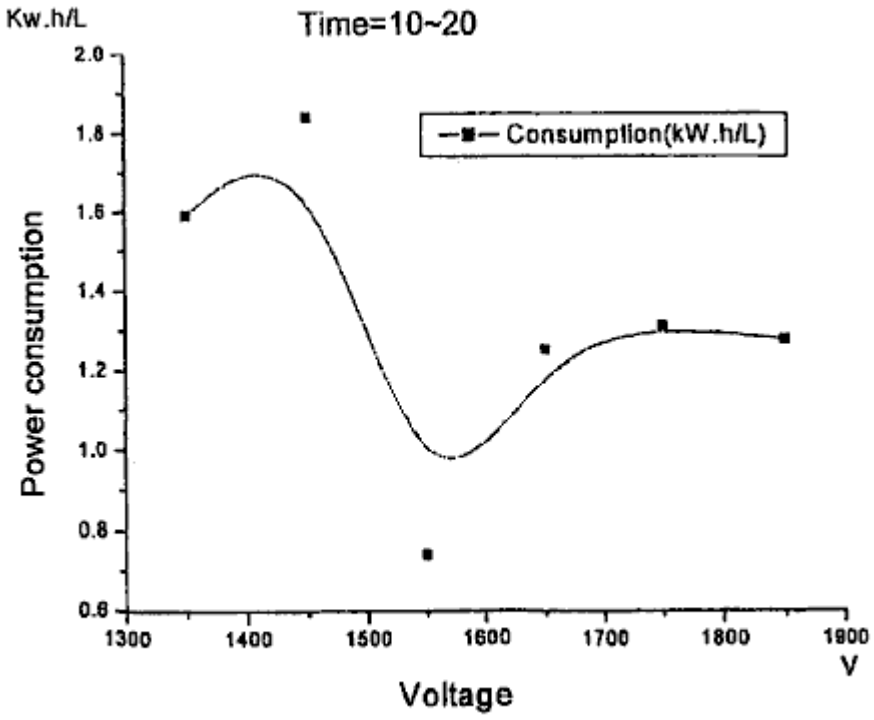
Kw.h/L
Time=10~20
Consumption(kW.h/L)
Power consumption
2.0
1.8
1.6
1.4
1.2
1.0
0.8
0.6
1300
1400
1500
1600
1700
1800
1900
V
Voltage

FIG. 32

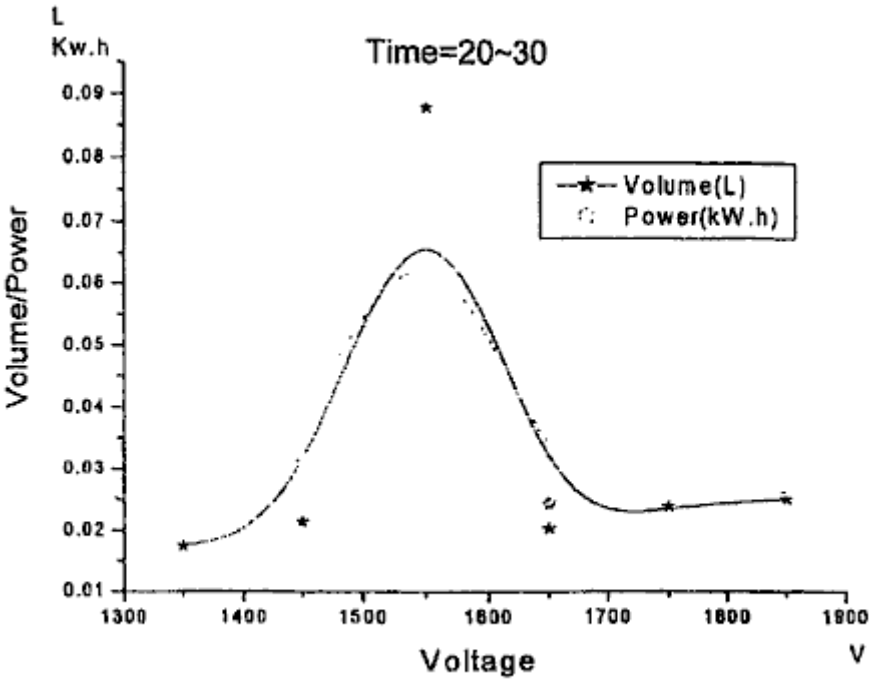
L
Kw.h
Time=20~30
Volume/Power
0.09
0.08
0.07
0.06
0.05
0.04
0.03
0.02
0.01
Volume(L)
Power(kW.h)
1300
1400
1500
1600
1700
1800
1900
Voltage
V

FIG. 33

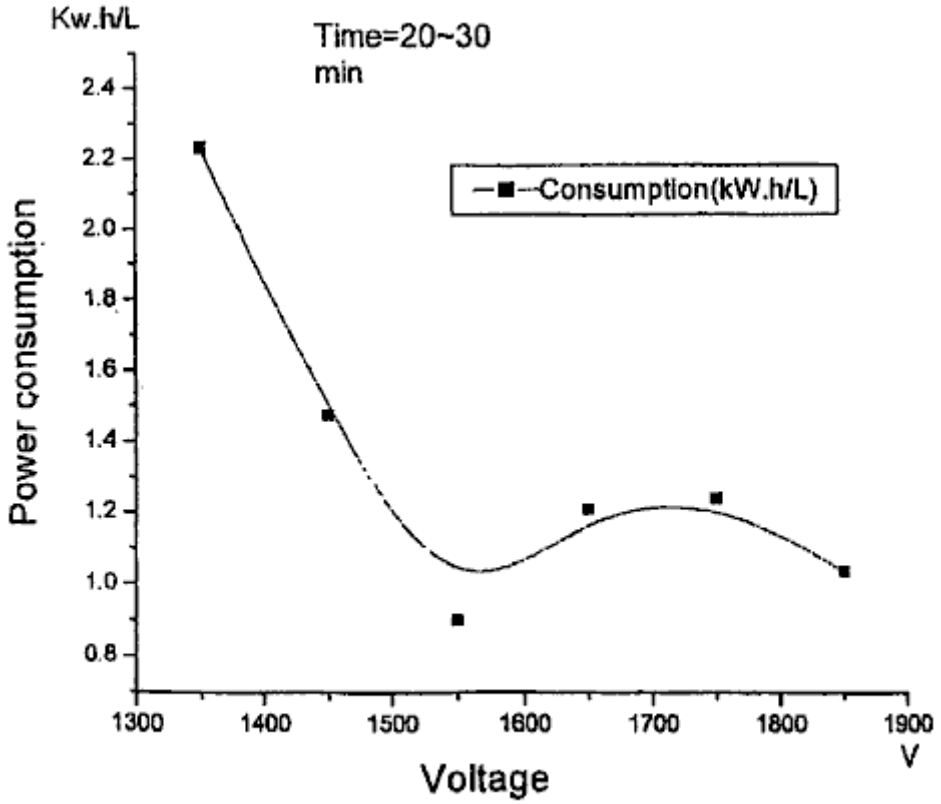
Kw.h/L
Time=20~30
min
Power consumption
2.4
2.2
2.0
1.8
1.6
1.4
1.2
1.0
0.8
Consumption(kW.h/L)
1300
1400
1500
1600
1700
1800
1900
V
Voltage

FIG. 34

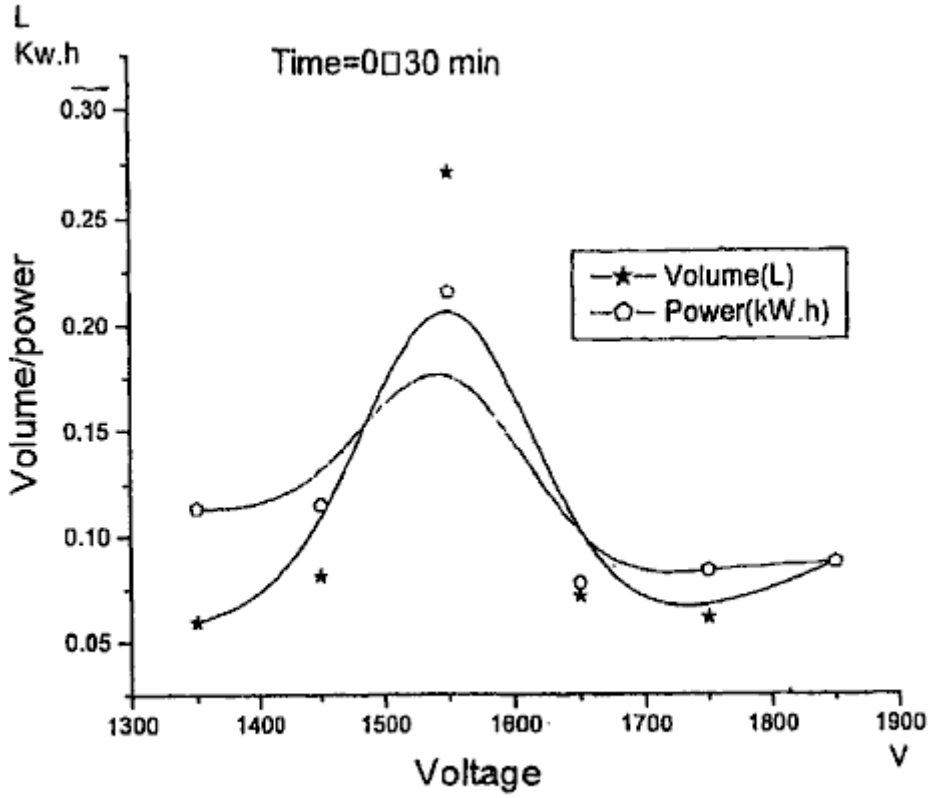
L
Kw.h
Time=0□30 min
Volume/power
0.30
0.25
0.20
0.15
0.10
0.05
Volume(L)
Power(kW.h)
1300
1400
1500
1600
1700
1800
1900
V
Voltage

FIG. 35

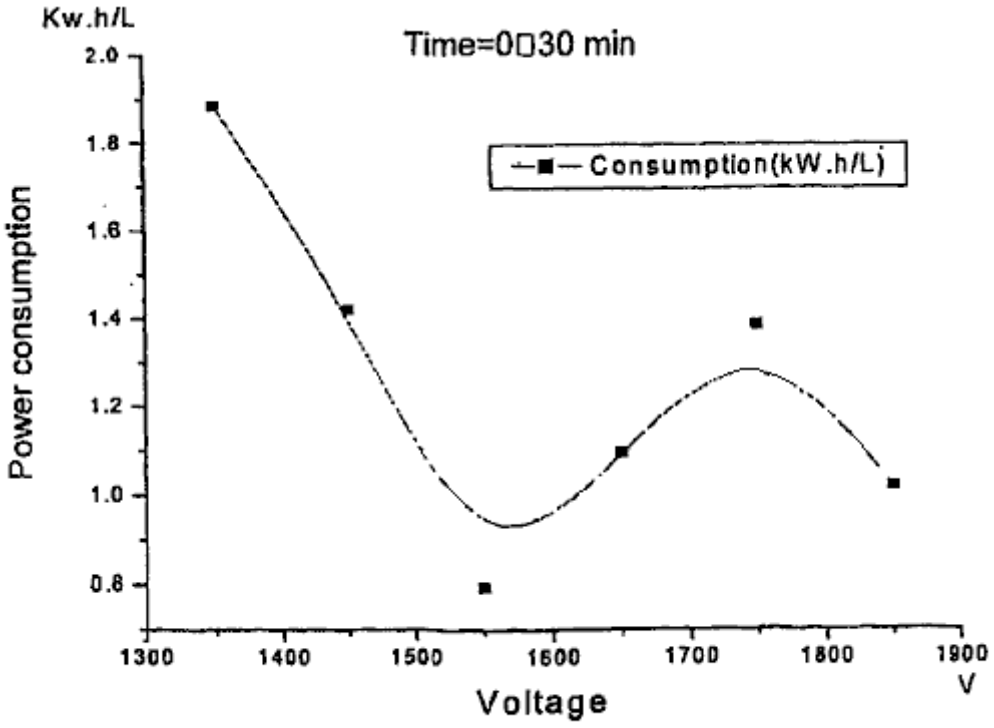
Kw.h/L
Time=0□30 min
Power consumption
2.0
1.8
1.6
1.4
1.2
1.0
0.8
Consumption(kW.h/L)
1300
1400
1500
1600
1700
1800
1900
V
Voltage

FIG. 36

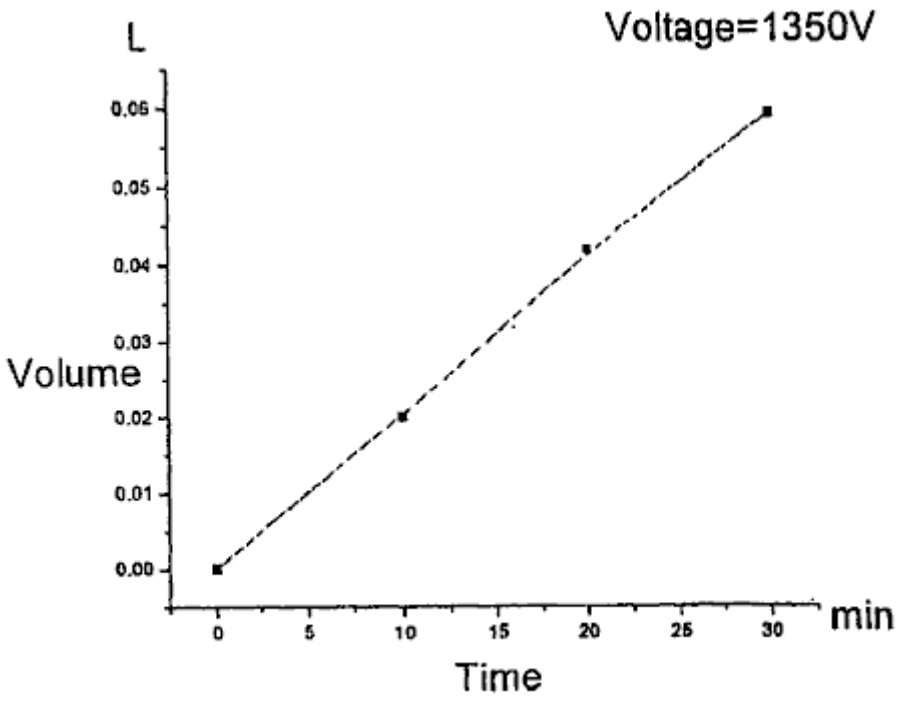
Voltage=1350V
L
0.06
0.05
0.04
0.03
Volume
0.02
0.01
0.00
0
5
10
15
20
25
30
min
Time

FIG. 37

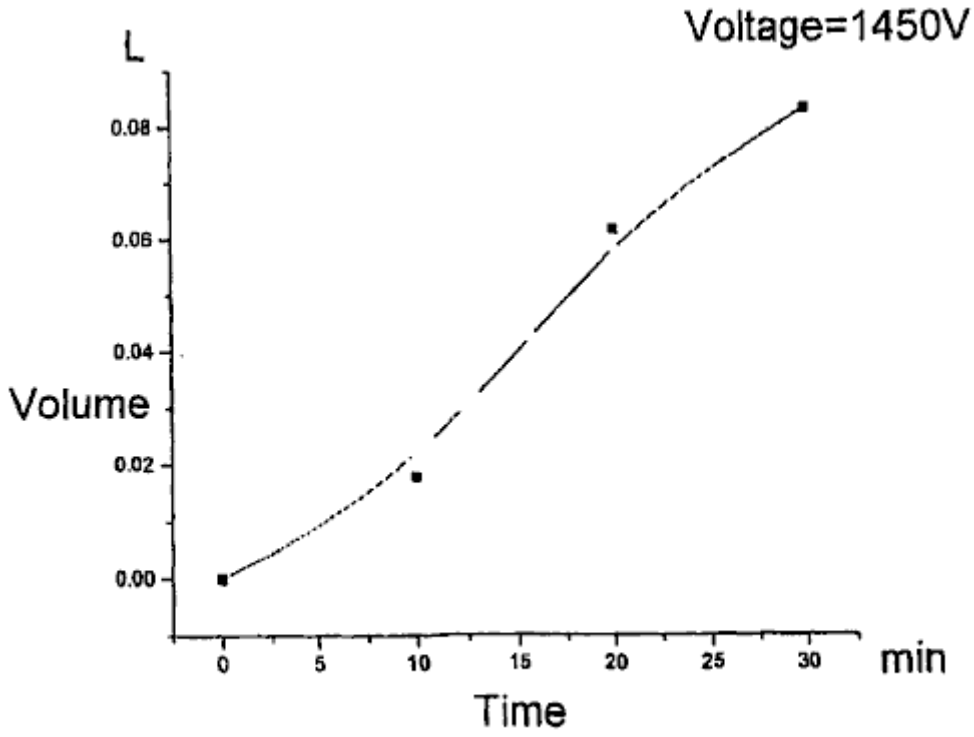
Voltage=1450V
L
0.08
0.06
0.04
Volume
0.02
0.00
0
5
10
15
20
25
30
min
Time

FIG. 38

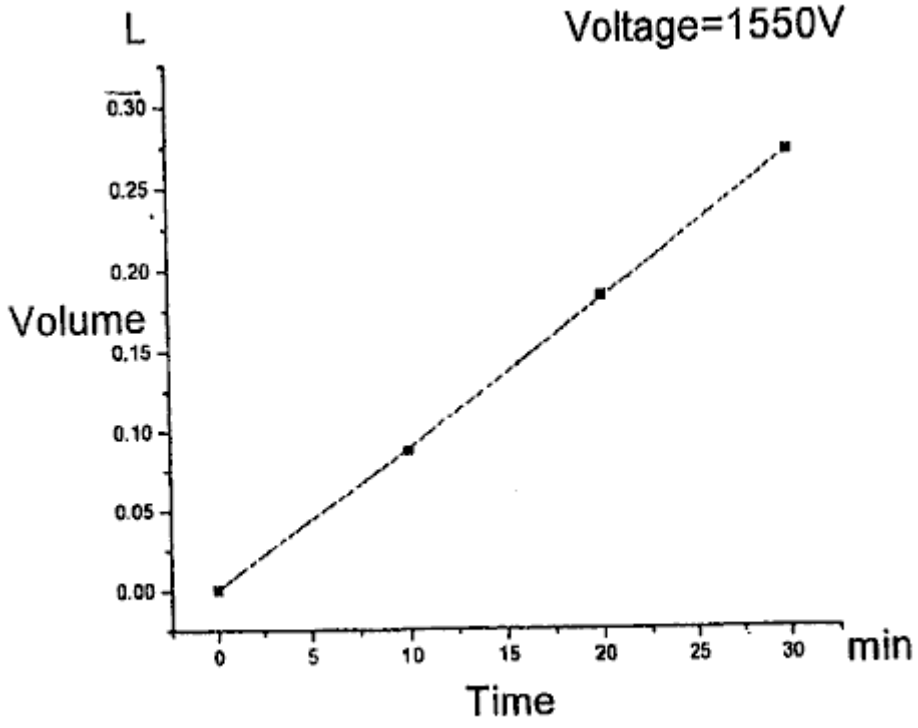
L
Voltage=1550V
0.30
0.25
0.20
Volume
0.15
0.10
0.05
0.00
0
5
10
15
20
25
30
min
Time

FIG. 39

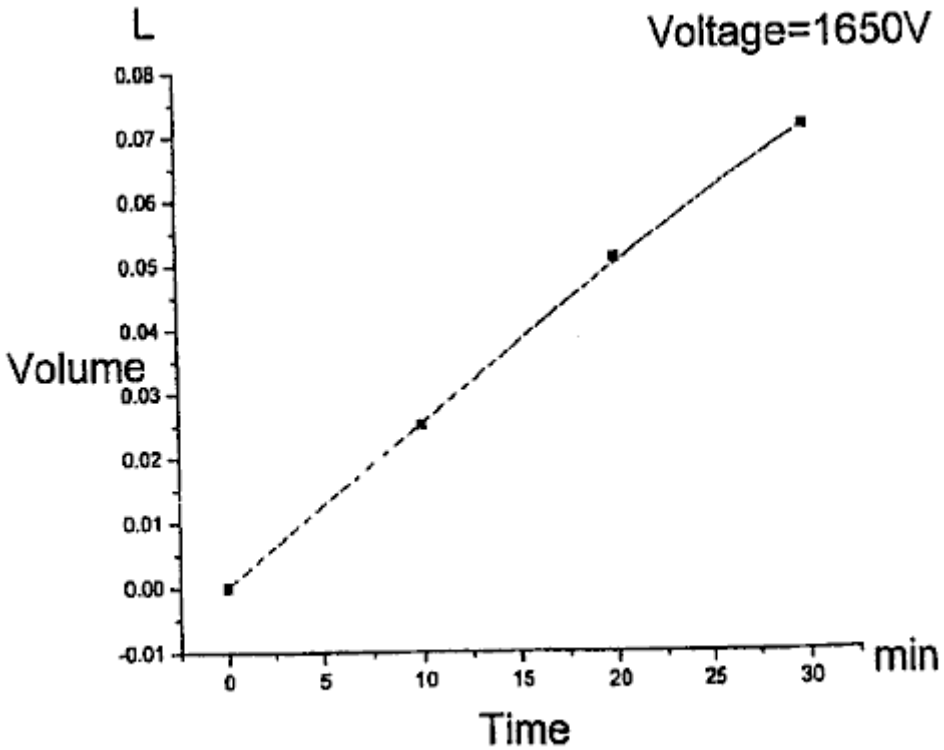
L
Voltage=1650V
0.08
0.07
0.06
0.05
0.04
Volume
0.03
0.02
0.01
0.00
-0.01
0
5
10
15
20
25
30
min
Time

FIG. 40

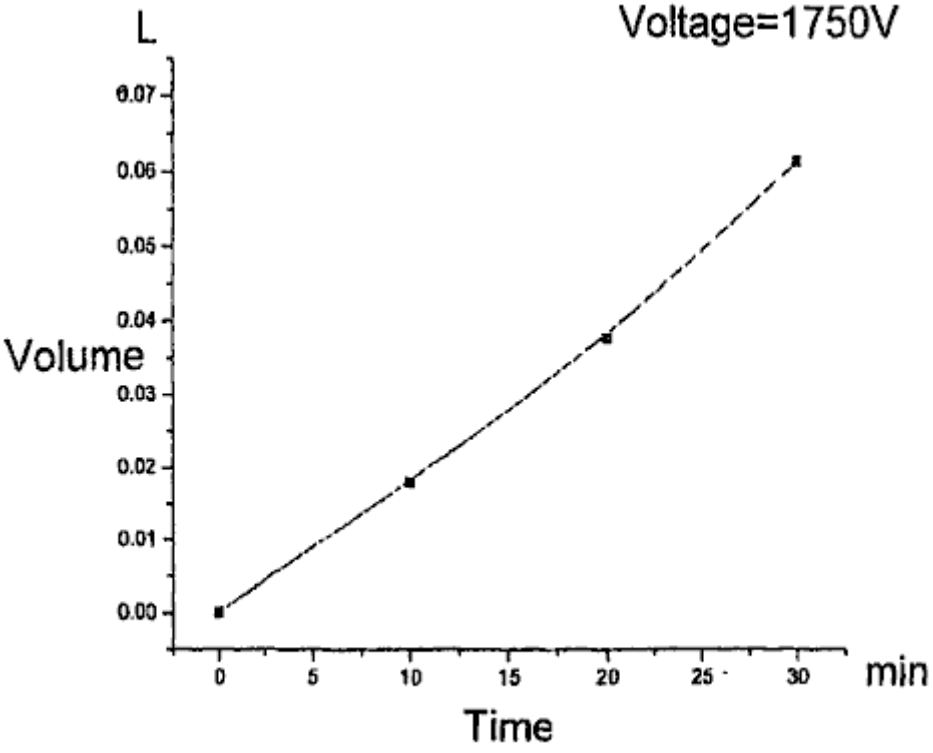
L
Voltage=1750V
0.07
0.06
0.05
0.04
Volume
0.03
0.02
0.01
0.00
0
5
10
15
20
25
30
min
Time

FIG. 41

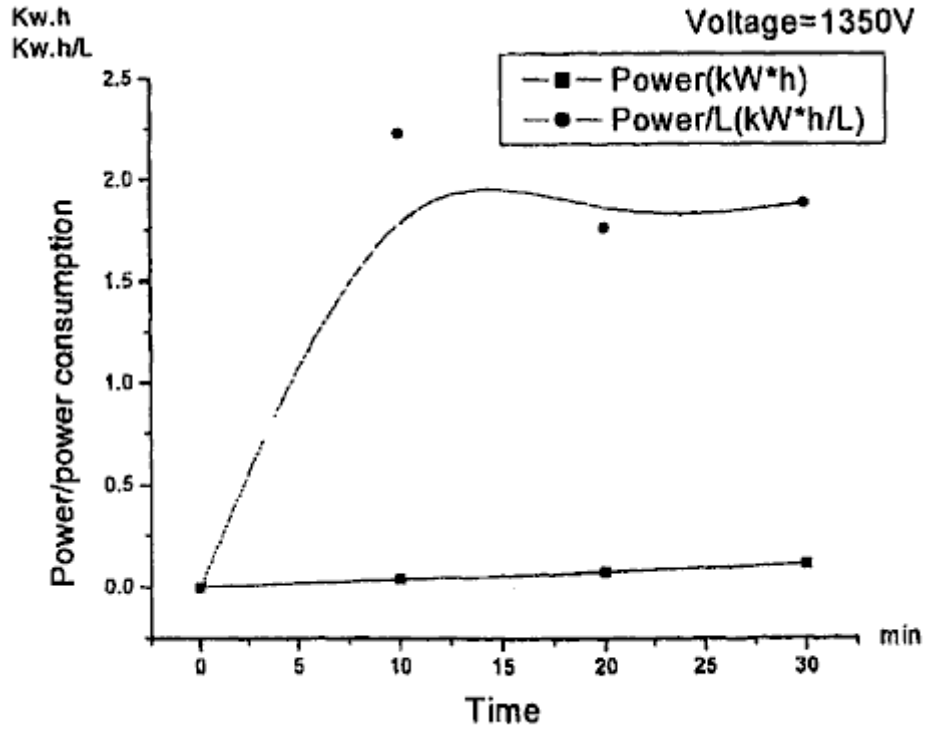
Kw.h
Kw.h/L
Voltage=1350V
Power(kW*h)
Power/L(kW*h/L)
2.5
2.0
1.5
1.0
0.5
0.0
Power/power consumption
0
5
10
15
20
25
30
min
Time

FIG. 42

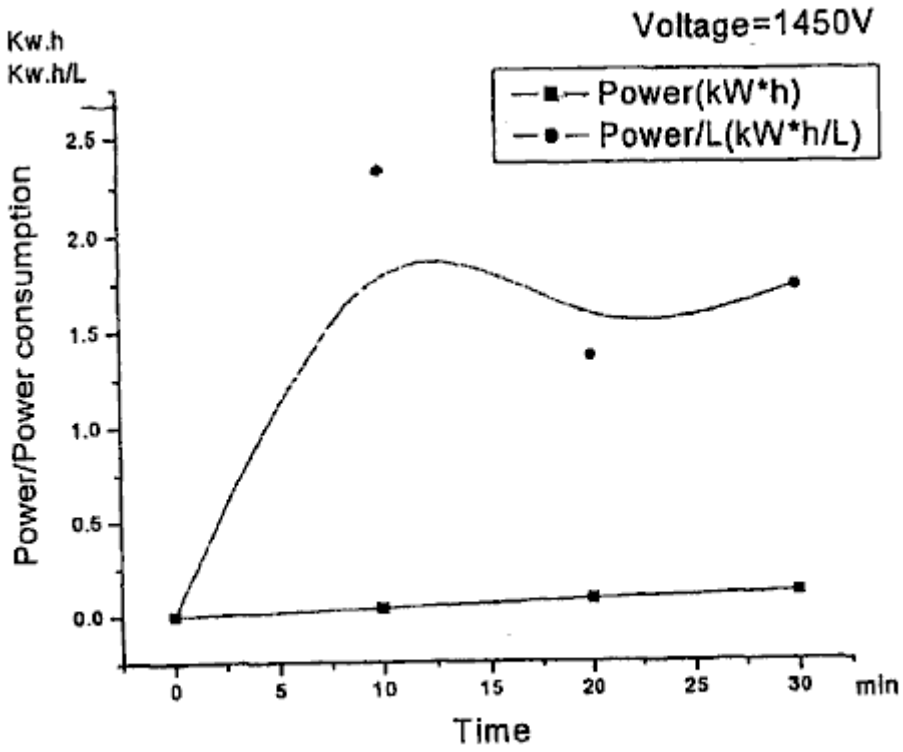
Voltage=1450V
Kw.h
Kw.h/L
Power(kW*h)
Power/L(kW*h/L)
Power/Power consumption
2.5
2.0
1.5
1.0
0.5
0.0
0
5
10
15
20
25
30
min
Time

FIG. 43

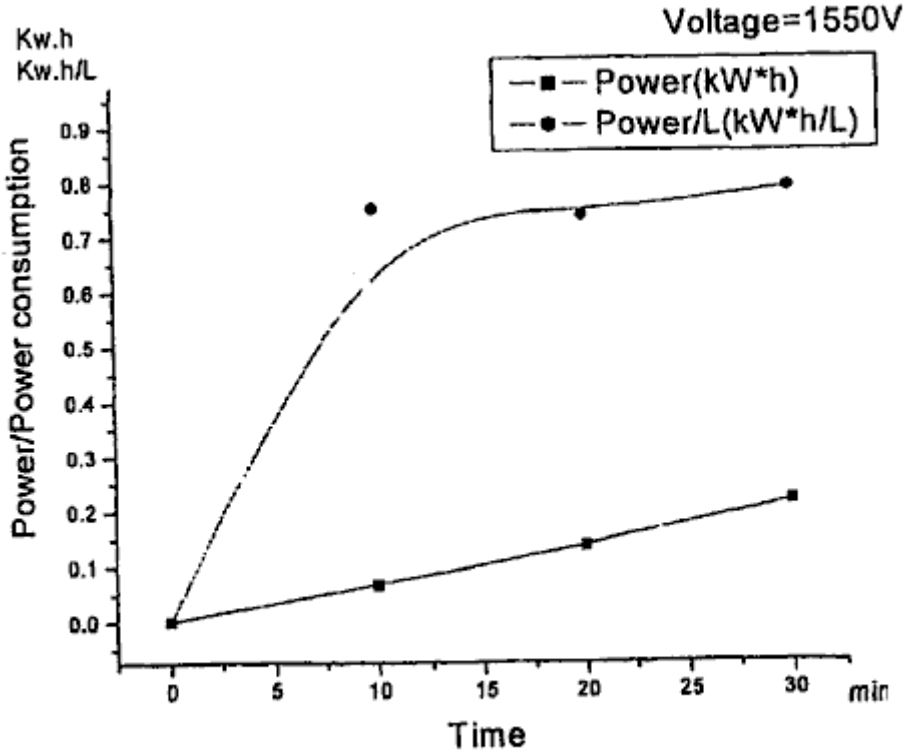
Voltage=1550V
Kw.h
Kw.h/L
Power(kW*h)
Power/L(kW*h/L)
Power/Power consumption
0.9
0.8
0.7
0.6
0.5
0.4
0.3
0.2
0.1
0.0
0
5
10
15
20
25
30
min
Time

FIG. 44

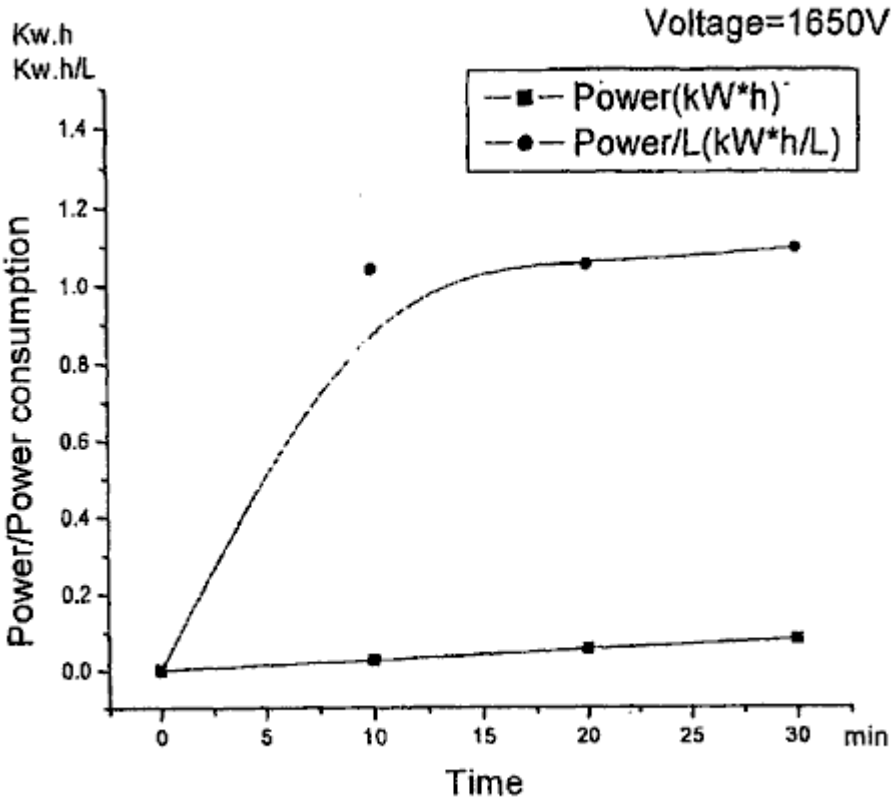
Voltage=1650V
Kw.h
Kw.h/L
Power(kW*h)
Power/L(kW*h/L)
Power/Power consumption
1.4
1.2
1.0
0.8
0.6
0.4
0.2
0.0
0
5
10
15
20
25
30
min
Time

FIG. 45

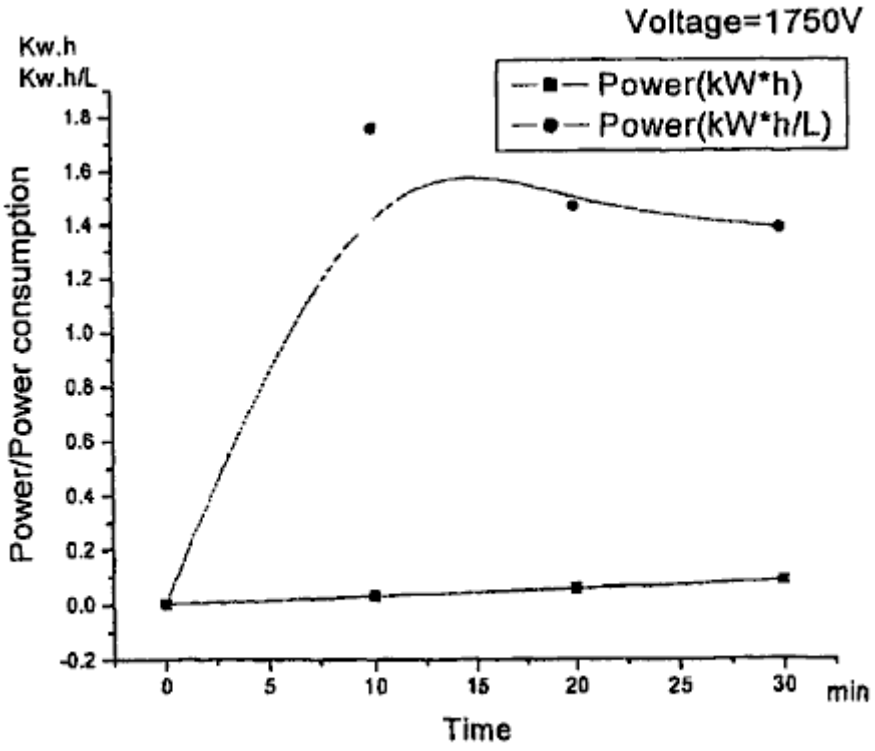
Voltage=1750V
Kw.h
Kw.h/L
Power(kW*h)
Power(kW*h/L)
Power/Power consumption
1.8
1.6
1.4
1.2
1.0
0.8
0.6
0.4
0.2
0.0
-0.2
0
5
10
15
20
25
30
min
Time

FIG. 46

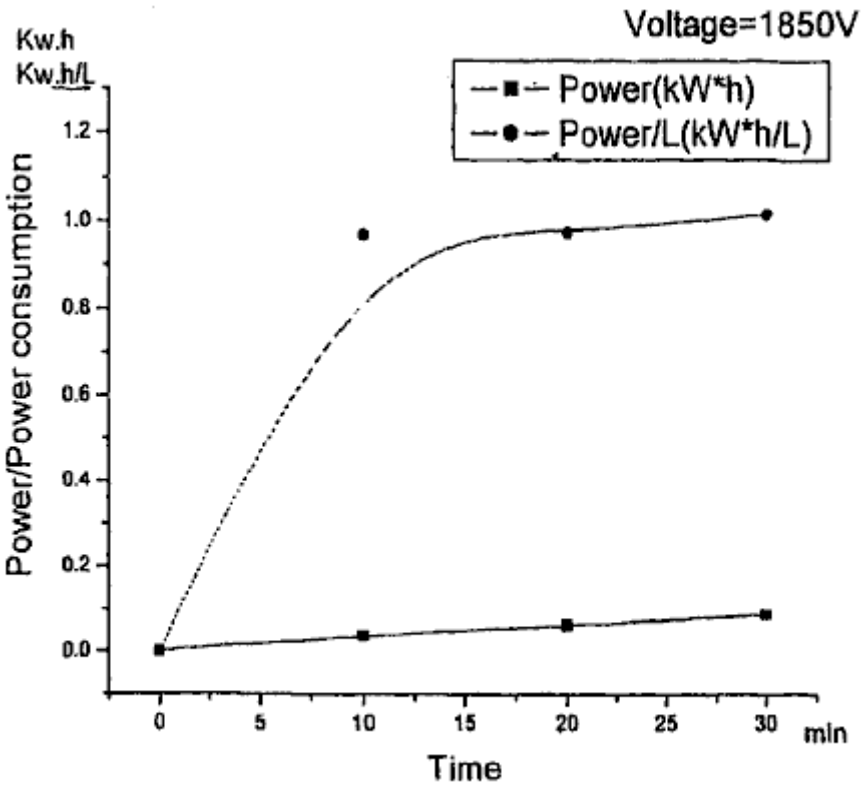
Voltage=1850V
Kw.h
Kw.h/L
Power(kW*h)
Power/L(kW*h/L)
Power/Power consumption
1.2
1.0
0.8
0.6
0.4
0.2
0.0
0
5
10
15
20
25
30
min
Time

FIG. 47

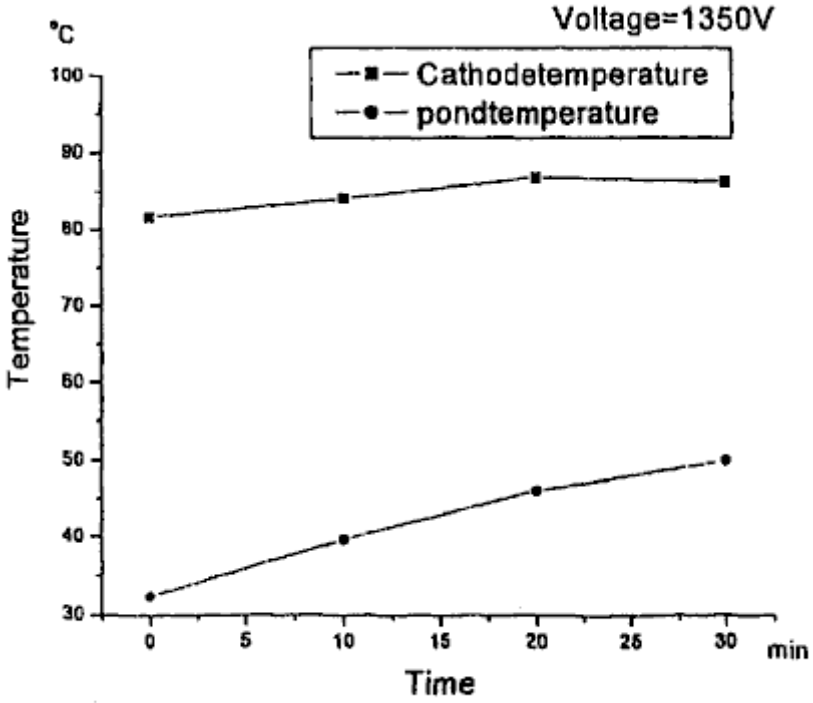
Voltage=1350V
°C
Cathodetemperature
pondtemperature
Temperature
100
90
80
70
60
50
40
30
0
5
10
15
20
25
30
min
Time

FIG. 48

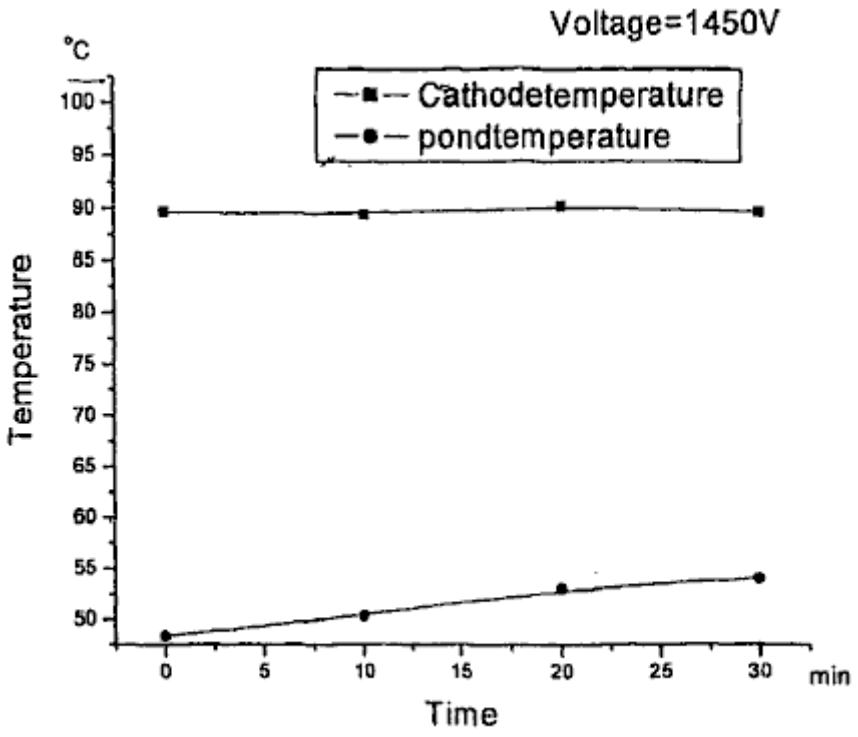
Voltage=1450V
°C
Cathodetemperature
pondtemperature
Temperature
100
95
90
85
80
75
70
65
60
55
50
0
5
10
15
20
25
30
min
Time

FIG. 49

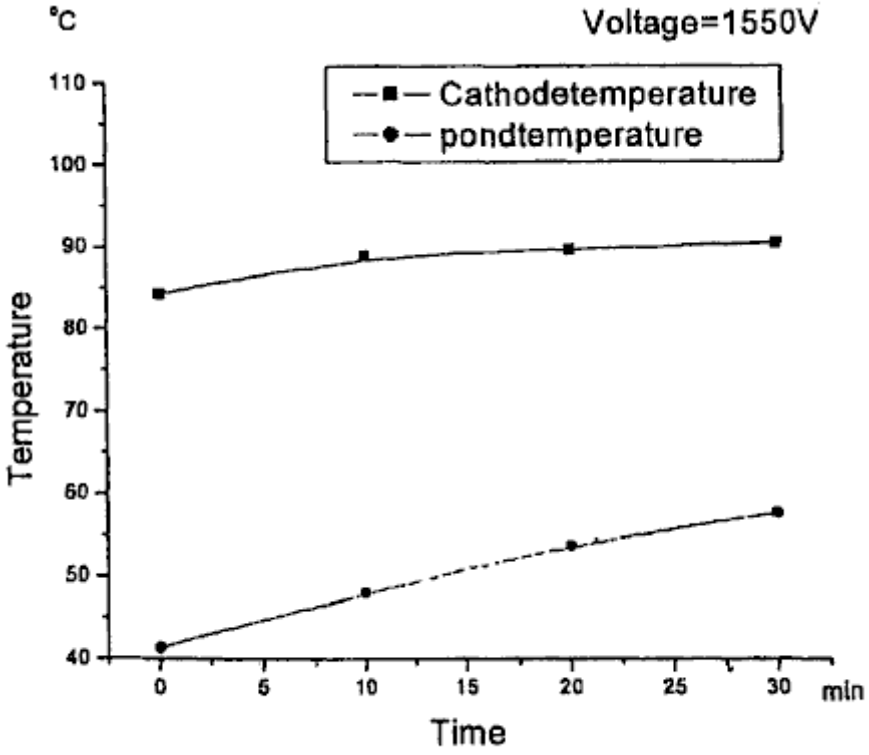
°C
Voltage=1550V
Cathodetemperature
pondtemperature
Temperature
110
100
90
80
70
60
50
40
0
5
10
15
20
25
30
min
Time

FIG. 50

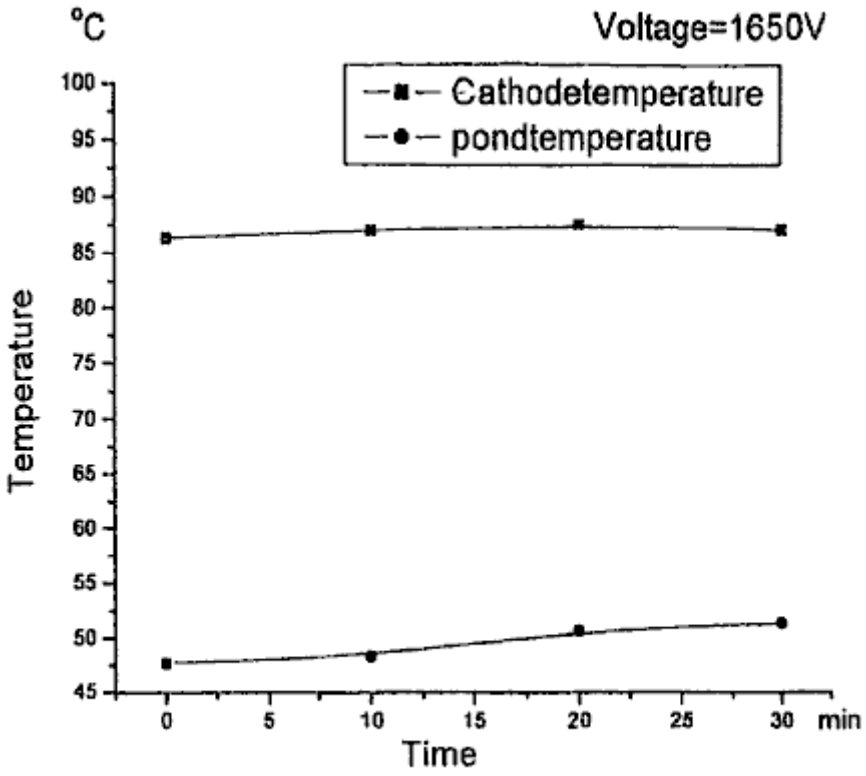
°C
Voltage=1650V
Cathodetemperature
pondtemperature
Temperature
100
95
90
85
80
75
70
65
60
55
50
45
0
5
10
15
20
25
30
min
Time

FIG. 51

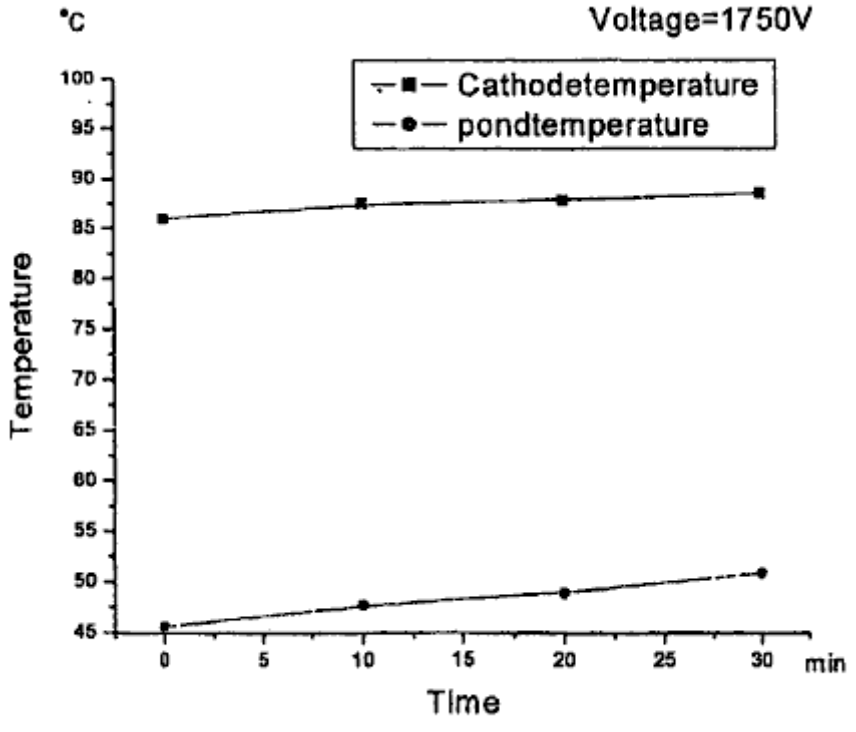
°C
Voltage=1750V
Cathodetemperature
pondtemperature
Temperature
100
95
90
85
80
75
70
65
60
55
50
45
0
5
10
15
20
25
30
min
Time

FIG. 52

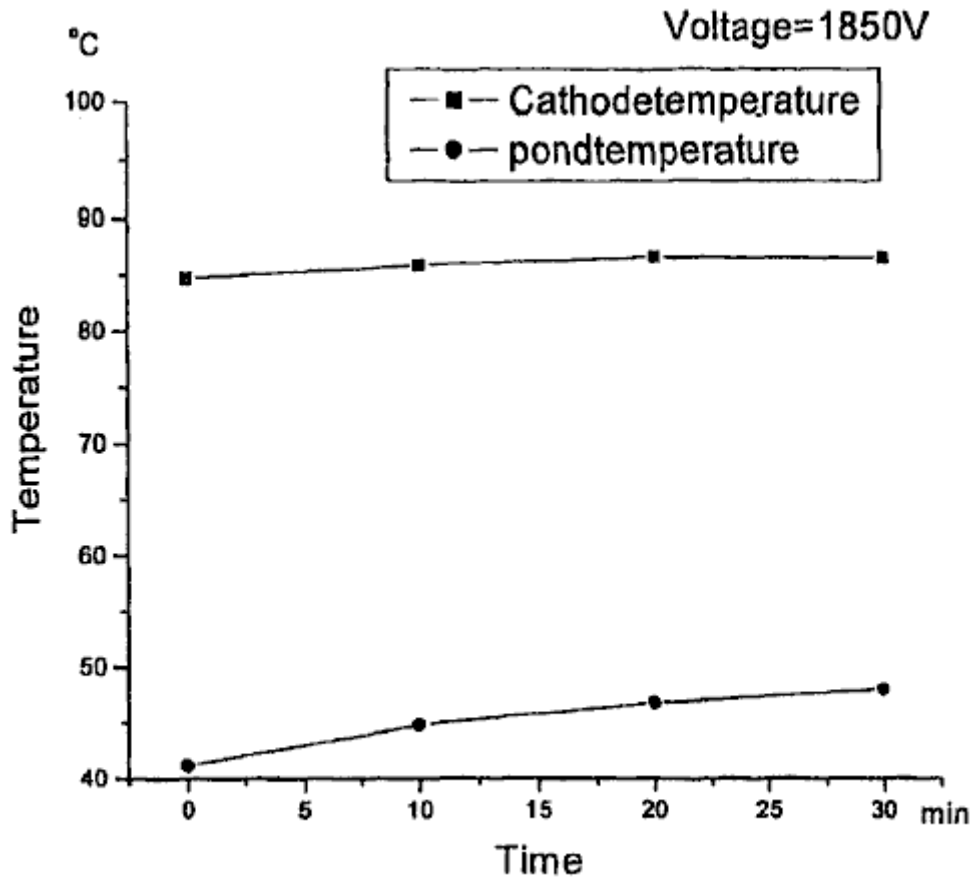
Voltage=1850V
°C
Cathodetemperature
pondtemperature
100
90
80
70
60
50
40
Temperature
0
5
10
15
20
25
30
min
Time
FIG. 53